THE ROLE OF CALCIUM HANDLING IN HEART FAILURE AND HEART FAILURE ASSOCIATED ARRHYTHMIAS

EDITED BY: Elisabetta Cerbai, Alessandro Mugelli and Daniel M. Johnson
PUBLISHED IN: Frontiers in Physiology

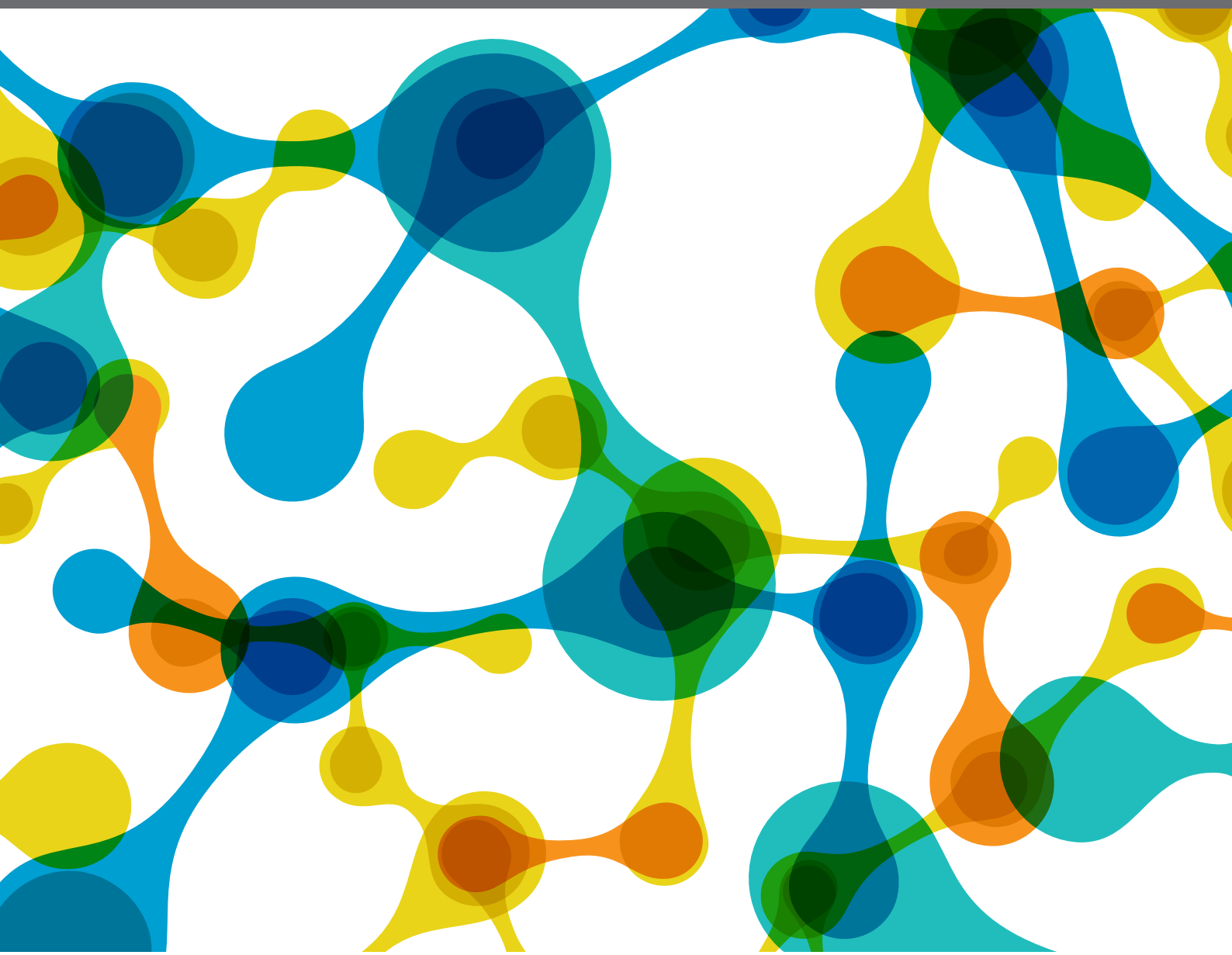

frontiers Research Topics

frontiers

ISSN 1664-8714
ISBN 978-2-88945-825-7
DOI 10.3389/978-2-88945-825-7

About Frontiers

Frontiers is more than just an open-access publisher of scholarly articles: it is a pioneering approach to the world of academia, radically improving the way scholarly research is managed. The grand vision of Frontiers is a world where all people have an equal opportunity to seek, share and generate knowledge. Frontiers provides immediate and permanent online open access to all its publications, but this alone is not enough to realize our grand goals.

Frontiers Journal Series

The Frontiers Journal Series is a multi-tier and interdisciplinary set of open-access, online journals, promising a paradigm shift from the current review, selection and dissemination processes in academic publishing. All Frontiers journals are driven by researchers for researchers; therefore, they constitute a service to the scholarly community. At the same time, the Frontiers Journal Series operates on a revolutionary invention, the tiered publishing system, initially addressing specific communities of scholars, and gradually climbing up to broader public understanding, thus serving the interests of the lay society, too.

Dedication to Quality

Each Frontiers article is a landmark of the highest quality, thanks to genuinely collaborative interactions between authors and review editors, who include some of the world's best academicians. Research must be certified by peers before entering a stream of knowledge that may eventually reach the public - and shape society; therefore, Frontiers only applies the most rigorous and unbiased reviews.
Frontiers revolutionizes research publishing by freely delivering the most outstanding research, evaluated with no bias from both the academic and social point of view. By applying the most advanced information technologies, Frontiers is catapulting scholarly publishing into a new generation.

What are Frontiers Research Topics?

Frontiers Research Topics are very popular trademarks of the Frontiers Journals Series: they are collections of at least ten articles, all centered on a particular subject. With their unique mix of varied contributions from Original Research to Review Articles, Frontiers Research Topics unify the most influential researchers, the latest key findings and historical advances in a hot research area! Find out more on how to host your own Frontiers Research Topic or contribute to one as an author by contacting the Frontiers Editorial Office: researchtopics@frontiersin.org

THE ROLE OF CALCIUM HANDLING IN HEART FAILURE AND HEART FAILURE ASSOCIATED ARRHYTHMIAS

Topic Editors:
Elisabetta Cerbai, University of Florence, Italy
Alessandro Mugelli, University of Florence, Italy
Daniel M. Johnson, University of Birmingham, United Kingdom

Under normal, healthy conditions, the contraction of cardiac myocytes, leading to the pump function of this organ, is driven by calcium-dependent mechanisms. Entry of calcium into the myocyte during the cardiac action potential causes activation of the ryanodine receptors and release of calcium from the sarcoplasmic reticulum. This process termed calcium-induced calcium release is essential for excitation-contraction coupling and enables each action potential to be transduced into a mechanical event. Indeed, in healthy myocytes, the calcium concentration in the cytosol of is elevated approximately 10-fold from a resting level of ~100 nM to ~1 μM. This process is finely orchestrated by a number of key proteins, which can be specifically regulated by various pathways depending on the oxygen demand. Furthermore, the specific structure of the myocyte allows certain calcium-dependent processes to be compartmentalised, increasing the efficiency and safety of this regulation.

Heart failure is a common, costly, and life-threatening condition. In 2015, for example, it affected around 40 million people globally. In patients with heart failure, the risk of sudden cardiac death and arrhythmias increases substantially. Cellular remodelling and alterations in calcium handling, which appear to contribute to the arrhythmogenic burden in heart failure, have been extensively reported. However, a number of unanswered questions remain, and each new study—while continuing to shed light on this subject—raises additional novel questions.

This current compendium of articles covers a number of aspects and comprehensively reviews current knowledge and perspectives regarding the link between calcium handling, arrhythmias and heart failure providing at the same time insights that may lead to novel therapeutic options for the future.

Citation: Cerbai, E., Mugelli, A., Johnson, D. M., eds. (2019). The Role of Calcium Handling in Heart Failure and Heart Failure Associated Arrhythmias. Lausanne: Frontiers Media. doi: 10.3389/978-2-88945-825-7

Table of Contents

frontiers in Physiology

EDITORIAL
published: 22 January 2019
doi: 10.3389/fphys.2019.00001

Editorial: The Role of Calcium Handling in Heart Failure and Heart Failure Associated Arrhythmias

Daniel M. Johnson[1]*, *Alessandro Mugelli*[2] *and Elisabetta Cerbai*[2]

[1] Institute of Cardiovascular Sciences, University of Birmingham, Birmingham, United Kingdom, [2] Department of Neuroscience, Psychology, Drug Research and Child Health (NeuroFarBa), University of Florence, Florence, Italy

Keywords: calcium, arrhythmia, heart failure, calcium signaling, ventricular, atrial

Editorial on the Research Topic

The Role of Calcium Handling in Heart Failure and Heart Failure Associated Arrhythmias

Over 20 years ago Heart Failure (HF) was described as an epidemic (Braunwald, 1997) and although we have made substantial progress in HF research and treatment since then, the prevalence of HF continues to rise. The estimated 6.5 million American adults over the age of 20 with HF between 2011 and 2014 (Benjamin Emelia et al., 2018) calls for a deeper understanding of mechanisms involved in this potentially life threatening syndrome.

Ever since Sydney Ringer's seminal work in the late 1800's proving the importance of Ca^{2+} in contractility (Miller, 2004), we have continued to be astounded by this multifaceted performer of cardiac function. In addition to sustaining the normal heartbeat, once dysregulated, Ca^{2+} handling and its associated proteins and pathways may turn into major driving factors toward mechanical and electrical dysfunction in HF.

Over recent years substantial progress has been made in understanding the links between Ca^{2+} handling and HF, including the arrhythmogenic predisposition. For these reasons the present Research Topic focuses on the interactions of Ca^{2+} with multiple players that can influence HF progression and arrhythmia liability. It contains both review articles as well as original research in this area which we believe could contribute to our understanding of HF and potential therapeutic targets.

The topic opens with two overview articles on Ca^{2+} handling and arrhythmogenesis in two relevant pathological conditions (Coppini et al.; Johnson and Antoons). Johnson and Antoons focus on the pathways likely contributing to ventricular arrhythmogenesis in HF with reduced ejection fraction (HFrEF) as a result of changes in both stretch and β-adrenergic signaling. These authors consider the changes in signaling at the level of the single cardiac myocyte in HF, looking at the crosstalk between the two complex signaling pathways associated with HF, Ca^{2+} handling and arrhythmogenesis, their disruption in HF and finally the consequence of changes in local Ca^{2+} microdomains (Johnson and Antoons). Coppini et al. describe changes in intracellular Na^{+} and Ca^{2+} in hypertrophic cardiomyopathy (HCM) using human ventricular tissue and single myocytes. HCM is one of the most common inherited cardiac diseases, generally due to mutations in sarcomeric proteins, and can lead to severe diastolic dysfunction and sudden death (Coppini et al.). In both papers, a number of potential therapeutic targets are proposed.

A link between atrial fibrillation (AF), HF and sudden cardiac death has been apparent for a number of years, (Lee Park and Anter, 2013; Reinier et al., 2014), and two articles aim to shed light into novel links between these "epidemics." Initially Denham et al. provide an excellent and extensive review of the literature linking AF and HF with altered Ca^{2+} handling, and discuss how these two "syndromes" feedback on each other eventually worsening the phenotype. Then,

Edited and reviewed by:
Ruben Coronel,
University of Amsterdam, Netherlands

***Correspondence:**
Daniel M. Johnson
danjohnsonmaastricht@gmail.com

Specialty section:
This article was submitted to Cardiac Electrophysiology, a section of the journal Frontiers in Physiology

Received: *13 December 2018*
Accepted: *04 January 2019*
Published: *22 January 2019*

Citation:
Johnson DM, Mugelli A and Cerbai E (2019) Editorial: The Role of Calcium Handling in Heart Failure and Heart Failure Associated Arrhythmias. Front. Physiol. 10:1. doi: 10.3389/fphys.2019.00001

Molina et al. provide novel insights into this subject using explanted tissue and myocytes isolated from patients with HFrEF alone or HFrEF with concomitant chronic AF. Interestingly, a number of differences were noted between these two populations, including increased spontaneous I_{NCX} and RyR2 open probability in patients with both AF and HFrEF when compared to patients with HFrEF alone (Molina et al.). These observations set a starting point in the "chicken and egg" history of AF, suggesting the occurrence of a specific substrate triggering AF in the context of HF-induced remodeling, that could be translated into improved therapeutic options.

Improvements in imaging techniques have speeded up our understanding of Ca^{2+} handling in multiple organ systems and pathologies, and HF has been no exception. Sacconi's lab has been amongst the pioneers in this area with the development of the ultrafast random access multiphoton (RAMP) microscope. This approach was used to simultaneously measure action potentials (AP) and intracellular Ca^{2+} transients at multiple sites, and in different sub-cellular domains within the myocyte (Crocini et al., 2014). Furthermore, this technique allows investigation of spatio-temporal relationships between local Ca^{2+} release and AP prolongation. Recent findings from this area are described in the current research topic by Scardigli et al. Ghouri et al. also utilize novel imaging techniques to optically image intact (infarcted) hearts. Using 2-photon microscopy, they visualize functional differences below the surface layers thus demonstrating electrophysiological abnormalities in infarcted areas when compared to the border zone and the non-infarcted area (Ghouri et al.).

In-silico investigations have also had a large impact on our understanding of cardiac electrophysiology over the years, as they allow dissecting of pathways to a resolution that may not be possible in the "wet-lab" (Quinn and Kohl, 2013). Mora et al. specifically look at the interactions between fibroblasts and myocytes using mathematical modeling and how these interactions can alter Ca^{2+} handling. Meanwhile, Tomek et al. expand our knowledge on how action potential alternans can be regulated by differential Ca^{2+} release from the sarcoplasmic reticulum (Mora et al.; Tomek et al.).

The search for unusual or veiled culprits—such as specific protein interactions or pathways—likely contributing to arrhythmia in HF is the common topic of three papers. Arvanitis et al. give an overview of the Histidine Rich Ca^{2+} binding protein (HRC) and its potential role in arrhythmogenesis. whilst Skogestad and Aronsen unravel alterations as a result of hypokalemia—a common syndrome amongst HF patients with life-threatening pro-arrhythmic consequences. Meanwhile, Ronchi et al. investigate how three factors often altered in HF-namely sympathetic pathways, AP duration and the renin-angiotensin system- can lead to altered Ca^{2+} release from the sarcoplasmic reticulum.

Finally, prediction of potential arrhythmias in HF patients remains challenging. Sprenkeler et al. use a large animal model with ventricular remodeling to demonstrate that differences in force-frequency relationships and mechanical restitution may be an interesting avenue to pursue. These data should ignite studies aimed at investigating the clinical relevance of such parameters (Sprenkeler et al.).

Overall, this issue of Frontiers has highlighted the fact that Ca^{2+} research in HF and the link to arrhythmogenesis is flourishing. There are still many unexplored avenues for research, exploiting state-of-the-art technologies to gain deeper insight into individual or common arrhythmogenic mechanisms in HF with different etiology and dysfunction (e.g., HFrEF vs. HFpEF).

We hope that this Topic will stimulate the development of future collaborative and interdisciplinary research ultimately leading to an increased therapeutic arsenal against life-threatening arrhythmias in HF.

AUTHOR CONTRIBUTIONS

All authors listed have made a substantial, direct and intellectual contribution to the work, and approved it for publication.

REFERENCES

Benjamin Emelia, J., Virani Salim, S., Callaway Clifton, W., Chamberlain Alanna, M., Chang Alexander, R., Cheng, S., et al. (2018). Heart disease and stroke statistics–2018 update: a report from the american heart association. *Circulation* 137, e67–e492. doi: 10.1161/CIR.0000000000000558

Braunwald, E. (1997). Cardiovascular medicine at the turn of the millennium: triumphs, concerns, and opportunities. *N. Engl. J. Med.* 337, 1360–1369. doi: 10.1056/NEJM199711063371906

Crocini, C., Coppini, R., Ferrantini, C., Pavone, F. S., and Sacconi, L. (2014). Functional cardiac imaging by random access microscopy. *Front. Physiol.* 5:403. doi: 10.3389/fphys.2014.00403

Lee Park, K., and Anter, E. (2013). Atrial fibrillation and heart failure: a review of the intersection of two cardiac epidemics. *J. Atr. Fibrillation* 6:751. doi: 10.4022/jafib.751

Miller, D. J. (2004). Sydney Ringer; physiological saline, calcium and the contraction of the heart. *J. Physiol.* 555, 585–587. doi: 10.1113/jphysiol.2004.060731

Quinn, T. A., and Kohl, P. (2013). Combining wet and dry research: experience with model development for cardiac mechano-electric structure-function studies. *Cardiovasc. Res.* 97, 601–611. doi: 10.1093/cvr/cvt003

Reinier, K., Marijon, E., Uy-Evanado, A., Teodorescu, C., Narayanan, K., Chugh, H., et al. (2014). The association between atrial fibrillation and sudden cardiac death: the relevance of heart failure. *JACC Heart Fail.* 2, 221–227. doi: 10.1016/j.jchf.2013.12.006

Conflict of Interest Statement: The authors declare that the research was conducted in the absence of any commercial or financial relationships that could be construed as a potential conflict of interest.

frontiers in Physiology

REVIEW
published: 16 October 2018
doi: 10.3389/fphys.2018.01453

Arrhythmogenic Mechanisms in Heart Failure: Linking β-Adrenergic Stimulation, Stretch, and Calcium

Daniel M. Johnson[1] and Gudrun Antoons[2]**

[1] Department of Cardiothoracic Surgery, Cardiovascular Research Institute Maastricht, Maastricht University, Maastricht, Netherlands, [2] Department of Physiology, Cardiovascular Research Institute Maastricht, Maastricht University, Maastricht, Netherlands

Heart failure (HF) is associated with elevated sympathetic tone and mechanical load. Both systems activate signaling transduction pathways that increase cardiac output, but eventually become part of the disease process itself leading to further worsening of cardiac function. These alterations can adversely contribute to electrical instability, at least in part due to the modulation of Ca^{2+} handling at the level of the single cardiac myocyte. The major aim of this review is to provide a definitive overview of the links and cross talk between β-adrenergic stimulation, mechanical load, and arrhythmogenesis in the setting of HF. We will initially review the role of Ca^{2+} in the induction of both early and delayed afterdepolarizations, the role that β-adrenergic stimulation plays in the initiation of these and how the propensity for these may be altered in HF. We will then go onto reviewing the current data with regards to the link between mechanical load and afterdepolarizations, the associated mechano-sensitivity of the ryanodine receptor and other stretch activated channels that may be associated with HF-associated arrhythmias. Furthermore, we will discuss how alterations in local Ca^{2+} microdomains during the remodeling process associated the HF may contribute to the increased disposition for β-adrenergic or stretch induced arrhythmogenic triggers. Finally, the potential mechanisms linking β-adrenergic stimulation and mechanical stretch will be clarified, with the aim of finding common modalities of arrhythmogenesis that could be targeted by novel therapeutic agents in the setting of HF.

Keywords: heart failure, myocytes, calcium, sympathetic stimulation, stretch, ryanodine, microdomains

OPEN ACCESS

Edited by:
Marcel van der Heyden, University Medical Center Utrecht, Netherlands

Reviewed by:
Rachel C. Myles, University of Glasgow, United Kingdom
Marina Cerrone, New York University, United States

****Correspondence:***
Daniel M. Johnson
danjohnsonmaastricht@gmail.com
Gudrun Antoons
g.antoons@maastrichtuniversity.nl

Specialty section:
This article was submitted to Cardiac Electrophysiology, a section of the journal Frontiers in Physiology

Received: *08 August 2018*
Accepted: *25 September 2018*
Published: *16 October 2018*

Citation:
Johnson DM and Antoons G (2018) Arrhythmogenic Mechanisms in Heart Failure: Linking β-Adrenergic Stimulation, Stretch, and Calcium. Front. Physiol. 9:1453. doi: 10.3389/fphys.2018.01453

Abbreviations: β-AR, β-adrenergic receptor; AC, adenyl cyclase; AP, action potential; BVR, beat-to-beat variability of repolarization; CaMKII, Ca^{2+}/calmodulin dependent protein kinase II; cAMP, cyclic adenosine 3′,5′-monophosphate; Casq2, cardiac calsequestrin; CICR, calcium induced calcium release; DAD, delayed afterdepolarization; EAD, early afterdepolarization; ECC, excitation contraction coupling; Epac, exchange protein activated by cAMP; HF, heart failure; I_{TI}, transient inward current; LTCC, L-type calcium channel; LVAD, left ventricular assist device; NCX, sodium/calcium exchanger; NO, nitric oxide; NOS, nitric oxide synthase; NOX2, NADPH oxidase 2; PI3K, phosphoinositide 3-kinase; PKA, protein kinase A; PLB, phospholamban; ROS, reactive oxygen species; RyR, ryanodine receptor; SACNS, stretch activated non-selective cation current; SERCA, SR Ca^{2+}-ATPase; SR, sarcoplasmic reticulum; INaL, late sodium current.

INTRODUCTION

Heart failure is a complex clinical syndrome with many contributory factors including ischemia, congenital heart disease, and pulmonary hypertension. HF can be defined as HF with preserved ejection fraction (HFpEF), when diastolic dysfunction plays a major role, or HF with reduced ejection fraction (HFrEF). HF with reduced ejection fraction has been associated with elevated sympathetic tone and mechanical load (Lohse et al., 2003). Both systems activate signaling transduction pathways that increase cardiac output, but adversely contribute to electrical instability, at least partially via modulation of Ca^{2+} handling.

The first documentation of alterations in the sympathetic signaling in chronic HF was when a decrease in concentrations of the sympathetic nervous neurotransmitter, norepinephrine, was shown in the failing human heart (Chidsey et al., 1963). Since that time, there has been accumulating evidence that the sympathetic nervous system plays a considerable role in HF (Port and Bristow, 2001) and this is highlighted by the continued use of β-receptor blockers as a favorable pharmacological treatment of HF (Waagstein et al., 1993; Ponikowski et al., 2016).

The hyperadrenergic state is in large part caused by an imbalance of autonomic reflex responses to early alterations in cardiac and peripheral hemodynamics (Toschi-Dias et al., 2017). In HF, vagal control by the baroreceptor reflex is reduced (Eckberg et al., 1971), while sympatho-excitatory reflexes are augmented, including the cardiac sympathetic afferent reflex (Wang and Zucker, 1996). The cardiac-specific reflex originates in the ventricle and is activated by elevated filling pressures (Malliani et al., 1973; Wang and Zucker, 1996), creating a positive feedback loop as its activation causes excessive sympathetic outflow to the heart and arteries (Chen et al., 2015). In turn, the heart readapts its systolic and diastolic force to the adrenergic-mediated increases in hemodynamic load via intrinsic autoregulatory mechanisms (Neves et al., 2015). Thus, adrenergic and hemodynamic regulatory systems tightly interact via a complex interplay of feedback mechanisms at the local and systemic level that are initially compensatory, but ultimately pathological.

Arrhythmias are a major cause of mortality in HF patients, and sudden cardiac death has previously been linked with a higher NYHA class (Saxon et al., 2006; Santangeli et al., 2017). Furthermore, in a recent study, ventricular arrhythmias were seen in up to 45% of patients who had received a LVAD (Garan et al., 2013). Although over the last decades remarkable advances have been made in terms of our understanding of risk factors and the efficacy of device therapy the underlying mechanisms responsible for arrhythmia induction and sudden cardiac death in this population remain elusive, and this is largely down to the complexity of the disease.

In this review, we will focus on the roles that altered sympathetic stimulation as well as mechanics may have on arrhythmogenic phenotype in patients with HF with reduced ejection fraction, concentrating on alterations of Ca^{2+} dynamics, β-adrenergic stimulation and stretch at the level of the single cardiac myocyte. It is hoped that information gained in this field will ultimately lead to novel strategies that could improve our therapeutic arsenal against HF.

BASIC PRINCIPLES OF CALCIUM-DEPENDENT ARRHYTHMOGENESIS-AFTERDEPOLARIZATIONS

Before discussing arrhythmogenic mechanisms in HF we need to understand the basic mechanisms of arrhythmogenesis and the link to Ca^{2+}.

Afterdepolarizations are thought to be one of the major mechanisms driving arrhythmogenesis in multiple patho-physiologies and we will concentrate on these in this review (**Figure 1**). These oscillations in the membrane potential can lead to either triggered activity and/or functional block which may encourage re-entry circuits (Wit and Rosen, 1983). These phenomena can be detected at multiple levels, ranging from the single cardiac myocyte to the tissue and can even be observed in the intact heart when monophasic APs are recorded (Priori et al., 1990). They are defined as depolarizations of the cardiac AP that can occur in phases 2, 3, or 4 of the AP (Cranefield, 1977). When they occur in phase 4 of the AP they are called DADs whereas if they occur earlier on the AP then they are termed EADs.

There is now a general consensus that DADs are a result of a I_{TI} activated by intracellular Ca^{2+} (Marban et al., 1986). This I_{TI} was originally described by Lederer and Tsien (1976) as a result of digitalis-induced arrhythmias and was later shown to be mainly due to activation of the electrogenic Na^{+}-Ca^{2+} exchanger (NCX), while the Ca^{2+}-activated Cl^{-} current (ICl_{Ca}) appears to contribute in some species (Fedida et al., 1987; Zygmunt et al., 1998). Interestingly a study from Verkerk et al. (2001) showed that I_{TI} in failing human cardiac myocytes was as a result of NCX alone. In addition to the potential of DADs to induce arrhythmias via triggered activity or functional block, recent work has also highlighted the potential of DADs to increase beat-to-beat variability of repolarization (BVR) which may also contribute to the arrhythmogenic nature of these afterdepolarizations (Johnson et al., 2013). The Ca^{2+} that activates these arrhythmogenic currents originate from the SR and is released via diastolic release events (Venetucci et al., 2008). For these reasons, when the SR is overloaded with Ca^{2+}, for example during intense β-adrenergic stimulation, the chance of spontaneous Ca^{2+} release is increased as is the likelihood for DADs (Yamada and Corr, 1992).

Mechanisms underlying EADs are much less clear cut however, and remain a topic of much debate. Early evidence suggested EADs were caused as a result of reactivation of I_{CaL} due to the prolonged plateau phase of the AP (January and Riddle, 1989; Zeng and Rudy, 1995). However, there is other experimental evidence that suggests that EADs may also be caused as a result of I_{TI} activation by intracellular Ca^{2+}, especially under conditions of Ca^{2+} overload (Priori et al.,

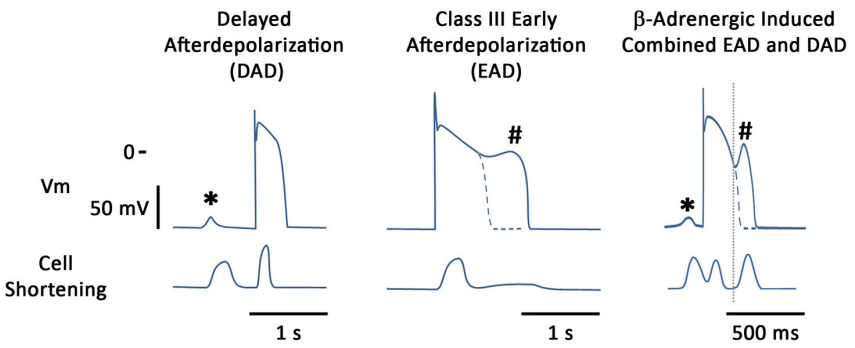

FIGURE 1 | Stylized examples of afterdepolarizations occurring in the single canine myocyte. Figure shows both membrane potentials and contraction for each situation. **(Left)** DAD (*) induced by the β-adrenergic agonist isoproterenol (ISO); **(Middle)** illustrates an EAD (#) induced by augmentation of the late sodium current, using ATX-II; **(Right)** illustrates that under certain conditions both types of afterdepolarizations can be seen in the same action potential. In this particular example, blockade of the potassium current, I_{Ks}, together with β-adrenergic stimulation are the proarrhythmic treatment and it can be seen that an early aftercontraction initiates prior to the upstroke of the EAD.

1990; Volders et al., 1997, 2000). Either way, it appears that EADs are modulated by systolic release of Ca^{2+} during the AP and are regulated by feedback on Ca^{2+} sensitive ion currents.

The link of afterdepolarizations at the single myocyte level to arrhythmogenesis at the whole heart level is extremely complex and incompletely understood. In the intact heart, myocytes are electrically coupled to each other, meaning that the membrane voltage is governed by not just one cell but multiple cells. Furthermore, the contribution of one afterdepolarization occurring in one cell (the source) will likely be negated by the neighboring cells not experiencing afterdepolarizations (the sink). Elegant work from the laboratory of James Weiss has investigated this phenomenon and has shown that chaotic EADs are able to synchronize globally when the tissue is smaller than a critical size. However, when the tissue is large enough, complete synchronization of EADs can no longer occur and this results in regions of partial synchronization that shift in time and space, that can act as foci for arrhythmia (Sato et al., 2009). Furthermore, work from the same group also estimated that the number of local myocyte DADs needed to be synchronized to induce a premature beat would be very large, however, this could be reduced structural and electrical remodeling (Xie et al., 2010). Finally, a recent study from the Bers' lab has also highlighted that in HF there is a much higher density of 'Ca^{2+} asynchronous' myocytes that are poorly coupled to the surrounding myocardium. These poorly coupled myocytes may also contribute to initiating triggered activity (Lang et al., 2017).

Over recent years it has become apparent that Ca^{2+} control of repolarization, and therefore also of arrhythmogenesis is more of a local rather than a global phenomenon. Both functional and structural microdomains dictate local Ca^{2+} concentrations, gradients and effector proteins. As these domains appear to be affected in HF, especially when we consider β-adrenergic stimulation and stretch we must also consider how this local control occurs.

LOCAL CONTROL OF Ca^{2+} RELEASE AT THE DYAD

In cardiac myocytes, Ca^{2+} is centrally involved in many processes including excitability, contraction, and regulation of gene expression. Such diversity of functional roles postulates the existence of dedicated microdomains in which Ca^{2+} signals are generated independently of cytosolic Ca^{2+} concentrations and sensed by macromolecular signaling components localized to these microdomains. Besides a functional component, Ca^{2+} microdomains are often physically delimited by specialized membrane structures and subcellular compartments. Specialized structures include dyadic junctions between transverse membrane invaginations (T-tubules) and SR, sarcolemmal domains outside dyads such as lipid rafts and caveolae, and intracellular structures such as tethered junctions between SR and mitochondria. Interestingly, compartmentalization of proteins that generate or regulate microdomain Ca^{2+} signaling is dynamic, often as a cause or consequence of disease. For example, the LTCC, or nNOS coupled to RyR, can translocate from the dyad to the sarcolemma which alters their function, presumably by coupling to different signaling complexes (Sanchez-Alonso et al., 2016; Carnicer et al., 2017).

Structural Organization

In the dyad, RyR in the SR juxtapose LTCC along T-tubules at close distances (∼12 nm) (Forbes and Sperelakis, 1983). Individual dyads control the process of Ca^{2+} induced Ca^{2+} release, or CICR. The elementary event is a Ca^{2+} spark released from the SR by the opening of RyR in a single Ca^{2+} release unit (Cheng and Lederer, 2008). When an LTCC opens during an AP, the local Ca^{2+} concentration in the dyad raises much more than cytosolic Ca^{2+}, from a diastolic level of 100 nM to more than 10 μM, sufficiently to activate RyR (Cannell and Kong, 2012). Not all RyR are localized at dyads; non-coupled RyR are activated through propagated Ca^{2+} release

with a delay. Therefore, a large heterogeneity of the tubular system (e.g., due to T-tubule loss in HF) causes dyssynchrony of subcellular Ca^{2+} release during systole (Heinzel et al., 2011). During diastole, few spontaneous Ca^{2+} sparks occur due to the relatively low sensitivity of RyR to resting Ca^{2+} levels. A spontaneous release event is spatially confined, but when the Ca^{2+} sensitivity or the RyR increases through phosphorylation or oxidation, or when SR Ca^{2+} load is high, more spontaneous Ca^{2+} sparks summate in time and space into propagating Ca^{2+} waves.

The structural design of the dyad also provides an optimal setting for feedback mechanisms of SR Ca^{2+} release on Ca^{2+}-regulated membrane currents. Negative feedback through Ca^{2+} release-dependent inactivation of LTCC serves as a mechanism to limit Ca^{2+} influx during the initial phase of the AP (Sham, 1997). As release-dependent inactivation is immediate, following the fast rise and decline of local Ca^{2+} near dyads, some of the LTCC may recover from inactivation within a single beat during the AP plateau (Acsai et al., 2011). The local feedback of Ca^{2+} on LTCC may contribute to the intrinsic BVR of the AP in normal physiology (Antoons et al., 2015). Interestingly, the same study did not find a major role for the NCX in BVR, although immunohistochemistry and functional studies have suggested colocalization of a fraction of NCX with LTCC (10–15% of total NCX) sensing local Ca^{2+} release in the dyadic subspace (Acsai et al., 2011; Scriven and Moore, 2013). In support of this notion, modulation of (dyadic) Ca^{2+} sparks by both reverse mode and forward mode NCX has been demonstrated (Neco et al., 2010; Biesmans et al., 2011).

To regulate CICR, the dyad harbors a repertoire of kinases and phosphatases that form macromolecular complexes with LTCC and RyR and regulate their levels of phosphorylation. PKA and CaMKII are key to the regulation of LTCC and RyR in the β-adrenergic and stretch response. PKA is targeted to LTCC and RyR via AKAPs, and transmits signals from β-ARs via cAMP (Catterall, 2015; Landstrom et al., 2017). Dyadic cAMP signals in the vicinity of LTCC and RyR are controlled by localized PDE activity (Kokkonen and Kass, 2017). It should be noted that exact mechanisms behind PKA regulation of RyR and its specific role in the β-adrenergic response are incompletely understood. Marx et al. (2000) proposed that PKA phosphorylation dissociates FKBP12.6 from RyR thereby enhancing RyR open probability. However, this mechanism remains questionable (Xiao et al., 2004). CaMKII is dually activated by Ca^{2+} and ROS (Maier and Bers, 2007), and possibly also by NO at high Ca^{2+} levels during β-adrenergic stimulation (Curran et al., 2014). Although CaMKII is targeted to both coupled and non-coupled RyR via unknown mechanisms, its activation is confined to the dyad, where it enhances the open probability of RyR and LTCC (Wehrens et al., 2004; Bers and Morotti, 2014).

Reactive Oxygen Species

In addition to phosphorylation mechanisms, ROS and NO have emerged as critical regulators of CICR. They modify LTCC and RyR function through redox modification of free cysteine residues. The action of ROS and NO is often multiphasic and bidirectional, depending on source, oxidant species, amount and timing and importantly, the local redox environment (Zima and Blatter, 2006). Typically, free radicals are short-lived and can only act on effectors in the close vicinity. Thus, redox modulation of Ca^{2+} in a cardiac myocyte is basically a tale of microdomain signaling of which the specific effects are determined by the subcellular location of the ROS/NO source and co-localization with its target proteins. Endogenous ROS are generated in the mitochondria as a by-product of respiration, and locally in the cytosol by specialized enzymes, such as NADPH oxidases (Burgoyne et al., 2012). Much of the O_2^- produced is rapidly converted to H_2O_2, a more stable and membrane permeable derivative. Endogenous NO is produced in relatively low concentrations by endothelial and neuronal isoforms of NOS (eNOS and nNOS, respectively) (Massion et al., 2003).

An important player in the redox control of dyadic Ca^{2+} is NOX2, a membrane-bound NADPH oxidase that resides in T-tubules. NOX2 is induced by fast pacing and stretch, and activates RyR via *S*-glutathionylation (Sánchez et al., 2005). RyR activation by rapid pacing also requires CaMKII, which itself is redox regulated (Erickson et al., 2008). Interestingly, the NOX2-CaMKII regulation of RyR is restricted to the dyadic cleft. In pig myocytes that resemble human and have a significant population of non-coupled RyR, faster pacing significantly increased Ca^{2+} spark activity of dyadic RyR, but not the activity of non-coupled RyR. Additionally, NOX2 and CaMKII inhibition abolished Ca^{2+} sparks in dyadic regions, but not near non-coupled regions (Dries et al., 2013). At this point it cannot be concluded if NOX2-derived ROS is upstream of CaMKII oxidation [as suggested in models of oxidative stress induced by angiotensin (Erickson et al., 2008; Purohit et al., 2013)] or whether NOX2 and CaMKII act in parallel. Furthermore, exact mechanisms of microdomain-specific activation of NOX2 and CaMKII in response to rapid pacing remain elusive. NOX2 is also activated by stretch. Prosser et al. (2011) have demonstrated that stretching a myocyte triggered an immediate burst of ROS and Ca^{2+} sparks. The ROS was derived from NOX2 as the response was sensitive to NOX2 inhibitors and absent in NOX2 deficient mice (Prosser et al., 2011).

In contrast to NOX2, mitochondria constitutively produce ROS. Mitochondria are located at a very short distance of dyadic regions [between 37 and 270 nm based on electron microscopy analysis of rat myocardium (Sharma et al., 2000)]. Several studies have shown that mitochondrial ROS can activate RyR (reviewed in Zhang H. et al., 2013), suggesting that basal ROS production by mitochondria is responsible for a significant portion of spontaneous Ca^{2+} sparks (Yan et al., 2008).

The LTCC also acts as a redox sensor due to free thiol groups in its α1-subunit (Muralidharan et al., 2016). Reported ROS effects on Ca^{2+} channel function are both stimulatory (Song et al., 2010), or inhibitory (Gill et al., 1995). This discrepancy might be due to differences in the phosphorylation state of the Ca^{2+} channel. Several serine/threonine kinases that regulate the channel are subjected to ROS modification, including PKA, PKC, and CaMKII (see Burgoyne et al., 2012, for review). The positive effects of phosphorylation might partially counterbalance the inhibitory effects of direct ROS oxidation of LTCC. During high oxidative stress, LTCC facilitation by CaMKII

is likely the predominant effect, since the calcium antagonist nifedipine could suppress the induction of EADs by H_2O_2 (Xie et al., 2009). ROS regulates many other proteins of the Ca^{2+} machinery outside the dyad. The overall effect of sustained ROS is Na^+ and Ca^{2+} overload promoting even more ROS production via positive feedback and predisposing the cell to afterdepolarizations (Wagner et al., 2013).

Nitric oxide is both a positive and a negative regulator of excitation–contraction (EC) coupling underscoring the complexity of cardiac NO signaling (Simon et al., 2014; Farah et al., 2018). NO exerts its action via two pathways: an indirect pathway by the activation of sGC producing cGMP, and a direct pathway by *S*-nitrosylation of proteins. High levels of NO would predominantly stimulate the cGMP pathway causing negative inotropy, while low levels activate nitrosylation processes leading to positive inotropy (González et al., 2008). The mechanisms of nitrosylation, and particularly its effects on EC coupling, remain poorly understood. Despite much controversy, some consensus has emerged on the specific roles of eNOS and nNOS highlighting the importance of their subcellular localization in modulating Ca^{2+} handling proteins. Colocalization of eNOS and LTCC in caveolae at the sarcolemma favors *S*-nitrosylation and inhibition of LTCC (Wang et al., 2008). nNOS is targeted to the SR where it colocalizes with RyR and is therefore considered the prime NO modulator of dyadic Ca^{2+} (Barouch et al., 2002). NO nitrosylates RyR and increases its activity (Wang et al., 2010, but see also Zahradníková et al., 1997). The notion that the positive effects of nNOS are linked to its specific localization on the SR has been supported by a recent study that developed a transgenic mouse model in which nNOS was targeted to the sarcolemma and no longer co-localized with RyR (Carnicer et al., 2017). Interestingly, relocalization of nNOS, as may occur in HF, produced the same negative effects on I_{CaL} and contraction as eNOS. In normal physiology, NOS activity is controlled by β-adrenergic stimulation and stretch, as will be discussed in the next paragraphs.

β-ADRENERGIC SIGNALING AND AFTERDEPOLARIZATIONS

In the heart, enhanced sympathetic activity is a potent stimulus for generation of arrhythmias. The relationship between sympathetic stimulation and triggered activity has long been recognized, *in vivo* (Priori et al., 1988, 1990) and *in vitro* (Lazzara and Marchi, 1989). During β-adrenergic stimulation, DADs and EADs often coexist. When Ca^{2+} overload plays a role in afterdepolarization formation, as could be the case under β-adrenergic stimulation, both EADs and DADs can be abolished by ryanodine, suggesting a common dependence of these on SR Ca^{2+} release under these conditions. In cardiac myocytes, β-ARs and their effector pathways targeting Ca^{2+} handling proteins are highly compartmentalized. In this paragraph, we will discuss the parallel activation of multiple molecular pathways by β-adrenergic subtypes, their specific end targets to controlling local and global Ca^{2+} release, and their impact on the generation of DADs and EADs.

β-Adrenergic Signaling Pathway

β-Adrenergic stimulation activates two pathways that operate in parallel: a PKA-dependent pathway that impacts on systolic Ca^{2+} through modulation of SR Ca^{2+} load, and a CaMKII pathway that regulates diastolic SR Ca^{2+} release (**Figure 2A**). Molecularly, the PKA signaling cascade is clearly defined. Upon activation, β-adrenergic agonists stimulate adenylate cyclase via Gs-coupled proteins raising cAMP levels that activates PKA (Bers, 2002). Subsequent phosphorylation of PKA substrates, including LTCC (causing increased Ca^{2+} influx) and PLB (accelerating SR Ca^{2+} uptake), results in enhancement of SR Ca^{2+} load. In cardiac myocytes, the compartmentation of cAMP signaling has been attributed to different β-AR subtypes that have distinct subcellular locations. β2 receptors are preferentially located at T-tubules where they co-localize with LTCC in caveolae, while β1 receptors are distributed more globally across T-tubules and surface sarcolemma. Using FRET sensors for cAMP, it was demonstrated that selective β1 stimulation generates cAMP signals that propagate throughout the cell, whereas the β2 AR signal is locally confined in T-tubules and specifically regulates LTCC during CICR (Nikolaev et al., 2006).

In vitro, PKA can also phosphorylate RyR (Marx et al., 2000), but in intact myocytes a functional role for PKA regulation of RyR remains controversial. Most evidence is in favor of CaMKII as the prime modulator of RyR during β-adrenergic stimulation. In response to adrenergic activation, CaMKII phosphorylates RyR and increases open probability when measured as SR Ca^{2+} leak (Curran et al., 2007) or diastolic Ca^{2+} sparks (Gutierrez et al., 2013). A recent study in pig myocytes suggested that CaMKII-dependent modulation of RyR during β-adrenergic stimulation was restricted to RyRs specifically in the dyadic cleft, and involved local activation of nNOS (Dries et al., 2016). The nNOS/CaMKII effects were not observed in RyR release sites that were not coupled to T-tubules. While there is conclusive evidence to support nNOS involvement in β-adrenergic modulation of RyR (Massion et al., 2003), the steps upstream from nNOS activation are less well defined. Some, but not all, studies suggested the involvement of Epac, a cAMP target parallel to PKA, leading to CaMKII autophosphorylation and downstream RyR phosphorylation (Pereira et al., 2007; Oestreich et al., 2009). A second pathway, independent of cAMP, involves PI3K and Akt as upstream activators of nNOS inducing CaMKII activation via nitrosylation (Curran et al., 2014). A recent study suggested that the Epac and nNOS pathway are interdependent and function largely in series (Pereira et al., 2017).

During β-adrenergic stimulation, the cAMP-PKA and nNOS-CaMKII pathways operate in parallel. From the current evidence it is clear that PKA signaling is distributed more globally with robust effects on LTCC and SERCA, whereas CaMKII is highly localized and exerts stronger effects than PKA on RyR. Ca^{2+} current facilitation by CaMKII under β-AR has also been demonstrated (Dries et al., 2016). The integrated response is

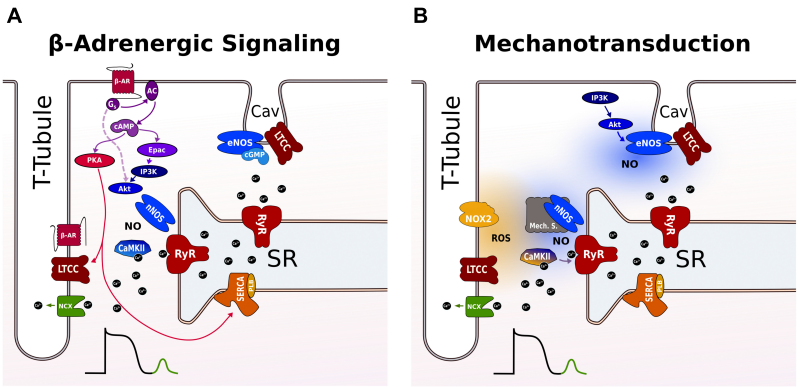

FIGURE 2 | Proposed pathways for inducing SR Ca^{2+} leak during β-adrenergic signaling and stretch in a ventricular cardiomyocyte. **(A)** β-AR raises cAMP levels via G_s-protein-dependent activation of AC that activates both PKA and Epac. PKA phosphorylates LTCC and PLB leading to more Ca^{2+} influx and faster uptake by SERCA into the SR. Epac activates nNOS and CaMKII via an PI3K and AkT signaling cascade promoting SR Ca^{2+} leak via RyR phosphorylation. The broken line indicates a cAMP and Epac-independent pathway for local activation of nNOS targeted to RyR in the dyad. RyR not coupled to LTCC in T-tubules are not modulated by CaMKII and nNOS. eNOS is localized to caveolae and exerts negative effects on LTCC during β-adrenergic stimulation. **(B)** Mechanotransduction involves ROS and NO for RyR activation. The ROS and NO pathway are independent and operate on different timescales via different mechanosensors. NOX2 produces ROS near RyR in the dyad increasing RyR activity possibly via oxidation of CaMKII. With a delay, nNOS is activated via an unknown mechanosensing mechanism. The enhanced SR Ca^{2+} leak promotes Ca^{2+} waves that activate a transient inward NCX current causing DAD. Caveolar eNOS is activated by stretch via PI3K-Akt and positively modulates EC coupling outside the dyad by mechanisms that are incompletely understood. See text for further details. AC, adenyl cyclase; β-AR, β-adrenergic receptor; cAMP, cyclic adenosine 3',5'-monophosphate; CaMKII, Ca^{2+}/calmodulin-dependent protein kinase II; EC, excitation contraction; DAD, delayed afterdepolarizations; eNOS, endothelial nitric oxide synthase; Epac, exchange protein activated by cAMP; LTCC, L-type Ca channel; NCX, Na^{+}/Ca^{2+} exchanger; NO, nitric oxide; NOX2, NADPH oxidase type 2; nNOS, neuronal nitric oxide synthase; PI3K, phosphoinositide 3-kinase; PKA, protein kinase A; PLB, phospholamban; ROS, reactive oxygen species; RyR, ryanodine receptor; SERCA, SR Ca^{2+}-ATPase; SR, sarcoplasmic reticulum.

enhancement of LTCC currents, SR Ca^{2+} load and leak. Together, these effects are able to favor both EADs and DADs.

Ca^{2+}-Dependent Mechanisms of Afterdepolarizations During β-Adrenergic Stimulation

The link between β-adrenergic stimulation, RyR-mediated Ca^{2+} leak and arrhythmogenesis has been most convincingly demonstrated in the clinical case of catecholaminergic polymorphic ventricular tachycardia (CPVT). Patients with CPVT carry mutations in RyR that increase the open probability of the receptor, or in calsequestrin (Casq2) where SR Ca^{2+} buffering is hindered and/or the interaction of Casq2 and RyR is altered (Cerrone et al., 2009). Introducing a CPVT associated RyR mutation in a mouse model, for example, resulted in a higher rate of Ca^{2+} sparks, waves and DADs in myocytes, and development of bidirectional ventricular tachycardia after exposure to catecholamines (Cerrone et al., 2005; Liu et al., 2006; Fernández-Velasco et al., 2009). The higher incidence of DADs and triggered activity has been attributed to increased RyR sensitization to Ca^{2+} (lowering the SR threshold for Ca^{2+} waves), and the enhanced SR Ca^{2+} by catecholamines (Fernández-Velasco et al., 2009; Kashimura et al., 2010). DAD occurrence also critically depends on the balance between SR Ca^{2+} load and the diastolic interval. Short durations reduce the time for SR refilling and recovery, and hence the likelihood of DADs. CPVT patients sometimes develop bradycardia. In this population the slow supraventricular rate has been suggested as the primary cause of ventricular arrhythmias (Faggioni et al., 2013), which may explain the reduced response of some patients to β-blockers (Priori et al., 2002). During bradycardia, particularly the Purkinje cells of the conduction system are prone to developing DADs and present a major source of focal activity in CPVT (Cerrone et al., 2007).

In conditions of excessive Ca^{2+} load, DADs and EADs often appear simultaneously (Priori and Corr, 1990; Volders et al., 1997; Antoons et al., 2007). A study by Johnson et al. (2013) in dog ventricular myocytes proposed a mechanism that coupled diastolic DADs to increased BVR and EADs. In the presence of isoproterenol, diastolic Ca^{2+} waves and DADs frequently appeared between beats. After a DAD, the duration of the next AP was consistently prolonged, related to an increase in I_{CaL}. The Ca transient during CICR was smaller after a DAD (presumably due to partial SR depletion), and modeling and voltage-clamp analysis explained the I_{CaL} facilitation by a reduction of Ca^{2+} dependent inactivation of I_{CaL}. The feedback of DAD on I_{CaL} caused significant BVR. Furthermore, because of the prolonged AP after a DAD, new Ca^{2+} waves could be generated before the end of repolarization and form EADs.

The phenomenal observation of Ca^{2+} sparks and waves that occur due to spontaneous (not triggered) openings of RyR clusters during diastole is well known (Cheng and Lederer, 2008). Triggered Ca^{2+} sparks, i.e., produced by LTCC openings during CICR, occur near-synchronously at the start of the Ca^{2+} transient and are not expected to occur during relaxation because of refractoriness of the RyR and SR Ca^{2+} content. However, using high sensitivity detectors during confocal imaging in rabbit ventricular myocytes, Fowler et al. (2018) detected Ca^{2+} sparks during the decay of the Ca^{2+} transient. They explained the

occurrence of these late Ca^{2+} sparks by the ability of release sites to recover from refractoriness during the plateau phase of the AP to become reactivated either by cytosolic Ca^{2+} itself, or by stochastic openings of LTCC. Late Ca^{2+} sparks are more readily observed when CaMKII activity is increased, as was reported in a mouse model of CaMKIIδc overexpression (Guo et al., 2012). CaMKII phosphorylation of LTCC causes a shift in the distribution of LTCC into high-activity gating modes and accelerates recovery from inactivation (Sham et al., 1995; Guo and Duff, 2006), which could explain the facilitation of late Ca^{2+} sparks by CaMKII. Interestingly, repetitively firing of late Ca^{2+} sparks produced microscopic waves of Ca^{2+} release presenting a new paradigm of electrical instability underlying BVR and EAD (induced by a DAD-like mechanism during the AP plateau), particularly in settings of HF with prolonged AP and increased CaMKII activity.

A final mechanism of EAD seen with β-AR relates to the dynamic modulation of Ca^{2+} window currents through Ca^{2+}-dependent feedback. The mechanism is independent of spontaneous Ca^{2+} events (unlike the mechanisms discussed above) but reflects local feedback of SR Ca^{2+} release on LTCC during CICR. In the classical view, EAD are caused by voltage-dependent recovery of inactivated LTCC. Inactivation and recovery of LTCC also have a Ca^{2+}-dependent component (Sipido et al., 1995; Sham, 1997), dynamically shaping Ca^{2+} window currents during a single beat. In dog and pig myocytes, we observed that under isoproterenol Ca^{2+}-dependent recovery of window currents was faster than the decay of global Ca^{2+} transients, relatively unaffected by slow Ca^{2+} buffers and absent when SR Ca^{2+} release was inhibited (Antoons et al., 2007; Acsai et al., 2011). These data strongly suggest that release-dependent recovery of window currents is driven by local changes in dyadic Ca^{2+}. The Ca^{2+}-dependent regulation of Ca^{2+} window currents seem to require sufficiently high levels of dyadic Ca^{2+}, or local activation of CaMKII, as the dynamic inactivation and recovery process was no longer observed in the absence of isoproterenol. Enhanced dynamic modulation of window LTCC by dyadic Ca^{2+} release is a suggested source of BVR (Antoons et al., 2015), and may contribute to an increased incidence of EADs under β-AR stimulation (Antoons et al., 2007).

MECHANICAL LOAD AND AFTERDEPOLARIZATIONS

Acute stretching of the heart destabilizes membrane potential and causes DADs and EADs (Franz et al., 1989). This arrhythmogenic activity is caused by negative feedback mechanisms that integrate mechanical and electrical activity of cardiac myocytes and presumably involve Ca^{2+} (Ravens, 2003). The myocardium responds to stretch by a more powerful contraction, a phenomenon referred to by Frank Starling (Sagawa et al., 1990). The intrinsic adaptation to changes in mechanical load has a second slower component of enhanced contractility described by the Anrep effect (von Anrep, 1912). Early work in intact cardiac muscle had not observed significant changes in diastolic and systolic global Ca^{2+} levels during the initial stretch response (Allen and Kurihara, 1982), which has argued against a major role for Ca^{2+} in stretch-induced arrhythmias. More recently, this view has been challenged by experiments that confocally monitored Ca^{2+} sparks and waves during stretch, suggesting that local Ca^{2+} release could account for at least part of the Frank Starling response (Petroff et al., 2001). Since then, a complex picture of mechanosensitive Ca^{2+} signaling has emerged that operates over a wide range of time scales. Within milliseconds, a small diastolic stretch triggers a burst of Ca^{2+} sparks (Iribe et al., 2009). When sustained, Ca^{2+} accumulates over minutes via stretch-induced autocrine/paracrine signaling participating in the Anrep effect (Cingolani et al., 2013). When stress becomes chronic, elevated Ca^{2+} influx activates gene expression leading to hypertrophy (Tavi et al., 2001; Gómez et al., 2013).

RyR Mechanosensitivity

Stretch-dependent regulation of the Ca^{2+} system is operated via the process of mechanotransduction. Its mechanisms involve many signaling cascades targeting a diversity of intracellular Ca^{2+} sources, including the SR and mitochondria (Schönleitner et al., 2017). Furthermore, mechanotransduction operates via different classes of mechanosensors of which the activation seems to depend on the mechanical environment of the myocyte, which in experimental settings is defined by the dimensionality of the stretch system (Chen-Izu and Izu, 2017). The modulation of RyR by mechanical force has been a focus of investigation after the first demonstration in a 3D cell-in-gel system that stretch can trigger Ca^{2+} sparks (Petroff et al., 2001). Subsequently, ROS and NO have been identified as key molecules in RyR mechanosensitivity (**Figure 2B**). NOX2 activation has been proposed as the principle mechanosensor underlying the initial fast response of Ca^{2+} sparks to stretch (Prosser et al., 2011). Stretch-induced ROS by NOX2 is fast, transient and confined near the dyad to permit rapid and reversible modification of RyR. It is therefore believed that the NOX2 pathway enhances CICR efficiency without changes in systolic Ca^{2+} and serves as an adaptation to beat-to-beat variations in preload contributing to the Frank Starling response.

Cardiac stretch also stimulates cardiomyocytes to produce NO (Khairallah et al., 2012). Mechanical stimulation of NO elevates the systolic Ca^{2+} transient and produces spontaneous Ca^{2+} sparks during diastole, as was demonstrated in myocytes contracting in-gel against a higher preload or afterload (Petroff et al., 2001; Jian et al., 2014). In these settings, NO was produced through activation of constitutive NOS by phosphorylation via the PI3K-Akt pathway (Petroff et al., 2001). Pharmacological inhibition or genetic deletion to differentiate between eNOS and nNOS pathways revealed that both isoforms were involved in the downstream effects on systolic Ca^{2+}, but only nNOS had a role in the induction of Ca^{2+} sparks (Jian et al., 2014). The divergent effects of eNOS and nNOS have been explained by their subcellular location. nNOS is localized at the dyad in close proximity of RyR, while eNOS is spatially confined in caveolae more distant from RyR release sites (Xu et al., 1999). Downstream from nNOS signaling, CaMKII was also found to modulate afterload-induced Ca^{2+} sparks. The mechanically

induced SR Ca^{2+} leak by nNOS is expected to deplete the SR of Ca^{2+}, however, SR Ca^{2+} content is maintained presumably via enhanced SERCA Ca^{2+} reuptake by nNOS (Vielma et al., 2016).

The NO-mediated increase of the Ca^{2+} transient to compensate for greater mechanical load typically appears with a delay of seconds and minutes, possibly participating in the Anrep effect. Trans-sarcolemmal Ca^{2+} influx also contributes to the slow Ca^{2+} loading during stretch. One of the proposed mechanisms is increased activity of Na^+/H^+ exchanger through mitochondrial ROS release downstream of stretch-induced angiotensin signaling (Cingolani et al., 2013). The result is an increase in intracellular Na^+ that stimulates reverse NCX loading the cell with Ca^{2+}. Na^+ and Ca^{2+} influx through non-selective cationic SAC may further contribute (Calaghan et al., 2004). Thus, slow adaptation to stretch is viewed as an enduring signal achieved by concerted action of local nNOS activity to fine-tune local Ca^{2+} release and transsarcolemmal Ca^{2+} and Na^+ influx to gain more Ca^{2+}.

Ca^{2+}-Dependent Mechanisms of Stretch-Induced Arrhythmias

While mechano-sensitization of RyR is part of an effective adaptation to preload and afterload by increasing the efficiency of local Ca^{2+} release, it also produces spontaneous Ca^{2+} sparks during diastole. In the normal heart, stretch-induced Ca^{2+} sparks are locally confined. Under certain conditions, when more Ca^{2+} sparks arise synchronously to form Ca^{2+} waves, the load-adaptive Ca^{2+} system could turn into an arrhythmogenic mechanism. The stretch-induced increase in ROS, Ca^{2+} sparks and velocity of propagating Ca^{2+} waves is graded, i.e., increases with increasing amount of stretch (Miura et al., 2015). Thus, large stretches, such as in dilated hearts, are more likely to trigger ventricular ectopy (Hansen et al., 1990). Mechanical dyssynchrony, often due to structural tissue heterogeneity, is a further compromising factor. In case of dyssynchronous contractions, Ca^{2+} waves arise from a non-SR source as result from Ca^{2+}-dissociation from the contractile filaments during late relaxation of the non-uniform cardiac muscle (Miura et al., 2008).

More ROS can also by produced by hypersensitivity of mechanosensitive signaling due to upregulation of a molecular component, as was demonstrated for a mouse model of Duchenne muscular dystrophy that showed upregulation of NOX2 and produced Ca^{2+} waves in response to moderate stretch (Prosser et al., 2011). In addition to DADs, ROS also activates EADs, via reactivation of I_{CaL} (Song et al., 2010), or enhanced late Na^+ current (Song Y. et al., 2006). While RyR, INaL, and LTCC can be directly activated by oxidation (Xu et al., 1998; Morita et al., 2003; Kassmann et al., 2008), redox modification of CaMKII seems to be crucially involved in ROS modulation of arrhythmogenic INaL and LTCC currents (Morita et al., 2009; Wagner et al., 2011). Of note, most electrophysiology studies applied H_2O_2 as an exogenous source of ROS. There are no current data to confirm if endogenous ROS produced by NOX2 during stretch behaves similarly. Source matters, as mitochondrial ROS caused a reduction of INa (Liu et al., 2010).

While ROS is a ubiquitous proarrhythmic signal, NO generate opposite pro- and antiarrhythmic signals that can be partly explained by divergent effects of eNOS and nNOS on Ca^{2+} handling proteins. Mice with targeted disruption of eNOS had a higher incidence of arrhythmias induced by ouabain (Rakhit et al., 2001) or β-adrenergic stimulation (Wang et al., 2008), confirming earlier work reporting on the protective effects of NO against ventricular arrhythmias in dogs (Vegh et al., 1992). The antiarrhythmic effects have been attributed to β-adrenergic antagonism of eNOS via reduction of I_{CaL} in a cGMP-dependent manner. Likewise, nNOS knockout mice suffered more from arrhythmias after myocardial infarction than their WT littermates. Because an I_{CaL} blocker reduced VF incidence, the authors concluded that nNOS is antiarrhythmic through I_{CaL} inhibition via direct nitrosylation (Burger et al., 2009). Nitrosylation of the Na^+ channel is also coupled to nNOS activity (Ahern et al., 2000). Conversely, when nNOS is activated by stretch or catecholamines in cardiac myocytes, local NO-CaMKII signals produce arrhythmogenic Ca^{2+} waves that originate from dyadic RyR (Curran et al., 2014; Jian et al., 2014). Giving the pro-arrhythmic actions of isoproterenol *in vivo*, it is reasonable to argue that during β-adrenergic stimulation in the presence of mechanical load, pro-arrhythmogenic nNOS signaling prevails.

In unloaded myocytes, the I_{TI} following a Ca^{2+} wave is mainly produced by NCX. In stretched myocytes, a significant contribution of stretch-activated channels is anticipated. Stretch-activated non-selective cation currents (SACNS) have been functionally demonstrated in ventricular myocytes at the whole-cell and single-level (Craelius et al., 1988). While it is unlikely that Na^+ and Ca^{2+} conducting SACNS participate in stretch-induced SR Ca^{2+} release in ventricular myocytes (Iribe et al., 2009), they may contribute to destabilize the resting membrane potential by generating inward current during diastole. Studies in whole hearts demonstrating anti-arrhythmic effects of GsMTx-4, a specific SACNS blocker, support the involvement of SAC in stretch-induced arrhythmias (Wang et al., 2016). The search for a 'true' SACNS, a structural homolog to the bacterial SAC that can be directly gated by membrane tension (Sukharev et al., 1994), is still ongoing. Interestingly in this regard is the discovery of Piezo channels in a neuroblastoma cell line (Coste et al., 2010). The biophysiological profile of Piezo matches endogenous cardiac SACNS, including weak voltage dependency, single channel conductance, inactivation, and sensitivity to GsMTx-4 (Gottlieb, 2017), and is therefore a promising candidate. Piezo is expressed at low levels in the heart (Coste et al., 2010), but its role in cardiac function has yet to be established.

In the heart, the search for cardiac SACNS has been largely focused on the transient receptor potential canonical (TRPC) channel family. The activation of TRP channels is polymodal, and some members are directly activated by membrane deformation (Inoue et al., 2009), although this remains somewhat controversial (Gottlieb et al., 2008). Two subtypes, TRPC3 and TRPC6, have been proposed as potential candidates participating in the slow force response (Yamaguchi et al., 2017). Hyperactive TRPC3 (Doleschal et al., 2015) or TRPC6 (Seo et al., 2014) amplified the slow inotropic response to stretch resulting in Ca^{2+}

overload and arrhythmogenesis. Doleschal et al. (2015) explained the pro-arrhythmia of TRPC3 by a Ca^{2+} overload dependent mechanism that involves spatial uncoupling between TRPC3 and NCX1 in specialized microdomains disrupting the tight regulation of NCX by local Ca^{2+} and Na^{+}. This thinking is in line with the conceptual view that TRPC channels have access to localized Ca^{2+} signaling microdomains that are separated from contractile dyadic signaling (Houser and Molkentin, 2008). The microdomain concept was initially proposed to explain the role of TRPC channels in the activation of the NFAT/calcineurin axis linking pathophysiological hypertrophy to chronic mechanical stretch (Kuwahara et al., 2006; Makarewich et al., 2014). It has been well established that structural and functional remodeling in pathological cardiovascular stress predisposes the heart to arrhythmias (Nattel et al., 2007; Orini et al., 2017).

Linking Mechanotransduction and Adrenergic Signaling

Thus far, ROS, NO, and CaMKII have been identified as the prime mediators of RyR mechanosensitivity in the intrinsic adaptation of contractile force to load. *In vivo*, intrinsic force adaptation is modulated by sympathetic activation by imposing a higher load on the heart through modulation of vascular tone. The myocyte can respond to higher mechanical and adrenergic stress through activation of mechanotransduction and adrenergic signaling networks, as discussed above and depicted in **Figure 2**, but interactions have not been systematically investigated. The mechanotransduction pathway shows both the rapid preload-induced NOX2 and slower afterload-induced NO branch, that most probably operate independently (Jian et al., 2014). It is also unlikely that NOX2 is directly involved in β-adrenergic signaling, since ROS scavengers failed to prevent increases in Ca^{2+} spark frequency in quiescent cells that were treated with isoproterenol (Gutierrez et al., 2013). It should be noted that NOX2 can possibly become activated during β-adrenergic signaling as an indirect consequence of chronotropic effects (Dries et al., 2013).

nNOS is centrally involved in both stretch- and adrenergically induced Ca^{2+} sparks, most likely via oxidation of downstream CaMKII (Gutierrez et al., 2013; Jian et al., 2014). It is therefore tempting to speculate that nNOS and CaMKII act as primary integrators of mechanotransduction and adrenergic RyR signaling networks. The assumption that co-activation of nNOS has a cumulative effect on RyR activity remains to be determined.

The eNOS effects are less clearly defined. eNOS is compartmentalized in caveolae at T-tubules and sarcolemma. In sarcolemmal caveolae, eNOS colocalizes with β-ARs and LTCC allowing NO to mitigate β-adrenergic inotropy through inhibition of LTCC by local cGMP (Wang et al., 2008). It is conceivable that a stretch activation of the eNOS-Akt-PI3K pathway positively modulates EC coupling gain in T-tubular caveolae, while negatively regulating the β-adrenergic response in a different subset of caveolae at the surface sarcolemma.

HEART FAILURE AND AFTERDEPOLARIZATIONS

Heart failure is associated with extensive cardiac remodeling, at both the structural and functional levels. Remodeling due to HF occurs for a number of reasons, however, it is in part, due to altered stress on the ventricular wall (Kehat and Molkentin, 2010).

Remodeling can lead to an increased propensity for complex ventricular arrhythmias and sudden cardiac death, and these are seen in over half of the patients presenting with HF with reduced ejection fraction. For these reasons it is imperative to understand the mechanisms that are responsible for the increased arrhythmia incidence in this population (Janse, 2004).

Purkinje fibers isolated from infarcted sections of human hearts have been shown to have significantly longer APD than those from non-infarcted zones, resulting in marked dispersion of APD in infarcted and adjacent zones. Furthermore, both epinephrine and the cardiac glycoside, ouabain, were able to induce DADs in these fibers (Dangman et al., 1982). Previous work using human trabeculae has also shown that there is an increased propensity for triggered activity in tissue from HF patients (Vermeulen et al., 1994). Further work from the Amsterdam group also showed that, in contrast to many animal species, norepinephrine induces APD prolongation in ventricular myocytes from human failing hearts, as well as EADs. These alterations were ascribed to an increase in both the calcium peak current and window current (Veldkamp et al., 2001).

In addition to the alterations in arrhythmia incidence in HF, it has been well described that the failing heart has a reduced responsiveness to elevated catecholamine levels, at least in end-stage HF, due to alterations in expression of β-ARs (Bristow et al., 1982; Ungerer et al., 1993). Interestingly, more recent work has also shown that in a patient cohort with HF, BVR of ventricular AP duration was increased during an autonomic challenge associated with increased sympathetic activity (Porter et al., 2017).

Taking these data together leads us to believe that modifications in signaling underlying β-adrenergic responsiveness and stretch may contribute to the increased occurrence of arrhythmias in these patient populations. Therefore, if we are able to understand the precise changes that occur in these systems during HF, we may get a better hold on the processed occurring, with an outlook of preventing and/or treating the, potentially, maladaptive remodeling (see below).

Global Remodeling

At the gross structural level, the geometry of the heart changes as a result of HF, becoming less elliptical and more spherical (Cohn et al., 2000). HF is associated with a progressive enlargement of the left ventricle, with increases in end-systolic left ventricular wall stress being seen (Florea et al., 1999), which may have detrimental effects on mechanosensitive mechanisms involved

in arrhythmia formation, and also contribute to the cellular arrhythmogenic remodeling.

Ion Channel Remodeling

At the level of the single myocyte, changes in HF include alterations in the densities of various membrane channels, which contributes to the increase in APD seen in the majority of HF models and in patients (Beuckelmann et al., 1993; Tomaselli and Marbán, 1999). One of the most consistent findings with regards to current alterations in HF is the decrease in the inwardly rectifying potassium current, I_{K1}, which contributes to maintaining the resting membrane potential as well as contributing to terminal repolarization (Beuckelmann et al., 1993; Nerbonne and Kass, 2005). Furthermore, the β-adrenergic regulation of I_{K1} has also been shown to be significantly reduced in myocytes isolated from HF patients (Koumi et al., 1995). Reduced I_{K1}, will mean that a smaller I_{TI} will be required to cause the same amplitude of DAD, or even triggered AP, and therefore altered regulation of this current in HF has major implications in the potential arrhythmogenic outcomes. An interesting recent study, however, showed that sympathetically -induced arrhythmias could not be induced when I_{K1} was inhibited in isolation in Langendorff-perfused rabbit hearts indicating that synergistic activity between multiple pathways, including altered RyR sensitivity, was required for arrhythmia induction (Myles et al., 2015).

Another potassium current that is of great interest when it comes to β-adrenergic modulation, is the slow rectifier, I_{Ks}. I_{Ks} function is prominent during β-adrenergic stimulation when it promotes AP shortening, to counteract the increase in inward Ca^{2+} current, thus providing critical "reserve" when other repolarizing currents are impaired (Jost et al., 2005; Varró et al., 2000; Volders et al., 2003). Although Veldkamp et al. (1995) could not detect this current in myocytes isolated from patients with cardiomyopathy, a number of animal models have indicated that this current is downregulated in HF (Tsuji et al., 2000; Li et al., 2002). A decrease in this current during intense sympathetic stimulation will lead to an increase in APD, and an increased tendency for afterdepolarizations. Furthermore, research from our own group has shown the key role that I_{Ks} plays in preventing excessive BVR during β-AR stimulation, which may also contribute to the arrhythmogenic substrate generated when this current is downregulated (Johnson et al., 2010, 2013).

The importance of both I_{K1} and I_{Ks} and their regulation by β-adrenergic stimulation in HF were recently highlighted by a study from the Bers' group. In this manuscript, the physiologically relevant AP-clamp technique was utilized to show that under β-adrenergic stimulation, reduced I_{Ks} responsiveness limits the integrated repolarizing potassium currents in a rabbit model of HF. Furthermore, an increase in APD BVR was seen in HF myocytes. Taken together these data illustrate the importance that these currents may play in arrhythmia generation in HF, especially under sympathetic stimulation (Hegyi et al., 2018a).

Apart from the acute effects of adrenergic stimulation on channel activity, one must also consider the effect of sustained sympathetic activation. A recent study did just this by investigating the effects of sustained adrenergic stimulation on I_{Ks} dynamics. In that particular study, they showed that I_{Ks} was reduced after continued β-AR stimulation, and this was mediated by CaMKII, a signaling molecule involved in both β-AR and mechanosensitive stimulated arrhythmias (Shugg et al., 2018). If this effect contributes to the increased incidence of arrhythmias in HF is currently unknown and should be the subject of further work.

With regards to the acute effect of HF on SACNS, that may also contribute to stretch-induced arrhythmias, multiple laboratories have shown that TRPC channel expression and activity are upregulated in pathological hypertrophy and HF (Eder and Molkentin, 2011). Furthermore, to our knowledge, to date only one study has investigated the level of Piezo channels in HF, with that study providing evidence of an upregulation in HF. However, the functional consequences of this upregulation are currently unknown and should be the subject of further research (Liang et al., 2017).

Excitation–Contraction Coupling Remodeling

As previously stated, the synchronous rises in Ca^{2+} leading to efficient ECC is due, in part, to the tight opposition of RyRs and LTCCs in the T-tubules in healthy ventricular myocytes. There is an abundance of literature describing a loss of T-tubules during HF (Lyon et al., 2009; Guo et al., 2013; Dries et al., 2018a), In addition to the loss of the concerted effort for successful ECC that the loss of T-tubules will bring, deleterious Ca^{2+} handling leading to arrhythmia may also result. A recent study investigated the potential mechanisms behind T-tubule disruption in post-infarction failing rat hearts. In that study, they showed that elevated wall stress was associated with disruption of the T-tubular structure and this was associated with decreased levels of junctophilin 2, which is a critical dyadic anchor. Furthermore, they carried out studies on loaded papillary muscles, which confirmed a direct role of wall stress on regulation of T-tubule organization (Frisk et al., 2016). Taken together these data indicate the importance that stretch has in developing the HF phenotype when it comes to subcellular structure of the myocyte. Alterations in location of relevant signaling pathways that may also be induced by this loss of cellular architecture will be discussed later (see the Section "Local (Microdomain) Remodeling").

As the current generated via the NCX appears to be the major player responsible for the I_{TI} that initiates DADs, and perhaps EADs, one also needs to consider how the function of this exchanger is altered in HF. Interestingly, a number of *in vitro* studies have suggested that stretch of adult myocytes increases NCX expression (Sipido et al., 2002). These data may lead us to believe that the increase stretch 'felt' by the *in situ* myocyte may also lead to an increase in NCX in HF. Indeed, the majority of studies have shown that NCX is increased in HF (Sipido et al., 2002; Schillinger et al., 2003), although we should approach these data with caution due to the fact that expression levels do not necessarily give an indication of activity, especially when considering an exchanger where ion concentrations, phosphorylation state [of partner proteins (e.g., phospholemman) as well as NCX itself] in addition to other

factors will ultimately influence the current generated by the exchanger.

One of the major influences on NCX activity is the intracellular Ca^{2+} concentration. It is well known that cardiomyocytes isolated from failing hearts (with reduced ejection fraction) show altered Na^{+} and Ca^{2+} haemostasis. The modified Ca^{2+} handling is characterized by decreased Ca^{2+} transients, enhanced diastolic SR Ca^{2+} release and diminished SR Ca^{2+} reuptake, which all contribute to altered Ca^{2+} concentrations 'seen' by the NCX (Hasenfuss and Pieske, 2002; Kho et al., 2012; Luo and Anderson, 2013) . Additionally, modeling studies have shown that that both dyadic and SR Ca^{2+} influence the appearance of DADs in addition to alterations in Ca^{2+} diffusion across the cell and Ca^{2+} uptake into the SR (Fink et al., 2011).

One of the first papers investigating Ca^{2+} sparks in myocytes from patients with HF indicated that alterations in the Ca^{2+} release mechanisms must be one of the mechanisms underlying EC coupling, in addition to alterations in SR Ca^{2+} load (Lindner et al., 2002). One of the driving forces behind this is the altered open probability of RyRs, which is governed by multiple factors, and has not been without controversy over the years (Dobrev and Wehrens, 2014). Interestingly, recent work has shown that stabilizing the RyR, using dantrolene, is able to prevent DADs in myocytes isolated from HF patients (Hartmann et al., 2017). Over the next few paragraphs, we will discuss how the major controllers of RyR stability, that also govern stretch and/or β-adrenergic signaling (namely CaMKII and ROS), can be affected in HF.

CaMKII phosphorylation of RyR appears to play an important role in arrhythmogenesis and sudden cardiac death in mice with HF (van Oort et al., 2010). Analysis from ventricular tissue from patients with either dilated or ischemic cardiomyopathy have shown that there is an increase in the levels of CaMKIIδ, the major isoform of CaMKII in the heart (Sossalla et al., 2010). Interestingly, single myocytes isolated from mice overexpressing CaMKIIδ are more liable to show DADs and spontaneous APs under β-adrenergic stimulation when compared to wild type mice (Sag et al., 2009). This increase in CaMKII seen in HF could directly promote arrhythmia formation by not only increasing diastolic Ca^{2+} leak via RyR phosphorylation, but also by promoting increases in the late Na^{+} current (Wagner et al., 2006), a current that has already been shown to be increased in HF, and incriminated in increased BVR and arrhythmia formation under these conditions (Maltsev et al., 2007).

The activity of CaMKII itself is under control of many different regulators, including ROS (as stated above and shown in **Figure 2**), which is detrimentally altered in HF. ROS also as having their own independent effects on RyR and other components of the Ca^{2+} handling machinery (dependent on the source of the ROS). In HF, just as in normal physiology, ROS has a number of different sources including NOX2, mitochondria and uncoupled NOS (Sag et al., 2013).

Interestingly, NOX2 expression and/or activity has also been shown to be increased in end-stage human HF in a number of studies, supporting the potential involvement of this pathway in the formation of ROS that may interfere with Ca^{2+} handling and lead to subsequent arrhythmias (Zhang M. et al., 2013). Furthermore, the elevated intracellular Na^{+} concentration seen in HF promotes the production of mitochondrial ROS (Kohlhaas et al., 2010; Viatchenko-Karpinski et al., 2014), which could ultimately lead to the potential for a vicious circle of proarrhythmic signaling via CaMKII.

Diseased hearts have been shown to have a significant increase in nNOS mRNA and protein expression (Damy et al., 2004). While on the other hand, several studies have provided evidence that NO production by eNOS is markedly diminished in HF, and an overexpression of eNOS has been shown to relieve cardiac dysfunction in a mouse model of HF (Katz et al., 1999; Jones et al., 2003; Damy et al., 2004). Under normal physiological conditions eNOS appears to decrease β-adrenergic responsiveness via inhibition of LTCC (Wang et al., 2008), therefore a reduction in this mechanism may be an additional driving force for β-adrenergic driven arrhythmias under these conditions. The overall increase in nNOS activity in HF, and the potentially altered signaling activity and targets (for example caveolae-associated molecules versus the RyR) resulting from the translocation of this molecule to the sarcolemma, may be important for deleterious Ca^{2+} handling and arrhythmia formation (Damy et al., 2004). Additionally, in HF it appears that NO production inducible NOS (iNOS) becomes of increased importance, although the role of this is currently less defined (Massion et al., 2003; Carnicer et al., 2013).

The activity of cAMP/PKA is tightly regulation by the activity of specific phosphodiesterases (PDEs) and protein phosphatases, however, the distribution of these is out of the scope of the present manuscript (see Guellich et al., 2014 for a review on this matter).

Finally, it is important to consider that the relative contribution of the different subtypes of β-ARs may also contribute to the increased arrhythmogenic phenotype observed in HF. As noted previously distinct pathways are associated with the different subtypes. Previous work has shown that the β_1 subtype of adrenoreceptors are especially downregulated in HF, while the coupling of the receptors to Gs, presumably via increased activity of the receptor kinases GRK2 and/or GRK5, is altered (Lohse et al., 2003). Interestingly, β_2-stimulation appears to be more arrhythmogenic in the failing heart when compared to the non-failing. Arrhythmogenesis appears to be driven by enhanced spontaneous SR Ca^{2+} release and aftercontractions, and is likely attributable, at least in part, to enhanced SR Ca^{2+} load secondary to PLB phosphorylation (DeSantiago et al., 2008). Away from the single cardiac myocyte, the requirement for β-Adrenergic stimulation to induce ectopic activity has also been shown in a human wedge preparation. Hearts from patients experiencing HF, exhibited ectopic beats and triggered activity in response to β_2-stimulation. The authors of this study ascribe the increase in arrhythmogenic activity due to the enhancement of transmural differences between Ca^{2+} and APD, facilitating the formation of DADs (Lang et al., 2015).

All of the data that has been discussed up till now has not considered the potential for regional differences in remodeling, which may be triggered by various stimuli, stresses and strains sensed at different anatomical locations. Taking this into account, a recent paper interestingly showed that in a porcine model

of myocardial infarction and HF, regional heterogeneities in arrhythmogenic remodeling do indeed exist. In this study, it was shown that changes in multiple currents lead to a shortening of AP at the border zone of the infarct, while APs recorded from the remote zone were prolonged. This will lead to a greater dispersion of repolarization across the ventricle, which could ultimately increase the arrhythmogenic substrate. Furthermore, these authors showed that cells isolated from the remote region showed DADs with a much higher frequency than in control, and amongst those cells, nearly half also showed triggered APs. Interestingly all HF-border cells showed DADs with over half showing triggered activity often with a superimposed EAD. In addition, inhibition of CaMKII decreased the occurrence of these DADs back to control levels, further indicating the importance of this multimodal signaling molecule in arrhythmia generation in this setting (Hegyi et al., 2018b). Although in this study these DADs were not induced by β-Adrenergic stimulation, but by burst pacing, one could also postulate that regional differences will also exist in terms of β-Adrenergic responsiveness in HF. In fact, a recent abstract from the Sipido group showed that in a pig model of MI, myocytes isolated from the peri-infarct region had a higher occurrence of isoproterenol induced DADs when compared to myocytes isolated from the region remote from the infarct (Dries et al., 2018b). These data pave the way for further research in this area.

Local (Microdomain) Remodeling

So far, we have only focussed on global remodeling, however, in addition to heterogeneity seen across the ventricular wall as just described, the myocyte in itself is not homogeneous, especially when the micro-architecture of the myocyte is altered as is seen in HF. For these reasons, we must also consider local subcellular alterations. Given the improvements in imaging techniques, and experimental advances over recent years we have gained greater insights into how alterations in these 'microdomains' may influence arrhythmogenic outcomes in HF. Over the next paragraphs, we will discuss a number of studies that have been carried out in an attempt to elucidate how these microdomains may influence stretch- or β-adrenergic-induced arrhythmia in HF, with a view on targeted therapeutics (see the Section "Therapeutic Interventions").

As noted previously, Ca^{2+} entry via the LTCC is the initial trigger for Ca^{2+} release from the SR, therefore it is important to discuss potential changes in this current in HF. At a global level, the majority of studies have shown that there is no alteration in whole cell Ca^{2+} current recorded from myocytes from HF patients or in animal models, although single channel studies have shown that the availability and open probability of the LTCC is increased in human HF myocytes (Beuckelmann and Erdmann, 1992; Mukherjee and Spinale, 1998; Schröder et al., 1998). However, over recent years a number of interesting observations have come to light indicating the location of LTCCs are different in HF myocytes. Alteration in the location of the LTCC will also have detrimental effects on the levels of Ca^{2+} the individual channels are exposed to. Therefore, Ca^{2+}-dependent inactivation of the current as well as the dynamic modulation of the window current are likely to be altered in HF. Both of these changes will contribute to the formation of afterdepolarizations and can be influenced by β-adrenergic stimulation.

Using a rat model, combined with osmotic detubulation, Bryant et al. (2015) showed that although no differences in total I_{CaL} density was seen between ventricular myocytes isolated from animals that had undergone a coronary artery ligation, this lack of change resulted from differential effects at the cell surface and the T-tubules. I_{CaL} current density was decreased at the T-tubules while it was increased at the cell surface (Bryant et al., 2015).

An additional study from the group of Gorelik, using the super-resolution scanning patch-clamp technique showed similar findings. They elegantly showed that in both human and rat HF there was a redistribution of functional LTCCs from their physiological T-tubular location to the non-native crest of the sarcolemma. They went on to show that the open probability of these redistributed channels was dramatically increased, and the high open probability was linked to enhanced CaMKII modulation in the 'new' location. The current at these non-native channels resulted in an elevated I_{CaL} window current, which contributed to the development of EADs. This remained true when these data were fed-into a 3-dimensional left ventricle model illustrating that the phenomenon occurring at the single cell level has far reaching arrhythmogenic implications (Sanchez-Alonso et al., 2016). Interestingly, work carried out over 20 years ago indicated that there was a frequency dependent decrease in I_{CaL} in human dilated cardiomyopathy (Sipido et al., 1998). If this is to do with the altered LTCC microdomains, potentially due to CaMKII, remains to be seen, but should be the subject of future studies.

Localization of the LTCC to the T-tubules has previously been shown to be under control of the membrane scaffolding protein BIN1, with the knockdown of this protein leading to a reduction in surface LTCC and alterations in Ca^{2+} handling within the myocyte (Hong et al., 2010). Interestingly, BIN1 has been shown to be decreased in human HF as well as in a number of animal models, which may contribute to the alterations in patterns seen in LTCC localization (Hong et al., 2012; Caldwell et al., 2014). A more recent study has implicated that the β-adrenergic stimulation of BIN1 leads to reorganization of LTCC/RyR microdomains by also recruiting phosphorylated RyRs into the dyads. When BIN1 is downregulated, therefore, these phosphorylated RyRs may not be recruited in the dyad and arrhythmias may be promoted due to the defective Ca^{2+} handling (Fu et al., 2016).

Over 10 years ago, it was shown that in the failing heart there are a number of RyRs that become 'orphaned' from their LTCC counterpart in the T-tubule in spontaneously hypertensive rats (Song L.S. et al., 2006). These investigators used this model to show that this loss of coupling between the LTCC and RyR led to Ca^{2+} instability in the heart. More recently, Dries et al. (2018a) showed that in human myocytes isolated from HF patients, there were more non-coupled (to LTCC) RyRs which had more spontaneous activity than in non-HF. Hyperactivity of these non-coupled RyRs

was reduced by CaMKII inhibition (Dries et al., 2018a). Previous work from the same group had illustrated that under healthy conditions, coupled (to LTCC) RyRs are distinctly modulated by CaMKII and ROS, while CaMKII and NOS1-dependent modulation of RyRs during β-adrenergic stimulation was also restricted to the dyadic cleft (Dries et al., 2013, 2016). The authors went on to use a pig model to further investigate alterations in coupled and non-coupled RyRs and their regulation in normal and pathophysiological conditions. However, after an MI, it was shown that under adrenergic stimulation using isoproterenol, Ca^{2+} waves were frequent and originated at non-coupled sites, generating larger NCX currents than in sham operated animals. Inhibition of CaMKII or mitochondrial-ROS scavenging reduced spontaneous Ca^{2+} waves, and improved excitation–contraction coupling, indicating that these could be interesting therapeutic targets (Dries et al., 2018a). A very recent paper corroborated the arrhythmogenic role of mitochondrial ROS in the formation of arrhythmias in a guinea pig model of non-ischemic HF (Dey et al., 2018). In this model, continuous telemetry recordings indicated a high frequency of premature ventricular complexes and spontaneous ventricular tachycardia/ventricular fibrillation in animals after aortic constriction and isoproterenol stimulation. Scavenging mitochondrial ROS using MitoTEMPO markedly suppressed arrhythmias as well as blunting QT prolongation and reducing QT variability. Taken all together these data indicate specific targeting of one source of ROS is adequate to reduce proarrhythmic outcomes.

In addition to alterations seen in the LTCC/RyR microdomain, and the control thereof, that may influence arrhythmogenesis we also need to consider alterations in the distribution of the different β-ARs themselves. One of the first reports investigating potential alterations was by Nikolaev et al. (2010). In that seminal study it was shown that, as opposed to the situation in healthy myocytes where β_1-adrenergic receptors are widely distributed at the cell crest and β_2-receptors (and their associated signaling pathways) are localized to the T-tubules, in HF β_2-receptors were redistributed from the transverse tubules to the cell crest, leading to a change in β_2-receptors associated compartmentation of cAMP (Nikolaev et al., 2010). These alterations lead to the β_2-receptors acting more like β_1-receptors and have detrimental effects on the cross-talk of adrenergic signaling and Ca^{2+} handling within the failing cell. Follow up studies have shown that the compartmentalization of the cAMP signaling from β_2-receptors is governed by caveolin 3, a protein that regulates the number of caveolae in the myocyte. Alteration in the T-tubule structure, levels of caveolin 3 and junctophilin 2 appear to be time-dependent, and gradually alter the β_2-signaling pathways. Furthermore, caveolin 3 overexpression in failing cells was able to restore, at least in part, the T-tubular location of the β_2-receptors (Wright et al., 2014; Schobesberger et al., 2017).

Interestingly, an additional study utilizing a rabbit model, also showed that reintroduction of caveolin-3 was able to normalizes β-adrenergic-induced contractile responses in HF myocytes, while also showing that in HF β2-induced signaling gains access to myofilament which may contribute to abnormal PKA phosphorylation of troponin I and contractile dysfunction (Barbagallo et al., 2016). In addition, work from the Sacconi group has shown that while cells from HF myocytes respond to β-adrenergic stimulation, this is not the case at the T-tubules that do not conduct APs, where the alterations seen in response may be caused by a lack of electrical activity. These data provide an alternative, or an additional, mechanism for the alterations seen in HF (Crocini et al., 2016).

THERAPEUTIC INTERVENTIONS

Despite advances in our knowledge of the pathophysiology underlying HF over the last 10 years, as outlined above, only a limited number of compounds have become available for the treatment of this debilitating disease (Gordin and Fonarow, 2016). Given the information in previous sections, we could consider targeting primary stressors (i.e., β-adrenergic stimulation or mechanical load) or downstream pathways. In **Figure 3**, we have summarized the most important mechanisms of afterdepolarizations, highlighting relationships between stimuli, key signaling molecules and targeted Ca^{2+} handling proteins and ion currents. Based on this scheme, we will discuss a number of (potential) interventions over the next few paragraphs that could be utilized to reduce the arrhythmogenic burden in HF patients.

Targeting Mechanical Load and Structural Remodeling

β-Blockers have been a mainstay of pharmacological treatment for HF for a number of years and are included in guidelines for treatment of HF, in part due to their antiarrhythmic properties (Funck-Brentano, 2006; Ponikowski et al., 2016). In addition to a reduction in β-adrenergic signaling that will be directly caused by β-blockers, they will also lead to a reduction of mechanical stressors that may also be responsible for the efficacy of β-blockers in preventing sudden cardiac death.

Not all β-blockers are equal, however, with some being selective at adrenoreceptor subtypes while others have additional actions at other ion channels. For instance, the antiarrhythmic effects of propranolol have also been ascribed to the potential of this compound to block Na^+ channels (Fabritz et al., 2014). In long QT syndrome, for instance, it has been shown that propranolol has a significantly better QTc shortening effect compared to metoprolol and nadolol, and this led to a higher risk of cardiac events in symptomatic patients receiving metoprolol (Chockalingam et al., 2012). Therefore, given the information we currently have regarding the alteration in the number and location of subtypes of the β- receptors in HF, specific targeting of β-ARs, perhaps differing over the course of HF progression, may offer an interesting solution.

An additional way that mechanical load can be reduced is by the used of LVADs. Previous work has shown that the use of a LVADs together with the use of a specific pharmacological regimen, including the use of β-blockers, can lead to the sustained reversal of severe HF secondary to non-ischemic cardiomyopathy, even when the LVAD is explanted (Birks et al., 2006). Interestingly, it appeared that the alterations seen in the

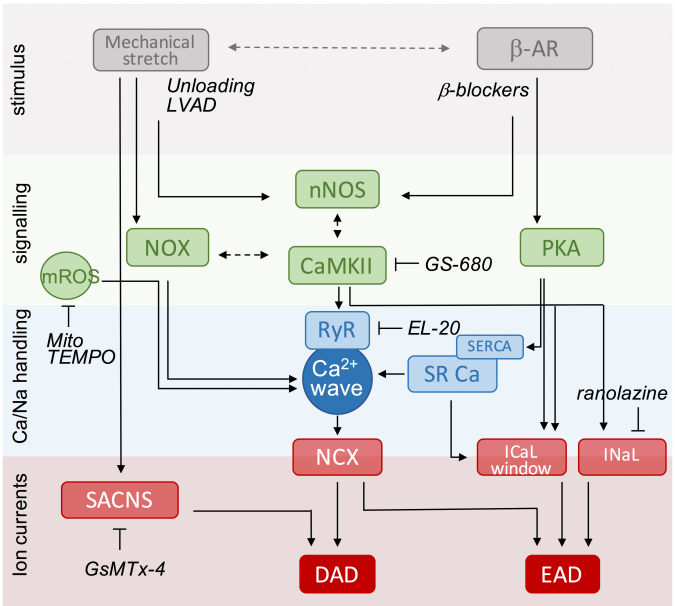

FIGURE 3 | Scheme of key events in β-adrenergic and stretch signaling for the induction of afterdepolarizations as potential targets for anti-arrhythmic therapy. The central event in the generation of afterdepolarizations is a Ca^{2+} wave that can produce DAD or EAD depending on the timing of NCX activation during the cardiac cycle (diastole or systole). Mechanical stretch and β-adrenergic agonists activate protein kinases (PKA, CaMKII) and free radicals (ROS, NO) that increase RyR activity and/or SR Ca^{2+} load to produce Ca^{2+} sparks and waves. Likewise, they increase the activity of late Na^{+} and Ca^{2+} currents promoting EADs, directly via phosphorylation and redox modification, or indirectly via modulation by increased SR Ca^{2+} release secondary to enhanced SR Ca^{2+} load. Stretch-activated ion channels further destabilize membrane potential during stretch. Anti-arrhythmic strategies include targeting of upstream stressors, downstream signaling components, and Ca handling proteins or currents. Specific examples under current investigation are indicated and further discussed in the text. DAD, delayed afterdepolarizations; EAD, early afterdepolarizations; LVAD, left ventricular assistant device; NCX, Na^{+}/Ca^{2+} exchanger; NO, nitric oxide; NOX, NADPH oxidase type; nNOS, neuronal nitric oxide synthase; PKA, protein kinase A; ROS, reactive oxygen species; RyR, ryanodine receptor; SACNS, stretch-activated non-selective cation currents; SR, sarcoplasmic reticulum; SERCA, SR Ca^{2+}-ATPase.

clinical phenotype in such patients was driven by modifications in ECC, and SR Ca^{2+} homeostasis in particular (Terracciano et al., 2004). More recent work has shown that mechanical unloading in a rat model (via heterotopic abdominal heart transplantation) reverses T-tubule remodeling, and normalizes local Ca^{2+} handling (Ibrahim et al., 2012).

Cardiac resynchronization therapy (CRT) is an alternative approach to alter mechanical loading and stretch and will assist to resynchronize ventricular wall motion. A recent meta-analysis indicated that this intervention may significantly reduce the risk of ventricular arrhythmias when compared with patients receiving ICDs. Interestingly the same study also showed that patients who were not-responsive to CRT may have had a significantly higher risk of ventricular arrhythmias (Saini et al., 2016). Furthermore, it was also shown that CRT was able to efficiently reduce subcellular heterogeneity of structure and function of RyRs and T-tubules in a canine model of HF, potentially due to the restoration of ventricular synchrony (Li et al., 2015).

Taking all of these data together it appears that alterations in mechanical load should be considered as a potential therapeutic strategy.

Another therapeutic strategy would be to potentially restrict remodeling in the first place. As previously mentioned, it appears there are a number of scaffolding proteins that are involved in the structural (and functional) remodeling of the Ca^{2+} microdomains in HF which could be the target for pharmaceutical intervention. For example, specific cardiac targeting of BIN1 could be an attractive option, although there are only limited data currently available and small molecules altering the activity of this protein are currently lacking. The potential for altering the T-tubule structure as a therapeutic intervention has recently been reviewed by Manfra et al. (2017).

Direct Targeting

It could also be possible to directly target proteins involved in arrhythmia formation under conditions of enhanced stretch or intense ß-adrenergic stimulation. For example, the potential to target stretch activated channels was recently reviewed by White (2006), however, it is perhaps of note to mention GsMTx-4, which is a peptide isolated from tarantula venom. Mixed results have been obtained with GsMTx-4 to date, with one study showing the potential for reducing the number of premature ventricular beats in an ischemia/reperfusion mouse model, while an additional study indicated no benefit in a swine model (Barrabés et al., 2015; Wang et al., 2016). Further studies are required using this compound, and derivatives of it, to truly delineate the utility of inhibition of these channels in prevention of arrhythmogenesis in HF.

Furthermore, the blockade of the components of I_{TI} which actually contributes to afterdepolarization could also be an interesting target. Inhibition of NCX as a target has been discussed previously (Antoons et al., 2012), however, progress in this area has been hampered the lack by selective, and/or mode selective inhibitors. More recently a number of more selective agents have been developed, including ORM-10103 which have shown their utility in preventing Ca^{2+} overload induced arrhythmias (Nagy et al., 2014). However, in a rabbit HF model NCX inhibition with ORM-10103 reduced premature ventricular beats but was unable to suppress secondary Ca^{2+} rise or the occurrence of EADs (Chang et al., 2018).

Direct inhibition of 'leaky' RyRs could also be an interesting target to diminish proarrhythmic Ca^{2+} leak. A recent paper showed the utility of a tetracaine-derived compound, EL20, which was able to limit arrhythmogenic Ca^{2+} waves in a CPVT model by only limiting Ca^{2+} release from RyRs associated with calmodulin (Klipp et al., 2018). Should this have utility in HF should be the subject of further investigation.

An alternative approach would be to alter the activity of SERCA in HF. A number of pre-clinical studies showed that there was anti-arrhythmic potential for increasing SERCA activity in HF using adeno-associated virus technology (Kawase et al., 2008; Lyon et al., 2011). Despite initial positive outcomes in small trials (Jessup et al., 2011), larger clinical trials have been unable to show the benefit of this approach (Greenberg et al., 2016; Hulot et al., 2017). Despite these disappointing results, further studies are still required to investigate the true utility of this approach. Activation of SERCA using small molecules may also be potentially interesting approach, and recently istaroxime has become a compound of interest (Ferrandi et al., 2013). A clinical trial using this compound is currently ongoing (ClinicalTrials.gov Identifier: NCT02617446) with the results being highly anticipated.

Targeting Downstream Modulation

An alternative avenue would be to target downstream signaling pathways that are involved. Perhaps one of the most investigated of these is the CaMKII pathway, perhaps due to the multimodal action of this kinase, and the fact that targeting this molecule may lead to selective modulation of proarrhythmic RyRs (Dries et al., 2018a). Interestingly it was recently shown that CaMKII activity persists even during chronic β-adrenergic blockade in HF, indicating that these two pathways could be targeted independently (Dewenter et al., 2017). To date, however, there are no clinically available CaMKII inhibitors, likely due to the lack of selective, bioavailable compounds. There are numerous reviews dealing with the potential of CaMKII inhibition as a potential treatment for HF, and for those reasons we will only discuss a couple of newer studies that have added fuel to the fire regarding the use of CaMKII inhibitors as antiarrhythmics (Swaminathan et al., 2012; Fischer et al., 2013; Westenbrink et al., 2013).

A recent study utilized the novel agent, GS-680, which is an ATP-dependent small molecule inhibitor of CaMKII, which appears to have good selectivity for CaMKII. In this study, this compound did not impair contractile function in failing human ventricular trabeculae and blunted the negative force-frequency relationship. Meanwhile, it increased the Ca^{2+} transient amplitude in isolated failing ventricular myocytes and reduced premature atrial contractions and afterdepolarizations in atrial cardiomyocytes (Lebek et al., 2018). Additionally, Dries et al. (2018a) recently showed that the specific CaMKII peptide inhibitor (AIP) significantly reduced the hyperactivity of RyRs in non-coupled regions without affecting spark frequency at coupled sites (Dries et al., 2018a). Finally, it has also been shown that inhibition of CaMKII is able to reduce the proarrhythmic effects of PDE-inhibitors, which act by increasing pools of cAMP (Bobin et al., 2016). If this is also true in HF should be the subject of future studies. If CaMKII inhibition will eventually function as an effective antiarrhythmic in HF still remains to be seen. While discussing CaMKII, it is also important to discuss the late Na^+ current. Recent work has shown that inhibition of this current is able to suppress Ca^{2+} related arrhythmias by reducing CaMKII phosphorylation (Wei et al., 2017). Furthermore, ranolazine, an agent that inhibits both late Na^+ and K^+ channels has been shown to have antiarrhythmic effects in the intact heart in CHF and, interestingly, was not associated with drug-induced proarrhythmia (Frommeyer et al., 2012). Once again, further work is required to determine the true utility of late Na^+ current inhibition under these circumstances.

Reactive oxygen species is one of the determinants of CaMKII activity, as well as having direct effects on Ca^{2+} handling proteins directly, so perhaps it is also possible to target ROS sources as an antiarrhythmic intervention. Interestingly the positive effect of the antioxidant vitamin C on the β-adrenergic response to dobutamine was blunted in HF patients, perhaps due to the global antioxidant properties of this agent (Mak and Newton, 2004), leading us to believe that a targeted approach may be required. The inhibition of NOX2 may be a promising approach although it may be necessary to avoid concurrent inhibition of other NADPHs which are required in other organ systems (Sag et al., 2014). Furthermore, supplementing with BH4, to 're-couple' uncoupled NOS has been proposed (Moens et al., 2008), however, there have been issues with the bio-availability of this compound (see Bendall et al., 2014). The final source of ROS that could be an interesting target in mitochondrial ROS, and as noted earlier a number of studies have shown the utility of mitoTEMPO in reducing arrhythmia in HF (Dey et al., 2018; Dries et al., 2018a). The development of bioavailable safe tools to directly alter mitochondrial ROS production is still in its infancy and efforts should be concentrated to develop these.

Finally, targeting Epac has also been proposed as a potential target for arrhythmias driven by β-adrenergic stimulation, although there is discussion about its role. A recent study showed that treatment with an Epac activator, 8-CPT, enhanced the late Na^+ current while inhibition of PKA (via PKI) did not affect the catecholamine induced increases in late Na^+ current, indicating that Epac alone plays a crucial role in these arrhythmias (Dybkova et al., 2014; Fujita et al., 2017).

CONCLUDING REMARKS

We still have a long way to go in treating ventricular arrhythmias that occur as a result of HF, however, concentrating on various microdomains within the cardiac myocytes that are under control of multiple pathways could be of great interest. Furthermore, linking the potential electro-mechanical and mechano-electro feedback loops could aid us in treating arrhythmias that occur as a result of this debilitating disease.

Is stretch sympathetic to HF? Only time and research will fully answer this question, but in the mean time we will have to be.

AUTHOR CONTRIBUTIONS

Both authors contributed to manuscript preparation and approved the final version of the manuscript.

ACKNOWLEDGMENTS

The authors would like to thank Roel Spätjens for the assistance in the preparation of **Figure 1** and Patrick Schönleitner for the assistance in the preparation of **Figure 2**.

REFERENCES

Acsai, K., Antoons, G., Livshitz, L., Rudy, Y., and Sipido, K. R. (2011). Microdomain [$Ca2^+$] near ryanodine receptors as reported by L-type $Ca2^+$ and $Na^+/Ca2^+$ exchange currents. *J. Physiol.* 589, 2569–2583. doi: 10.1113/jphysiol.2010.202663

Ahern, G. P., Hsu, S.-F., Klyachko, V. A., and Jackson, M. B. (2000). Induction of persistent sodium current by exogenous and endogenous nitric oxide. *J. Biol. Chem.* 275, 28810–28815. doi: 10.1074/jbc.M003090200

Allen, D. G., and Kurihara, S. (1982). The effects of muscle length on intracellular calcium transients in mammalian cardiac muscle. *J. Physiol.* 327, 79–94. doi: 10.1113/jphysiol.1982.sp014221

Antoons, G., Johnson, D. M., Dries, E., Santiago, D. J., Ozdemir, S., Lenaerts, I., et al. (2015). Calcium release near l-type calcium channels promotes beat-to-beat variability in ventricular myocytes from the chronic AV block dog. *J. Mol. Cell. Cardiol.* 89(Part B), 326–334. doi: 10.1016/j.yjmcc.2015.10.008

Antoons, G., Volders, P. G., Stankovicova, T., Bito, V., Stengl, M., Vos, M. A., et al. (2007). Window $Ca2^+$ current and its modulation by $Ca2^+$ release in hypertrophied cardiac myocytes from dogs with chronic atrioventricular block. *J. Physiol.* 579, 147–160. doi: 10.1113/jphysiol.2006.124222

Antoons, G., Willems, R., and Sipido, K. R. (2012). Alternative strategies in arrhythmia therapy: evaluation of Na/Ca exchange as an anti-arrhythmic target. *Pharmacol. Ther.* 134, 26–42. doi: 10.1016/j.pharmthera.2011.12.001

Barbagallo, F., Xu, B., Reddy, G. R., West, T., Wang, Q., Fu, Q., et al. (2016). Genetically encoded biosensors reveal PKA hyperphosphorylation on the myofilaments in rabbit heart failure. *Circ. Res.* 119, 931–943. doi: 10.1161/CIRCRESAHA.116.308964

Barouch, L. A., Harrison, R. W., Skaf, M. W., Rosas, G. O., Cappola, T. P., Kobeissi, Z. A., et al. (2002). Nitric oxide regulates the heart by spatial confinement of nitric oxide synthase isoforms. *Nature* 416, 337–339. doi: 10.1038/416005a

Barrabés, J. A., Inserte, J., Agulló, L., Rodríguez-Sinovas, A., Alburquerque-Béjar, J. J., and Garcia-Dorado, D. (2015). Effects of the selective stretch-activated channel blocker GsMtx4 on stretch-induced changes in refractoriness in isolated rat hearts and on ventricular premature beats and arrhythmias after coronary occlusion in swine. *PLoS One* 10:e0125753. doi: 10.1371/journal.pone.0125753

Bendall, J. K., Douglas, G., McNeill, E., Channon, K. M., and Crabtree, M. J. (2014). Tetrahydrobiopterin in cardiovascular health and disease. *Antioxid. Redox Signal.* 20, 3040–3077. doi: 10.1089/ars.2013.5566

Bers, D. M. (2002). Cardiac excitation–contraction coupling. *Nature* 415, 198–205. doi: 10.1038/415198a

Bers, D. M., and Morotti, S. (2014). $Ca2^+$ current facilitation is CaMKII-dependent and has arrhythmogenic consequences. *Front. Pharmacol.* 5:144. doi: 10.3389/fphar.2014.00144

Beuckelmann, D. J., and Erdmann, E. (1992). $Ca2^+$-currents and intracellular [$Ca2^+$]i-transients in single ventricular myocytes isolated from terminally failing human myocardium. *Basic Res. Cardiol.* 87(Suppl. 1), 235–243.

Beuckelmann, D. J., Näbauer, M., and Erdmann, E. (1993). Alterations of K^+ currents in isolated human ventricular myocytes from patients with terminal heart failure. *Circ. Res.* 73, 379–385. doi: 10.1161/01.RES.73.2.379

Biesmans, L., Macquaide, N., Heinzel, F. R., Bito, V., Smith, G. L., and Sipido, K. R. (2011). Subcellular heterogeneity of ryanodine receptor properties in ventricular myocytes with low T-tubule density. *PLoS One* 6:e25100. doi: 10.1371/journal.pone.0025100

Birks, E. J., Tansley, P. D., Hardy, J., George, R. S., Bowles, C. T., Burke, M., et al. (2006). Left ventricular assist device and drug therapy for the reversal of heart failure. *N. Engl. J. Med.* 355, 1873–1884. doi: 10.1056/NEJMoa053063

Bobin, P., Varin, A., Lefebvre, F., Fischmeister, R., Vandecasteele, G., and Leroy, J. (2016). Calmodulin kinase II inhibition limits the pro-arrhythmic $Ca2^+$ waves induced by cAMP-phosphodiesterase inhibitors. *Cardiovasc. Res.* 110, 151–161. doi: 10.1093/cvr/cvw027

Bristow, M. R., Ginsburg, R., Minobe, W., Cubicciotti, R. S., Sageman, W. S., Lurie, K., et al. (1982). Decreased catecholamine sensitivity and beta-adrenergic-receptor density in failing human hearts. *N. Engl. J. Med.* 307, 205–211. doi: 10.1056/NEJM198207223070401

Bryant, S. M., Kong, C. H., Watson, J., Cannell, M. B., James, A. F., and Orchard, C. H. (2015). Altered distribution of ICa impairs Ca release at the t-tubules of ventricular myocytes from failing hearts. *J. Mol. Cell. Cardiol.* 86, 23–31. doi: 10.1016/j.yjmcc.2015.06.012

Burger, D. E., Lu, X., Lei, M., Xiang, F.-L., Hammoud, L., Jiang, M., et al. (2009). Neuronal nitric oxide synthase protects against myocardial infarction-induced ventricular arrhythmia and mortality in mice. *Circulation* 120, 1345–1354. doi: 10.1161/CIRCULATIONAHA.108.846402

Burgoyne, J. R., Mongue-Din, H., Eaton, P., and Shah, A. M. (2012). Redox signaling in cardiac physiology and pathology. *Circ. Res.* 111, 1091–1106. doi: 10.1161/CIRCRESAHA.111.255216

Calaghan, S. C., Le Guennec, J.-Y., and White, E. (2004). Cytoskeletal modulation of electrical and mechanical activity in cardiac myocytes. *Prog. Biophys. Mol. Biol.* 84, 29–59. doi: 10.1016/S0079-6107(03)00057-9

Caldwell, J. L., Smith, C. E., Taylor, R. F., Kitmitto, A., Eisner, D. A., Dibb, K. M., et al. (2014). Dependence of cardiac transverse tubules on the BAR domain protein amphiphysin II (BIN-1). *Circ. Res.* 115, 986–996. doi: 10.1161/CIRCRESAHA.116.303448

Cannell, M. B., and Kong, C. H. (2012). Local control in cardiac E-C coupling. *J. Mol. Cell. Cardiol.* 52, 298–303. doi: 10.1016/j.yjmcc.2011.04.014

Carnicer, R., Crabtree, M. J., Sivakumaran, V., Casadei, B., and Kass, D. A. (2013). Nitric oxide synthases in heart failure. *Antioxid. Redox Signal.* 18, 1078–1099. doi: 10.1089/ars.2012.4824

Carnicer, R., Suffredini, S., Liu, X., Reilly, S., Simon, J. N., Surdo, N. C., et al. (2017). The subcellular localisation of neuronal nitric oxide synthase determines the downstream effects of no on myocardial function. *Cardiovasc. Res.* doi: 10.1093/cvr/cvx002 [Epub ahead of print].

Catterall, W. A. (2015). Regulation of cardiac calcium channels in the fight-or-flight response. *Curr. Mol. Pharmacol.* 8, 12–21. doi: 10.2174/1874467208666150507103417

Cerrone, M., Colombi, B., Santoro, M., di Barletta, M. R., Scelsi, M., Villani, L., et al. (2005). Bidirectional ventricular tachycardia and fibrillation elicited in a knock-in mouse model carrier of a mutation in the cardiac ryanodine receptor. *Circ. Res.* 96, e77–e82. doi: 10.1161/01.RES.0000169067.51055.72

Cerrone, M., Napolitano, C., and Priori, S. G. (2009). Catecholaminergic polymorphic ventricular tachycardia: a paradigm to understand mechanisms of arrhythmias associated to impaired $Ca2^+$ regulation. *Heart Rhythm* 6, 1652–1659. doi: 10.1016/j.hrthm.2009.06.033

Cerrone, M., Noujaim, S. F., Tolkacheva, E. G., Talkachou, A., O'Connell, R., Berenfeld, O., et al. (2007). Arrhythmogenic mechanisms in a mouse model of catecholaminergic polymorphic ventricular tachycardia. *Circ. Res.* 101, 1039–1048. doi: 10.1161/CIRCRESAHA.107.148064

Chang, P.-C., Lu, Y.-Y., Lee, H.-L., Lin, S.-F., Chu, Y., Wen, M.-S., et al. (2018). Paradoxical effects of sodium-calcium exchanger inhibition on torsade de pointes and early afterdepolarization in a heart failure rabbit model. *J. Cardiovasc. Pharmacol.* 72, 97–105. doi: 10.1097/FJC.0000000000000598

Chen, W.-W., Xiong, X.-Q., Chen, Q., Li, Y.-H., Kang, Y.-M., and Zhu, G.-Q. (2015). Cardiac sympathetic afferent reflex and its implications for sympathetic activation in chronic heart failure and hypertension. *Acta Physiol.* 213, 778–794. doi: 10.1111/apha.12447

Cheng, H., and Lederer, W. J. (2008). Calcium sparks. *Physiol. Rev.* 88, 1491–1545. doi: 10.1152/physrev.00030.2007

Chen-Izu, Y., and Izu, L. T. (2017). Mechano-chemo-transduction in cardiac myocytes. *J. Physiol.* 595, 3949–3958. doi: 10.1113/JP273101

Chidsey, C. A., Braunwald, E., Morrow, A. G., and Mason, D. T. (1963). Myocardial norepinephrine concentration in man. effects of reserpine and of congestive heart failure. *N. Engl. J. Med.* 269, 653–658. doi: 10.1056/NEJM196309262691302

Chockalingam, P., Crotti, L., Girardengo, G., Johnson, J. N., Harris, K. M., van der Heijden, J. F., et al. (2012). Not all beta-blockers are equal in the management of long QT syndrome types 1 and 2: higher recurrence of events under metoprolol. *J. Am. Coll. Cardiol.* 60, 2092–2099. doi: 10.1016/j.jacc.2012.07.046

Cingolani, H. E., Pérez, N. G., Cingolani, O. H., and Ennis, I. L. (2013). The Anrep effect: 100 years later. *Am. J. Physiol. Heart Circ. Physiol.* 304, H175–H182. doi: 10.1152/ajpheart.00508.2012

Cohn, J. N., Ferrari, R., Sharpe, N., and on Behalf of an International Forum on Cardiac Remodeling (2000). Cardiac remodeling—concepts and clinical implications: a consensus paper from an international forum on cardiac remodeling. *J. Am. Coll. Cardiol.* 35, 569–582. doi: 10.1016/S0735-1097(99)00630-0

Coste, B., Mathur, J., Schmidt, M., Earley, T. J., Ranade, S., Petrus, M. J., et al. (2010). Piezo1 and Piezo2 are essential components of distinct mechanically activated cation channels. *Science* 330, 55–60. doi: 10.1126/science.1193270

Craelius, W., Chen, V., and el-Sherif, N. (1988). Stretch activated ion channels in ventricular myocytes. *Biosci. Rep.* 8, 407–414. doi: 10.1007/BF01121637

Cranefield, P. F. (1977). Action potentials, afterpotentials, and arrhythmias. *Circ. Res.* 41, 415–423. doi: 10.1161/01.RES.41.4.415

Crocini, C., Coppini, R., Ferrantini, C., Yan, P., Loew, L. M., Poggesi, C., et al. (2016). T-tubular electrical defects contribute to blunted β-adrenergic response in heart failure. *Int. J. Mol. Sci.* 17:E1471. doi: 10.3390/ijms17091471

Curran, J., Hinton, M. J., Ríos, E., Bers, D. M., and Shannon, T. R. (2007). β-adrenergic enhancement of sarcoplasmic reticulum calcium leak in cardiac myocytes is mediated by calcium/calmodulin-dependent protein kinase. *Circ. Res.* 100, 391–398. doi: 10.1161/01.RES.0000258172.74570.e6

Curran, J., Tang, L., Roof, S. R., Velmurugan, S., Millard, A., Shonts, S., et al. (2014). Nitric oxide-dependent activation of CaMKII increases diastolic sarcoplasmic reticulum calcium release in cardiac myocytes in response to adrenergic stimulation. *PLoS One* 9:e87495. doi: 10.1371/journal.pone.0087495

Damy, T., Ratajczak, P., Shah, A. M., Camors, E., Marty, I., Hasenfuss, G., et al. (2004). Increased neuronal nitric oxide synthase-derived NO production in the failing human heart. *Lancet* 363, 1365–1367. doi: 10.1016/S0140-6736(04)16048-0

Dangman, K. H., Danilo, P., Hordof, A. J., Mary-Rabine, L., Reder, R. F., and Rosen, M. R. (1982). Electrophysiologic characteristics of human ventricular and Purkinje fibers. *Circulation* 65, 362–368. doi: 10.1161/01.CIR.65.2.362

DeSantiago, J., Ai, X., Islam, M., Acuna, G., Ziolo, M. T., Bers, D. M., et al. (2008). Arrhythmogenic effects of β2-adrenergic stimulation in the failing heart are attributable to enhanced sarcoplasmic reticulum Ca load. *Circ. Res.* 102, 1389–1397. doi: 10.1161/CIRCRESAHA.107.169011

Dewenter, M., Neef, S., Vettel, C., Lämmle, S., Beushausen, C., Zelarayan, L. C., et al. (2017). Calcium/calmodulin-dependent protein kinase II activity persists during chronic β-adrenoceptor blockade in experimental and human heart failureclinical perspective. *Circ. Heart Fail.* 10:e003840. doi: 10.1161/CIRCHEARTFAILURE.117.003840

Dey, S., DeMazumder, D., Sidor, A., Foster, D. B., and O'Rourke, B. (2018). Mitochondrial ROS drive sudden cardiac death and chronic proteome remodeling in heart failure. *Circ. Res.* 123, 356–371. doi: 10.1161/CIRCRESAHA.118.312708

Dobrev, D., and Wehrens, X. H. (2014). Role of RyR2 phosphorylation in heart failure and arrhythmias: controversies around ryanodine receptor phosphorylation in cardiac disease. *Circ. Res.* 114, 1311–1319. doi: 10.1161/CIRCRESAHA.114.300568

Doleschal, B., Primessnig, U., Wölkart, G., Wolf, S., Schernthaner, M., Lichtenegger, M., et al. (2015). TRPC3 contributes to regulation of cardiac contractility and arrhythmogenesis by dynamic interaction with NCX1. *Cardiovasc. Res.* 106, 163–173. doi: 10.1093/cvr/cvv022

Dries, E., Bito, V., Lenaerts, I., Antoons, G., Sipido, K. R., and Macquaide, N. (2013). Selective modulation of coupled ryanodine receptors during microdomain activation of calcium/calmodulin-dependent kinase II in the dyadic cleft. *Circ. Res.* 113, 1242–1252. doi: 10.1161/CIRCRESAHA.113.301896

Dries, E., Santiago, D. J., Gilbert, G., Lenaerts, I., Vandenberk, B., Nagaraju, C. K., et al. (2018a). Hyperactive ryanodine receptors in human heart failure and ischemic cardiomyopathy reside outside of couplons. *Cardiovasc. Res.* 114, 1512–1524. doi: 10.1093/cvr/cvy088

Dries, E., Vandenberk, B., Gilbert, G., Amoni, M., Holemans, P., Willems, R., et al. (2018b). P519Regional heterogeneity of hyperactive non-coupled ryanodine receptors makes the peri-infarct region more prone to triggered activities after myocardial infarction. *Cardiovasc. Res.* 114, S126–S127. doi: 10.1093/cvr/cvy060.376

Dries, E., Santiago, D. J., Johnson, D. M., Gilbert, G., Holemans, P., Korte, S. M., et al. (2016). Calcium/calmodulin-dependent kinase II and nitric oxide synthase 1-dependent modulation of ryanodine receptors during β-adrenergic stimulation is restricted to the dyadic cleft. *J. Physiol.* 594, 5923–5939. doi: 10.1113/JP271965

Dybkova, N., Wagner, S., Backs, J., Hund, T. J., Mohler, P. J., Sowa, T., et al. (2014). Tubulin polymerization disrupts cardiac β-adrenergic regulation of late INa. *Cardiovasc. Res.* 103, 168–177. doi: 10.1093/cvr/cvu120

Eckberg, D. L., Drabinsky, M., and Braunwald, E. (1971). Defective cardiac parasympathetic control in patients with heart disease. *N. Engl. J. Med.* 285, 877–883. doi: 10.1056/NEJM197110142851602

Eder, P., and Molkentin, J. D. (2011). TRPC channels as effectors of cardiac hypertrophy. *Circ. Res.* 108, 265–272. doi: 10.1161/CIRCRESAHA.110.225888

Erickson, J. R., Joiner, M. A., Guan, X., Kutschke, W., Yang, J., Oddis, C. V., et al. (2008). A dynamic pathway for calcium-independent activation of CaMKII by methionine oxidation. *Cell* 133, 462–474. doi: 10.1016/j.cell.2008.02.048

Fabritz, L., Franz, M. R., Carmeliet, E., and Kirchhof, P. (2014). To the Editor–Propranolol, a β-adrenoreceptor blocker, prevents arrhythmias also by its sodium channel blocking effect. *Heart Rhythm* 11:e1. doi: 10.1016/j.hrthm.2013.12.027

Faggioni, M., Hwang, H. S., van der Werf, C., Nederend, I., Kannankeril, P. J., Wilde, A. A., et al. (2013). Accelerated sinus rhythm prevents catecholaminergic polymorphic ventricular tachycardia in mice and in patients. *Circ. Res.* 112, 689–697. doi: 10.1161/CIRCRESAHA.111.300076

Farah, C., Michel, L. Y. M., and Balligand, J.-L. (2018). Nitric oxide signalling in cardiovascular health and disease. *Nat. Rev. Cardiol.* 15, 292–316. doi: 10.1038/nrcardio.2017.224

Fedida, D., Noble, D., Rankin, A. C., and Spindler, A. J. (1987). The arrhythmogenic transient inward current iTI and related contraction in isolated guinea-pig ventricular myocytes. *J. Physiol.* 392, 523–542. doi: 10.1113/jphysiol.1987.sp016795

Fernández-Velasco, M., Rueda, A., Rizzi, N., Benitah, J.-P., Colombi, B., Napolitano, C., et al. (2009). Increased $Ca2^+$ sensitivity of the ryanodine receptor mutant RyR2R4496C underlies catecholaminergic polymorphic ventricular tachycardia. *Circ. Res.* 104, 201–209. doi: 10.1161/CIRCRESAHA.108.177493

Ferrandi, M., Barassi, P., Tadini-Buoninsegni, F., Bartolommei, G., Molinari, I., Tripodi, M. G., et al. (2013). Istaroxime stimulates SERCA2a and accelerates calcium cycling in heart failure by relieving phospholamban inhibition. *Br. J. Pharmacol.* 169, 1849–1861. doi: 10.1111/bph.12278

Fink, M., Noble, P. J., and Noble, D. (2011). $Ca2^+$-induced delayed afterdepolarizations are triggered by dyadic subspace $Ca2^+$ affirming that

increasing SERCA reduces aftercontractions. *Am. J. Physiol. Heart Circ. Physiol.* 301, H921–H935. doi: 10.1152/ajpheart.01055.2010

Fischer, T. H., Neef, S., and Maier, L. S. (2013). The Ca-calmodulin dependent kinase II: a promising target for future antiarrhythmic therapies? *J. Mol. Cell. Cardiol.* 58, 182–187. doi: 10.1016/j.yjmcc.2012.11.003

Florea, V. G., Mareyev, V. Y., Samko, A. N., Orlova, I. A., Coats, A. J., and Belenkov, Y. N. (1999). Left ventricular remodelling: common process in patients with different primary myocardial disorders. *Int. J. Cardiol.* 68, 281–287. doi: 10.1016/S0167-5273(98)00362-3

Forbes, M. S., and Sperelakis, N. (1983). The membrane systems and cytoskeletal elements of mammalian myocardial cells. *Cell Muscle Motil.* 3, 89–155. doi: 10.1007/978-1-4615-9296-9_5

Fowler, E. D., Kong, C. H. T., Hancox, J. C., and Cannell, M. B. (2018). Late $Ca2^+$ sparks and ripples during the systolic $Ca2^+$ transient in heart muscle cellsnovelty and significance. *Circ. Res.* 122, 473–478. doi: 10.1161/CIRCRESAHA.117.312257

Franz, M. R., Burkhoff, D., Yue, D. T., and Sagawa, K. (1989). Mechanically induced action potential changes and arrhythmia in isolated and in situ canine hearts. *Cardiovasc. Res.* 23, 213–223. doi: 10.1093/cvr/23.3.213

Frisk, M., Ruud, M., Espe, E. K. S., Aronsen, J. M., Røe, Å. T., Zhang, L., et al. (2016). Elevated ventricular wall stress disrupts cardiomyocyte t-tubule structure and calcium homeostasis. *Cardiovasc. Res.* 112, 443–451. doi: 10.1093/cvr/cvw111

Frommeyer, G., Rajamani, S., Grundmann, F., Stypmann, J., Osada, N., Breithardt, G., et al. (2012). New insights into the beneficial electrophysiologic profile of ranolazine in heart failure: prevention of ventricular fibrillation with increased postrepolarization refractoriness and without drug-induced proarrhythmia. *J. Card. Fail.* 18, 939–949. doi: 10.1016/j.cardfail.2012.10.017

Fu, Y., Shaw, S. A., Naami, R., Vuong, C. L., Basheer, W. A., Guo, X., et al. (2016). Isoproterenol promotes rapid ryanodine receptor movement to bridging integrator 1 (BIN1)-organized dyads. *Circulation* 133, 388–397. doi: 10.1161/CIRCULATIONAHA.115.018535

Fujita, T., Umemura, M., Yokoyama, U., Okumura, S., and Ishikawa, Y. (2017). The role of Epac in the heart. *Cell. Mol. Life Sci.* 74, 591–606. doi: 10.1007/s00018-016-2336-5

Funck-Brentano, C. (2006). Beta-blockade in CHF: from contraindication to indication. *Eur. Heart J. Suppl.* 8, C19–C27. doi: 10.1093/eurheartj/sul010

Garan, A. R., Yuzefpolskaya, M., Colombo, P. C., Morrow, J. P., Te-Frey, R., Dano, D., et al. (2013). Ventricular arrhythmias and implantable cardioverter-defibrillator therapy in patients with continuous-flow left ventricular assist devices. *J. Am. Coll. Cardiol.* 61, 2542–2550. doi: 10.1016/j.jacc.2013.04.020

Gill, J. S., McKenna, W. J., and Camm, A. J. (1995). Free radicals irreversibly decrease $Ca2^+$ currents in isolated guinea-pig ventricular myocytes. *Eur. J. Pharmacol.* 292, 337–340.

Gómez, A. M., Ruiz-Hurtado, G., Benitah, J.-P., and Domínguez-Rodríguez, A. (2013). $Ca(2^+)$ fluxes involvement in gene expression during cardiac hypertrophy. *Curr. Vasc. Pharmacol.* 11, 497–506. doi: 10.2174/1570161111311040013

González, D. R., Fernández, I. C., Ordenes, P. P., Treuer, A. V., Eller, G., and Boric, M. P. (2008). Differential role of S-nitrosylation and the NO-cGMP-PKG pathway in cardiac contractility. *Nitric Oxide* 18, 157–167. doi: 10.1016/j.niox.2007.09.086

Gordin, J. S., and Fonarow, G. C. (2016). New medications for heart failure. *Trends Cardiovasc. Med.* 26, 485–492. doi: 10.1016/j.tcm.2016.02.008

Gottlieb, P., Folgering, J., Maroto, R., Raso, A., Wood, T. G., Kurosky, A., et al. (2008). Revisiting TRPC1 and TRPC6 mechanosensitivity. *Pflugers Arch.* 455, 1097–1103. doi: 10.1007/s00424-007-0359-3

Gottlieb, P. A. (2017). A tour de force: the discovery, properties, and function of piezo channels. *Curr. Top. Membr.* 79, 1–36. doi: 10.1016/bs.ctm.2016.11.007

Greenberg, B., Butler, J., Felker, G. M., Ponikowski, P., Voors, A. A., Desai, A. S., et al. (2016). Calcium upregulation by percutaneous administration of gene therapy in patients with cardiac disease (CUPID 2): a randomised, multinational, double-blind, placebo-controlled, phase 2b trial. *Lancet* 387, 1178–1186. doi: 10.1016/S0140-6736(16)00082-9

Guellich, A., Mehel, H., and Fischmeister, R. (2014). Cyclic AMP synthesis and hydrolysis in the normal and failing heart. *Pflugers Arch.* 466, 1163–1175. doi: 10.1007/s00424-014-1515-1

Guo, A., Zhang, C., Wei, S., Chen, B., and Song, L.-S. (2013). Emerging mechanisms of T-tubule remodelling in heart failure. *Cardiovasc. Res.* 98, 204–215. doi: 10.1093/cvr/cvt020

Guo, J., and Duff, H. J. (2006). Calmodulin kinase II accelerates L-type $Ca2^+$ current recovery from inactivation and compensates for the direct inhibitory effect of $[Ca2^+]$i in rat ventricular myocytes. *J. Physiol.* 574, 509–518. doi: 10.1113/jphysiol.2006.109199

Guo, T., Zhang, T., Ginsburg, K. S., Mishra, S., Brown, J. H., and Bers, D. M. (2012). CaMKIIδC slows [Ca]i decline in cardiac myocytes by promoting Ca sparks. *Biophys. J.* 102, 2461–2470. doi: 10.1016/j.bpj.2012.04.015

Gutierrez, D. A., Fernandez-Tenorio, M., Ogrodnik, J., and Niggli, E. (2013). NO-dependent CaMKII activation during β-adrenergic stimulation of cardiac muscle. *Cardiovasc. Res.* 100, 392–401. doi: 10.1093/cvr/cvt201

Hansen, D. E., Craig, C. S., and Hondeghem, L. M. (1990). Stretch-induced arrhythmias in the isolated canine ventricle. Evidence for the importance of mechanoelectrical feedback. *Circulation* 81, 1094–1105. doi: 10.1161/01.CIR.81.3.1094

Hartmann, N., Pabel, S., Herting, J., Schatter, F., Renner, A., Gummert, J., et al. (2017). Antiarrhythmic effects of dantrolene in human diseased cardiomyocytes. *Heart Rhythm* 14, 412–419. doi: 10.1016/j.hrthm.2016.09.014

Hasenfuss, G., and Pieske, B. (2002). Calcium cycling in congestive heart failure. *J. Mol. Cell. Cardiol.* 34, 951–969. doi: 10.1006/jmcc.2002.2037

Hegyi, B., Bossuyt, J., Ginsburg, K. S., Mendoza, L. M., Talken, L., Ferrier, W. T., et al. (2018a). Altered repolarization reserve in failing rabbit ventricular myocytes: calcium and β-adrenergic effects on delayed- and inward-rectifier potassium currents. *Circ. Arrhythm. Electrophysiol.* 11:e005852. doi: 10.1161/CIRCEP.117.005852

Hegyi, B., Bossuyt, J., Griffiths, L. G., Shimkunas, R., Coulibaly, Z., Jian, Z., et al. (2018b). Complex electrophysiological remodeling in postinfarction ischemic heart failure. *Proc. Natl. Acad. Sci. U.S.A.* 115, E3036–E3044. doi: 10.1073/pnas.1718211115

Heinzel, F. R., MacQuaide, N., Biesmans, L., and Sipido, K. (2011). Dyssynchrony of $Ca2^+$ release from the sarcoplasmic reticulum as subcellular mechanism of cardiac contractile dysfunction. *J. Mol. Cell. Cardiol.* 50, 390–400. doi: 10.1016/j.yjmcc.2010.11.008

Hong, T.-T., Cogswell, R., James, C. A., Kang, G., Pullinger, C. R., Malloy, M. J., et al. (2012). Plasma BIN1 correlates with heart failure and predicts arrhythmia in patients with arrhythmogenic right ventricular cardiomyopathy. *Heart Rhythm* 9, 961–967. doi: 10.1016/j.hrthm.2012.01.024

Hong, T.-T., Smyth, J. W., Gao, D., Chu, K. Y., Vogan, J. M., Fong, T. S., et al. (2010). BIN1 localizes the L-type calcium channel to cardiac T-tubules. *PLoS Biol.* 8:e1000312. doi: 10.1371/journal.pbio.1000312

Houser, S. R., and Molkentin, J. D. (2008). Does contractile $Ca2^+$ control calcineurin-NFAT signaling and pathological hypertrophy in cardiac myocytes? *Sci. Signal.* 1:e31. doi: 10.1126/scisignal.125pe31

Hulot, J.-S., Salem, J.-E., Redheuil, A., Collet, J.-P., Varnous, S., Jourdain, P., et al. (2017). Effect of intracoronary administration of AAV1/SERCA2a on ventricular remodelling in patients with advanced systolic heart failure: results from the AGENT-HF randomized phase 2 trial. *Eur. J. Heart Fail.* 19, 1534–1541. doi: 10.1002/ejhf.826

Ibrahim, M., Navaratnarajah, M., Siedlecka, U., Rao, C., Dias, P., Moshkov, A. V., et al. (2012). Mechanical unloading reverses transverse tubule remodelling and normalizes local $Ca2^+$-induced $Ca2^+$ release in a rodent model of heart failure. *Eur. J. Heart Fail.* 14, 571–580. doi: 10.1093/eurjhf/hfs038

Inoue, R., Jian, Z., and Kawarabayashi, Y. (2009). Mechanosensitive TRP channels in cardiovascular pathophysiology. *Pharmacol. Ther.* 123, 371–385. doi: 10.1016/j.pharmthera.2009.05.009

Iribe, G., Ward, C. W., Camelliti, P., Bollensdorff, C., Mason, F., Burton, R. A., et al. (2009). Axial stretch of rat single ventricular cardiomyocytes causes an acute and transient increase in $Ca2^+$ spark rate. *Circ. Res.* 104, 787–795. doi: 10.1161/CIRCRESAHA.108.193334

Janse, M. J. (2004). Electrophysiological changes in heart failure and their relationship to arrhythmogenesis. *Cardiovasc. Res.* 61, 208–217. doi: 10.1016/j.cardiores.2003.11.018

January, C. T., and Riddle, J. M. (1989). Early afterdepolarizations: mechanism of induction and block. A role for L-type $Ca2^+$ current. *Circ. Res.* 64, 977–990. doi: 10.1161/01.RES.64.5.977

Jessup, M., Greenberg, B., Mancini, D., Cappola, T., Pauly, D. F., Jaski, B., et al. (2011). Calcium upregulation by percutaneous administration of gene therapy in cardiac disease (CUPID): a phase 2 trial of intracoronary gene therapy of sarcoplasmic reticulum $Ca2^+$ -ATPase in patients with advanced heart failure. *Circulation* 124, 304–313. doi: 10.1161/CIRCULATIONAHA.111.022889

Jian, Z., Han, H., Zhang, T., Puglisi, J., Izu, L. T., Shaw, J. A., et al. (2014). Mechanochemotransduction during cardiomyocyte contraction is mediated by localized nitric oxide signaling. *Sci. Signal.* 7:ra27. doi: 10.1126/scisignal.2005046

Johnson, D. M., Heijman, J., Bode, E. F., Greensmith, D. J., van der Linde, H., Abi-Gerges, N., et al. (2013). Diastolic spontaneous calcium release from the sarcoplasmic reticulum increases beat-to-beat variability of repolarization in canine ventricular myocytes after β-adrenergic stimulation. *Circ. Res.* 112, 246–256. doi: 10.1161/CIRCRESAHA.112.275735

Johnson, D. M., Heijman, J., Pollard, C. E., Valentin, J.-P., Crijns, H. J. G. M., Abi-Gerges, N., et al. (2010). I(Ks) restricts excessive beat-to-beat variability of repolarization during beta-adrenergic receptor stimulation. *J. Mol. Cell. Cardiol.* 48, 122–130. doi: 10.1016/j.yjmcc.2009.08.033

Jones, S. P., Greer, J. J. M., van Haperen, R., Duncker, D. J., de Crom, R., and Lefer, D. J. (2003). Endothelial nitric oxide synthase overexpression attenuates congestive heart failure in mice. *Proc. Natl. Acad. Sci. U.S.A.* 100, 4891–4896. doi: 10.1073/pnas.0837428100

Jost, N., Virág, L., Bitay, M., Takács, J., Lengyel, C., Biliczki, P., et al. (2005). Restricting excessive cardiac action potential and QT prolongation: a vital role for IKs in human ventricular muscle. *Circulation* 112, 1392–1399. doi: 10.1161/CIRCULATIONAHA.105.550111

Kashimura, T., Briston, S. J., Trafford, A. W., Napolitano, C., Priori, S. G., Eisner, D. A., et al. (2010). In the RyR2R4496C mouse model of CPVT, β-adrenergic stimulation induces Ca waves by increasing SR Ca content and not by decreasing the threshold for Ca waves novelty and significance. *Circ. Res.* 107, 1483–1489. doi: 10.1161/CIRCRESAHA.110.227744

Kassmann, M., Hansel, A., Leipold, E., Birkenbeil, J., Lu, S.-Q., Hoshi, T., et al. (2008). Oxidation of multiple methionine residues impairs rapid sodium channel inactivation. *Pflugers Arch.* 456, 1085–1095. doi: 10.1007/s00424-008-0477-6

Katz, S. D., Khan, T., Zeballos, G. A., Mathew, L., Potharlanka, P., Knecht, M., et al. (1999). Decreased activity of the L-arginine-nitric oxide metabolic pathway in patients with congestive heart failure. *Circulation* 99, 2113–2117. doi: 10.1161/01.CIR.99.16.2113

Kawase, Y., Ly, H. Q., Prunier, F., Lebeche, D., Shi, Y., Jin, H., et al. (2008). Reversal of cardiac dysfunction after long-term expression of SERCA2a by gene transfer in a pre-clinical model of heart failure. *J. Am. Coll. Cardiol.* 51, 1112–1119. doi: 10.1016/j.jacc.2007.12.014

Kehat, I., and Molkentin, J. D. (2010). Molecular pathways underlying cardiac remodeling during pathophysiologic stimulation. *Circulation* 122, 2727–2735. doi: 10.1161/CIRCULATIONAHA.110.942268

Khairallah, R. J., Shi, G., Sbrana, F., Prosser, B. L., Borroto, C., Mazaitis, M. J., et al. (2012). Microtubules underlie dysfunction in duchenne muscular dystrophy. *Sci. Signal.* 5:ra56. doi: 10.1126/scisignal.2002829

Kho, C., Lee, A., and Hajjar, R. J. (2012). Altered sarcoplasmic reticulum calcium cycling–targets for heart failure therapy. *Nat. Rev. Cardiol.* 9, 717–733. doi: 10.1038/nrcardio.2012.145

Klipp, R. C., Li, N., Wang, Q., Word, T. A., Sibrian-Vazquez, M., Strongin, R. M., et al. (2018). EL20, a potent antiarrhythmic compound, selectively inhibits calmodulin-deficient ryanodine receptor type 2. *Heart Rhythm* 15, 578–586. doi: 10.1016/j.hrthm.2017.12.017

Kohlhaas, M., Liu, T., Knopp, A., Zeller, T., Ong, M. F., Böhm, M., et al. (2010). Elevated cytosolic Na^+ increases mitochondrial formation of reactive oxygen species in failing cardiac myocytes. *Circulation* 121, 1606–1613. doi: 10.1161/CIRCULATIONAHA.109.914911

Kokkonen, K., and Kass, D. A. (2017). Nanodomain regulation of cardiac cyclic nucleotide signaling by phosphodiesterases. *Annu. Rev. Pharmacol. Toxicol.* 57, 455–479. doi: 10.1146/annurev-pharmtox-010716-104756

Koumi, S., Backer, C. L., Arentzen, C. E., and Sato, R. (1995). beta-Adrenergic modulation of the inwardly rectifying potassium channel in isolated human ventricular myocytes. Alteration in channel response to beta-adrenergic stimulation in failing human hearts. *J. Clin. Invest.* 96, 2870–2881. doi: 10.1172/JCI118358

Kuwahara, K., Wang, Y., McAnally, J., Richardson, J. A., Bassel-Duby, R., Hill, J. A., et al. (2006). TRPC6 fulfills a calcineurin signaling circuit during pathologic cardiac remodeling. *J. Clin. Invest.* 116, 3114–3126. doi: 10.1172/JCI27702

Landstrom, A. P., Dobrev, D., and Wehrens, X. H. T. (2017). Calcium signaling and cardiac arrhythmias. *Circ. Res.* 120, 1969–1993. doi: 10.1161/CIRCRESAHA.117.310083

Lang, D., Holzem, K., Kang, C., Xiao, M., Hwang, H. J., Ewald, G. A., et al. (2015). Arrhythmogenic remodeling of β2 versus β1 adrenergic signaling in the human failing heart. *Circ. Arrhythm. Electrophysiol.* 8, 409–419. doi: 10.1161/CIRCEP.114.002065

Lang, D., Sato, D., Jiang, Y., Ginsburg, K. S., Ripplinger, C. M., and Bers, D. M. (2017). Calcium-dependent arrhythmogenic foci created by weakly coupled myocytes in the failing heart. *Circ. Res.* 121, 1379–1391. doi: 10.1161/CIRCRESAHA.117.312050

Lazzara, R., and Marchi, S. (1989). "Electrophysiologic mechanisms for the generation of arrhythmias with adrenergic stimulation," in *Adrenergic System and Ventricular Arrhythmias in Myocardial Infarction*, eds J. Brachmann and A. Schömig (Berlin: Springer), 231–238. doi: 10.1007/978-3-642-74317-7_19

Lebek, S., Plößl, A., Baier, M., Mustroph, J., Tarnowski, D., Lücht, C. M., et al. (2018). The novel CaMKII inhibitor GS-680 reduces diastolic SR Ca leak and prevents CaMKII-dependent pro-arrhythmic activity. *J. Mol. Cell. Cardiol.* 118, 159–168. doi: 10.1016/j.yjmcc.2018.03.020

Lederer, W. J., and Tsien, R. W. (1976). Transient inward current underlying arrhythmogenic effects of cardiotonic steroids in Purkinje fibres. *J. Physiol.* 263, 73–100. doi: 10.1113/jphysiol.1976.sp011622

Li, G.-R., Lau, C.-P., Ducharme, A., Tardif, J.-C., and Nattel, S. (2002). Transmural action potential and ionic current remodeling in ventricles of failing canine hearts. *Am. J. Physiol. Heart Circ. Physiol.* 283, H1031–H1041. doi: 10.1152/ajpheart.00105.2002

Li, H., Lichter, J. G., Seidel, T., Tomaselli, G. F., Bridge, J. H. B., and Sachse, F. B. (2015). Cardiac resynchronization therapy reduces subcellular heterogeneity of ryanodine receptors, T-tubules, and $Ca2^+$ sparks produced by dyssynchronous heart failure. *Circ. Heart Fail.* 8, 1105–1114. doi: 10.1161/CIRCHEARTFAILURE.115.002352

Liang, J., Huang, B., Yuan, G., Chen, Y., Liang, F., Zeng, H., et al. (2017). Stretch-activated channel Piezo1 is up-regulated in failure heart and cardiomyocyte stimulated by AngII. *Am. J. Transl. Res.* 9, 2945–2955.

Lindner, M., Brandt, M. C., Sauer, H., Hescheler, J., Böhle, T., and Beuckelmann, D. J. (2002). Calcium sparks in human ventricular cardiomyocytes from patients with terminal heart failure. *Cell Calcium* 31, 175–182. doi: 10.1054/ceca.2002.0272

Liu, M., Liu, H., and Dudley, S. C. (2010). Reactive oxygen species originating from mitochondria regulate the cardiac sodium channel. *Circ. Res.* 107, 967–974. doi: 10.1161/CIRCRESAHA.110.220673

Liu, N., Colombi, B., Memmi, M., Zissimopoulos, S., Rizzi, N., Negri, S., et al. (2006). Arrhythmogenesis in catecholaminergic polymorphic ventricular tachycardia: insights from a RyR2 R4496C knock-in mouse model. *Circ. Res.* 99, 292–298. doi: 10.1161/01.RES.0000235869.50747.e1

Lohse, M. J., Engelhardt, S., and Eschenhagen, T. (2003). What is the role of β-adrenergic signaling in heart failure? *Circ. Res.* 93, 896–906. doi: 10.1161/01.RES.0000102042.83024.CA

Luo, M., and Anderson, M. E. (2013). Mechanisms of altered $Ca2^+$ handling in heart failure. *Circ. Res.* 113, 690–708. doi: 10.1161/CIRCRESAHA.113.301651

Lyon, A. R., Bannister, M. L., Collins, T., Pearce, E., Sepehripour, A. H., Dubb, S. S., et al. (2011). SERCA2a gene transfer decreases sarcoplasmic reticulum calcium leak and reduces ventricular arrhythmias in a model of chronic heart failure. *Circ. Arrhythm. Electrophysiol.* 4, 362–372. doi: 10.1161/CIRCEP.110.961615

Lyon, A. R., MacLeod, K. T., Zhang, Y., Garcia, E., Kanda, G. K., Lab, M. J., et al. (2009). Loss of T-tubules and other changes to surface topography in ventricular myocytes from failing human and rat heart. *Proc. Natl. Acad. Sci. U.S.A.* 106, 6854–6859. doi: 10.1073/pnas.0809777106

Maier, L. S., and Bers, D. M. (2007). Role of $Ca2^+$/calmodulin-dependent protein kinase (CaMK) in excitation-contraction coupling in the heart. *Cardiovasc. Res.* 73, 631–640. doi: 10.1016/j.cardiores.2006.11.005

Mak, S., and Newton, G. E. (2004). Redox modulation of the inotropic response to dobutamine is impaired in patients with heart failure. *Am. J. Physiol. Heart Circ. Physiol.* 286, H789–H795. doi: 10.1152/ajpheart.00633.2003

Makarewich, C. A., Zhang, H., Davis, J., Correll, R. N., Trappanese, D. M., Hoffman, N. E., et al. (2014). Transient receptor potential channels contribute to pathological structural and functional remodeling after myocardial infarction. *Circ. Res.* 115, 567–580. doi: 10.1161/CIRCRESAHA.115.303831

Malliani, A., Recordati, G., and Schwartz, P. J. (1973). Nervous activity of afferent cardiac sympathetic fibres with atrial and ventricular endings. *J. Physiol.* 229, 457–469. doi: 10.1113/jphysiol.1973.sp010147

Maltsev, V. A., Silverman, N., Sabbah, H. N., and Undrovinas, A. I. (2007). Chronic heart failure slows late sodium current in human and canine ventricular myocytes: implications for repolarization variability. *Eur. J. Heart Fail.* 9, 219–227. doi: 10.1016/j.ejheart.2006.08.007

Manfra, O., Frisk, M., and Louch, W. E. (2017). Regulation of cardiomyocyte T-tubular structure: opportunities for therapy. *Curr. Heart Fail. Rep.* 14, 167–178. doi: 10.1007/s11897-017-0329-9

Marban, E., Robinson, S. W., and Wier, W. G. (1986). Mechanisms of arrhythmogenic delayed and early afterdepolarizations in ferret ventricular muscle. *J. Clin. Invest.* 78, 1185–1192. doi: 10.1172/JCI112701

Marx, S. O., Reiken, S., Hisamatsu, Y., Jayaraman, T., Burkhoff, D., Rosemblit, N., et al. (2000). PKA phosphorylation dissociates FKBP12.6 from the calcium release channel (ryanodine receptor): defective regulation in failing hearts. *Cell* 101, 365–376. doi: 10.1016/S0092-8674(00)80847-8

Massion, P. B., Feron, O., Dessy, C., and Balligand, J.-L. (2003). Nitric oxide and cardiac function: ten years after, and continuing. *Circ. Res.* 93, 388–398. doi: 10.1161/01.RES.0000088351.58510.21

Miura, M., Taguchi, Y., Nagano, T., Sasaki, M., Handoh, T., and Shindoh, C. (2015). Effect of myofilament Ca(2^+) sensitivity on Ca(2^+) wave propagation in rat ventricular muscle. *J. Mol. Cell. Cardiol.* 84, 162–169. doi: 10.1016/j.yjmcc.2015.04.027

Miura, M., Wakayama, Y., Endoh, H., Nakano, M., Sugai, Y., Hirose, M., et al. (2008). Spatial non-uniformity of excitation-contraction coupling can enhance arrhythmogenic-delayed afterdepolarizations in rat cardiac muscle. *Cardiovasc. Res.* 80, 55–61. doi: 10.1093/cvr/cvn162

Moens, A. L., Takimoto, E., Tocchetti, C. G., Chakir, K., Bedja, D., Cormaci, G., et al. (2008). Reversal of cardiac hypertrophy and fibrosis from pressure overload by tetrahydrobiopterin: efficacy of recoupling nitric oxide synthase as a therapeutic strategy. *Circulation* 117, 2626–2636. doi: 10.1161/CIRCULATIONAHA.107.737031

Morita, H., Suzuki, G., Haddad, W., Mika, Y., Tanhehco, E. J., Sharov, V. G., et al. (2003). Cardiac contractility modulation with nonexcitatory electric signals improves left ventricular function in dogs with chronic heart failure. *J. Card. Fail.* 9, 69–75. doi: 10.1054/jcaf.2003.8

Morita, N., Sovari, A. A., Xie, Y., Fishbein, M. C., Mandel, W. J., Garfinkel, A., et al. (2009). Increased susceptibility of aged hearts to ventricular fibrillation during oxidative stress. *Am. J. Physiol. Heart Circ. Physiol.* 297, H1594–H1605. doi: 10.1152/ajpheart.00579.2009

Mukherjee, R., and Spinale, F. G. (1998). L-type calcium channel abundance and function with cardiac hypertrophy and failure: a review. *J. Mol. Cell. Cardiol.* 30, 1899–1916. doi: 10.1006/jmcc.1998.0755

Muralidharan, P., Szappanos, H. C., Ingley, E., and Hool, L. (2016). Evidence for redox sensing by a human cardiac calcium channel. *Sci. Rep.* 6:19067. doi: 10.1038/srep19067

Myles, R. C., Wang, L., Bers, D. M., and Ripplinger, C. M. (2015). Decreased inward rectifying K^+ current and increased ryanodine receptor sensitivity synergistically contribute to sustained focal arrhythmia in the intact rabbit heart. *J. Physiol.* 593, 1479–1493. doi: 10.1113/jphysiol.2014.279638

Nagy, N., Kormos, A., Kohajda, Z., Szebeni, Á., Szepesi, J., Pollesello, P., et al. (2014). Selective Na^+/$Ca2^+$ exchanger inhibition prevents $Ca2^+$ overload-induced triggered arrhythmias. *Br. J. Pharmacol.* 171, 5665–5681. doi: 10.1111/bph.12867

Nattel, S., Maguy, A., Le Bouter, S., and Yeh, Y.-H. (2007). Arrhythmogenic ion-channel remodeling in the heart: heart failure, myocardial infarction, and atrial fibrillation. *Physiol. Rev.* 87, 425–456. doi: 10.1152/physrev.00014.2006

Neco, P., Rose, B., Huynh, N., Zhang, R., Bridge, J. H. B., Philipson, K. D., et al. (2010). Sodium-calcium exchange is essential for effective triggering of calcium release in mouse heart. *Biophys. J.* 99, 755–764. doi: 10.1016/j.bpj.2010.04.071

Nerbonne, J. M., and Kass, R. S. (2005). Molecular physiology of cardiac repolarization. *Physiol. Rev.* 85, 1205–1253. doi: 10.1152/physrev.00002.2005

Neves, J. S., Leite-Moreira, A. M., Neiva-Sousa, M., Almeida-Coelho, J., Castro-Ferreira, R., and Leite-Moreira, A. F. (2015). Acute myocardial response to stretch: what we (don't) know. *Front. Physiol.* 6:408. doi: 10.3389/fphys.2015.00408

Nikolaev, V. O., Bünemann, M., Schmitteckert, E., Lohse, M. J., and Engelhardt, S. (2006). Cyclic AMP imaging in adult cardiac myocytes reveals far-reaching β1-adrenergic but locally confined β2-adrenergic receptor–mediated signaling. *Circ. Res.* 99, 1084–1091. doi: 10.1161/01.RES.0000250046.69918.d5

Nikolaev, V. O., Moshkov, A., Lyon, A. R., Miragoli, M., Novak, P., Paur, H., et al. (2010). Beta2-adrenergic receptor redistribution in heart failure changes cAMP compartmentation. *Science* 327, 1653–1657. doi: 10.1126/science.1185988

Oestreich, E. A., Malik, S., Goonasekera, S. A., Blaxall, B. C., Kelley, G. G., Dirksen, R. T., et al. (2009). Epac and phospholipase Cε regulate $Ca2^+$ release in the heart by activation of protein kinase Cε and calcium-calmodulin kinase II. *J. Biol. Chem.* 284, 1514–1522. doi: 10.1074/jbc.M806994200

Orini, M., Nanda, A., Yates, M., Di Salvo, C., Roberts, N., Lambiase, P. D., et al. (2017). Mechano-electrical feedback in the clinical setting: current perspectives. *Prog. Biophys. Mol. Biol.* 130, 365–375. doi: 10.1016/j.pbiomolbio.2017.06.001

Pereira, L., Bare, D. J., Galice, S., Shannon, T. R., and Bers, D. M. (2017). β-Adrenergic induced SR $Ca2^+$ leak is mediated by an Epac-NOS pathway. *J. Mol. Cell. Cardiol.* 108, 8–16. doi: 10.1016/j.yjmcc.2017.04.005

Pereira, L., Métrich, M., Fernández-Velasco, M., Lucas, A., Leroy, J., Perrier, R., et al. (2007). The cAMP binding protein Epac modulates $Ca2^+$ sparks by a $Ca2^+$/calmodulin kinase signalling pathway in rat cardiac myocytes. *J. Physiol.* 583, 685–694. doi: 10.1113/jphysiol.2007.133066

Petroff, M. G., Kim, S. H., Pepe, S., Dessy, C., Marbán, E., Balligand, J. L., et al. (2001). Endogenous nitric oxide mechanisms mediate the stretch dependence of $Ca2^+$ release in cardiomyocytes. *Nat. Cell Biol.* 3, 867–873. doi: 10.1038/ncb1001-867

Ponikowski, P., Voors, A. A., Anker, S. D., Bueno, H., Cleland, J. G., Coats, A. J., et al. (2016). 2016 ESC Guidelines for the diagnosis and treatment of acute and chronic heart failure: the Task Force for the diagnosis and treatment of acute and chronic heart failure of the European Society of Cardiology (ESC) Developed with the special contribution of the Heart Failure Association (HFA) of the ESC. *Eur. Heart J.* 37, 2129–2200. doi: 10.1093/eurheartj/ehw128

Port, J. D., and Bristow, M. R. (2001). Altered beta-adrenergic receptor gene regulation and signaling in chronic heart failure. *J. Mol. Cell. Cardiol.* 33, 887–905. doi: 10.1006/jmcc.2001.1358

Porter, B., Bishop, M. J., Claridge, S., Behar, J., Sieniewicz, B. J., Webb, J., et al. (2017). Autonomic modulation in patients with heart failure increases beat-to-beat variability of ventricular action potential duration. *Front. Physiol.* 8:328. doi: 10.3389/fphys.2017.00328

Priori, S. G., and Corr, P. B. (1990). Mechanisms underlying early and delayed afterdepolarizations induced by catecholamines. *Am. J. Physiol.* 258, H1796–H1805. doi: 10.1152/ajpheart.1990.258.6.H1796

Priori, S. G., Mantica, M., Napolitano, C., and Schwartz, P. J. (1990). Early afterdepolarizations induced in vivo by reperfusion of ischemic myocardium. A possible mechanism for reperfusion arrhythmias. *Circulation* 81, 1911–1920. doi: 10.1161/01.CIR.81.6.1911

Priori, S. G., Mantica, M., and Schwartz, P. J. (1988). Delayed afterdepolarizations elicited in vivo by left stellate ganglion stimulation. *Circulation* 78, 178–185. doi: 10.1161/01.CIR.78.1.178

Priori, S. G., Napolitano, C., Memmi, M., Colombi, B., Drago, F., Gasparini, M., et al. (2002). Clinical and molecular characterization of patients with catecholaminergic polymorphic ventricular tachycardia. *Circulation* 106, 69–74. doi: 10.1161/01.CIR.0000020013.73106.D8

Prosser, B. L., Ward, C. W., and Lederer, W. J. (2011). X-ROS signaling: rapid mechano-chemo transduction in heart. *Science* 333, 1440–1445. doi: 10.1126/science.1202768

Purohit, A., Rokita, A. G., Guan, X., Chen, B., Koval, O. M., Voigt, N., et al. (2013). Oxidized $Ca2^+$/calmodulin-dependent protein kinase II triggers atrial fibrillation. *Circulation* 128, 1748–1757. doi: 10.1161/CIRCULATIONAHA.113.003313

Rakhit, A., Maguire, C. T., Wakimoto, H., Gehrmann, J., Li, G. K., Kelly, R. A., et al. (2001). In vivo electrophysiologic studies in endothelial nitric oxide synthase (eNOS)-deficient mice. *J. Cardiovasc. Electrophysiol.* 12, 1295–1301. doi: 10.1046/j.1540-8167.2001.01295.x

Ravens, U. (2003). Mechano-electric feedback and arrhythmias. *Prog. Biophys. Mol. Biol.* 82, 255–266. doi: 10.1016/S0079-6107(03)00026-9

Sag, C. M., Santos, C. X., and Shah, A. M. (2014). Redox regulation of cardiac hypertrophy. *J. Mol. Cell. Cardiol.* 73, 103–111. doi: 10.1016/j.yjmcc.2014.02.002

Sag, C. M., Wadsack, D. P., Khabbazzadeh, S., Abesser, M., Grefe, C., Neumann, K., et al. (2009). Calcium/calmodulin-dependent protein kinase II contributes to cardiac arrhythmogenesis in heart failure. *Circ. Heart Fail.* 2, 664–675. doi: 10.1161/CIRCHEARTFAILURE.109.865279

Sag, C. M., Wagner, S., and Maier, L. S. (2013). Role of oxidants on calcium and sodium movement in healthy and diseased cardiac myocytes. *Free Radic. Biol. Med.* 63, 338–349. doi: 10.1016/j.freeradbiomed.2013.05.035

Sagawa, K., Lie, R. K., and Schaefer, J. (1990). Translation of Otto frank's paper "Die Grundform des arteriellen Pulses" zeitschrift für biologie 37: 483–526 (1899). *J. Mol. Cell. Cardiol.* 22, 253–254. doi: 10.1016/0022-2828(90)91459-K

Saini, A., Kannabhiran, M., Reddy, P., Gopinathannair, R., Olshansky, B., and Dominic, P. (2016). Cardiac resynchronization therapy may be antiarrhythmic particularly in responders: a systematic review and meta-analysis. *JACC Clin. Electrophysiol.* 2, 307–316. doi: 10.1016/j.jacep.2015.10.007

Sánchez, G., Pedrozo, Z., Domenech, R. J., Hidalgo, C., and Donoso, P. (2005). Tachycardia increases NADPH oxidase activity and RyR2 S-glutathionylation in ventricular muscle. *J. Mol. Cell. Cardiol.* 39, 982–991. doi: 10.1016/j.yjmcc.2005.08.010

Sanchez-Alonso, J. L., Bhargava, A., O'Hara, T., Glukhov, A. V., Schobesberger, S., Bhogal, N., et al. (2016). Microdomain-specific modulation of L-type calcium channels leads to triggered ventricular arrhythmia in heart failurenovelty and significance. *Circ. Res.* 119, 944–955. doi: 10.1161/CIRCRESAHA.116.308698

Santangeli, P., Rame, J. E., Birati, E. Y., and Marchlinski, F. E. (2017). Management of ventricular arrhythmias in patients with advanced heart failure. *J. Am. Coll. Cardiol.* 69, 1842–1860. doi: 10.1016/j.jacc.2017.01.047

Sato, D., Xie, L.-H., Sovari, A. A., Tran, D. X., Morita, N., Xie, F., et al. (2009). Synchronization of chaotic early afterdepolarizations in the genesis of cardiac arrhythmias. *Proc. Natl. Acad. Sci. U.S.A.* 106, 2983–2988. doi: 10.1073/pnas.0809148106

Saxon, L. A., Bristow, M. R., Boehmer, J., Krueger, S., Kass, D. A., De Marco, T., et al. (2006). Predictors of sudden cardiac death and appropriate shock in the comparison of medical therapy, pacing, and defibrillation in heart failure (COMPANION) trial. *Circulation* 114, 2766–2772. doi: 10.1161/CIRCULATIONAHA.106.642892

Schillinger, W., Fiolet, J. W., Schlotthauer, K., and Hasenfuss, G. (2003). Relevance of Na^+–$Ca2^+$ exchange in heart failure. *Cardiovasc. Res.* 57, 921–933. doi: 10.1016/S0008-6363(02)00826-X

Schobesberger, S., Wright, P., Tokar, S., Bhargava, A., Mansfield, C., Glukhov, A. V., et al. (2017). T-tubule remodelling disturbs localized β2-adrenergic signalling in rat ventricular myocytes during the progression of heart failure. *Cardiovasc. Res.* 113, 770–782. doi: 10.1093/cvr/cvx074

Schönleitner, P., Schotten, U., and Antoons, G. (2017). Mechanosensitivity of microdomain calcium signalling in the heart. *Prog. Biophys. Mol. Biol.* 130, 288–301. doi: 10.1016/j.pbiomolbio.2017.06.013

Schröder, F., Handrock, R., Beuckelmann, D. J., Hirt, S., Hullin, R., Priebe, L., et al. (1998). Increased availability and open probability of single L-type calcium channels from failing compared with nonfailing human ventricle. *Circulation* 98, 969–976. doi: 10.1161/01.CIR.98.10.969

Scriven, D. R., and Moore, E. D. (2013). $Ca2^+$ channel and Na^+/$Ca2^+$ exchange localization in cardiac myocytes. *J. Mol. Cell. Cardiol.* 58, 22–31. doi: 10.1016/j.yjmcc.2012.11.022

Seo, K., Rainer, P. P., Lee, D.-I., Hao, S., Bedja, D., Birnbaumer, L., et al. (2014). Hyperactive adverse mechanical stress responses in dystrophic heart are coupled to transient receptor potential canonical 6 and blocked by cGMP-protein kinase G modulation. *Circ. Res.* 114, 823–832. doi: 10.1161/CIRCRESAHA.114.302614

Sham, J. S. (1997). $Ca2^+$ release-induced inactivation of $Ca2^+$ current in rat ventricular myocytes: evidence for local $Ca2^+$ signalling. *J. Physiol.* 500(Pt 2), 285–295.

Sham, J. S., Cleemann, L., and Morad, M. (1995). Functional coupling of $Ca2^+$ channels and ryanodine receptors in cardiac myocytes. *Proc. Natl. Acad. Sci. U.S.A.* 92, 121–125. doi: 10.1073/pnas.92.1.121

Sharma, V. K., Ramesh, V., Franzini-Armstrong, C., and Sheu, S.-S. (2000). Transport of $Ca2^+$ from sarcoplasmic reticulum to mitochondria in rat ventricular myocytes. *J. Bioenerg. Biomembr.* 32, 97–104. doi: 10.1023/A:1005520714221

Shugg, T., Johnson, D. E., Shao, M., Lai, X., Witzmann, F., Cummins, T. R., et al. (2018). Calcium/calmodulin-dependent protein kinase II regulation of IKs during sustained β-adrenergic receptor stimulation. *Heart Rhythm* 15, 895–904. doi: 10.1016/j.hrthm.2018.01.024

Simon, J. N., Duglan, D., Casadei, B., and Carnicer, R. (2014). Nitric oxide synthase regulation of cardiac excitation-contraction coupling in health and disease. *J. Mol. Cell. Cardiol.* 73, 80–91. doi: 10.1016/j.yjmcc.2014.03.004

Sipido, K. R., Callewaert, G., and Carmeliet, E. (1995). Inhibition and rapid recovery of $Ca2^+$ current during $Ca2^+$ release from sarcoplasmic reticulum in guinea pig ventricular myocytes. *Circ. Res.* 76, 102–109. doi: 10.1161/01.RES.76.1.102

Sipido, K. R., Stankovicova, T., Vanhaecke, J., Flameng, W., and Verdonckc, F. (1998). A critical role for L-type $Ca2^+$ current in the regulation of $Ca2^+$ release from the sarcoplasmic reticulum in human ventricular myocytes from dilated cardiomyopathy. *Ann. N. Y. Acad. Sci.* 853, 353–356. doi: 10.1111/j.1749-6632.1998.tb08298.x

Sipido, K. R., Volders, P. G. A., Vos, M. A., and Verdonck, F. (2002). Altered Na/Ca exchange activity in cardiac hypertrophy and heart failure: a new target for therapy? *Cardiovasc. Res.* 53, 782–805. doi: 10.1016/S0008-6363(01)00470-9

Song, L.-S., Sobie, E. A., McCulle, S., Lederer, W. J., Balke, C. W., and Cheng, H. (2006). Orphaned ryanodine receptors in the failing heart. *Proc. Natl. Acad. Sci. U.S.A.* 103, 4305–4310. doi: 10.1073/pnas.0509324103

Song, Y., Shryock, J. C., Wagner, S., Maier, L. S., and Belardinelli, L. (2006). Blocking late sodium current reduces hydrogen peroxide-induced arrhythmogenic activity and contractile dysfunction. *J. Pharmacol. Exp. Ther.* 318, 214–222. doi: 10.1124/jpet.106.101832

Song, Y.-H., Cho, H., Ryu, S.-Y., Yoon, J.-Y., Park, S.-H., Noh, C.-I., et al. (2010). L-type $Ca2^+$ channel facilitation mediated by H_2O_2-induced activation of CaMKII in rat ventricular myocytes. *J. Mol. Cell. Cardiol.* 48, 773–780. doi: 10.1016/j.yjmcc.2009.10.020

Sossalla, S., Fluschnik, N., Schotola, H., Ort, K. R., Neef, S., Schulte, T., et al. (2010). Inhibition of elevated $Ca2^+$/calmodulin-dependent protein kinase II improves contractility in human failing myocardium. *Circ. Res.* 107, 1150–1161. doi: 10.1161/CIRCRESAHA.110.220418

Sukharev, S. I., Blount, P., Martinac, B., Blattner, F. R., and Kung, C. (1994). A large-conductance mechanosensitive channel in *E. coli* encoded by mscL alone. *Nature* 368, 265–268. doi: 10.1038/368265a0

Swaminathan, P. D., Purohit, A., Hund, T. J., and Anderson, M. E. (2012). Calmodulin-dependent protein kinase II: linking heart failure and arrhythmias. *Circ. Res.* 110, 1661–1677. doi: 10.1161/CIRCRESAHA.111.243956

Tavi, P., Laine, M., Weckström, M., and Ruskoaho, H. (2001). Cardiac mechanotransduction: from sensing to disease and treatment. *Trends Pharmacol. Sci.* 22, 254–260. doi: 10.1016/S0165-6147(00)01679-5

Terracciano, C. M., Hardy, J., Birks, E. J., Khaghani, A., Banner, N. R., and Yacoub, M. H. (2004). Clinical recovery from end-stage heart failure using left-ventricular assist device and pharmacological therapy correlates with increased sarcoplasmic reticulum calcium content but not with regression of cellular hypertrophy. *Circulation* 109, 2263–2265. doi: 10.1161/01.CIR.0000129233.51320.92

Tomaselli, G. F., and Marbán, E. (1999). Electrophysiological remodeling in hypertrophy and heart failure. *Cardiovasc. Res.* 42, 270–283. doi: 10.1016/S0008-6363(99)00017-6

Toschi-Dias, E., Rondon, M. U. P. B., Cogliati, C., Paolocci, N., Tobaldini, E., and Montano, N. (2017). Contribution of autonomic reflexes to the hyperadrenergic state in heart failure. *Front. Neurosci.* 11:162. doi: 10.3389/fnins.2017.00162

Tsuji, Y., Opthof, T., Kamiya, K., Yasui, K., Liu, W., Lu, Z., et al. (2000). Pacing-induced heart failure causes a reduction of delayed rectifier potassium currents along with decreases in calcium and transient outward currents in rabbit ventricle. *Cardiovasc. Res.* 48, 300–309. doi: 10.1016/S0008-6363(00)00180-2

Ungerer, M., Böhm, M., Elce, J. S., Erdmann, E., and Lohse, M. J. (1993). Altered expression of beta-adrenergic receptor kinase and beta 1-adrenergic receptors in the failing human heart. *Circulation* 87, 454–463. doi: 10.1161/01.CIR.87.2.454

van Oort, R. J., McCauley, M. D., Dixit, S. S., Pereira, L., Yang, Y., Respress, J. L., et al. (2010). Ryanodine receptor phosphorylation by CaMKII promotes life-threatening ventricular arrhythmias in mice with heart failure. *Circulation* 122, 2669–2679. doi: 10.1161/CIRCULATIONAHA.110.982298

Varró, A., Baláti, B., Iost, N., Takács, J., Virág, L., Lathrop, D. A., et al. (2000). The role of the delayed rectifier component IKs in dog ventricular muscle and Purkinje fibre repolarization. *J. Physiol.* 523, 67–81. doi: 10.1111/j.1469-7793.2000.00067.x

Vegh, A., Szekeres, L., and Parratt, J. (1992). Preconditioning of the ischaemic myocardium; involvement of the L-arginine nitric oxide pathway. *Br. J. Pharmacol.* 107, 648–652. doi: 10.1111/j.1476-5381.1992.tb14501.x

Veldkamp, M. W., van Ginneken, A. C., Opthof, T., and Bouman, L. N. (1995). Delayed rectifier channels in human ventricular myocytes. *Circulation* 92, 3497–3504. doi: 10.1161/01.CIR.92.12.3497

Veldkamp, M. W., Verkerk, A. O., van Ginneken, A. C. G., Baartscheer, A., Schumacher, C., de Jonge, N., et al. (2001). Norepinephrine induces action potential prolongation and early afterdepolarizations in ventricular myocytes isolated from human end-stage failing hearts. *Eur. Heart J.* 22, 955–963. doi: 10.1053/euhj.2000.2499

Venetucci, L. A., Trafford, A. W., O'Neill, S. C., and Eisner, D. A. (2008). The sarcoplasmic reticulum and arrhythmogenic calcium release. *Cardiovasc. Res.* 77, 285–292. doi: 10.1093/cvr/cvm009

Verkerk, A. O., Veldkamp, M. W., Baartscheer, A., Schumacher, C. A., Klöpping, C., van Ginneken, A. C. G., et al. (2001). Ionic mechanism of delayed afterdepolarizations in ventricular cells isolated from human end-stage failing hearts. *Circulation* 104, 2728–2733. doi: 10.1161/hc4701.099577

Vermeulen, J. T., Mcguire, M. A., Opthof, T., Coronel, R., de Bakker, J. M., Klöpping, C., et al. (1994). Triggered activity and automaticity in ventricular trabeculae of failing human and rabbit hearts. *Cardiovasc. Res.* 28, 1547–1554. doi: 10.1093/cvr/28.10.1547

Viatchenko-Karpinski, S., Kornyeyev, D., El-Bizri, N., Budas, G., Fan, P., Jiang, Z., et al. (2014). Intracellular Na^+ overload causes oxidation of CaMKII and leads to $Ca2^+$ mishandling in isolated ventricular myocytes. *J. Mol. Cell. Cardiol.* 76, 247–256. doi: 10.1016/j.yjmcc.2014.09.009

Vielma, A. Z., León, L., Fernández, I. C., González, D. R., and Boric, M. P. (2016). Nitric oxide synthase 1 modulates basal and β-adrenergic-stimulated contractility by rapid and reversible redox-dependent S-nitrosylation of the heart. *PLoS One* 11:e0160813. doi: 10.1371/journal.pone.0160813

Volders, P. G., Kulcśar, A., Vos, M. A., Sipido, K. R., Wellens, H. J., Lazzara, R., et al. (1997). Similarities between early and delayed afterdepolarizations induced by isoproterenol in canine ventricular myocytes. *Cardiovasc. Res.* 34, 348–359. doi: 10.1016/S0008-6363(96)00270-2

Volders, P. G., Stengl, M., van Opstal, J. M., Gerlach, U., Spätjens, R. L., Beekman, J. D., et al. (2003). Probing the contribution of IKs to canine ventricular repolarization: key role for beta-adrenergic receptor stimulation. *Circulation* 107, 2753–2760. doi: 10.1161/01.CIR.0000068344.54010.B3

Volders, P. G., Vos, M. A., Szabo, B., Sipido, K. R., de Groot, S. H., Gorgels, A. P., et al. (2000). Progress in the understanding of cardiac early afterdepolarizations and torsades de pointes: time to revise current concepts. *Cardiovasc. Res.* 46, 376–392. doi: 10.1016/S0008-6363(00)00022-5

von Anrep, G. (1912). On the part played by the suprarenals in the normal vascular reactions of the body. *J. Physiol.* 45, 307–317. doi: 10.1113/jphysiol.1912.sp001553

Waagstein, F., Bristow, M. R., Swedberg, K., Camerini, F., Fowler, M. B., Silver, M. A., et al. (1993). Beneficial effects of metoprolol in idiopathic dilated cardiomyopathy. Metoprolol in Dilated Cardiomyopathy (MDC) Trial Study Group. *Lancet* 342, 1441–1446. doi: 10.1016/0140-6736(93)92930-R

Wagner, S., Dybkova, N., Rasenack, E. C. L., Jacobshagen, C., Fabritz, L., Kirchhof, P., et al. (2006). $Ca2^+$/calmodulin-dependent protein kinase II regulates cardiac Na^+ channels. *J. Clin. Invest.* 116, 3127–3138. doi: 10.1172/JCI26620

Wagner, S., Rokita, A. G., Anderson, M. E., and Maier, L. S. (2013). Redox regulation of sodium and calcium handling. *Antioxid. Redox Signal.* 18, 1063–1077. doi: 10.1089/ars.2012.4818

Wagner, S., Ruff, H. M., Weber, S. L., Bellmann, S., Sowa, T., Schulte, T., et al. (2011). Reactive oxygen species-activated Ca/calmodulin kinase IIδ is required for late I(Na) augmentation leading to cellular Na and Ca overload. *Circ. Res.* 108, 555–565. doi: 10.1161/CIRCRESAHA.110.221911

Wang, H., Kohr, M. J., Wheeler, D. G., and Ziolo, M. T. (2008). Endothelial nitric oxide synthase decreases beta-adrenergic responsiveness via inhibition of the L-type $Ca2^+$ current. *Am. J. Physiol. Heart Circ. Physiol.* 294, H1473–H1480. doi: 10.1152/ajpheart.01249.2007

Wang, H., Viatchenko-Karpinski, S., Sun, J., Györke, I., Benkusky, N. A., Kohr, M. J., et al. (2010). Regulation of myocyte contraction via neuronal nitric oxide synthase: role of ryanodine receptor S-nitrosylation. *J. Physiol.* 588, 2905–2917. doi: 10.1113/jphysiol.2010.192617

Wang, J., Ma, Y., Sachs, F., Li, J., and Suchyna, T. M. (2016). GsMTx4-D is a cardioprotectant against myocardial infarction during ischemia and reperfusion. *J. Mol. Cell. Cardiol.* 98, 83–94. doi: 10.1016/j.yjmcc.2016.07.005

Wang, W., and Zucker, I. H. (1996). Cardiac sympathetic afferent reflex in dogs with congestive heart failure. *Am. J. Physiol.* 271, R751–R756. doi: 10.1152/ajpregu.1996.271.3.R751

Wehrens, X. H., Lehnart, S. E., Reiken, S. R., and Marks, A. R. (2004). $Ca2^+$/calmodulin-dependent protein kinase II phosphorylation regulates the cardiac ryanodine receptor. *Circ. Res.* 94, e61–e70. doi: 10.1161/01.RES.0000125626.33738.E2

Wei, X.-H., Yu, S.-D., Ren, L., Huang, S.-H., Yang, Q.-M., Wang, P., et al. (2017). Inhibition of late sodium current suppresses calcium-related ventricular arrhythmias by reducing the phosphorylation of CaMK-II and sodium channel expressions. *Sci. Rep.* 7:981. doi: 10.1038/s41598-017-01056-0

Westenbrink, B. D., Edwards, A. G., McCulloch, A. D., and Brown, J. H. (2013). The promise of CaMKII inhibition for heart disease: preventing heart failure and arrhythmias. *Expert Opin. Ther. Targets* 17, 889–903. doi: 10.1517/14728222.2013.809064

White, E. (2006). Mechanosensitive channels: therapeutic targets in the myocardium? *Curr. Pharm. Des.* 12, 3645–3663.

Wit, A. L., and Rosen, M. R. (1983). Pathophysiologic mechanisms of cardiac arrhythmias. *Am. Heart J.* 106, 798–811. doi: 10.1016/0002-8703(83)90003-0

Wright, P. T., Nikolaev, V. O., O'Hara, T., Diakonov, I., Bhargava, A., Tokar, S., et al. (2014). Caveolin-3 regulates compartmentation of cardiomyocyte beta2-adrenergic receptor-mediated cAMP signaling. *J. Mol. Cell. Cardiol.* 67, 38–48. doi: 10.1016/j.yjmcc.2013.12.003

Xiao, B., Sutherland, C., Walsh, M. P., and Chen, S. R. W. (2004). Protein kinase A phosphorylation at serine-2808 of the cardiac $Ca2^+$-release channel (ryanodine receptor) does not dissociate 12.6-kDa FK506-binding protein (FKBP12.6). *Circ. Res.* 94, 487–495. doi: 10.1161/01.RES.0000115945.89741.22

Xie, L.-H., Chen, F., Karagueuzian, H. S., and Weiss, J. N. (2009). Oxidative-stress-induced afterdepolarizations and calmodulin kinase II signaling. *Circ. Res.* 104, 79–86. doi: 10.1161/CIRCRESAHA.108.183475

Xie, Y., Sato, D., Garfinkel, A., Qu, Z., and Weiss, J. N. (2010). So little source, so much sink: requirements for afterdepolarizations to propagate in tissue. *Biophys. J.* 99, 1408–1415. doi: 10.1016/j.bpj.2010.06.042

Xu, K. Y., Huso, D. L., Dawson, T. M., Bredt, D. S., and Becker, L. C. (1999). Nitric oxide synthase in cardiac sarcoplasmic reticulum. *Proc. Natl. Acad. Sci. U.S.A.* 96, 657–662. doi: 10.1073/pnas.96.2.657

Xu, L., Eu, J. P., Meissner, G., and Stamler, J. S. (1998). Activation of the cardiac calcium release channel (ryanodine receptor) by poly-S-nitrosylation. *Science* 279, 234–237. doi: 10.1126/science.279.5348.234

Yamada, K. A., and Corr, P. B. (1992). Effects of β-adrenergic receptor activation on intracellular calcium and membrane potential in adult cardiac myocytes. *J. Cardiovasc. Electrophysiol.* 3, 209–224. doi: 10.1111/j.1540-8167.1992.tb00968.x

Yamaguchi, Y., Iribe, G., Nishida, M., and Naruse, K. (2017). Role of TRPC3 and TRPC6 channels in the myocardial response to stretch: linking physiology and pathophysiology. *Prog. Biophys. Mol. Biol.* 130, 264–272. doi: 10.1016/j.pbiomolbio.2017.06.010

Yan, Y., Liu, J., Wei, C., Li, K., Xie, W., Wang, Y., et al. (2008). Bidirectional regulation of $Ca2^+$ sparks by mitochondria-derived reactive oxygen species in cardiac myocytes. *Cardiovasc. Res.* 77, 432–441. doi: 10.1093/cvr/cvm047

Zahradníková, A., Minarovic, I., Venema, R. C., and Mészáros, L. G. (1997). Inactivation of the cardiac ryanodine receptor calcium release channel

by nitric oxide. *Cell Calcium* 22, 447–454. doi: 10.1016/S0143-4160(97)90072-5

Zeng, J., and Rudy, Y. (1995). Early afterdepolarizations in cardiac myocytes: mechanism and rate dependence. *Biophys. J.* 68, 949–964. doi: 10.1016/S0006-3495(95)80271-7

Zhang, H., Gomez, A. M., Wang, X., Yan, Y., Zheng, M., and Cheng, H. (2013). ROS regulation of microdomain $Ca2^{+}$ signalling at the dyads. *Cardiovasc. Res.* 98, 248–258. doi: 10.1093/cvr/cvt050

Zhang, M., Perino, A., Ghigo, A., Hirsch, E., and Shah, A. M. (2013). NADPH oxidases in heart failure: poachers or gamekeepers? *Antioxid. Redox Signal.* 18, 1024–1041. doi: 10.1089/ars.2012.4550

Zima, A. V., and Blatter, L. A. (2006). Redox regulation of cardiac calcium channels and transporters. *Cardiovasc. Res.* 71, 310–321. doi: 10.1016/j.cardiores.2006.02.019

Zygmunt, A. C., Goodrow, R. J., and Weigel, C. M. (1998). INaCa and ICl(Ca) contribute to isoproterenol-induced delayed after depolarizations in midmyocardial cells. *Am. J. Physiol.* 275, H1979–H1992.

Conflict of Interest Statement: The authors declare that the research was conducted in the absence of any commercial or financial relationships that could be construed as a potential conflict of interest.

frontiers in Physiology

HYPOTHESIS AND THEORY
published: 16 October 2018
doi: 10.3389/fphys.2018.01391

Altered Ca^{2+} and Na^{+} Homeostasis in Human Hypertrophic Cardiomyopathy: Implications for Arrhythmogenesis

Raffaele Coppini[1], Cecilia Ferrantini[2], Alessandro Mugelli[1], Corrado Poggesi[2] and Elisabetta Cerbai[1]*

[1] *Department of Neuroscience, Psychology, Drug Sciences and Child Health (NEUROFARBA), University of Florence, Florence, Italy,* [2] *Department of Experimental and Clinical Medicine, University of Florence, Florence, Italy*

Hypertrophic cardiomyopathy (HCM) is the most common mendelian heart disease, with a prevalence of 1/500. HCM is a primary cause of sudden death, due to an heightened risk of ventricular tachyarrhythmias that often occur in young asymptomatic patients. HCM can slowly progress toward heart failure, either with preserved or reduced ejection fraction, due to worsening of diastolic function. Accumulation of intra-myocardial fibrosis and replacement scars underlies heart failure progression and represents a substrate for sustained arrhythmias in end-stage patients. However, arrhythmias and mechanical abnormalities may occur in hearts with little or no fibrosis, prompting toward functional pathomechanisms. By studying viable cardiomyocytes and trabeculae isolated from inter-ventricular septum samples of non-failing HCM patients with symptomatic obstruction who underwent myectomy operations, we identified that specific abnormalities of intracellular Ca^{2+} handling are associated with increased cellular arrhytmogenesis and diastolic dysfunction. In HCM cardiomyocytes, diastolic Ca^{2+} concentration is increased both in the cytosol and in the sarcoplasmic reticulum and the rate of Ca^{2+} transient decay is slower, while the amplitude of Ca^{2+}-release is preserved. Ca^{2+} overload is the consequence of an increased Ca^{2+} entry via L-type Ca^{2+}-current [due to prolongation the action potential (AP) plateau], combined with a reduced rate of Ca^{2+}-extrusion through the Na^{+}/Ca^{2+} exchanger [due to increased cytosolic (Na^{+})] and a lower expression of SERCA. Increased late Na^{+} current (I_{NaL}) plays a major role, as it causes both AP prolongation and Na^{+} overload. Intracellular Ca^{2+} overload determines an higher frequency of Ca^{2+} waves leading to delayed-afterdepolarizations (DADs) and premature contractions, but is also linked with the increased diastolic tension and slower relaxation of HCM myocardium. Sustained increase of intracellular [Ca^{2+}] goes hand-in-hand with the increased activation of Ca^{2+}/calmodulin-dependent protein-kinase-II (CaMKII) and augmented phosphorylation of its targets, including Ca^{2+} handling proteins. In transgenic HCM mouse models, we found that Ca^{2+} overload, CaMKII and increased I_{NaL} drive myocardial remodeling since

OPEN ACCESS

Edited by:
Gaetano Santulli,
Columbia University, United States

Reviewed by:
Dmitry Terentyev,
Brown University, United States
Jordi Heijman,
Maastricht University, Netherlands

****Correspondence:***
Raffaele Coppini
raffaele.coppini@unifi.it

Specialty section:
This article was submitted to Cardiac Electrophysiology, a section of the journal Frontiers in Physiology

Received: *29 June 2018*
Accepted: *13 September 2018*
Published: *16 October 2018*

Citation:
Coppini R, Ferrantini C, Mugelli A, Poggesi C and Cerbai E (2018) Altered Ca^{2+} and Na^{+} Homeostasis in Human Hypertrophic Cardiomyopathy: Implications for Arrhythmogenesis. Front. Physiol. 9:1391. doi: 10.3389/fphys.2018.01391

the earliest stages of disease and underlie the development of hypertrophy, diastolic dysfunction and the arrhythmogenic substrate. In conclusion, diastolic dysfunction and arrhythmogenesis in human HCM myocardium are driven by functional alterations at cellular and molecular level that may be targets of innovative therapies.

Keywords: cardiac hypertrophy, ion channels, ranolazine, arrhythmias, afterdepolarization, calmodulin kinase (CaMKII), T-tubules, beta adrenergic

INTRODUCTION: ARRHYTHMIC SUBSTRATE IN HCM, FROM TISSUE TO THE SINGLE MYOCYTE

Hypertrophic cardiomyopathy (HCM) is the most common monogenic inheritable heart disease (Maron et al., 2000; Gersh et al., 2011; Authors/Task Force Members et al., 2014), with a prevalence of 1:500. HCM is a leading cause of sudden cardiac death in the young (Maron et al., 2000) and a prevalent cause of heart failure and stroke in all age groups (Maron et al., 2003). Mutations in genes coding for sarcomeric proteins are found in over 60% of patients with HCM, the most commonly involved genes being *MYH7* (β-myosin heavy-chain) and *MYBPC3* (cardiac myosin-binding protein-C). Increased ventricular arrhythmogenesis is one of the main pathophysiological features of this disease (Olivotto et al., 2009) and is responsible for the heightened risk of lethal arrhythmias in HCM patients. Despite being only mildly symptomatic in about 2/3 of patients (Maron et al., 2016), HCM can slowly progress toward heart failure, either with preserved or reduced ejection fraction, due to worsening of diastolic and/or systolic function (Olivotto et al., 2012). Accumulation of intra-myocardial fibrosis and replacement scars underlies heart failure progression and represents a substrate for sustained arrhythmias (Galati et al., 2016). Late gadolinium enhancement (LGE) at cardiac magnetic resonance, an index of cardiac fibrosis, is widely used to stratify the severity of disease progression (Authors/Task Force Members et al., 2014) and to help defining the risk of lethal arrhythmias and terminal heart failure (Chan et al., 2014). However, LGE only identifies extensive replacement scars and well predicts the risk of arrhythmias only at the advanced stages of the disease (Chan et al., 2014). Replacement fibrosis in HCM appears to be related with local myocardial ischemia, caused by microvascular dysfunction (Sotgia et al., 2008), as myocardial tissue in regions with severe microvascular ischemia is slowly replaced by collagen. The degree of microvascular dysfunction, as assessed by positron emission tomography with labeled ammonia measuring the reduction of local myocardial blood flow, is related with patient outcome, including the risk of arrhythmias at advanced disease stages (Cecchi et al., 2003). Replacement fibrosis and microvascular ischemia are strongly related with the risk of ventricular arrhythmias because they create a stable substrate for reentry circuits, the main drivers of sustained ventricular arrhythmias (Pogwizd and Corr, 1987). In order for a reentry circuit to be established, an area of conduction block adjacent to a region of slower, unidirectional conduction is needed: indeed, in HCM myocardium, patchy replacement fibrosis generates areas of no-conduction, while the surrounding ischemic regions (due to microvascular dysfunction) cause slower, altered conduction, and transient local alterations of repolarization (Hurtado-de-Mendoza et al., 2017). Following these observation, the simplest conclusion would be that structural left ventricular remodeling at macroscopic myocardial level, featuring replacement fibrosis and microvascular dysfunction, is the main determinant of arrhythmias in HCM. However, a clear relationship between fibrosis (measured with LGE), microvascular dysfunction (measured by PET) and arrhythmic risk is observed only in the minority of patients (10–15%) that experience a slow progression toward end-stage HCM, an highly arrhythmogenic condition not unlike terminal ischemic heart failure, thus requiring aggressive preventive strategies (Priori et al., 2015). On the contrary, the majority of sudden cardiac death events due to lethal ventricular arrhythmias occur in patients at earlier stages of disease progression, often in the absence of marked structural abnormalities besides left-ventricular (LV) hypertrophy, also in very young patients (Maurizi et al., 2018). In early stages of hypertrophic cardiomyopathies, replacement scars are absent and only microscopic intramyocardial fibrosis is present, and its extent can be assessed by CMR using T1-mapping (Dass et al., 2012) or extracellular volume (ECV) measurements with gadolinium contrast, both altered even before the onset of hypertrophy in HCM-mutation carriers (Ho et al., 2013). However, the link between the degree of ECV expansion and the risk of arrhythmias in early stage HCM is still uncertain (Avanesov et al., 2017). Therefore, arrhythmias in HCM cannot be the sole consequence of the substrate for re-entry circuits at tissue level. On the contrary, the main determinants of arrhythmogenesis in HCM are to be found within the affected cardiomyocytes, a consequence of the alterations of ion currents and intracellular Ca^{2+} handling that occur as a part of HCM-related ventricular cardiomyocyte remodeling (Coppini et al., 2013; Coppini et al., 2017; Ferrantini et al., 2017; Ferrantini et al., 2018). Indeed, from a pathophysiological standpoint, the vast majority of ventricular tachycardia episodes begin with one or more premature ectopic ventricular beats (Ulus et al., 2013). Premature ventricular activations are essential to initiate the abnormal rotating conduction of the re-entry circuits in the presence of an appropriate substrate. Even in the presence of extended structural alterations, such as large scars and diffuse interstitial fibrosis, ectopic premature activations initiating in abnormal cardiomyocytes could be essential triggers to initiate the re-entry that is then maintained by the structural substrate. Interestingly, ectopic activity is the primary event producing local unidirectional block, which is an essential prerequisite for the establishment of a re-entry

circuit. Ectopic ventricular beats are very common in HCM patients (Adabag et al., 2005) and originate from the premature spontaneous premature activation of a group of adjacent synchronized ventricular cardiomyocytes within the ventricular mass, which is then propagated to the whole surrounding ventricular mass, often in a chaotic and unpredictable manner (Sato et al., 2009). Early- and delayed- afterdepolarizations are the cellular arrhythmic events that may result into the spontaneous generation of premature action potentials in the affected cardiomyocytes. The following part of this review will illustrate how an increased likelihood of early and delayed after-depolarizations in HCM cardiomyocytes is a consequence of specific alterations of ion currents and intracellular Ca^{2+}-handling.

MATERIALS AND METHODS

Most of the results presented in the figures were previously published in Coppini et al. (2013) and in Ferrantini et al. (2018). Previously unpublished results are presented in **Figures 3**, **4**. Cardiomyocytes and intact trabeculae were freshly isolated as previously described (Coppini et al., 2013; Ferrantini et al., 2018), using surgical upper inter-ventricular septum samples excised from HCM patients who underwent myectomy operation for the relief of severe symptoms due to obstruction of the LV outflow tract. Notably, all recruited patients had preserved systolic function but impaired diastole and most of them have a history of documented non-sustained ventricular tachycardia at Holter monitoring. The experimental protocols were approved by the ethical committee of Careggi University-Hospital of Florence (2006/0024713, renewed May 2009; 2013/0035305). In single cardiomyocytes, APs and Ca^{2+} transients were simultaneously measured using combined patch-clamp and Ca^{2+}-fluorescence measurements, during stimulation at different frequencies. Cell capacitance was measured in voltage-clamp mode. Isometric force was measured from intact trabeculae during electrical field stimulation. Cells/trabeculae were exposed to test drugs for at least 5 min prior to recordings. Number of cells/trabeculae for each comparison, as well as the statistical tests used, are indicated in the respective figure legends.

REMODELING OF ION CURRENTS IN HCM CARDIOMYOCYTES

Hypertrophic cardiomyopathy (HCM) cellular pathophysiology is characterized by the interplay between primary alterations (direct consequences of causal sarcomeric mutations altering myofilament function) and a large number of secondary myocardial modifications, comprising cellular electrophysiological remodeling (changes in transmembrane currents) and alterations of intracellular Ca^{2+} handling [Ca^{2+} transients and diastolic (Ca^{2+})] (Coppini et al., 2013; Coppini et al., 2017; Ferrantini et al., 2017; Ferrantini et al., 2018). Due to the profound electrophysiological differences between mouse and human cardiomyocytes, studies conducted on transgenic rodent models did not help to identify the features if ion-current remodeling occurring in HCM myocardium (van der Velden et al., 2015). To overcome this limitation, we investigated the abnormalities of electrical function, Ca^{2+} handling and contraction of human HCM myocardium as coexisting contributing factors for contractile dysfunction and arrhythmias in this disease (Coppini et al., 2013). We used isolated myocytes and intact trabeculae from fresh myocardial samples from the interventricular septum of HCM patients undergoing surgical myectomy operation for refractory symptoms related to severe obstruction of the left ventricular outflow tract, compared with septal samples from non-hypertrophic surgical patients (Coppini et al., 2013; Ferrantini et al., 2018). Overall, we performed patch-clamp and ion-fluorescence studies in over 200 cardiomyocytes from 43 HCM patients (Coppini et al., 2013; Ferrantini et al., 2018). Results of patch clamp studies in isolated ventricular cardiomyocytes showed that the duration of action potentials (APD), recorded at various pacing rates, was significantly prolonged in cardiomyocytes from HCM cardiomyocytes, with regards to controls (**Figure 1A**). As expected, prolongation of APD was associated with prolonged QTc in patients from the HCM cohort (average QTc = 470 ms). Of note, a recent large multi-center observational study on HCM patients suggested that mild QT prolongation is a common observation in those patients (Johnson et al., 2011). Prolonged APD was the main determinant of the increased risk of early afterdepolarisations (EADs) (Antzelevitch and Belardinelli, 2006), that is, spontaneous depolarisations occurring before the end of the repolarization phase: the occurrence of this type of cellular arrhythmias was 6-fold more frequent in HCM vs. control cardiomyocytes (**Figure 1B**). Interestingly, the frequency of EADs and the degree of APD prolongation went hand in hand with the incidence of ventricular arrhythmias in patients: patients whose cells show markedly prolonged APDs had a higher rate of documented non-sustained ventricular tachycardia at 24 h ECG (Coppini et al., 2013; **Figure 1C**). APD prolongation in HCM cardiomyocytes is caused by a combination of decreased repolarizing potassium currents and increased depolarizing (Ca^{2+} and Na^{+}) currents: transient outward K^{+} current (I_{to}), inward-rectifier current (I_{K1}), as well as delayed rectifier K^{+} currents were significantly reduced, while both L-Type Ca^{2+} current (I_{CaL}) and late Na^{+} current (I_{NaL}) were increased in HCM cells, as compared to control cardiomyocytes (Coppini et al., 2013; **Figures 1D–H**). Pathological changes of the density of ion currents in HCM cardiomyocytes were caused by different mechanisms. The reduced density of potassium currents in HCM cardiomyocytes was the consequence of the lower levels of expression of K^{+} channel genes (**Figures 1D,E**), as observed in several human and animal models of cardiac hypertrophy and heart failure (Ravens and Cerbai, 2008), including heart failure with preserved ejection fraction (HFpEF) (Cho et al., 2017). In line with other models of LV hypertrophy and diastolic dysfunction (Cho et al., 2017), in human HCM myocardium the ion-channel genes with the most severely depressed expression were I_{to}

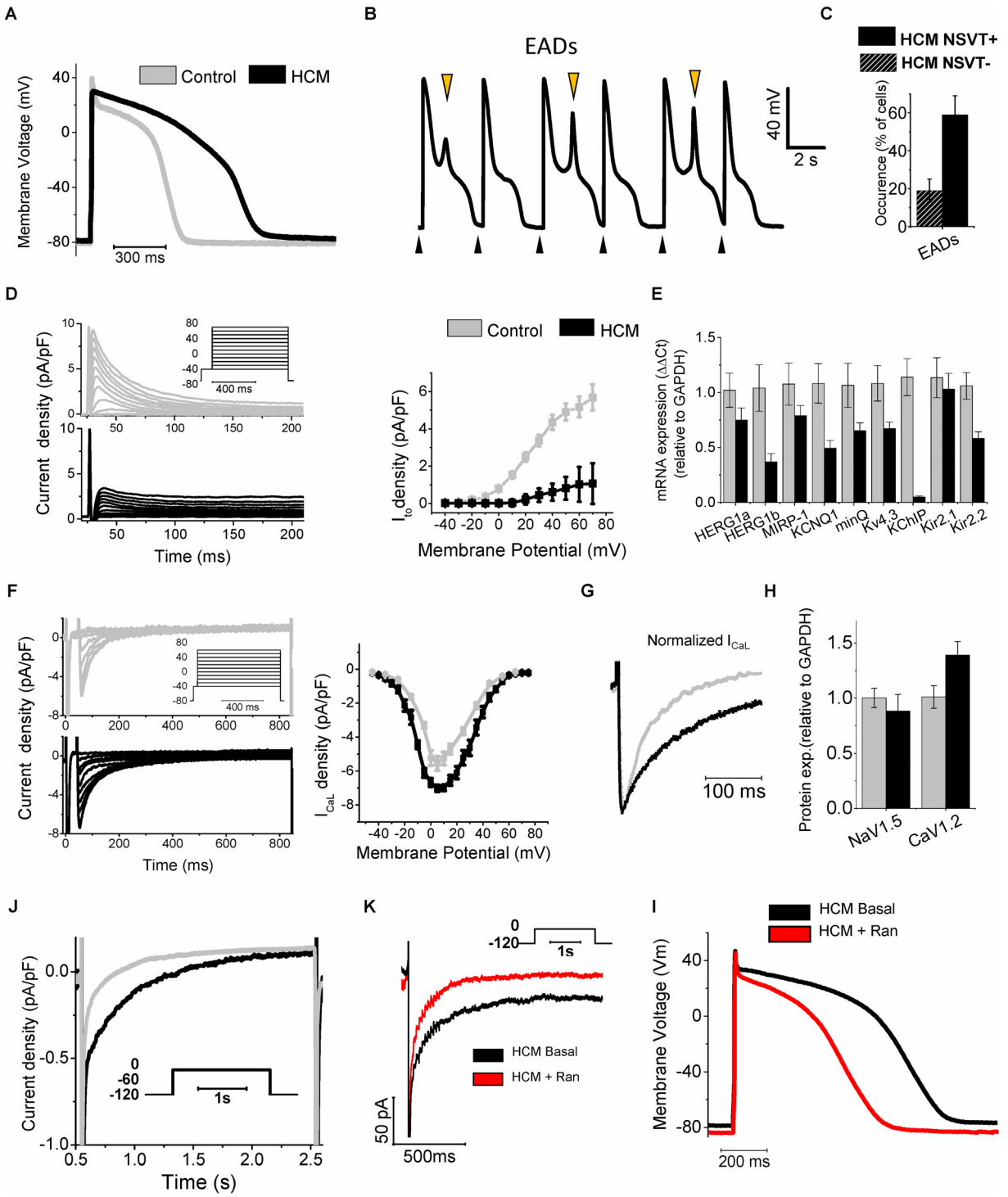

FIGURE 1 | Remodeling of ion currents in HCM cardiomyocytes **(A)** Superimposed representative action potentials recorded during stimulation at 0.2 Hz from HCM and control cardiomyocytes. **(B)** Representative recording from an HCM cardiomyocyte paced at 0.2 Hz, showing EADs. Black arrows mark stimuli. Orange arrows mark EADs. **(C)** Occurrence of EADs in 23 cells from patients without NSVT (NSVT−) and 29 from patients with NSVT (NSVT+). **(D)** Representative traces (left, top panel control, bottom panel HCM) and average I_{to} activation curves from control and HCM cardiomyocytes (right panel). **(E)** RNA expression of potassium current genes, relative to GAPDH in control (N = 11, gray) and HCM (N = 15, black) samples. **(F)** Left: representative I_{CaL} traces at different voltages. Right: I_{CaL} activation curves. **(G)** Superimposed normalized I_{CaL} recordings at 0 mV. **(H)** Protein expression of I_{CaL} and I_{Na} main channel subunits (Cav1.2 and Nav1.5). **(J)** Representative I_{NaL} traces from control and HCM cardiomyocytes. **(K)** Ranolazine inhibits I_{NaL} in HCM cardiomyocytes: representative I_{NaL} traces from an HCM cardiomyocyte during depolarization to −20 mV in the absence (Basal) or presence of Ran. **(I)** Action potentials at 0.2 Hz from an HCM cardiomyocyte before (Basal) and after exposure to 10 μmol/L ranolazine (Ran). Modified from Coppini et al., 2013 (ref. 19).

and I_{K1} (Coppini et al., 2013): this might be a consequence of the increased activity of Ca^{2+}/calmodulin-dependent protein-kinase II (CaMKII) in HCM cardiomyocytes (Coppini et al., 2013), which is able to down-regulate I_{to} and I_{K1} currents by reducing the expression of functional channels (Wagner et al., 2009). Moreover, the down-regulation of I_{K1} (Kir2.1) may also be related with the increased expression of micro-RNA miR-1 (Yang et al., 2007) observed in HCM specimens (Coppini et al., 2013). The small increase of I_{CaL} density in HCM cardiomyocytes is likely determined by the slightly higher expression of CACNA1.2 gene and CaV1.2 protein (**Figures 1F–H**). In addition, the inactivation kinetics of I_{CaL} is markedly slower in HCM vs. control cardiomyocytes (Coppini et al., 2013; Ferrantini et al., 2018; **Figure 1G**), contributing to prolong I_{CaL} activation during the AP plateau, thus delaying repolarization. Interestingly, we found that the slower inactivation of I_{CaL} observed in HCM cardiomyocytes may be related with the increased phosphorylation of L-type Ca^{2+} channel β-subunit by CaMKII (Hudmon et al., 2005), observed in HCM myocardium (**Figure 3**). Finally, I_{NaL} was consistently increased in all studied HCM myocytes: I_{NaL} integral (estimating the total Na^+ flow upon a single current activation) was 2–3 times larger in HCM as compared with control cells (**Figure 1J**). As I_{NaL} is the slowly inactivating or non-inactivating component of Na^+ current that remains active as a depolarizing current during the AP plateau, it directly contributes to prolong APD in HCM cardiomyocytes, as previously shown in human and animal models of cardiac hypertrophy and heart failure (Maltsev et al., 1998; Pieske and Houser, 2003; Pogwizd et al., 2003). The aforementioned changes in Ca^{2+}, late Na^+ and K^+ current densities were quantitatively introduced into validated mathematical models of human ventricular myocyte (Grandi et al., 2010; Coppini et al., 2013; Passini et al., 2016): these studies confirmed that the observed ion current changes are sufficient to explain the prolongation of APD in human HCM cardiomyocytes. Also, modeling studies suggested that increased I_{NaL} plays a pivotal role as determinant of APD prolongation and EADs in HCM (Passini et al., 2016), as repolarization reserve is extremely reduced by the down-regulation of K^+ currents. In support of this hypothesis, we studied the effects of I_{NaL} inhibition by ranolazine (Antzelevitch et al., 2004) or GS-967 (Sicouri et al., 2013) (a potent and selective I_{NaL} blocker) in HCM cardiomyocytes (Coppini et al., 2013; Ferrantini et al., 2018): I_{NaL} inhibition significantly reduced APD by approximately 30% in all HCM cardiomyocytes (**Figure 1**). Of note, ranolazine (at the clinically relevant concentration of 10 μM) and GS-967 (at 0.5 μM) reduced I_{NaL} by 70% in HCM cardiomyocytes. Consistently, the likelyhood of EADs in HCM cardiomyocytes was nearly halved by ranolazine or GS-967. In agreement with the increased role of I_{NaL} as a determinant of APD in the presence of an impaired repolarization reserve, the efficacy of ranolazine in shortening APD was more pronounced at low pacing frequencies and in cells with a longer APD at baseline. Studies in a mathematical cardiomyocyte model (Passini et al., 2016) confirmed that inhibition of 70% of I_{NaL} in HCM myocytes is sufficient to reduce APD, abolish EADs and reduce APD dispersion, as experimentally observed with pharmacological blockers.

REMODELING OF Ca^{2+} HANDLING IN HCM CARDIOMYOCYTES

Notwithstanding the large variabilities observed among different disease models, the common feature that is described in all transgenic animal models, human samples and cellular models of HCM is the sustained increase of diastolic intracellular calcium concentration $[(Ca^{2+})]_i$ within ventricular cardiomyocytes (Knollmann et al., 2003; Haim et al., 2007; Ashrafian et al., 2011; Fraysse et al., 2012; Lan et al., 2013). The increase of $[Ca^{2+}]_i$ is likely to be a direct consequence of some of the sarcomere mutations that cause the disease and thus it may among the first pathological changes in the hearts of HCM-mutation carriers. Indeed, the majority of HCM-related mutations cause an increase of the Ca^{2+}-sensitivity of the myofilaments and determine an increased ATP-consumption by the cardiac sarcomeres (Ashrafian et al., 2011), thus reducing the energetic efficiency of force production by the myocardium. Both these primary sarcomeric changes are associated with an increase of $[Ca^{2+}]_i$: the increased myofilament Ca^{2+}- sensitivity determines a slower release of Ca^{2+} from Troponin-C that in turn prolongs the decay of Ca^{2+}-transients and leads to elevated diastolic $[Ca^{2+}]_i$ (Baudenbacher et al., 2008). ATP depletion caused by the reduced efficiency of mutated myofilaments can reduce the function of the sarcoplasmic reticulum Ca^{2+}-ATPase (SERCA), thus reducing the rate of Ca^{2+} reuptake from the cytosol during relaxation (Ashrafian et al., 2003). Regardless of the cause that primarily increases $[Ca^{2+}]_i$, the complex remodeling of the Ca^{2+}-handling apparatus in the cardiomyocytes of HCM hearts determines a global alteration of intracellular Ca^{2+} fluxes, ultimately contributing to aggravate Ca^{2+} overload in the cytosol and in the sarcoplasmic reticulum (SR) (**Figure 2**).

In human HCM cardiomyocytes, abnormalities of APD and ion current were paralleled by marked alterations of intracellular Ca^{2+} handling (Coppini et al., 2013; Ferrantini et al., 2018), as studied by virtue of fluorescence measurements using Ca^{2+}-sensitive dyes. Ca^{2+} transient amplitude was similar in HCM and control myocytes. Conversely, Ca^{2+} transient kinetics was significantly slower and intracellular diastolic Ca^{2+} concentration ($[Ca^{2+}]_i$) was higher in HCM cells as compared to control cardiomyocytes, especially at higher rates of stimulation (**Figures 2A–C**). The elevated $[Ca^{2+}]_i$ contributed to the abnormally high rate of spontaneous Ca^{2+} releases from the SR observed in HCM myocytes, resulting in diastolic Ca^{2+}-waves and delayed after-depolarizations (DADs), thus contributing to cellular arrhythmogenesis (**Figure 2D**). Additionally, SR Ca^{2+} content was slightly increased in HCM cardiomyocytes (**Figure 2F**), at variance with human and animal models of heart failure with reduced systolic function, where decreased SR Ca^{2+} content and Ca^{2+} transients amplitude are common observations (Beuckelmann et al., 1992; Shan et al., 2010). The altered Ca^{2+} fluxes in HCM myocytes

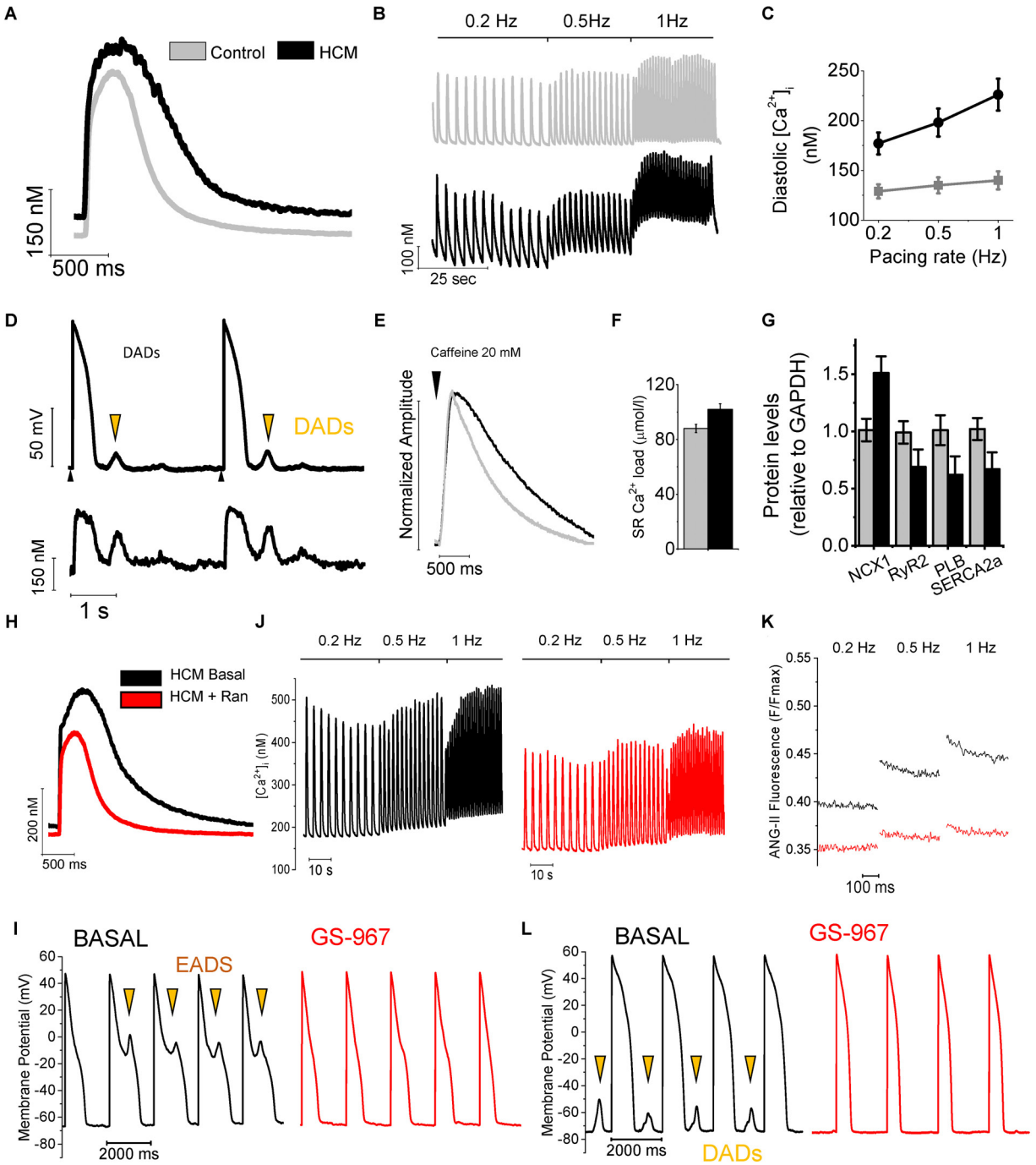

FIGURE 2 | Remodeling of Ca^{2+} handling in HCM cardiomyocytes. **(A)** Superimposed representative $Ca^{2+}{}_i$ transients recorded during stimulation at 0.2 Hz. from control and HCM cardiomyocytes. **(B)** Continuous recordings of $Ca^{2+}{}_i$ transients elicited at 0.2, 0.5, and 1 Hz frequency of stimulation, from a control (above) and an HCM (below) cardiomyocyte. **(C)** Average diastolic $Ca^{2+}{}_i$ fluorescence levels at increasing pacing frequencies. **(D)** Representative recording from an HCM cardiomyocyte, showing DADs, occurring in response to spontaneous Ca^{2+} release (calcium waves). Black arrows mark stimuli. Orange arrows mark DADs. **(E)** Ca^{2+} fluorescence traces during the protocol to measure SR Ca^{2+} content with caffeine: superimposed normalized caffeine-induced calcium transients from HCM and control cardiomyocytes. **(F)** SR Ca^{2+} content (left) in control and HCM cardiomyocytes. **(G)** Protein expression of NCX1, SERCA2a, RYR2 and PLB in HCM (N = 10) and control (N = 10) specimens. **(H)** Superimposed representative $Ca^{2+}{}_i$ transients at 0.2 Hz from an HCM cardiomyocyte at baseline and with ranolazine. **(J)** Trains of $Ca^{2+}{}_i$ transients elicited at 0.2, 0.5, and 1 Hz in an HCM myocyte before (left) and following (right) exposure to Ran. **(K)** Representative traces of ANG-II florescence (intracellular sodium) during diastole, recorded at steady state stimulation of 0.2, 0.5, and 1 Hz in the absence (black) and presence (red) of 10 µM Ran. **(I)** Representative trains of action potentials elicited at 0.5 Hz at baseline (black traces) and in the presence of GS-967 0.5 µM (red traces). Early after-depolarizations (EADs) are marked by arrows. **(L)** Representative trains of action potentials elicited at 0.5 Hz. Delayed after-depolarizations (DADs) are marked by arrows. Modified from Coppini et al. (2013) and from Ferrantini et al. (2018).

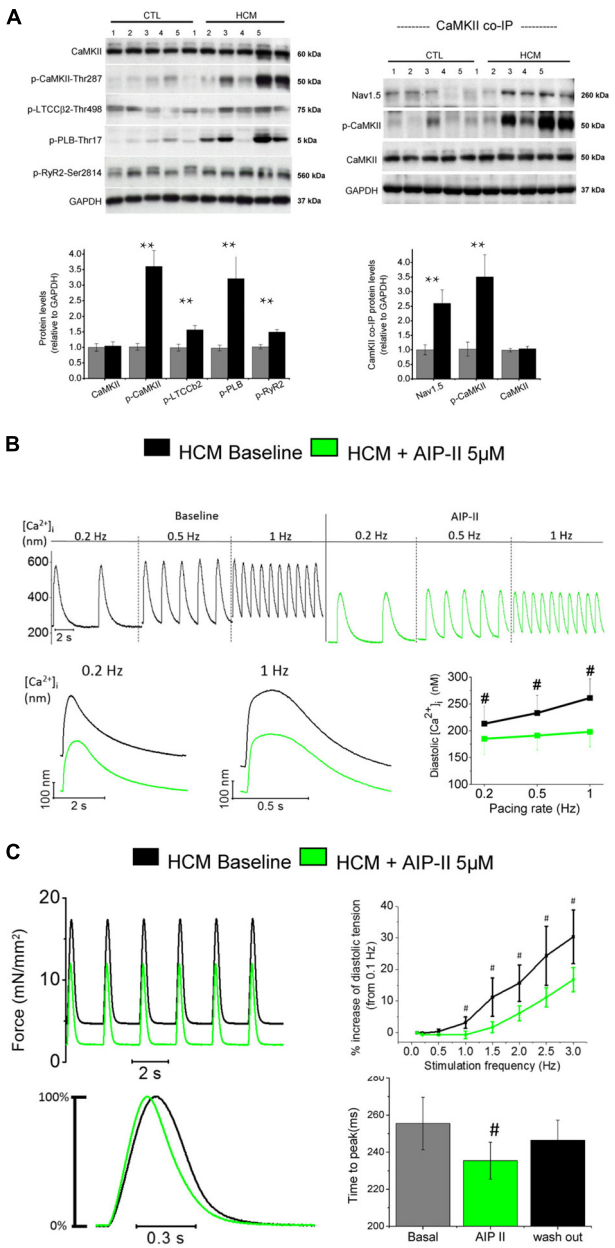

FIGURE 3 | Increased CaMKII activity underlies electro-mechanical remodeling in HCM cardiomyocytes: acute effects of CaMKII block with Autocamtide 2-related inhibitory peptide II (AIP II) on Ca^{2+} transients and twitch force. **(A)** Right: Representative Western blots (above) for total CaMKII, *(Continued)*

FIGURE 3 | Continued
phosphorylated CaMKII at threonine 287 (p-CaMKII), phosphorylated L-type $Ca2^{+}$ channel β2 subunit at threonine 498 (p-LTCCb2), phosphorylated phospholamban at threonine 17 (p-PLB) and phosphorylated ryanodine receptor 2 at serine 2814 (p-RyR2). Average values from septum of control (n = 10) and HCM patients (n = 10) are reported below. Left: Representative Western blots (above) and mean values (below) for Co-IP of Nav1.5 with CaMKII from control (n = 10) and HCM patients (n = 10), probed with antibodies for Nav1.5, p-CaMKII and total CaMKII. **(A,B)** For each protein, 5 blots representative of the 10 are shown. Relative intensity of individual bands was quantitated and normalized to GAPDH. The ratio for control was assigned a value of 1. $^{**}P < 0.01$, t-test. Modified from Coppini et al., 2013. **(B)** Representative Ca^{2+} transients recorded from an HCM cardiomyocytes in the absence and in the presence of AIP II, showing a reduction of diastolic $[Ca^{2+}]_i$ levels upon administration of AIP II. Data from 19 cells from 4 patients **(C)** Top: Representative force traces from an HCM trabecula in the absence and in the presence of AIPII, showing a reduction of diastolic tension after AIPII and mean diastolic tension at various frequency from 6 HCM trabeculae (5 patients), in the absence and in the presence of AIP II. Bottom: Normalized representative force traces highlighting the effects of AIPII on twitch kinetics and mean data for contraction peak time, at baseline, under AIP II and after washout of the drug **(B,C)**. $^{\#}P < 0.05$ in paired t-test. Previously unpublished data.

are the result of several concurrent alterations: (i)increased amplitude and slower inactivation kinetics of L-Type Ca^{2+}-current (see above), (ii)reduced expression of SERCA and reduced SERCA/phospholamban ratio (**Figure 2G**), (iii)loss or disorganization of t-tubules (see below), (iv) increase leakage of Ca^{2+} from the SR, and (v)abnormal function of the Na^{+}/Ca^{2+} exchanger (NCX). The latter is the consequence of the increased intracellular concentration of Na^{+} ($[Na^{+}]_i$). In agreement with these results, we calculated a negative shift of the NCX reversal potential (E_{NCX}), suggesting increased $[Na^{+}]_i$. Indeed, we directly observed an increase of $[Na^{+}]_i$ in HCM myocytes, as measured in human HCM myocytes using the Na^{+}-selective fluorescent dye Asante Natrium Green II (**Figure 2K**). Based on this observation, we proposed that enhanced Na^{+} influx mediated by the larger I_{NaL} leads to a sustained increase in cytosolic $[Na^{+}]_i$, providing the driving force for an increased rate of Ca^{2+} entry trough NCX, as previously observed in secondary LV hypertrophy (Terracciano et al., 2001), albeitnot in heart failure. Combined with the increased expression of NCX and the prolongation of APs, this mechanism leads to an increased total Ca^{2+} entry during the plateau of the AP, thus helping HCM cardiomyocytes to maintain normal SR Ca^{2+} load, Ca^{2+} transients amplitude and contractility (Weisser-Thomas et al., 2003) despite SERCA down-regulation. This is at variance with reports on human failing cardiomyocytes (Beuckelmann et al., 1992), where SERCA down-regulation reduces SR Ca^{2+} load and Ca^{2+} release. However, the increased cytosolic $[Na^{+}]_i$ in HCM myocytes also reduces forward-mode NCX activity, thus determining the observed decrease of Ca^{2+} extrusion rate during exposure to caffeine (**Figure 2E**) and likely contributing to prolong Ca^{2+} transient decay and increase diastolic $[Ca^{2+}]_i$, in combination with the reduced activity of SERCA. Notably, prolongation of APs likely contributes to reduce Ca^{2+} extrusion through the NCX, as the exchanger can effectively work in forward mode only at diastolic potentials. The central role of the increased I_{NaL} in determining Na^{+} and Ca^{2+} overload in HCM cardiomyocytes is highlighted by the effects of I_{NaL} inhibition by ranolazine or GS-967 (Coppini et al., 2013; Ferrantini et al., 2018). In human HCM cardiomyocytes, besides shortening APD, I_{NaL} inhibition reduced intracellular $[Na^{+}]$ (**Figure 2K**), as directly assessed using fluorescence measurements. The reduction of $[Na^{+}]_i$ shifted E_{NCX} back to positive levels; this in turn led to a potentiation of the forward-mode activity of the NCX

(Ca^{2+} extrusion/Na^{+} entry), while it decreased the reverse-mode function (Ca^{2+} entry/Na^{+} extrusion). The enhanced Ca^{2+} extrusion via the NCX resulted in an acceleration of Ca^{2+}-transient decay, determined a reduction of diastolic $[Ca^{2+}]_i$, and lessened diastolic $[Ca^{2+}]_i$ rise in response to increases of pacing frequency (**Figures 2H–J**). In keeping with these observations, we observed that ranolazine hastened the decay of caffeine-induced Ca^{2+} transients and slightly reduced SR Ca^{2+}-content in HCM cardiomyocytes (Coppini et al., 2013). Interestingly, the reduction of diastolic $[Ca^{2+}]_i$ by ranolazine or GS-967 reduced the occurrence of spontaneous diastolic Ca^{2+} waves, DADs and triggered activity (**Figures 2I–L**).

Intracellular Ca^{2+} overload negatively affected diastolic function in HCM myocardium: kinetics of relaxation was slower in HCM vs. control trabeculae and diastolic tension was higher, especially at high stimulation frequencies. Ranolazine and GS-967, by lowering diastolic $[Ca^{2+}]_i$, accelerated relaxation of HCM myocardium (Coppini et al., 2013; Ferrantini et al., 2018). Of note, when used in control myocytes and trabeculae, we observed none of the effects shown by ranolazine and GS-967 on action potentials, Ca^{2+}-handling and contraction in HCM myocardium (Coppini et al., 2013; Ferrantini et al., 2018); these results highlight the selectivity of these compounds for I_{NaL} over peak I_{Na} and support the idea that I_{NaL} augmentation plays a leading role in the remodeling of cardiac electro-mechanical function in HCM.

Most of the abnormalities of Ca^{2+} handling and contraction we observed in human cardiomyocytes and trabeculae were present also in cardiomyocytes isolated from the hearts of transgenic mice carrying the clinically relevant R92Q mutation of the Troponin T gene (Coppini et al., 2017; Ferrantini et al., 2017): these include slower Ca^{2+}-transients, elevated $[Ca^{2+}]_i$, increased I_{NaL} and $[Na^{+}]_i$, as well as impaired relaxation and elevated diastolic tension. Interestingly, in cardiomyocytes from the R92Q mouse, ranolazine hastened Ca^{2+} transients, normalized $[Ca^{2+}]_i$ and $[Na^{+}]_i$ and reduced Ca^{2+}-dependent arrhythmias. The observed antiarrhythmic effect of ranolazine may, at least in part, depend on the direct stabilization of ryanodine receptors by the drug (Parikh et al., 2012), which may have contributed to reduce spontaneous diastolic Ca^{2+} release and arrhythmogenic Ca^{2+} waves in human and mouse HCM cardiomyocytes.

ROLE OF CAMKII IN HCM PATHOPHYSIOLOGY

Sustained activation of the signaling pathways driven by calcium-calmodulin dependent protein kinase II (CaMKII) appear to play a central role as a determinant of cardiomyocyte remodeling and dysfunction in HCM myocardium (**Figure 3**), as observed in several human and animal models of cardiac hypertrophy and heart failure (Ling et al., 2009; Toischer et al., 2010; Fischer et al., 2013). Sustained activation of CaMKII in disease conditions is driven by the increase of cytosolic $[Ca^{2+}]_I$ within the cardiomyocyte, as Ca^{2+}-bound calmodulin is the most important activator of this kinase (Hudmon and Schulman, 2002). Additionally, enhanced generation of reactive oxygen species in diseased myocytes, a likely consequence of myocardial energetic derangement, can be a strong contributor to CaMKII over-activation in HCM cardiac muscle (Erickson et al., 2011). Once activated, CaMKII then phosphorylates itself (at threonine 286 site), thereby prolonging and potentiating its activated state. In HCM vs. control specimens (Coppini et al., 2013), CaMKII auto-phosphorylation was increased 3.5-fold (**Figure 3A**), indicating increased activity (Lai et al., 1986). This in turn potentiates the phosphorylation of all the downstream targets of CaMKII (Toischer et al., 2010; Anderson et al., 2011; Fischer et al., 2013). CaMKII targets several proteins involved in the regulation of cardiomyocyte electrophysiology and calcium fluxes. The observed 2.5-fold higher phosphorylation of cardiac Na^{+} channel (NaV1.5) by CaMKII in HCM samples (**Figure 3A**; Coppini et al., 2013) may have significantly contributed to increase I_{NaL} in HCM cardiomyocytes (Wagner et al., 2006); this suggests that CaMKII activation is the most relevant cause of I_{NaL} augmentation in HCM cardiac myocytes, although additional mechanisms might be involved (e.g., oxidation of Na^{+}channels) (Lu et al., 1999). The increased phosphorylation of L-Type Ca^{2+} channel (**Figure 3A**) may have contributed to slow down I_{CaL} inactivation in HCM cells (Hudmon et al., 2005; Xu et al., 2010). The slower I_{CaL} inactivation may also be a consequence of the loss of T-tubules observed in HCM cardiomyocytes (see below) (Brette et al., 2004). Moreover, the observed 1.5-fold higher CaMKII-dependent phosphorylation of RyR2 (**Figure 3A**) may have contributed to increase the rate of spontaneous releases during diastole (Shannon et al., 2003) and DADs (Curran et al., 2010) in HCM myocytes. Finally, the observed 3-fold higher phosphorylation of PLB at CaMKII site (**Figure 3A**), via reduced SERCA inhibition, may have partially counteracted the consequences of reduced SERCA expression in terms of SR Ca^{2+} reuptake, ultimately contributing to maintain SR Ca^{2+} content and steady state Ca^{2+}-transient amplitude in HCM cardiomyocytes (Mattiazzi and Kranias, 2011). In support of the previous observations, we here tested the effects of the acute inhibition of CaMKII in HCM cardiomyocytes and trabeculae by using the cell-permeant version of Autocamtide-related inhibitory peptide II (AIP-II, see **Figures 3B–C**). In single human HCM cardiomyocytes, AIP-II reduced diastolic $[Ca^{2+}]_i$ and limited the increase of diastolic $[Ca^{2+}]_i$ at higher stimulation frequencies, without affecting the amplitude or the kinetics of Ca^{2+}-transients (**Figure 3B**). In line with that, when used in intact human HCM while measuring twitch force, AIP-II reduced diastolic tension and limited the increase of diastolic tension upon increase of pacing rate (**Figure 3C**). Interestingly, AIP-II accelerated time-to-peak contraction in HCM trabeculae, suggesting that acute inhibition of CaMKII may directly affect the kinetics of force generation by the myofilaments.

Besides the direct effects on cardiomyocyte function, CaMKII is able to alter the expression of genes involved in the hypertrophic remodeling process of cardiomyocytes, and to facilitate the production of collagen, the increase of extracellular matrix volume and the growth of cardiac fibroblasts (Kreusser and Backs, 2014). We verified that CaMKII participates in the development and progression of cardiac functional and

structural phenotype in HCM by studying the transgenic R92Q-TnT mouse model. In the R92Q-TnT mouse, CaMKII activity, increased I_{NaL} and cardiomyocyte Ca^{2+} overload go hand in hand during disease development and are present since the earliest stages of disease development (Coppini et al., 2017; Ferrantini et al., 2017). In this mouse model, lifelong treatment with ranolazine prevented the development of all features of HCM-specific cardiac phenotype, including LV thickening, progression of LV diastolic dysfunction and intra-myocardial fibrosis and the establishment of an arrhythmogenic substrate (Coppini et al., 2017). The mechanism by which ranolazine prevents the hypertrophic HCM phenotype is related to the inhibition of the enhanced I_{NaL}, leading to decreased intracellular $[Na^+]$ and diastolic $[Ca^{2+}]_i$, eventually avoiding the pathological intensification of CaMKII function in treated mice (Coppini et al., 2017). The reduction of CaMKII-activity in treated mice prevented the progression of the hypertrophic remodeling in mutant hearts, thereby reducing the morphological and functional cardiac HCM-phenotype in mutation-carrier mice.

LOSS OF T-TUBULES IN HCM CARDIOMYOCYTES

T-tubules (Ferrantini et al., 2013) play a fundamental role in myocardial function because they allow a quick propagation of APs within the inner portions of cardiac myocytes. The simultaneous electrical activation of the whole t-tubular system allows for a synchronous triggering of Ca^{2+}release from the SR across the whole myocytes, even the central regions that are farther away from surface sarcolemma. This is essential to achieve an homogeneous activation of all myofilaments and thus a rapid simultaneous shortening of the entire cardiac cell. As a proof of concept, by acutely disrupting T-tubules trough osmotic-shock, Ca^{2+}release was rendered asynchronous (Brette et al., 2005), resulting in a clear impairment of contractile function and a slower relaxation (Ferrantini et al., 2014). In cardiomyocytes from animal models of cardiac hypertrophy and heart failure, a delay of local Ca^{2+}release was observed both in areas where t-tubules are disrupted (Song et al., 2006) and in regions adjacent to electrically uncoupled T-tubules (Sacconi et al., 2012; Crocini et al., 2014). Lyon et al. (2009) studied T-tubular structures in myocardial specimens from patients with HF caused by different diseases (i.e., post-ischemic HF, dilated cardiomyopathy and HCM) and observed a significant reduction of T-tubule density in all failing human hearts regardless of the underlying disease, including in end-stage HCM. In a mouse model of HCM we used Random Access Multi Photon (RAMP) microscopy to measure the local propagation of APs in the T-tubule and the correspondent release of Ca^{2+}in the adjacent junctional area by simultaneously mapping multiple sites of an isolated cell. With this technique, we found that more than 20% of T-tubules are unable to propagate AP and the surrounding junctional regions display a significantly delayed local Ca^{2+}release (Crocini et al., 2016). In this mouse model, asynchronous intracellular Ca^{2+} release due to altered T-tubules contribute to slow down Ca^{2+}-transient kinetics and impair diastolic function.

In all cardiomyocytes subjected to patch-clamp measurements, we measured cell capacitance, an index of sarcolemma extension, and compared with cell volume, as estimated by cell surface (**Figure 4A**). The ratio between cell capacitance and volume (surface/volume ratio) was reduced in HCM vs. control human cardiomyocytes, suggesting reduction of T-tubules. In addition, we recently performed a preliminary assessment of the density of T-tubules in cardiomyocytes isolated from surgical septal samples of 10 HCM patient (Ferrantini et al., 2018; **Figures 4B,C**): in all the myocytes studied under the confocal microscope after membrane fluorescent labeling, we observed a very low density of T-tubules, much lower than what is expected in healthy human cardiomyocytes (Lyon et al., 2009). We previously demonstrated that the loss of t-tubules may directly contribute to slow down the kinetics of Ca^{2+} transients (Ferrantini et al., 2014), thus delaying relaxation, with possible detrimental effects on diastolic function. However, it is unclear whether and how loss of t-tubules affects the propensity toward arrhythmias of HCM cardiomyocytes. Loss of t-tubules could be protective against arrhythmias because orphan RyR channels (RyR uncoupled from t-tubules) have a reduced likelihood of diastolic spontaneous opening (Brette et al., 2005); however, the rate of Ca^{2+} waves is increased in human HCM. Loss of t-tubules leads to reduction of capacitance/volume ratio, thus increasing conduction velocity in detubulated myocardial tissue: this effect may prevent the formation of small re-entry circuits. On the contrary, loss of t-tubules may promote arrhythmias because it reduces synchronicity of Ca^{2+} release, thus raising the likelihood of APD and effective-refractory-period (ERP) temporal fluctuations (alternans): APD and ERP alternans facilitate the formation of dynamic reentry circuits (Heinzel et al., 2011). In support of this, we found that Ca^{2+} release is indeed asynchronous in human HCM cardiomyocytes (**Figure 4D**). Moreover, loss of t-tubules reduces Ca^{2+}-dependent inactivation of I_{CaL}, as subsarcolemmal systolic $[Ca^{2+}]$ is lower below surface sarcolemma than in proximity of T-tubules (Morotti et al., 2012): indeed, I_{CaL} inactivation is slower in human HCM cells as compared with controls. Finally, the presence of dysfunctional residual t-tubules within the myocyte may facilitate spontaneous Ca^{2+}-release events at SR sites adjacent to those tubules, as we previously showed in a model of heart failure (Crocini et al., 2014), increasing the overall risk of Ca^{2+} waves and DADs.

ABNORMAL RESPONSE OF HCM MYOCARDIUM TO BETA-ADRENERGIC STIMULATION

We recently investigated the characteristics and anomalies of β-adrenergic signaling in the myocardium of HCM patients by comparing the response of control cardiac muscle to β-adrenergic stimulation with that observed in HCM cardiomyocytes or trabeculae (Ferrantini et al., 2018; **Figure 5**). In particular, we observed that the mechanical response to the β-adrenergic agonist isoproterenol (that is, augmentation of twitch force amplitude and acceleration of relaxation) was qualitatively similar in HCM and control trabeculae, albeit the kinetics

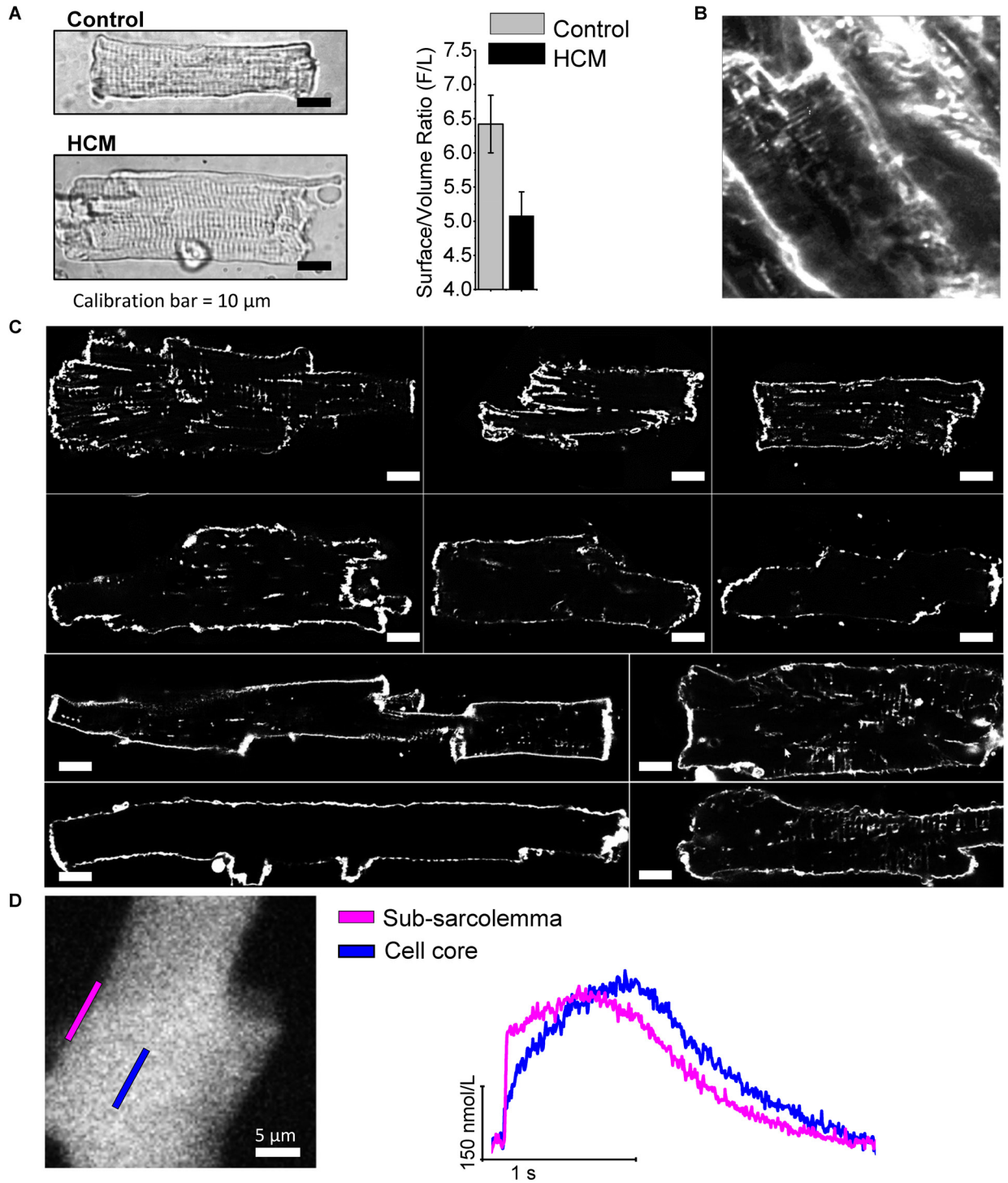

FIGURE 4 | The density of T-tubules is markedly low in HCM cardiomyocytes. **(A)** Left: Representative images of a control (top) and an HCM(bottom) cardiomyocyte, showing cell hypertrophy in HCM. Right: surface/volume ratio in HCM and control cardiomyocytes;surface is derived from cell capacitance, volume estimated from cell area. Data from 64 cells (14 patients). Previously unpublished data. **(B)** 2-photon image recorded in HCM intact tissue after membrane labeling with anepp dyes, showing a severe reduction of T-tubules. **(C)**Each cell derives from a different patient sample (ID of the patient is indicated next to the cell in each respective image). Cells were stained with Di-3-ANEPPDHQ (Thermo-Fisher) and imaged with a Leica Confocal microscope using the 488 nm laser line. Sections were taken at mid cell. While the outer sarcolemma is well stained in all myocytes, T-tubules are barely visible in most of them and some cells are completely devoid of T-tubules. White bars equal 10 µm. **(D)** Recordings of intracellular calcium from an HCM myocytes using a fast camera; right: calcium variations during an elicited electrical activation in the subsarcolemma and in the cell core. In agreement with the loss of t-tubule, calcium rise in the core is significantly delayed. Previously unpublished data.

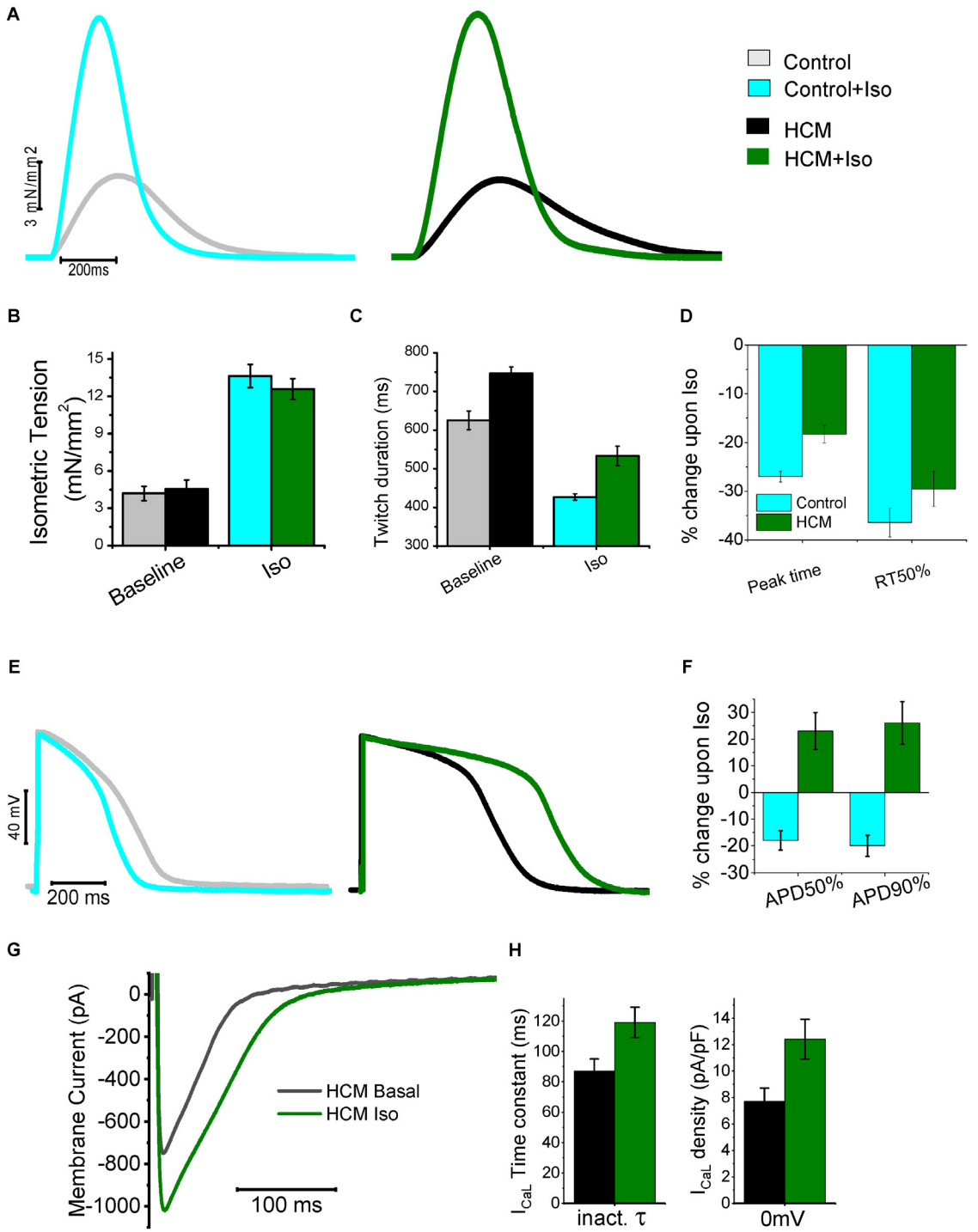

FIGURE 5 | Mechanical and electrical response to β-adrenergic stimulation of HCM myocardium. **(A)** Representative superimposed force twitches elicited at 0.5 Hz in control (left) and HCM (right) trabeculae in the absence and presence of Isoproterenol 10^{-7}M (Iso). **(B)** Isometric tension during steady state stimulation at 0.5 in the absence and presence of Iso in control and HCM trabeculae. **(C)** Duration of force twitches (from stimulus to 90% of relaxation) elicited at 0.5 Hz in the absence and presence of Isoproterenol 10^{-7}M. **(D)** Percentages of Change in the parameters of twitch kinetics (0.5 Hz) upon exposure to Iso in Control (cyan) and HCM (green) trabeculae: time from stimulus to peak contraction (peak time) and time from peak to 50% of relaxation (RT50%). **(E)** Representative superimposed action potentials elicited at 0.5 Hz in control (left) and HCM (right) cardiomyocytes, in the absence and presence of Iso. **(F)** Percentages of Change in the parameters of action potential kinetics upon exposure to Iso in Control (cyan) and HCM (green) cardiomyocytes: time from stimulus to 50% repolarization (APD50%) and time from peak to 90% of repolarization (APD90%). **(G)** Representative superimposed L-Type Ca-current traces at baseline (black traces) and in the presence of Iso (green). **(H)** L-Type Ca-current inactivation time-constant(left) and density (right) at baseline (black) and with Iso (green) in HCM cells. Modified from Ferrantini et al. (2018).

of contraction and relaxation remained slower in HCM myocardium, even upon maximal β-adrenergic activation (Ferrantini et al., 2018; **Figures 5A–D**). These results suggest that the molecular mechanisms responsible for the acceleration of relaxation upon β-adrenergic activation [i.e., myofilament $Ca2^{+}$-desensitization (Sequeira et al., 2013) and phospholamban phosphorylation (Coppini et al., 2013; Helms et al., 2016)] are preserved in HCM myocardium.

On the contrary The electrical response to isoprenalin observed in single HCM cardiomyocytes was profoundly different as compared with control cardiac cells (**Figures 5E–G**). Activation of β-adrenergic receptors physiologically leads to the enhancement of both I_{CaL} and the slow delayed-rectifier K^+ current (I_{Ks}). In healthy human cardiomyocytes the increase of repolarizing K^+ currents prevails over the augmentation of I_{CaL} (Terrenoire et al., 2005), thus determining a net reduction of AP duration (Taggart et al., 2003; **Figure 5E**). In HCM cardiomyocytes, however, we observed unbalanced changes in the expression of Ca^{2+} and K^+ currents (Coppini et al., 2013). As shown in **Figure 1**, we observed a reduction of the expression of all K^+ channels (including I_{Ks}) while the expression of Ca^{2+} channels and the density of I_{CaL} was slightly increased. Therefore, in response to β-stimulation, the potentiation of I_{CaL} prevails over the increase of K^+ currents, ultimately causing a net increase of inward currents during the plateau of the AP, thus determining a "paradoxical" prolongation of APD in HCM cardiomyocytes (Ferrantini et al., 2018; **Figures 5E,F**). Moreover, we observed that β-adrenergic stimulation in HCM cardiomyocytes not only increased peak I_{CaL} amplitude, but also slowed down I_{CaL} inactivation (Ferrantini et al., 2018; **Figures 5G,H**), further contribute to the prolongation of APs by β-adrenergic agonists. Additionally, recent work suggested that β-adrenergic stimulation is able to rapidly and transiently increase I_{NaL} in cardiac myocytes (Dybkova et al., 2014): a further augmentation of the already increased I_{NaL} in HCM myocytes may have played a relevant role in the paradoxical prolongation of APs with isoprenaline. As expected, AP prolongation by β-adrenergic agonists further increased the occurrence of arrhythmogenic early afterdepolarizations, triggered activity and spontaneous premature contractions in HCM cardiomyocytes and trabeculae (Ferrantini et al., 2018). This paradoxical electrical response may have severe consequences in HCM patients, that is, it may increase the risk of exercise/stress-induced arrhythmias in HCM patients.

In parallel, the response of HCM cardiomyocytes to β-adrenergic stimulation in terms of Ca^{2+}-handling changes was also abnormal. In HCM cardiomyocytes the β-adrenergic-induced increase of Ca^{2+} release may primarily rely on the prolongation of Ca^{2+} entry via I_{CaL} channels caused by the slower current inactivation. In addition to the increase of net Ca^{2+} influx through I_{CaL}, the potentiation of Ca^{2+}-entry via reverse-mode NCX may have contributed to the augmentation of Ca^{2+}-transients β-receptor activation (Perchenet et al., 2000). The increase of NCX-mediated Ca^{2+}-entry upon β-adrenergic stimulation is probably caused by the rise of intracellular $[Na^+]$ in response to the transient augmentation of I_{NaL} and by the further prolongation of AP plateau, as reverse-mode NCX is only active at positive membrane potentials (Coppini et al., 2013; Dybkova et al., 2014). The idea that the increase of contractile tension in response to β-adrenergic activation mainly depends on the larger Ca^{2+}-entry through the sarcolemma apparently contrasts with the largely accepted idea that the inotropic response of β-stimulus mainly stems from the increase of SR Ca^{2+} content (Desantiago et al., 2008), mediated by the enhancement of SR Ca^{2+}-uptake by SERCA via PKA-dependent phospholamban phosphorylation, ultimately causing an enhanced release of Ca^{2+} from the SR. The hastening of Ca-transient decay in response to isoprenaline in HCM cardiomyocytes (Ferrantini et al., 2018) suggests that the β-adrenergic-induced increase of SERCA function (via PkA-mediated phospholamban phosphorylation) is preserved in HCM myocardium, as Ca-transient decay is physiologically accelerated by isoproterenol. Despite the shortening of Ca^{2+} transient decay, their rise-time is so prolonged that the total duration of Ca^{2+}-transients is not reduced upon β-stimulation. The rise of SR Ca^{2+} load upon exposure to isoprenaline in HCM myocytes may be limited by the increased phosphorylation of ryanodine receptors (due to the higher CaMKII activity), which in turn causes a larger rate of Ca^{2+} leakage from the SR during the diastolic period. This may render positive inotropic responses more dependent on the increase of Ca^{2+} entry from the sarcolemma, as the possibility to accumulate Ca^{2+} in the SR is limited. An additional contributor to this aberrant behavior is the lower density of t-tubules observed in HCM myocytes (see above) (Orchard and Brette, 2008). The physiological response to β-adrenergic activation may be radically different in disease-remodeled myocytes showing a sparse and disorganized the T-tubular system. In HCM cells, where T-tubules are nearly absent, we expect a large redistribution of I_{CaL} channels to the surface sarcolemma (Coppini et al., 2013). Under such conditions, modulation of cellularinotropism essentially relies on the magnitude of sarcolemmal Ca^{2+} triggers (Ferrantini et al., 2014), that is, the amplitude and duration of I_{CaL} plus the rate of NCX-mediated Ca^{2+} entry (reverse mode). The prolongation of APs causing increased sarcolemmal Ca^{2+}-entry appears to be an essential requisite for the preservation of the positive-inotropic effect of β-adrenergic stimulation in HCM myocardium. In line with that hypothesis, the application of ranolazine or GS-967 on top of isoproterenol, which prevented the β-adrenergic-induced AP prolongation, also greatly reduced the positive inotropic response to β-stimulation in HCM myocardium (Ferrantini et al., 2018). The preservation of inotropic response in HCM myocardium comes at the expense of a further impairment of diastolic function (due to prolonged Ca^{2+} transient rise-time) and a further increase of the likelihood of cellular arrhythmias (due to increased cytosolic Ca^{2+} accumulation and AP prolongation).

CONCLUSION

Hypertrophic remodeling in the myocardium of patients with HCM features several pathological alterations of cardiomyocyte electrical function and intracellular Ca^{2+}-handling (**Figure 6**), that contribute to increase the likelihood of EADs, DADs and

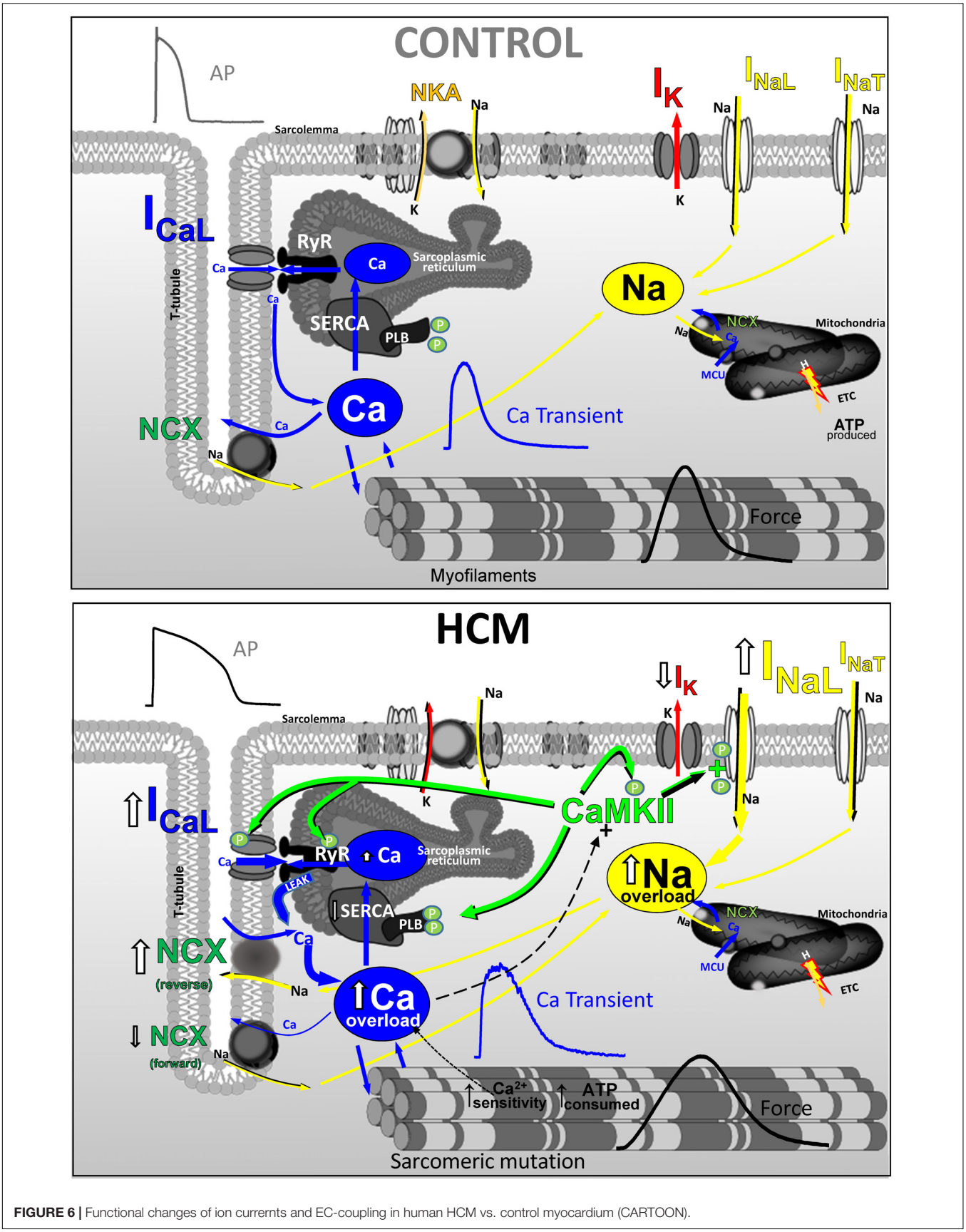

FIGURE 6 | Functional changes of ion currernts and EC-coupling in human HCM vs. control myocardium (CARTOON).

premature contractions. Such arrhythmogenic changes occur since the early stages of HCM disease development and may explain the occurrence of ventricular arrhythmias and cardiac arrest in young HCM patients who lack advanced structural alterations of myocardial structure (e.g., diffuse fibrosis, myocardial scars, massive hypertrophy, severe microvascular abnormalities). Changes of the expression and function of ion channels and EC-coupling proteins in HCM myocardium concur to generate an "acquired channelopathy" phenotype in HCM patients that raises the risk of arrhythmias even before the establishment of a structural substrate for sustained arrhythmias. Among the several molecular determinants of cellular arrrhythmogenesis, increased I_{NaL} appear to play a leading role in HCM and may represent a selective target for pharmacological prevention of arrhythmias in this disease, with possible clinical implications. Although targeting I_{NaL} is proven to be effective antiarrhytmic approach, one cannot discount NCX (Passini et al., 2016), leaky RyR channels or cardiac CaMKII as potential targets to reduce Ca^{2+}-dependent arrhythmias in HCM.

AUTHOR CONTRIBUTIONS

RC performed most of the original experiments described in this review and drafted this manuscript. CF contributed to the original data presented and discussed here, drafted the figures and copyedited the manuscript. AM, CP, and EC supervised the original projects that led to production of the results shown here; moreover, they critically reviewed and edited the manuscript. All authors concur with the current submitted version.

FUNDING

Original data described in the review are from research work supported by: the Regione Toscana (FAS-Salute 2014, ToRSADE project), Telethon Italy (GGP13162), the EU (STREP Project 241577 BIG HEART, 7th European Framework Program and project SILICOFCM, grant agreement N. 777204, Horizon 2020 research and innovation program) and the Italian Ministry of Health (RF 2010-2313451, RF-2013-02356787, and GR-2011-02350583).

REFERENCES

Adabag, A. S., Casey, S. A., Kuskowski, M. A., Zenovich, A. G., and Maron, B. J. (2005). Spectrum and prognostic significance of arrhythmias on ambulatory Holter electrocardiogram in hypertrophic cardiomyopathy. *J. Am. Coll. Cardiol.* 45, 697–704. doi: 10.1016/j.jacc.2004.11.043

Anderson, M. E., Brown, J. H., and Bers, D. M. (2011). CaMKII in myocardial hypertrophy and heart failure. *J. Mol. Cell Cardiol.* 51, 468–473. doi: 10.1016/j.yjmcc.2011.01.012

Antzelevitch, C., and Belardinelli, L. (2006). The role of sodium channel current in modulating transmural dispersion of repolarization and arrhythmogenesis. *J. Cardiovasc. Electrophysiol.* 17(Suppl. 1), S79–S85. doi: 10.1111/j.1540-8167.2006.00388.x

Antzelevitch, C., Belardinelli, L., Zygmunt, A. C., Burashnikov, A., Di Diego, J. M., Fish, J. M., et al. (2004). Electrophysiological effects of ranolazine, a novel antianginal agent with antiarrhythmic properties. *Circulation* 110, 904–910. doi: 10.1161/01.CIR.0000139333.83620.5D

Ashrafian, H., McKenna, W. J., and Watkins, H. (2011). Disease pathways and novel therapeutic targets in hypertrophic cardiomyopathy. *Circ. Res.* 109, 86–96. doi: 10.1161/CIRCRESAHA.111.242974

Ashrafian, H., Redwood, C., Blair, E., and Watkins, H. (2003). Hypertrophic cardiomyopathy:a paradigm for myocardial energy depletion. *Trends Genet.* 19, 263–268. doi: 10.1016/S0168-9525(03)00081-87

Authors/Task Force Members Elliott, P. M., Anastasakis, A., Borger, M. A., Borggrefe, M., Cecchi, F., et al. (2014). 2014 ESC Guidelines on diagnosis and management of hypertrophic cardiomyopathy: the Task Force for the Diagnosis and Management of Hypertrophic Cardiomyopathy of the European Society of Cardiology (ESC). *Eur. Heart J.* 35, 2733–2779. doi: 10.1093/eurheartj/ehu284

Avanesov, M., Munch, J., Weinrich, J., Well, L., Saring, D., Stehning, C., et al. (2017). Prediction of the estimated 5-year risk of sudden cardiac death and syncope or non-sustained ventricular tachycardia in patients with hypertrophic cardiomyopathy using late gadolinium enhancement and extracellular volume CMR. *Eur. Radiol.* 27, 5136–5145. doi: 10.1007/s00330-017-4869-x

Baudenbacher, F., Schober, T., Pinto, J. R., Sidorov, V. Y., Hilliard, F., Solaro, R. J., et al. (2008). Myofilament Ca^{2+} sensitization causes susceptibility to cardiac arrhythmia in mice. *J. Clin. Invest.* 118, 3893–3903. doi: 10.1172/JCI36642

Beuckelmann, D. J., Nabauer, M., and Erdmann, E. (1992). Intracellular calcium handling in isolated ventricular myocytes from patients with terminal heart failure. *Circulation* 85, 1046–1055. doi: 10.1161/01.CIR.85.3.1046

Brette, F., Despa, S., Bers, D. M., and Orchard, C. H. (2005). Spatiotemporal characteristics of SR Ca^{2+} uptake and release in detubulated rat ventricular myocytes. *J. Mol. Cell Cardiol.* 39, 804–812. doi: 10.1016/j.yjmcc.2005.08.005

Brette, F., Salle, L., and Orchard, C. H. (2004). Differential modulation of L-type Ca2 + current by SR Ca^{2+} release at the T-tubules and surface membrane of rat ventricular myocytes. *Circ. Res.* 95, e1–e7. doi: 10.1161/01.RES.0000135547.53927.F6

Cecchi, F., Olivotto, I., Gistri, R., Lorenzoni, R., Chiriatti, G., and Camici, P. G. (2003). Coronary microvascular dysfunction and prognosis in hypertrophic cardiomyopathy. *N. Engl. J. Med.* 349, 1027–1035. doi: 10.1056/NEJMoa025050

Chan, R. H., Maron, B. J., Olivotto, I., Pencina, M. J., Assenza, G. E., Haas, T., et al. (2014). Prognostic value of quantitative contrast-enhanced cardiovascular magnetic resonance for the evaluation of sudden death risk in patients with hypertrophic cardiomyopathy. *Circulation* 130, 484–495. doi: 10.1161/CIRCULATIONAHA.113.007094

Cho, J. H., Zhang, R., Kilfoil, P. J., Gallet, R., de Couto, G., Bresee, C., et al. (2017). Delayed repolarization underlies ventricular arrhythmias in rats with heart failure and preserved ejection fraction. *Circulation* 136, 2037–2050. doi: 10.1161/CIRCULATIONAHA.117.028202

Coppini, R., Ferrantini, C., Yao, L., Fan, P., Del Lungo, M., Stillitano, F., et al. (2013). Late sodium current inhibition reverses electromechanical dysfunction in human hypertrophic cardiomyopathy. *Circulation* 127, 575–584. doi: 10.1161/CIRCULATIONAHA.112.134932

Coppini, R., Mazzoni, L., Ferrantini, C., Gentile, F., Pioner, J. M., Laurino, A., et al. (2017). Ranolazine prevents phenotype development in a mouse model of hypertrophic cardiomyopathy. *Circ. Heart Fail.* 10:e003565. doi: 10.1161/CIRCHEARTFAILURE.116.003565

Crocini, C., Coppini, R., Ferrantini, C., Yan, P., Loew, L. M., Tesi, C., et al. (2014). Defects in T-tubular electrical activity underlie local alterations of calcium release in heart failure. *Proc. Natl. Acad. Sci. U.S.A.* 111, 15196–15201. doi: 10.1073/pnas.1411557111

Crocini, C., Ferrantini, C., Scardigli, M., Coppini, R., Mazzoni, L., Lazzeri, E., et al. (2016). Novel insights on the relationship between T-tubular defects and contractile dysfunction in a mouse model of hypertrophic cardiomyopathy. *J. Mol. Cell Cardiol.* 91, 42–51. doi: 10.1016/j.yjmcc.2015.12.013

Curran, J., Brown, K. H., Santiago, D. J., Pogwizd, S., Bers, D. M., and Shannon, T. R. (2010). Spontaneous Ca waves in ventricular myocytes from failing hearts depend on Ca^{2+}-calmodulin-dependent protein kinase II. *J. Mol. Cell Cardiol.* 49, 25–32. doi: 10.1016/j.yjmcc.2010.03.013

Dass, S., Suttie, J. J., Piechnik, S. K., Ferreira, V. M., Holloway, C. J., Banerjee, R., et al. (2012). Myocardial tissue characterization using magnetic resonance

noncontrast t1 mapping in hypertrophic and dilated cardiomyopathy. *Circ. Cardiovasc. Imaging* 5, 726–733. doi: 10.1161/CIRCIMAGING.112.976738

Desantiago, J., Ai, X., Islam, M., Acuna, G., Ziolo, M. T., Bers, D. M., et al. (2008). Arrhythmogenic effects of beta2-adrenergic stimulation in the failing heart are attributable to enhanced sarcoplasmic reticulum Ca load. *Circ. Res.* 102, 1389–1397. doi: 10.1161/CIRCRESAHA.107.169011

Dybkova, N., Wagner, S., Backs, J., Hund, T. J., Mohler, P. J., Sowa, T., et al. (2014). Tubulin polymerization disrupts cardiac beta-adrenergic regulation of late INa. *Cardiovasc. Res.* 103, 168–177. doi: 10.1093/cvr/cvu120

Erickson, J. R., He, B. J., Grumbach, I. M., and Anderson, M. E. (2011). CaMKII in the cardiovascular system: sensing redox states. *Physiol. Rev.* 91, 889–915. doi: 10.1152/physrev.00018.2010

Ferrantini, C., Coppini, R., Pioner, J. M., Gentile, F., Tosi, B., Mazzoni, L., et al. (2017). Pathogenesis of hypertrophic cardiomyopathy is mutation rather than disease specific: a comparison of the cardiac troponin T E163R and R92Q mouse models. *J. Am. Heart Assoc.* 6, e005407. doi: 10.1161/JAHA.116.005407

Ferrantini, C., Coppini, R., Sacconi, L., Tosi, B., Zhang, M. L., Wang, G. L., et al. (2014). Impact of detubulation on force and kinetics of cardiac muscle contraction. *J. Gen. Physiol.* 143, 783–797. doi: 10.1085/jgp.201311125

Ferrantini, C., Crocini, C., Coppini, R., Vanzi, F., Tesi, C., Cerbai, E., et al. (2013). The transverse-axial tubular system of cardiomyocytes. *Cell Mol. Life Sci.* 70, 4695–4710. doi: 10.1007/s00018-013-1410-1415

Ferrantini, C., Pioner, J. M., Mazzoni, L., Gentile, F., Tosi, B., Rossi, A., et al. (2018). Late sodium current inhibitors to treat exercise-induced obstruction in hypertrophic cardiomyopathy: an in vitro study in human myocardium. *Br. J. Pharmacol.* 175, 2635–2652. doi: 10.1111/bph.14223

Fischer, T. H., Herting, J., Tirilomis, T., Renner, A., Neef, S., Toischer, K., et al. (2013). Ca2 + /calmodulin-dependent protein kinase II and protein kinase A differentially regulate sarcoplasmic reticulum Ca2 + leak in human cardiac pathology. *Circulation* 128, 970–981. doi: 10.1161/CIRCULATIONAHA.113.001746

Fraysse, B., Weinberger, F., Bardswell, S. C., Cuello, F., Vignier, N., Geertz, B., et al. (2012). Increased myofilament Ca^{2+} sensitivity and diastolic dysfunction as early consequences of Mybpc3 mutation in heterozygous knock-in mice. *J. Mol. Cell Cardiol.* 52, 1299–1307. doi: 10.1016/j.yjmcc.2012.03.009

Galati, G., Leone, O., Pasquale, F., Olivotto, I., Biagini, E., Grigioni, F., et al. (2016). Histological and histometric characterization of myocardial fibrosis in end-stage hypertrophic cardiomyopathy: a clinical-pathological study of 30 explanted hearts. *Circ. Heart Fail.* 9:e003090. doi: 10.1161/CIRCHEARTFAILURE.116.003090

Gersh, B. J., Maron, B. J., Bonow, R. O., Dearani, J. A., Fifer, M. A., Link, M. S., et al. (2011). 2011 ACCF/AHA guideline for the diagnosis and treatment of hypertrophic cardiomyopathy: a report of the American College of Cardiology Foundation/American Heart Association Task Force on Practice Guidelines. *Circulation* 124, e783–e831. doi: 10.1161/CIR.0b013e318223e2bd

Grandi, E., Pasqualini, F. S., and Bers, D. M. (2010). A novel computational model of the human ventricular action potential and Ca transient. *J. Mol. Cell Cardiol.* 48, 112–121. doi: 10.1016/j.yjmcc.2009.09.019

Haim, T. E., Dowell, C., Diamanti, T., Scheuer, J., and Tardiff, J. C. (2007). Independent FHC-related cardiac troponin T mutations exhibit specific alterations in myocellular contractility and calcium kinetics. *J. Mol. Cell Cardiol.* 42, 1098–1110. doi: 10.1016/j.yjmcc.2007.03.906

Heinzel, F. R., MacQuaide, N., Biesmans, L., and Sipido, K. (2011). Dyssynchrony of Ca^{2+} release from the sarcoplasmic reticulum as subcellular mechanism of cardiac contractile dysfunction. *J. Mol. Cell Cardiol.* 50, 390–400. doi: 10.1016/j.yjmcc.2010.11.008

Helms, A. S., Alvarado, F. J., Yob, J., Tang, V. T., Pagani, F., Russell, M. W., et al. (2016). Genotype-dependent and -independent calcium signaling dysregulation in human hypertrophic cardiomyopathy. *Circulation* 134, 1738–1748. doi: 10.1161/CIRCULATIONAHA.115.020086

Ho, C. Y., Abbasi, S. A., Neilan, T. G., Shah, R. V., Chen, Y., Heydari, B., et al. (2013). T1 measurements identify extracellular volume expansion in hypertrophic cardiomyopathy sarcomere mutation carriers with and without left ventricular hypertrophy. *Circ. Cardiovasc. Imaging* 6, 415–422. doi: 10.1161/CIRCIMAGING.112.000333

Hudmon, A., and Schulman, H. (2002). Structure-function of the multifunctional Ca2 + /calmodulin-dependent protein kinase II. *Biochem. J.* 364(Pt 3), 593–611. doi: 10.1042/BJ20020228

Hudmon, A., Schulman, H., Kim, J., Maltez, J. M., Tsien, R. W., and Pitt, G. S. (2005). CaMKII tethers to L-type Ca^{2+} channels, establishing a local and dedicated integrator of Ca^{2+} signals for facilitation. *J. Cell Biol.* 171, 537–547. doi: 10.1083/jcb.200505155

Hurtado-de-Mendoza, D., Corona-Villalobos, C. P., Pozios, I., Gonzales, J., Soleimanifard, Y., Sivalokanathan, S., et al. (2017). Diffuse interstitial fibrosis assessed by cardiac magnetic resonance is associated with dispersion of ventricular repolarization in patients with hypertrophic cardiomyopathy. *J. Arrhythm* 33, 201–207. doi: 10.1016/j.joa.2016.10.005

Johnson, J. N., Grifoni, C., Bos, J. M., Saber-Ayad, M., Ommen, S. R., Nistri, S., et al. (2011). Prevalence and clinical correlates of QT prolongation in patients with hypertrophic cardiomyopathy. *Eur. Heart J.* 32, 1114–1120. doi: 10.1093/eurheartj/ehr021

Knollmann, B. C., Kirchhof, P., Sirenko, S. G., Degen, H., Greene, A. E., Schober, T., et al. (2003). Familial hypertrophic cardiomyopathy-linked mutant troponin T causes stress-induced ventricular tachycardia and Ca^{2+}-dependent action potential remodeling. *Circ. Res.* 92, 428–436. doi: 10.1161/01.RES.0000059562.91384.1A

Kreusser, M. M., and Backs, J. (2014). Integrated mechanisms of CaMKII-dependent ventricular remodeling. *Front. Pharmacol.* 5:36. doi: 10.3389/fphar.2014.00036

Lai, Y., Nairn, A. C., and Greengard, P. (1986). Autophosphorylation reversibly regulates the Ca^{2+}/calmodulin-dependence of Ca^{2+}/calmodulin-dependent protein kinase II. *Proc. Natl. Acad. Sci. U.S.A.* 83, 4253–4257. doi: 10.1073/pnas.83.12.4253

Lan, F., Lee, A. S., Liang, P., Sanchez-Freire, V., Nguyen, P. K., Wang, L., et al. (2013). Abnormal calcium handling properties underlie familial hypertrophic cardiomyopathy pathology in patient-specific induced pluripotent stem cells. *Cell Stem Cell* 12, 101–113. doi: 10.1016/j.stem.2012.10.010

Ling, H., Zhang, T., Pereira, L., Means, C. K., Cheng, H., Gu, Y., et al. (2009). Requirement for Ca^{2+}/calmodulin-dependent kinase II in the transition from pressure overload-induced cardiac hypertrophy to heart failure in mice. *J. Clin. Invest.* 119, 1230–1240. doi: 10.1172/JCI38022

Lu, T., Lee, H. C., Kabat, J. A., and Shibata, E. F. (1999). Modulation of rat cardiac sodium channel by the stimulatory G protein alpha subunit. *J. Physiol.* 518(Pt 2), 371–384.

Lyon, A. R., MacLeod, K. T., Zhang, Y., Garcia, E., Kanda, G. K., Lab, M. J., et al. (2009). Loss of T-tubules and other changes to surface topography in ventricular myocytes from failing human and rat heart. *Proc. Natl. Acad. Sci. U.S.A.* 106, 6854–6859. doi: 10.1073/pnas.0809777106

Maltsev, V. A., Sabbah, H. N., Higgins, R. S., Silverman, N., Lesch, M., and Undrovinas, A. I. (1998). Novel, ultraslow inactivating sodium current in human ventricular cardiomyocytes. *Circulation* 98, 2545–2552. doi: 10.1161/01.CIR.98.23.2545

Maron, B. J., McKenna, W. J., Danielson, G. K., Kappenberger, L. J., Kuhn, H. J., Seidman, C. E., et al. (2003). American College of Cardiology/European Society of Cardiology clinical expert consensus document on hypertrophic cardiomyopathy. A report of the American College of Cardiology Foundation Task Force on Clinical Expert Consensus Documents and the European Society of Cardiology Committee for Practice Guidelines. *J. Am. Coll. Cardiol.* 42, 1687–1713. doi: 10.1016/S0735-1097(03)00941-0

Maron, B. J., Olivotto, I., Spirito, P., Casey, S. A., Bellone, P., Gohman, T. E., et al. (2000). Epidemiology of hypertrophic cardiomyopathy-related death: revisited in a large non-referral-based patient population. *Circulation* 102, 858–864. doi: 10.1161/01.CIR.102.8.858

Maron, M. S., Rowin, E. J., Olivotto, I., Casey, S. A., Arretini, A., Tomberli, B., et al. (2016). Contemporary natural history and management of nonobstructive hypertrophic cardiomyopathy. *J. Am. Coll. Cardiol.* 67, 1399–1409. doi: 10.1016/j.jacc.2016.01.023

Mattiazzi, A., and Kranias, E. G. (2011). CaMKII regulation of phospholamban and SR Ca^{2+} load. *Heart Rhythm* 8, 784–787. doi: 10.1016/j.hrthm.2010.11.035

Maurizi, N., Passantino, S., Spaziani, G., Girolami, F., Arretini, A., Targetti, M., et al. (2018). Long-term outcomes of pediatric-onset hypertrophic cardiomyopathy and age-specific risk factors for lethal arrhythmic events. *JAMA Cardiol.* 3, 520–525. doi: 10.1001/jamacardio.2018.0789

Morotti, S., Grandi, E., Summa, A., Ginsburg, K. S., and Bers, D. M. (2012). Theoretical study of L-type Ca^{2+} current inactivation kinetics during

action potential repolarization and early afterdepolarizations. *J. Physiol.* 590, 4465–4481. doi: 10.1113/jphysiol.2012.231886

Olivotto, I., Cecchi, F., Poggesi, C., and Yacoub, M. H. (2012). Patterns of disease progression in hypertrophic cardiomyopathy: an individualized approach to clinical staging. *Circ. Heart Fail.* 5, 535–546. doi: 10.1161/CIRCHEARTFAILURE.112.967026

Olivotto, I., Girolami, F., Nistri, S., Rossi, A., Rega, L., Garbini, F., et al. (2009). The many faces of hypertrophic cardiomyopathy: from developmental biology to clinical practice. *J. Cardiovasc. Transl. Res.* 2, 349–367. doi: 10.1007/s12265-009-9137-9132

Orchard, C., and Brette, F. (2008). t-Tubules and sarcoplasmic reticulum function in cardiac ventricular myocytes. *Cardiovasc. Res.* 77, 237–244. doi: 10.1093/cvr/cvm002

Parikh, A., Mantravadi, R., Kozhevnikov, D., Roche, M. A., Ye, Y., Owen, L. J., et al. (2012). Ranolazine stabilizes cardiac ryanodine receptors: a novel mechanism for the suppression of early afterdepolarization and torsades de pointes in long QT type 2. *Heart Rhythm* 9, 953–960. doi: 10.1016/j.hrthm.2012.01.010

Passini, E., Minchole, A., Coppini, R., Cerbai, E., Rodriguez, B., Severi, S., et al. (2016). Mechanisms of pro-arrhythmic abnormalities in ventricular repolarisation and anti-arrhythmic therapies in human hypertrophic cardiomyopathy. *J. Mol. Cell Cardiol.* 96, 72–81. doi: 10.1016/j.yjmcc.2015.09.003

Perchenet, L., Hinde, A. K., Patel, K. C., Hancox, J. C., and Levi, A. J. (2000). Stimulation of Na/Ca exchange by the beta-adrenergic/protein kinase A pathway in guinea-pig ventricular myocytes at 37 degrees C. *Pflugers Arch.* 439, 822–828.

Pieske, B., and Houser, S. R. (2003). [Na +]i handling in the failing human heart. *Cardiovasc. Res.* 57, 874–886. doi: 10.1016/S0008-6363(02)00841-6

Pogwizd, S. M., and Corr, P. B. (1987). Electrophysiologic mechanisms underlying arrhythmias due to reperfusion of ischemic myocardium. *Circulation* 76, 404–426. doi: 10.1161/01.CIR.76.2.404

Pogwizd, S. M., Sipido, K. R., Verdonck, F., and Bers, D. M. (2003). Intracellular Na in animal models of hypertrophy and heart failure: contractile function and arrhythmogenesis. *Cardiovasc. Res.* 57, 887–896. doi: 10.1016/S0008-6363(02)00735-6

Priori, S. G., Blomstrom-Lundqvist, C., Mazzanti, A., Blom, N., Borggrefe, M., Camm, J., et al. (2015). 2015 ESC Guidelines for the management of patients with ventricular arrhythmias and the prevention of sudden cardiac death: the task force for the management of patients with ventricular arrhythmias and the prevention of sudden cardiac death of the European Society of Cardiology (ESC). Endorsed by: Association for European Paediatric and Congenital Cardiology (AEPC). *Eur Heart J.* 36, 2793–2867. doi: 10.1093/eurheartj/ehv316

Ravens, U., and Cerbai, E. (2008). Role of potassium currents in cardiac arrhythmias. *Europace* 10, 1133–1137. doi: 10.1093/europace/eun193

Sacconi, L., Ferrantini, C., Lotti, J., Coppini, R., Yan, P., Loew, L. M., et al. (2012). Action potential propagation in transverse-axial tubular system is impaired in heart failure. *Proc. Natl. Acad. Sci. U.S.A.* 109, 5815–5819. doi: 10.1073/pnas.1120188109

Sato, D., Xie, L. H., Sovari, A. A., Tran, D. X., Morita, N., Xie, F., et al. (2009). Synchronization of chaotic early afterdepolarizations in the genesis of cardiac arrhythmias. *Proc. Natl. Acad. Sci. U.S.A.* 106, 2983–2988. doi: 10.1073/pnas.0809148106

Sequeira, V., Wijnker, P. J., Nijenkamp, L. L., Kuster, D. W., Najafi, A., Witjas-Paalberends, E. R., et al. (2013). Perturbed length-dependent activation in human hypertrophic cardiomyopathy with missense sarcomeric gene mutations. *Circ. Res.* 112, 1491–1505. doi: 10.1161/CIRCRESAHA.111.300436

Shan, J., Betzenhauser, M. J., Kushnir, A., Reiken, S., Meli, A. C., Wronska, A., et al. (2010). Role of chronic ryanodine receptor phosphorylation in heart failure and beta-adrenergic receptor blockade in mice. *J. Clin. Invest.* 120, 4375–4387. doi: 10.1172/JCI37649

Shannon, T. R., Pogwizd, S. M., and Bers, D. M. (2003). Elevated sarcoplasmic reticulum Ca2 + leak in intact ventricular myocytes from rabbits in heart failure. *Circ. Res.* 93, 592–594. doi: 10.1161/01.RES.0000093399.11734.B3

Sicouri, S., Belardinelli, L., and Antzelevitch, C. (2013). Antiarrhythmic effects of the highly selective late sodium channel current blocker GS-458967. *Heart Rhythm* 10, 1036–1043. doi: 10.1016/j.hrthm.2013.03.023

Song, L. S., Sobie, E. A., McCulle, S., Lederer, W. J., Balke, C. W., and Cheng, H. (2006). Orphaned ryanodine receptors in the failing heart. *Proc. Natl. Acad. Sci. U.S.A.* 103, 4305–4310. doi: 10.1073/pnas.0509324103

Sotgia, B., Sciagra, R., Olivotto, I., Casolo, G., Rega, L., Betti, I., et al. (2008). Spatial relationship between coronary microvascular dysfunction and delayed contrast enhancement in patients with hypertrophic cardiomyopathy. *J. Nucl. Med.* 49, 1090–1096. doi: 10.2967/jnumed.107.050138

Taggart, P., Sutton, P., Chalabi, Z., Boyett, M. R., Simon, R., Elliott, D., et al. (2003). Effect of adrenergic stimulation on action potential duration restitution in humans. *Circulation* 107, 285–289. doi: 10.1161/01.CIR.0000044941.13346.74

Terracciano, C. M., Philipson, K. D., and MacLeod, K. T. (2001). Overexpression of the Na^+/Ca^{2+} exchanger and inhibition of the sarcoplasmic reticulum Ca^{2+}-ATPase in ventricular myocytes from transgenic mice. *Cardiovasc. Res.* 49, 38–47. doi: 10.1016/S0008-6363(00)00205-4

Terrenoire, C., Clancy, C. E., Cormier, J. W., Sampson, K. J., and Kass, R. S. (2005). Autonomic control of cardiac action potentials: role of potassium channel kinetics in response to sympathetic stimulation. *Circ. Res.* 96, e25–e34. doi: 10.1161/01.RES.0000160555.58046.9a

Toischer, K., Rokita, A. G., Unsold, B., Zhu, W., Kararigas, G., Sossalla, S., et al. (2010). Differential cardiac remodeling in preload versus afterload. *Circulation* 122, 993–1003. doi: 10.1161/CIRCULATIONAHA.110.943431

Ulus, T., Kudaiberdieva, G., and Gorenek, B. (2013). The onset mechanisms of ventricular tachycardia. *Int. J. Cardiol.* 167, 619–623. doi: 10.1016/j.ijcard.2012.09.034

van der Velden, J., Ho, C. Y., Tardiff, J. C., Olivotto, I., Knollmann, B. C., and Carrier, L. (2015). Research priorities in sarcomeric cardiomyopathies. *Cardiovasc. Res.* 105, 449–456. doi: 10.1093/cvr/cvv019

Wagner, S., Dybkova, N., Rasenack, E. C., Jacobshagen, C., Fabritz, L., Kirchhof, P., et al. (2006). Ca^{2+}/calmodulin-dependent protein kinase II regulates cardiac Na^+ channels. *J. Clin. Invest.* 116, 3127–3138. doi: 10.1172/JCI26620

Wagner, S., Hacker, E., Grandi, E., Weber, S. L., Dybkova, N., Sossalla, S., et al. (2009). Ca/calmodulin kinase II differentially modulates potassium currents. *Circ. Arrhythm Electrophysiol.* 2, 285–294. doi: 10.1161/CIRCEP.108.842799

Weisser-Thomas, J., Piacentino, V. III, Gaughan, J. P., Margulies, K., and Houser, S. R. (2003). Calcium entry via Na/Ca exchange during the action potential directly contributes to contraction of failing human ventricular myocytes. *Cardiovasc. Res.* 57, 974–985. doi: 10.1016/S0008-6363(02)00732-0

Xu, L., Lai, D., Cheng, J., Lim, H. J., Keskanokwong, T., Backs, J., et al. (2010). Alterations of L-type calcium current and cardiac function in CaMKII{delta} knockout mice. *Circ. Res.* 107, 398–407. doi: 10.1161/CIRCRESAHA.110.222562

Yang, B., Lin, H., Xiao, J., Lu, Y., Luo, X., Li, B., et al. (2007). The muscle-specific microRNA miR-1 regulates cardiac arrhythmogenic potential by targeting GJA1 and KCNJ2. *Nat. Med.* 13, 486–491. doi: 10.1038/nm1569

Conflict of Interest Statement: The authors declare that the research was conducted in the absence of any commercial or financial relationships that could be construed as a potential conflict of interest.

frontiers in Physiology

REVIEW
published: 04 October 2018
doi: 10.3389/fphys.2018.01380

Calcium in the Pathophysiology of Atrial Fibrillation and Heart Failure

Nathan C. Denham, Charles M. Pearman, Jessica L. Caldwell, George W. P. Madders, David A. Eisner, Andrew W. Trafford and Katharine M. Dibb**

Unit of Cardiac Physiology, Division of Cardiovascular Sciences, Manchester Academic Health Science Centre, University of Manchester, Manchester, United Kingdom

Atrial fibrillation (AF) is commonly associated with heart failure. A bidirectional relationship exists between the two—AF exacerbates heart failure causing a significant increase in heart failure symptoms, admissions to hospital and cardiovascular death, while pathological remodeling of the atria as a result of heart failure increases the risk of AF. A comprehensive understanding of the pathophysiology of AF is essential if we are to break this vicious circle. In this review, the latest evidence will be presented showing a fundamental role for calcium in both the induction and maintenance of AF. After outlining atrial electrophysiology and calcium handling, the role of calcium-dependent afterdepolarizations and atrial repolarization alternans in triggering AF will be considered. The atrial response to rapid stimulation will be discussed, including the short-term protection from calcium overload in the form of calcium signaling silencing and the eventual progression to diastolic calcium leak causing afterdepolarizations and the development of an electrical substrate that perpetuates AF. The role of calcium in the bidirectional relationship between heart failure and AF will then be covered. The effects of heart failure on atrial calcium handling that promote AF will be reviewed, including effects on both atrial myocytes and the pulmonary veins, before the aspects of AF which exacerbate heart failure are discussed. Finally, the limitations of human and animal studies will be explored allowing contextualization of what are sometimes discordant results.

Keywords: atrial fibrillation, pathophysiology, calcium, heart failure, t-tubules

OPEN ACCESS

Edited by:
Alessandro Mugelli, Università degli Studi di Firenze, Italy

Reviewed by:
Richard Leonard Verrier, Beth Israel Deaconess Medical Center, Harvard Medical School, United States
David R. Van Wagoner, Cleveland Clinic Lerner College of Medicine, United States

****Correspondence:***
Katharine M. Dibb
Katharine.dibb@manchester.ac.uk
Nathan C. Denham
nathan.denham@manchester.ac.uk

Specialty section:
This article was submitted to Cardiac Electrophysiology, a section of the journal Frontiers in Physiology

Received: *17 July 2018*
Accepted: *11 September 2018*
Published: *04 October 2018*

Citation:
Denham NC, Pearman CM, Caldwell JL, Madders GWP, Eisner DA, Trafford AW and Dibb KM (2018) Calcium in the Pathophysiology of Atrial Fibrillation and Heart Failure. Front. Physiol. 9:1380. doi: 10.3389/fphys.2018.01380

INTRODUCTION

Two highly prevalent forms of cardiovascular disease are atrial fibrillation (AF) and heart failure, and in spite of recent advances in treatment these conditions remain important causes of morbidity and mortality. AF is an abnormal heart rhythm affecting more than 30 million patients worldwide (Chugh et al., 2014), and is characterized by rapid and disorganized electrical activity within the cardiac atria (Kirchhof et al., 2016). This results in the loss of atrial contraction, irregular ventricular contractions, and has a detrimental effect on the lives of those who suffer from it ranging from a reduction in day-to-day quality of life secondary to symptoms such as palpitations and exercise intolerance (Thrall et al., 2006), and an increased risk of heart failure (Stewart et al., 2002), stroke (Wolf et al., 1991), and premature death (Benjamin et al., 1998). Heart failure is defined as the presence of symptoms such as breathlessness resulting from cardiac structural or functional abnormalities that in general cause impaired contraction and/or relaxation of the myocardium (Ponikowski et al., 2016). This life-threatening condition affects 1–2% of the general population in the developed world (Mosterd and Hoes, 2007), and carries higher mortality rates than many

cancers (Mamas et al., 2017). Of increasing importance is the bidirectional relationship between AF and heart failure. To put it simply, those with AF are more likely to develop heart failure and vice versa.

Heart failure occurs in up to one third of patients with AF (Santhanakrishnan et al., 2016), which may be as a direct result of rapid ventricular rates in AF [known as a tachycardia-induced cardiomyopathy (Fujino et al., 2007)] or the association of risk factors common to both conditions such as hypertension (Benjamin et al., 1994; Levy et al., 1996). If heart failure occurs in those with AF, the patient is likely to face an increased burden of symptoms, more admissions to hospital and a lower chance of restoring sinus rhythm (Silva-Cardoso et al., 2013; Odutayo et al., 2017). On the other hand, in those who initially have a normal cardiac rhythm, heart failure is associated with a 5-fold increase in the risk of developing new AF (Benjamin et al., 1994) due to electrical and structural remodeling in the atria (Nattel et al., 2007; Nattel and Harada, 2014), which can also increase rates of hospitalization, stroke, and death (Dries et al., 1998; McManus et al., 2013; Odutayo et al., 2017).

Disordered calcium handling is a key link in the bidirectional relationship between AF and heart failure and it is the aim of this review to provide the reader with an up-to-date overview of this important topic. We will start by exploring the role of calcium in excitation-contraction coupling in healthy atria followed by an overview of the general mechanisms of arrhythmias. While the effects of AF on calcium handling have been reviewed recently e.g., Dobrev and Wehrens (2017) and Landstrom et al. (2017), here we focus firstly on the pathological remodeling of calcium handling which determines the progression of AF from short-lived paroxysms to longer durations of persistent AF. To achieve this, we have attempted to stratify studies in terms of the stage of AF (from early remodeling to persistent AF). Secondly, we examine how heart failure promotes AF with an emphasis on calcium cycling in the atria, providing an insight into the fundamental changes which drive both conditions, including the role played by t-tubules. In addition, we describe the mechanisms by which AF exacerbates heart failure, and how a vicious circle can be generated. Finally, this review provides a critical appraisal of both human and animal studies in this field, to highlight limitations that should influence future research.

CALCIUM, EXCITATION-CONTRACTION COUPLING, AND ARRHYTHMIAS

To appreciate the association between AF, heart failure, and disturbances in calcium handling, we must first understand the role of calcium in excitation contraction coupling in healthy atrial tissue. The action potential is initiated by the rapid influx of sodium (I_{Na}) resulting in membrane depolarization. The shape of the atrial action potential differs from that of the ventricle, at least in larger species, where generally the atrial action potential is shorter and more triangulated (Hume and Uehara, 1985; Giles and Imaizumi, 1988; Amos et al., 1996; Xu et al., 1999) as reviewed in Nerbonne and Kass (2005). Depolarization activates L-type calcium channels (LTCCs) allowing a small amount of calcium to enter the cell. ($I_{Ca(L)}$) (Bers, 2002; Eisner et al., 2017).

As in ventricular myocytes, a small influx of calcium via $I_{Ca(L)}$ triggers the release of a larger quantity of calcium from the sarcoplasmic reticulum (SR) into the cytoplasm via ryanodine receptors (RyRs) in a process known as calcium-induced calcium release (CICR; **Figure 1A**) (Bers, 2002; Eisner et al., 2017). It is important to mention that although this process is mechanistically similar, the relative contributions of the individual components differ (Walden et al., 2009).

CICR is rapid and in the healthy ventricle occurs near-simultaneously throughout the cell due to two main factors. Firstly, LTCCs on the cell membrane and RyRs on the SR membrane associate closely to form dyads allowing efficient triggering of calcium release. Secondly, deep invaginations of the surface membrane known as transverse (t)-tubules allow dyads to occur not only at the cell periphery but throughout the cell interior, such that calcium rises in a more synchronous manner in ventricular myocytes (**Figure 1A**). Calcium release is not completely synchronous in atrial cells as there are fewer t-tubules than in ventricular myocytes (Dibb et al., 2009; Caldwell et al., 2014), and their abundance changes with cell width, species, and location in the atria (Richards et al., 2011; Frisk et al., 2014; Glukhov et al., 2015; Gadeberg et al., 2016). These factors likely contribute to the diversity of atrial t-tubule density reported, particularly in small mammalian species, where t-tubules are either lacking (Huser et al., 1996; Brette et al., 2002), sparse, and often longitudinally orientated (Kirk et al., 2003; Woo et al., 2005) or can be more abundant (Frisk et al., 2014; Glukhov et al., 2015). It is generally well established that atrial t-tubules are common in large mammalian species e.g., sheep, cow, horse, dog, and pig although t-tubule levels are heterogeneous between cells and species (Wakili et al., 2010; Richards et al., 2011; Frisk et al., 2014; Gadeberg et al., 2016). Since many of these species are used as models of AF it is important that atrial t-tubule levels mimic those found in the human. T-tubules have been shown to be present to some extent in almost 70% of human atrial cells (Richards et al., 2011) although only sparse t-tubules have been reported in isolated human atrial cells (Greiser et al., 2014). Differences between studies may arise due to t-tubule damage, suggested to occur as a result of enzymatic digestion (Chen et al., 2015), or to differences in the underlying pathophysiology of patient samples and therefore the reliance of systolic calcium on human atrial t-tubules is not well understood.

Following the release of calcium from the SR, free intracellular calcium is then available to bind to troponin C, causing myocyte contraction. Relaxation is brought about by the removal of calcium from the cytosol which occurs via two main mechanisms: reuptake into the SR by the sarcoplasmic reticulum calcium ATPase pump (SERCA) regulated by the inhibitory proteins phospholamban and sarcolipin, and removal from the cell via the sodium-calcium exchanger (NCX) on the plasma membrane (**Figure 1A**). Minor contributions to calcium removal come from the plasma membrane calcium ATPase pump and the mitochondrial

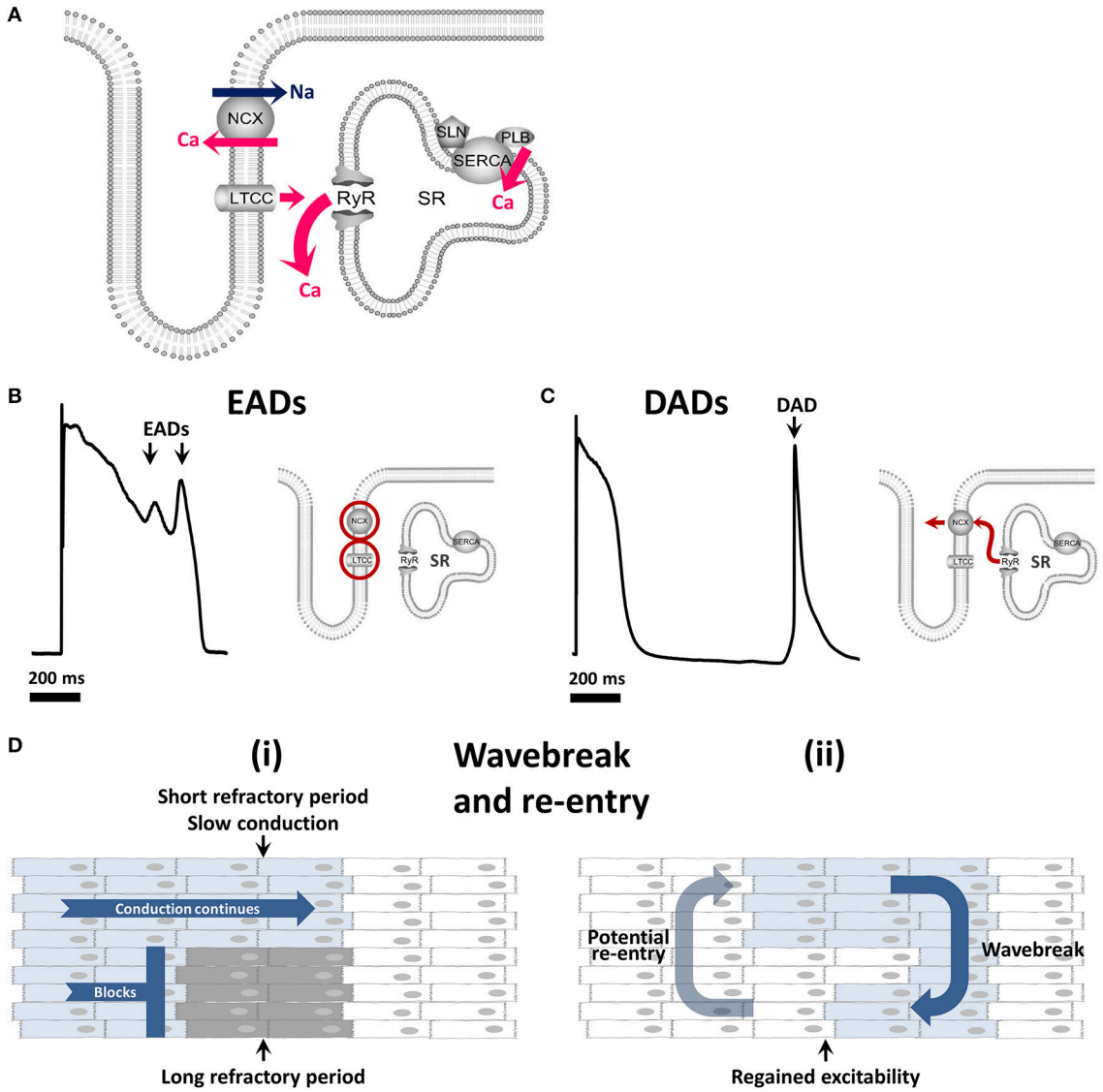

FIGURE 1 | Calcium cycling and mechanisms of arrhythmia. **(A)** The role of the calcium cycling mechanism in calcium induced calcium release **(B)** Early afterdepolarizations arise through reactivation of $I_{Ca(L)}$ and / or I_{Na} and are facilitated by I_{NCX}. **(C)** Delayed afterdepolarizations arise through spontaneous calcium release from the sarcoplasmic reticulum. **(D)** (i) Wavebreak occurs when a smooth depolarizing wave front encounters an area of inexcitable tissue (ii) which may progress to re-entry whereby the depolarizing wave continues to rotate around an inexcitable core. EAD, early afterdepolarization; DAD, delayed afterdepolarization; LTCC, L-type calcium channel; RyR, ryanodine receptor; SR, sarcoplasmic reticulum; NCX, sodium/calcium exchanger; SERCA, sarco-endoplasmic reticulum calcium ATPase.

calcium uniporter. When free cytoplasmic calcium falls, it dissociates from troponin C, bringing about relaxation during the diastolic phase of the action potential (phase 4) (Bers, 2001).

In the steady state, calcium influx and efflux are maintained in balance. Any increase in calcium influx e.g., during beta adrenergic stimulation, is met by a corresponding increase in calcium efflux (Trafford et al., 1997; Eisner et al., 2013). Under normal conditions, this ensures cells do not become overloaded with calcium. SR calcium content can be increased but only if influx exceeds efflux until a new steady state of influx and efflux is achieved (Trafford et al., 1997). In conditions such as AF and heart failure, pathological remodeling of calcium handling can promote arrhythmias.

The Basis of Arrhythmias

Like all tachyarrhythmias, the onset and maintenance of AF is dependent on three key mechanisms: automaticity, triggered activity, and re-entry (Antzelevitch and Burashnikov, 2011). Automaticity, whereby an excitable tissue spontaneously depolarizes, is an inherent property of the specialized tissue

within the cardiac conduction system. Abnormal automaticity occurs when an area outside the conduction system becomes capable of automatic activity faster than the leading pacemaker site, or less commonly when disease accelerates the firing rate of nodal tissue.

Triggered activity refers to additional impulses triggered by an initial action potential, known as afterdepolarizations. Although several mechanisms can lead to afterdepolarizations, many of these relate to abnormalities in calcium handling. There are two types of afterdepolarization termed "early" or "delayed" afterdepolarizations. Early afterdepolarizations (EADs; **Figure 1B**), occur within the action potential (phases 2–3) and may arise from reactivation of $I_{Ca(L)}$ or spontaneous calcium release (Qi et al., 2009) driving reverse mode I_{NCX} as reviewed by Weiss et al. (2010). Delayed afterdepolarizations (DADs; **Figure 1C**), occurring after the action potential (within phase 4) arise from spontaneous calcium release from the SR in the form of a calcium wave (Venetucci et al., 2008). This spontaneous calcium transient leaves the cell via NCX in exchange for sodium, creating a transient inward current (I_{ti}). If the depolarizations induced by EADs or DADs are large enough they may lead to one or more additional premature action potentials.

Both normal and arrhythmogenic calcium release from the SR occurs via RyRs. Calcium sparks are the elementary calcium release events of the SR which occur when RyRs within a cluster open (Cheng et al., 1993; Rajagopal et al., 2015; Walker et al., 2015). Under conditions of increased calcium loading, spark frequency increases and calcium sparks are able to trigger propagating calcium waves (Cheng et al., 1993). Therefore calcium waves occur when the SR reaches a threshold calcium content (Diaz et al., 1997; Venetucci et al., 2007). The calcium release kinetics of the RyR can be modified by phosphorylation at the protein kinase A site or at the CaMKII site resulting in increased RyR calcium sensitivity and open probability (Wehrens et al., 2004; Vest et al., 2005; Huke and Bers, 2008). In addition, accessory proteins such as junctophilin (Beavers et al., 2013), FKBP-12.6 (Marx et al., 2000), calsequestrin, triadin, and junctin (Gyorke et al., 2004) can all modulate RyR open probability.

The third main arrhythmic mechanism is re-entry whereby waves of depolarization circle around an obstacle, continuously reinitiating in the manner of a dog chasing its tail (**Figure 1D**). This obstacle may be anatomical, such as scar tissue, but functional obstacles such as a core of tissue rendered inexcitable by continuous depolarization can also permit re-entry. This functional re-entry is of particular importance in AF (Allessie et al., 1977; Comtois et al., 2005).

These fundamental mechanisms feed into several models of AF including the classical model of multiple re-entrant circuits continually forming and extinguishing (Allessie et al., 1996) and the more recent view of one or more primary re-entrant drivers or rotors which break down to fibrillatory conduction at the peripheries (Berenfeld and Jalife, 2014). A discussion on the merits of these models can be found elsewhere (Allessie and de Groot, 2014; Narayan and Jalife, 2014).

THE PATHOPHYSIOLOGY OF ATRIAL FIBRILLATION

The Natural History of Atrial Fibrillation

In many patients who are otherwise free from cardiovascular disease, AF is first seen as short bursts of fibrillation that last from minutes to hours before reverting spontaneously to a normal sinus rhythm in a pattern known as paroxysmal AF (Kirchhof et al., 2016). These bursts are initiated by electrical impulses known as triggers, most commonly arising from the pulmonary veins (Haissaguerre et al., 1998). Over time, the frequency and duration of AF tends to increase until eventually the arrhythmia becomes both continuous and self-sustaining (Gillis and Rose, 2000), and is known as persistent AF. The electrical properties and structure of the atria that determine how well the atria support AF are together known as the atrial substrate. The increasing tendency to AF occurs due to changes in the atrial substrate brought about by the rapid stimulation of the atria during bouts of AF, and are summed up by the phrase "AF begets AF" (Wijffels et al., 1995). However, the stepwise progression from paroxysmal to persistent AF is not universal, as those who have structural heart disease such as heart failure may have developed a pro-arrhythmic substrate before AF arises, and may therefore immediately present with persistent AF (Leclercq et al., 2014). Dysregulation of calcium is involved both in the triggering of AF, and the progression of the atrial substrate that facilitates AF. In this section, we aim to describe the time course of key changes in calcium cycling with regard to the stage of AF, highlighting not only how "calcium cycling remodeling begets further remodeling" but what may drive the atria down this path rather than be bystander effects.

What Triggers Atrial Fibrillation?

In patients with "lone AF," the early stages of the disease are predominantly due to abnormally frequent triggering impulses. In humans, the commonest sites for triggers are the pulmonary veins from which rapid electrical activity can both initiate and sustain AF (Oral et al., 2002). The pulmonary veins are estimated to be the source of triggers in $\sim$ 90% of patients with paroxysmal AF. This has led to the development of ablation therapy which aims to electrically isolate the pulmonary veins from the left atrium and thereby prevent triggers from reaching the myocardium (Haissaguerre et al., 1998). Although triggers can arise from other areas of the atria such as the left atrial appendage (Santangeli et al., 2016), the key role of the pulmonary vein sleeves is supported by mechanistic studies demonstrating features that predispose these tissues to abnormal firing (Arora et al., 2003).

The myocytes which extend up the pulmonary vein sleeves can fire independently (Perez-Lugones et al., 2003), potentially due to automaticity, triggered activity, and micro re-entry [as reviewed in Takahara et al. (2014)]. These myocytes are electrophysiologically distinct from those in the atria. For example canine pulmonary vein sleeves display both decreased I_{K1} and $I_{Ca(L)}$ but increased delayed rectifier currents compared to atrial myocardium (Ehrlich et al., 2003). The net effect of these differences is a shorter action potential duration and less negative

resting membrane potential which together facilitate calcium-dependent afterdepolarizations and triggered activity (Patterson et al., 2006).

The automaticity and triggered activity seen in pulmonary vein myocytes may be calcium dependent, as some studies report asynchronous spontaneous calcium transients in myocytes in intact pulmonary veins (Chou et al., 2005; Logantha et al., 2010; Rietdorf et al., 2014). Some have found that these spontaneously active cells have higher SR calcium content and a corresponding increase in the frequency of calcium sparks compared to atrial myocytes which could contribute to these spontaneous events (Chang et al., 2008). However, spontaneous pulmonary vein activity has not been found in all studies, and the calcium handling properties of canine pulmonary vein myocytes are generally unaltered compared to those from the atria (Hocini et al., 2002; Perez-Lugones et al., 2003; Coutu et al., 2006). Increased firing from the veins has been reported during periods of tachycardia (Chen et al., 2000; Honjo et al., 2003) and during rapid changes in autonomic tone (Zimmermann and Kalusche, 2001; Tomita et al., 2003; Patterson et al., 2005) due to an increase in the predisposition to calcium-dependent afterdepolarizations at these times.

In addition to the electrophysiological and calcium handling differences, the anatomy of the veins also promotes re-entry due to the combination of abrupt changes in fiber orientation and reduced electrical connectivity between muscle bundles creating areas of heterogeneous conduction velocity and localized block (Hocini et al., 2002; Arora et al., 2003). Calcium may also play a role in the propagation of triggered impulses from the pulmonary veins to the atria via small conductance calcium-activated potassium channels. Rapid stimulation increases the expression of these channels and shortens the action potential in the pulmonary veins. However, the effect of blocking these channels is unclear as both pro-arrhythmic (Hsueh et al., 2013) and antiarrhythmic effects (Ozgen et al., 2007; Qi et al., 2014) have been described.

Taken together, the available evidence supports a greater propensity for the pulmonary veins to generate spontaneous activity although the precise mechanism is controversial.

What Makes an Atrial Substrate Vulnerable to Atrial Fibrillation?

The atrial substrate refers to the sum of all atrial characteristics that influence how readily the atria support fibrillation. In response to triggering impulses, a healthy atrial substrate may generate fibrillation that extinguishes after a very short period, or may not support fibrillation at all. On the other hand, a diseased, remodeled and thence vulnerable atrial substrate will often manifest prolonged fibrillation in response to the same triggering impulses (Sanders et al., 2003; Cha et al., 2004a; Todd et al., 2004). The atrial substrate changes over time and in response to high atrial rates as seen during fibrillation, in part mediated by intracellular calcium.

Many of the characteristics that contribute to the vulnerability of the atrial substrate can be understood using the classical multiple-wavelet paradigm of AF in which AF results from many wavelets following re-entrant circuits that continuously form and extinguish in a chaotic manner (Moe et al., 1964). The size of these wavelets is a product of the conduction velocity of the tissue and the effective refractory period (ERP), referred to as the wavelength. The atrial ERP is primarily determined by the action potential duration (Bode et al., 2001). Atrial tissue with properties that support a shorter wavelength exhibit wavelets that rotate around a smaller volume of tissue (Zou et al., 2005). In this model, AF terminates when all wavelets have extinguished at a single time-point, which becomes increasingly unlikely the more wavelets the atria can sustain.

Structural aspects of the atria therefore influence atrial vulnerability. Larger atria as found in heart failure can sustain more wavelets simultaneously, and are therefore more vulnerable to AF (Sridhar et al., 2009; Melenovsky et al., 2015). Fibrosed atria, arising as a consequence of heart failure (Li et al., 1999) or obesity (Fukui et al., 2013), conduct electrical impulses more slowly, leading to a shorter wavelength and allowing more re-entrant circuits to co-exist in a given mass of tissue (Van Wagoner and Nerbonne, 2000). Electrophysiological properties such as the atrial refractory period also feed into to this model as a shorter action potential (and thus shorter refractory period) leads to a shorter wavelength permitting a greater number of re-entrant wavelets and facilitating AF. Mechanisms to shorten action potential duration include a decrease in $I_{Ca(L)}$, decreased forward mode I_{NCX} or an increase in potassium currents (Johannsson and Wohlfart, 1980; Fermini and Schanne, 1991; Viswanathan et al., 1999; Armoundas et al., 2003). To generate these wavelets, the normally smooth and regular waves of depolarization traversing the atria must be disrupted (Zhao et al., 2013). Wavebreak occurs when a wavefront can pass in one region of tissue but is blocked in an adjacent region, causing the wavefront to begin to rotate. This wavebreak is more likely to occur if the refractory periods of the atrial tissue differ markedly from region to region, referred to as a dispersion of repolarization (Allessie et al., 1977). While this dispersion can be fixed, an important dynamic determinant of the dispersion of repolarization is action potential alternans, often driven by calcium dynamics.

Action potential alternans refers to a phenomenon whereby a single cell or region of tissue generates action potentials in a repeated long-short-long-short pattern when stimulated, as reviewed by (Weiss et al., 2011). As this alternating sequence passes through the myocardial tissue, it creates a discordant pattern whereby at a single point in time the action potentials in some regions will be short but in neighboring regions will be long. If a premature triggering impulse occurs, it may potentially block in regions with long action potentials but continue to conduct where action potentials are short, creating wavebreak and re-entry. In this context therefore atrial alternans acts as a substrate for AF. Although action potential alternans can arise from properties of the sarcolemmal ion channels, it can also be driven by instabilities in calcium handling (Eisner et al., 2005). Alternating calcium transient amplitudes can occur due to high stimulation rates, elevated SR calcium content, and alterations to RyR refractoriness, as reviewed by Qu et al. (2013). These then lead to alternation of the action potential: large transients increase calcium-dependent inactivation of $I_{Ca(L)}$ and enhance calcium efflux through NCX, simultaneously shortening

the plateau of the action potential and extending terminal repolarisation, while small calcium transients produce a longer plateau but shorter terminal repolarization. Atrial alternans can be measured in patients using standard electrophysiological catheters and correlates with vulnerability to AF (Verrier et al., 2016). It has been shown to track the progression of AF in a sheep tachypacing model, to precede the transition from atrial flutter to fibrillation in man, and to occur more frequently in the atria of patients with AF than those without (Narayan et al., 2002, 2008, 2011; Monigatti-Tenkorang et al., 2014).

Another calcium-dependent aspect of the vulnerability of the atrial substrate to AF is calcium loading of the cell during brief periods of rapid atrial stimulation. When the atria are exposed to rapid rates such as triggers from the pulmonary veins, or artificially from rapid pacing, there is a net influx of calcium into the cell via the more frequently activated $I_{Ca(L)}$ (Sun et al., 2001). This is presumably primarily driven by the increased stimulation rate increasing influx per unit time because with increasing rates, calcium entry via $I_{Ca(L)}$ decreases per beat (Dibb et al., 2007). This increased influx of calcium leads to increased reuptake via SERCA, loading the SR. A new steady state of calcium flux is created at a higher SR calcium content when an increase in the fractional release of calcium during the transient enables sufficient efflux to balance the increased influx. The higher SR calcium content also increases the frequency of RyR opening during diastole promoting a greater I_{ti} and increasing the probability of inducing an afterdepolarization (Cheng, H. et al., 1996). Triggers therefore produce immediate pro-arrhythmogenic changes in the atrium encouraging calcium-dependent afterdepolarizations (Ferrier et al., 1973; Terracciano et al., 1995; Santiago et al., 2013) leading to additional action potentials (Burashnikov and Antzelevitch, 2003), further increasing the atrial rate and calcium influx into the cell.

Calcium handling is additionally remodeled as a consequence of t-tubule loss which is evident following 7 days of atrial pacing (Wakili et al., 2010) (classified in **Table 1** as paroxysmal AF), during persistent AF (Lenaerts et al., 2009) and during heart failure induced by both rapid ventricular pacing (Dibb et al., 2009) and myocardial infarction (Kettlewell et al., 2013). An overview of all changes can be observed in **Figure 2**. While t-tubule loss occurs as a consequence of AF, it may also either facilitate AF occurrence in heart failure or arrhythmia progression (in the absence of heart failure) by a number of the mechanisms discussed above. Electrically, t-tubule loss, at least in the ventricle, decreases the duration of the action potential (Brette et al., 2006) and if a similar phenomenon occurs in the atria then t-tubule loss may exacerbate action potential shortening in AF and shorten the atrial refractory period. Loss of t-tubular $I_{Ca(L)}$ likely contributes to action potential shortening (Brette et al., 2006) and also promotes the decrease in $I_{Ca(L)}$ (Lenaerts et al., 2009) which is a hallmark feature of AF.

Structurally, the loss or remodeling of t-tubules results in RyRs becoming "orphaned" and producing dyssyncronous calcium sparks which may promote calcium dependant arrhythmias in the ventricle (Song et al., 2006). However the role of orphaned ventricular RyRs is unclear since in dyssyncronous heart failure loss of t-tubules from the cell ends is associated with higher RyR density and a decrease in calcium sparks (Li et al., 2015). While orphaned RyRs will inevitably arise following atrial t-tubule loss, whether they promote atrial arrhythmias has not yet been shown. It is well known that t-tubule loss reduces the synchrony of ventricular calcium release (Louch et al., 2006; Heinzel et al., 2008) which is aggravated by failed action potential propagation into remodeled t-tubules (Sacconi et al., 2012). Similarly, in the atria, t-tubule loss is associated with impaired calcium release in the cell interior (Dibb et al., 2009; Lenaerts et al., 2009; Wakili et al., 2010). Both orphaned RyRs and heterogeneous calcium release have been suggested to contribute to the increased alternans susceptibility which computer models predict to occur due to t-tubule disruption and loss (Li Q. et al., 2012; Nivala et al., 2015) providing a mechanism by which t-tubule associated changes in calcium handling may facilitate AF.

How do the Atria Respond to Excess Calcium Influx Acutely?

Rapid atrial stimulation by triggering impulses increases cellular calcium loading in the atria (Sun et al., 2001). It might be expected that the heart would have a mechanism to protect itself against rapid stimulation that would otherwise cause uncontrolled calcium overload, and this could be achieved by reducing calcium influx or increasing calcium efflux. To explore whether such a mechanism does indeed exist, animal models of short-term rapid atrial pacing have been used. One adaptive mechanism that has recently come to light is calcium signal silencing (Greiser et al., 2014) which affects both calcium influx and efflux.

Calcium influx is primarily determined by $I_{Ca(L)}$ which is decreased in the early stages of rapid atrial pacing both in terms of current density and LTCC expression (**Table 1**). Studies investigating rapid pacing (up to 7 days duration) show a progressive reduction in $I_{Ca(L)}$ (Bosch et al., 2003; Qi et al., 2008) with decreased mRNA encoding the alpha subunit of the LTCC seen after just 24 h (Bosch et al., 2003). The downregulation in mRNA transcription is believed to be mediated by the acute increase in intracellular calcium acting via the calcium calmodulin-calcineurin-NFAT pathway to help keep cells in calcium balance (Qi et al., 2008).

Calcium efflux is also increased in these early stages of tachypacing. This occurs via an increase in NCX current for a given level of intracellular calcium as opposed to any change in NCX expression (Greiser et al., 2014). Taken alone this might be expected to increase both action potential duration and DADs via increased I_{ti}, depolarizing the sarcolemma reaching the threshold for triggering additional action potentials, however, neither of these occur. Signal silencing firstly involves shortening of the action potential where presumably factors which include decreased $I_{Ca(L)}$ offset any increase in I_{NCX}. Secondly, the rate of arrhythmogenic calcium release in the form of sparks is unaltered since increased I_{NCX} is balanced by protective changes such as decreased RyR expression and

TABLE 1 | A table showing all studies which have investigated changes in calcium cycling in the atrium in either the various stages of atrial fibrillation (**AF**) or in heart failure with a reduced ejection fraction.

		Early	pAF	PerAF	Heart failure
Sarcoplasmic Reticulum Calcium Content		↑ Sun et al., 2001 ↔ Greiser et al., 2014	↑ Voigt et al., 2014 ↔ Hove-Madsen et al., 2004 ↓ Greiser et al., 2009; Wakili et al., 2010	↔ Kneller et al., 2002; Lenaerts et al., 2009; Neef et al., 2010; Voigt et al., 2012; Macquaide et al., 2015	↑ Yeh et al., 2008; Clarke et al., 2015; Aistrup et al., 2017 ↓ Saba et al., 2005; Johnsen et al., 2013
LTCC and $I_{Ca(L)}$	*α1 subunit mRNA*	↓ Bosch et al., 2003	↓ Brundel et al., 2001 ↔ Brundel et al., 1999	↓ Brundel et al., 1999; Lai et al., 1999; Van Gelder et al., 1999; Yue et al., 1999; van der Velden et al., 2000b; Gaborit et al., 2005	–
	α1 subunit protein expression	–	↓ Brundel et al., 2001; Lugenbiel et al., 2015 ↔ Brundel et al., 1999	↓ Brundel et al., 1999; Klein et al., 2003; Lenaerts et al., 2009 ↔ Schotten et al., 2003b; Christ et al., 2004 ↑ Dai et al., 2016	↔ Ouadid et al., 1995; Boixel et al., 2001
	$I_{Ca(L)}$ *density*	↓ Bosch et al., 2003; Qi et al., 2008; Greiser et al., 2014	↓ Yagi et al., 2002; Cha et al., 2004a; Wakili et al., 2010 ↔ Voigt et al., 2014	↓ Yue et al., 1997; Van Wagoner et al., 1999; Workman et al., 2001; Yagi et al., 2002; Christ et al., 2004; Lenaerts et al., 2009; Voigt et al., 2012 ↑ (single channel only) Klein et al., 2003	↓ Ouadid et al., 1995; Li et al., 2000; Boixel et al., 2001; Cha et al., 2004a,b; Dinanian et al., 2008; Sridhar et al., 2009; Clarke et al., 2015 ↔ Cheng T. H. et al., 1996; Workman et al., 2009
SERCA and accessory proteins	*SERCA2A mRNA*	–	↔ Brundel et al., 1999	↓ Brundel et al., 1999; Lai et al., 1999; Ohkusa et al., 1999; Cao et al., 2002 ↔ Van Gelder et al., 1999	–
	SERCA protein expression	↓ Greiser et al., 2014	↓ Voigt et al., 2014; Lugenbiel et al., 2015; Wang et al., 2017 ↔ Brundel et al., 1999; Wakili et al., 2010	↔ Hoit et al., 2002; Schotten et al., 2002; El-Armouche et al., 2006; Lenaerts et al., 2009; Neef et al., 2010; Dai et al., 2016 ↓ Brundel et al., 1999	↔ Shanmugam et al., 2011; Clarke et al., 2015 ↓ Yeh et al., 2008
	SERCA function	–	↑ Xie et al., 2012; Voigt et al., 2014	↑ Shanmugam et al., 2011 ↔ Kneller et al., 2002 ↓ Voigt et al., 2012	↓ Yeh et al., 2008; Johnsen et al., 2013; Clarke et al., 2015; Hohendanner et al., 2016
	PLB mRNA	–	–	↔ Lai et al., 1999; Van Gelder et al., 1999 ↓ Gaborit et al., 2005	–
	PLB protein expression	↔ Greiser et al., 2014	↔ Brundel et al., 1999; Voigt et al., 2014	↔ Brundel et al., 1999; Schotten et al., 2002; Uemura et al., 2004; El-Armouche et al., 2006; Lenaerts et al., 2009; Neef et al., 2010 ↓ Hoit et al., 2002	↔ Yeh et al., 2008; Shanmugam et al., 2011; Clarke et al., 2015
	PLB phosphorylation (Ser16)	↔ Greiser et al., 2014	↓ Greiser et al., 2009; Lugenbiel et al., 2015 ↑ Voigt et al., 2014	↑ El-Armouche et al., 2006; Dai et al., 2016 ↔ Lenaerts et al., 2009	↓ Shanmugam et al., 2011
	PLB phosphorylation (Thr17)	↔ Greiser et al., 2014	↔ Voigt et al., 2014 ↑ Chelu et al., 2009 ↓ Lugenbiel et al., 2015	↑ El-Armouche et al., 2006 ↔ Neef et al., 2010	↑ Yeh et al., 2008; Clarke et al., 2015
	Sarcolipin mRNA	–	–	↓ Uemura et al., 2004	–

(Continued)

TABLE 1 | Continued

		Early	pAF	PerAF	Heart failure
	Sarcolipin protein expression	–	↓ Xie et al., 2012	↓ Shanmugam et al., 2011	↓ Shanmugam et al., 2011
RyR	*RyR mRNA*	–	↔ Brundel et al., 1999	↔ Brundel et al., 1999; Lai et al., 1999	–
				↓ Ohkusa et al., 1999	
	RyR protein expression	↓ Greiser et al., 2014	↑ Voigt et al., 2014	↓ Ohkusa et al., 1999; Lenaerts et al., 2009; Neef et al., 2010	↔ Yeh et al., 2008; Shanmugam et al., 2011
			↔ Brundel et al., 1999; Wakili et al., 2010	↔ Brundel et al., 1999; Schotten et al., 2002; Voigt et al., 2012	↓ Brandenburg et al., 2016
				↑ Dai et al., 2016	
	RyR phosphorylation (Ser2808)	↑ Greiser et al., 2014	↔ Chelu et al., 2009; Wakili et al., 2010; Chiang et al., 2014b; Voigt et al., 2014	↑ Vest et al., 2005; Voigt et al., 2012	↑ Brandenburg et al., 2016
			↑ Li et al., 2014		
			↓ Lugenbiel et al., 2015		↓ Yeh et al., 2008
	RyR phosphorylation (Ser2814)	↓ Greiser et al., 2014	↑ Chelu et al., 2009; Greiser et al., 2009; Chiang et al., 2014b	↑ Neef et al., 2010; Voigt et al., 2012	↔ Yeh et al., 2008; Brandenburg et al., 2016
			↔ Wakili et al., 2010; Voigt et al., 2014; Lugenbiel et al., 2015		
	Single channel open probability	–	↑ Beavers et al., 2013; Chiang et al., 2014b; Voigt et al., 2014	↑ Vest et al., 2005; Neef et al., 2010; Voigt et al., 2012; Macquaide et al., 2015	–
				↔ Lenaerts et al., 2009	
NCX	*NCX mRNA*	–	↔ Brundel et al., 1999	↔ Brundel et al., 1999; Van Gelder et al., 1999; Yue et al., 1999; Uemura et al., 2004	–
	NCX protein expression	↔ Greiser et al., 2014	↔ Brundel et al., 1999; Wakili et al., 2010; Voigt et al., 2014	↑ Schotten et al., 2002; El-Armouche et al., 2006; Lenaerts et al., 2009; Voigt et al., 2012	↑ Li et al., 2000
			↑ Lugenbiel et al., 2015	↔ Brundel et al., 1999; Hoit et al., 2002	
	I_{ti}	↑ Greiser et al., 2014	↔ Cha et al., 2004a; Wakili et al., 2010; Voigt et al., 2014	↑ Lenaerts et al., 2009; Voigt et al., 2012	↑ Li et al., 2000; Cha et al., 2004a,b; Johnsen et al., 2013; Hohendanner et al., 2015, 2016
				↔ Kneller et al., 2002	↓ Clarke et al., 2015
Calcium Transient Amplitude		↓ Sun et al., 1998; Greiser et al., 2014	↔ Voigt et al., 2014	↓ Schotten et al., 2002; Lenaerts et al., 2009; Voigt et al., 2012	↓ Saba et al., 2005; Bonilla et al., 2014; Clarke et al., 2015
		↔ Wakili et al., 2010		↑ Yeh et al., 2008; Hohendanner et al., 2016	
Afterdepolarizations	*Spark and wave frequency*	↔ Greiser et al., 2014	↑ Hove-Madsen et al., 2004; Sood et al., 2008; Chelu et al., 2009; Li N. et al., 2012; Shan et al., 2012; Beavers et al., 2013; Chiang et al., 2014a,b; Faggioni et al., 2014; Li et al., 2014; Voigt et al., 2014	↑ Neef et al., 2010; Voigt et al., 2012; Purohit et al., 2013; Macquaide et al., 2015	↑ Saba et al., 2005; Yeh et al., 2008; Johnsen et al., 2013; Hohendanner et al., 2015, 2016; Aistrup et al., 2017
	EADs	–	↑ Burashnikov and Antzelevitch, 2003	–	–
	DADs	–	↑ Li N. et al., 2012; Chiang et al., 2014a; Faggioni et al., 2014; Li et al., 2014; Voigt et al., 2014	↑ Voigt et al., 2012; Purohit et al., 2013	Yeh et al., 2008; Hohendanner et al., 2015, 2016; Aistrup et al., 2017

Early = Animal models with <7 days atrial tachycardia pacing. pAF (paroxysmal atrial fibrillation) = Animal models with 7–28 days of atrial tachycardia pacing OR a genetically modified mouse model of AF OR a human study detailing paroxysmal AF in the baseline characteristics. PerAF (persistent atrial fibrillation) = Animal models with >28 days of atrial tachycardia pacing OR human studies with either: persistent AF reported in baseline characteristics or assumed persistent in absence of description.

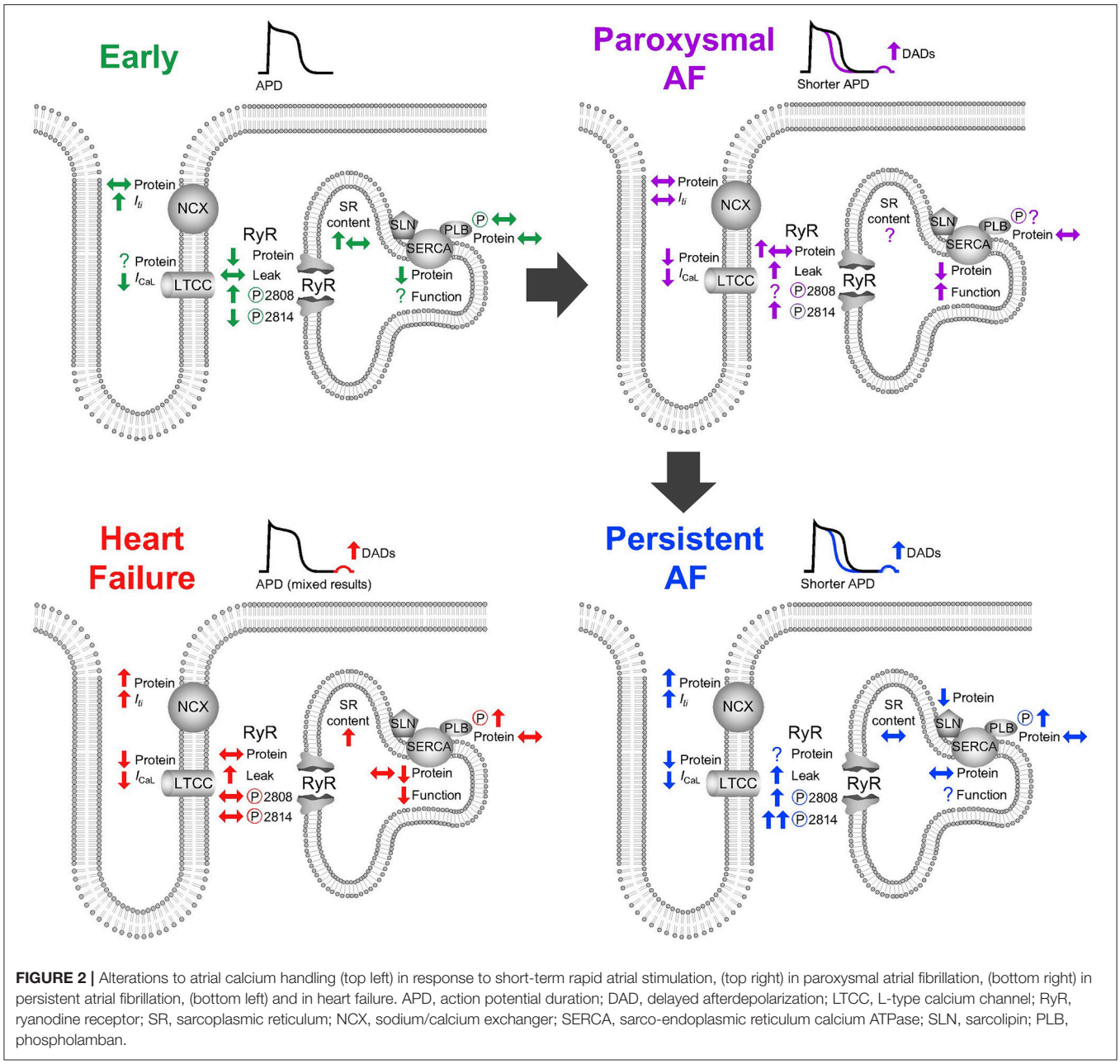

FIGURE 2 | Alterations to atrial calcium handling (top left) in response to short-term rapid atrial stimulation, (top right) in paroxysmal atrial fibrillation, (bottom right) in persistent atrial fibrillation, (bottom left) and in heart failure. APD, action potential duration; DAD, delayed afterdepolarization; LTCC, L-type calcium channel; RyR, ryanodine receptor; SR, sarcoplasmic reticulum; NCX, sodium/calcium exchanger; SERCA, sarco-endoplasmic reticulum calcium ATPase; SLN, sarcolipin; PLB, phospholamban.

reduced phosphorylation by calcium calmodulin dependent kinase two (CaMKII), decreased intracellular sodium, and increasing intracellular calcium buffering (Greiser, 2017). Overall these factors in combination with a lack of change in SR calcium content are the hallmarks of silencing that result in no observable change in calcium sparks and a reduction in calcium transient amplitude (Sun et al., 2001; Greiser et al., 2014).

Calcium signal silencing has, to the best of our knowledge, only been studied in a species where atrial t-tubules are generally absent (Greiser et al., 2014). It is therefore unknown if early t-tubule loss, as a result of rapid atrial stimulation (Wakili et al., 2010), could facilitate signal silencing by reducing central calcium release or if early t-tubule loss promotes calcium dependent arrhythmias favoring the progression from signal silencing to AF.

Which Aspects of Calcium Cycling Promote Paroxysmal Atrial Fibrillation?

Paroxysmal AF, characterized by initially short periods of self-terminating AF, can be found when the triggers for AF are present but the atrial substrate has not yet remodeled to an extent that supports persistent AF. Remodeling of calcium cycling is an important step in the temporal progression to paroxysmal AF. This will involve additional changes in calcium handling not seen in silencing which ultimately lead to arrhythmogenic calcium release and triggered activity thereby promoting AF.

Paroxysmal Atrial Fibrillation Is Associated With Diastolic Leak From Ryanodine Receptors

A key concept in the pathophysiology of paroxysmal AF is increased diastolic leak of calcium from the SR, which can be quantified by assessing the frequency of calcium sparks and arrhythmogenic calcium waves. An increase in calcium sparks and waves is well known to occur in paroxysmal AF (**Table 1**) and is associated with RyR remodeling in a manner that favors calcium release. Whereas in the early stages of rapid atrial stimulation that lead to signal silencing RyR expression was decreased, in paroxysmal AF the trend is toward an increase in expression (Brundel et al., 1999; Greiser et al., 2014; Voigt et al., 2014) with an increase in channel open probability (Beavers et al., 2013; Chiang et al., 2014b; Voigt et al., 2014). In these studies the main driver was thought to be an increase in RyR phosphorylation. RyRs can be phosphorylated by both PKA (at Ser2808) and CaMKII (at Ser2814). In paroxysmal AF increased RyR open probability appears to arise from phosphorylation at the CaMKII site whereas results regarding phosphorylation at the PKA site are mixed (Chelu et al., 2009; Wakili et al., 2010; Chiang et al., 2014b; Li et al., 2014; Voigt et al., 2014; Lugenbiel et al., 2015). In terms of the CaMKII site evidence suggests a progression from the earliest effects of signal silencing in which RyR phosphorylation decreases (Greiser et al., 2014), to the majority of papers in paroxysmal AF reporting an increase in RyR phosphorylation (Chelu et al., 2009; Greiser et al., 2009; Chiang et al., 2014b). For sustained calcium leak to occur a mechanism is required to maintain SR calcium loading and this is discussed in the following section. It is unknown if t-tubule loss (Wakili et al., 2010), orphaned RyRs or RyR remodeling (Song et al., 2006; Li et al., 2015) play a role in increased calcium sparks and waves in paroxysmal AF. Following myocardial infarction in the ventricle, CaMKII modulates only non-coupled RyRs (Dries et al., 2013) but whether this mechanism promotes calcium leak in the atria at sites following t-tubule loss remains unknown.

Diastolic leak may also be implicated in rare inherited forms of paroxysmal AF. Expressing mutations found in families with inherited AF syndromes in mouse models has found that these variants are frequently associated with RyR remodeling. Knock-out of spinophilin-1 (a protein that links RyRs to protein phosphatase (1) in mice leads to hyperphosphorylation of RyRs at the CaMKII site and an increase in leak (Chiang et al., 2014b). Mice with a loss of function mutation in junctophilin (a protein which normally binds and stabilizes RyRs) show reduced junctophilin binding to RyR, with a secondary increase in open probability and leak (Beavers et al., 2013). Knock-out mice for FKBP-12.6 (a protein which binds and stabilizes RyRs in their unphosphorylated state) show increased leak (Sood et al., 2008), which can be reversed by inhibiting CaMKII phosphorylation of RyR (Li N. et al., 2012). Finally, a genetic mutation resulting in loss of miRNA-106b-25 cluster increases vulnerability to AF by increasing RyR expression (Chiang et al., 2014a). Overall, increased leak in paroxysmal AF appears to be via CaMKII phosphorylation of RyRs. As paroxysms of AF continue to increase cellular calcium concentrations, and as CaMKII activity is regulated by the concentration of calcium, it is easy to imagine how this could result in a positive feedback loop perpetuating AF.

How Is RyR Leak Maintained and Translated to Triggered Activity in Paroxysmal Atrial Fibrillation?

In addition to the properties of RyRs, diastolic leak is also dependent on SR calcium content, with higher SR calcium content leading to greater diastolic leak (Lukyanenko et al., 1996). Importantly, simply making the RyR leaky without otherwise manipulating SR content will not produce calcium waves in the steady state—while this decreases the threshold for a calcium wave, it also decreases SR calcium content below the threshold (Diaz et al., 1997; Venetucci et al., 2007). Studies investigating the absolute SR content in paroxysmal AF are inconsistent (Hove-Madsen et al., 2004; Greiser et al., 2009; Wakili et al., 2010; Voigt et al., 2014) and the relationship to threshold is unknown. However, all studies we refer to in (**Table 1**) report an increase in diastolic calcium leak in paroxysmal AF therefore we assume SR calcium content must be above threshold.

For calcium waves to occur a mechanism is required to maintain SR calcium content above threshold (Venetucci et al., 2007; Ho et al., 2016). SERCA function increases in paroxysmal AF (Xie et al., 2012; Voigt et al., 2014) which would explain how SR calcium content could be maintained in spite of an increase in RyR mediated calcium leak. The increase in SERCA function occurs despite decreased expression of SERCA protein (Voigt et al., 2014; Lugenbiel et al., 2015; Wang et al., 2017), potentially caused by changes in regulatory proteins. Phospholamban (PLB) inhibits SERCA function although this inhibition can be relieved by phosphorylation by PKA (Ser16 site) or CaMKII (Thr17 site). PLB protein expression does not change in paroxysmal AF and investigation of its phosphorylation status has produced inconsistent results (Brundel et al., 1999; Chelu et al., 2009; Greiser et al., 2009; Voigt et al., 2014; Lugenbiel et al., 2015). In the atria, in addition to PLB, sarcolipin can also slow calcium reuptake by SERCA. We are unaware of any studies measuring sarcolipin levels in paroxysmal AF. However, sarcolipin knock-out mice show increased SERCA function and an increased frequency of afterdepolarizations, supporting the concept of maintained SR calcium content to promote leak (Babu et al., 2007; Xie et al., 2012). It is important to appreciate that increasing SERCA function can have either pro- or anti-arrhythmic effects in different contexts. While increasing SERCA function could overload the SR with calcium and thereby promote afterdepolarizations, increased SERCA function might also be expected to increased calcium buffering and thereby increase the threshold for calcium waves (Briston et al., 2014). Reflecting these different possibilities, while increasing SERCA by gene transfer in the failing ventricle is anti-arrhythmic (Lyon et al., 2011), overexpressing SERCA in mouse atria promotes cellular correlates of AF (Nassal et al., 2015).

NCX is important in the conversion of calcium leak to arrhythmias as the calcium released by a wave is removed from the cytosol by NCX to generate the transient inward current I_{ti} which can trigger additional action potentials (Ferrier et al., 1973). The increase in calcium sparks and waves in paroxysmal

AF is associated with an increase in afterdepolarizations (Li N. et al., 2012; Chiang et al., 2014a; Faggioni et al., 2014; Li et al., 2014; Voigt et al., 2014). NCX remains relatively unchanged in paroxysmal AF compared to sinus rhythm (**Table 1**), although as NCX increased in the early stages of rapid atrial stimulation that led to calcium signal silencing, the normalization of NCX in paroxysmal AF may represent a fall from an initial rise. However, insufficient evidence exists at this time to form firm conclusions particularly around what drives the initial rise and subsequent fall in NCX function as this does not relate to expression levels (**Table 1**).

Similar to the acute response to rapid atrial pacing, both the current density of $I_{Ca(L)}$ and the expression of LTCCs are reduced in paroxysmal AF (Brundel et al., 2001; Yagi et al., 2002; Cha et al., 2004a; Wakili et al., 2010; Lugenbiel et al., 2015). It is important to recognize that although $I_{Ca(L)}$ density is generally decreased, consistent with protection against calcium overload, this is offset by rapid atrial rates during paroxysms of AF which would be expected to promote calcium loading. Additionally decreased $I_{Ca(L)}$ could have further pro-arrhythmic effects due to a shortening of the action potential duration, decreasing the refractory period and therefore the wavelength of potential re-entrant circuits.

Overall, paroxysmal AF is associated with increased RyR diastolic leak, increased SERCA function despite unchanged SERCA expression, decreased $I_{Ca(L)}$ and t-tubule loss. These changes appear to initiate a stepwise progression of remodeling toward persistent AF in which an atrial substrate develops which can support increasing durations of AF. This remodeling includes a positive feedback mechanism in which activation of CaMKII phosphorylates RyRs increasing diastolic leak and encouraging further rises in intracellular calcium (Qi et al., 2008), and substrate development by upregulation of pro-fibrotic pathways such as the calcium calmodulin-calcineurin-NFAT pathway (Lin et al., 2004; Wakili et al., 2011). A major question remains namely by what mechanism does early silencing progress to paroxysmal AF or, alternatively, why do some patients develop AF and others not? One possible explanation may lie in the ability of the heart to prevent calcium overload. Interestingly, when considering susceptibility to AF, it was the patients with the greatest $I_{Ca(L)}$ who had an increased incidence of post-operative AF (Van Wagoner et al., 1999). We might speculate that a lack of ability to adapt to high rate by decreasing $I_{Ca(L)}$ and protecting the atria from excessive calcium loading could potentiate the development of paroxysms of AF via calcium dependant arrhythmias.

How Does Remodeling of Calcium Cycling Allow Paroxysmal Atrial Fibrillation to Progress to Persistent Atrial Fibrillation?

The duration of the paroxysms of AF tends to prolong until persistent AF develops, defined clinically as episodes of arrhythmia that last more than seven days before returning to sinus rhythm spontaneously, if at all (Kirchhof et al., 2016). The progression to persistent AF involves alterations in the atrial substrate and calcium handling such that ongoing elevations in cytosolic calcium concentrations activate pathways leading to structural remodeling of the atria. This, coupled with the continued decrease in refractory period leads to the atrial substrate becoming more vulnerable and assuming a greater role in the maintenance of the arrhythmia (Cha et al., 2004b).

SR Calcium Leak in Persistent Atrial Fibrillation Is Associated With RyR Phosphorylation at Both PKA and CaMKII Sites

The enhanced diastolic leak of calcium found in paroxysmal AF continues as AF becomes persistent, and continues to promote triggered activity (Voigt et al., 2012; Purohit et al., 2013). RyR expression tends to be unaltered or downregulated (Brundel et al., 1999; Ohkusa et al., 1999; Schotten et al., 2002; Lenaerts et al., 2009; Neef et al., 2010; Voigt et al., 2012) and is unlikely to be a major factor in the increased SR calcium leak observed in persistent AF. Instead, leak may be due altered kinetics of RyR opening. As was seen in paroxysmal AF, RyR single channel open probability is increased in persistent AF (Vest et al., 2005; Neef et al., 2010; Voigt et al., 2012; Macquaide et al., 2015), which may be due to RyR phosphorylation.

Persistent AF is associated with increased phosphorylation at both the PKA and CaMKII site as well as hyperphosphorylation at the CaMKII site (Vest et al., 2005; Neef et al., 2010; Voigt et al., 2012). Hyperphosphorylation is thought to arise when all four RyR subunits are phosphorylated instead of just two (Marx et al., 2000; Voigt et al., 2012) further increasing their diastolic open probability and leading to a higher frequency of calcium sparks, waves and afterdepolarizations (Vest et al., 2005; Voigt et al., 2012). This is in contrast to paroxysmal AF where RyR leak appeared to be predominantly via CaMKII phosphorylation (**Table 1**).

Experiments blocking RyR phosphorylation suggest that the CaMKII site may be more important than the PKA site in determining SR calcium leak in persistent AF (Neef et al., 2010; Voigt et al., 2012), although the relative role of PKA vs. CaMKII in promoting SR calcium leak is controversial. Evidence of the importance of RyR phosphorylation by PKA come from studies suggesting that PKA phosphorylation leads to dissociation of FKBP12.6 from the RyR, enhancing the open probability of the channel and facilitating SR calcium leak and arrhythmias (Marx et al., 2000; Lehnart et al., 2006). However, this is not universally accepted as other laboratories suggest that hyperphosphorylation of RyR by PKA is not involved in cardiac dysfunction (Benkusky et al., 2007; Zhang et al., 2012). For detailed reviews on this topic we refer the reader to Houser (2014), Dobrev and Wehrens (2014) or Landstrom et al. (2017).

The Mechanisms Maintaining SR Calcium Content Despite Increased Leak in Persistent Atrial Fibrillation Are Unclear

As was seen in paroxysmal AF, maintaining SR calcium leak requires a mechanism to maintain SR calcium content. Despite the increase in diastolic leak, SR calcium content does not change in persistent AF (Lenaerts et al., 2009; Neef et al., 2010; Voigt et al., 2012). While in paroxysmal AF this is likely to be due to increased SERCA function, the mechanism responsible for maintaining SR calcium content in persistent AF is unclear. In

persistent AF, SERCA protein and mRNA levels are generally similar to control (Hoit et al., 2002; Schotten et al., 2002; El-Armouche et al., 2006; Lenaerts et al., 2009; Neef et al., 2010; Dai et al., 2016) or may even decrease (Brundel et al., 1999; Lai et al., 1999; Ohkusa et al., 1999; Cao et al., 2002) While expression of PLB does not appear to change (Brundel et al., 1999; Lai et al., 1999; Van Gelder et al., 1999; Schotten et al., 2002; Uemura et al., 2004; El-Armouche et al., 2006; Lenaerts et al., 2009; Neef et al., 2010), phosphorylation of PLB may increase (El-Armouche et al., 2006; Dai et al., 2016) but this is not universally reported (Lenaerts et al., 2009; Neef et al., 2010). It is also unclear why differential CaMKII phosphorylation of PLB and RyR can occur within the same atria (Neef et al., 2010) raising the possibility that CaMKII signaling is compartmentalized (Mishra et al., 2011). It has also been shown that sarcolipin expression is reduced in persistant AF, providing an additional mechanism to increase SERCA function (Uemura et al., 2004; Shanmugam et al., 2011). However, inconsistent results have been reported when SERCA function has been directly measured in persistent AF (Kneller et al., 2002; Shanmugam et al., 2011; Voigt et al., 2012).

How Does the Structure and Function of the Sarcolemma Remodel in Persistant Atrial Fibrillation?

NCX expression and current may increase in response to high burdens of persistent AF although these findings are not universal (Brundel et al., 1999; Hoit et al., 2002; Kneller et al., 2002; Schotten et al., 2002; El-Armouche et al., 2006; Lenaerts et al., 2009; Voigt et al., 2012). A trend toward an increase in I_{ti} would support the hypothesis that an increase in diastolic leak may result in the increased occurrence of afterdepolarizations that might reinitiate or sustain persistent AF (Burashnikov and Antzelevitch, 2003, 2006). However NCX expression is not associated with the duration of AF in man (Brundel et al., 1999; Van Gelder et al., 1999).

The decrease in $I_{Ca(L)}$ seen early in response to rapid atrial stimulation continues in response to repeated episodes of AF (Yue et al., 1997; Van Wagoner et al., 1999; Workman et al., 2001; Yagi et al., 2002; Christ et al., 2004; Lenaerts et al., 2009; Voigt et al., 2012), potentially caused by lower levels of mRNA for the alpha subunit (Brundel et al., 1999, 2001; Lai et al., 1999; Van Gelder et al., 1999; van der Velden et al., 2000b; Gaborit et al., 2005), reduced LTCC protein expression (Brundel et al., 1999, 2001; Lenaerts et al., 2009), a shift in single channel gating (Lenaerts et al., 2009) and potentially a reduction in single channel open probability due to reduced phosphorylation (Christ et al., 2004). The time course over which these changes occur has been variably reported as between 2 and 6 months (Van Gelder et al., 1999; van der Velden et al., 2000b), which may reflect differences in AF burden between studies. Studies investigating LTCCs during the progression of AF report decreased expression in persistent AF but not in paroxysmal AF suggesting $I_{Ca(L)}$ might decrease over the time course of the disease (Brundel et al., 1999; Van Gelder et al., 1999). However others report no change in $I_{Ca(L)}$ between paroxysmal and persistent AF (Yagi et al., 2002). This discrepancy between decreased expression and current density might be in part due to the reduction in calcium transient amplitude in persistent AF (Schotten et al., 2002; Lenaerts et al., 2009; Voigt et al., 2012) resulting in decreased calcium dependent inactivation of $I_{Ca(L)}$ maintaining current amplitude. These differences may also explain why some studies report the nadir of $I_{Ca(L)}$ is reached quickly before remaining stable, while others reported a slow downward trend inversely proportional to increasing amounts of time in AF (Yagi et al., 2002; Cha et al., 2004a; Wakili et al., 2010).

While atrial t-tubule loss contributes to the decrease of $I_{Ca(L)}$ in AF in some species (Lenaerts et al., 2009), the absence of atrial t-tubules at baseline in other species precludes the involvement of this mechanism e.g., Greiser et al. (2014) and likely contributes to disparity between studies regarding the time course of $I_{Ca(L)}$ loss. While t-tubule loss could increase as AF develops and contribute to the progressive loss of $I_{Ca(L)}$ the available data does not support this concept. Following 7 days of rapid atrial pacing in the dog t-tubules were reduced by 60% (Wakili et al., 2010) but only by ∼45% following 182 days of rapid atrial pacing in the sheep (Lenaerts et al., 2009) suggesting t-tubule loss may facilitate AF in the early stages but not the subsequent progression of AF.

Electrically, the decrease in $I_{Ca(L)}$ contributes to the progressive shortening of action potential duration seen in persistent AF (Bosch et al., 1999; Workman et al., 2001; Kneller et al., 2002; Wakili et al., 2010; Schmidt et al., 2015). This shortening decreases the refractory period of the atrial myocytes, in turn reducing the wavelength of potential re-entrant circuits, allowing more circuits to co-exist within a given mass of atrial tissue and reducing the likelihood of AF terminating. The refractory period not only decreases, but also loses the ability to adapt to changes in heart rate (Wijffels et al., 1995; Gaspo et al., 1997b; Bosch et al., 1999; Willems et al., 2001; Workman et al., 2001; Cha et al., 2004a; Todd et al., 2004; Anne et al., 2007). These changes in action potential duration and refractory period are also contributed to by a reduction in I_{Na} (Gaspo et al., 1997a) and I_{to} (Le Grand et al., 1994; Yue et al., 1997; Bosch et al., 2003) and an increase in I_{K1} (Workman et al., 2001; Dobrev et al., 2005). A full review of all ion channel remodeling at the various stages of AF is beyond the scope of this article and the reader is directed to Nattel et al. (2007).

Elevated Cytosolic Calcium Activates Pro-Fibrotic Pathways Leading to Structural Remodeling

Calcium also plays a key role in the structural changes in the atria caused by and facilitating the progression of persistent AF. Despite the efforts of the myocyte to minimize calcium entry via $I_{Ca(L)}$, if calcium silencing fails then cytosolic calcium concentrations inevitably rise. This rise activates intracellular signaling pathways such as the pro-fibrotic Wnt pathway via calcium sensitive enzymes such as protein kinase C, CaMKII and calcineurin, and leads to myocyte hypertrophy, fibrosis and atrial dilatation (Bukowska et al., 2006; De, 2011; Tao et al., 2016). The consequence of atrial dilatation is a greater mass of tissue able to harbor more simultaneous re-entrant circuits, stabilizing the arrhythmia. In response to increased oxidative stress and angiotensin-II levels in AF (Tsai et al., 2011), pro-fibrotic pathways including the fibroblast transforming growth factor beta pathway (Harada et al., 2012) encourage expansion of the extracellular matrix with deposition of fibrillin and

fibronectin, providing a substrate for re-entry by increasing heterogeneity of impulse conduction (Spach et al., 1982; Li et al., 1999). Furthermore, the gap junctions that electrically connect adjacent myocytes are remodeled by AF, altering the relative expression of their constituent proteins connexins 40, 43, and 45 and further disturbing atrial conduction (Elvan et al., 1997; van der Velden, et al., 2000a; Dupont et al., 2001). Atrial structural remodeling may be facilitated in part by changes in calcium cycling within fibroblasts. For reviews of the role of calcium in dictating structural remodeling in atrial myocytes and fibroblasts we refer the interested reader to reviews by Wakili et al. (2011) and Nattel (2017).

Elevated Intracellular Calcium Promotes Mitochondrial Dysfunction

An additional effect of increasing intracellular calcium concentrations is disturbed mitochondrial function. Calcium cycling is an energetic process which is dependent upon the bidirectional relationship between the SR and the mitochondria (as reviewed in Dorn and Maack, 2013). Mitochondria act as a calcium buffer, and the increased cytosolic calcium also leads to increased calcium concentrations within the mitochondria (Ausma et al., 2000). This increases the open probability of the calcium-sensitive mitochondrial permeability transition pore resulting in increased proton leak and disrupting ATP synthesis (Parks et al., 2018). The proton leak in turn generates reactive oxygen species (ROS) and promotes cell death (reviewed in Griffiths, 2012). The mitochondrial dysfunction that can occur at times of calcium overload is compounded by the increased energy demand of active transporters such as SERCA which are trying to restore homeostatic balance. If these energy demands are not met, mitochondrial dysfunction can contribute to calcium cycling remodeling including increasing RyR leak (Anzai et al., 1998; Xie et al., 2015) and a greater frequency of DADs (Beresewicz and Horackova, 1991).

The effects of mitochondrial dysfunction, increased ROS production and increased oxidative stress have been observed in patients with persistent AF (Mihm et al., 2001; Bukowska et al., 2008; Yongjun et al., 2013; Xie et al., 2015) and can also can predict vulnerability to AF following cardiac surgery (Carnes et al., 2001; Montaigne et al., 2013; Anderson et al., 2014). A full review of ROS and oxidative stress in AF can be found in Sovari et al. (Sovari and Dudley, 2012).

Summary of the Role of Calcium Handling in Atrial Fibrillation

In summary, triggering impulses, arising most commonly from the pulmonary veins, lead to short bursts of rapid atrial activity and an increase in the influx of calcium. The response of the healthy atrium is to offset this net influx by increasing efflux in calcium signal silencing. However since some patients develop AF there must be factors which promote paroxysmal AF rather than signal silencing. We speculate that this could include (i) a failure in the ability of the calcium cycling mechanism to adapt to increased rate, (ii) the presence of pre-existing structural heart disease or, (iii) early loss of atrial t-tubules promoting arrhythmogenic calcium release. Other, extra cardiac factors, may also also determine the vulnerability to AF and include roles for obesity (Goudis et al., 2015), aging (Steenman and Lande, 2017) or alcohol (Voskoboinik et al., 2016), which could further promote arrhythmogenic calcium release. These factors, either individually or in combination may determine the probability of developing persistent AF as well as the rate of progression of the disease. It is clear that changes to calcium cycling are a key component of this progression encouraging electrical remodeling, structural remodeling, and mitochondrial dysfunction, and ultimately promoting further AF. A downward spiral ensues until the atrium is capable of sustaining AF indefinitely, making it harder to restore and sustain sinus rhythm.

THE INTERPLAY BETWEEN HEART FAILURE AND ATRIAL FIBRILLATION

Heart failure is a leading cause of death worldwide that arises as an endpoint of many cardiovascular diseases including ischaemic heart disease, valvular heart disease, hypertension, and inherited cardiomyopathies (Ziaeian and Fonarow, 2016). In addition to ventricular arrhythmias that can lead to sudden cardiac death (Bardy et al., 2005), heart failure is also associated with an increased risk of atrial arrhythmias including AF (Benjamin et al., 1994). AF, if seen, is associated with a worsening of symptoms and prognosis (Dries et al., 1998; McManus et al., 2013; Odutayo et al., 2017). The relationship between heart failure and AF is summarized in **Figure 3**.

Heart failure is defined as the presence of symptoms such as breathlessness resulting from structural or functional abnormalities that in general cause impaired contraction and / or relaxation of the myocardium (Ponikowski et al., 2016). This broad definition aids clinicians in adopting a standard approach to patient investigation and treatment, but generates a heterogeneous group that requires further subdivision in order to make sense of the range of human and animal studies performed. The commonest way of subdividing heart failure based on cardiac performance is into two groups: heart failure with a reduced ejection fraction vs. heart failure with a preserved ejection fraction (Ponikowski et al., 2016). The majority of studies examining calcium handling in the atria in heart failure have focused on those with reduced ejection fraction and we will therefore focus on this group, although it is important to remember that all types of heart failure are associated with AF (McManus et al., 2013).

In this section, we will not only show that the atria in heart failure undergo remodeling in calcium cycling, but this bears a number of similarities to the remodeling in AF presented in the previous section and that the two conditions are inexorably linked.

Does Heart Failure Promote Atrial Fibrillation Through Changes in Atrial Calcium Cycling?

In contrast to the large body of work exploring the role of calcium handling in AF, far less has been published regarding the effects of heart failure on atrial calcium handling. However,

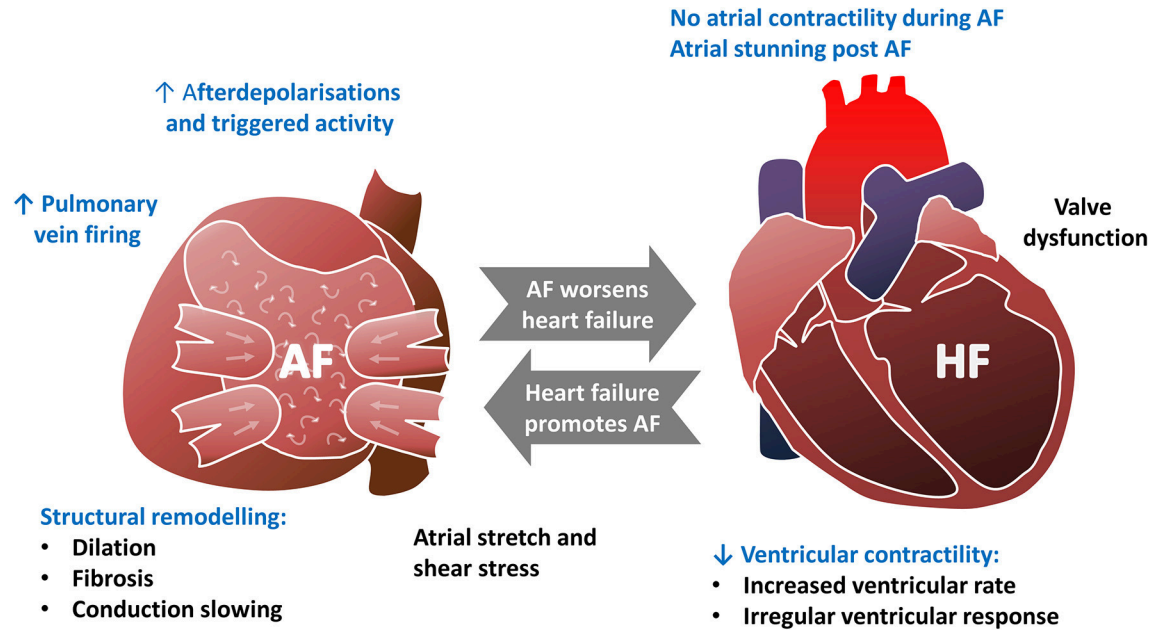

FIGURE 3 | The bidirectional relationship between atrial fibrillation and heart failure. Text highlighted in Blue indicates that perturbed calcium handling is implicated in this aspect of the pathophysiology.

heart failure appears to be associated with changes to atrial calcium cycling with decreased $I_{Ca(L)}$ contributed to by loss of atrial t-tubules, increased SR calcium content despite unchanged or lower calcium reuptake by SERCA, and increased diastolic calcium leak. These effects may be mediated by atrial stretch caused by elevated intra-atrial pressure (Eckstein et al., 2008). Heart failure also affects the pulmonary veins, increasing their spontaneous activity (Lin et al., 2016). Overall many aspects of calcium handling remodeling are common to both AF and heart failure and therefore it is plausible that AF could exacerbate heart failure remodeling and vice versa.

Heart Failure Is Associated With Decreased Atrial $I_{Ca(L)}$ and Increased Sarcoplasmic Reticulum Calcium Content

Atrial $I_{Ca(L)}$ has generally been found to decrease in heart failure (Ouadid et al., 1995; Li et al., 2000; Boixel et al., 2001; Cha et al., 2004a,b; Sridhar et al., 2009; Clarke et al., 2015) although these findings have not been universally replicated in human studies (Cheng T. H. et al., 1996; Workman et al., 2009). Interestingly, this reduction in $I_{Ca(L)}$ has also been found in those with dilated atria and other forms of structural heart disease associated with an increased susceptibility to AF (Le Grand et al., 1994; Deroubaix et al., 2004; Dinanian et al., 2008). The reduction in $I_{Ca(L)}$ appears to be due to a reduction in the expression of LTCCs (Ouadid et al., 1995). Decreased atrial t-tubule density may contribute to the reduced abundance of LTCCs (Dibb et al., 2009; Lenaerts et al., 2009). T-tubules are disordered in hypertrophied atria (Brandenburg et al., 2016) and lost in heart failure and myocardial infarction (Dibb et al., 2009; Kettlewell et al., 2013; Caldwell et al., 2014) to a greater extent than is seen in the ventricle (Dibb et al., 2009; Caldwell et al., 2014). In addition the amplitude of $I_{Ca(L)}$ on the t-tubules that remain in heart failure is also reduced (Glukhov et al., 2015) further decreasing overall $I_{Ca(L)}$. The decrease in atrial $I_{Ca(L)}$ is contributed to by a reduced baseline response to beta stimulation (Boixel et al., 2001), while single channel voltage gating and recovery from inactivation do not appear to change (Li et al., 2000; Boixel et al., 2001; Cha et al., 2004b). Overall, there appears to be a decrease in atrial $I_{Ca(L)}$ in heart failure (Ouadid et al., 1995; Li et al., 2000; Boixel et al., 2001; Cha et al., 2004a,b,b; Dinanian et al., 2008; Sridhar et al., 2009; Clarke et al., 2015) which can also have effects on SR calcium content (Trafford et al., 2001; Clarke et al., 2015, 2017).

Increasing SR calcium content is generally pro-arrhythmic as this can lead to an increased frequency of delayed afterdepolarizations, and this is often seen in the atria of those with heart failure (Yeh et al., 2008; Hohendanner et al., 2015, 2016; Aistrup et al., 2017). While in rodents a decrease in SR calcium content (Saba et al., 2005) is associated with reduced SERCA, PLB, and sarcolipin expression (Shanmugam et al., 2011), a somewhat different story predominates in large mammals in which atrial SR calcium content increases in heart failure (Yeh et al., 2008; Clarke et al., 2015; Aistrup et al., 2017) despite decreased calcium reuptake by SERCA (Clarke et al., 2015; Hohendanner et al., 2016). This apparently paradoxical finding has been explained by the decrease in atrial $I_{Ca(L)}$ where inhibiting $I_{Ca(L)}$ in control cells reproduces the increase in SR calcium content. Here, decreased $I_{Ca(L)}$ can paradoxically increase SR calcium content (Trafford et al., 2001; Clarke et al., 2015, 2017). It is less clear how SERCA function is reduced in these models of heart failure. Generally in large mammals and man, SERCA and PLB levels remain unchanged but can decrease

(Yeh et al., 2008; Shanmugam et al., 2011; Clarke et al., 2015). However, other changes have been observed which would be expected to increase SERCA function in heart failure including an increase in phosphorylation of PLB at the CaMKII site (Yeh et al., 2008; Clarke et al., 2015) and a decrease in sarcolipin levels (Shanmugam et al., 2011).

In keeping with the recurring theme seen in paroxysmal and persistent AF, heart failure is also associated with increased diastolic calcium leak (Saba et al., 2005; Yeh et al., 2008; Johnsen et al., 2013; Hohendanner et al., 2015, 2016; Aistrup et al., 2017). The increase in leak appears to occur despite no change or even a decrease in RyR expression (Yeh et al., 2008; Shanmugam et al., 2011; Brandenburg et al., 2016). Unlike in AF, the phosphorylation of RyRs does not appear to change in heart failure (Yeh et al., 2008; Brandenburg et al., 2016), and the increased leak is therefore likely to be caused by the increased atrial SR calcium content generally reported in large mammals with heart failure (Yeh et al., 2008; Clarke et al., 2015; Aistrup et al., 2017). As opposed to AF, atrial t-tubule loss in heart failure may facilitate calcium dependant arrhythmias by "orphaning" RyRs, promoting heterogenous calcium release and facilitating atrial alternans as has observed in the ventricle (Louch et al., 2006; Song et al., 2006; Heinzel et al., 2008; Li Q. et al., 2012; Nivala et al., 2015). It is noteworthy that atrial t-tubule loss in heart failure appears more severe than that observed in AF [at least in the sheep (Dibb et al., 2009; Lenaerts et al., 2009)] although whether the greater loss of t-tubules in heart failure increases the likelihood of AF remains to be determined.

In heart failure the amplitude of the calcium transient is important since impaired ventricular filling results in a greater reliance on atrial contraction (Kono et al., 1992). While it is clear that SR function is remodeled in heart failure, how decreased $I_{Ca(L)}$ and increased SR calcium content interact to give rise to the systolic calcium transient is unclear, with both increased and decreased calcium transient amplitude reported (**Table 1**). One discrepancy may lie in experimental conditions. Under voltage clamp conditions decreased $I_{Ca(L)}$ may decrease calcium transient amplitude (Clarke et al., 2015) whereas prolongation of the heart failure atrial action potential in current clamp recordings (Koumi et al., 1994) would be expected to promote $I_{Ca(L)}$ or reverse mode I_{NCX} which together with increased SR calcium content could increase calcium transient amplitude (Yeh et al., 2008). This effect however does not explain all discrepancies.

Compounding the increased SR calcium content, atrial NCX activity generally increases in heart failure (Li et al., 2000; Cha et al., 2004a,b; Hohendanner et al., 2015, 2016) although some have found otherwise (Clarke et al., 2015). The combination of elevated SR calcium content and increased NCX favors the generation of delayed afterdepolarizations, and an increase in atrial afterdepolarizations in heart failure is indeed consistently reported (Yeh et al., 2008; Hohendanner et al., 2015, 2016; Aistrup et al., 2017), along with a higher propensity for these calcium waves to trigger action potentials (Hohendanner et al., 2016) potentially leading to re-initiation of AF.

Atrial Stretch may Mediate the Changes in Calcium Cycling

One of the mechanisms by which heart failure induces changes in atrial calcium cycling is the mechanical stress placed on the atrial wall, caused by the increase in left ventricular end diastolic pressure elevating left atrial pressure. This mechanical stress takes two forms, and both have important effects on calcium cycling. Stretch is the result of tension placed on the atrial myocyte as the left atrium dilates, while shear stress results from elevated pressure in the atrium deforming the myocyte (Schonleitner et al., 2017).

Atrial stretch increases contractility acutely under physiological conditions and is commonly known as the Frank-Starling mechanism [as reviewed in Sequeira et al. (Sequeira and van der Velden, 2015)]. This rapid increase in contractile force is due to an increase in the myofilament calcium sensitivity and was originally described in the ventricle (Allen and Kurihara, 1982; Hibberd and Jewell, 1982) although the same mechanism has been shown to occur in the atria (Tavi et al., 1998). A second, slower increase in contractility also occurs in response to myocardial stretch and is known as the slow force response (Parmley and Chuck, 1973; von Lewinski et al., 2004). Much of the initial work characterizing this phenomenon focused on the ventricle and showed it was brought about by an increase in the calcium transient (Alvarez et al., 1999), whereby myocyte stretch activates the sodium-proton exchanger increasing intracellular sodium providing a gradient to increase calcium influx via reverse NCX (Alvarez et al., 1999; von Lewinski et al., 2003; Kockskamper et al., 2008). In ventricular myocytes, this is associated with an increase in the frequency of sparks (Iribe and Kohl, 2008; Iribe et al., 2009) with one potential mechanism being via enhanced ROS production leading to increased open probability of RyRs (Prosser et al., 2013). This NCX dependant mechanism however has not been shown to occur in the atria, with instead a dependence on angiotensin II and endothelin-1 signaling (Kockskamper et al., 2008).

Both acute (Bode et al., 2000; Eijsbouts et al., 2003; Kuijpers et al., 2011) and chronic (Solti et al., 1989) atrial stretch have been shown to promote AF and are comprehensively reviewed in Eckstein et al. (2008) and Nazir and Lab (1996). One of the better described mechanisms of AF vulnerability in chronic atrial stretch is dependent upon endothelin-1 signaling [as reviewed in Drawnel et al (Drawnel et al., 2013)]. Endothelin-1 concentrations in the left atrium increase in both AF and heart failure (Mayyas et al., 2010) and this may act locally to enhance diastolic leak and ectopy via inositol 1,4,5-triphosphate signaling (Proven et al., 2006; Tinker et al., 2016), as well as by upregulating profibrotic pathways implicated in structural remodeling (Ruwhof and van der Laarse, 2000; Burstein et al., 2008).

Atrial shear stress has also been shown to increase calcium sparks and waves (Woo et al., 2007; Kim and Woo, 2015; Son et al., 2016), but is less well studied than stretch. It is also unclear whether stretch and shear stress can produce additive effects on calcium cycling. Although the increase in calcium sparks is not believed to be pro-arrhythmic in the absence of structural

heart disease (Schonleitner et al., 2017), the greater degree of stretch in heart failure compounded by the loss of atrial t-tubules (Dibb et al., 2009) may contribute to an increased frequency of afterdepolarizations. For comprehensive reviews of atrial stretch and shear stress see Thanigaimani et al. (2017) or Ravelli (2003).

Impaired Energy Supply may Also Contribute to the Changes in Calcium Cycling and Ion Channel Homeostasis

Heart failure may also cause changes in atrial calcium cycling through mitochondrial dysfunction. Mitochondrial dysfunction, increased ROS production and increased oxidative stress occur in heart failure and have been extensively reviewed elsewhere (Dorn and Maack, 2013; Bertero and Maack, 2018). The mitochondrial dysfunction that occurs in failing ventricular myocytes also occurs in the atria of those with heart failure (Cha et al., 2003; Marin-Garcia et al., 2009). This results in a mismatch of energy demand and supply within the myocyte and necessitates a change in cellular metabolism to try to correct this (Fukushima et al., 2015). There is evidence in both heart failure and AF that myocytes undergo a change in transcription of key metabolic and cell signaling pathways (Barth et al., 2011, 2016). The downregulation of the metabolic pathways correlates with a reduction in transcription of calcium cycling proteins such as the LTCC, RyR, SERCA, and PLB, which suggests the metabolic shift in response to an energy deficit is associated with changes in calcium cycling although a direct cause has not been established (Barth et al., 2016). The upregulation of calcium-dependent signaling pathways such as the Wnt pathway may encourage further structural remodeling to occur to support AF (Barth et al., 2011).

Pulmonary Vein Firing Accelerates in Heart Failure

In addition to its effects on the atrial myocardium, heart failure also influences the pulmonary veins, potentially increasing their spontaneous firing rate. Increasing intra-atrial pressure, as found in heart failure, accelerates pulmonary vein firing in intact sheep hearts (Kalifa et al., 2003). While this increase appears to be mediated by changes in calcium cycling leading to more delayed afterdepolarizations (Chang et al., 2008; Loh et al., 2009; Lin et al., 2016), the cellular changes responsible for this are unclear. While increased levels of circulating B-type natriuretic peptide have been suggested to increase the rate of spontaneous firing due to increased $I_{Ca(L)}$ and I_{NCX} but decreased late I_{Na} (Lin et al., 2016), others report an increase in DADs in the setting of heart failure with decreased $I_{Ca(L)}$ and increased late I_{Na} (Chang et al., 2008). Overall, heart failure appears to increase the rate of pulmonary vein firing, but the discordant results and lack of studies in large mammals make the precise mechanism underlying this unclear.

The Effects of Heart Failure on the Atrial Action Potential Are Unclear

Heart failure has been shown to affect atrial electrophysiology although the current evidence is inconsistent. Some describe a prolongation of the atrial action potential in heart failure (Koumi et al., 1994; Li et al., 2000; Yeh et al., 2008) associated with prolongation of the refractory period, which has been suggested to promote AF by facilitating early afterdepolarizations. However, others have described shorter action potentials and refractory periods in association with heart failure (Koumi et al., 1997; Schreieck et al., 2000; Sridhar et al., 2009; Workman et al., 2009; Clarke et al., 2015) and argued that this might facilitate AF by decreasing the wavelength of re-entrant circuits allowing a greater number to co-exist. While experimental differences between studies such as species, rate of stimulation, stage of heart failure and level of t-tubule loss likely contribute to the disparate literature this suggests that the influence of heart failure on action potential duration and refractory period may be of secondary importance in the initiation of AF. This is supported by evidence from models of heart failure that have not found any difference in refractory period but still shown markedly increased vulnerability to AF (Li et al., 1999), and from tachy-paced models of heart failure that have been allowed to recover demonstrating that increased vulnerability to AF remains despite the refractory period returning to baseline (Cha et al., 2004b).

Heart Failure Promotes Structural Remodeling of the Atria

A major determinant of the susceptibility to AF in those with heart failure is remodeling of the atrial structure in the form of atrial dilatation (Sridhar et al., 2009; Melenovsky et al., 2015) and fibrosis (Li et al., 1999; Shinagawa et al., 2002; Cha et al., 2004a,b; Todd et al., 2004). While similar structural changes can occur in AF, the structural remodeling associated with heart failure is more extensive and progresses more rapidly than is seen as a response to AF (Li et al., 1999). Macroscopically, this remodeling takes the form of left atrial dilatation, which regardless of its underlying cause is associated with an increased risk of developing AF (Solti et al., 1989; Huang et al., 2003) and can be used clinically to predict the success of treatments aimed at restoring sinus rhythm (Brodsky et al., 1989; Helms et al., 2009; Montefusco et al., 2010). In heart failure, this dilatation occurs due to a rise in left ventricular end diastolic pressure (Melenovsky et al., 2015). At a microscopic scale, the dilatation is accompanied by atrial fibrosis. The atrial fibrosis induced by heart failure leads to slower, heterogeneous conduction promoting wavebreak and re-entry (Li et al., 1999; Sanders et al., 2003; Akkaya et al., 2013). In an effort to prevent the deleterious effects of structural remodeling, anti-fibrotic agents have been explored and shown to reduce atrial fibrosis and vulnerability to AF in models of heart failure (Lee et al., 2006; Le Grand et al., 2014) and appear to reduce the incidence of AF in clinical trials (Chaugai et al., 2016).

How Does Atrial Fibrillation Exacerbate Heart Failure?

When AF develops in those with heart failure it is associated with worsening symptoms and prognosis, in part due to a loss of atrial contraction further impairing ventricular filling. However, other factors influencing the worsening of heart failure include rapid heart rates and an irregular ventricular response compromising ventricular performance, atrial stunning, and

valvular dysfunction, mediated in part by alterations in both atrial and ventricular calcium handling.

Cardiac Output Is Impaired During Atrial Fibrillation

In sinus rhythm, atrial contraction contributes to ventricular filling. Loss of meaningful atrial contraction during AF can reduce cardiac output by up to 25% (Hecht and Lange, 1956; Naito et al., 1983). Many of those with heart failure are less able to increase their cardiac output in response to exercise (Mc et al., 1939), or may even have a lower cardiac output at rest (Stead et al., 1948), and the additional loss from AF exacerbates symptoms such as breathlessness and exercise tolerance (Ponikowski et al., 2016).

In addition to the loss of atrial contractility, the rapid ventricular rates which frequently occur in untreated AF reduce ventricular diastolic filling compared to a physiological heart rate (Raymond et al., 1998), further decreasing cardiac output. If these episodes of rapid ventricular rates are prolonged, they can impair ventricular function, although this can be reversed by restoring sinus rhythm or by slowing the ventricular rate in AF (Khan et al., 2008). The impaired ventricular function may be a primary cause for heart failure (a tachycardia-induced cardiomyopathy), or may be appreciated as a worsening of left ventricular function that is already impaired for another reason (Grogan et al., 1992; Fujino et al., 2007; Simantirakis et al., 2012). Rapid cardiac stimulation reliably induces dilated cardiomyopathy and end stage heart failure and is therefore commonly used as an experimental model of heart failure (Li et al., 2000; He et al., 2001; Cha et al., 2004a; Clarke et al., 2015). In this context, impaired ventricular systolic function is associated with remodeling of calcium handling—the high ventricular rates lead to t-tubule loss and a decreased ventricular calcium transient amplitude which can arise by a decrease in either SR calcium content or peak $I_{Ca(L)}$ (He et al., 2001; Hobai and O'Rourke, 2001; Briston et al., 2011). It seems likely that the effects of tachycardia (as a result of AF) on ventricular function seen clinically may be mediated by a similar mechanism although these animal models do not take into account any change in rhythm which can occur in AF.

AF also results in an irregular ventricular response which has compounding effects on cardiac output. Short-term irregularity in ventricular contraction is associated with lower cardiac output independently of heart rate in dogs (Naito et al., 1983), and impaired systolic function in man (Sramko et al., 2016). The effects of an irregular ventricular rate may develop further over time driven by changes in calcium handling, as ventricular myocytes paced in an irregular rhythm for 24 h demonstrate lower calcium transient amplitude, reduced expression of SERCA, and reduced phosphorylation of phospholamban compared to control (Ling et al., 2012).

AF is also associated with the development of valve dysfunction in the form of mitral regurgitation (Skinner et al., 1964). While mitral regurgitation can affect atrial structure in ways which promote AF, AF also appears to promote mitral regurgitation (Liang and Silvestry, 2016). The irregular ventricular response acutely influences mitral regurgitation (Naito et al., 1983), while in the longer term, persistent AF causes dilatation of the mitral valve annulus leading to functional mitral regurgitation (Liang and Silvestry, 2016). Mitral regurgitation contributes to the increase in pulmonary capillary wedge pressure associated with AF (Clark et al., 1997) which leads to fluid leaking from the pulmonary capillaries to cause pulmonary oedema giving rise to breathlessness.

Overall, the decrease in cardiac output due to a combination of: loss of atrial function, loss of regular ventricular contraction and increased mitral regurgitation can exacerbate pre-existing heart failure.

Atrial Function Remains Depressed After Atrial Fibrillation has Terminated

Atrial function remains temporarily depressed following the restoration of sinus rhythm in patients who have periods of AF, known as atrial stunning (Schotten et al., 2003a). This effect is unsurprising, as the changes in calcium handling that take place during AF which lead to decreased calcium transient amplitude and hence decreased contractility require time to resolve (Schotten et al., 2002; Lenaerts et al., 2009; Voigt et al., 2012). The effects of stunning can last for up to a month, and the time to recovery is proportional to the duration of AF prior to cardioversion (Harjai et al., 1997; Sparks et al., 1999). It appears that a major determinant of the residual decreased contractility seen in stunned atrial myocytes is decreased $I_{Ca(L)}$, although pathological remodeling of contractile proteins contributes to this process (Schotten et al., 2001). While electrical reverse remodeling can occur between short bouts of AF (Todd et al., 2004), it is possible that the structural remodeling that occurs in persistent AF may have an irreversible effect on atrial contraction despite restoration of sinus rhythm, but evidence for this is lacking.

IS THE PATHOPHYSIOLOGY OF ATRIAL FIBRILLATION IN HEART FAILURE DIFFERENT TO ATRIAL FIBRILLATION IN THE ABSENCE OF STRUCTURAL HEART DISEASE?

AF can also develop in the absence of heart failure, and one subtype of AF which has historically been described in the literature is that of lone AF. "Lone AF," defined by the absence of overt heart disease or precipitating illness is relatively unusual, accounting for only 10% of new diagnoses of AF (Kim et al., 2016). Some argue that even this figure may be an overestimate as more thorough investigation might reveal underlying disease in many of these patients (Wyse et al., 2014). Even in the absence of overt heart disease, many young patients who develop AF may still have an underlying cause in the form of a genetic predisposition caused by variants in ion channels (Weng et al., 2017). We recognize the term "lone AF" is controversial based on inconsistencies in the definition and a lack of a distinct pathophysiological mechanism (Potpara and Lip, 2014; Wyse et al., 2014). For that reason, we have compared AF that occurs on the background of heart failure vs. AF in the absence of structural heart disease or a major risk factor.

The abnormalities in atrial calcium handling that occur in response to heart failure have some similarities with those that occur in AF (**Table 1**). The decrease in atrial $I_{Ca(L)}$ in heart failure mirrors that seen in both paroxysmal and persistent AF. SR calcium content increases in heart failure as some studies report in early or paroxysmal AF although this is not found in persistent AF. There is limited data on the effects of heart failure on atrial RyRs but, unlike in AF, heart failure does do not appear to lead to RyR phosphorylation. However, the net effect of these modifications leads to a similar endpoint of increased RyR leak and afterdepolarizations in heart failure and AF. Although the pulmonary veins are the source of triggers for AF in the majority of patients with lone AF (Haissaguerre et al., 1998), the remodeling of atrial calcium cycling that promotes afterdepolarizations throughout the atria theoretically increases the chance of triggers occurring from non-pulmonary vein sources, potentially diminishing the relative importance of the pulmonary veins in patients with heart failure. This may be of significant practical importance as it may influence the ablation strategies used in clinical practice which typically focus on the pulmonary veins, and may contribute to the lower success rates of ablation described in those with heart failure (Anselmino et al., 2014).

A major difference between the AF that occurs alongside heart failure and the early stages of AF that occurs without evidence of overt heart disease is the atrial structure. As we have seen, heart failure leads to atrial dilatation and fibrosis, promoting heterogeneous conduction, wavebreak, and a substrate that supports multiple simultaneous re-entrant circuits. The atrial structural remodeling found in heart failure occurs more rapidly and to a greater extent than in AF without heart failure (Li et al., 1999). This appears to be an important determinant of atrial vulnerability in canine models of heart failure, in which far longer durations of AF were observed in dogs with heart failure compared to control animals (Li et al., 1999). This experimental work has parallels with epidemiological studies in man. Patients with heart failure are less likely to have a paroxysmal form of the disease and more likely to have persistent or permanent AF than those without heart failure (Silva-Cardoso et al., 2013). Although this data does not describe the initial presentation of patients with AF, it is possible that while the natural history of lone AF typically begins with paroxysmal AF in structurally normal atria, in those with heart failure AF may be more likely to present with persistent AF. Structural remodeling of the atria is associated with a lower chance of maintaining sinus rhythm in response to medication, cardioversion, or ablation when assessed using left atrial diameter e.g., (Nedios et al., 2015) or fibrosis assessed by MRI scanning (Marrouche et al., 2014). Maintaining sinus rhythm is accordingly less likely in those with heart failure than those without (Anselmino et al., 2014; Fredersdorf et al., 2014). Even though these structural changes occur more rapidly in heart failure, atrial dilatation and fibrosis also occur in advanced forms of AF in those without heart failure (Schotten et al., 2003a).

Overall, the pathophysiology of AF in those with heart failure shares many similarities to the advanced AF seen in those without heart failure. Heart failure patients often present with AF some distance along their journey of atrial remodeling.

WHAT ARE THE LIMITATIONS OF RESEARCH IN UNDERSTANDING THE PATHOPHYSIOLOGY OF ATRIAL FIBRILLATION?

Although there is strong evidence to support the role of calcium remodeling as a whole in AF and heart failure, some aspects of this process show wide variation in the experimental data which often produces conflicting results. There are a number of potential reasons for the differences in findings, and herein we provide a critical review of these.

Studies of Human Myocytes Are Hampered by Comorbid Conditions and Medications

Obtaining human atrial myocytes to study calcium handling can be performed by using samples of atrial appendage that are routinely discarded following cardiac surgery (Voigt et al., 2015). While patient samples offer a unique opportunity to study the disease in which we are interested this approach suffers from several disadvantages. Research participants need to have an indication for cardiac surgery and therefore have other cardiovascular conditions that confound interpretation of results. Common indications for surgery include coronary artery bypass grafting for ischaemic heart disease and valve replacement for mitral valve disease, both of which are independently associated with structural remodeling of the atria and an increased vulnerability to AF. Furthermore, these patients are often taking medications that influence cellular electrophysiology and calcium handling such as beta-adrenoceptor blockers. While atrial tissue would ideally be obtained from humans without pre-existing cardiac disease, access to this tissue is extremely limited as the risks associated with an atrial biopsy far outweigh any potential benefit (From et al., 2011).

Some Animal Models may not be Fully Representative of Human Atrial Fibrillation

To avoid the limitations of using human tissue, animal models are frequently used which include rodents and large mammals such as dogs, sheep, or goats. However, spontaneously occurring AF in these animal models is rare (Heijman et al., 2016) and an artificial trigger is required. The artificial trigger is often in the form of rapid atrial pacing which mimics pulmonary vein triggers (Morillo et al., 1995), although other models such as vagal stimulation are also used and are reviewed further by Nishida et al. (2010). These models have been helpful in characterizing the early steps in the development of AF, as episodes of AF early on in the disease course in humans may occur infrequently and take months or years to diagnose (Kirchhof et al., 2016).

Animal models of AF benefit from the fact that the frequency and duration of arrhythmia can be quantified allowing a time course of remodeling to be determined. However, it is uncertain whether the atrial changes induced artificially by rapid atrial

pacing which produce persistent AF within days to weeks are truly comparable to the human condition in which persistent AF typically develops over months to years. Furthermore, the atrial arrhythmias seen in rodents may be a poor comparator for human AF due to the differences in ion channel expression between rodents and man (Gussak et al., 2000), the differences in the relative importance of SERCA and NCX in clearing cytosolic calcium (Bassani et al., 1994), and the lack of an extensive t-tubule network in rodents that is found in larger mammals (Richards et al., 2011). On the other hand genetic manipulation of rodents can result in powerful models for understanding arrhythmic mechanisms.

The results from animal models of atrial electrophysiology in heart failure may also be confounded by the technique used to induce ventricular dysfunction. Many large animal models use ventricular tachypacing to produce a dilated cardiomyopathy. While this technique is likely to be representative of end stage heart failure, it must be borne in mind that tachycardiompathy accounts for only a minority of the causes of heart failure seen in humans (Mosterd and Hoes, 2007) and may therefore differ in important regards from more representative aetiologies of heart failure such as ischaemic heart disease. For example, ventricular tachypacing may inadvertently cause rapid atrial pacing via retrograde conduction through the atrioventricular node, mimicking AF. It is therefore important that this potential confounder is pre-empted, measured, and if necessary addressed by blocking the AV node (Li et al., 1999).

Overall, interpreting the results of studies of calcium handling in AF requires careful attention to the methods used including species, duration of AF, and confounding comorbidities and medications.

CONCLUSIONS

Calcium plays a fundamental role in the pathophysiology of AF, as well as in the bidirectional relationship between AF and heart failure. Remodeling of calcium cycling in response to rapid atrial stimulation can be seen within days in the form of calcium signaling silencing. However, these initially protective changes eventually become pathological as paroxysmal AF develops and can facilitate the progression to persistent AF. A recurring theme throughout this progression is increased diastolic leak of calcium from RyRs which promotes afterdepolarizations. The rise in intracellular calcium concentrations also activates pro-fibrotic pathways leading to structural remodeling in the atria that produces a substrate that can support the complex re-entry seen in AF. This review has provided a comprehensive stepwise description of the fundamental aspects of calcium cycling remodeling.

Heart failure leads to remodeling of calcium cycling and structural changes within the atria which support persistent AF. In return, AF exacerbates heart failure by reducing cardiac output, due in part to a loss of atrial contraction but also by affecting ventricular calcium cycling. A vicious circle ensues whereby one condition begets the other. Questions remain surrounding the complex interaction between AF and heart failure, but the undeniable importance of calcium cycling remodeling in both conditions should prompt the exploration of these mechanisms as potential novel therapeutic targets.

AUTHOR CONTRIBUTIONS

ND prepared the first draft of the manuscript, which was critically revised by CP, JC, GM, DE, AT, and KD. JC produced the figures. All authors agree with its final content.

FUNDING

The authors ND, CP, JC, AT, DE, and AT, are supported by funding from the British Heart Foundation (FS/17/54/33126; FS/15/28/31476; FS12/34/29565; FS12/57/29717; PG/12/89/29970 and FS/09/002/26487). GM is funded by a Medical Research Council Award 1637974. CP is a clinical lecturer funded by the National Institute for Health Research.

REFERENCES

Aistrup, G. L., Arora, R., Grubb, S., Yoo, S., Toren, B., Kumar, M., et al. (2017). Triggered intracellular calcium waves in dog and human left atrial myocytes from normal and failing hearts. *Cardiovasc. Res.* 113, 1688–1699. doi: 10.1093/cvr/cvx167

Akkaya, M., Higuchi, K., Koopmann, M., Damal, K., Burgon, N. S., Kholmovski, E., et al. (2013). Higher degree of left atrial structural remodeling in patients with atrial fibrillation and left ventricular systolic dysfunction. *J. Cardiovasc. Electrophysiol.* 24, 485–491. doi: 10.1111/jce.12090

Allen, D. G., and Kurihara, S. (1982). The effects of muscle length on intracellular calcium transients in mammalian cardiac muscle. *J. Physiol.* 327, 79–94. doi: 10.1113/jphysiol.1982.sp014221

Allessie, M., and de Groot, N. (2014). CrossTalk opposing view: rotors have not been demonstrated to be the drivers of atrial fibrillation. *J. Physiol.* 592, 3167–3170. doi: 10.1113/jphysiol.2014.271809

Allessie, M. A., Bonke, F. I., and Schopman, F. J. (1977). Circus movement in rabbit atrial muscle as a mechanism of tachycardia. III. The "leading circle" concept: a new model of circus movement in cardiac tissue without the involvement of an anatomical obstacle. *Circ. Res.* 41, 9–18. doi: 10.1161/01.RES.41.1.9

Allessie, M. A., Konings, K., Kirchhof, C. J., and Wijffels, M. (1996). Electrophysiologic mechanisms of perpetuation of atrial fibrillation. *Am. J. Cardiol.* 77, 10a−23a. doi: 10.1016/S0002-9149(97)89114-X

Alvarez, B. V., Perez, N. G., Ennis, I. L., Camilion de Hurtado, M. C., and Cingolani, H. E. (1999). Mechanisms underlying the increase in force and Ca^{2+} transient that follow stretch of cardiac muscle: a possible explanation of the Anrep effect. *Circ. Res.* 85, 716–722. doi: 10.1161/01.RES.85.8.716

Amos, G. J., Wettwer, E., Metzger, F., Li, Q., Himmel, H. M., and Ravens, U. (1996). Differences between outward currents of human atrial and subepicardial ventricular myocytes. *J. Physiol.* 491(Pt. 1), 31–50.

Anderson, E. J., Efird, J. T., Davies, S. W., O'Neal, W. T., Darden, T. M., Thayne, K. A., et al. (2014). Monoamine oxidase is a major determinant of redox balance in human atrial myocardium and is associated with postoperative atrial fibrillation. *J. Am. Heart Assoc.* 3:e000713. doi: 10.1161/JAHA.113.000713

Anne, W., Willems, R., Holemans, P., Beckers, F., Roskams, T., Lenaerts, I., et al. (2007). Self-terminating AF depends on electrical remodeling while persistent AF depends on additional structural changes in a rapid atrially paced sheep model. *J. Mol. Cell. Cardiol.* 43, 148–158. doi: 10.1016/j.yjmcc.2007.05.010

Anselmino, M., Matta, M., D'Ascenzo, F., Bunch, T. J., Schilling, R. J., Hunter, R. J., et al. (2014). Catheter ablation of atrial fibrillation in patients with

left ventricular systolic dysfunction: a systematic review and meta-analysis. *Circ. Arrhythm. Electrophysiol.* 7, 1011–1018. doi: 10.1161/CIRCEP.114.001938

Antzelevitch, C., and Burashnikov, A. (2011). Overview of basic mechanisms of cardiac arrhythmia. *Card. Electrophysiol. Clin.* 3, 23–45. doi: 10.1016/j.ccep.2010.10.012

Anzai, K., Ogawa, K., Kuniyasu, A., Ozawa, T., Yamamoto, H., and Nakayama, H. (1998). Effects of hydroxyl radical and sulfhydryl reagents on the open probability of the purified cardiac ryanodine receptor channel incorporated into planar lipid bilayers. *Biochem. Biophys. Res. Commun.* 249, 938–942. doi: 10.1006/bbrc.1998.9244

Armoundas, A. A., Hobai, I. A., Tomaselli, G. F., Winslow, R. L., and O'Rourke, B. (2003). Role of sodium-calcium exchanger in modulating the action potential of ventricular myocytes from normal and failing hearts. *Circ. Res.* 93, 46–53. doi: 10.1161/01.RES.0000080932.98903.D8

Arora, R., Verheule, S., Scott, L., Navarrete, A., Katari, V., Wilson, E., et al. (2003). Arrhythmogenic substrate of the pulmonary veins assessed by high-resolution optical mapping. *Circulation* 107, 1816–1821. doi: 10.1161/01.CIR.0000058461.86339.7E

Ausma, J., Dispersyn, G. D., Duimel, H., Thone, F., Ver Donck, L., Allessie, M. A., et al. (2000). Changes in ultrastructural calcium distribution in goat atria during atrial fibrillation. *J. Mol. Cell. Cardiol.* 32, 355–364. doi: 10.1006/jmcc.1999.1090

Babu, G. J., Bhupathy, P., Timofeyev, V., Petrashevskaya, N. N., Reiser, P. J., Chiamvimonvat, N., et al. (2007). Ablation of sarcolipin enhances sarcoplasmic reticulum calcium transport and atrial contractility. *Proc. Natl. Acad. Sci. U. S. A.* 104, 17867–17872. doi: 10.1073/pnas.0707722104

Bardy, G. H., Lee, K. L., Mark, D. B., Poole, J. E., Packer, D. L., Boineau, R., et al. (2005). Amiodarone or an implantable cardioverter-defibrillator for congestive heart failure. *N. Engl. J. Med.* 352, 225–237. doi: 10.1056/NEJMoa043399

Barth, A. S., Kumordzie, A., Frangakis, C., Margulies, K. B., Cappola, T. P., and Tomaselli, G. F. (2011). Reciprocal transcriptional regulation of metabolic and signaling pathways correlates with disease severity in heart failure. *Circ. Cardiovasc. Genet.* 4, 475–483. doi: 10.1161/CIRCGENETICS.110.957571

Barth, A. S., Kumordzie, A., and Tomaselli, G. F. (2016). Orchestrated regulation of energy supply and energy expenditure: transcriptional coexpression of metabolism, ion homeostasis, and sarcomeric genes in mammalian myocardium. *Heart Rhythm* 13, 1131–1139. doi: 10.1016/j.hrthm.2016.01.009

Bassani, J. W., Bassani, R. A., and Bers, D. M. (1994). Relaxation in rabbit and rat cardiac cells: species-dependent differences in cellular mechanisms. *J. Physiol.* 476, 279–293. doi: 10.1113/jphysiol.1994.sp020130

Beavers, D. L., Wang, W., Ather, S., Voigt, N., Garbino, A., Dixit, S. S., et al. (2013). Mutation E169K in junctophilin-2 causes atrial fibrillation due to impaired RyR2 stabilization. *J. Am. Coll. Cardiol.* 62, 2010–2019. doi: 10.1016/j.jacc.2013.06.052

Benjamin, E. J., Levy, D., Vaziri, S. M., D'Agostino, R. B., Belanger, A. J., and Wolf, P. A. (1994). Independent risk factors for atrial fibrillation in a population-based cohort. The Framingham Heart Study. *JAMA.* 271, 840–844.

Benjamin, E. J., Wolf, P. A., D'Agostino, R. B., Silbershatz, H., Kannel, W. B., and Levy, D. (1998). Impact of atrial fibrillation on the risk of death: the Framingham Heart Study. *Circulation* 98, 946–952. doi: 10.1161/01.CIR.98.10.946

Benkusky, N. A., Weber, C. S., Scherman, J. A., Farrell, E. F., Hacker, T. A., John, M. C., et al. (2007). Intact beta-adrenergic response and unmodified progression toward heart failure in mice with genetic ablation of a major protein kinase A phosphorylation site in the cardiac ryanodine receptor. *Circ. Res.* 101, 819–829. doi: 10.1161/CIRCRESAHA.107.153007

Berenfeld, O., and Jalife, J. (2014). Mechanisms of atrial fibrillation: rotors, ionic determinants, and excitation frequency. *Cardiol. Clin.* 32, 495–506. doi: 10.1016/j.ccl.2014.07.001

Beresewicz, A., and Horackova, M. (1991). Alterations in electrical and contractile behavior of isolated cardiomyocytes by hydrogen peroxide: possible ionic mechanisms. *J. Mol. Cell. Cardiol.* 23, 899–918. doi: 10.1016/0022-2828(91)90133-7

Bers, D. M. (2001). *Excitation-Contraction Coupling and Cardiac Contractile Force. 2nd Edn*. Dordrecht; London: Kluwer Academic.

Bers, D. M. (2002). Cardiac excitation-contraction coupling. *Nature* 415, 198–205. doi: 10.1038/415198a

Bertero, E., and Maack, C. (2018). Calcium signaling and reactive oxygen species in mitochondria. *Circ. Res.* 122, 1460–1478. doi: 10.1161/CIRCRESAHA.118.310082

Bode, F., Katchman, A., Woosley, R. L., and Franz, M. R. (2000). Gadolinium decreases stretch-induced vulnerability to atrial fibrillation. *Circulation* 101, 2200–2205. doi: 10.1161/01.CIR.101.18.2200

Bode, F., Kilborn, M., Karasik, P., and Franz, M. R. (2001). The repolarization-excitability relationship in the human right atrium is unaffected by cycle length, recording site and prior arrhythmias. *J. Am. Coll. Cardiol.* 37, 920–925. doi: 10.1016/S0735-1097(00)01189-X

Boixel, C., Gonzalez, W., Louedec, L., and Hatem, S. N. (2001). Mechanisms of L-type Ca^{2+} current downregulation in rat atrial myocytes during heart failure. *Circ. Res.* 89, 607–613. doi: 10.1161/hh1901.096702

Bonilla, I. M., Long, V. P. III., Vargas-Pinto, P., Wright, P., Belevych, A., Lou, Q., et al. (2014). Calcium-activated potassium current modulates ventricular repolarization in chronic heart failure. *PLoS ONE* 9:e108824. doi: 10.1371/journal.pone.0108824

Bosch, R. F., Scherer, C. R., Rub, N., Wohrl, S., Steinmeyer, K., Haase, H., et al. (2003). Molecular mechanisms of early electrical remodeling: transcriptional downregulation of ion channel subunits reduces I(Ca,L) and I(to) in rapid atrial pacing in rabbits. *J. Am. Coll. Cardiol.* 41, 858–869. doi: 10.1016/S0735-1097(02)02922-4

Bosch, R. F., Zeng, X., Grammer, J. B., Popovic, K., Mewis, C., and Kuhlkamp, V. (1999). Ionic mechanisms of electrical remodeling in human atrial fibrillation. *Cardiovasc. Res.* 44, 121–131. doi: 10.1016/S0008-6363(99)00178-9

Brandenburg, S., Kohl, T., Williams, G. S., Gusev, K., Wagner, E., Rog-Zielinska, E. A., et al. (2016). Axial tubule junctions control rapid calcium signaling in atria. *J. Clin. Invest.* 126, 3999–4015. doi: 10.1172/JCI88241

Brette, F., Komukai, K., and Orchard, C. H. (2002). Validation of formamide as a detubulation agent in isolated rat cardiac cells. *Am. J. Physiol. Heart Circ. Physiol.* 283, H1720–H1728. doi: 10.1152/ajpheart.00347.2002

Brette, F., Salle, L., and Orchard, C. H. (2006). Quantification of calcium entry at the T-tubules and surface membrane in rat ventricular myocytes. *Biophys. J.* 90, 381–389. doi: 10.1529/biophysj.105.069013

Briston, S. J., Caldwell, J. L., Horn, M. A., Clarke, J. D., Richards, M. A., Greensmith, D. J., et al. (2011). Impaired beta-adrenergic responsiveness accentuates dysfunctional excitation-contraction coupling in an ovine model of tachypacing-induced heart failure. *J. Physiol.* 589 (Pt. 6), 1367–1382. doi: 10.1113/jphysiol.2010.203984

Briston, S. J., Dibb, K. M., Solaro, R. J., Eisner, D. A., and Trafford, A. W. (2014). Balanced changes in Ca buffering by SERCA and troponin contribute to Ca handling during beta-adrenergic stimulation in cardiac myocytes. *Cardiovasc. Res.* 104, 347–354. doi: 10.1093/cvr/cvu201

Brodsky, M. A., Allen, B. J., Capparelli, E. V., Luckett, C. R., Morton, R., and Henry, W. L. (1989). Factors determining maintenance of sinus rhythm after chronic atrial fibrillation with left atrial dilatation. *Am. J. Cardiol.* 63, 1065–1068. doi: 10.1016/0002-9149(89)90079-9

Brundel, B. J., Van Gelder, I. C., Henning, R. H., Tieleman, R. G., Tuinenburg, A. E., Wietses, M., et al. (2001). Ion channel remodeling is related to intraoperative atrial effective refractory periods in patients with paroxysmal and persistent atrial fibrillation. *Circulation* 103, 684–690. doi: 10.1161/01.CIR.103.5.684

Brundel, B. J., van Gelder, I. C., Henning, R. H., Tuinenburg, A. E., Deelman, L. E., Tieleman, R. G., et al. (1999). Gene expression of proteins influencing the calcium homeostasis in patients with persistent and paroxysmal atrial fibrillation. *Cardiovasc. Res.* 42, 443–454. doi: 10.1016/S0008-6363(99)00045-0

Bukowska, A., Lendeckel, U., Hirte, D., Wolke, C., Striggow, F., Rohnert, P., et al. (2006). Activation of the calcineurin signaling pathway induces atrial hypertrophy during atrial fibrillation. *Cell. Mol. Life Sci.* 63, 333–342. doi: 10.1007/s00018-005-5353-3

Bukowska, A., Schild, L., Keilhoff, G., Hirte, D., Neumann, M., Gardemann, A., et al. (2008). Mitochondrial dysfunction and redox signaling in atrial tachyarrhythmia. *Exp. Biol. Med.* 233, 558–574. doi: 10.3181/0706-RM-155

Burashnikov, A., and Antzelevitch, C. (2003). Reinduction of atrial fibrillation immediately after termination of the arrhythmia is mediated by late phase 3 early afterdepolarization-induced triggered activity. *Circulation* 107, 2355–2360. doi: 10.1161/01.CIR.0000065578.00869.7C

Burashnikov, A., and Antzelevitch, C. (2006). Late-phase 3 EAD. A unique mechanism contributing to initiation of atrial fibrillation. *Pacing Clin. Electrophysiol.* 29, 290–295. doi: 10.1111/j.1540-8159.2006.00336.x

Burstein, B., Libby, E., Calderone, A., and Nattel, S. (2008). Differential behaviors of atrial versus ventricular fibroblasts: a potential role for platelet-derived growth factor in atrial-ventricular remodeling differences. *Circulation* 117, 1630–1641. doi: 10.1161/CIRCULATIONAHA.107.748053

Caldwell, J. L., Smith, C. E., Taylor, R. F., Kitmitto, A., Eisner, D. A., Dibb, K. M., et al. (2014). Dependence of cardiac transverse tubules on the BAR domain protein amphiphysin II (BIN-1). *Circ. Res.* 115, 986–996. doi: 10.1161/CIRCRESAHA.116.303448

Cao, K., Xia, X., Shan, Q., Chen, Z., Chen, X., and Huang, Y. (2002). Changes of sarcoplamic reticular Ca^{2+}-ATPase and IP(3)-I receptor mRNA expression in patients with atrial fibrillation. *Chin. Med. J.* 115, 664–667. Available online at: http://124.205.33.103:81/ch/reader/view_abstract.aspx?file_no=20025664&flag=1

Carnes, C. A., Chung, M. K., Nakayama, T., Nakayama, H., Baliga, R. S., Piao, S., et al. (2001). Ascorbate attenuates atrial pacing-induced peroxynitrite formation and electrical remodeling and decreases the incidence of postoperative atrial fibrillation. *Circ. Res.* 89, E32–E38. doi: 10.1161/hh1801.097644

Cha, T. J., Ehrlich, J. R., Zhang, L., and Nattel, S. (2004a). Atrial ionic remodeling induced by atrial tachycardia in the presence of congestive heart failure. *Circulation* 110, 1520–1526. doi: 10.1161/01.CIR.0000142052.03565.87

Cha, T. J., Ehrlich, J. R., Zhang, L., Shi, Y. F., Tardif, J. C., Leung, T. K., et al. (2004b). Dissociation between ionic remodeling and ability to sustain atrial fibrillation during recovery from experimental congestive heart failure. *Circulation* 109, 412–418. doi: 10.1161/01.CIR.0000109501.47603.0C

Cha, Y. M., Dzeja, P. P., Shen, W. K., Jahangir, A., Hart, C. Y., Terzic, A., et al. (2003). Failing atrial myocardium: energetic deficits accompany structural remodeling and electrical instability. *Am. J. Physiol. Heart Circ. Physiol.* 284, H1313–H1320. doi: 10.1152/ajpheart.00337.2002

Chang, S. H., Chen, Y. C., Chiang, S. J., Higa, S., Cheng, C. C., Chen, Y. J., et al. (2008). Increased Ca^{2+} sparks and sarcoplasmic reticulum Ca^{2+} stores potentially determine the spontaneous activity of pulmonary vein cardiomyocytes. *Life Sci.* 83, 284–292. doi: 10.1016/j.lfs.2008.06.014

Chaugai, S., Meng, W. Y., and Ali Sepehry, A. (2016). Effects of RAAS blockers on atrial fibrillation prophylaxis: an updated systematic review and meta-analysis of randomized controlled trials. *J. Cardiovasc. Pharmacol. Ther.* 21, 388–404. doi: 10.1177/1074248415619490

Chelu, M. G., Sarma, S., Sood, S., Wang, S., van Oort, R. J., Skapura, D. G., et al. (2009). Calmodulin kinase II-mediated sarcoplasmic reticulum Ca^{2+} leak promotes atrial fibrillation in mice. *J. Clin. Invest.* 119, 1940–1951. doi: 10.1172/JCI37059

Chen, B., Zhang, C., Guo, A., and Song, L. S. (2015). *In situ* single photon confocal imaging of cardiomyocyte T-tubule system from Langendorff-perfused hearts. *Front. Physiol.* 6:134. doi: 10.3389/fphys.2015.00134

Chen, Y. J., Chen, S. A., Chang, M. S., and Lin, C. I. (2000). Arrhythmogenic activity of cardiac muscle in pulmonary veins of the dog: implication for the genesis of atrial fibrillation. *Cardiovasc. Res.* 48, 265–273. doi: 10.1016/S0008-6363(00)00179-6

Cheng, H., Lederer, M. R., Lederer, W. J., and Cannell, M. B. (1996). Calcium sparks and $[Ca^{2+}]$i waves in cardiac myocytes. *Am. J. Physiol.* 270 (Pt. 1), C148–C159. doi: 10.1152/ajpcell.1996.270.1.C148

Cheng, H., Lederer, W. J., and Cannell, M. B. (1993). Calcium sparks: elementary events underlying excitation-contraction coupling in heart muscle. *Science* 262, 740–744. doi: 10.1126/science.8235594

Cheng, T. H., Lee, F. Y., Wei, J., and Lin, C. I. (1996). Comparison of calcium-current in isolated atrial myocytes from failing and nonfailing human hearts. *Mol. Cell. Biochem.* 157, 157–162.

Chiang, D. Y., Kongchan, N., Beavers, D. L., Alsina, K. M., Voigt, N., Neilson, J. R., et al. (2014a). Loss of microRNA-106b-25 cluster promotes atrial fibrillation by enhancing ryanodine receptor type-2 expression and calcium release. *Circ. Arrhythm. Electrophysiol.* 7, 1214–1222. doi: 10.1161/CIRCEP.114.001973

Chiang, D. Y., Li, N., Wang, Q., Alsina, K. M., Quick, A. P., Reynolds, J. O., et al. (2014b). Impaired local regulation of ryanodine receptor type 2 by protein phosphatase 1 promotes atrial fibrillation. *Cardiovasc. Res.* 103, 178–187. doi: 10.1093/cvr/cvu123

Chou, C. C., Nihei, M., Zhou, S., Tan, A., Kawase, A., Macias, E. S., et al. (2005). Intracellular calcium dynamics and anisotropic reentry in isolated canine pulmonary veins and left atrium. *Circulation* 111, 2889–2897. doi: 10.1161/CIRCULATIONAHA.104.498758

Christ, T., Boknik, P., Wohrl, S., Wettwer, E., Graf, E. M., Bosch, R. F., et al. (2004). L-type Ca^{2+} current downregulation in chronic human atrial fibrillation is associated with increased activity of protein phosphatases. *Circulation* 110, 2651–2657. doi: 10.1161/01.CIR.0000145659.80212.6A

Chugh, S. S., Havmoeller, R., Narayanan, K., Singh, D., Rienstra, M., Benjamin, E. J., et al. (2014). Worldwide epidemiology of atrial fibrillation: a Global Burden of Disease 2010 Study. *Circulation* 129, 837–847. doi: 10.1161/CIRCULATIONAHA.113.005119

Clark, D. M., Plumb, V. J., Epstein, A. E., and Kay, G. N. (1997). Hemodynamic effects of an irregular sequence of ventricular cycle lengths during atrial fibrillation. *J. Am. Coll. Cardiol.* 30, 1039–1045. doi: 10.1016/S0735-1097(97)00254-4

Clarke, J. D., Caldwell, J. L., Horn, M. A., Bode, E. F., Richards, M. A., Hall, M. C., et al. (2015). Perturbed atrial calcium handling in an ovine model of heart failure: potential roles for reductions in the L-type calcium current. *J. Mol. Cell. Cardiol.* 79, 169–179. doi: 10.1016/j.yjmcc.2014.11.017

Clarke, J. D., Caldwell, J. L., Pearman, C. M., Eisner, D. A., Trafford, A. W., and Dibb, K. M. (2017). Increased Ca buffering underpins remodelling of Ca^{2+} handling in old sheep atrial myocytes. *J. Physiol.* 595, 6263–6279. doi: 10.1113/JP274053

Comtois, P., Kneller, J., and Nattel, S. (2005). Of circles and spirals: bridging the gap between the leading circle and spiral wave concepts of cardiac reentry. *Europace* 7 (Suppl. 2), 10–20. doi: 10.1016/j.eupc.2005.05.011

Coutu, P., Chartier, D., and Nattel, S. (2006). Comparison of Ca^{2+}-handling properties of canine pulmonary vein and left atrial cardiomyocytes. *Am. J. Physiol. Heart Circ. Physiol.* 291, H2290–H2300. doi: 10.1152/ajpheart.00730.2005

Dai, J., Zhang, H., Chen, Y., Chang, Y., Yuan, Q., Ji, G., et al. (2016). Characterization of Ca+ handling proteins and contractile proteins in patients with lone atrial fibrillation. *Int. J. Cardiol.* 202, 749–751. doi: 10.1016/j.ijcard.2015.10.010

De, A. (2011). Wnt/Ca^{2+} signaling pathway: a brief overview. *Acta Biochim. Biophys. Sin.* 43, 745–756. doi: 10.1093/abbs/gmr079

Deroubaix, E., Folliguet, T., Rucker-Martin, C., Dinanian, S., Boixel, C., Validire, P., et al. (2004). Moderate and chronic hemodynamic overload of sheep atria induces reversible cellular electrophysiologic abnormalities and atrial vulnerability. *J. Am. Coll. Cardiol.* 44, 1918–1926. doi: 10.1016/j.jacc.2004.07.055

Diaz, M. E., Trafford, A. W., O'Neill, S. C., and Eisner, D. A. (1997). Measurement of sarcoplasmic reticulum Ca^{2+} content and sarcolemmal Ca^{2+} fluxes in isolated rat ventricular myocytes during spontaneous Ca^{2+} release. *J. Physiol.* 501, 3–16.

Dibb, K. M., Clarke, J. D., Horn, M. A., Richards, M. A., Graham, H. K., Eisner, D. A., et al. (2009). Characterization of an extensive transverse tubular network in sheep atrial myocytes and its depletion in heart failure. *Circ. Heart Fail.* 2, 482–489. doi: 10.1161/CIRCHEARTFAILURE.109.852228

Dibb, K. M., Eisner, D. A., and Trafford, A. W. (2007). Regulation of systolic $[Ca^{2+}]$i and cellular Ca^{2+} flux balance in rat ventricular myocytes by SR Ca^{2+}, L-type Ca^{2+} current and diastolic $[Ca^{2+}]$i. *J. Physiol.* 585 (Pt. 2), 579–592. doi: 10.1113/jphysiol.2007.141473

Dinanian, S., Boixel, C., Juin, C., Hulot, J. S., Coulombe, A., Rucker-Martin, C., et al. (2008). Downregulation of the calcium current in human right atrial myocytes from patients in sinus rhythm but with a high risk of atrial fibrillation. *Eur. Heart J.* 29, 1190–1197. doi: 10.1093/eurheartj/ehn140

Dobrev, D., Friedrich, A., Voigt, N., Jost, N., Wettwer, E., Christ, T., et al. (2005). The G protein-gated potassium current I(K,ACh) is constitutively active in patients with chronic atrial fibrillation. *Circulation* 112, 3697–3706. doi: 10.1161/CIRCULATIONAHA.105.575332

Dobrev, D., and Wehrens, X. H. (2014). Role of RyR2 phosphorylation in heart failure and arrhythmias: Controversies around ryanodine receptor phosphorylation in cardiac disease. *Circ. Res.* 114, 1311–1319. doi: 10.1161/CIRCRESAHA.114.300568

Dobrev, D., and Wehrens, X. H. T. (2017). Calcium-mediated cellular triggered activity in atrial fibrillation. *J. Physiol.* 595, 4001–4008. doi: 10.1113/JP273048

Dorn, G. W. II., and Maack, C. (2013). SR and mitochondria: calcium cross-talk between kissing cousins. *J. Mol. Cell. Cardiol.* 55, 42–49. doi: 10.1016/j.yjmcc.2012.07.015

Drawnel, F. M., Archer, C. R., and Roderick, H. L. (2013). The role of the paracrine/autocrine mediator endothelin-1 in regulation of cardiac contractility and growth. *Br. J. Pharmacol.* 168, 296–317. doi: 10.1111/j.1476-5381.2012.02195.x

Dries, D. L., Exner, D. V., Gersh, B. J., Domanski, M. J., Waclawiw, M. A., and Stevenson, L. W. (1998). Atrial fibrillation is associated with an increased risk for mortality and heart failure progression in patients with asymptomatic and symptomatic left ventricular systolic dysfunction: a retrospective analysis of the SOLVD trials. Studies of Left Ventricular Dysfunction. *J. Am. Coll. Cardiol.* 32, 695–703. doi: 10.1016/S0735-1097(98)00297-6

Dries, E., Bito, V., Lenaerts, I., Antoons, G., Sipido, K. R., and Macquaide, N. (2013). Selective modulation of coupled ryanodine receptors during microdomain activation of calcium/calmodulin-dependent kinase II in the dyadic cleft. *Circ. Res.* 113, 1242–1252. doi: 10.1161/CIRCRESAHA.113.301896

Dupont, E., Ko, Y., Rothery, S., Coppen, S. R., Baghai, M., Haw, M., et al. (2001). The gap-junctional protein connexin40 is elevated in patients susceptible to postoperative atrial fibrillation. *Circulation* 103, 842–849. doi: 10.1161/01.CIR.103.6.842

Eckstein, J., Verheule, S., de Groot, N. M., Allessie, M., and Schotten, U. (2008). Mechanisms of perpetuation of atrial fibrillation in chronically dilated atria. *Prog. Biophys. Mol. Biol.* 97, 435–451. doi: 10.1016/j.pbiomolbio.2008.02.019

Ehrlich, J. R., Cha, T. J., Zhang, L., Chartier, D., Melnyk, P., Hohnloser, S. H., et al. (2003). Cellular electrophysiology of canine pulmonary vein cardiomyocytes: action potential and ionic current properties. *J. Physiol.* 551 (Pt. 3), 801–813. doi: 10.1113/jphysiol.2003.046417

Eijsbouts, S. C., Majidi, M., van Zandvoort, M., and Allessie, M. A. (2003). Effects of acute atrial dilation on heterogeneity in conduction in the isolated rabbit heart. *J. Cardiovasc. Electrophysiol.* 14, 269–278. doi: 10.1046/j.1540-8167.2003.02280.x

Eisner, D., Bode, E., Venetucci, L., and Trafford, A. (2013). Calcium flux balance in the heart. *J. Mol. Cell. Cardiol.* 58, 110–117. doi: 10.1016/j.yjmcc.2012.11.017

Eisner, D. A., Caldwell, J. L., Kistamas, K., and Trafford, A. W. (2017). Calcium and excitation-contraction coupling in the heart. *Circ. Res.* 121, 181–195. doi: 10.1161/CIRCRESAHA.117.310230

Eisner, D. A., Diaz, M. E., Li, Y., O'Neill, S. C., and Trafford, A. W. (2005). Stability and instability of regulation of intracellular calcium. *Exp. Physiol.* 90, 3–12. doi: 10.1113/expphysiol.2004.029231

El-Armouche, A., Boknik, P., Eschenhagen, T., Carrier, L., Knaut, M., Ravens, U., et al. (2006). Molecular determinants of altered Ca^{2+} handling in human chronic atrial fibrillation. *Circulation* 114, 670–680. doi: 10.1161/CIRCULATIONAHA.106.636845

Elvan, A., Huang, X. D., Pressler, M. L., and Zipes, D. P. (1997). Radiofrequency catheter ablation of the atria eliminates pacing-induced sustained atrial fibrillation and reduces connexin 43 in dogs. *Circulation* 96, 1675–1685. doi: 10.1161/01.CIR.96.5.1675

Faggioni, M., Savio-Galimberti, E., Venkataraman, R., Hwang, H. S., Kannankeril, P. J., Darbar, D., et al. (2014). Suppression of spontaneous ca elevations prevents atrial fibrillation in calsequestrin 2-null hearts. *Circ. Arrhythm. Electrophysiol.* 7, 313–320. doi: 10.1161/CIRCEP.113.000994

Fermini, B., and Schanne, O. F. (1991). Determinants of action potential duration in neonatal rat ventricle cells. *Cardiovasc. Res.* 25, 235–243. doi: 10.1093/cvr/25.3.235

Ferrier, G. R., Saunders, J. H., and Mendez, C. (1973). A cellular mechanism for the generation of ventricular arrhythmias by acetylstrophanthidin. *Circ. Res.* 32, 600–609. doi: 10.1161/01.RES.32.5.600

Fredersdorf, S., Ucer, E., Jungbauer, C., Dornia, C., Eglmeier, J., Eissnert, C., et al. (2014). Lone atrial fibrillation as a positive predictor of left atrial volume reduction following ablation of atrial fibrillation. *Europace* 16, 26–32. doi: 10.1093/europace/eut152

Frisk, M., Koivumaki, J. T., Norseng, P. A., Maleckar, M. M., Sejersted, O. M., and Louch, W. E. (2014). Variable t-tubule organization and Ca^{2+} homeostasis across the atria. *Am. J. Physiol.Heart Circ. Physiol.* 307, H609–H620. doi: 10.1152/ajpheart.00295.2014

From, A. M., Maleszewski, J. J., and Rihal, C. S. (2011). Current status of endomyocardial biopsy. *Mayo Clin. Proc.* 86, 1095–1102. doi: 10.4065/mcp.2011.0296

Fujino, T., Yamashita, T., Suzuki, S., Sugiyma, H., Sagara, K., Sawada, H., et al. (2007). Characteristics of congestive heart failure accompanied by atrial fibrillation with special reference to tachycardia-induced cardiomyopathy. *Circ. J.* 71, 936–940. doi: 10.1253/circj.71.936

Fukui, A., Takahashi, N., Nakada, C., Masaki, T., Kume, O., Shinohara, T., et al. (2013). Role of leptin signaling in the pathogenesis of angiotensin II-mediated atrial fibrosis and fibrillation. *Circ. Arrhythm. Electrophysiol.* 6, 402–409. doi: 10.1161/CIRCEP.111.000104

Fukushima, A., Milner, K., Gupta, A., and Lopaschuk, G. D. (2015). Myocardial energy substrate metabolism in heart failure : from pathways to therapeutic targets. *Curr. Pharm. Des.* 21, 3654–3664. doi: 10.2174/1381612821666150710150445

Gaborit, N., Steenman, M., Lamirault, G., Le Meur, N., Le Bouter, S., Lande, G., et al. (2005). Human atrial ion channel and transporter subunit gene-expression remodeling associated with valvular heart disease and atrial fibrillation. *Circulation* 112, 471–481. doi: 10.1161/CIRCULATIONAHA.104.506857

Gadeberg, H. C., Bond, R. C., Kong, C. H., Chanoit, G. P., Ascione, R., Cannell, M. B., et al. (2016). Heterogeneity of T-tubules in pig hearts. *PLoS ONE* 11:e0156862. doi: 10.1371/journal.pone.0156862

Gaspo, R., Bosch, R. F., Bou-Abboud, E., and Nattel, S. (1997a). Tachycardia-induced changes in Na+ current in a chronic dog model of atrial fibrillation. *Circ. Res.* 81, 1045–1052. doi: 10.1161/01.RES.81.6.1045

Gaspo, R., Bosch, R. F., Talajic, M., and Nattel, S. (1997b). Functional mechanisms underlying tachycardia-induced sustained atrial fibrillation in a chronic dog model. *Circulation* 96, 4027–4035. doi: 10.1161/01.CIR.96.11.4027

Giles, W. R., and Imaizumi, Y. (1988). Comparison of potassium currents in rabbit atrial and ventricular cells. *J. Physiol.* 405, 123–145. doi: 10.1113/jphysiol.1988.sp017325

Gillis, A. M., and Rose, M. S. (2000). Temporal patterns of paroxysmal atrial fibrillation following DDDR pacemaker implantation. *Am. J. Cardiol.* 85, 1445–1450. doi: 10.1016/S0002-9149(00)00792-X

Glukhov, A. V., Balycheva, M., Sanchez-Alonso, J. L., Ilkan, Z., Alvarez-Laviada, A., Bhogal, N., et al. (2015). Direct evidence for microdomain-specific localization and remodeling of functional L-type calcium channels in rat and human atrial myocytes. *Circulation* 132, 2372–2384. doi: 10.1161/CIRCULATIONAHA.115.018131

Goudis, C. A., Korantzopoulos, P., Ntalas, I. V., Kallergis, E. M., and Ketikoglou, D. G. (2015). Obesity and atrial fibrillation: a comprehensive review of the pathophysiological mechanisms and links. *J. Cardiol.* 66, 361–369. doi: 10.1016/j.jjcc.2015.04.002

Greiser, M. (2017). Calcium signalling silencing in atrial fibrillation. *J. Physiol.* 595, 4009–4017. doi: 10.1113/JP273045

Greiser, M., Kerfant, B. G., Williams, G. S., Voigt, N., Harks, E., Dibb, K. M., et al. (2014). Tachycardia-induced silencing of subcellular Ca^{2+} signaling in atrial myocytes. *J. Clin. Invest.* 124, 4759–4772. doi: 10.1172/JCI70102

Greiser, M., Neuberger, H. R., Harks, E., El-Armouche, A., Boknik, P., de Haan, S., et al. (2009). Distinct contractile and molecular differences between two goat models of atrial dysfunction: AV block-induced atrial dilatation and atrial fibrillation. *J. Mol. Cell. Cardiol.* 46, 385–394. doi: 10.1016/j.yjmcc.2008.11.012

Griffiths, E. J. (2012). Mitochondria and heart disease. *Adv. Exp. Med. Biol.* 942, 249–267. doi: 10.1007/978-94-007-2869-1_11

Grogan, M., Smith, H. C., Gersh, B. J., and Wood, D. L. (1992). Left ventricular dysfunction due to atrial fibrillation in patients initially believed to have idiopathic dilated cardiomyopathy. *Am. J. Cardiol.* 69, 1570–1573. doi: 10.1016/0002-9149(92)90705-4

Gussak, I., Chaitman, B. R., Kopecky, S. L., and Nerbonne, J. M. (2000). Rapid ventricular repolarization in rodents: electrocardiographic manifestations, molecular mechanisms, and clinical insights. *J. Electrocardiol.* 33, 159–170. doi: 10.1016/S0022-0736(00)80072-2

Gyorke, I., Hester, N., Jones, L. R., and Gyorke, S. (2004). The role of calsequestrin, triadin, and junctin in conferring cardiac ryanodine receptor responsiveness to luminal calcium. *Biophys. J.* 86, 2121–2128. doi: 10.1016/S0006-3495(04)74271-X

Haissaguerre, M., Jais, P., Shah, D. C., Takahashi, A., Hocini, M., Quiniou, G., et al. (1998). Spontaneous initiation of atrial fibrillation by ectopic beats originating in the pulmonary veins. *N. Engl. J. Med.* 339, 659–666. doi: 10.1056/NEJM199809033391003

Harada, M., Luo, X., Qi, X. Y., Tadevosyan, A., Maguy, A., Ordog, B., et al. (2012). Transient receptor potential canonical-3 channel-dependent fibroblast regulation in atrial fibrillation. *Circulation* 126, 2051–2064. doi: 10.1161/CIRCULATIONAHA.112.121830

Harjai, K. J., Mobarek, S. K., Cheirif, J., Boulos, L. M., Murgo, J. P., and Abi-Samra, F. (1997). Clinical variables affecting recovery of left atrial mechanical function after cardioversion from atrial fibrillation. *J. Am. Coll. Cardiol.* 30, 481–486. doi: 10.1016/S0735-1097(97)00173-3

He, J., Conklin, M. W., Foell, J. D., Wolff, M. R., Haworth, R. A., Coronado, R., et al. (2001). Reduction in density of transverse tubules and L-type Ca^{2+} channels in canine tachycardia-induced heart failure. *Cardiovasc. Res.* 49, 298–307. doi: 10.1016/S0008-6363(00)00256-X

Hecht, H. H., and Lange, R. L. (1956). The hemodynamic consequences of atrial fibrillation. *Mod. Concepts Cardiovasc. Dis.* 25, 351–353.

Heijman, J., Algalarrondo, V., Voigt, N., Melka, J., Wehrens, X. H., Dobrev, D., et al. (2016). The value of basic research insights into atrial fibrillation mechanisms as a guide to therapeutic innovation: a critical analysis. *Cardiovasc. Res.* 109, 467–479. doi: 10.1093/cvr/cvv275

Heinzel, F. R., Bito, V., Biesmans, L., Wu, M., Detre, E., von Wegner, F., et al. (2008). Remodeling of T-tubules and reduced synchrony of Ca^{2+} release in myocytes from chronically ischemic myocardium. *Circ. Res.* 102, 338–346. doi: 10.1161/CIRCRESAHA.107.160085

Helms, A. S., West, J. J., Patel, A., Lipinski, M. J., Mangrum, J. M., Mounsey, J. P., et al. (2009). Relation of left atrial volume from three-dimensional computed tomography to atrial fibrillation recurrence following ablation. *Am. J. Cardiol.* 103, 989–993. doi: 10.1016/j.amjcard.2008.12.021

Hibberd, M. G., and Jewell, B. R. (1982). Calcium- and length-dependent force production in rat ventricular muscle. *J. Physiol.* 329, 527–540. doi: 10.1113/jphysiol.1982.sp014317

Ho, H. T., Belevych, A. E., Liu, B., Bonilla, I. M., Radwanski, P. B., Kubasov, I. V., et al. (2016). Muscarinic stimulation facilitates sarcoplasmic reticulum Ca release by modulating ryanodine receptor 2 phosphorylation through protein kinase, G., and Ca/calmodulin-dependent protein kinase, II. *Hypertension* 68, 1171–1178. doi: 10.1161/HYPERTENSIONAHA.116.07666

Hobai, I. A., and O'Rourke, B. (2001). Decreased sarcoplasmic reticulum calcium content is responsible for defective excitation-contraction coupling in canine heart failure. *Circulation* 103, 1577–1584. doi: 10.1161/01.CIR.103.11.1577

Hocini, M., Ho, S. Y., Kawara, T., Linnenbank, A. C., Potse, M., Shah, D., et al. (2002). Electrical conduction in canine pulmonary veins: electrophysiological and anatomic correlation. *Circulation* 105, 2442–2448. doi: 10.1161/01.CIR.0000016062.80020.11

Hohendanner, F., DeSantiago, J., Heinzel, F. R., and Blatter, L. A. (2016). Dyssynchronous calcium removal in heart failure-induced atrial remodeling. *Am. J. Physiol. Heart Circ. Physiol.* 311, H1352–H1359. doi: 10.1152/ajpheart.00375.2016

Hohendanner, F., Walther, S., Maxwell, J. T., Kettlewell, S., Awad, S., Smith, G. L., et al. (2015). Inositol-1,4,5-trisphosphate induced Ca^{2+} release and excitation-contraction coupling in atrial myocytes from normal and failing hearts. *J. Physiol.* 593, 1459–1477. doi: 10.1113/jphysiol.2014.283226

Hoit, B. D., Takeishi, Y., Cox, M. J., Gabel, M., Kirkpatrick, D., Walsh, R. A., et al. (2002). Remodeling of the left atrium in pacing-induced atrial cardiomyopathy. *Mol. Cell. Biochem.* 238, 145–150. doi: 10.1023/A:1019988024077

Honjo, H., Boyett, M. R., Niwa, R., Inada, S., Yamamoto, M., Mitsui, K., et al. (2003). Pacing-induced spontaneous activity in myocardial sleeves of pulmonary veins after treatment with ryanodine. *Circulation* 107, 1937–1943. doi: 10.1161/01.CIR.0000062645.38670.BD

Houser, S. R. (2014). Role of RyR2 phosphorylation in heart failure and arrhythmias: protein kinase A-mediated hyperphosphorylation of the ryanodine receptor at serine 2808 does not alter cardiac contractility or cause heart failure and arrhythmias. *Circ. Res.* 114, 1320–1327. doi: 10.1161/CIRCRESAHA.114.300569

Hove-Madsen, L., Llach, A., Bayes-Genis, A., Roura, S., Rodriguez Font, E., Aris, A., et al. (2004). Atrial fibrillation is associated with increased spontaneous calcium release from the sarcoplasmic reticulum in human atrial myocytes. *Circulation* 110, 1358–1363. doi: 10.1161/01.CIR.0000141296.59876.87

Hsueh, C. H., Chang, P. C., Hsieh, Y. C., Reher, T., Chen, P. S., and Lin, S. F. (2013). Proarrhythmic effect of blocking the small conductance calcium activated potassium channel in isolated canine left atrium. *Heart Rhythm* 10, 891–898. doi: 10.1016/j.hrthm.2013.01.033

Huang, J. L., Tai, C. T., Chen, J. T., Ting, C. T., Chen, Y. T., Chang, M. S., et al. (2003). Effect of atrial dilatation on electrophysiologic properties and inducibility of atrial fibrillation. *Basic Res. Cardiol.* 98, 16–24. doi: 10.1007/s00395-003-0385-z

Huke, S., and Bers, D. M. (2008). Ryanodine receptor phosphorylation at Serine 2030, 2808 and 2814 in rat cardiomyocytes. *Biochem. Biophys. Res. Commun.* 376, 80–85. doi: 10.1016/j.bbrc.2008.08.084

Hume, J. R., and Uehara, A. (1985). Ionic basis of the different action potential configurations of single guinea-pig atrial and ventricular myocytes. *J. Physiol.* 368, 525–544. doi: 10.1113/jphysiol.1985.sp015874

Huser, J., Lipsius, S. L., and Blatter, L. A. (1996). Calcium gradients during excitation-contraction coupling in cat atrial myocytes. *J. Physiol.* 494 (Pt. 3), 641–51.

Iribe, G., and Kohl, P. (2008). Axial stretch enhances sarcoplasmic reticulum Ca^{2+} leak and cellular Ca^{2+} reuptake in guinea pig ventricular myocytes: experiments and models. *Prog. Biophys. Mol. Biol.* 97, 298–311. doi: 10.1016/j.pbiomolbio.2008.02.012

Iribe, G., Ward, C. W., Camelliti, P., Bollensdorff, C., Mason, F., Burton, R. A., et al. (2009). Axial stretch of rat single ventricular cardiomyocytes causes an acute and transient increase in Ca^{2+} spark rate. *Circ. Res.* 104, 787–795. doi: 10.1161/CIRCRESAHA.108.193334

Johannsson, M., and Wohlfart, B. (1980). Cellular calcium as a determinant of action potential duration in rabbit myocardium. *Acta Physiol. Scand.* 110, 241–247. doi: 10.1111/j.1748-1716.1980.tb06660.x

Johnsen, A. B., Hoydal, M., Rosbjorgen, R., Stolen, T., and Wisloff, U. (2013). Aerobic interval training partly reverse contractile dysfunction and impaired Ca^{2+} handling in atrial myocytes from rats with post infarction heart failure. *PLoS ONE* 8:e66288. doi: 10.1371/journal.pone.0066288

Kalifa, J., Jalife, J., Zaitsev, A. V., Bagwe, S., Warren, M., Moreno, J., et al. (2003). Intra-atrial pressure increases rate and organization of waves emanating from the superior pulmonary veins during atrial fibrillation. *Circulation* 108, 668–671. doi: 10.1161/01.CIR.0000086979.39843.7B

Kettlewell, S., Burton, F. L., Smith, G. L., and Workman, A. J. (2013). Chronic myocardial infarction promotes atrial action potential alternans, after depolarizations, and fibrillation. *Cardiovasc. Res.* 99, 215–224. doi: 10.1093/cvr/cvt087

Khan, M. N., Jais, P., Cummings, J., Di Biase, L., Sanders, P., Martin, D. O., et al. (2008). Pulmonary-vein isolation for atrial fibrillation in patients with heart failure. *N. Engl. J. Med.* 359, 1778–1785. doi: 10.1056/NEJMoa0708234

Kim, E. J., Yin, X., Fontes, J. D., Magnani, J. W., Lubitz, S. A., McManus, D. D., et al. (2016). Atrial fibrillation without comorbidities: prevalence, incidence and prognosis (from the Framingham Heart Study). *Am. Heart J.* 177, 138–144. doi: 10.1016/j.ahj.2016.03.023

Kim, J. C., and Woo, S. H. (2015). Shear stress induces a longitudinal Ca^{2+} wave via autocrine activation of P2Y1 purinergic signalling in rat atrial myocytes. *J. Physiol.* 593, 5091–5109. doi: 10.1113/JP271016

Kirchhof, P., Benussi, S., Kotecha, D., Ahlsson, A., Atar, D., Casadei, B., et al. (2016). 2016 ESC Guidelines for the management of atrial fibrillation developed in collaboration with EACTS. *Eur. Heart J.* 37, 2893–2962. doi: 10.1093/eurheartj/ehw210

Kirk, M. M., Izu, L. T., Chen-Izu, Y., McCulle, S. L., Wier, W. G., Balke, C. W., et al. (2003). Role of the transverse-axial tubule system in generating calcium sparks and calcium transients in rat atrial myocytes. *J. Physiol.* 547 (Pt. 2), 441–451. doi: 10.1113/jphysiol.2002.034355

Klein, G., Schroder, F., Vogler, D., Schaefer, A., Haverich, A., Schieffer, B., et al. (2003). Increased open probability of single cardiac L-type calcium channels in patients with chronic atrial fibrillation. role of phosphatase 2A. *Cardiovasc. Res.* 59, 37–45. doi: 10.1016/S0008-6363(03)00357-2

Kneller, J., Sun, H., Leblanc, N., and Nattel, S. (2002). Remodeling of Ca^{2+}-handling by atrial tachycardia: evidence for a role in loss of rate-adaptation. *Cardiovasc. Res.* 54, 416–426. doi: 10.1016/S0008-6363(02)00274-2

Kockskamper, J., von Lewinski, D., Khafaga, M., Elgner, A., Grimm, M., Eschenhagen, T., et al. (2008). The slow force response to stretch in atrial and ventricular myocardium from human heart: functional relevance and subcellular mechanisms. *Prog. Biophys. Mol. Biol.* 97, 250–267. doi: 10.1016/j.pbiomolbio.2008.02.026

Kono, T., Sabbah, H. N., Rosman, H., Alam, M., Stein, P. D., and Goldstein, S. (1992). Left atrial contribution to ventricular filling during the course of evolving heart failure. *Circulation* 86, 1317–1322. doi: 10.1161/01.CIR.86.4.1317

Koumi, S., Arentzen, C. E., Backer, C. L., and Wasserstrom, J. A. (1994). Alterations in muscarinic K+ channel response to acetylcholine and to G protein-mediated activation in atrial myocytes isolated from failing human hearts. *Circulation* 90, 2213–2224. doi: 10.1161/01.CIR.90.5.2213

Koumi, S. I., Martin, R. L., and Sato, R. (1997). Alterations in ATP-sensitive potassium channel sensitivity to ATP in failing human hearts. *Am. J. Physiol.* 272, H1656–H1665.

Kuijpers, N. H., Potse, M., van Dam, P. M., ten Eikelder, H. M., Verheule, S., Prinzen, F. W., et al. (2011). Mechanoelectrical coupling enhances initiation and affects perpetuation of atrial fibrillation during acute atrial dilation. *Heart Rhythm* 8, 429–436. doi: 10.1016/j.hrthm.2010.11.020

Lai, L. P., Su, M. J., Lin, J. L., Lin, F. Y., Tsai, C. H., Chen, Y. S., et al. (1999). Down-regulation of L-type calcium channel and sarcoplasmic reticular Ca^{2+}-ATPase mRNA in human atrial fibrillation without significant change in the mRNA of ryanodine receptor, calsequestrin and phospholamban: an insight into the mechanism of atrial electrical remodeling. *J. Am. Coll. Cardiol.* 33, 1231–1237. doi: 10.1016/S0735-1097(99)00008-X

Landstrom, A. P., Dobrev, D., and Wehrens, X. H. T. (2017). Calcium signaling and cardiac arrhythmias. *Circ. Res.* 120, 1969–1993. doi: 10.1161/CIRCRESAHA.117.310083

Le Grand, B., Letienne, R., Dupont-Passelaigue, E., Lantoine-Adam, F., Longo, F., David-Dufilho, M., et al. (2014). F 16915 prevents heart failure-induced atrial fibrillation: a promising new drug as upstream therapy. *Naunyn Schmiedeberg's Arch. Pharmacol.* 387, 667–677. doi: 10.1007/s00210-014-0975-3

Le Grand, B. L., Hatem, S., Deroubaix, E., Couetil, J. P., and Coraboeuf, E. (1994). Depressed transient outward and calcium currents in dilated human atria. *Cardiovasc. Res.* 28, 548–556. doi: 10.1093/cvr/28.4.548

Leclercq, J. F., Halimi, F., Fiorello, P., Bertrand, C., and Attuel, P. (2014). Evaluation of time course and predicting factors of progression of paroxysmal or persistent atrial fibrillation to permanent atrial fibrillation. *Pacing Clin. Electrophysiol.* 37, 345–355. doi: 10.1111/pace.12264

Lee, K. W., Everett, T. H IV., Rahmutula, D., Guerra, J. M., Wilson, E., Ding, C., et al. (2006). Pirfenidone prevents the development of a vulnerable substrate for atrial fibrillation in a canine model of heart failure. *Circulation* 114, 1703–1712. doi: 10.1161/CIRCULATIONAHA.106.624320

Lehnart, S. E., Terrenoire, C., Reiken, S., Wehrens, X. H., Song, L. S., Tillman, E. J., et al. (2006). Stabilization of cardiac ryanodine receptor prevents intracellular calcium leak and arrhythmias. *Proc. Natl. Acad. Sci. U. S. A.* 103, 7906–7910. doi: 10.1073/pnas.0602133103

Lenaerts, I., Bito, V., Heinzel, F. R., Driesen, R. B., Holemans, P., D'Hooge, J., et al. (2009). Ultrastructural and functional remodeling of the coupling between Ca^{2+} influx and sarcoplasmic reticulum Ca^{2+} release in right atrial myocytes from experimental persistent atrial fibrillation. *Circ. Res.* 105, 876–885. doi: 10.1161/CIRCRESAHA.109.206276

Levy, D., Larson, M. G., Vasan, R. S., Kannel, W. B., and Ho, K. K. (1996). The progression from hypertension to congestive heart failure. *JAMA.* 275, 1557–1562. doi: 10.1001/jama.1996.03530440037034

Li, D., Fareh, S., Leung, T. K., and Nattel, S. (1999). Promotion of atrial fibrillation by heart failure in dogs: atrial remodeling of a different sort. *Circulation* 100, 87–95. doi: 10.1161/01.CIR.100.1.87

Li, D., Melnyk, P., Feng, J., Wang, Z., Petrecca, K., Shrier, A., et al. (2000). Effects of experimental heart failure on atrial cellular and ionic electrophysiology. *Circulation* 101, 2631–2638. doi: 10.1161/01.CIR.101.22.2631

Li, H., Lichter, J. G., Seidel, T., Tomaselli, G. F., Bridge, J. H., and Sachse, F. B. (2015). Cardiac resynchronization therapy reduces subcellular heterogeneity of ryanodine receptors, T-Tubules, and Ca^{2+} sparks produced by dyssynchronous heart failure. *Circ. Heart Fail.* 8, 1105–1114. doi: 10.1161/CIRCHEARTFAILURE.115.002352

Li, N., Chiang, D. Y., Wang, S., Wang, Q., Sun, L., Voigt, N., et al. (2014). Ryanodine receptor-mediated calcium leak drives progressive development of an atrial fibrillation substrate in a transgenic mouse model. *Circulation* 129, 1276–1285. doi: 10.1161/CIRCULATIONAHA.113.006611

Li, N., Wang, T., Wang, W., Cutler, M. J., Wang, Q., Voigt, N., et al. (2012). Inhibition of CaMKII phosphorylation of RyR2 prevents induction of atrial fibrillation in FKBP12.6 knockout mice. *Circ. Res.* 110, 465–470. doi: 10.1161/CIRCRESAHA.111.253229

Li, Q., O'Neill, S. C., Tao, T., Li, Y., Eisner, D., and Zhang, H. (2012). Mechanisms by which cytoplasmic calcium wave propagation and alternans are generated in cardiac atrial myocytes lacking T-tubules-insights from a simulation study. *Biophys. J.* 102, 1471–1482. doi: 10.1016/j.bpj.2012.03.007

Liang, J. J., and Silvestry, F. E. (2016). Mechanistic insights into mitral regurgitation due to atrial fibrillation: "atrial functional mitral regurgitation". *Trends Cardiovasc. Med.* 26, 681–689. doi: 10.1016/j.tcm.2016.04.012

Lin, C. C., Lin, J. L., Lin, C. S., Tsai, M. C., Su, M. J., Lai, L. P., et al. (2004). Activation of the calcineurin-nuclear factor of activated T-cell signal transduction pathway in atrial fibrillation. *Chest* 126, 1926–1932. doi: 10.1016/S0012-3692(15)31443-4

Lin, Y. K., Chen, Y. C., Chen, Y. A., Yeh, Y. H., Chen, S. A., and Chen, Y. J. (2016). B-type natriuretic peptide modulates pulmonary vein arrhythmogenesis: a novel potential contributor to the genesis of atrial tachyarrhythmia in heart failure. *J. Cardiovasc. Electrophysiol.* 27, 1462–1471. doi: 10.1111/jce.13093

Ling, L. H., Khammy, O., Byrne, M., Amirahmadi, F., Foster, A., Li, G., et al. (2012). Irregular rhythm adversely influences calcium handling in ventricular myocardium: implications for the interaction between heart failure and atrial fibrillation. *Circ. Heart Fail.* 5, 786–793. doi: 10.1161/CIRCHEARTFAILURE.112.968321

Logantha, S. J., Cruickshank, S. F., Rowan, E. G., and Drummond, R. M. (2010). Spontaneous and electrically evoked Ca^{2+} transients in cardiomyocytes of the rat pulmonary vein. *Cell Calcium* 48, 150–160. doi: 10.1016/j.ceca.2010.08.002

Loh, Y. X., Wu, K. H., Chen, Y. C., Hsu, C. H., Wei, J., and Lin, C. I. (2009). Reduced Ca^{2+} transport across sarcolemma but enhanced spontaneous activity in cardiomyocytes isolated from left atrium-pulmonary veins tissue of myopathic hamster. *J. Biomed. Sci.* 16:114. doi: 10.1186/1423-0127-16-114

Louch, W. E., Mork, H. K., Sexton, J., Stromme, T. A., Laake, P., Sjaastad, I., et al. (2006). T-tubule disorganization and reduced synchrony of Ca^{2+} release in murine cardiomyocytes following myocardial infarction. *J. Physiol.* 574 (Pt. 2), 519–533. doi: 10.1113/jphysiol.2006.107227

Lugenbiel, P., Wenz, F., Govorov, K., Schweizer, P. A., Katus, H. A., and Thomas, D. (2015). Atrial fibrillation complicated by heart failure induces distinct remodeling of calcium cycling proteins. *PLoS ONE* 10:e0116395. doi: 10.1371/journal.pone.0116395

Lukyanenko, V., Gyorke, I., and Gyorke, S. (1996). Regulation of calcium release by calcium inside the sarcoplasmic reticulum in ventricular myocytes. *Pflugers Arch.* 432, 1047–1054. doi: 10.1007/s004240050233

Lyon, A. R., Bannister, M. L., Collins, T., Pearce, E., Sepehripour, A. H., Dubb, S. S., et al. (2011). SERCA2a gene transfer decreases sarcoplasmic reticulum calcium leak and reduces ventricular arrhythmias in a model of chronic heart failure. *Circ. Arrhythm. Electrophysiol.* 4, 362–372. doi: 10.1161/CIRCEP.110.961615

Macquaide, N., Tuan, H. T., Hotta, J., Sempels, W., Lenaerts, I., Holemans, P., et al. (2015). Ryanodine receptor cluster fragmentation and redistribution in persistent atrial fibrillation enhance calcium release. *Cardiovasc. Res.* 108, 387–398. doi: 10.1093/cvr/cvv231

Mamas, M. A., Sperrin, M., Watson, M. C., Coutts, A., Wilde, K., Burton, C., et al. (2017). Do patients have worse outcomes in heart failure than in cancer? A primary care-based cohort study with 10-year follow-up in Scotland. *Eur. J. Heart Fail.* 19, 1095–1104. doi: 10.1002/ejhf.822

Marin-Garcia, J., Goldenthal, M. J., Damle, S., Pi, Y., and Moe, G. W. (2009). Regional distribution of mitochondrial dysfunction and apoptotic remodeling in pacing-induced heart failure. *J. Card. Fail.* 15, 700–708. doi: 10.1016/j.cardfail.2009.04.010

Marrouche, N. F., Wilber, D., Hindricks, G., Jais, P., Akoum, N., Marchlinski, F., et al. (2014). Association of atrial tissue fibrosis identified by delayed enhancement MRI and atrial fibrillation catheter ablation: the DECAAF study. *JAMA.* 311, 498–506. doi: 10.1001/jama.2014.3

Marx, S. O., Reiken, S., Hisamatsu, Y., Jayaraman, T., Burkhoff, D., Rosemblit, N., et al. (2000). PKA phosphorylation dissociates FKBP12.6 from the calcium

release channel (ryanodine receptor): defective regulation in failing hearts. *Cell* 101, 365–376. doi: 10.1016/S0092-8674(00)80847-8

Mayyas, F., Niebauer, M., Zurick, A., Barnard, J., Gillinov, A. M., Chung, M. K., et al. (2010). Association of left atrial endothelin-1 with atrial rhythm, size, and fibrosis in patients with structural heart disease. *Circ. Arrhythm. Electrophysiol.* 3, 369–379. doi: 10.1161/CIRCEP.109.924985

Mc, G. J., Shore, R., Hauenstein, V., and Goldman, F. (1939). Influence of exercise on cardiac output in congestive heart failure. *Arch. Intern. Med.* 63, 469–475. doi: 10.1001/archinte.1939.00180200038004

McManus, D. D., Hsu, G., Sung, S. H., Saczynski, J. S., Smith, D. H., Magid, D. J., et al. (2013). Atrial fibrillation and outcomes in heart failure with preserved versus reduced left ventricular ejection fraction. *J. Am. Heart Assoc.* 2:e005694. doi: 10.1161/JAHA.112.005694

Melenovsky, V., Hwang, S. J., Redfield, M. M., Zakeri, R., Lin, G., and Borlaug, B. A. (2015). Left atrial remodeling and function in advanced heart failure with preserved or reduced ejection fraction. *Circ. Heart Fail.* 8, 295–303. doi: 10.1161/CIRCHEARTFAILURE.114.001667

Mihm, M. J., Yu, F., Carnes, C. A., Reiser, P. J., McCarthy, P. M., Van Wagoner, D. R., et al. (2001). Impaired myofibrillar energetics and oxidative injury during human atrial fibrillation. *Circulation* 104, 174–180. doi: 10.1161/01.CIR.104.2.174

Mishra, S., Gray, C. B., Miyamoto, S., Bers, D. M., and Brown, J. H. (2011). Location matters: clarifying the concept of nuclear and cytosolic CaMKII subtypes. *Circ. Res.* 109, 1354–1362. doi: 10.1161/CIRCRESAHA.111.248401

Moe, G. K., Rheinboldt, W. C., and Abildskov, J. A. (1964). A computer model of atrial fibrillation. *Am. Heart J.* 67, 200–220. doi: 10.1016/0002-8703(64)90371-0

Monigatti-Tenkorang, J., Jousset, F., Pascale, P., Vesin, J. M., Ruchat, P., Fromer, M., et al. (2014). Intermittent atrial tachycardia promotes repolarization alternans and conduction slowing during rapid rates, and increases susceptibility to atrial fibrillation in a free-behaving sheep model. *J. Cardiovasc. Electrophysiol.* 25, 418–427. doi: 10.1111/jce.12353

Montaigne, D., Marechal, X., Lefebvre, P., Modine, T., Fayad, G., Dehondt, H., et al. (2013). Mitochondrial dysfunction as an arrhythmogenic substrate: a translational proof-of-concept study in patients with metabolic syndrome in whom post-operative atrial fibrillation develops. *J. Am. Coll. Cardiol.* 62, 1466–1473. doi: 10.1016/j.jacc.2013.03.061

Montefusco, A., Biasco, L., Blandino, A., Cristoforetti, Y., Scaglione, M., Caponi, D., et al. (2010). Left atrial volume at MRI is the main determinant of outcome after pulmonary vein isolation plus linear lesion ablation for paroxysmal-persistent atrial fibrillation. *J. Cardiovasc. Med.* 11, 593–598. doi: 10.2459/JCM.0b013e32833831e4

Morillo, C. A., Klein, G. J., Jones, D. L., and Guiraudon, C. M. (1995). Chronic rapid atrial pacing. Structural, functional, and electrophysiological characteristics of a new model of sustained atrial fibrillation. *Circulation* 91, 1588–1595. doi: 10.1161/01.CIR.91.5.1588

Mosterd, A., and Hoes, A. W. (2007). Clinical epidemiology of heart failure. *Heart* 93, 1137–1146. doi: 10.1136/hrt.2003.025270

Naito, M., David, D., Michelson, E. L., Schaffenburg, M., and Dreifus, L. S. (1983). The hemodynamic consequences of cardiac arrhythmias: evaluation of the relative roles of abnormal atrioventricular sequencing, irregularity of ventricular rhythm and atrial fibrillation in a canine model. *Am. Heart J.* 106, 284–291. doi: 10.1016/0002-8703(83)90194-1

Narayan, S. M., Bode, F., Karasik, P. L., and Franz, M. R. (2002). Alternans of atrial action potentials during atrial flutter as a precursor to atrial fibrillation. *Circulation* 106, 1968–1973. doi: 10.1161/01.CIR.0000037062.35762.B4

Narayan, S. M., Franz, M. R., Clopton, P., Pruvot, E. J., and Krummen, D. E. (2011). Repolarization alternans reveals vulnerability to human atrial fibrillation. *Circulation* 123, 2922–2930. doi: 10.1161/CIRCULATIONAHA.110.977827

Narayan, S. M., and Jalife, J. (2014). CrossTalk proposal: rotors have been demonstrated to drive human atrial fibrillation. *J. Physiol.* 592, 3163–3166. doi: 10.1113/jphysiol.2014.271031

Narayan, S. M., Kazi, D., Krummen, D. E., and Rappel, W. J. (2008). Repolarization and activation restitution near human pulmonary veins and atrial fibrillation initiation: a mechanism for the initiation of atrial fibrillation by premature beats. *J. Am. Coll. Cardiol.* 52, 1222–1230. doi: 10.1016/j.jacc.2008.07.012

Nassal, M. M., Wan, X., Laurita, K. R., and Cutler, M. J. (2015). Atrial SERCA2a overexpression has no affect on cardiac alternans but promotes arrhythmogenic SR Ca^{2+} triggers. *PLoS ONE* 10:e0137359. doi: 10.1371/journal.pone.0137359

Nattel, S. (2017). Molecular and cellular mechanisms of atrial fibrosis in atrial fibrillation. *JACC Clin. Electrophysiol.* 3, 425–435. doi: 10.1016/j.jacep.2017.03.002

Nattel, S., and Harada, M. (2014). Atrial remodeling and atrial fibrillation: recent advances and translational perspectives. *J. Am. Coll. Cardiol.* 63, 2335–2345. doi: 10.1016/j.jacc.2014.02.555

Nattel, S., Maguy, A., Le Bouter, S., and Yeh, Y. H. (2007). Arrhythmogenic ion-channel remodeling in the heart: heart failure, myocardial infarction, and atrial fibrillation. *Physiol. Rev.* 87, 425–456. doi: 10.1152/physrev.00014.2006

Nazir, S. A., and Lab, M. J. (1996). Mechanoelectric feedback and atrial arrhythmias. *Cardiovasc. Res.* 32, 52–61. doi: 10.1016/S0008-6363(96)00054-5

Nedios, S., Kosiuk, J., Koutalas, E., Kornej, J., Sommer, P., Arya, A., et al. (2015). Comparison of left atrial dimensions in CT and echocardiography as predictors of long-term success after catheter ablation of atrial fibrillation. *J. Interv. Card. Electrophysiol.* 43, 237–244. doi: 10.1007/s10840-015-0010-8

Neef, S., Dybkova, N., Sossalla, S., Ort, K. R., Fluschnik, N., Neumann, K., et al. (2010). CaMKII-dependent diastolic SR Ca^{2+} leak and elevated diastolic Ca^{2+} levels in right atrial myocardium of patients with atrial fibrillation. *Circ. Res.* 106, 1134–1144. doi: 10.1161/CIRCRESAHA.109.203836

Nerbonne, J. M., and Kass, R. S. (2005). Molecular physiology of cardiac repolarization. *Physiol. Rev.* 85, 1205–1253. doi: 10.1152/physrev.00002.2005

Nishida, K., Michael, G., Dobrev, D., and Nattel, S. (2010). Animal models for atrial fibrillation: clinical insights and scientific opportunities. *Europace* 12, 160–172. doi: 10.1093/europace/eup328

Nivala, M., Song, Z., Weiss, J. N., and Qu, Z. (2015). T-tubule disruption promotes calcium alternans in failing ventricular myocytes: mechanistic insights from computational modeling. *J. Mol. Cell. Cardiol.* 79, 32–41. doi: 10.1016/j.yjmcc.2014.10.018

Odutayo, A., Wong, C. X., Williams, R., Hunn, B., and Emdin, C. A. (2017). Prognostic importance of atrial fibrillation timing and pattern in adults with congestive heart failure: a systematic review and meta-analysis. *J. Card. Fail.* 23, 56–62. doi: 10.1016/j.cardfail.2016.08.005

Ohkusa, T., Ueyama, T., Yamada, J., Yano, M., Fujumura, Y., Esato, K., et al. (1999). Alterations in cardiac sarcoplasmic reticulum Ca^{2+} regulatory proteins in the atrial tissue of patients with chronic atrial fibrillation. *J. Am. Coll. Cardiol.* 34, 255–263. doi: 10.1016/S0735-1097(99)00169-2

Oral, H., Ozaydin, M., Tada, H., Chugh, A., Scharf, C., Hassan, S., et al. (2002). Mechanistic significance of intermittent pulmonary vein tachycardia in patients with atrial fibrillation. *J. Cardiovasc. Electrophysiol.* 13, 645–650. doi: 10.1046/j.1540-8167.2002.00645.x

Ouadid, H., Albat, B., and Nargeot, J. (1995). Calcium currents in diseased human cardiac cells. *J. Cardiovasc. Pharmacol.* 25, 282–291. doi: 10.1097/00005344-199502000-00014

Ozgen, N., Dun, W., Sosunov, E. A., Anyukhovsky, E. P., Hirose, M., Duffy, H. S., et al. (2007). Early electrical remodeling in rabbit pulmonary vein results from trafficking of intracellular SK2 channels to membrane sites. *Cardiovasc. Res.* 75, 758–769. doi: 10.1016/j.cardiores.2007.05.008

Parks, R. J., Murphy, E., and Liu, J. C. (2018). Mitochondrial permeability transition pore and calcium handling. *Methods Mol. Biol.* 1782, 187–196. doi: 10.1007/978-1-61779-382-0_15

Parmley, W. W., and Chuck, L. (1973). Length-dependent changes in myocardial contractile state. *Am. J. Physiol.* 224, 1195–1199.

Patterson, E., Lazzara, R., Szabo, B., Liu, H., Tang, D., Li, Y. H., et al. (2006). Sodium-calcium exchange initiated by the Ca^{2+} transient: an arrhythmia trigger within pulmonary veins. *J. Am. Coll. Cardiol.* 47, 1196–1206. doi: 10.1016/j.jacc.2005.12.023

Patterson, E., Po, S. S., Scherlag, B. J., and Lazzara, R. (2005). Triggered firing in pulmonary veins initiated by *in vitro* autonomic nerve stimulation. *Heart Rhythm* 2, 624–631. doi: 10.1016/j.hrthm.2005.02.012

Perez-Lugones, A., McMahon, J. T., Ratliff, N. B., Saliba, W. I., Schweikert, R. A., Marrouche, N. F., et al. (2003). Evidence of specialized conduction cells in human pulmonary veins of patients with atrial fibrillation. *J. Cardiovasc. Electrophysiol.* 14, 803–809. doi: 10.1046/j.1540-8167.2003.03075.x

Ponikowski, P., Voors, A. A., Anker, S. D., Bueno, H., Cleland, J. G., Coats, A. J., et al. (2016). 2016 ESC guidelines for the diagnosis and treatment of acute and

chronic heart failure: the task force for the diagnosis and treatment of acute and chronic heart failure of the European Society of Cardiology (ESC). *Eur Heart J.* 18, 891–975. doi: 10.1002/ejhf.592

Potpara, T. S., and Lip, G. Y. (2014). Lone atrial fibrillation - an overview. *Int. J. Clin. Pract.* 68, 418–433. doi: 10.1111/ijcp.12281

Prosser, B. L., Ward, C. W., and Lederer, W. J. (2013). X-ROS signalling is enhanced and graded by cyclic cardiomyocyte stretch. *Cardiovasc. Res.* 98, 307–314. doi: 10.1093/cvr/cvt066

Proven, A., Roderick, H. L., Conway, S. J., Berridge, M. J., Horton, J. K., Capper, S. J., et al. (2006). Inositol 1,4,5-trisphosphate supports the arrhythmogenic action of endothelin-1 on ventricular cardiac myocytes. *J. Cell Sci.* 119 (Pt. 16), 3363–3375. doi: 10.1242/jcs.03073

Purohit, A., Rokita, A. G., Guan, X., Chen, B., Koval, O. M., Voigt, N., et al. (2013). Oxidized Ca^{2+}/calmodulin-dependent protein kinase II triggers atrial fibrillation. *Circulation* 128, 1748–1757. doi: 10.1161/CIRCULATIONAHA.113.003313

Qi, X., Yeh, Y. H., Chartier, D., Xiao, L., Tsuji, Y., Brundel, B. J., et al. (2009). The calcium/calmodulin/kinase system and arrhythmogenic afterdepolarizations in bradycardia-related acquired long-QT syndrome. *Circ. Arrhythm. Electrophysiol.* 2, 295–304. doi: 10.1161/CIRCEP.108.815654

Qi, X. Y., Diness, J. G., Brundel, B. J., Zhou, X. B., Naud, P., Wu, C. T., et al. (2014). Role of small-conductance calcium-activated potassium channels in atrial electrophysiology and fibrillation in the dog. *Circulation* 129, 430–440. doi: 10.1161/CIRCULATIONAHA.113.003019

Qi, X. Y., Yeh, Y. H., Xiao, L., Burstein, B., Maguy, A., Chartier, D., et al. (2008). Cellular signaling underlying atrial tachycardia remodeling of L-type calcium current. *Circ. Res.* 103, 845–854. doi: 10.1161/CIRCRESAHA.108.175463

Qu, Z., Nivala, M., and Weiss, J. N. (2013). Calcium alternans in cardiac myocytes: order from disorder. *J. Mol. Cell. Cardiol.* 58, 100–109. doi: 10.1016/j.yjmcc.2012.10.007

Rajagopal, V., Bass, G., Walker, C. G., Crossman, D. J., Petzer, A., Hickey, A., et al. (2015). Examination of the effects of heterogeneous organization of RyR clusters, myofibrils and mitochondria on Ca^{2+} release patterns in cardiomyocytes. *PLoS Comput. Biol.* 11:e1004417. doi: 10.1371/journal.pcbi.1004417

Ravelli, F. (2003). Mechano-electric feedback and atrial fibrillation. *Prog. Biophys. Mol. Biol.* 82, 137–149. doi: 10.1016/S0079-6107(03)00011-7

Raymond, R. J., Lee, A. J., Messineo, F. C., Manning, W. J., and Silverman, D. I. (1998). Cardiac performance early after cardioversion from atrial fibrillation. *Am. Heart J.* 136, 435–442. doi: 10.1016/S0002-8703(98)70217-0

Richards, M. A., Clarke, J. D., Saravanan, P., Voigt, N., Dobrev, D., Eisner, D. A., et al. (2011). Transverse tubules are a common feature in large mammalian atrial myocytes including human. *Am. J. Physiol. Heart Circ. Physiol.* 301, H1996–H2005. doi: 10.1152/ajpheart.00284.2011

Rietdorf, K., Bootman, M. D., and Sanderson, M. J. (2014). Spontaneous, pro-arrhythmic calcium signals disrupt electrical pacing in mouse pulmonary vein sleeve cells. *PLoS ONE* 9:e88649. doi: 10.1371/journal.pone.0088649

Ruwhof, C., and van der Laarse, A. (2000). Mechanical stress-induced cardiac hypertrophy: mechanisms and signal transduction pathways. *Cardiovasc. Res.* 47, 23–37. doi: 10.1016/S0008-6363(00)00076-6

Saba, S., Janczewski, A. M., Baker, L. C., Shusterman, V., Gursoy, E. C., Feldman, A. M., et al. (2005). Atrial contractile dysfunction, fibrosis, and arrhythmias in a mouse model of cardiomyopathy secondary to cardiac-specific overexpression of tumor necrosis factor-{alpha}. *Am. J. Physiol. Heart Circ. Physiol.* 289, H1456–H1467. doi: 10.1152/ajpheart.00733.2004

Sacconi, L., Ferrantini, C., Lotti, J., Coppini, R., Yan, P., Loew, L. M., et al. (2012). Action potential propagation in transverse-axial tubular system is impaired in heart failure. *Proc. Natl. Acad. Sci. U. S. A.* 109, 5815–5819. doi: 10.1073/pnas.1120188109

Sanders, P., Morton, J. B., Davidson, N. C., Spence, S. J., Vohra, J. K., Sparks, P. B., et al. (2003). Electrical remodeling of the atria in congestive heart failure: electrophysiological and electroanatomic mapping in humans. *Circulation* 108, 1461–1468. doi: 10.1161/01.CIR.0000090688.49283.67

Santangeli, P., Zado, E. S., Hutchinson, M. D., Riley, M. P., Lin, D., Frankel, D. S., et al. (2016). Prevalence and distribution of focal triggers in persistent and long-standing persistent atrial fibrillation. *Heart Rhythm* 13, 374–382. doi: 10.1016/j.hrthm.2015.10.023

Santhanakrishnan, R., Wang, N., Larson, M. G., Magnani, J. W., McManus, D. D., Lubitz, S. A., et al. (2016). Atrial fibrillation begets heart failure and vice versa: temporal associations and differences in preserved versus reduced ejection fraction. *Circulation* 133, 484–492. doi: 10.1161/CIRCULATIONAHA.116.022835

Santiago, D. J., Rios, E., and Shannon, T. R. (2013). Isoproterenol increases the fraction of spark-dependent RyR-mediated leak in ventricular myocytes. *Biophys. J.* 104, 976–985. doi: 10.1016/j.bpj.2013.01.026

Schmidt, C., Wiedmann, F., Voigt, N., Zhou, X. B., Heijman, J., Lang, S., et al. (2015). Upregulation of K(2P)3.1 K+ current causes action potential shortening in patients with chronic atrial fibrillation. *Circulation* 132, 82–92. doi: 10.1161/CIRCULATIONAHA.114.012657

Schonleitner, P., Schotten, U., and Antoons, G. (2017). Mechanosensitivity of microdomain calcium signalling in the heart. *Prog. Biophys. Mol. Biol.* 130 (Pt. B), 288–301. doi: 10.1016/j.pbiomolbio.2017.06.013

Schotten, U., Ausma, J., Stellbrink, C., Sabatschus, I., Vogel, M., Frechen, D., et al. (2001). Cellular mechanisms of depressed atrial contractility in patients with chronic atrial fibrillation. *Circulation* 103, 691–698. doi: 10.1161/01.CIR.103.5.691

Schotten, U., Duytschaever, M., Ausma, J., Eijsbouts, S., Neuberger, H. R., and Allessie, M. (2003a). Electrical and contractile remodeling during the first days of atrial fibrillation go hand in hand. *Circulation* 107, 1433–1439. doi: 10.1161/01.CIR.0000055314.10801.4F

Schotten, U., Greiser, M., Benke, D., Buerkel, K., Ehrenteidt, B., Stellbrink, C., et al. (2002). Atrial fibrillation-induced atrial contractile dysfunction: a tachycardiomyopathy of a different sort. *Cardiovasc. Res.* 53, 192–201. doi: 10.1016/S0008-6363(01)00453-9

Schotten, U., Haase, H., Frechen, D., Greiser, M., Stellbrink, C., Vazquez-Jimenez, J. F., et al. (2003b). The L-type Ca^{2+}-channel subunits alpha1C and beta2 are not downregulated in atrial myocardium of patients with chronic atrial fibrillation. *J. Mol. Cell. Cardiol.* 35, 437–443. doi: 10.1016/S0022-2828(03)00012-9

Schreieck, J., Wang, Y., Overbeck, M., Schomig, A., and Schmitt, C. (2000). Altered transient outward current in human atrial myocytes of patients with reduced left ventricular function. *J. Cardiovasc. Electrophysiol.* 11, 180–192. doi: 10.1111/j.1540-8167.2000.tb00318.x

Sequeira, V., and van der Velden, J. (2015). Historical perspective on heart function: the Frank-Starling Law. *Biophys. Rev.* 7, 421–447. doi: 10.1007/s12551-015-0184-4

Shan, J., Xie, W., Betzenhauser, M., Reiken, S., Chen, B. X., Wronska, A., et al. (2012). Calcium leak through ryanodine receptors leads to atrial fibrillation in 3 mouse models of catecholaminergic polymorphic ventricular tachycardia. *Circ. Res.* 111, 708–717. doi: 10.1161/CIRCRESAHA.112.273342

Shanmugam, M., Molina, C. E., Gao, S., Severac-Bastide, R., Fischmeister, R., and Babu, G. J. (2011). Decreased sarcolipin protein expression and enhanced sarco(endo)plasmic reticulum Ca^{2+} uptake in human atrial fibrillation. *Biochem. Biophys. Res. Commun.* 410, 97–101. doi: 10.1016/j.bbrc.2011.05.113

Shinagawa, K., Shi, Y. F., Tardif, J. C., Leung, T. K., and Nattel, S. (2002). Dynamic nature of atrial fibrillation substrate during development and reversal of heart failure in dogs. *Circulation.*105, 2672–2678. doi: 10.1161/01.CIR.0000016826.62813.F5

Silva-Cardoso, J., Zharinov, O. J., Ponikowski, P., Naditch-Brule, L., Lewalter, T., Brette, S., et al. (2013). Heart failure in patients with atrial fibrillation is associated with a high symptom and hospitalization burden: the RealiseAF survey. *Clin. Cardiol.* 36, 766–774. doi: 10.1002/clc.22209

Simantirakis, E. N., Koutalas, E. P., and Vardas, P. E. (2012). Arrhythmia-induced cardiomyopathies: the riddle of the chicken and the egg still unanswered? *Europace* 14, 466–473. doi: 10.1093/europace/eur348

Skinner, N. S. Jr., Mitchell, J. H., Wallace, A. G., and Sarnoff, S. J. (1964). Hemodynamic consequences of atrial fibrillation at constant ventricular rates. *Am. J. Med.* 36, 342–350. doi: 10.1016/0002-9343(64)90160-3

Solti, F., Vecsey, T., Kekesi, V., and Juhasz-Nagy, A. (1989). The effect of atrial dilatation on the genesis of atrial arrhythmias. *Cardiovasc. Res.* 23, 882–886. doi: 10.1093/cvr/23.10.882

Son, M. J., Kim, J. C., Kim, S. W., Chidipi, B., Muniyandi, J., Singh, T. D., et al. (2016). Shear stress activates monovalent cation channel transient receptor potential melastatin subfamily 4 in rat atrial myocytes via type 2 inositol

1,4,5-trisphosphate receptors and Ca^{2+} release. *J. Physiol.* 594, 2985–3004. doi: 10.1113/JP270887

Song, L. S., Sobie, E. A., McCulle, S., Lederer, W. J., Balke, C. W., and Cheng, H. (2006). Orphaned ryanodine receptors in the failing heart. *Proc. Natl. Acad. Sci. U. S. A.* 103, 4305–4310. doi: 10.1073/pnas.0509324103

Sood, S., Chelu, M. G., van Oort, R. J., Skapura, D., Santonastasi, M., Dobrev, D., et al. (2008). Intracellular calcium leak due to FKBP12.6 deficiency in mice facilitates the inducibility of atrial fibrillation. *Heart Rhythm* 5, 1047–1054. doi: 10.1016/j.hrthm.2008.03.030

Sovari, A. A., Dudley, S. C. Jr. (2012). Reactive oxygen species-targeted therapeutic interventions for atrial fibrillation. *Front. Physiol.* 3:311. doi: 10.3389/fphys.2012.00311

Spach, M. S., Miller, W. T. III, Dolber, P. C., Kootsey, J. M., Sommer, J. R., Mosher, C. E., et al. (1982). The functional role of structural complexities in the propagation of depolarization in the atrium of the dog. Cardiac conduction disturbances due to discontinuities of effective axial resistivity. *Circ. Res.* 50, 175–191. doi: 10.1161/01.RES.50.2.175

Sparks, P. B., Jayaprakash, S., Mond, H. G., Vohra, J. K., Grigg, L. E., and Kalman, J. M. (1999). Left atrial mechanical function after brief duration atrial fibrillation. *J. Am. Coll. Cardiol.* 33, 342–349. doi: 10.1016/S0735-1097(98)00585-3

Sramko, M., Wichterle, D., and Kautzner, J. (2016). Feasibility of *in-vivo* simulation of acute hemodynamics in human atrial fibrillation. *PLoS ONE* 11:e0165241. doi: 10.1371/journal.pone.0165241

Sridhar, A., Nishijima, Y., Terentyev, D., Khan, M., Terentyeva, R., Hamlin, R. L., et al. (2009). Chronic heart failure and the substrate for atrial fibrillation. *Cardiovasc. Res.* 84, 227–236. doi: 10.1093/cvr/cvp216

Stead, E. A. Jr., Warren, J. V., and Brannon, E. S. (1948). Cardiac output in congestive heart failure; an analysis of the reasons for lack of close correlation between the symptoms of heart failure and the resting cardiac output. *Am. Heart J.* 35, 529–541. doi: 10.1016/0002-8703(48)90640-1

Steenman, M., and Lande, G. (2017). Cardiac aging and heart disease in humans. *Biophys. Rev.* 9, 131–137. doi: 10.1007/s12551-017-0255-9

Stewart, S., Hart, C. L., Hole, D. J., and McMurray, J. J. (2002). A population-based study of the long-term risks associated with atrial fibrillation: 20-year follow-up of the Renfrew/Paisley study. *Am. J. Med.* 113, 359–364. doi: 10.1016/S0002-9343(02)01236-6

Sun, H., Chartier, D., Leblanc, N., and Nattel, S. (2001). Intracellular calcium changes and tachycardia-induced contractile dysfunction in canine atrial myocytes. *Cardiovasc. Res.* 49, 751–761. doi: 10.1016/S0008-6363(00)00294-7

Sun, H., Gaspo, R., Leblanc, N., and Nattel, S. (1998). Cellular mechanisms of atrial contractile dysfunction caused by sustained atrial tachycardia. *Circulation* 98, 719–727. doi: 10.1161/01.CIR.98.7.719

Takahara, A., Hagiwara, M., Namekata, I., and Tanaka, H. (2014). Pulmonary vein myocardium as a possible pharmacological target for the treatment of atrial fibrillation. *J. Pharmacol. Sci.* 126, 1–7. doi: 10.1254/jphs.14R09CP

Tao, H., Yang, J. J., Shi, K. H., and Li, J. (2016). Wnt signaling pathway in cardiac fibrosis: new insights and directions. *Metab. Clin. Exp.* 65, 30–40. doi: 10.1016/j.metabol.2015.10.013

Tavi, P., Han, C., and Weckstrom, M. (1998). Mechanisms of stretch-induced changes in $[Ca^{2+}]$i in rat atrial myocytes: role of increased troponin C affinity and stretch-activated ion channels. *Circ. Res.* 83, 1165–1177. doi: 10.1161/01.RES.83.11.1165

Terracciano, C. M., Naqvi, R. U., and MacLeod, K. T. (1995). Effects of rest interval on the release of calcium from the sarcoplasmic reticulum in isolated guinea pig ventricular myocytes. *Circ. Res.* 77, 354–360. doi: 10.1161/01.RES.77.2.354

Thanigaimani, S., McLennan, E., Linz, D., Mahajan, R., Agbaedeng, T. A., Lee, G., et al. (2017). Progression and reversibility of stretch induced atrial remodeling: characterization and clinical implications. *Prog. Biophys.Mol. Biol.* 130 (Pt. B), 376–86. doi: 10.1016/j.pbiomolbio.2017.07.010

Thrall, G., Lane, D., Carroll, D., and Lip, G. Y. (2006). Quality of life in patients with atrial fibrillation: a systematic review. *Am. J. Med.* 119, 448.e1–19. doi: 10.1016/j.amjmed.2005.10.057

Tinker, A., Finlay, M., Nobles, M., and Opel, A. (2016). The contribution of pathways initiated via the Gq\11 G-protein family to atrial fibrillation. *Pharmacol. Res.* 105, 54–61. doi: 10.1016/j.phrs.2015.11.008

Todd, D. M., Fynn, S. P., Walden, A. P., Hobbs, W. J., Arya, S., and Garratt, C. J. (2004). Repetitive 4-week periods of atrial electrical remodeling promote stability of atrial fibrillation: time course of a second factor involved in the self-perpetuation of atrial fibrillation. *Circulation* 109, 1434–1439. doi: 10.1161/01.CIR.0000124006.84596.D9

Tomita, T., Takei, M., Saikawa, Y., Hanaoka, T., Uchikawa, S., Tsutsui, H., et al. (2003). Role of autonomic tone in the initiation and termination of paroxysmal atrial fibrillation in patients without structural heart disease. *J. Cardiovasc. Electrophysiol.* 14, 559–564. doi: 10.1046/j.1540-8167.2003.02462.x

Trafford, A. W., Diaz, M. E., and Eisner, D. A. (2001). Coordinated control of cell Ca^{2+} loading and triggered release from the sarcoplasmic reticulum underlies the rapid inotropic response to increased L-type Ca^{2+} current. *Circ. Res.* 88, 195–201. doi: 10.1161/01.RES.88.2.195

Trafford, A. W., Diaz, M. E., Negretti, N., and Eisner, D. A. (1997). Enhanced Ca^{2+} current and decreased Ca^{2+} efflux restore sarcoplasmic reticulum Ca^{2+} content after depletion. *Circ. Res.* 81, 477–484. doi: 10.1161/01.RES.81.4.477

Tsai, C. T., Tseng, C. D., Hwang, J. J., Wu, C. K., Yu, C. C., Wang, Y. C., et al. (2011). Tachycardia of atrial myocytes induces collagen expression in atrial fibroblasts through transforming growth factor beta1. *Cardiovasc. Res.* 89, 805–815. doi: 10.1093/cvr/cvq322

Uemura, N., Ohkusa, T., Hamano, K., Nakagome, M., Hori, H., Shimizu, M., et al. (2004). Down-regulation of sarcolipin mRNA expression in chronic atrial fibrillation. *Eur. J. Clin. Invest.* 34, 723–730. doi: 10.1111/j.1365-2362.2004.01422.x

van der Velden, H. M., Ausma, J., Rook, M. B., Hellemons, A. J., van Veen, T. A., Allessie, M. A., et al. (2000a). Gap junctional remodeling in relation to stabilization of atrial fibrillation in the goat. *Cardiovasc. Res.* 46, 476–486. doi: 10.1016/S0008-6363(00)00026-2

van der Velden, H. M. W., van der Zee, L., Wijffels, M. C., van Leuven, C., Dorland, R., Vos, M. A., et al. (2000b). Atrial fibrillation in the goat induces changes in monophasic action potential and mRNA expression of ion channels involved in repolarization. *J. Cardiovasc. Electrophysiol.* 11, 1262–1269. doi: 10.1046/j.1540-8167.2000.01262.x

Van Gelder, I. C., Brundel, B. J., Henning, R. H., Tuinenburg, A. E., Tieleman, R. G., Deelman, L., et al. (1999). Alterations in gene expression of proteins involved in the calcium handling in patients with atrial fibrillation. *J. Cardiovasc. Electrophysiol.* 10, 552–560. doi: 10.1111/j.1540-8167.1999.tb00712.x

Van Wagoner, D. R., and Nerbonne, J. M. (2000). Molecular basis of electrical remodeling in atrial fibrillation. *J. Mol. Cell. Cardiol.* 32, 1101–1117. doi: 10.1006/jmcc.2000.1147

Van Wagoner, D. R., Pond, A. L., Lamorgese, M., Rossie, S. S., McCarthy, P. M., and Nerbonne, J. M. (1999). Atrial L-type Ca^{2+} currents and human atrial fibrillation. *Circ. Res.* 85, 428–436. doi: 10.1161/01.RES.85.5.428

Venetucci, L. A., Trafford, A. W., and Eisner, D. A. (2007). Increasing ryanodine receptor open probability alone does not produce arrhythmogenic calcium waves: threshold sarcoplasmic reticulum calcium content is required. *Circ. Res.* 100, 105–111. doi: 10.1161/01.RES.0000252828.17939.00

Venetucci, L. A., Trafford, A. W., O'Neill, S. C., and Eisner, D. A. (2008). The sarcoplasmic reticulum and arrhythmogenic calcium release. *Cardiovasc. Res.* 77, 285–292. doi: 10.1093/cvr/cvm009

Verrier, R. L., Fuller, H., Justo, F., Nearing, B. D., Rajamani, S., and Belardinelli, L. (2016). Unmasking atrial repolarization to assess alternans, spatiotemporal heterogeneity, and susceptibility to atrial fibrillation. *Heart Rhythm* 13, 953–961. doi: 10.1016/j.hrthm.2015.11.019

Vest, J. A., Wehrens, X. H., Reiken, S. R., Lehnart, S. E., Dobrev, D., Chandra, P., et al. (2005). Defective cardiac ryanodine receptor regulation during atrial fibrillation. *Circulation* 111, 2025–2032. doi: 10.1161/01.CIR.0000162461.67140.4C

Viswanathan, P. C., Shaw, R. M., and Rudy, Y. (1999). Effects of IKr and IKs heterogeneity on action potential duration and its rate dependence: a simulation study. *Circulation* 99, 2466–2474. doi: 10.1161/01.CIR.99.18.2466

Voigt, N., Heijman, J., Wang, Q., Chiang, D. Y., Li, N., Karck, M., et al. (2014). Cellular and molecular mechanisms of atrial arrhythmogenesis in patients with paroxysmal atrial fibrillation. *Circulation* 129, 145–156. doi: 10.1161/CIRCULATIONAHA.113.006641

Voigt, N., Li, N., Wang, Q., Wang, W., Trafford, A. W., Abu-Taha, I., et al. (2012). Enhanced sarcoplasmic reticulum Ca^{2+} leak and increased Na^{+}-Ca^{2+} exchanger function underlie delayed afterdepolarizations in patients with chronic atrial fibrillation. *Circulation* 125, 2059–2070. doi: 10.1161/CIRCULATIONAHA.111.067306

Voigt, N., Pearman, C. M., Dobrev, D., and Dibb, K. M. (2015). Methods for isolating atrial cells from large mammals and humans. *J. Mol. Cell. Cardiol.* 86, 187–198. doi: 10.1016/j.yjmcc.2015.07.006

von Lewinski, D., Stumme, B., Fialka, F., Luers, C., and Pieske, B. (2004). Functional relevance of the stretch-dependent slow force response in failing human myocardium. *Circ. Res.* 94, 1392–1398. doi: 10.1161/01.RES.0000129181.48395.ff

von Lewinski, D., Stumme, B., Maier, L. S., Luers, C., Bers, D. M., and Pieske, B. (2003). Stretch-dependent slow force response in isolated rabbit myocardium is Na+ dependent. *Cardiovasc. Res.* 57, 1052–1061. doi: 10.1016/S0008-6363(02)00830-1

Voskoboinik, A., Prabhu, S., Ling, L. H., Kalman, J. M., and Kistler, P. M. (2016). Alcohol and atrial fibrillation: a sobering review. *J. Am. Coll. Cardiol.* 68, 2567–2576. doi: 10.1016/j.jacc.2016.08.074

Wakili, R., Voigt, N., Kaab, S., Dobrev, D., and Nattel, S. (2011). Recent advances in the molecular pathophysiology of atrial fibrillation. *J. Clin. Invest.* 121, 2955–2968. doi: 10.1172/JCI46315

Wakili, R., Yeh, Y. H., Yan Qi, X., Greiser, M., Chartier, D., Nishida, K., et al. (2010). Multiple potential molecular contributors to atrial hypocontractility caused by atrial tachycardia remodeling in dogs. *Circ. Arrhythm. Electrophysiol.* 3, 530–541. doi: 10.1161/CIRCEP.109.933036

Walden, A. P., Dibb, K. M., and Trafford, A. W. (2009). Differences in intracellular calcium homeostasis between atrial and ventricular myocytes. *J. Mol. Cell. Cardiol.* 46, 463–473. doi: 10.1016/j.yjmcc.2008.11.003

Walker, M. A., Kohl, T., Lehnart, S. E., Greenstein, J. L., Lederer, W. J., and Winslow, R. L. (2015). On the adjacency matrix of RyR2 cluster structures. *PLoS Comput. Biol.* 11:e1004521. doi: 10.1371/journal.pcbi.1004521

Wang, H. L., Zhou, X. H., Li, Z. Q., Fan, P., Zhou, Q. N., Li, Y. D., et al. (2017). Prevention of atrial fibrillation by using sarcoplasmic reticulum calcium ATPase pump overexpression in a rabbit model of rapid atrial pacing. *Med. Sci. Monit.* 23, 3952–3960. doi: 10.12659/MSM.904824

Wehrens, X. H., Lehnart, S. E., Reiken, S. R., and Marks, A. R. (2004). Ca^{2+}/calmodulin-dependent protein kinase II phosphorylation regulates the cardiac ryanodine receptor. *Circ. Res.* 94, e61–e70. doi: 10.1161/01.RES.0000125626.33738.E2

Weiss, J. N., Garfinkel, A., Karagueuzian, H. S., Chen, P. S., and Qu, Z. (2010). Early afterdepolarizations and cardiac arrhythmias. *Heart Rhythm* 7, 1891–1899. doi: 10.1016/j.hrthm.2010.09.017

Weiss, J. N., Nivala, M., Garfinkel, A., and Qu, Z. (2011). Alternans and arrhythmias: from cell to heart. *Circ. Res.* 108, 98–112. doi: 10.1161/CIRCRESAHA.110.223586

Weng, L. C., Choi, S. H., Klarin, D., Smith, J. G., Loh, P. R., Chaffin, M., et al. (2017). Heritability of atrial fibrillation. *Circ. Cardiovasc. Genet.* 10:e001838. doi: 10.1161/CIRCGENETICS.117.001838

Wijffels, M. C., Kirchhof, C. J., Dorland, R., and Allessie, M. A. (1995). Atrial fibrillation begets atrial fibrillation. A study in awake chronically instrumented goats. *Circulation* 92, 1954–1968. doi: 10.1161/01.C. I. R.92.7.1954

Willems, R., Sipido, K. R., Holemans, P., Ector, H., Van de Werf, F., and Heidbuchel, H. (2001). Different patterns of angiotensin II and atrial natriuretic peptide secretion in a sheep model of atrial fibrillation. *J. Cardiovasc. Electrophysiol.* 12, 1387–1392. doi: 10.1046/j.1540-8167.2001.01387.x

Wolf, P. A., Abbott, R. D., and Kannel, W. B. (1991). Atrial fibrillation as an independent risk factor for stroke: the Framingham Study. *Stroke* 22, 983–988. doi: 10.1161/01.STR.22.8.983

Woo, S. H., Cleemann, L., and Morad, M. (2005). Diversity of atrial local Ca^{2+} signalling: evidence from 2-D confocal imaging in Ca^{2+}-buffered rat atrial myocytes. *J. Physiol.* 567 (Pt. 3), 905–921. doi: 10.1113/jphysiol.2005.092270

Woo, S. H., Risius, T., and Morad, M. (2007). Modulation of local Ca^{2+} release sites by rapid fluid puffing in rat atrial myocytes. *Cell Calcium* 41, 397–403. doi: 10.1016/j.ceca.2006.09.005

Workman, A. J., Kane, K. A., and Rankin, A. C. (2001). The contribution of ionic currents to changes in refractoriness of human atrial myocytes associated with chronic atrial fibrillation. *Cardiovasc. Res.* 52, 226–235. doi: 10.1016/S0008-6363(01)00380-7

Workman, A. J., Pau, D., Redpath, C. J., Marshall, G. E., Russell, J. A., Norrie, J., et al. (2009). Atrial cellular electrophysiological changes in patients with ventricular dysfunction may predispose to AF. *Heart Rhythm* 6, 445–451. doi: 10.1016/j.hrthm.2008.12.028

Wyse, D. G., Van Gelder, I. C., Ellinor, P. T., Go, A. S., Kalman, J. M., Narayan, S. M., et al. (2014). Lone atrial fibrillation: does it exist? *J. Am. Coll. Cardiol.* 63, 1715–1723. doi: 10.1016/j.jacc.2014.01.023

Xie, L. H., Shanmugam, M., Park, J. Y., Zhao, Z., Wen, H., Tian, B., et al. (2012). Ablation of sarcolipin results in atrial remodeling. *Am. J. Physiol. Cell physiol.* 302, C1762–C1771. doi: 10.1152/ajpcell.00425.2011

Xie, W., Santulli, G., Reiken, S. R., Yuan, Q., Osborne, B. W., Chen, B. X., et al. (2015). Mitochondrial oxidative stress promotes atrial fibrillation. *Sci. Rep.* 5:11427. doi: 10.1038/srep11427

Xu, H., Li, H., and Nerbonne, J. M. (1999). Elimination of the transient outward current and action potential prolongation in mouse atrial myocytes expressing a dominant negative Kv4 alpha subunit. *J. Physiol.* 519 (Pt. 1), 11–21. doi: 10.1111/j.1469-7793.1999.0011o.x

Yagi, T., Pu, J., Chandra, P., Hara, M., Danilo, P. Jr., Rosen, M. R., et al. (2002). Density and function of inward currents in right atrial cells from chronically fibrillating canine atria. *Cardiovasc. Res.* 54, 405–415. doi: 10.1016/S0008-6363(02)00279-1

Yeh, Y. H., Wakili, R., Qi, X. Y., Chartier, D., Boknik, P., Kaab, S., et al. (2008). Calcium-handling abnormalities underlying atrial arrhythmogenesis and contractile dysfunction in dogs with congestive heart failure. *Circ. Arrhythm. Electrophysiol.* 1, 93–102. doi: 10.1161/CIRCEP.107.754788

Yongjun, Q., Huanzhang, S., Wenxia, Z., Hong, T., and Xijun, X. (2013). Histopathological characteristics and oxidative injury secondary to atrial fibrillation in the left atrial appendages of patients with different forms of mitral valve disease. *Cardiovasc. Pathol.* 22, 211–218. doi: 10.1016/j.carpath.2012.10.002

Yue, L., Feng, J., Gaspo, R., Li, G. R., Wang, Z., and Nattel, S. (1997). Ionic remodeling underlying action potential changes in a canine model of atrial fibrillation. *Circ. Res.* 81, 512–525. doi: 10.1161/01.RES.81.4.512

Yue, L., Melnyk, P., Gaspo, R., Wang, Z., and Nattel, S. (1999). Molecular mechanisms underlying ionic remodeling in a dog model of atrial fibrillation. *Circ. Res.* 84, 776–784. doi: 10.1161/01.RES.84.7.776

Zhang, H., Makarewich, C. A., Kubo, H., Wang, W., Duran, J. M., Li, Y., et al. (2012). Hyperphosphorylation of the cardiac ryanodine receptor at serine 2808 is not involved in cardiac dysfunction after myocardial infarction. *Circ. Res.* 110, 831–840. doi: 10.1161/CIRCRESAHA.111.255158

Zhao, J., Butters, T. D., Zhang, H., LeGrice, I. J., Sands, G. B., and Smaill, B. H. (2013). Image-based model of atrial anatomy and electrical activation: a computational platform for investigating atrial arrhythmia. *IEEE Trans. Med. Imaging* 32, 18–27. doi: 10.1109/TMI.2012.2227776

Ziaeian, B., and Fonarow, G. C. (2016). Epidemiology and aetiology of heart failure. *Nat. Rev. Cardiol.* 13, 368–378. doi: 10.1038/nrcardio.2016.25

Zimmermann, M., and Kalusche, D. (2001). Fluctuation in autonomic tone is a major determinant of sustained atrial arrhythmias in patients with focal ectopy originating from the pulmonary veins. *J. Cardiovasc. Electrophysiol.* 12, 285–291. doi: 10.1046/j.1540-8167.2001.00285.x

Zou, R., Kneller, J., Leon, L. J., and Nattel, S. (2005). Substrate size as a determinant of fibrillatory activity maintenance in a mathematical model of canine atrium. *Am. J. Physiol. Heart Circ. Physiol.* 289, H1002–H1012. doi: 10.1152/ajpheart.00252.2005

Conflict of Interest Statement: The authors declare that the research was conducted in the absence of any commercial or financial relationships that could be construed as a potential conflict of interest.

frontiers in Physiology

ORIGINAL RESEARCH
published: 09 October 2018
doi: 10.3389/fphys.2018.01383

Profibrotic, Electrical, and Calcium-Handling Remodeling of the Atria in Heart Failure Patients With and Without Atrial Fibrillation

*Cristina E. Molina[1,2,3†], Issam H. Abu-Taha[1†], Qiongling Wang[4], Elena Roselló-Díez[5], Marcus Kamler[6], Stanley Nattel[1,7,8], Ursula Ravens[9,10], Xander H. T. Wehrens[4], Leif Hove-Madsen[2], Jordi Heijman[11] and Dobromir Dobrev[1]**

[1] Institute of Pharmacology, West German Heart and Vascular Center, University Duisburg-Essen, Essen, Germany, [2] Biomedical Research Institute Barcelona (IIBB-CSIC) and Biomedical Research Institute Sant Pau, Hospital de Sant Pau, Barcelona, Spain, [3] Institute of Experimental Cardiovascular Research, University Medical Center Hamburg-Eppendorf, Hamburg, Germany, [4] Cardiovascular Research Institute – Department of Molecular Physiology and Biophysics, Baylor College of Medicine, Houston, TX, United States, [5] Cardiac Surgery Department, Hospital de la Santa Creu i Sant Pau, Barcelona, Spain, [6] Department of Thoracic and Cardiovascular Surgery, West German Heart and Vascular Center Essen, University Hospital Essen, Essen, Germany, [7] Department of Medicine, Montreal Heart Institute and Université de Montréal, Montreal, QC, Canada, [8] Department of Pharmacology and Therapeutics, McGill University, Montreal, QC, Canada, [9] Institute of Experimental Cardiovascular Medicine, University Heart Center Freiburg, University of Freiburg, Bad Krozingen, Germany, [10] Institute of Physiology, Medical Faculty Carl Gustav Carus, TU Dresden, Dresden, Germany, [11] Department of Cardiology, CARIM School for Cardiovascular Diseases, Maastricht University, Maastricht, Netherlands

OPEN ACCESS

Edited by:
Elisabetta Cerbai, Università degli Studi di Firenze, Italy

Reviewed by:
Stefan Dhein, Leipzig University, Germany
Cecilia Ferrantini, Università degli Studi di Firenze, Italy

***Correspondence:**
Dobromir Dobrev
dobromir.dobrev@uk-essen.de

† These authors have contributed equally to this work

Specialty section:
This article was submitted to Cardiac Electrophysiology, a section of the journal Frontiers in Physiology

Received: *12 June 2018*
Accepted: *11 September 2018*
Published: *09 October 2018*

Citation:
Molina CE, Abu-Taha IH, Wang Q, Roselló-Díez E, Kamler M, Nattel S, Ravens U, Wehrens XHT, Hove-Madsen L, Heijman J and Dobrev D (2018) Profibrotic, Electrical, and Calcium-Handling Remodeling of the Atria in Heart Failure Patients With and Without Atrial Fibrillation. Front. Physiol. 9:1383. doi: 10.3389/fphys.2018.01383

Atrial fibrillation (AF) and heart failure (HF) are common cardiovascular diseases that often co-exist. Animal models have suggested complex AF-promoting atrial structural, electrical, and Ca^{2+}-handling remodeling in the setting of HF, but data in human samples are scarce, particularly regarding Ca^{2+}-handling remodeling. Here, we evaluated atrial remodeling in patients with severe left ventricular (LV) dysfunction (HFrEF), long-standing persistent ('chronic') AF (cAF) or both (HFrEF-cAF), and sinus rhythm controls with normal LV function (Ctl) using western blot in right-atrial tissue, sharp-electrode action potential (AP) measurements in atrial trabeculae and voltage-clamp experiments in isolated right-atrial cardiomyocytes. Compared to Ctl, expression of profibrotic markers (collagen-1a, fibronectin, periostin) was higher in HFrEF and HFrEF-cAF patients, indicative of structural remodeling. Connexin-43 expression was reduced in HFrEF patients, but not HFrEF-cAF patients. AP characteristics were unchanged in HFrEF, but showed classical indices of electrical remodeling in cAF and HFrEF-cAF (prolonged AP duration at 20% and shorter AP duration at 50% and 90% repolarization). L-type Ca^{2+} current ($I_{Ca,L}$) was significantly reduced in HFrEF, cAF and HFrEF-cAF, without changes in voltage-dependence. Potentially proarrhythmic spontaneous transient-inward currents were significantly more frequent in HFrEF and HFrEF-cAF compared to Ctl, likely resulting from increased sarcoplasmic reticulum (SR) Ca^{2+} load (integrated caffeine-induced current) in HFrEF and increased ryanodine-receptor (RyR2) single-channel open probability in HFrEF and HFrEF-cAF. Although expression and phosphorylation of the SR Ca^{2+}-ATPase type-2a (SERCA2a) regulator phospholamban were unchanged in HFrEF and HFrEF-cAF patients, protein levels of SERCA2a were increased in HFrEF-cAF and

sarcolipin expression was decreased in both HFrEF and HFrEF-cAF, likely increasing SR Ca^{2+} uptake and load. RyR2 protein levels were decreased in HFrEF and HFrEF-cAF patients, but junctin levels were higher in HFrEF and relative Ser2814-RyR2 phosphorylation levels were increased in HFrEF-cAF, both potentially contributing to the greater RyR2 open probability. These novel insights into the molecular substrate for atrial arrhythmias in HF-patients position Ca^{2+}-handling abnormalities as a likely trigger of AF in HF patients, which subsequently produces electrical remodeling that promotes the maintenance of the arrhythmia. Our new findings may have important implications for the development of novel treatment options for AF in the context of HF.

Keywords: atrial fibrillation, heart failure, heart failure with reduced ejection fraction, human atrial cardiomyocytes, Ca^{2+} handling

INTRODUCTION

Atrial fibrillation (AF) and heart failure (HF) are common cardiovascular diseases, negatively affecting morbidity and mortality of millions of patients worldwide (Benjamin et al., 2018). AF and HF frequently co-exist, and HF is a strong independent risk factor for the development of AF (Ling et al., 2016; Sartipy et al., 2017). AF prevalence increases with the severity of HF, ranging from 5% in NYHA Class I to 40–50% in NYHA Class IV (Andrade et al., 2014). The presence of AF in HF patients is associated with a worse prognosis (Wang et al., 2003; Mogensen et al., 2017). In agreement, the CASTLE-AF study has recently demonstrated that maintenance of sinus rhythm in HF patients with reduced left ventricular (LV) ejection fraction (HFrEF) through catheter ablation of AF significantly reduces mortality (Marrouche et al., 2018).

The common clinical coincidence of AF and HF may in part be due to their shared dependence on risk factors such as hypertension and diabetes. In addition, several bidirectional mechanistic interactions between AF and HF may promote the co-existence of both diseases in patients (Heijman et al., 2013; Hohendanner et al., 2018). For example, the atrial contribution to cardiac output is lost in the setting of AF and AF may promote ventricular dysfunction when ventricular rate is not well controlled. On the other hand, HF chronically elevates atrial pressure and causes atrial stretch, while activating systemic neurohumoral signaling pathways that affect the atria. Both components are expected to produce AF-promoting atrial remodeling. Indeed, AF is increasingly regarded as a symptom of an atrial cardiomyopathy produced by a wide variety of pathophysiological processes (Goette et al., 2017), which might be the first clinical sign of compromised ventricular function.

Animal models have identified complex atrial electrical remodeling in HF, which differs depending on species, as well as type (myocardial infarction vs. ventricular tachypacing) and duration of HF (Pandit and Workman, 2016). By contrast, structural remodeling, including activation of profibrotic signaling pathways, is a consistent finding in most HF models (Li et al., 1999; Cardin et al., 2003; Milliez et al., 2005; Yamada et al., 2017). Finally, accumulating evidence also suggests an important role for Ca^{2+}-handling abnormalities in the increased susceptibility to AF in various HF models (Yeh et al., 2008; Lugenbiel et al., 2015; Pluteanu et al., 2018).

Multiple components of atrial remodeling in patients have been characterized for different forms of AF (Brundel et al., 2002; Schotten et al., 2011; Jalife and Kaur, 2015; Simon et al., 2016). Electrical remodeling (notably shortening of action potential [AP] duration [APD]) (Dobrev et al., 2001; Voigt et al., 2012; Schmidt et al., 2015) and structural remodeling (hypertrophy and increased fibrosis) are consistent findings in patients with long-standing persistent ('chronic') AF (cAF) (Polyakova et al., 2008; Cao et al., 2010). Ca^{2+}-handling abnormalities have been identified in both paroxysmal AF and cAF, although the underlying molecular mechanisms are distinct (Voigt et al., 2012, 2014; Beavers et al., 2013). However, information about AF-promoting atrial remodeling in HFrEF patients is limited and inconsistent (Ling et al., 2016; Pandit and Workman, 2016), with reduced, unchanged or prolonged cardiomyocyte APD being reported in HFrEF patients (Schreieck et al., 2000; Workman et al., 2009; Schmidt et al., 2017). On electroanatomical mapping, APDs are rather prolonged in HF patients (Sanders et al., 2003), paralleling findings in animal models (Li et al., 2000). Similar to animal models, atrial structural remodeling, including fibrosis, is commonly observed in HF patients (Xu et al., 2004; Akkaya et al., 2013). However, whether HF is associated with atrial Ca^{2+}-handling abnormalities in humans and whether the underlying mechanisms are similar to those observed in patients with AF is not known. Moreover, patients with HF-dependent AF are subjected to both HF- and AF-related remodeling. Due to the cross-talk between both processes, the resulting remodeling is likely different from and more complex than the sum of the individual processes (Cha et al., 2004; Heijman et al., 2013; Goette et al., 2017), but has not yet been characterized in atrial samples from patients.

Here, we assessed for the first time atrial profibrotic, electrical and Ca^{2+}-handling remodeling in atrial samples from patients

Abbreviations: AF, atrial fibrillation; AP, action potential; APD, AP duration; αSMA, α smooth muscle actin; cAF, long-standing persistent ('chronic') AF; Col1a, collagen 1a; CSQ, calsequestrin; Cx40/43, connexin-40/connexin-43; ERP, effective refractory period; HF, heart failure; HFrEF, heart failure with reduced ejection fraction; $I_{Ca,L}$, L-type Ca^{2+} current; I_{TI}, transient-inward current; LV, left ventricle; MMP9, matrix metallopeptidase 9; NCX1, Na^{+}-Ca^{2+}-exchanger type-1; NYHA, New York Heart Association; PLB, phospholamban; RA, right atrium; RyR2, ryanodine receptor type-2; SERCA2a, sarcoplasmic reticulum Ca^{2+}-ATPase type-2a; SR, sarcoplasmic reticulum; TGF-β1, transforming growth factor β1.

with HFrEF and HFrEF-cAF to sinus-rhythm patients with normal LV ejection fraction (Ctl). We obtained evidence for substantial profibrotic and Ca^{2+}-handling remodeling in HFrEF patients, but did not find indices of classical electrical remodeling. Proarrhythmic diastolic Ca^{2+}-release events and profibrotic remodeling were similarly observed in HFrEF-cAF patients, along with classical AF-related electrical remodeling, consistent with the more complex pathophysiology present in these patients. Overall, our new data position Ca^{2+}-handling abnormalities as a potential early component of HF-related atrial remodeling, which in fibrotic atria may initiate AF episodes that induce electrical remodeling, promoting arrhythmia-stabilizing reentry and AF persistence.

MATERIALS AND METHODS

Human Tissue Samples

Right-atrial (RA) appendages were obtained from 79 Ctl patients (LV ejection fraction > 50%), 40 patients with HFrEF, 35 patients with cAF and 36 HFrEF-cAF undergoing open-heart surgery. Mean LV ejection fraction was <35% for HFrEF and HFrEF-cAF. Patient characteristics are provided in **Tables 1–3**. Experimental protocols were approved by ethical review boards of Dresden University of Technology, Hospital de la Santa Creu i Sant Pau and University Hospital Essen, and were conducted in accordance with the Declaration of Helsinki. Each patient gave written informed consent. The tissue samples were collected just prior to atrial cannulation for extracorporeal circulatory bypass, stored in Tyrode solution and transferred to the laboratory for AP recordings in trabeculae, cardiomyocyte isolation for voltage-clamp studies, or freezing in liquid nitrogen for biochemical and biophysical experiments, as detailed below.

Western Blot Analysis

Western blot analyses were performed as previously described (El-Armouche et al., 2006; Shanmugam et al., 2011). In brief, atrial lysates were subjected to electrophoresis on 5% or 10% acrylamide gels, or 10% Bis-Tris gels (Thermo Fisher Scientific, Waltham, MA, United States) for analyses of sarcolipin, followed by transfer onto polyvinyl difluoride (PVDF) or nitrocellulose membranes. Protein levels of α smooth-muscle actin (αSMA, 1:500, A5228, Sigma-Aldrich, St. Louis, MO, United States), calsequestrin (CSQ, 1:2,500, PA1-913, Thermo Fisher Scientific), collagen 1α (Col1a, 1:1,000, sc-293182, Santa Cruz Biotechnology, Santa Cruz, CA, United States), connexin-40 (Cx40, 1:1,000, ab1726, Merck Millipore, Burlington, MA, United States), total and Ser368-phosphorylated connexin-43 (Cx43, 1:1,000, 3511, Cell Signaling Technology, Danvers, MA, United States), fibronectin (1:1,000, sc-8422, Santa Cruz Biotechnology), GAPDH (1:20,000, 5G4 6C5, HyTest, Turku, Finland), junctin (1:2,000, LS-C196703, LifeSpan BioSciences, Seattle, WA, United States), junctophilin-2 (1:1,000, sc-134875, Santa Cruz), matrix metallopeptidase 9 (MMP9, 1:200, ab38898, Abcam, Cambridge, United Kingdom), Na^{+}-Ca^{2+}-exchanger type-1 (NCX1, 1:1,000, R3F1, Swant,

TABLE 1 | Clinical characteristics of patient samples employed for multicellular action potential recordings.

	Ctl	HFrEF	cAF	HFrEF-cAF
Patients (*n*)	15	15	15	15
Female gender	5 (33.3%)	5 (33.3%)	3 (20.0%)	2 (13.3%)
Age (years)	67.7 ± 2.43	68.2 ± 1.31	73.1 ± 1.63	71.1 ± 1.73
BMI (kg/m^2)	28.3 ± 0.93	27.1 ± 1.37	28.4 ± 1.26	27.5 ± 1.10
CAD	7 (46.7%)	8 (53.3%)	4 (26.7%)	2 (13.3%)
AVD/MVD	3 (20.0%)	4 (26.7%)	9 (60.0%)	9 (60.0%)
CAD + AVD/MVD	5 (33.3%)	3 (20.0%)	2 (13.3%)	4 (26.7%)
Hypertension	14 (93.3%)	13 (86.7%)	15 (100%)	14 (93.3%)
Diabetes	6 (40.0%)	7 (46.7%)	6 (40.0%)	6 (40.0%)
Dyslipidemia	11 (73.3%)	10 (66.7%)	11 (78.6%)	11 (78.6%)
LAD (mm)	44.0 ± 1.44	44.6 ± 1.58	50.38 ± 1.57[1]	54.3 ± 1.93*,#
LVEF (%)	60.9 ± 1.81	27.8 ± 1.57*	61.73 ± 1.85#	29.5 ± 1.55*,$
Digitalis	0 (0.0%)	1 (6.7%)	5 (33.3%)	3 (20.0%)
ACE inhibitors	8 (53.3%)	9 (60.0%)	8 (53.3%)	11 (73.3%)
AT_1 blockers	4 (26.7%)	7 (46.7%)	7 (46.7%)	1 (6.7%)
Beta-blockers	13 (86.7%)	14 (93.3%)	10 (66.7%)	14 (93.3%)
Calcium-antagonists	2 (13.3%)	0 (0.0%)	3 (20.0%)	0 (0.0%)
Diuretics	7 (46.7%)	11 (73.3%)	14 (93.3%)	11 (73.3%)
Nitrates	3 (20.0%)	0 (0.0%)	2 (13.3%)	2 (13.3%)
Lipid-lowering drugs	14 (93.3%)	7 (46.7%)	10 (66.7%)	9 (60.0%)

*Values are presented as mean ± SEM or number of patients (%). ACE, angiotensin-converting enzyme; AT, angiotensin receptor; AVD/MVD, aortic/mitral valve disease; BMI, body mass index; CAD, coronary artery disease; LAD, left atrial diameter; LVEF, left ventricular ejection fraction. * indicates P < 0.01 vs. Ctl, # indicates P < 0.01 vs. HFrEF, $ indicates P < 0.01 vs. cAF. [1]LAD in cAF is borderline significantly increased vs. Ctl (P = 0.051). CAD, AVD/MVD, and CAD + AVD/MVD reflect the indications for cardiac surgery (bypass surgery, valve replacement or a combination of both).*

TABLE 2 | Clinical characteristics of patient samples used for voltage-clamp recordings in isolated atrial cardiomyocytes.

	Ctl	HFrEF	cAF	HFrEF-cAF
Patients (*n*)	37	8	20	8
Female gender	22 (59.5%)	5 (62.5%)	12 (60.0%)	2 (25.0%)
Age (years)	62.6 ± 2.20	69.9 ± 4.10	69.0 ± 1.83	64.8 ± 7.20
BMI (kg/m^2)	N/A	N/A	N/A	N/A
CAD	11 (29.7%)	4 (50.0%)	3 (15.0%)	1 (12.5%)
AVD/MVD	19 (51.4%)	2 (25.0%)	13 (65.0%)	5 (62.5%)
CAD + AVD/MVD	7 (18.9%)	2 (25.0%)	4 (20.0%)	2 (25.0%)
Hypertension	18 (48.6%)	4 (50%)	14 (70.0%)	3 (37.5%)
Diabetes	11 (29.7%)	3 (37.5%)	7 (35.0%)	1 (12.5%)
Dyslipidemia	20 (54.1%)	5 (62.5%)	9 (45.0%)	3 (37.5%)
LAD (mm)	39.5 ± 1.3	43.3 ± 5.1	52.3 ± 3.04*	47.7 ± 4.2
LVEF (%)	64.5 ± 1.9	25.1 ± 2.4*	52.4 ± 1.40*,#	28.7 ± 4.4*,$
Digitalis	1 (2.7%)	0 (0.0%)	6 (30.0%)*	4 (50.0%)*
ACE inhibitors	10 (27.0%)	3(37.5%)	8 (40.0%)	2 (25.0%)
AT_1 blockers	8 (21.6%)	0 (0.0%)	6 (30.0%)	1 (12.5%)
Beta-blockers	13 (35.1%)	5 (62.5%)	10 (50.0%)	3 (37.5%)
Calcium-antagonists	0 (0.0%)	0 (0.0%)	0 (0.0%)	0 (0.0%)
Diuretics	8 (21.6%)	3 (37.5%)	10 (50.0%)	5 (62.5%)
Nitrates	13 (35.1%)	0 (0.0%)	7 (35.0%)	0 (0.0%)
Lipid-lowering drugs	19 (51.3%)	4 (50%)	9 (45.0%)	2 (25%)

*Values are presented as mean ± SEM or number of patients (%). ACE, angiotensin-converting enzyme; AT, angiotensin receptor; AVD/MVD, aortic/mitral valve disease; BMI, body mass index; CAD, coronary artery disease; LAD, left atrial diameter; LVEF, left ventricular ejection fraction; N/A, not available. * indicates $P < 0.05$ vs. Ctl, # indicates $P < 0.05$ vs. HFrEF, $ indicates $P < 0.05$ vs. cAF. CAD, AVD/MVD, and CAD + AVD/MVD reflect the indications for cardiac surgery (bypass surgery, valve replacement or a combination of both).*

Marly, Switzerland), periostin (1:1,000, sc-134875, Santa Cruz Biotechnology), total, Ser16- and Thr17-phosphorylated phospholamban (PLB, all 1:1,000, ab2865 and ab92697, Abcam, Cambridge, United Kingdom and A010-13, Badrilla Ltd., Leeds, United Kingdom), total ryanodine receptor type-2 channel (RyR2, 1:1,000, MA3-916, Thermo Fisher Scientific), sarcolipin (1:100, ABT13, Merck Millipore), sarcoplasmic reticulum (SR) Ca^{2+}-ATPase type-2a (SERCA2a; 1:2,000, sc-8095, Santa Cruz Biotechnology), transforming growth factor β1 (TGF-β1, 1:1000, ab9758, Abcam), and vimentin (1:1,000, sc373717, Santa Cruz Biotechnology) were determined using appropriate primary antibodies. The Ser2808-RyR2 and Ser2814-RyR2 phospho-epitope-specific antibodies (both 1:2,000) were custom generated, as previously described (Voigt et al., 2012). Appropriate near-infrared fluorophore dyes (IRDye, all 1:20,000, LI-COR Biosciences, Lincoln, NE, United States) were employed as secondary antibodies and imaged with an Odyssey Infrared Imaging System (LI-COR Biosciences). Protein expression was normalized to GAPDH.

Electrophysiological Recordings

Action potentials were recorded in trabeculae isolated from RA appendages using the standard microelectrode technique as previously described, with microelectrode tip resistance of 10–25 MΩ and 1 ms stimulus, 25% above threshold intensity applied at a frequency of 1 Hz (Wettwer et al., 2004; Loose et al., 2014). The bath solution contained (in mmol/L): NaCl 127, KCl 4.5, $MgCl_2$ 1.5, $CaCl_2$ 1.8, glucose 10, $NaHCO_3$ 22, and NaH_2PO_4 0.42, equilibrated with O_2/CO_2 (95:5) at 35 ± 2°C and pH = 7.4.

Cardiomyocyte isolation was performed according to previously established protocols (Llach et al., 2011; Molina et al., 2012; Voigt et al., 2015). Briefly, enzymatic digestion was carried out in a Ca^{2+}-free Tyrode solution containing 0.5 mg/ml collagenase (Worthington type 2, 300 u/mg), 0.25 mg/ml proteinase (Sigma type XXIV, 11 u/mg solid) and 5% bovine fatty acid-free albumin. After 30 min at 37°C, the tissue was removed from the enzyme solution, and cells were disaggregated in Ca^{2+}-free solution. The remaining tissue was digested for 3 × 15 min in a fresh Ca^{2+}-free solution containing 0.4 mg/ml collagenase. Only elongated cells with clear cross striations and without granulation were used for experiments. Total membrane currents were measured at room temperature in the perforated-patch configuration with an EPC-10 amplifier (HEKA Elektronik, Germany), as previously described (Llach et al., 2011; Molina et al., 2012). The extracellular solution contained (in mmol/L): NaCl 127, TEA 5, HEPES 10, $NaHCO_3$ 4, NaH_2PO_4 0.33, glucose 10, pyruvic acid 5, $CaCl_2$ 2, $MgCl_2$ 1.8 (pH = 7.4) and the pipette solution contained (in mmol/L): aspartic acid 109, CsCl 47, Mg_2ATP 3, $MgCl_2$ 1, Na_2-phosphocreatine 5, Li_2GTP 0.42, HEPES 10 (pH = 7.2 with CsOH). Amphotericin B (250 μg/ml) was added to the pipette solution before starting the experiment. All chemicals were acquired from Sigma-Aldrich.

The L-type calcium current ($I_{Ca,L}$) was measured using a 50 ms prepulse from −80 to −45 mV to inactivate the fast Na^+ current, followed by a 200 ms depolarization to +10 mV and $I_{Ca,L}$ amplitude was determined as the difference between the peak inward current and the current at the end of the depolarization (Llach et al., 2011; Molina et al., 2012). The current–voltage

TABLE 3 | Clinical characteristics of patient samples employed for biochemical experiments.

	Ctl	HFrEF	HFrEF-cAF
Patients (*n*)	27	17	13
Female gender	11 (40.7%)	3 (17.6%)	4 (30.8%)
Age (years)	69.6 ± 2.37	63.4 ± 3.10	71.4 ± 1.51
BMI (kg/m^2)	29.3 ± 0.91	27.9 ± 1.19	27.9 ± 2.02
CAD	3 (11.1%)	7 (46.7%)*	4 (30.8%)
AVD/MVD	19 (70.4%)	4 (26.7%)*	8 (61.5%)
CAD + AVD/MVD	5 (18.5%)	4 (26.7%)*	1 (7.7%)
Hypertension[1]	21 (77.8%)	7 (50.0%)	9 (69.2%)
Diabetes[1]	8 (30.8%)	4 (30.8%)	4 (30.8%)
Dyslipidemia[1]	14 (58.3%)	7 (50.0%)	2 (16.7%)
LAD (mm)	39.5 ± 0.57	43.9 ± 1.04*	47.0 ± 1.30*
LVEF (%)	62.7 ± 1.22	33.3 ± 1.09*	34.2 ± 1.74*
Digitalis	0 (0.0%)	0 (0.0%)	1 (7.7%)
ACE inhibitors	7 (25.9%)	10 (58.8%)	5 (38.5%)
AT_1 blockers	5 (18.5%)	0 (0.0%)	2 (15.4%)
Beta-blockers	15 (55.6%)	16 (94.1%)*	9 (69.2%)
Calcium-antagonists	9 (33.3%)	2 (11.8%)	1 (7.7%)
Diuretics	12 (44.4%)	13 (76.5%)	7 (53.8%)
Nitrates	2 (7.4%)	0 (0.0%)	0 (0.0%)
Lipid-lowering drugs	11 (40.7%)	10 (58.8%)	4 (30.8%)

*Values are presented as mean ± SEM or number of patients (%). ACE, angiotensin-converting enzyme; AT, angiotensin receptor; AVD/MVD, aortic/mitral valve disease; BMI, body mass index; CAD, coronary artery disease; LAD, left atrial diameter; LVEF, left ventricular ejection fraction. * indicates $P < 0.05$ vs. Ctl. [1]Information on hypertension, diabetes and dyslipidemia was available for 27, 26, and 24 of the 27 Ctl patients, for 14, 13, and 14 of the 17 HFrEF patients, and for 13, 13, and 12 of the 13 HFrEF-cAF patients, respectively. CAD, AVD/MVD, and CAD + AVD/MVD reflect the indications for cardiac surgery (bypass surgery, valve replacement or a combination of both).*

relationship for $I_{Ca,L}$ and the voltage-dependent inactivation were obtained using test potentials between −40 and +50 mV. The time constants of $I_{Ca,L}$ inactivation were determined from a bi-exponential fit of the decaying phase of $I_{Ca,L}$. Recovery of $I_{Ca,L}$ from inactivation was assessed using a two-pulse protocol with increasing intervals between the first and the second pulse used to elicit $I_{Ca,L}$.

The SR Ca^{2+} content was measured at room temperature as the time integral of the current elicited by rapid exposure to 10 mmol/L caffeine to release all Ca^{2+} from the SR, activating NCX1, and was converted to amoles (10^{-18} mol) of calcium released from the SR, assuming a stoichiometry of 3 Na^+ to 1 Ca^{2+} for NCX1. Spontaneous calcium releases were examined as transient-inward currents (I_{NCX}) with the membrane potential clamped at −80 mV, as previously described (Hove-Madsen et al., 2004; Llach et al., 2011; Molina et al., 2012; Voigt et al., 2012).

RyR2 Single-Channel Recordings

RyR2 single-channel recordings were obtained as previously described (Wehrens et al., 2003). In brief, SR membrane-preparations were incorporated into lipid-bilayer membranes made of a 3:1 mixture of phosphatidylethanolamine and phosphatidylserine (Avanti Polar Lipids, Alabaster, AL, United States) dissolved in *n*-decane (25 mg/ml). Bilayers were formed across a 150 μm aperture of a polystyrene cuvette. The *trans* chamber (luminal side of the SR) contained (in mmol/L): HEPES 250, KCl 50 and $Ca(OH)_2$ 53. The *cis* chamber (cytosolic side of the SR) contained (in mmol/L): HEPES 250, Tris-base 125, KCl 50, EGTA 1, $CaCl_2$ 0.5 (pH = 7.35). At the end of each experiment, ryanodine (5 μmol/L) was applied to the *cis* chamber to confirm identity of RyR2 channels. Data were collected using Digidata 1322A (Molecular Devices, Sunnyvale, CA, United States) and Warner Bilayer Clamp Amplifier BC-535 (Warner Instruments, Hamden, CT, United States) at 0 mV under voltage-clamp conditions. Cytosolic free Ca^{2+} was calculated with WinMax32. Data were analyzed from digitized current recordings using pCLAMP-9.2 software (Molecular Devices).

Data Analysis and Statistics

Data are presented as mean ± standard error (SEM) or scatter plots of individual measurements with 95% confidence interval and interquartile ranges. Normality was assessed using D'Agostino and Pearson omnibus test. For multicellular AP recordings, biochemical experiments, and clinical parameters, for which each patient contributed a single data point, one-way ANOVA followed by a *post hoc* Bonferroni *t*-test was used to compare means between groups for normally distributed continuous data. Continuous data which did not follow a normal distribution or for which normality could not be assessed were compared using a Kruskal–Wallis test with Dunn's multiple comparison *t*-test. Categorical data were analyzed using a Chi-squared test with Bonferroni correction for multiple comparisons when comparing more than two groups. For patch-clamp and RyR2 single-channel recordings, in which each patient may contribute multiple data points, hierarchical statistics were employed according to recently published methods (Sikkel et al., 2017). Logarithmic transformations were applied to non-normal-distributed data (RyR2 properties and frequency of spontaneous SR Ca^{2+}-release events) before applying hierarchical statistical analyses. $P < 0.05$ was considered statistically significant.

RESULTS

Patient Characteristics

Major clinical parameters for all patient groups are provided in **Table 1** (for patient samples employed for multicellular AP recordings), **Table 2** (for patient samples used for cardiomyocyte isolation and voltage-clamp experiments), and **Table 3** (for patient samples used for biochemical experiments). By definition, LV ejection fractions were significantly lower in HFrEF and HFrEF-cAF groups compared to Ctl and cAF. In addition, there was a strong trend toward increased left atrial diameter in HFrEF patients, which was even more pronounced in cAF and HFrEF-cAF patients. As expected, HFrEF patients also tended to take more β-blockers, whereas AF patients more often received digitalis. There were no other major differences in clinical parameters between the three groups.

Profibrotic Remodeling

Patients with HFrEF have increased macroscopic fibrosis and conduction slowing (Sanders et al., 2003; Akkaya et al., 2013). Moreover, animal models of HF consistently show increased molecular markers of profibrotic remodeling (Cardin et al., 2003). We evaluated protein expression levels of key extracellular matrix components (col1a, fibronectin, MMP9), activated fibroblast/(myo)fibroblast markers (vimentin, periostin, αSMA) and profibrotic signaling molecules (TGF-β1) in atrial tissue homogenates of Ctl, HFrEF and HFrEF-cAF patients (**Figure 1A**). Compared to Ctl patients, col1a, fibronectin and periostin were significantly increased in HFrEF and HFrEF-cAF patients, consistent with increased fibrosis in these patients.

Electrical Remodeling

First we assessed the protein expression of connexin isoforms contributing to electrical cell-to-cell coupling and signaling. Protein levels of Cx40 were not different between the three groups, whereas protein expression of total Cx43 was reduced by ∼41% ($P = 0.078$) in atrial homogenates of HFrEF patients, but was not different between Ctl and HFrEF-cAF patients (**Figure 1B**). Similarly, steady-state phosphorylation levels of Cx43 at Ser368, which control internalization of connexins (Cone et al., 2014), were reduced by ∼36% in HFrEF only (**Figure 1B**), potentially contributing to the conduction slowing observed *in vivo* (Sanders et al., 2003).

Next, we recorded APs in multicellular preparations from Ctl, HFrEF, cAF and HFrEF-cAF patients (**Figure 2A**). There were no significant differences in resting membrane potential, upstroke velocity (maximum dV/dt), conduction time, plateau potential or APD at 20%, 50%, or 90% of repolarization between Ctl and HFrEF patients (**Figure 2B**). By contrast, patients with cAF or HFrEF-cAF had a significantly increased plateau potential, significantly prolonged APD at 20% repolarization, and significantly shorter APD at 50% and 90% repolarization compared to Ctl ($P < 0.01$ for all; **Figure 2B**). There was a trend toward an increased AP amplitude in HFrEF ($P = 0.077$ vs. Ctl), which was significant in patients with cAF or HFrEF-cAF.

Then, we investigated $I_{Ca,L}$ properties in isolated human atrial cardiomyocytes as a potential contributor to electrical remodeling and marker of Ca^{2+}-handling remodeling. HFrEF, cAF and HFrEF-cAF patients all had a significant decrease in peak $I_{Ca,L}$ amplitude (**Figure 3A**). Voltage-dependence of peak $I_{Ca,L}$ (**Figure 3B**), inactivation (**Figures 3C,D**), and the time constant of recovery from inactivation (**Figure 3F**) were not different between Ctl, HFrEF, cAF and HFrEF-cAF patients. We determined the fast and slow time constants of $I_{Ca,L}$ inactivation through a biexponential fit. Although the fast time constant was not different between Ctl, HFrEF and HFrEF-cAF (Ctl: 13.6 ± 0.95 ms, HFrEF: 18.8 ± 4.2 ms, and HFrEF-cAF: 18.1 ± 1.2 ms), it was increased in cAF (20.7 ± 2.9 ms). The slow time constant was significantly larger in HFrEF-cAF patients (131.8 ± 12.1 ms) and slightly increased in HFrEF (90.1 ± 3.2 ms; P = 0.058) compared to Ctl patients (63.2 ± 2.2 ms; **Figure 3E**). Taken together, these data point to potential remodeling of atrial Ca^{2+} handling in patients with HFrEF and HFrEF-cAF.

Ca^{2+}-Handling Remodeling

We first assessed indices of dysfunctional diastolic Ca^{2+} handling by measuring spontaneous occurrence of depolarizing transient-inward currents at −80 mV with perforated patch-clamp technique (**Figure 4A**), as described (Hove-Madsen et al., 2004). These currents, which are mediated by NCX, represent a well-accepted proarrhythmic consequence of spontaneous SR Ca^{2+}-release events (Hove-Madsen et al., 2004; Llach et al., 2011; Heijman et al., 2014). The frequency of spontaneous I_{NCX} was larger in HFrEF (2.3 ± 0.49 min^{-1}), cAF (2.0 ± 0.41 min^{-1}), and HFrEF-cAF (1.5 ± 0.42 min^{-1}) compared to Ctl (0.51 ± 0.14 min^{-1}; **Figure 4B**), with unchanged I_{NCX} amplitude between the groups (**Figure 4C**).

Spontaneous SR Ca^{2+}-release events could be promoted by an increased SR Ca^{2+} load. Therefore, we quantified SR Ca^{2+} load during caffeine-mediated SR Ca^{2+} release, which produces a large I_{NCX}, the integral of which is a reliable measure of SR Ca^{2+} content (Hove-Madsen et al., 2004; Voigt et al., 2012, 2014). SR Ca^{2+} load was significantly larger in HFrEF (10.1 ± 0.75 amol/pF) compared to Ctl (6.6 ± 0.50 amol/pF; $P < 0.01$; **Figures 5A,B**), but unchanged in cAF or HFrEF-cAF. The time constant of the caffeine-induced I_{NCX} was not different between the groups, pointing to an unaltered NCX function (**Figure 5C**). Accordingly, NCX1 protein expression was unchanged in HFrEF and HFrEF-cAF patients (**Figure 6**).

The increased SR Ca^{2+} load could be mediated by increased SR Ca^{2+} uptake via SERCA2a. Protein levels of SERCA2a were unchanged in HFrEF, but strongly increased in patients with HFrEF-cAF (**Figure 6**). Protein expression of the inhibitory SERCA2a regulator PLB, along with phosphorylation of PLB at the protein kinase-A site (Ser16) or the Ca^{2+}/calmodulin-dependent protein kinase-II site (Thr17) were not different between Ctl, HFrEF and HFrEF-cAF patients (**Figure 6**). By contrast, expression of the atrial-specific SERCA2a inhibitor sarcolipin was decreased by ∼66% in HFrEF and by ∼72% in HFrEF-cAF ($P < 0.05$ vs. Ctl for both), likely increasing SR Ca^{2+} uptake.

Besides increased SR Ca^{2+} load, spontaneous SR Ca^{2+}-release events often result from RyR2 dysfunction (Voigt et al., 2012, 2014; Beavers et al., 2013; Li et al., 2014). To address this directly we investigated RyR2 single-channel open probability in lipid bilayer experiments (**Figure 7A**). At 150 nmol/L intracellular [Ca^{2+}], mimicking diastolic conditions, RyR2 open probability was significantly larger in both HFrEF (5.7 ± 1.6%) and HFrEF-cAF (30.9 ± 11.8%) patients compared to Ctl (0.6 ± 0.2%) patients ($P < 0.05$ for both; **Figure 7B**). The increased open probability was primarily due to a decrease in closed time (**Figure 7D**), although single-channel open time was significantly prolonged in HFrEF-cAF patients (**Figure 7C**), further increasing open probability. Finally, we assessed the molecular basis of the increased RyR2 open probability using Western blotting (**Figure 8A**). Compared to Ctl the relative RyR2 protein levels were decreased by ∼45% in HFrEF patients ($P < 0.01$), along with a similar non-significant trend (∼28% reduction) in HFrEF-cAF ($P = 0.10$; **Figure 8B**). Phosphorylation levels at Ser2808-RyR2 normalized to total RyR2

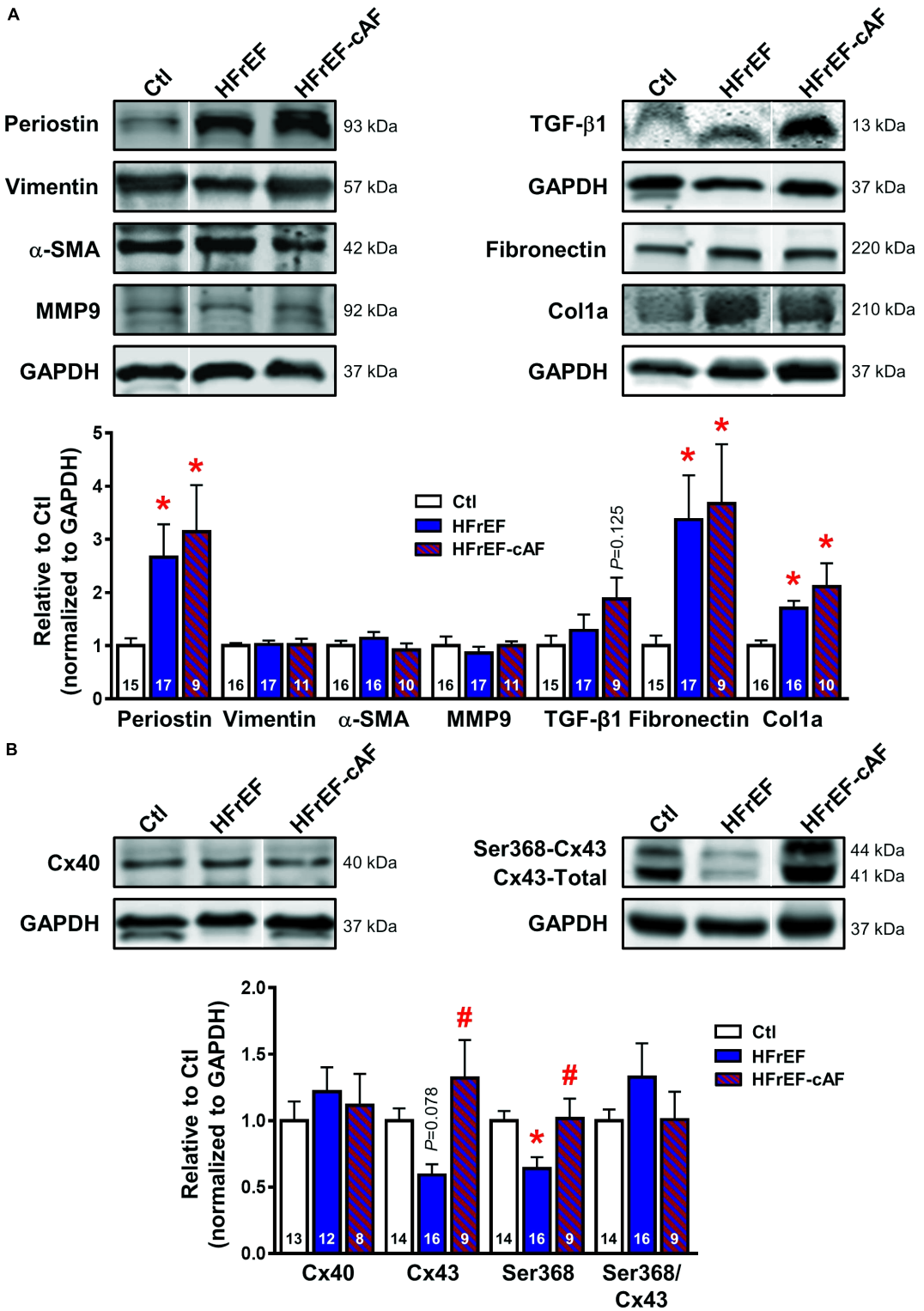

FIGURE 1 | Atrial profibrotic and connexin remodeling. **(A)** Representative Western blot examples (top) and quantification of protein expression (bottom; mean ± SEM) of periostin, vimentin, α-smooth muscle actin (α-SMA), matrix metallopeptidase 9 (MMP9), transforming growth factor-β1 (TGF-β1), fibronectin and collagen 1α (col1a) in right-atrial tissue homogenates from Ctl (white bars), HFrEF (blue bars) or HFrEF-cAF (red/blue-striped bars) patients. Vertical white lines separate non-adjacent lanes on the same blot. **(B)** Representative Western blot examples (top) and quantification of protein expression (bottom; mean ± SEM) of total connexin-40 (Cx40), total and Ser368-phosphorylated connexin-43 (Cx43). GAPDH was used as loading control and is shown for the samples used for Western blots of periostin, vimentin, α-SMA and MMP9, for TGF-β1, and for fibronectin and col1a. Numbers in bars indicate number of patients. * indicates $P < 0.05$ vs. Ctl, # indicates $P < 0.05$ vs. HFrEF.

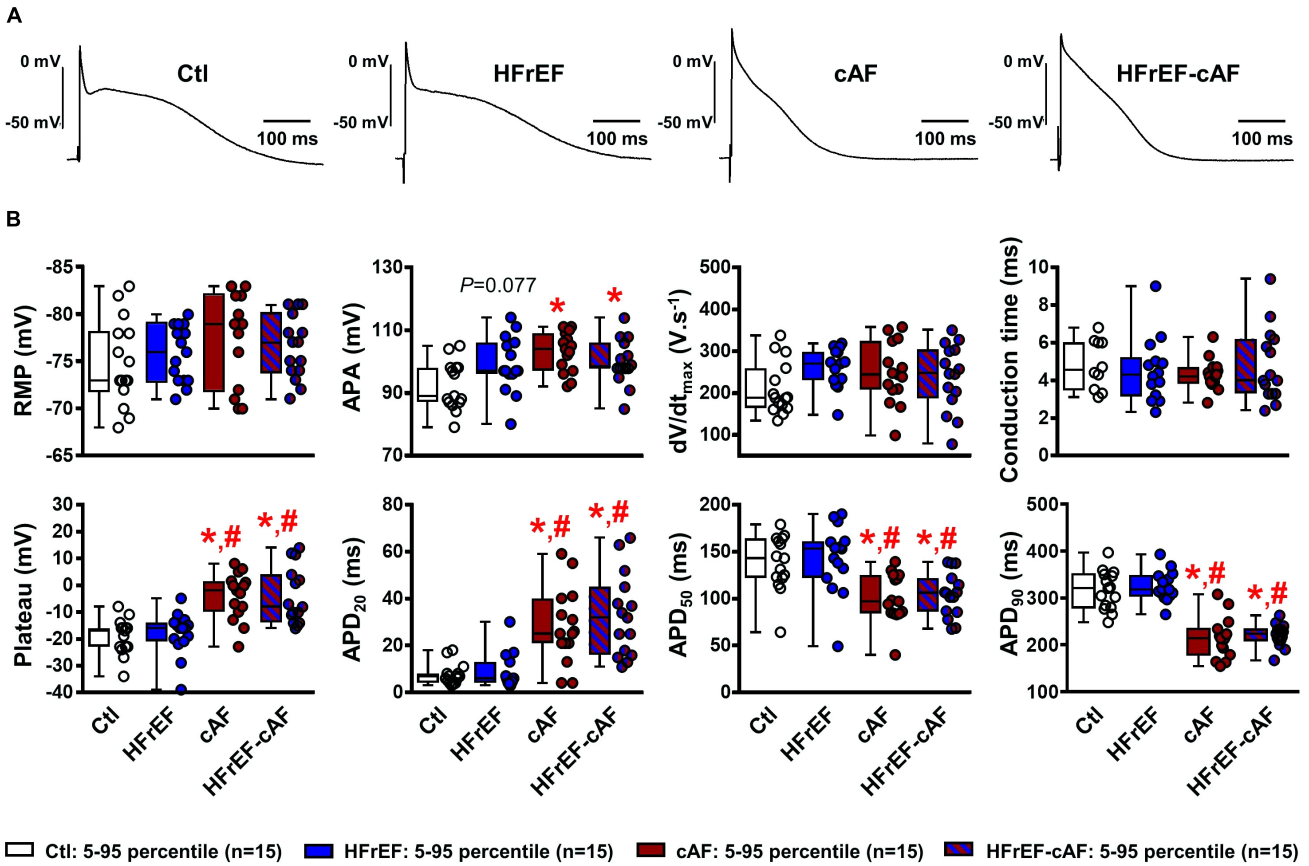

FIGURE 2 | Electrical remodeling in multicellular human atrial trabeculae. **(A)** Representative action potential (AP) recordings in multicellular preparations from Ctl, HFrEF, cAF or HFrEF-cAF patients (from left to right). **(B)** Quantification of AP parameters in Ctl (white bars), HFrEF (blue bars), cAF (red bars) or HFrEF-cAF (red/blue-striped bars) patients. Top row shows (from left to right): resting membrane potential (RMP), AP amplitude (APA), maximal AP upstroke velocity (dV/dt_{max}) and conduction time (note different n-numbers). Bottom row shows (from left to right): level of AP plateau and AP duration (APD) at 20%, 50%, and 90% of repolarization. * indicates $P < 0.05$ vs. Ctl, # indicates $P < 0.05$ vs. HFrEF. Numbers indicate number of patients.

were not different between the three groups, whereas relative phosphorylation at Ser2814-RyR2 was increased by ∼97% in HFrEF-cAF compared to Ctl or HFrEF patients ($P < 0.05$ for both), potentially underlying the increased RyR2 open probability in these patients (**Figure 8B**). We also investigated the protein levels of other validated components of the RyR2 macromolecular complex (CSQ, junctin, and junctophilin-2) (Landstrom et al., 2017). Protein levels of CSQ were unchanged in HFrEF or HFrEF-cAF compared to Ctl (**Figure 8C**), whereas junctin expression was ∼65% higher in HFrEF vs Ctl patients ($P = 0.011$) and there was a trend toward increased levels of junctophilin-2 in HFrEF compared to Ctl patients ($P = 0.059$; **Figure 8C**).

DISCUSSION

In the present study, we have detailed for the first time profibrotic, electrical and Ca^{2+}-handling remodeling in patients with HFrEF alone and HFrEF-cAF. Our data show (1) that profibrotic markers are upregulated in patients with HFrEF, independent of the presence of AF; (2) that protein expression and phosphorylation of connexin-43 are reduced in HFrEF only; (3) that classical indices of AF-related atrial electrical remodeling only occur in cAF and HFrEF-cAF; and (4) that potentially proarrhythmic atrial Ca^{2+}-handling abnormalities are a typical finding in both HFrEF and HFrEF-cAF patients. Together, these data provide novel insights into the cellular and molecular mechanisms of AF in patients with HFrEF and HFrEF-cAF, which may have important implications for the development of novel therapeutic option for AF patients in the context of HF.

Comparison to Previous Work

Atrial structural remodeling is a consistent finding in patients with HFrEF. At the tissue level, increased atrial fibrosis assessed using late gadolinium enhancement magnetic resonance imaging has been reported (Akkaya et al., 2013). Atrial fibrosis is also a common finding in animal models of HFrEF (Li et al., 1999; Milliez et al., 2005; Yamada et al., 2017; Pluteanu et al., 2018), and the underlying pathways have been investigated in detail (Cardin et al., 2003). Our data similarly point to prominent profibrotic remodeling, with increased expression of

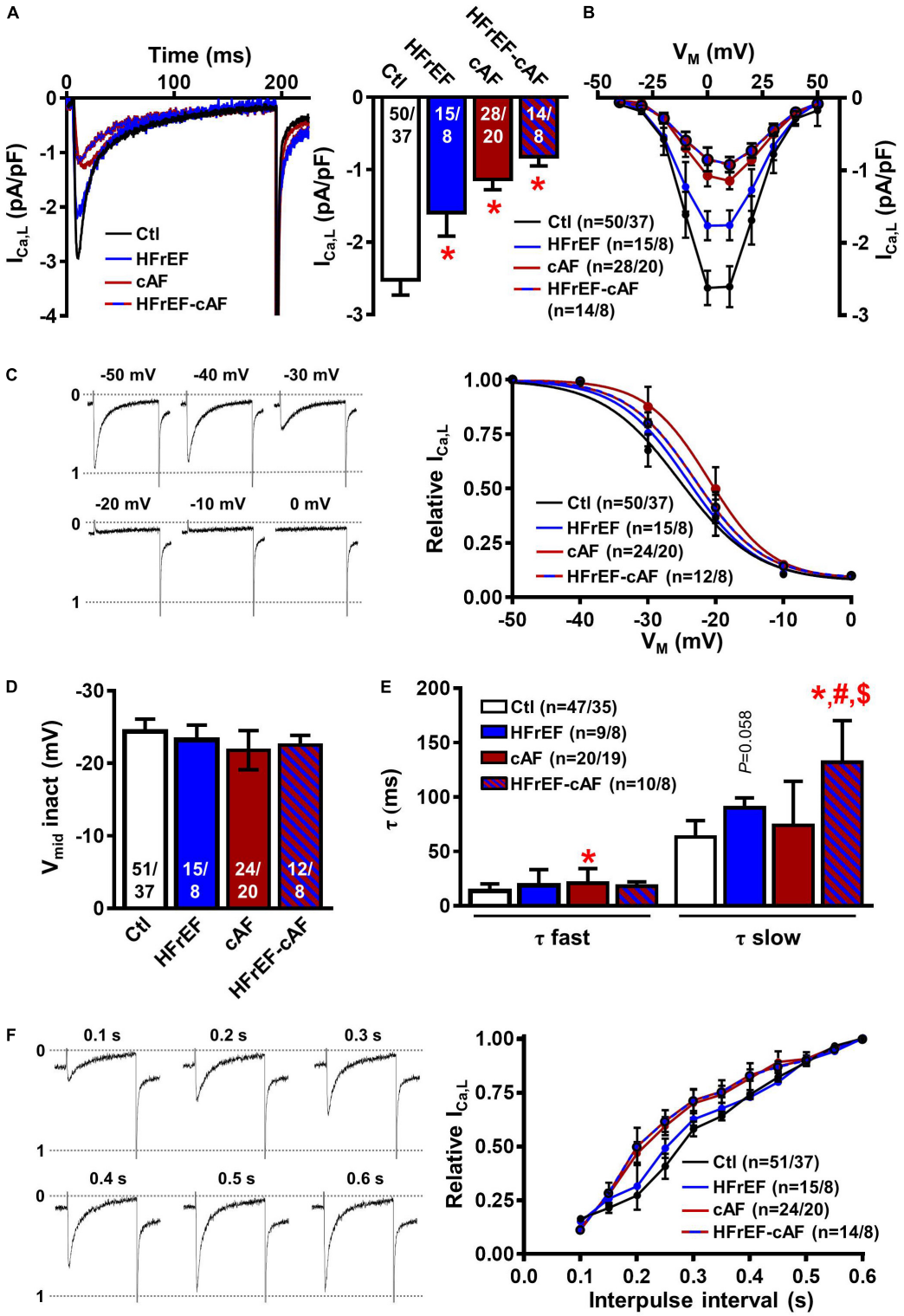

FIGURE 3 | L-type Ca^{2+} current ($I_{Ca,L}$) measurements in isolated human atrial cardiomyocytes. **(A)** Representative $I_{Ca,L}$ recording during a 200-ms depolarizing pulse to +10 mV in a Ctl (black), HFrEF (blue), cAF (red) or HFrEF-cAF (blue/red) atrial cardiomyocyte (left) and quantification of I_{CaL} amplitude (right). **(B)** Current-voltage relationship of peak $I_{Ca,L}$. **(C)** Representative examples of $I_{Ca,L}$ inactivation protocol (left) and voltage dependence of inactivation (right) **(D)** midpoint of inactivation in Ctl, HFrEF, cAF and HFrEF-cAF patients. **(E)** Fast and slow time constants of inactivation during a depolarization to +10 mV in Ctl, HFrEF, cAF and HFrEF-cAF patients. **(F)** Representative examples (left) and quantification (right) of $I_{Ca,L}$ recovery from inactivation with various interpulse intervals. Numbers in bars indicate number of cells/number of patients. * indicates $P < 0.05$ vs. Ctl, # indicates $P < 0.05$ vs. HFrEF, $ indicates $P < 0.05$ vs. cAF.

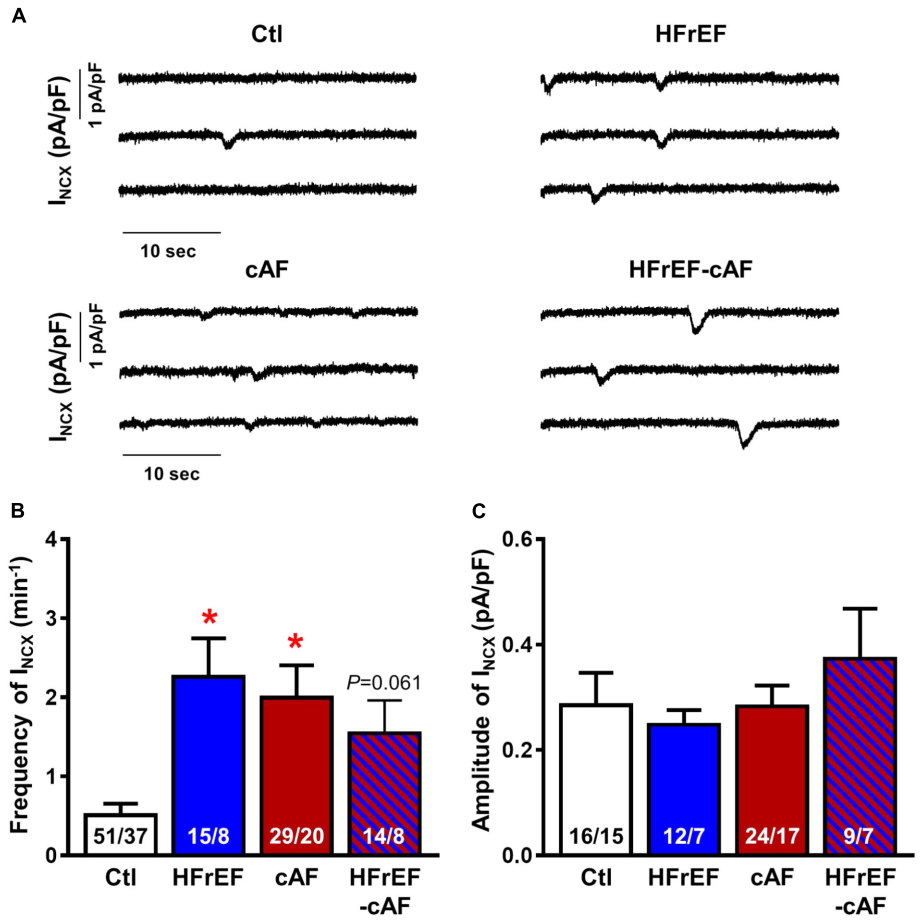

FIGURE 4 | Spontaneous Ca^{2+}-release events in isolated human atrial cardiomyocytes. **(A)** Representative recordings of NCX-mediated transient-inward current (I_{NCX}) in atrial cardiomyocytes from Ctl, HFrEF, cAF or HFrEF-cAF patients. **(B,C)** Frequency **(B)** and amplitude **(C)** of spontaneous I_{NCX} in the four groups. Numbers in bars indicate number of cells/number of patients. * indicates $P < 0.05$ vs. Ctl.

col1a, periostin and fibronectin. The associated alterations in atrial structure are expected to cause reentry-promoting slow, heterogeneous conduction, which has been directly observed *in vivo* in atria of HFrEF patients (Sanders et al., 2003). We also identified reduced expression and Ser368 phosphorylation of Cx43 in HFrEF patients, which may also contribute to conduction abnormalities.

Reentry-promoting electrical remodeling, characterized by shortening of APD and hyperpolarization of the resting membrane potential, is a hallmark of cAF and is a consistent finding in animal models with atrial tachycardia remodeling (Heijman et al., 2014). By contrast, APD and resting membrane potential of patients with paroxysmal AF are not different from Ctl patients (Voigt et al., 2014; Schmidt et al., 2015). Similarly, in the present study we found no significant differences in AP properties in patients with HFrEF only, suggesting that electrical remodeling may be primarily a consequence of the rapid atrial rate during cAF. At the cardiomyocyte level various inconsistent results have been published about atrial electrical remodeling in the setting of HF. Workman et al. (2009) reported shortened APD and effective refractory period (ERP) in atrial cardiomyocytes from HFrEF patients undergoing cardiac surgery, whereas Schreieck et al. (2000) detected no differences in atrial cardiomyocyte APD between HFrEF and Ctl patients or healthy donors. Finally, other studies in atrial cardiomyocytes (Koumi et al., 1994), *ex vivo* multicellular preparations (Fedorov et al., 2011) and *in vivo* recordings in patients (Sanders et al., 2003) have reported prolonged APD and/or ERP.

The inconsistent results between studies related to APD in HFrEF patients might at least in part be explained by the use of isolated cardiomyocytes vs. multicellular preparations and the techniques used to assess APD/ERP. Cardiomyocyte isolation procedures from human atria are known to affect function of a number of ion channels, often resulting in depolarized resting membrane potentials that require injection of a hyperpolarizing current in order to record APs. Such a current may differentially affect APs from Ctl or HFrEF patients. In addition, remodeling of individual ion currents in HFrEF patients appears highly variable between studies. For example, both reduced and unchanged inward-rectifier K^+ current, as well as reduced, unchanged and increased transient-outward K^+ current have been reported (Koumi

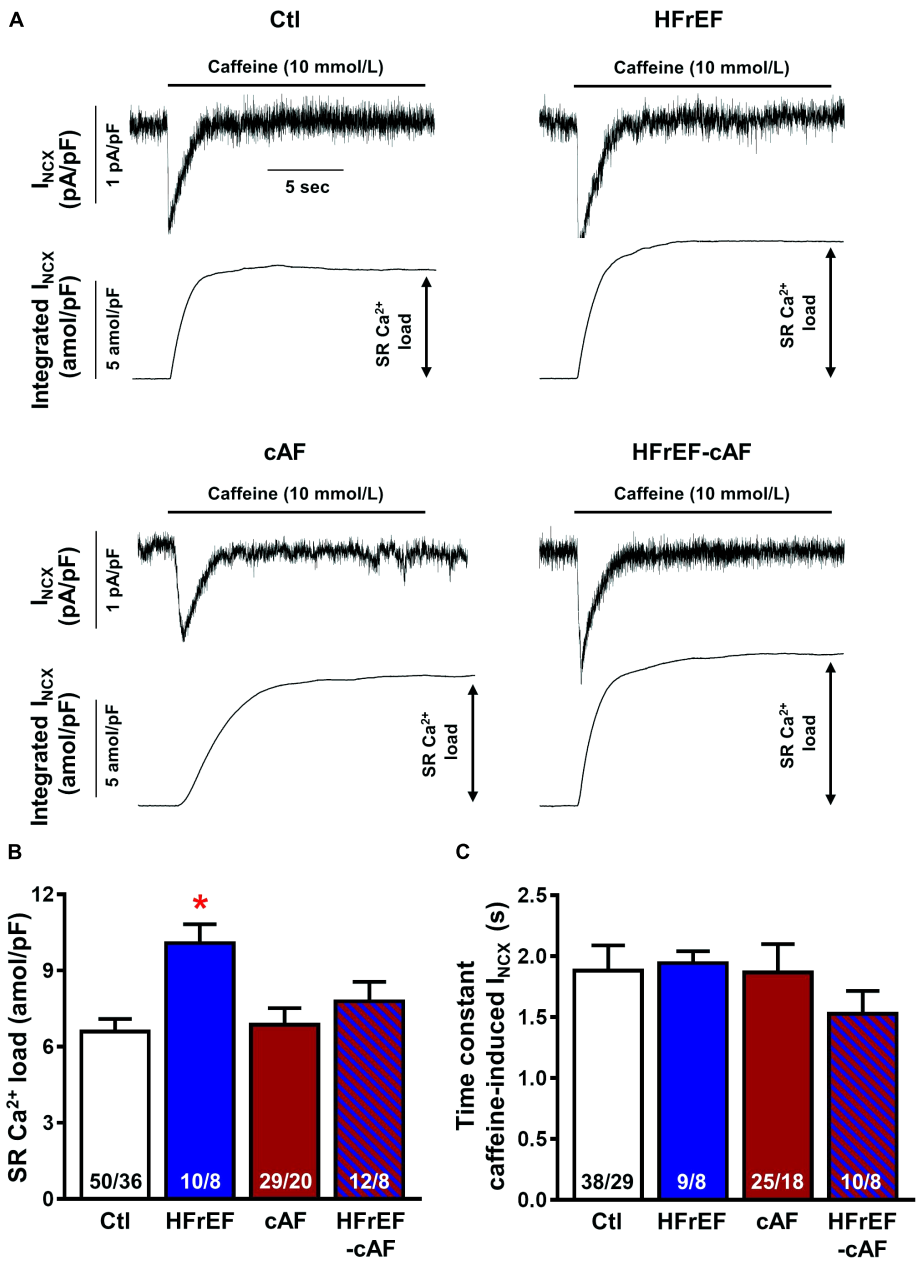

FIGURE 5 | Sarcoplasmic reticulum (SR) Ca^{2+} load in isolated human atrial cardiomyocytes. **(A)** Representative recordings of NCX-mediated inward current (I_{NCX}) induced by caffeine (10 mmol/l) application in atrial cardiomyocytes from Ctl, HFrEF, cAF or HFrEF-cAF patients (top panels). The bottom panels show the integral of membrane current over time, the amplitude of which is an accepted index of SR Ca^{2+} load. **(B,C)** SR Ca^{2+} load **(B)** and time constant of caffeine-induced I_{NCX} (an indicator of NCX function) in the four groups. Numbers in bars indicate number of cells/number of patients. * indicates $P < 0.05$ vs. Ctl.

et al., 1994; Van Wagoner et al., 1997; Schreieck et al., 2000; Workman et al., 2009). Differences in patient characteristics, including the use of explanted end-stage failing hearts and healthy donor hearts in some studies (Koumi et al., 1994; Van Wagoner et al., 1997; Fedorov et al., 2011), compared to patients undergoing open-heart surgery with normal or impaired LV function in our and other studies (Schreieck et al., 2000; Workman et al., 2009), may also contribute to the variable findings. Similarly, work from animal models suggest that the duration of HF differentially affects electrical remodeling, with 2 weeks of ventricular tachypacing resulting in ERP prolongation (Cha et al., 2004), 5 weeks of ventricular tachypacing associating with unchanged ERP (Li et al., 1999) and 4 months of ventricular tachypacing abbreviating atrial ERP (Sridhar et al., 2009). Since the duration of HFrEF is usually not controlled in patients, differences in HFrEF duration between the human studies are expected. Here we employed sharp-electrode AP recordings in multicellular preparations, which avoided cell-isolation-induced

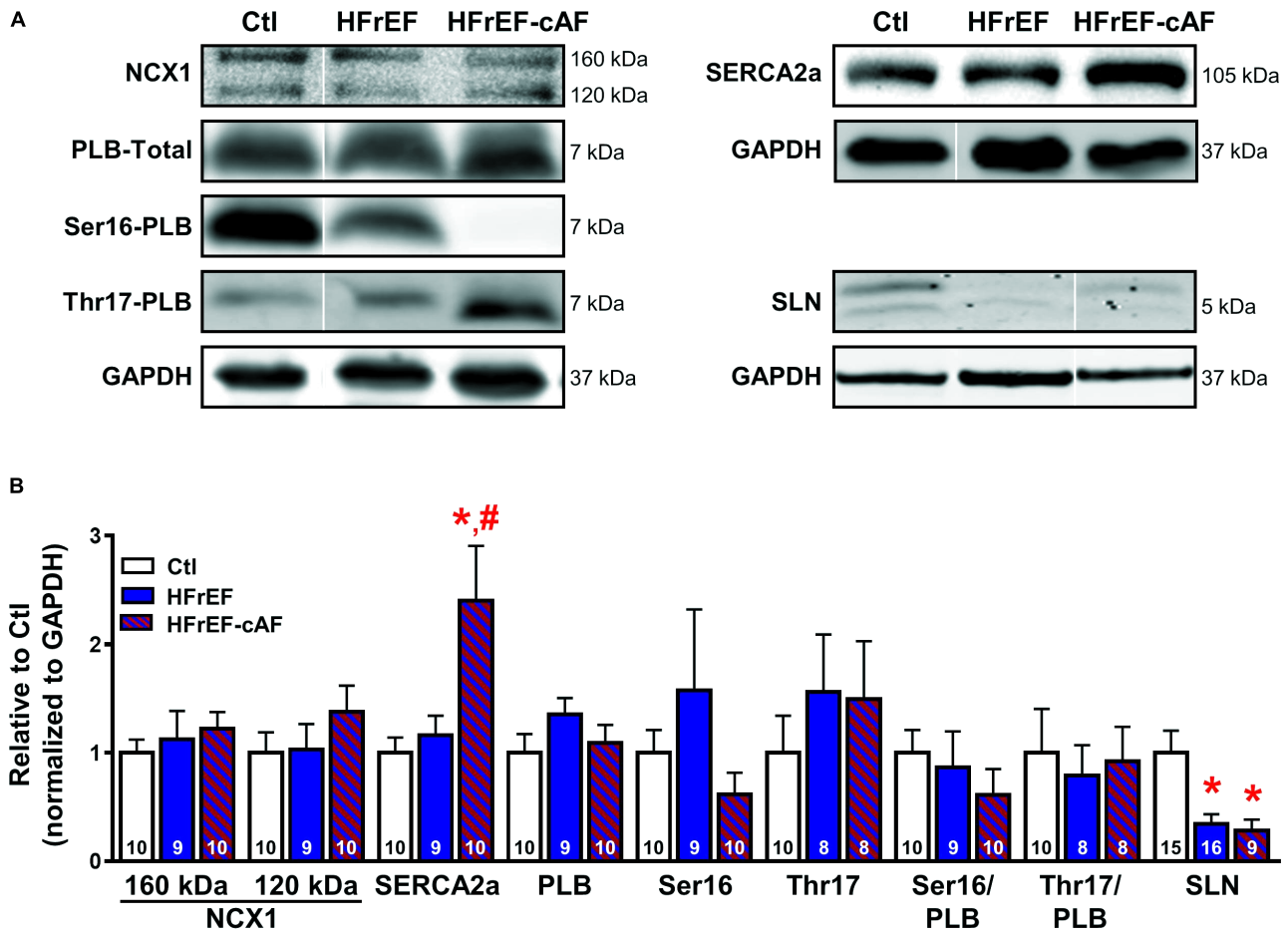

FIGURE 6 | Molecular determinants of increased sarcoplasmic reticulum (SR) Ca^{2+} load. **(A)** Representative Western blot examples of protein expression of Na^{+}-Ca^{2+}-exchanger type-1 (NCX1; full-length protein of 160 kDa with proteolytic fragment at 120 kDa), SR Ca^{2+}-ATPase type-2a (SERCA2a) and its inhibitory regulators phospholamban (PLB; total PLB as well as Ser16- and Thr17-phosphorylated PLB) and sarcolipin (SLN). GAPDH was used as loading control. Ser16-PLB of HFrEF-cAF represents an extreme example. **(B)** Quantification of NCX1, SERCA2a, total PLB, Ser16- and Thr17-phosphorylated PLB, Ser16/total PLB, Thr17/total PLB, and SLN in right-atrial tissue homogenates of Ctl (white bars), HFrEF (blue bars) or HFrEF-cAF (red/blue-striped bars). Numbers in bars indicate number of patients. * indicates $P < 0.05$ vs. Ctl, # indicates $P < 0.05$ vs. HFrEF.

effects, minimized the variability in individual ion currents and produced stable resting membrane potentials at physiological levels. Our results suggest that even if remodeling in some ion currents might exist in HFrEF patients, resting membrane potential and APD shape do not differ between Ctl and HFrEF patients. Clearly, validation of our multicellular findings in other patient cohorts is needed to confirm whether alterations in atrial APD occur with HFrEF.

Our current data indicate that also in the presence of HFrEF, AF produces typical atrial tachycardia-related remodeling, including reentry-promoting APD shortening. These data are consistent with results from Cha et al. who showed that atrial tachycardia shortened ERP in dogs with pacing-induced HF, albeit to a lesser degree than dogs with normal LV function (Cha et al., 2004). By contrast, in a pig model the combined presence of AF and HF resulted in prolonged APD (Lugenbiel et al., 2015). However, in this model AF was the primary initiator of a (mild) ventricular tachycardiomyopathy, which is different from patients in whom HF is mainly due to advanced cardiovascular disease, notably hypertension and myocardial infarction (Benjamin et al., 2018), as in our study. Overall, despite the fact that potential APD changes can occur with HFrEF, once AF develops it produces the APD shortening that typifies the electrophysiological profile in patients with cAF.

To the best of our knowledge, functional Ca^{2+}-handling remodeling has not been studied in atria of patients with HFrEF. Here we identified extensive indices of abnormal Ca^{2+}-handling in these patients, both in the absence and presence of AF, including greater incidence of spontaneous I_{NCX}, increased SR Ca^{2+} load, and RyR2 dysfunction. Protein levels of sarcolipin and RyR2 were decreased in HFrEF patients, but we did not find significant changes in SERCA2a or NCX1 expression, PLB expression or phosphorylation, or RyR2 phosphorylation in these patients. Our results are consistent with data from Shanmugam et al. (2011) who also identified decreased sarcolipin

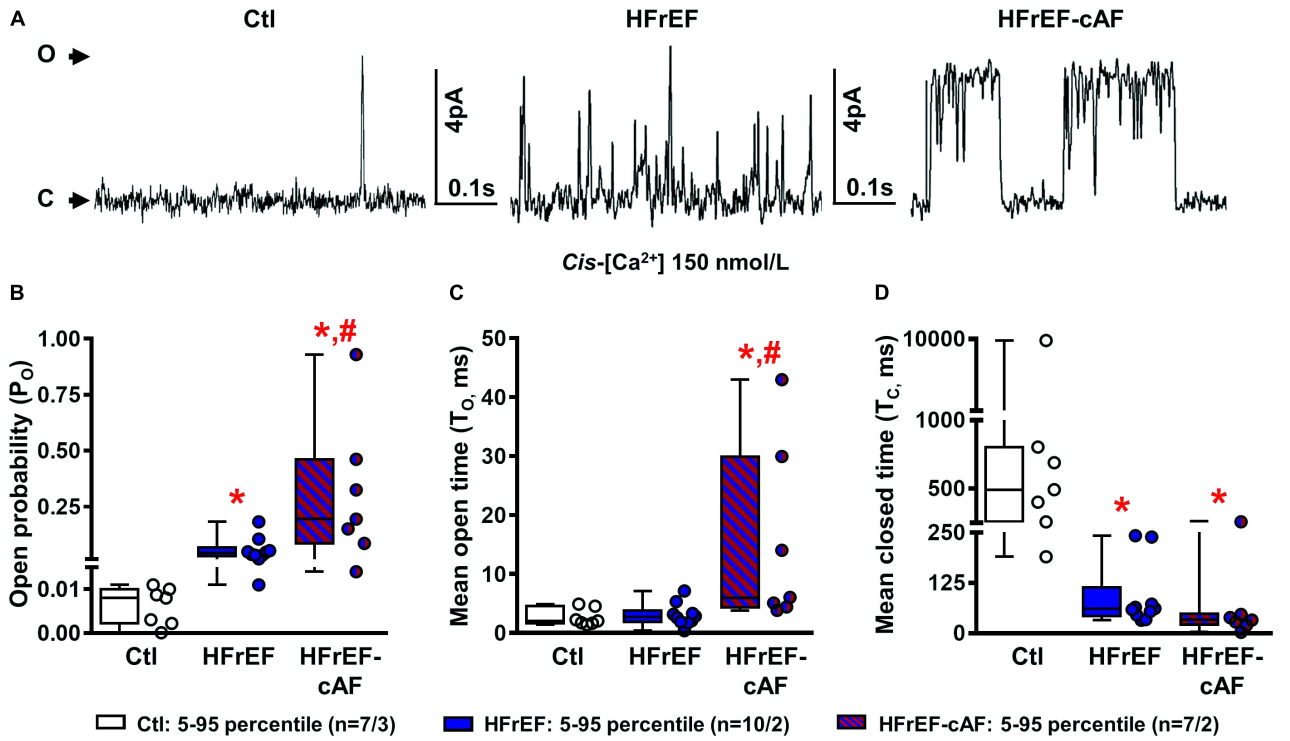

FIGURE 7 | Single-channel recordings of cardiac ryanodine receptor type-2 (RyR2) channels. **(A)** Representative RyR2 single-channel recording in a right-atrial sample from a Ctl, HFrEF or HFrEF-cAF patient. Upward deflections reflect channel opening. **(B–D)** Quantification of open probability **(B)**, mean open time **(C)**, and mean closed time **(D)** of single RyR2 channels from Ctl (white bars/symbols), HFrEF (blue bars/symbols) or HFrEF-cAF (red/blue-striped bars/symbols) patients. Numbers represent number of channels/number of patients. * indicates $P < 0.05$ vs. Ctl, # indicates $P < 0.05$ vs. HFrEF.

expression, unchanged SERCA2a expression and a tendency toward decreased RyR2 expression in atria from HF patients. The present results are also in line with data in atrial cardiomyocytes from rabbits with chronic myocardial infarction (Kettlewell et al., 2013), failing hearts from spontaneously hypertensive rats (Pluteanu et al., 2018), and a dog model of ventricular tachypacing-induced HF (Stambler et al., 2003; Yeh et al., 2008), all of which showed an increased incidence of spontaneous SR Ca^{2+}-release events. Moreover, HF dogs also had increased SR Ca^{2+} load, decreased RyR2 expression, unaltered RyR2 phosphorylation and unchanged expression of PLB or NCX1 (Yeh et al., 2008), similar to our data. In contrast to our findings, SERCA2a expression was decreased in this model and the significantly increased SR Ca^{2+} load was explained by an increase in PLB phosphorylation at Thr17 (Yeh et al., 2008). Finally, our data in HFrEF patients are similar to our previous findings in patients with paroxysmal AF (Voigt et al., 2014). Paroxysmal AF patients also exhibited increased SR Ca^{2+} load and spontaneous SR Ca^{2+}-release events, although the underlying molecular mechanisms appear somewhat distinct, involving increased RyR2 expression and decreased SERCA2a expression. Interestingly, despite a similar functional phenotype, there also appear to be mechanistic differences at the molecular level between HFrEF and HFrEF-cAF patients. For example, although protein levels of sarcolipin and RyR2 are decreased in both HFrEF and HFrEF-cAF patients, only the latter group have upregulated SERCA2a expression along with increased RyR2-Ser2814 phosphorylation, which sensitizes RyR2 to cytosolic Ca^{2+}. The higher RyR2-Ser2814 phosphorylation level is consistent with the significantly greater RyR2 single-channel open probability in HFrEF-cAF compared to Ctl or HFrEF patients, likely explaining why SR Ca^{2+} load is not increased in HFrEF-cAF. The increased SERCA2a expression might also help to maintain SR Ca^{2+} load despite the strong increase in RyR2 open probability, which is expected to increase SR Ca^{2+} leak and to decrease SR Ca^{2+} load. Finally, protein levels of junctin were higher in HFrEF, but not HFrEF-cAF patients and mice with cardiac restricted junctin overexpression develop spontaneous AF (Hong et al., 2002). Thus junctin-mediated RyR2 dysfunction might contribute to the development of AF in the context of HF.

Clinical Implications

Despite the important progress being made in our understanding, diagnosis and treatment of AF, it remains a major clinical problem (Heijman et al., 2018). Basic science has provided a lot of insights about the fundamental mechanisms underlying AF, identifying ectopic (triggered) activity promoted by Ca^{2+}-handling abnormalities and reentry promoted by APD shortening and slow, heterogeneous conduction as the major arrhythmia mechanisms (Heijman et al., 2014, 2016). Nonetheless, a number of important translational challenges remain (Heijman et al., 2018), including the

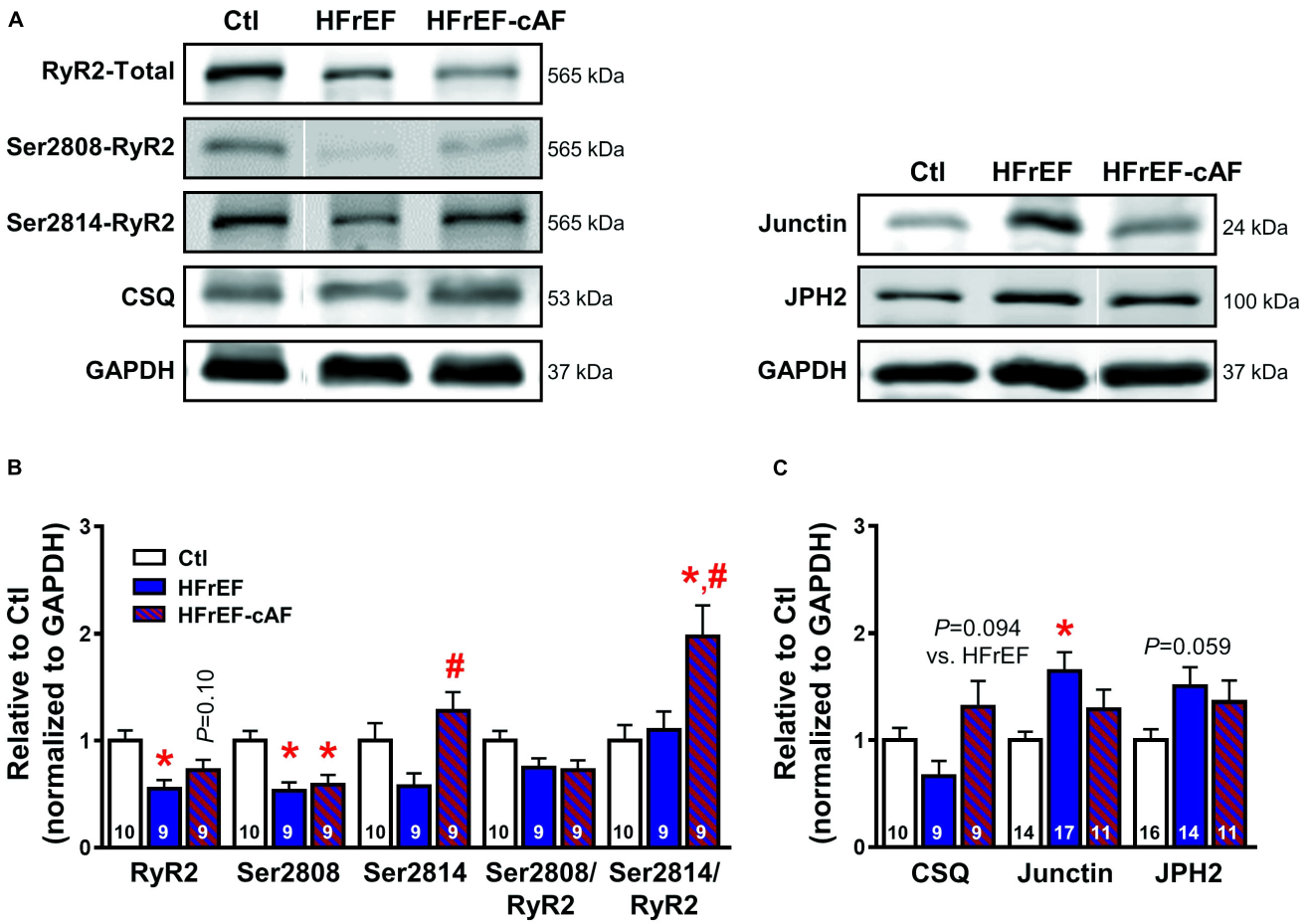

FIGURE 8 | Molecular determinants of ryanodine receptor type-2 (RyR2) dysfunction. **(A)** Representative Western blot examples of total RyR2, Ser2808-, and Ser2814-phosphorylated RyR2 and calsequestrin (CSQ; left), as well as junctin and junctophilin-2 (JPH2; right) protein expression levels. GAPDH was used as loading control. **(B)** Quantification of total RyR2, Ser2808-, and Ser2814-phosphorylated RyR2, Ser2808/total RyR2, and Ser2814/total RyR2 protein expression levels in Ctl (white bars), HFrEF (blue bars) and HFrEF-cAF (red/blue-striped bars) patients. **(C)** Protein expression levels of the RyR2-interacting proteins CSQ, junctin, and JPH2 in Ctl, HFrEF and HFrEF-cAF patients. Data are shown relative to Ctl. Numbers in bars indicate number of patients. * indicates $P < 0.05$ vs. Ctl, # indicates $P < 0.05$ vs. HFrEF.

identification of the dominant arrhythmia mechanisms in specific subgroups of AF patients to enable tailored therapy. There is increasing awareness that AF is a common endpoint of many different pathophysiological processes that promote an atrial cardiomyopathy (Andrade et al., 2014; Goette et al., 2017). However, the nature of the underlying atrial remodeling is likely distinct for different comorbidities, risk factors and stages of the disease. In agreement, we have previously shown that there are important differences in atrial remodeling between patients with paroxysmal AF and those with cAF (Voigt et al., 2012, 2014; Beavers et al., 2013). Atrial remodeling in patients with HFrEF or HFrEF-cAF has not previously been characterized in detail, particularly with respect to atrial Ca^{2+}-handling, despite the very common clinical coexistence of AF and HF (Ling et al., 2016; Sartipy et al., 2017).

Together with previous studies, our current data suggest that Ca^{2+}-handling abnormalities and Ca^{2+}-mediated triggered activity are a common motif shared by cAF patients and HF patients in sinus rhythm, who are at an increased risk of developing AF. Atrial arrhythmias have a focal initiation pattern in dogs with ventricular tachypacing-induced HF (Fenelon et al., 2003) and their inducibility is suppressed by Ca^{2+}-antagonists (Stambler et al., 2003), supporting a major role for Ca^{2+}-mediated ectopic activity in the initiation of AF in the setting of HF. In addition, there is evidence for a significant role of focal ectopy in AF patients (Haissaguerre et al., 1998; Lee et al., 2015).

Accumulating evidence suggests that Ca^{2+}-handling abnormalities may promote structural remodeling. For example, CREM-IbΔC-X transgenic mice develop progressive atrial remodeling and spontaneous AF, which is prevented by genetic inhibition of RyR2 dysfunction and associated SR Ca^{2+} leak (Li et al., 2014). Similarly, the PLB-R14del mutation produces Ca^{2+}-handling abnormalities and exhibits a clinical phenotype characterized initially by an increased risk of ventricular arrhythmias at young age, with a subsequent predisposition

to dilated cardiomyopathy and HF (van Rijsingen et al., 2014). Thus, abnormal Ca^{2+}-handling might be an early event in the pathogenesis of AF, apart from promotion of ectopic activity *per se*. In particular, the HFrEF-induced atrial Ca^{2+}-handling remodeling that we identified may serve both as an initiator of AF episodes and a promoter of atrial electrical and structural remodeling, creating a substrate for the maintenance and progression of AF. Thus, our present findings may have important clinical implications. They point to an urgent need for methods to assess potential cardiomyocyte Ca^{2+}-handling abnormalities in patients during the early stages of the remodeling process, when the disease is still amenable to therapy, and a need for better therapeutic options to treat these abnormalities based on our understanding of the underlying molecular mechanisms in specific patient subgroups (Heijman et al., 2018). Moreover, since atrial Ca^{2+}-handling remodeling in HFrEF patients is characterized by both RyR2 and SERCA2a dysfunction, a therapeutic intervention modulating only a single target may not be sufficient to normalize altered atrial Ca^{2+} handling. Indeed, we have previously shown in paroxysmal AF patients with a similar phenotype that RyR2 and SERCA2a dysfunction can each promote proarrhythmic spontaneous SR Ca^{2+}-release events and that the combination of both factors is significantly more proarrhythmic than each individually (Voigt et al., 2014). Technological advances such as catheter-based photoacoustic imaging with cell-permeable Ca^{2+} indicators (Roberts et al., 2018) may in the future enable *in vivo* imaging of Ca^{2+}-handling abnormalities in large animal models or patients (Heijman et al., 2018).

Potential Limitations

Although our data provide an extensive characterization of atrial remodeling in HFrEF and HFrEF-cAF patients, we did not address ion-channel remodeling in detail. Despite absence of AP changes in multicellular preparations, $I_{Ca,L}$ was reduced in HFrEF patients, in line with previous findings (Ouadid et al., 1995). Thus, alterations in K^+ channels may balance the reduction in $I_{Ca,L}$, resulting in unaltered AP properties, as previously observed in other studies (Koumi et al., 1994; Schreieck et al., 2000; Workman et al., 2009).

We did not measure Ca^{2+}-handling abnormalities directly using Ca^{2+} imaging with fluorescent indicators. Instead, we employed spontaneous I_{NCX} during voltage-clamp at -80 mV as an accepted marker of spontaneous SR-derived Ca^{2+} release and we characterized Ca^{2+}-handling remodeling through changes in RyR2 single-channel properties. Of note, the use of perforated-patch techniques with preserved physiological intracellular milieu, along with the absence of fluorescent Ca^{2+} indicators, which buffer intracellular Ca^{2+}, are expected to result in a more precise detection of the consequences of abnormal SR Ca^{2+} releases. Nevertheless, subsequent work employing Ca^{2+} imaging should further dissect the precise abnormalities of atrial Ca^{2+}-handling in the context of HFrEF with and without AF.

The present work is necessarily restricted to RA appendage tissue obtained from patients undergoing open-heart surgery. Our findings may not hold for other regions of the atria, which may be exposed to different levels of stretch or neurohumoral factors, and may not be applicable to HFrEF patients without an indication for open-heart surgery.

We have previously shown that there are important differences in Ca^{2+}-handling abnormalities between paroxysmal AF and cAF (Voigt et al., 2012, 2014). Similarly, there are notable differences in the epidemiology, pathophysiology and therapeutic management of HF patients with reduced, mid-range and preserved LV ejection fraction, although AF is common in all variants (Lam and Solomon, 2014; Sartipy et al., 2017). Our results were obtained in patients with significantly impaired LV function (mean LV ejection fractions ∼30%) with or without cAF. Although the clinical characteristics of the HFrEF population employed in this population make an ischemic etiology very likely, we were unable to establish the exact etiology of HF for individual patients. Results might be different for other types of AF and HF, which could produce distinct forms of atrial remodeling and show complex patterns in their interaction. Furthermore, there were some differences in clinical characteristics (e.g., regarding the indication for surgery) among the patient groups and the different data sets for the same subgroup (i.e., between **Tables 1–3**), which might influence our findings. Finally, our study is concerned with the potential molecular and cellular mechanisms of AF in HFrEF patients, but although we were able to include data from cAF without HFrEF in our functional analyses, we did not have samples from cAF patients without HFrEF to include in the Western-blot experiments. Furthermore, our work does not address the additional tissue-level properties, such as fibrosis and conduction velocity patterns or autonomic innervation, which play a key role in cardiac arrhythmogenesis in patients. For example, we did not observe significant differences in maximum dV/dt_{max} (reflecting Na^+-channel function) and conduction time, which also reflects connexin function, in multicellular preparations of HFrEF patients, despite reduced Cx43 protein levels and reports of reduced conduction velocity *in vivo* (Sanders et al., 2003), suggesting a role for regional differences and additional regulatory mechanisms of atrial conduction in the intact heart.

CONCLUSION

In this study, we provide the first detailed characterization of atrial remodeling in the setting of HFrEF with and without cAF. Spontaneous I_{NCX} currents, likely mediated by Ca^{2+}-handling abnormalities, are increased and might act as triggers of AF in HFrEF patients with profibrotic and connexin remodeling. AF subsequently produces atrial electrical remodeling that stabilizes the arrhythmia by promoting AF-maintaining reentry. These novel findings may have important implications for the development of new treatment options for AF in the context of HF.

AUTHOR CONTRIBUTIONS

CM and DD conceived the research. CM, IA-T, and QW performed the experiments. ER-D and MK provided reagents

and samples. CM, IA-T, QW, SN, UR, XW, JH, and DD analyzed the data. XW, LH-M, and DD handled funding and project management. JH, SN, and DD drafted and revised the manuscript. All authors approved the final version of the manuscript.

FUNDING

This work was supported by Marie Curie IEF Grant (PIEF-GA-2012-331241 to CM), the Netherlands Organization for Scientific Research (ZonMW Veni 91616057 to JH), the National Institutes of Health (R01-HL131517 and R01-HL136389 to DD; and R01-HL089598, R01-HL-091947, R01-HL117641, and R01-HL134824 to XW), the DZHK (German Center for Cardiovascular Research, 81X2800108, 81X2800161, and 81X2800136 to DD), Spanish Ministry for Science, Innovation and Universities (SAF2014-58286-C2-1-R and SAF2017-88019-C3-1-R to LH-M) and Marató TV3 foundation (2015-2-30 to LH-M) and the German Research Foundation (DFG, Do 769/4-1 to DD), and the Canadian Institutes of Health Research (1484011) and Heart and Stroke Foundation of Canada (16-12708) to SN.

ACKNOWLEDGMENTS

The authors thank Ramona Nagel and Konstanze Fischer for excellent technical assistance.

REFERENCES

Akkaya, M., Higuchi, K., Koopmann, M., Damal, K., Burgon, N. S., Kholmovski, E., et al. (2013). Higher degree of left atrial structural remodeling in patients with atrial fibrillation and left ventricular systolic dysfunction. *J. Cardiovasc. Electrophysiol.* 24, 485–491. doi: 10.1111/jce.12090

Andrade, J., Khairy, P., Dobrev, D., and Nattel, S. (2014). The clinical profile and pathophysiology of atrial fibrillation: relationships among clinical features, epidemiology, and mechanisms. *Circ. Res.* 114, 1453–1468. doi: 10.1161/CIRCRESAHA.114.303211

Beavers, D. L., Wang, W., Ather, S., Voigt, N., Garbino, A., Dixit, S. S., et al. (2013). Mutation E169K in junctophilin-2 causes atrial fibrillation due to impaired RyR2 stabilization. *J. Am. Coll. Cardiol.* 62, 2010–2019. doi: 10.1016/j.jacc.2013.06.052

Benjamin, E. J., Virani, S. S., Callaway, C. W., Chamberlain, A. M., Chang, A. R., Cheng, S., et al. (2018). Heart disease and stroke statistics-2018 update: a report from the American heart association. *Circulation* 137, e67–e492. doi: 10.1161/CIR.0000000000000558

Brundel, B. J., Henning, R. H., Kampinga, H. H., Van Gelder, I. C., and Crijns, H. J. (2002). Molecular mechanisms of remodeling in human atrial fibrillation. *Cardiovasc. Res.* 54, 315–324.

Cao, H., Xue, L., Wu, Y., Ma, H., Chen, L., Wang, X., et al. (2010). Natriuretic peptides and right atrial fibrosis in patients with paroxysmal versus persistent atrial fibrillation. *Peptides* 31, 1531–1539. doi: 10.1016/j.peptides.2010.04.019

Cardin, S., Li, D., Thorin-Trescases, N., Leung, T. K., Thorin, E., and Nattel, S. (2003). Evolution of the atrial fibrillation substrate in experimental congestive heart failure: angiotensin-dependent and -independent pathways. *Cardiovasc. Res.* 60, 315–325.

Cha, T. J., Ehrlich, J. R., Zhang, L., and Nattel, S. (2004). Atrial ionic remodeling induced by atrial tachycardia in the presence of congestive heart failure. *Circulation* 110, 1520–1526. doi: 10.1161/01.CIR.0000142052.03565.87

Cone, A. C., Cavin, G., Ambrosi, C., Hakozaki, H., Wu-Zhang, A. X., Kunkel, M. T., et al. (2014). Protein kinase Cδ-mediated phosphorylation of Connexin43 gap junction channels causes movement within gap junctions followed by vesicle internalization and protein degradation. *J. Biol. Chem.* 289, 8781–8798. doi: 10.1074/jbc.M113.533265

Dobrev, D., Graf, E., Wettwer, E., Himmel, H. M., Hala, O., Doerfel, C., et al. (2001). Molecular basis of downregulation of G-protein-coupled inward rectifying K^+ current ($I_{K,ACh}$) in chronic human atrial fibrillation: decrease in GIRK4 mRNA correlates with reduced $I_{K,ACh}$ and muscarinic receptor–mediated shortening of action potentials. *Circulation* 104, 2551–2557.

El-Armouche, A., Boknik, P., Eschenhagen, T., Carrier, L., Knaut, M., Ravens, U., et al. (2006). Molecular determinants of altered Ca^{2+} handling in human chronic atrial fibrillation. *Circulation* 114, 670–680. doi: 10.1161/CIRCULATIONAHA.106.636845

Fedorov, V. V., Glukhov, A. V., Ambrosi, C. M., Kostecki, G., Chang, R., Janks, D., et al. (2011). Effects of KATP channel openers diazoxide and pinacidil in coronary-perfused atria and ventricles from failing and non-failing human hearts. *J. Mol. Cell Cardiol.* 51, 215–225. doi: 10.1016/j.yjmcc.2011.04.016

Fenelon, G., Shepard, R. K., and Stambler, B. S. (2003). Focal origin of atrial tachycardia in dogs with rapid ventricular pacing-induced heart failure. *J. Cardiovasc. Electrophysiol.* 14, 1093–1102.

Goette, A., Kalman, J. M., Aguinaga, L., Akar, J., Cabrera, J. A., Chen, S. A., et al. (2017). EHRA/HRS/APHRS/SOLAECE expert consensus on atrial cardiomyopathies: Definition, characterization, and clinical implication. *Heart Rhythm* 14, e3–e40. doi: 10.1016/j.hrthm.2016.05.028

Haissaguerre, M., Jais, P., Shah, D. C., Takahashi, A., Hocini, M., Quiniou, G., et al. (1998). Spontaneous initiation of atrial fibrillation by ectopic beats originating in the pulmonary veins. *N. Engl. J. Med.* 339, 659–666. doi: 10.1056/NEJM199809033391003

Heijman, J., Algalarrondo, V., Voigt, N., Melka, J., Wehrens, X. H., Dobrev, D., et al. (2016). The value of basic research insights into atrial fibrillation mechanisms as a guide to therapeutic innovation: a critical analysis. *Cardiovasc. Res.* 109, 467–479. doi: 10.1093/cvr/cvv275

Heijman, J., Guichard, J. B., Dobrev, D., and Nattel, S. (2018). Translational challenges in atrial fibrillation. *Circ. Res.* 122, 752–773. doi: 10.1161/CIRCRESAHA.117.311081

Heijman, J., Voigt, N., Abu-Taha, I. H., and Dobrev, D. (2013). Rhythm control of atrial fibrillation in heart failure. *Heart Fail. Clin.* 9, 407–415. doi: 10.1016/j.hfc.2013.06.001

Heijman, J., Voigt, N., Nattel, S., and Dobrev, D. (2014). Cellular and molecular electrophysiology of atrial fibrillation initiation, maintenance, and progression. *Circ. Res.* 114, 1483–1499. doi: 10.1161/CIRCRESAHA.114.302226

Hohendanner, F., Messroghli, D., Bode, D., Blaschke, F., Parwani, A., Boldt, L. H., et al. (2018). Atrial remodelling in heart failure: recent developments and relevance for heart failure with preserved ejection fraction. *ESC Heart Fail.* 5, 211–221. doi: 10.1002/ehf2.12260

Hong, C. S., Cho, M. C., Kwak, Y. G., Song, C. H., Lee, Y. H., Lim, J. S., et al. (2002). Cardiac remodeling and atrial fibrillation in transgenic mice overexpressing junction. *FASEB J.* 16, 1310–1312. doi: 10.1096/fj.01-0908fje

Hove-Madsen, L., Llach, A., Bayes-Genis, A., Roura, S., Rodriguez Font, E., Aris, A., et al. (2004). Atrial fibrillation is associated with increased spontaneous calcium release from the sarcoplasmic reticulum in human atrial myocytes. *Circulation* 110, 1358–1363. doi: 10.1161/01.CIR.0000141296.59876.87

Jalife, J., and Kaur, K. (2015). Atrial remodeling, fibrosis, and atrial fibrillation. *Trends Cardiovasc. Med.* 25, 475–484. doi: 10.1016/j.tcm.2014.12.015

Kettlewell, S., Burton, F. L., Smith, G. L., and Workman, A. J. (2013). Chronic myocardial infarction promotes atrial action potential alternans, afterdepolarizations, and fibrillation. *Cardiovasc. Res.* 99, 215–224. doi: 10.1093/cvr/cvt087

Koumi, S., Arentzen, C. E., Backer, C. L., and Wasserstrom, J. A. (1994). Alterations in muscarinic K^+ channel response to acetylcholine and to G protein-mediated activation in atrial myocytes isolated from failing human hearts. *Circulation* 90, 2213–2224.

Lam, C. S., and Solomon, S. D. (2014). The middle child in heart failure: heart failure with mid-range ejection fraction (40-50%). *Eur. J. Heart Fail.* 16, 1049–1055. doi: 10.1002/ejhf.159

Landstrom, A. P., Dobrev, D., and Wehrens, X. H. T. (2017). Calcium signaling and cardiac arrhythmias. *Circ. Res.* 120, 1969–1993. doi: 10.1161/CIRCRESAHA.117.310083

Lee, S., Sahadevan, J., Khrestian, C. M., Cakulev, I., Markowitz, A., and Waldo, A. L. (2015). Simultaneous biatrial high-density (510-512 electrodes) epicardial mapping of persistent and long-standing persistent atrial fibrillation in patients: new insights into the mechanism of its maintenance. *Circulation* 132, 2108–2117. doi: 10.1161/CIRCULATIONAHA.115.017007

Li, D., Fareh, S., Leung, T. K., and Nattel, S. (1999). Promotion of atrial fibrillation by heart failure in dogs: atrial remodeling of a different sort. *Circulation* 100, 87–95.

Li, D., Melnyk, P., Feng, J., Wang, Z., Petrecca, K., Shrier, A., et al. (2000). Effects of experimental heart failure on atrial cellular and ionic electrophysiology. *Circulation* 101, 2631–2638.

Li, N., Chiang, D. Y., Wang, S., Wang, Q., Sun, L., Voigt, N., et al. (2014). Ryanodine receptor-mediated calcium leak drives progressive development of an atrial fibrillation substrate in a transgenic mouse model. *Circulation* 129, 1276–1285. doi: 10.1161/CIRCULATIONAHA.113.006611

Ling, L. H., Kistler, P. M., Kalman, J. M., Schilling, R. J., and Hunter, R. J. (2016). Comorbidity of atrial fibrillation and heart failure. *Nat. Rev. Cardiol.* 13, 131–147. doi: 10.1038/nrcardio.2015.191

Llach, A., Molina, C. E., Prat-Vidal, C., Fernandes, J., Casado, V., Ciruela, F., et al. (2011). Abnormal calcium handling in atrial fibrillation is linked to up-regulation of adenosine A2A receptors. *Eur. Heart J.* 32, 721–729. doi: 10.1093/eurheartj/ehq464

Loose, S., Mueller, J., Wettwer, E., Knaut, M., Ford, J., Milnes, J., et al. (2014). Effects of I_{Kur} blocker MK-0448 on human right atrial action potentials from patients in sinus rhythm and in permanent atrial fibrillation. *Front. Pharmacol.* 5:26. doi: 10.3389/fphar.2014.00026

Lugenbiel, P., Wenz, F., Govorov, K., Schweizer, P. A., Katus, H. A., and Thomas, D. (2015). Atrial fibrillation complicated by heart failure induces distinct remodeling of calcium cycling proteins. *PLoS One* 10:e0116395. doi: 10.1371/journal.pone.0116395

Marrouche, N. F., Brachmann, J., Andresen, D., Siebels, J., Boersma, L., Jordaens, L., et al. (2018). Catheter ablation for atrial fibrillation with heart failure. *N. Engl. J. Med.* 378, 417–427. doi: 10.1056/NEJMoa1707855

Milliez, P., Deangelis, N., Rucker-Martin, C., Leenhardt, A., Vicaut, E., Robidel, E., et al. (2005). Spironolactone reduces fibrosis of dilated atria during heart failure in rats with myocardial infarction. *Eur. Heart J.* 26, 2193–2199. doi: 10.1093/eurheartj/ehi478

Mogensen, U. M., Jhund, P. S., Abraham, W. T., Desai, A. S., Dickstein, K., Packer, M., et al. (2017). Type of atrial fibrillation and outcomes in patients with heart failure and reduced ejection fraction. *J. Am. Coll. Cardiol.* 70, 2490–2500. doi: 10.1016/j.jacc.2017.09.027

Molina, C. E., Leroy, J., Richter, W., Xie, M., Scheitrum, C., Lee, I. O., et al. (2012). Cyclic adenosine monophosphate phosphodiesterase type 4 protects against atrial arrhythmias. *J. Am. Coll. Cardiol.* 59, 2182–2190. doi: 10.1016/j.jacc.2012.01.060

Ouadid, H., Albat, B., and Nargeot, J. (1995). Calcium currents in diseased human cardiac cells. *J. Cardiovasc. Pharmacol.* 25, 282–291.

Pandit, S. V., and Workman, A. J. (2016). Atrial electrophysiological remodeling and fibrillation in heart failure. *Clin. Med. Insights Cardiol.* 10(Suppl 1), 41–46. doi: 10.4137/CMC.S39713

Pluteanu, F., Nikonova, Y., Holzapfel, A., Herzog, B., Scherer, A., Preisenberger, J., et al. (2018). Progressive impairment of atrial myocyte function during left ventricular hypertrophy and heart failure. *J. Mol. Cell Cardiol.* 114, 253–263. doi: 10.1016/j.yjmcc.2017.11.020

Polyakova, V., Miyagawa, S., Szalay, Z., Risteli, J., and Kostin, S. (2008). Atrial extracellular matrix remodelling in patients with atrial fibrillation. *J. Cell Mol. Med.* 12, 189–208. doi: 10.1111/j.1582-4934.2008.00219.x

Roberts, S., Seeger, M., Jiang, Y., Mishra, A., Sigmund, F., Stelzl, A., et al. (2018). Calcium sensor for photoacoustic imaging. *J. Am. Chem. Soc.* 140, 2718–2721. doi: 10.1021/jacs.7b03064

Sanders, P., Morton, J. B., Davidson, N. C., Spence, S. J., Vohra, J. K., Sparks, P. B., et al. (2003). Electrical remodeling of the atria in congestive heart failure: electrophysiological and electroanatomic mapping in humans. *Circulation* 108, 1461–1468. doi: 10.1161/01.CIR.0000090688.49283.67

Sartipy, U., Dahlstrom, U., Fu, M., and Lund, L. H. (2017). Atrial fibrillation in heart failure with preserved, mid-range, and reduced ejection fraction. *JACC Heart Fail.* 5, 565–574. doi: 10.1016/j.jchf.2017.05.001

Schmidt, C., Wiedmann, F., Voigt, N., Zhou, X. B., Heijman, J., Lang, S., et al. (2015). Upregulation of $K_{2P}3.1$ K^+ current causes action potential shortening in patients with chronic atrial fibrillation. *Circulation* 132, 82–92. doi: 10.1161/CIRCULATIONAHA.114.012657

Schmidt, C., Wiedmann, F., Zhou, X. B., Heijman, J., Voigt, N., Ratte, A., et al. (2017). Inverse remodelling of $K_{2P}3.1$ K^+ channel expression and action potential duration in left ventricular dysfunction and atrial fibrillation: implications for patient-specific antiarrhythmic drug therapy. *Eur. Heart J.* 38, 1764–1774. doi: 10.1093/eurheartj/ehw559

Schotten, U., Verheule, S., Kirchhof, P., and Goette, A. (2011). Pathophysiological mechanisms of atrial fibrillation: a translational appraisal. *Physiol. Rev.* 91, 265–325. doi: 10.1152/physrev.00031.2009

Schreieck, J., Wang, Y., Overbeck, M., Schomig, A., and Schmitt, C. (2000). Altered transient outward current in human atrial myocytes of patients with reduced left ventricular function. *J. Cardiovasc. Electrophysiol.* 11, 180–192.

Shanmugam, M., Molina, C. E., Gao, S., Severac-Bastide, R., Fischmeister, R., and Babu, G. J. (2011). Decreased sarcolipin protein expression and enhanced sarco(endo)plasmic reticulum Ca^{2+} uptake in human atrial fibrillation. *Biochem. Biophys. Res. Commun.* 410, 97–101. doi: 10.1016/j.bbrc.2011.05.113

Sikkel, M. B., Francis, D. P., Howard, J., Gordon, F., Rowlands, C., Peters, N. S., et al. (2017). Hierarchical statistical techniques are necessary to draw reliable conclusions from analysis of isolated cardiomyocyte studies. *Cardiovasc. Res.* 113, 1743–1752. doi: 10.1093/cvr/cvx151

Simon, J. N., Ziberna, K., and Casadei, B. (2016). Compromised redox homeostasis, altered nitroso-redox balance, and therapeutic possibilities in atrial fibrillation. *Cardiovasc. Res.* 109, 510–518. doi: 10.1093/cvr/cvw012

Sridhar, A., Nishijima, Y., Terentyev, D., Khan, M., Terentyeva, R., Hamlin, R. L., et al. (2009). Chronic heart failure and the substrate for atrial fibrillation. *Cardiovasc. Res.* 84, 227–236. doi: 10.1093/cvr/cvp216

Stambler, B. S., Fenelon, G., Shepard, R. K., Clemo, H. F., and Guiraudon, C. M. (2003). Characterization of sustained atrial tachycardia in dogs with rapid ventricular pacing-induced heart failure. *J. Cardiovasc. Electrophysiol.* 14, 499–507.

van Rijsingen, I. A., Van Der Zwaag, P. A., Groeneweg, J. A., Nannenberg, E. A., Jongbloed, J. D., Zwinderman, A. H., et al. (2014). Outcome in phospholamban R14del carriers: results of a large multicentre cohort study. *Circ. Cardiovasc. Genet.* 7, 455–465. doi: 10.1161/CIRCGENETICS.113.000374

Van Wagoner, D. R., Pond, A. L., Mccarthy, P. M., Trimmer, J. S., and Nerbonne, J. M. (1997). Outward K^+ current densities and Kv1.5 expression are reduced in chronic human atrial fibrillation. *Circ. Res.* 80, 772–781.

Voigt, N., Heijman, J., Wang, Q., Chiang, D. Y., Li, N., Karck, M., et al. (2014). Cellular and molecular mechanisms of atrial arrhythmogenesis in patients with paroxysmal atrial fibrillation. *Circulation* 129, 145–156. doi: 10.1161/CIRCULATIONAHA.113.006641

Voigt, N., Li, N., Wang, Q., Wang, W., Trafford, A. W., Abu-Taha, I., et al. (2012). Enhanced sarcoplasmic reticulum Ca^{2+} leak and increased Na^+-Ca^{2+} exchanger function underlie delayed afterdepolarizations in patients with chronic atrial fibrillation. *Circulation* 125, 2059–2070. doi: 10.1161/CIRCULATIONAHA.111.067306

Voigt, N., Pearman, C. M., Dobrev, D., and Dibb, K. M. (2015). Methods for isolating atrial cells from large mammals and humans. *J. Mol. Cell Cardiol.* 86, 187–198. doi: 10.1016/j.yjmcc.2015.07.006

Wang, T. J., Larson, M. G., Levy, D., Vasan, R. S., Leip, E. P., Wolf, P. A., et al. (2003). Temporal relations of atrial fibrillation and congestive heart failure and their joint influence on mortality: the framingham heart study. *Circulation* 107, 2920–2925. doi: 10.1161/01.CIR.0000072767.89944.6E

Wehrens, X. H., Lehnart, S. E., Huang, F., Vest, J. A., Reiken, S. R., Mohler, P. J., et al. (2003). FKBP12.6 deficiency and defective calcium release channel (ryanodine receptor) function linked to exercise-induced sudden cardiac death. *Cell* 113, 829–840.

Wettwer, E., Hala, O., Christ, T., Heubach, J. F., Dobrev, D., Knaut, M., et al. (2004). Role of I_{Kur} in controlling action potential shape and contractility in the human atrium: influence of chronic atrial fibrillation. *Circulation* 110, 2299–2306. doi: 10.1161/01.CIR.0000145155.60288.71

Workman, A. J., Pau, D., Redpath, C. J., Marshall, G. E., Russell, J. A., Norrie, J., et al. (2009). Atrial cellular electrophysiological changes in patients with ventricular dysfunction may predispose to AF. *Heart Rhythm* 6, 445–451. doi: 10.1016/j.hrthm.2008.12.028

Xu, J., Cui, G., Esmailian, F., Plunkett, M., Marelli, D., Ardehali, A., et al. (2004). Atrial extracellular matrix remodeling and the maintenance of atrial fibrillation. *Circulation* 109, 363–368. doi: 10.1161/01.CIR.0000109495.02213.52

Yamada, S., Lo, L. W., Chou, Y. H., Lin, W. L., Chang, S. L., Lin, Y. J., et al. (2017). Renal denervation regulates the atrial arrhythmogenic substrates through reverse structural remodeling in heart failure rabbit model. *Int. J. Cardiol.* 235, 105–113. doi: 10.1016/j.ijcard.2017.02.085

Yeh, Y. H., Wakili, R., Qi, X. Y., Chartier, D., Boknik, P., Kaab, S., et al. (2008). Calcium-handling abnormalities underlying atrial arrhythmogenesis and contractile dysfunction in dogs with congestive heart failure. *Circ. Arrhythm. Electrophysiol.* 1, 93–102. doi: 10.1161/CIRCEP.107.754788

Conflict of Interest Statement: XW is a founding partner of Elex Biotech, a start-up company that developed drug molecules that target ryanodine receptors for the treatment of cardiac arrhythmia disorders. DD is a member of the scientific advisory board of OMEICOS Therapeutics GmbH, a company developing small molecules mimicking the effects of omega-3 fatty acids, and of Acesion Pharma, a company developing selective blockers of small-conductance calcium dependent potassium channels.

The remaining authors declare that the research was conducted in the absence of any commercial or financial relationships that could be construed as a potential conflict of interest.

frontiers in Physiology

PERSPECTIVE
published: 25 October 2018
doi: 10.3389/fphys.2018.01474

Interplay Between Sub-Cellular Alterations of Calcium Release and T-Tubular Defects in Cardiac Diseases

Marina Scardigli[1,2], Cecilia Ferrantini[2,3], Claudia Crocini[4], Francesco S. Pavone[1,2,5] and Leonardo Sacconi[1,2]**

[1] National Institute of Optics, National Research Council, Florence, Italy, [2] European Laboratory for Non-Linear Spectroscopy, Florence, Italy, [3] Division of Physiology, Department of Experimental and Clinical Medicine, University of Florence, Florence, Italy, [4] Department of Molecular, Cellular, and Developmental Biology & BioFrontiers Institute, University of Colorado Boulder, Boulder, CO, United States, [5] Department of Physics and Astronomy, University of Florence, Florence, Italy

Asynchronous Ca^{2+} release promotes non-homogeneous myofilament activation, leading to mechanical dysfunction, as well as initiation of propagated calcium waves and arrhythmias. Recent advances in microscopy techniques have allowed for optical recordings of local Ca^{2+} fluxes and action potentials from multiple sub-cellular domains within cardiac cells with unprecedented spatial and temporal resolution. Since then, sub-cellular local information of the spatio-temporal relationship between Ca^{2+} release and action potential propagation have been unlocked, providing novel mechanistic insights in cardiac excitation-contraction coupling (ECC). Here, we review the promising perspectives arouse from repeatedly probing Ca^{2+} release at the same sub-cellular location while simultaneously probing multiple locations at the same time within a single cardiac cell. We also compare the results obtained in three different rodent models of cardiac diseases, highlighting disease-specific mechanisms. Slower local Ca^{2+} release has been observed in regions with defective action potential conduction in diseased cardiac cells. Moreover, significant increment of Ca^{2+} variability (both in time and in space) has been found in diseased cardiac cells but does not directly correlate with local electrical defects nor with the degree of structural aberrations of the cellular membrane system, suggesting a role for other players of the ECC machinery. We finally explore exciting opportunities provided by the technology for studying different cardiomyocyte populations, as well as for dissecting the mechanisms responsible for subcellular spatio-temporal variability of Ca^{2+} release.

Keywords: t-tubule, excitation-contraction coupling, calcium imaging, voltage imaging, microscopy

OPEN ACCESS

Edited by:
Alessandro Mugelli,
Università degli Studi di Firenze, Italy

Reviewed by:
Peter Kohl,
Imperial College London,
United Kingdom
Gudrun Antoons,
Maastricht University, Netherlands

***Correspondence:**
Claudia Crocini
claudia.crocini@colorado.edu
Leonardo Sacconi
sacconi@lens.unifi.it

Specialty section:
This article was submitted to Cardiac Electrophysiology, a section of the journal Frontiers in Physiology

Received: *10 July 2018*
Accepted: *28 September 2018*
Published: *25 October 2018*

Citation:
Scardigli M, Ferrantini C, Crocini C, Pavone FS and Sacconi L (2018) Interplay Between Sub-Cellular Alterations of Calcium Release and T-Tubular Defects in Cardiac Diseases. Front. Physiol. 9:1474. doi: 10.3389/fphys.2018.01474

INTRODUCTION

In cardiac cell, Ca^{2+} release mediates the transduction of an action potential (AP) generated at the cellular membrane (sarcolemma) into contraction of the sarcomeres, in a process called excitation-contraction coupling (ECC) (Bers, 2002). During the AP, Dihydropyridine receptors (DHPR) located on the sarcolemma open, generating an inward Ca^{2+} current (I_{caL}), which in turns activate a massive release of Ca^{2+} from the sarcoplasmic reticulum (SR) through ryanodine receptor (RyR)

2 (Kushnir and Marks, 2010). This mechanism is called calcium induced calcium release (CICR) and occurs in the dyads, where RyRs are clustered in release units on the SR juxtaposing DHPRs on the sarcolemma (Scriven et al., 2013). When a DHPR opens, local $[Ca^{2+}]_i$ rises up to 10–20 μM in less than 1 ms in the junctional cleft and triggers approximately 6–20 RyRs to release at each couplon (Bers, 2001). This increases $[Ca^{2+}]_i$ in the cleft to 200–400 μM. Ca^{2+} diffuses in the cell as the spatial and temporal summation of each local Ca^{2+} release unit (CRU) (Wier and Balke, 1999) and activates myofilaments that are the end effector of ECC (Bers, 2002). During systole, the strength of twitch depends on SR Ca^{2+} release, which in turn depends on SR Ca^{2+} content and the extent of the Ca^{2+} trigger (Bassani et al., 1995; Hobai and O'Rourke, 2001). After each contraction, $[Ca^{2+}]_i$ must decrease, so that cardiac cycle is enabled again. There are two main mechanisms to reduce $[Ca^{2+}]_i$: SR Ca^{2+}-ATPase (SERCA) and sarcolemmal Na^+/ Ca^{2+} exchanger (NCX). The first pumps Ca^{2+} back into the SR consuming ATP, the latter extrudes the cation in the extracellular space, exploiting the electrochemical gradient of Na^+, with a stoichiometry of 3Na:1Ca (Eisner et al., 1998). This balance between *trans*-sarcolemmal and SR Ca^{2+} influx and efflux is very highly maintained and it is essential for homogeneous myofilaments contraction and relaxation. The two main features of cardiac diseases, such as contractile dysfunction and arrhythmias, are correlated with ECC abnormalities (Ter Keurs and Boyden, 2007). To ensure a homogenous contraction of the entire cardiomyocyte, the AP is rapidly propagated toward the cell core thanks to a complex network of sarcolemmal invaginations named transverse-axial tubular system (TATS) or t-tubules. In control ventricular myocytes containing t-tubules, SR Ca^{2+} release is spatially and temporally synchronized (Cheng et al., 1994; Haddock et al., 1999; Brette et al., 2002, 2004, 2005; Yang et al., 2002).

Ca^{2+} transient desynchronization can be experimentally reproduced in myocytes acutely detubulated through osmotic shock (Brette et al., 2002; Yang et al., 2002) or in cultured myocytes (Louch et al., 2004), mimicking pathological conditions in which t-tubules are disrupted (Kostin et al., 1998; He et al., 2001; Louch et al., 2006; Song et al., 2006; Heinzel et al., 2008; Dibb et al., 2009; Sacconi et al., 2012; Crocini et al., 2016c). The loss of TATS determines a Ca^{2+}release initially triggered at sites where t-tubules are present, followed by propagation into regions without TATS, where RyR2 are orphan of their corresponding Ca^{2+} channels (Heinzel et al., 2002).

A common trait of ECC abnormalities consists in the loss of the perfect synchrony between membrane voltage and Ca^{2+} fluxes (Gomez et al., 1997). The interaction between RyR2 and Ca^{2+} channels is finely regulated (Ibrahim et al., 2011) as any spatio-temporal alteration may generate "waves" or "foci" leading to abrupt arrhythmias or, if persisting, to ineffective ECC and severe failure. However, electrical properties of TATS are often studied using indirect or macroscopic observations rather than on direct measurements.

In the last few years, the combination of advanced optical microscopy with novel functional reporters opened the possibility to better understand the role of TATS in both healthy and disease, by unveiling functional features with an unprecedented spatio-temporal resolution. In this regard, our group has recently developed an ultrafast random access two-photon microscope (Sacconi et al., 2012). Combining this technology with novel fluorinated voltage sensitive dyes with improved photostability (Yan et al., 2012) and calcium probes, we have simultaneously measured action potentials (APs) and intracellular calcium release at multiple sites within the TATS with sub-millisecond temporal and sub-micrometer spatial resolution. In the present work, we will review the capability of this method in providing important insights on sub-cellular alterations of calcium release and in dissecting their relationship with TATS morpho-functional defects found in different cardiac diseases.

SUB-CELLULAR RECORDINGS OF CALCIUM RELEASE AND ACTION POTENTIALS

In the last few decades, several techniques have been developed in order to get functional information of the TATS in isolated cardiomyocytes. In particular, optical methodologies have met the need to reduce invasiveness of traditional methods and have undergone a wide evolution. The major limiting factor to optically record fast physiological events, like AP and Ca^{2+} release in multiple site of the same cardiomyocyte, has been the scanning time that restricts recordings to only a single position of the cell at the time, i.e., line scanning approach. A strategy to overcome this limitation could consist in spending more time just to collect as many photons as possible from selected positions. We have recently implemented a new technique based on Random Access Multiphoton (RAMP) (Iyer et al., 2006) microscopy to record AP propagation and Ca^{2+} release at different domains of the same cardiomyocyte in a simultaneous fashion (Sacconi et al., 2012; Crocini et al., 2014a,b,2016c). In detail, the RAMP microscope is a two-photon microscope provided with an ultrafast scanning head made of two orthogonal acousto-optic deflectors (AODs) that diffract a laser beam at a precise angle, which can be changed within a few microseconds. Based on the velocity of sound propagation in the crystal present in the AODs and the dimension of the laser beam, a commutation time of about 4 μs can be estimated between a scanning line and the next in multiplexed modality. In order to get information about the two main actors of ECC, isolated cardiomyocytes from rodents were stained with FluoForte GFP-certified, a fluorescent Ca^{2+} indicator, and di-4-AN(F)EPPTEA, a fluorinated voltage-sensitive dye (VSD) (Yan et al., 2012): the RAMP microscope was used to simultaneously excite both dyes and, thanks to the large Stokes shift of the fluorinated VSD, the two fluorescence signals were easily distinguished using appropriate optical tools. **Figures 1A,B** illustrates the real-time simultaneous optical recording of AP and Ca^{2+} transients in isolated cardiomyocytes at different non-contiguous domains. Isolated cardiac cells were field stimulated at room temperature (Sacconi et al., 2012; Crocini et al., 2014b) to reach steady state. Then, we performed real-time simultaneous optical recordings

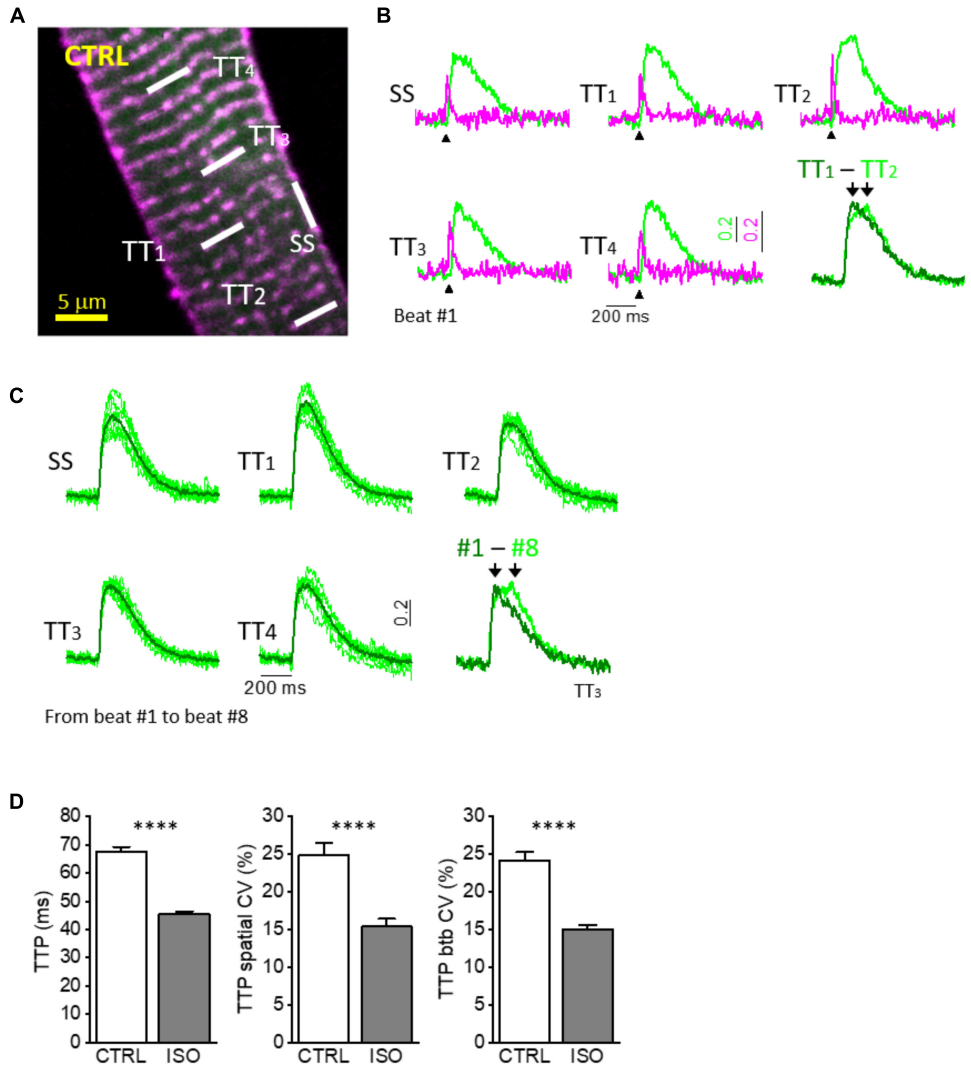

FIGURE 1 | Simultaneous multisite voltage and Ca^{2+} recordings. **(A)** Two-photon fluorescence (TPF) image of a stained rat ventricular myocyte: sarcolemma in magenta (di-4-ANE(F)PTEA) and $[Ca^{2+}]_i$ in green (GFP-certified Fluoforte). Modified from Crocini et al. (2014b). **(B)** Normalized fluorescence traces ($\Delta F/F_0$) simultaneously recorded from the scanned sites indicated in white in **A**: surface sarcolemma (SS) and four T-tubules (TTi). AP is elicited at 200 ms (black arrowheads). Membrane voltage (magenta) and $[Ca^{2+}]_i$ (green). The last is a superimposition of two simultaneous Ca^{2+} transients. Modified from Crocini et al. (2014b). **(C)** Superimposition of ten subsequent Ca^{2+} transients recorded from five scanned sites in a CTRL cardiomyocyte. The last is a superimposition of one scanned t-tubule obtained from different subsequent beating (recording #1 and recording #8). **(D)** Graphs showing mean values for Ca^{2+} transient time-to-peak (TTP), time-to-peak spatial variability coefficient (TTP spatial CV), and time-to-peak beat-to-beat variability coefficient (TTP btb CV) of Ca^{2+} release. Data reported as mean ± SEM from 122 TTs (27 CTRL cells from 10 rats) and 48 TTs (11 ISO cells from 3 rats). Student's *t*-test applied, $^{****}P < 0.0001$.

consisting of 10 consecutive recordings, where we probed 5–10 different tubular membrane sites per recording (TTi, $i = 1$ to 10) (**Figure 1C**). The length of scanning lines for each membrane site ranged from 2 to 10 µm with an integration time of 200 µs per line, leading to a temporal resolution of 0.4–2 ms. The signal-to-noise ratio (S/N) was sufficient to detect the presence of an AP occurring at sarcolemma and to assess the temporal features of the Ca^{2+} transient in the surrounding cytoplasm. Local calcium transients at each TTi were analyzed in terms of amplitude and kinetics and we calculated a coefficient of variability (CV) as the ratio between the standard deviation and the mean of a specific parameter, namely the time to peak of Ca^{2+} release.

Of note, by averaging the 10 consecutive RAMP measurements performed at each site, we have demonstrated the tight electrical coupling between surface sarcolemma (SS) and t-tubules (TTs) (Sacconi et al., 2012), as well as the perfect overlap of Ca^{2+} transients originating close to SS and TTs during steady-state stimulations in control ventricular cardiomyocytes (Crocini et al., 2014b). These results have demonstrated the uniformity of Ca^{2+} release across the entire cardiomyocyte and highlighted the crucial role of the TATS in propagating AP into the whole cell ensuring a synchronous Ca^{2+} release. Exploiting the possibility to simultaneously and consecutively perform several measurements of selected regions, we obtained

information regarding Ca^{2+} release variability in both space and time. These two parameters appeared to be of peculiar interest:

1. The spatial CV of time to peak (spatial CV of TTP), that is the ratio of the standard deviation to the mean between TTi = 1 to 10 recorded during a single activation (e.g., trial 1 or trial 2 or trial 3, etc.).
2. The beat-to-beat CV of time to peak (btb CV of TTP), that is the ratio of the standard deviation to the mean between consecutive activations (trial 1, trial 2, trial 3 etc.) calculated at a specific membrane site (e.g., TT1 or TT2 or TT3, etc.).

Regarding the mechanisms underlying the observed spatio-temporal variability, we first hypothesized that the presence of a non-negligible spatial CV (approximately 25%; **Figures 1C,D**) between far apart TT_i in control rat ventricular cardiomyocytes could be related to heterogeneous functional or structural characteristics at different calcium release sites. Non-homogeneous phosphorylation levels of RYR2 or DHPRs in space, for instance, or variability in the dyadic cleft dimensions/structure could lead to a large spatial CV even in control cells. This hypothesis was denied when we observed a quantitatively similar variability of Ca^{2+} release in time, i.e., when we compared consecutive activations at the same single t-tubule site. In control rat ventricular cardiomyocytes btb CV of TTP was also in the order of 25% (**Figures 1C,D**) On a beat-to-beat basis, no functional or structural changes at the calcium release sites may occur that could account for a relatively large (25%) CV and, in our view, the sole possible mechanism underlying the phenomenon is the stochastic nature of Ca^{2+} release itself, that our RAMP technique appears able to detect. Indeed, only a few Ca^{2+} release units (CRUs) reside within the volume probed by each scanned line (5–10 CRUs in $\sim$10 μm^3) (Franzini-Armstrong et al., 1999; Soeller et al., 2007). A typical CRU hosts about 50–200 RyRs and 10–25 Ca^{2+} release channels (Franzini-Armstrong et al., 1999). During normal twitch activation (at low inotropic levels) only a small fraction of RyR2 is recruited (e.g., of the total $\sim$3 million of RyR2 in the cell, less than 2–5% would open during a regular twitch) (Wier et al., 1994; Bers, 2001). This low open probability (Po) of the RyR2 explains the high variability of Ca^{2+} release that we observed. We expected that by increasing RyR2 Po the spatial and btb CV of TTP would decrease. In order to enhance RyR2 Po, we performed measurements in the presence of a β-adrenergic agonist, isoproterenol (ISO, 10^{-7} M), that acutely promotes RyR2 hyperphosphorylation at Protein Kinase A (PKA) sites, thus prolonging the duration of RyR2 opening (RyR2 t_{on}) and enhancing RyR2 cytosolic and luminal Ca^{2+} sensitivity (Eisner et al., 2004; Ferrantini et al., 2016). As expected, we found that both spatial and btb CV of TTP were markedly reduced under ISO: the extent of the reduction (**Figure 1D**) was similar for the two parameters. This result suggests that the local variability of TTP (in space and time) is tightly related to the functional state of RyR2s and reflects the stochastic nature of their openings. Of note, to some extent, the synchronization of local Ca^{2+} release under ISO could be attributed to a more intense trigger (i.e., slower I_{CaL} inactivation), and further experiments with a direct RyR2 agonist would be helpful to define the reciprocal role of the two mechanisms (Ca^{2+} channels *vs*. RyR2 PKA-mediated phosphorylation).

T-TUBULE STRUCTURAL REMODELING AND CALCIUM ALTERATIONS IN CARDIAC DISEASES

The ability of our method to probe the spatiotemporal relationship between Ca^{2+} and electrical activity was then explored in three models of cardiac disease characterized by TATS morpho-functional remodeling.

All animal handling and procedures were performed in accordance with the guidelines from Directive 2010/63/EU of the European Parliament on the protection of animals used for scientific purposes and conformed to the principles and regulations as described in the editorial by Grundy (2015). The experimental protocol was approved by the Italian Ministry of Health (protocol number 647/2015-PR).

We compared the following pathological settings:

- a rat model of ischemic heart failure (HF-ischemic), in which myocardial infarction was induced by ligation of the left anterior coronary artery as previously described (Lyon et al., 2009); the animals were studied 8–10 weeks after the ischemic damage, when echocardiographic signs of heart failure were (such as left ventricle (LV) dilation and reduced LV contractility) easily revealed.
- a rat model of left ventricular hypertrophy induced by spontaneous hypertension (i.e., spontaneously hypertensive rats, SHR). Notably we analyzed the late-stage of the disease, when LV dilation and failure occurred. Thus, this model represents a second example of overt heart failure (HF-SHR) (Okamoto and Aoki, 1963).
- a mouse model of hypertrophic cardiomyopathy (HCM), expressing a human mutated cardiac troponin T (deletion of a codon at position 160 of the protein, cTnT Δ160E), associated with high risk of sudden cardiac death and severe diastolic dysfunction in patients (Pasquale et al., 2012; Coppini et al., 2014). Mice employed were 6–8 months old, reflecting early stages of the disease, when LV function is compensated (Moore et al., 2013).

In order to quantify the loss of TATS transverse components (TT) from confocal images of isolated cardiomyocytes, we used AutoTT, a software developed specifically for quantitative analysis of the TATS architecture (Guo and Song, 2014). Cardiomyocytes isolated from the three pathological models introduced above showed different levels of t-tubular remodeling (**Figure 2**). In particular, we found a variable reduction of TT density, more accentuated in the HF-ischemic model (HF-ischemic > HF-SHR > HCM). Disruption of TT in failing cardiomyocyte was previously reported in a number of animal models and in human myocytes (He et al., 2001;

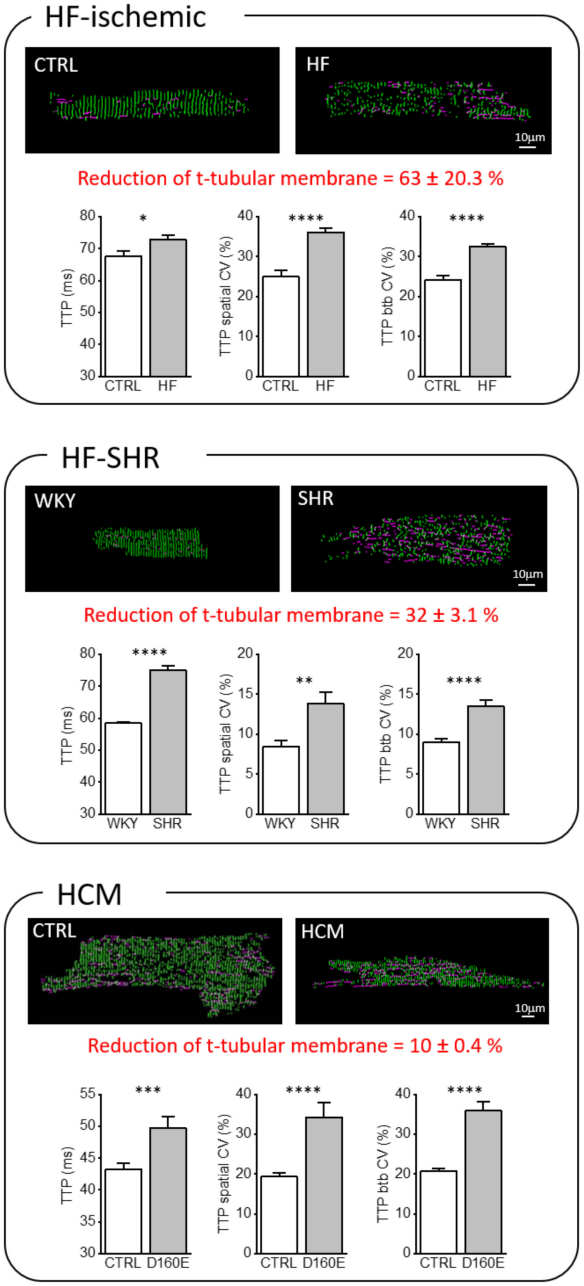

FIGURE 2 | Transverse-axial tubular system architecture and Ca^{2+} kinetics in ischemic heart failure (HF-ischemic), spontaneously hypertensive rats in overt heart failure (HF-SHR), and hypertrophic cardiomyopathy (HCM). On the top, representative images of cellsshowing skeletonized T-tubular system, obtained with AUTO-TT. Transverse elements are shown in green and axial ones in magenta. On the bottom, Graphs showing mean values for Ca^{2+} transient time-to-peak (TTP), time-to-peak spatial variability coefficient (TTP spatial CV), and time-to-peak beat-to-beat variability coefficient (TTP btb CV) of Ca^{2+} release. Data reported as mean ± SEM from 122 TTs (27 CTRL cells from 10 rats), 364 TTs (59 HF cells from 12 rats), 87 TTs (25 WKY cells from 8 rats), 87 TTs (23 SHR cells from 8 rats), 101 TTs (28 CTRL cells from 10 mice), and 66 TTs (17 Δ160E cells from 7 mice). Auto TT images of: HF-SHR from Scardigli et al. (2017); of CTRL and HCM from Crocini et al. (2016c). Student's *t*-test applied, $^{*}P < 0.05$, $^{**}P < 0.01$, $^{***}P < 0.001$, $^{****}P < 0.0001$.

Song et al., 2006). In a rat model of left ventricular hypertrophy, the loss of t-tubules was described as a marker of the transition from compensated hypertrophy to HF (Wei et al., 2010). Our genetic-based model of LV hypertrophy (HCM) demonstrates that t-tubule disruption can occur also during the compensated stages of LV hypertrophy (Crocini et al., 2016c), highlighting the "detubulation" process as an early event of cardiomyocyte remodeling.

Most of the studies regarding membrane architecture in pathological conditions have been conducted with lipophilic membrane-selective fluorescent dyes and reported a reduction of t-tubule staining. Two distinct possibilities underlie this observation. First, t-tubules may seal off from the surface membrane and remain as (permanent or transitory) sealed-off intracellular membrane structures. Alternatively, t-tubules could be truly depleted from the "diseased" cells with a real loss of membrane domains and associated proteins. Discrimination between these possibilities would be crucial to acquire new insights about pathological t-tubular turnover, but rather difficult to explore experimentally. We instead focused our attention on the function of the "residual" remodeled TATS elements. Besides a reduction of transverse components, remodeled TATS show: (1) a reduction in the number of t-tubular openings on the surface (mouths) (Wagner et al., 2012), (2) a greater proportion of tubules running in the longitudinal and oblique directions (Louch et al., 2006; Swift et al., 2008), (3) increased mean t-tubular diameter and length (Maron et al., 1975; Kaprielian et al., 2000), and (4) tubular proliferation, with enhanced t-tubular tortuosity, increased number of constrictions and branches (Kostin et al., 1998). These geometrical changes, characterized with nanometric resolution by STED microscopy (Wagner et al., 2012; Kohl et al., 2013), go hand in hand with structural alterations of the dyadic cleft, as well as changes of membrane channels density and function. In failing myocytes, an expansion of the dyadic cleft occurs, resulting in a greater distance between Ca^{2+} channels and RyR2 (Gomez et al., 1997; Wei et al., 2010; van Oort et al., 2011). Recently, an increased variability in dyadic cleft distance has been also described (Wei et al., 2010). There is a general consensus that I_{CaL} density is unchanged in HF and HCM cardiomyocytes when measured during voltage-clamp steps (Bers, 2006; Coppini et al., 2013), but the number of Ca^{2+}channels is reportedly reduced (He et al., 2001). Increased single Ca^{2+}channel activity appears to maintain normal Ca^{2+} current density in HF (Schroder et al., 1998), and this may result from increased phosphorylation of the Ca^{2+}channel by PKA and/or Ca^{2+}/calmodulin kinase II (CaMKII) (Chen et al., 2002). Similarly, RyR2 density in HF and HCM cardiomyocytes appear to be unchanged (Gomez et al., 2001; Benitah et al., 2002; Coppini et al., 2013) but channel function is enhanced by post-translational modifications. For instance, chronic "hyper-phosphorylation" of RyR2 by PKA (Marx et al., 2000) and CaMKII (Ai et al., 2005; Curran et al., 2010; Grimm et al., 2015; Pereira et al., 2017) that occurs in HF causes dissociation of FKBP12.6 from RyR2, destabilizes the RyR2 complex and causes functional uncoupling of neighboring RyRs.

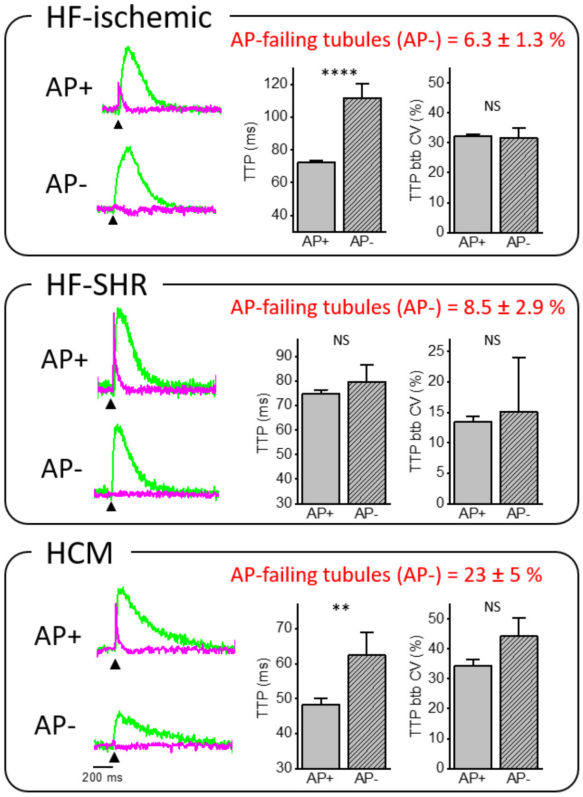

FIGURE 3 | Relationship between electrical defects and Ca^{2+} kinetics in ischemic heart failure (HF-ischemic), spontaneously hypertensive rats in overt heart failure (HF-SHR), and hypertrophic cardiomyopathy (HCM). On the left, normalized fluorescence traces ($\Delta F/F_0$) of voltage (magenta) and $[Ca^{2+}]_i$ (green) recorded from the two scanned sites. An action potential (elicited at 200 ms, black arrowheads) is clearly visible in AP+ but absent in AP– within the same cell. On the right, graphs showing mean values for Ca^{2+} transient time-to-peak (TTP) and time-to-peak beat-to-beat variability coefficient (TTP btb CV) of Ca^{2+} release in AP+ and AP–. Data reported as mean ± SEM from 341 AP+ and 23 AP– (59 HF cells from 12 rats), 80 AP+ and 7 AP– (23 SHR cells from 8 rats), and 51 AP+ and 15 AP– (17 Δ160E cells from 7 mice). Traces of HCM from Crocini et al. (2016c) Student's *t*-test applied, NS $P > 0.05$, $^{**}P < 0.01$, $^{****}P < 0.0001$.

In addition to phosphorylation (Marx et al., 2000; Braz et al., 2004; Wehrens et al., 2004), RYR2 is regulated by other post-translational modifications such as oxidation and S-nitrosylation (Xu et al., 1998; Eu et al., 2000; Barouch et al., 2002; Santos et al., 2011) as well as accessory and structural proteins (e.g., triadin, junctin, and junctophilin-2) (van Oort et al., 2011). Every level of RyR2 regulation can be impaired in HF (Yano et al., 2005), with the functional effect of destabilizing RYR2 closed states.

Thus, while arrays of RyR2s normally tend to open and close together, RyR2 functional uncoupling in failing myocytes is proposed to result in a greater open probability during diastole and desynchronised channels opening during systole. Increased dyadic cleft distance associated with impaired Ca^{2+} channels and, more importantly, impaired RyR2 function in the CRUs may lead to a general disruption of local Ca^{2+} release synchronicity in remodeled TATS.

Using the RAMP microscope, we have directly addressed this issue and observed that a number of functional abnormalities are common in "residual" TATS of HF-ischemic, HF-SHR, and HCM cardiomyocytes: Ca^{2+} transient TTPs are prolonged and both the spatial and btb CV (of TTPs) are increased (**Figure 2**). We believe that the structural TATS and dyadic changes combined with the impaired RyR2 regulation described above play a major role in the increased local variability of TTP observed in the three diseases. However, exploiting the possibility of RAMP technique to simultaneously map local TATS electrical activity and measure corresponding Ca^{2+} fluxes, we found that the increased TTPs could be also correlated to electrical abnormalities occurring at the single t-tubular level (Sacconi et al., 2012; Crocini et al., 2014b; 2016c; Scardigli et al., 2017).

RELATIONSHIP BETWEEN ELECTRICAL T-TUBULAR DEFECTS AND LOCAL ALTERATIONS OF CALCIUM RELEASE

Our laboratory has demonstrated that loss of the TATS leads to alteration of AP propagation. A number of t-tubules fail to propagate AP from the surface sarcolemma into the cell core (failing T-tubule; AP−) (**Figure 3**) in diseased cardiomyocytes. In two different rat models of heart failure, HF-ischemic and HF-SHR, (6.3 ± 1.3)% and (8.5 ± 2.9)% of t-tubules, respectively, were not able to conduct the AP, while a regular stimulated AP occured on the surface sarcolemma and neighbor t-tubules. Interestingly, in cTnT Δ160E ventricular cardiomyocytes, we observed (23 ± 5)% of AP-failing t-tubules, while TATS morphological alterations were minimal (Crocini et al., 2016c). This result suggests that the number of failing t-tubules is not correlated with the degree of lost t-tubular elements, but is due to local ultrastructural alterations (Crocini et al., 2016b; Scardigli et al., 2017). Further support comes from our findings regarding acutely detubulated cardiomyocytes, in which a dramatic detachment of t-tubules was associated with only (12 ± 4)% of failing t-tubules among the remaining connected elements (Sacconi et al., 2012). Based on the pathological substrate, electrical defects may profoundly impair local Ca^{2+} release determining significant differences of Ca^{2+} release TTP between coupled (AP+) and uncoupled (AP−) t-tubules. Ca^{2+} transient TTPs were significantly prolonged in AP− as compared to corresponding AP+ in HF-ischemic and HCM myocytes. These results strongly suggest that the Ca^{2+} transient detected at AP− tubules originates from the Ca^{2+} signal propagating from neighboring electrically coupled sites (AP+). This phenomenon was confirmed by a follow-up work, in which we employed a β-adrenergic agonist in HF-ischemic myocytes (Crocini et al., 2016a). At variance with AP+ tubules, Ca^{2+} transient TTPs at AP− sites were not affected by β-adrenergic stimulation, validating the propagative Ca^{2+}-cascade. In fact, β-adrenergic signaling does not regulate the velocity of Ca^{2+} propagation in the cell.

Interestingly, btb CV of TTP was not affected by the electrical coupling of the corresponding t-tubule in all of the disease settings we have investigated. Importantly, this result indicates

that local Ca^{2+} release variability measured with our technique is determined by RyR2 functional state rather than propagative Ca^{2+}-cascade from functioning AP+ sites to AP−. Again, this result has been confirmed by acute treatment of HF-ischemic myocytes with β-adrenergic agonist (Crocini et al., 2016a), in which btb CV of TTP was reduced upon β-adrenergic stimulation. We can conclude that β-adrenergic signaling can regulate RyR2 functional states, resulting in a reduced CV in any location of the cell. Differently from HF-ischemic and HCM, Ca^{2+} kinetics did not show a statistical difference between AP+ and AP− in SHR/HF cardiomyocytes. This result remains of difficult interpretation and may be related to the pronounced delay of the overall Ca^{2+} transient that involves the whole cell in SHR (Bing et al., 1991).

CONCLUSION AND PRESPECTIVES

We employed the RAMP microscope to simultaneously and consecutively measure local TATS activity and obtain information regarding Ca^{2+} release kinetics and variability of Ca^{2+} transient time to peak both in space (spatial CV) and in time (btb CV). We found that, in control cardiomyocytes, space and btb CV of TTP are similar one other (approximately ∼25%) and are both reduced by half upon isoproterenol treatment. Starting from the consideration that a relative small number of RyR2 are located in the scanned regions, our results in control cardiomyocytes suggest that the local variability of TTP may be tightly related to the stochastic opening of RyR2s and is influenced by the channel functional state. The beat-to-beat variability at single membrane domains strongly exclude the presence of systematic structural or functional factors underlying the variability in space. The stochastic nature of Ca^{2+} release is further confirmed by the fact that mean local Ca^{2+} transients, resulting from averaging 10 consecutively measurements, perfectly overlap in terms of amplitude and kinetics between SS and TT. In our view, the fact that an average "in time" abolishes the spatial variability is a further demonstration that the mechanisms underlying this variability is the stochasticity of Ca^{2+} release.

We next studied the electrical function and associated Ca^{2+} fluxes of "residual" structurally remodeled TATS in three pathological conditions (HF-ischemic, HF-SHR, HCM) and found a number of common changes as well as disease-specific alterations: prolonged local Ca^{2+} transients TTPs and markedly increased spatial and temporal variability of TTPs. Despite different numbers, we found a population of "residual" t-tubules failing to propagating AP in all three pathological settings. We found two main results. The first (expected) was an increased spatial and btb CV of TTPs in disease remodeled TATS. The second (unexpected) was that the electrical coupling of t-tubules (AP+ and AP−) does not influence the variability of Ca^{2+} release.

At glance, the spatial CV appears to be the more relevant parameter in terms of functional implications for non-homogenous sarcomere activation and the generation of pro-arrhythmogenic triggers through mechano-electric feedback. In diseased myocardium, where t-tubules are structurally and functionally remodeled and the spatial variability of Ca^{2+} release is increased, the coexistence of "in parallel" myofibril layers with different timing of initial activation would result in reduced force development and overall slower kinetics. However, we can speculate that the increased temporal variability of Ca^{2+} release may generate also the coexistence of "in series" myofibrils with different timing of activation, eventually promoting arrhythmias by favoring AP alternans. These new pro-arrhythmogenic mechanisms that occur in remodeled t-tubules may be added to those previously described (Orchard et al., 2013; Crocini et al., 2014a).

A number of mechanisms may contribute to the increased spatial and btb CV of TTPs of remodeled TATS, including dyadic structural changes and alterations of Ca^{2+} channels density and regulation. However, the absence of difference in btb CV of TTPs between AP+ and AP−, conditions where local I_{CaL} triggers are present (AP+) and absent (AP−), respectively, exclude a major role of Ca^{2+} channels function and indicates that the main player in the local variability of Ca^{2+} release is the RyR2 functional state. While RyR2 function resulting from targeted single post-translational modification (e.g., the effects of single phosphorylation at specific sites) has been largely studied in channels re-expressed in bilayers, the complex RyR2 alterations that occur in cardiac diseases cannot be reproduced *in vitro*. Preserving the manifold context of pathological settings is therefore essential to accurately investigate disease-related channel alternations. Thanks to our RAMP approach, a novel set of information may become accessible, allowing for unprecedented exploration of RyR2 function in living cardiomyocytes. Distinct modulation of different subpopulations of RyR2 clusters, those coupled to the t-tubules (dyadic RyR2) and those non-coupled (corbular RyR2), has been recently highlighted in a number of studies (Dries et al., 2013, 2016). CaMKII-dependent potentiation of RyR2 activity, for instance, is restricted to coupled RyRs in the dyadic cleft (Dries et al., 2013), while PKA phosphorylation occur at all RyRs concurrently, including those "non-coupled" to the sarcolemmal membrane (Dries et al., 2013, 2016). In addition to the subcellular microdomain compartmentalization, the phosphorylations by CaMKII and PKA differently affect RyR2 gating as well as its modulation by a number of factors (e.g., cytosolic and luminal calcium, regulatory proteins) (Bers, 2001). As an example, the mean open probability (Po) is increased by both kinases, but the effects on channel open times (To) and channel closed times (Tc) are specific and may directly affect the stochasticity of Ca^{2+} release and its subcellular spatio-temporal variability. The scenario of RyR2 subpopulations at different microdomains is even more complex in cells that exhibit a t-tubular network poor of transverse elements but enriched of other components (e.g., axial tubules, AT).

In the absence of abundant transverse membrane invaginations, as in atrial cells or in disease-remodeled ventricular cardiomyocytes, we can configure the presence

of at list other three populations of RyR2 in addition to those mentioned above:

- RyR2s that are coupled to axial tubules, well represented in atrial cells.

- RyR2s that are "orphaned" of their t-tubules because of t-tubule disruption in disease-associated structural remodeling.

- RyR2s that are coupled to non-propagating (AP-) t-tubules, as observed in disease-remodeled myocytes and described in detail above.

The study of subcellular spatio-temporal variability of Ca^{2+} release with the RAMP technique may provide significant insights to clarify the functional characteristics of these RyR2 populations. For instance, in mouse atrial myocytes, Ca^{2+} release from the SR in axial tubules is approximately two times faster at the center of the cell as compared to Ca^{2+} release at the surface. Rapid Ca^{2+} release correlated with colocalization of highly phosphorylated (highphos) RyR2 clusters at junctions between axial tubules and SR junctions (Brandenburg et al., 2016). Novel evidence of atrial "super-hub" Ca^{2+} signaling has been recently reported across different species (Brandenburg et al., 2018), possibly establishing a new paradigm for atrial Ca^{2+} release. We can speculate that the spatio-temporal variability of Ca^{2+} release could be reduced at the highphos RyR2 clusters and our approach may help establishing the role of axial tubules, highphos RyR2 clusters, and non-junctional Ca^{2+} release. RAMP measurements can be extended to the intact tissue in order to study subcellular Ca^{2+} release spatio-temporal variability in various cells at the same time (Sacconi et al., 2012; Ferrantini et al., 2014). These studies could include human myocardium, whose characteristics are only partly reproduced by murine models, thus providing an even further interesting perspective to dissect RyR2 function in a physiological environment. In fact, recent studies in failing human hearts agree on the reduction of t-tubule density, which was two to three times lower in failing ventricular myocytes from HF patients with different aetiologies than in healthy donors (Cannell et al., 2006; Lyon et al., 2009). Loss of t-tubules have been also described in patients with genetic-based cardiomyopathies (Maron et al., 1975; Kaprielian et al., 2000; Ferrantini et al., 2018). We believe that our studies on rodent models of HF and congenital cardiac diseases could (qualitatively) reflect the spatio-temporal variability of Ca^{2+} release that may occur in human cardiomyocytes. Though, direct RAMP measurements of Ca^{2+} release in human t-tubules are needed, and may represent the most exciting perspective for this technology.

AUTHOR CONTRIBUTIONS

MS analyzed the data. MS, CC, CF, FP, and LS wrote the paper.

FUNDING

This work was supported by the European Union Horizon 2020 research and innovation program under grant agreement no. 654148 Laserlab-Europe, by the Italian Ministry for Education, University and Research in the framework of the Flagship Project NanoMAX, by the Italian Ministry of Health (WFR GR-2011-02350583), by Telethon–Italy (GGP13162), by Ente Cassa di Risparmio di Firenze (private foundation), and by FAS-Salute ToRSADE project. CC holds a long-term fellowship from the Human Frontiers Science Program Organization (LT001449/2017-L).

REFERENCES

Ai, X., Curran, J. W., Shannon, T. R., Bers, D. M., and Pogwizd, S. M. (2005). Ca2 + /calmodulin-dependent protein kinase modulates cardiac ryanodine receptor phosphorylation and sarcoplasmic reticulum Ca2 + leak in heart failure. *Circ. Res.* 97, 1314–1322. doi: 10.1161/01.RES.0000194329.41863.89

Barouch, L. A., Harrison, R. W., Skaf, M. W., Rosas, G. O., Cappola, T. P., Kobeissi, Z. A., et al. (2002). Nitric oxide regulates the heart by spatial confinement of nitric oxide synthase isoforms. *Nature* 416, 337–339.

Bassani, J. W., Yuan, W., and Bers, D. M. (1995). Fractional SR Ca release is regulated by trigger Ca and SR Ca content in cardiac myocytes. *Am. J. Physiol.* 268(5 Pt 1), C1313–C1319. doi: 10.1152/ajpcell.1995.268.5.C1313

Benitah, J. P., Kerfant, B. G., Vassort, G., Richard, S., and Gomez, A. M. (2002). Altered communication between L-type calcium channels and ryanodine receptors in heart failure. *Front. Biosci.* 7:e21. doi: 10.2741/benitah

Bers, D. M. (2001). *Excitation-Contraction Coupling and Cardiac Contractile Force*. Norwell, MA: Kluwer Academic Publishers. doi: 10.1007/978-94-010-0658-3

Bers, D. M. (2002). Cardiac excitation-contraction coupling. *Nature* 415, 198–205. doi: 10.1038/415198a

Bers, D. M. (2006). Altered cardiac myocyte Ca regulation in heart failure. *Physiology* 21, 380–387. doi: 10.1152/physiol.00019.2006

Bing, O. H., Brooks, W. W., Conrad, C. H., Sen, S., Perreault, C. L., and Morgan, J. P. (1991). Intracellular calcium transients in myocardium from spontaneously hypertensive rats during the transition to heart failure. *Circ. Res.* 68, 1390–1400. doi: 10.1161/01.RES.68.5.1390

Brandenburg, S., Kohl, T., Williams, G. S., Gusev, K., Wagner, E., Rog-Zielinska, E. A., et al. (2016). Axial tubule junctions control rapid calcium signaling in atria. *J. Clin. Invest.* 126, 3999–4015. doi: 10.1172/JCI88241

Brandenburg, S., Pawlowitz, J., Fakuade, F. E., Kownatzki-Danger, D., Kohl, T., Mitronova, G., et al. (2018). Axial tubule junctions activate atrial Ca^{2+} release across specie. *Front. Physiol.* 9:1227. doi: 10.3389/fphys.2018.01227

Braz, J. C., Gregory, K., Pathak, A., Zhao, W., Sahin, B., Klevitsky, R., et al. (2004). PKC-alpha regulates cardiac contractility and propensity toward heart failure. *Nat. Med.* 10, 248–254. doi: 10.1038/nm1000

Brette, F., Despa, S., Bers, D. M., and Orchard, C. H. (2005). Spatiotemporal characteristics of SR Ca(2 +) uptake and release in detubulated rat ventricular myocytes. *J. Mol. Cell Cardiol.* 39, 804–812. doi: 10.1016/j.yjmcc.2005.08.005

Brette, F., Komukai, K., and Orchard, C. H. (2002). Validation of formamide as a detubulation agent in isolated rat cardiac cells. *Am. J. Physiol. Heart Circ. Physiol.* 283, H1720–H1728. doi: 10.1152/ajpheart.00347.2002

Brette, F., Rodriguez, P., Komukai, K., Colyer, J., and Orchard, C. H. (2004). beta-adrenergic stimulation restores the Ca transient of ventricular myocytes lacking t-tubules. *J. Mol. Cell Cardiol.* 36, 265–275. doi: 10.1016/j.yjmcc.2003.11.002

Cannell, M. B., Crossman, D. J., and Soeller, C. (2006). Effect of changes in action potential spike configuration, junctional sarcoplasmic reticulum micro-architecture and altered t-tubule structure in human heart failure. *J. Muscle Res. Cell Motil.* 27, 297–306. doi: 10.1007/s10974-006-9089-y

Chen, X., Piacentino, V. III, Furukawa, S., Goldman, B., Margulies, K. B., and Houser, S. R. (2002). L-type Ca2 + channel density and regulation are altered in failing human ventricular myocytes and recover after support with mechanical assist devices. *Circ. Res.* 91, 517–524. doi: 10.1161/01.RES.0000033988.13062.7C

Cheng, H., Cannell, M. B., and Lederer, W. J. (1994). Propagation of excitation-contraction coupling into ventricular myocytes. *Pflugers Arch.* 428, 415–417. doi: 10.1007/BF00724526

Coppini, R., Ferrantini, C., Aiazzi, A., Mazzoni, L., Sartiani, L., Mugelli, A., et al. (2014). Isolation and functional characterization of human ventricular cardiomyocytes from fresh surgical samples. *J. Vis. Exp.* 21:86. doi: 10.3791/51116

Coppini, R., Ferrantini, C., Yao, L., Fan, P., Del Lungo, M., Stillitano, F., et al. (2013). Late sodium current inhibition reverses electromechanical dysfunction in human hypertrophic cardiomyopathy. *Circulation* 127, 575–584. doi: 10.1161/CIRCULATIONAHA.112.134932

Crocini, C., Coppini, R., Ferrantini, C., Pavone, F. S., and Sacconi, L. (2014a). Functional cardiac imaging by random access microscopy. *Front. Physiol.* 5:403. doi: 10.3389/fphys.2014.00403

Crocini, C., Coppini, R., Ferrantini, C., Yan, P., Loew, L. M., Tesi, C., et al. (2014b). Defects in T-tubular electrical activity underlie local alterations of calcium release in heart failure. *Proc. Natl. Acad. Sci. U.S.A.* 111, 15196–15201. doi: 10.1073/pnas.1411557111

Crocini, C., Coppini, R., Ferrantini, C., Yan, P., Loew, L. M., Poggesi, C., et al. (2016a). T-tubular electrical defects contribute to blunted beta-adrenergic response in heart failure. *Int. J. Mol. Sci.* 17, 1410–1471. doi: 10.3390/ijms17091471

Crocini, C., Ferrantini, C., Coppini, R., and Sacconi, L. (2016b). Electrical defects of the transverse-axial tubular system in cardiac diseases. *J. Physiol.* 595, 3815–3822. doi: 10.1113/JP273042

Crocini, C., Ferrantini, C., Scardigli, M., Coppini, R., Mazzoni, L., Lazzeri, E., et al. (2016c). Novel insights on the relationship between T-tubular defects and contractile dysfunction in a mouse model of hypertrophic cardiomyopathy. *J. Mol. Cell Cardiol.* 91, 42–51. doi: 10.1016/j.yjmcc.2015.12.013

Curran, J., Brown, K. H., Santiago, D. J., Pogwizd, S., Bers, D. M., and Shannon, T. R. (2010). Spontaneous Ca waves in ventricular myocytes from failing hearts depend on Ca(2 +)-calmodulin-dependent protein kinase II. *J. Mol. Cell Cardiol.* 49, 25–32. doi: 10.1016/j.yjmcc.2010.03.013

Dibb, K. M., Clarke, J. D., Horn, M. A., Richards, M. A., Graham, H. K., Eisner, D. A., et al. (2009). Characterization of an extensive transverse tubular network in sheep atrial myocytes and its depletion in heart failure. *Circ. Heart Fail.* 2, 482–489. doi: 10.1161/CIRCHEARTFAILURE.109.852228

Dries, E., Bito, V., Lenaerts, I., Antoons, G., Sipido, K. R., and Macquaide, N. (2013). Selective modulation of coupled ryanodine receptors during microdomain activation of calcium/calmodulin-dependent kinase II in the dyadic cleft. *Circ. Res.* 113, 1242–1252. doi: 10.1161/CIRCRESAHA.113.301896

Dries, E., Santiago, D. J., Johnson, D. M., Gilbert, G., Holemans, P., Korte, S. M., et al. (2016). Calcium/calmodulin-dependent kinase II and nitric oxide synthase 1-dependent modulation of ryanodine receptors during beta-adrenergic stimulation is restricted to the dyadic cleft. *J. Physiol.* 594, 5923–5939. doi: 10.1113/JP271965

Eisner, D. A., Diaz, M. E., O'Neill, S. C., and Trafford, A. W. (2004). Physiological and pathological modulation of ryanodine receptor function in cardiac muscle. *Cell Calcium* 35, 583–589. doi: 10.1016/j.ceca.2004.01.012

Eisner, D. A., Trafford, A. W., Diaz, M. E., Overend, C. L., and O'Neill, S. C. (1998). The control of Ca release from the cardiac sarcoplasmic reticulum: regulation versus autoregulation. *Cardiovasc. Res.* 38, 589–604. doi: 10.1016/S0008-6363(98)00062-5

Eu, J. P., Sun, J., Xu, L., Stamler, J. S., and Meissner, G. (2000). The skeletal muscle calcium release channel: coupled O2 sensor and NO signaling functions. *Cell* 102, 499–509. doi: 10.1016/S0092-8674(00)00054-4

Ferrantini, C., Coppini, R., Sacconi, L., Tosi, B., Zhang, M. L., Wang, G. L., et al. (2014). Impact of detubulation on force and kinetics of cardiac muscle contraction. *J. Gen. Physiol.* 143, 783–797. doi: 10.1085/jgp.201311125

Ferrantini, C., Coppini, R., Scellini, B., Ferrara, C., Pioner, J. M., Mazzoni, L., et al. (2016). R4496C RyR2 mutation impairs atrial and ventricular contractility. *J. Gen. Physiol.* 147, 39–52. doi: 10.1085/jgp.201511450

Ferrantini, C., Pioner, J. M., Mazzoni, L., Gentile, F., Tosi, B., Rossi, A., et al. (2018). Late sodium current inhibitors to treat exercise-induced obstruction in hypertrophic cardiomyopathy: an in vitro study in human myocardium. *Br. J. Pharmacol.* 175, 2635–2652. doi: 10.1111/bph.14223

Franzini-Armstrong, C., Protasi, F., and Ramesh, V. (1999). Shape, size, and distribution of Ca(2 +) release units and couplons in skeletal and cardiac muscles. *Biophys. J.* 77, 1528–1539. doi: 10.1016/S0006-3495(99)77000-1

Gomez, A. M., Guatimosim, S., Dilly, K. W., Vassort, G., and Lederer, W. J. (2001). Heart failure after myocardial infarction: altered excitation-contraction coupling. *Circulation* 104, 688–693. doi: 10.1161/hc3201.092285

Gomez, A. M., Valdivia, H. H., Cheng, H., Lederer, M. R., Santana, L. F., Cannell, M. B., et al. (1997). Defective excitation-contraction coupling in experimental cardiac hypertrophy and heart failure. *Science* 276, 800–806. doi: 10.1126/science.276.5313.800

Grimm, M., Ling, H., Willeford, A., Pereira, L., Gray, C. B., Erickson, J. R., et al. (2015). CaMKIIdelta mediates beta-adrenergic effects on RyR2 phosphorylation and SR Ca(2 +) leak and the pathophysiological response to chronic beta-adrenergic stimulation. *J. Mol. Cell Cardiol.* 85, 282–291. doi: 10.1016/j.yjmcc.2015.06.007

Grundy, D. (2015). Principles and standards for reporting animal experiments in *The Journal of Physiology and Experimental Physiology*. *J. Physiol.* 593, 2547–2549. doi: 10.1113/JP270818

Guo, A., and Song, L. S. (2014). AutoTT: automated detection and analysis of T-tubule architecture in cardiomyocytes. *Biophys. J.* 106, 2729–2736. doi: 10.1016/j.bpj.2014.05.013

Haddock, P. S., Coetzee, W. A., Cho, E., Porter, L., Katoh, H., Bers, D. M., et al. (1999). Subcellular [Ca2 +]i gradients during excitation-contraction coupling in newborn rabbit ventricular myocytes. *Circ. Res.* 85, 415–427. doi: 10.1161/01.RES.85.5.415

He, J., Conklin, M. W., Foell, J. D., Wolff, M. R., Haworth, R. A., Coronado, R., et al. (2001). Reduction in density of transverse tubules and L-type Ca(2 +) channels in canine tachycardia-induced heart failure. *Cardiovasc. Res.* 49, 298–307. doi: 10.1016/S0008-6363(00)00256-X

Heinzel, F. R., Bito, V., Biesmans, L., Wu, M., Detre, E., von Wegner, F., et al. (2008). Remodeling of T-tubules and reduced synchrony of Ca2 + release in myocytes from chronically ischemic myocardium. *Circ. Res.* 102, 338–346. doi: 10.1161/CIRCRESAHA.107.160085

Heinzel, F. R., Bito, V., Volders, P. G., Antoons, G., Mubagwa, K., and Sipido, K. R. (2002). Spatial and temporal inhomogeneities during Ca2 + release from the sarcoplasmic reticulum in pig ventricular myocytes. *Circ. Res.* 91, 1023–1030. doi: 10.1161/01.RES.0000045940.67060.DD

Hobai, I. A., and O'Rourke, B. (2001). Decreased sarcoplasmic reticulum calcium content is responsible for defective excitation-contraction coupling in canine heart failure. *Circulation* 103, 1577–1584. doi: 10.1161/01.CIR.103.11.1577

Ibrahim, M., Gorelik, J., Yacoub, M. H., and Terracciano, C. M. (2011). The structure and function of cardiac t-tubules in health and disease. *Proc. Biol. Sci.* 278, 2714–2723. doi: 10.1098/rspb.2011.0624

Iyer, V., Hoogland, T. M., and Saggau, P. (2006). Fast functional imaging of single neurons using random-access multiphoton (RAMP) microscopy. *J. Neurophysiol.* 95, 535–545. doi: 10.1152/jn.00865.2005

Kaprielian, R. R., Stevenson, S., Rothery, S. M., Cullen, M. J., and Severs, N. J. (2000). Distinct patterns of dystrophin organization in myocyte sarcolemma and transverse tubules of normal and diseased human myocardium. *Circulation* 101, 2586–2594. doi: 10.1161/01.CIR.101.22.2586

Kohl, T., Westphal, V., Hell, S. W., and Lehnart, S. E. (2013). Superresolution microscopy in heart - cardiac nanoscopy. *J. Mol. Cell Cardiol.* 58, 13–21. doi: 10.1016/j.yjmcc.2012.11.016

Kostin, S., Scholz, D., Shimada, T., Maeno, Y., Mollnau, H., Hein, S., et al. (1998). The internal and external protein scaffold of the T-tubular system in cardiomyocytes. *Cell Tissue Res.* 294, 449–460. doi: 10.1007/s004410051196

Kushnir, A., and Marks, A. R. (2010). The ryanodine receptor in cardiac physiology and disease. *Adv. Pharmacol.* 59, 1–30. doi: 10.1016/S1054-3589(10)59001-X

Louch, W. E., Bito, V., Heinzel, F. R., Macianskiene, R., Vanhaecke, J., Flameng, W., et al. (2004). Reduced synchrony of Ca2 + release with loss of T-tubules-a comparison to Ca2 + release in human failing cardiomyocytes. *Cardiovasc. Res.* 62, 63–73. doi: 10.1016/j.cardiores.2003.12.031

Louch, W. E., Mork, H. K., Sexton, J., Stromme, T. A., Laake, P., Sjaastad, I., et al. (2006). T-tubule disorganization and reduced synchrony of Ca2 + release in murine cardiomyocytes following myocardial infarction. *J. Physiol.* 574(Pt 2), 519–533. doi: 10.1113/jphysiol.2006.107227

Lyon, A. R., MacLeod, K. T., Zhang, Y., Garcia, E., Kanda, G. K., Lab, M. J., et al. (2009). Loss of T-tubules and other changes to surface topography in ventricular myocytes from failing human and rat heart. *Proc. Natl. Acad. Sci. U.S.A.* 106, 6854–6859. doi: 10.1073/pnas.0809777106

Maron, B. J., Ferrans, V. J., and Roberts, W. C. (1975). Ultrastructural features of degenerated cardiac muscle cells in patients with cardiac hypertrophy. *Am. J. Pathol.* 79, 387–434.

Marx, S. O., Reiken, S., Hisamatsu, Y., Jayaraman, T., Burkhoff, D., Rosemblit, N., et al. (2000). PKA phosphorylation dissociates FKBP12.6 from the calcium release channel (ryanodine receptor): defective regulation in failing hearts. *Cell* 101, 365–376. doi: 10.1016/S0092-8674(00)80847-8

Moore, R. K., Grinspan, L. T., Jimenez, J., Guinto, P. J., Ertz-Berger, B., and Tardiff, J. C. (2013). HCM-linked 160E cardiac troponin T mutation causes unique progressive structural and molecular ventricular remodeling in transgenic mice. *J. Mol. Cell Cardiol.* 58, 188–198. doi: 10.1016/j.yjmcc.2013.02.004

Okamoto, K., and Aoki, K. (1963). Development of a strain of spontaneously hypertensive rats. *Jpn. Circ. J.* 27, 282–293. doi: 10.1253/jcj.27.282

Orchard, C. H., Bryant, S. M., and James, A. F. (2013). Do t-tubules play a role in arrhythmogenesis in cardiac ventricular myocytes? *J. Physiol.* 591, 4141–4147. doi: 10.1113/jphysiol.2013.254540

Pasquale, F., Syrris, P., Kaski, J. P., Mogensen, J., McKenna, W. J., and Elliott, P. (2012). Long-term outcomes in hypertrophic cardiomyopathy caused by mutations in the cardiac troponin T gene. *Circ. Cardiovasc. Genet.* 5, 10–17. doi: 10.1161/CIRCGENETICS.111.959973

Pereira, L., Bare, D. J., Galice, S., Shannon, T. R., and Bers, D. M. (2017). beta-Adrenergic induced SR Ca(2 +) leak is mediated by an Epac-NOS pathway. *J. Mol. Cell Cardiol.* 108, 8–16. doi: 10.1016/j.yjmcc.2017.04.005

Sacconi, L., Ferrantini, C., Lotti, J., Coppini, R., Yan, P., Loew, L. M., et al. (2012). Action potential propagation in transverse-axial tubular system is impaired in heart failure. *Proc. Natl. Acad. Sci. U.S.A.* 109, 5815–5819. doi: 10.1073/pnas.1120188109

Santos, C. X., Anilkumar, N., Zhang, M., Brewer, A. C., and Shah, A. M. (2011). Redox signaling in cardiac myocytes. *Free Radic. Biol. Med.* 50, 777–793. doi: 10.1016/j.freeradbiomed.2011.01.003

Scardigli, M., Crocini, C., Ferrantini, C., Gabbrielli, T., Silvestri, L., Coppini, R., et al. (2017). Quantitative assessment of passive electrical properties of the cardiac T-tubular system by FRAP microscopy. *Proc. Natl. Acad. Sci. U.S.A.* 114, 5737–5742. doi: 10.1073/pnas.1702188114

Schroder, F., Handrock, R., Beuckelmann, D. J., Hirt, S., Hullin, R., Priebe, L., et al. (1998). Increased availability and open probability of single L-type calcium channels from failing compared with nonfailing human ventricle. *Circulation* 98, 969–976. doi: 10.1161/01.CIR.98.10.969

Scriven, D. R., Asghari, P., and Moore, E. D. (2013). Microarchitecture of the dyad. *Cardiovasc. Res.* 98, 169–176. doi: 10.1093/cvr/cvt025

Soeller, C., Crossman, D., Gilbert, R., and Cannell, M. B. (2007). Analysis of ryanodine receptor clusters in rat and human cardiac myocytes. *Proc. Natl. Acad. Sci. U.S.A.* 104, 14958–14963. doi: 10.1073/pnas.0703016104

Song, L. S., Sobie, E. A., McCulle, S., Lederer, W. J., Balke, C. W., and Cheng, H. (2006). Orphaned ryanodine receptors in the failing heart. *Proc. Natl. Acad. Sci. U.S.A.* 103, 4305–4310. doi: 10.1073/pnas.0509324103

Swift, F., Birkeland, J. A., Tovsrud, N., Enger, U. H., Aronsen, J. M., Louch, W. E., et al. (2008). Altered Na + /Ca2 + -exchanger activity due to downregulation of Na + /K + -ATPase alpha2-isoform in heart failure. *Cardiovasc. Res.* 78, 71–78. doi: 10.1093/cvr/cvn013

Ter Keurs, H. E., and Boyden, P. A. (2007). Calcium and arrhythmogenesis. *Physiol. Rev.* 87, 457–506. doi: 10.1152/physrev.00011.2006

van Oort, R. J., Garbino, A., Wang, W., Dixit, S. S., Landstrom, A. P., Gaur, N., et al. (2011). Disrupted junctional membrane complexes and hyperactive ryanodine receptors after acute junctophilin knockdown in mice. *Circulation* 123, 979–988. doi: 10.1161/CIRCULATIONAHA.110.006437

Wagner, E., Lauterbach, M. A., Kohl, T., Westphal, V., Williams, G. S., Steinbrecher, J. H., et al. (2012). Stimulated emission depletion live-cell super-resolution imaging shows proliferative remodeling of T-tubule membrane structures after myocardial infarction. *Circ. Res.* 111, 402–414. doi: 10.1161/CIRCRESAHA.112.274530

Wehrens, X. H., Lehnart, S. E., Reiken, S. R., and Marks, A. R. (2004). Ca2 + /calmodulin-dependent protein kinase II phosphorylation regulates the cardiac ryanodine receptor. *Circ. Res.* 94, e61–e70. doi: 10.1161/01.RES.0000125626.33738.E2

Wei, S., Guo, A., Chen, B., Kutschke, W., Xie, Y. P., Zimmerman, K., et al. (2010). T-tubule remodeling during transition from hypertrophy to heart failure. *Circ. Res.* 107, 520–531. doi: 10.1161/CIRCRESAHA.109.212324

Wier, W. G., and Balke, C. W. (1999). Ca(2 +) release mechanisms, Ca(2 +) sparks, and local control of excitation-contraction coupling in normal heart muscle. *Circ. Res.* 85, 770–776. doi: 10.1161/01.RES.85.9.770

Wier, W. G., Egan, T. M., Lopez-Lopez, J. R., and Balke, C. W. (1994). Local control of excitation-contraction coupling in rat heart cells. *J. Physiol.* 474, 463–471. doi: 10.1113/jphysiol.1994.sp020037

Xu, L., Eu, J. P., Meissner, G., and Stamler, J. S. (1998). Activation of the cardiac calcium release channel (ryanodine receptor) by poly-S-nitrosylation. *Science* 279, 234–237. doi: 10.1126/science.279.5348.234

Yan, P., Acker, C. D., Zhou, W. L., Lee, P., Bollensdorff, C., Negrean, A., et al. (2012). Palette of fluorinated voltage-sensitive hemicyanine dyes. *Proc. Natl. Acad. Sci. U.S.A.* 109, 20443–20448. doi: 10.1073/pnas.1214850109

Yang, Z., Pascarel, C., Steele, D. S., Komukai, K., Brette, F., and Orchard, C. H. (2002). Na + -Ca2 + exchange activity is localized in the T-tubules of rat ventricular myocytes. *Circ. Res.* 91, 315–322. doi: 10.1161/01.RES.0000030180.06028.23

Yano, M., Okuda, S., Oda, T., Tokuhisa, T., Tateishi, H., Mochizuki, M., et al. (2005). Correction of defective interdomain interaction within ryanodine receptor by antioxidant is a new therapeutic strategy against heart failure. *Circulation* 112, 3633–3643. doi: 10.1161/CIRCULATIONAHA.105.555623

Conflict of Interest Statement: The authors declare that the research was conducted in the absence of any commercial or financial relationships that could be construed as a potential conflict of interest.

The handling Editor declared a shared affiliation, though no other collaboration, with several of the authors CF, FP, and LS at the time of review.

frontiers in Physiology

ORIGINAL RESEARCH
published: 17 October 2018
doi: 10.3389/fphys.2018.01454

Characterization of Electrical Activity in Post-myocardial Infarction Scar Tissue in Rat Hearts Using Multiphoton Microscopy

*Iffath A. Ghouri[1], Allen Kelly[1], Simona Salerno[2], Karin Garten[2], Tomas Stølen[2], Ole-Johan Kemi[1] and Godfrey L. Smith[1]**

[1] Institute of Cardiovascular & Medical Sciences, University of Glasgow, Glasgow, United Kingdom, [2] Department of Circulation and Medical Imaging, St. Olav's Hospital, Norwegian University of Science and Technology, Trondheim, Norway

Background: The origin of electrical behavior in post-myocardial infarction scar tissue is still under debate. This study aims to examine the extent and nature of the residual electrical activity within a stabilized ventricular infarct scar.

Methods and Results: An apical infarct was induced in the left ventricle of Wistar rats by coronary artery occlusion. Five weeks post-procedure, hearts were Langendorff-perfused, and optically mapped using di-4-ANEPPS. Widefield imaging of optical action potentials (APs) on the left ventricular epicardial surface revealed uniform areas of electrical activity in both normal zone (NZ) and infarct border zone (BZ), but only limited areas of low-amplitude signals in the infarct zone (IZ). 2-photon (2P) excitation of di-4-ANEPPS and Fura-2/AM at discrete layers in the NZ revealed APs and Ca^{2+} transients (CaTs) to 500–600 μm below the epicardial surface. 2P imaging in the BZ revealed superficial connective tissue structures lacking APs or CaTs. At depths greater than approximately 300 μm, myocardial structures were evident that supported normal APs and CaTs. In the IZ, although 2P imaging did not reveal clear myocardial structures, low-amplitude AP signals were recorded at discrete layers. No discernible Ca^{2+} signals could be detected in the IZ. AP rise times in BZ were slower than NZ (3.50 ± 0.50 ms vs. 2.23 ± 0.28 ms) and further slowed in IZ (9.13 ± 0.56 ms). Widefield measurements of activation delay between NZ and BZ showed negligible difference (3.37 ± 1.55 ms), while delay values in IZ showed large variation (11.88 ± 9.43 ms).

Conclusion: These AP measurements indicate that BZ consists of an electrically inert scar above relatively normal myocardium. Discrete areas/layers of IZ displayed entrained APs with altered electrophysiology, but the structure of this tissue remains to be elucidated.

Keywords: myocardial infarction, optical mapping, two-photon microscopy, intracellular calcium, border zone

OPEN ACCESS

Edited by:
Daniel M. Johnson, Maastricht University, Netherlands

Reviewed by:
William Louch, University of Oslo, Norway
Richard David Walton, Université de Bordeaux, France

***Correspondence:**
Godfrey L. Smith
godfrey.smith@glasgow.ac.uk

Specialty section:
This article was submitted to Cardiac Electrophysiology, a section of the journal Frontiers in Physiology

Received: *01 June 2018*
Accepted: *25 September 2018*
Published: *17 October 2018*

Citation:
Ghouri IA, Kelly A, Salerno S, Garten K, Stølen T, Kemi O-J and Smith GL (2018) Characterization of Electrical Activity in Post-myocardial Infarction Scar Tissue in Rat Hearts Using Multiphoton Microscopy. Front. Physiol. 9:1454. doi: 10.3389/fphys.2018.01454

INTRODUCTION

Interruption of myocardial blood flow due to narrowing or blocking of coronary arteries leads to cell damage and death in the areas of tissue supplied by these vessels. Following this myocardial infarction (MI), ischemia of the underlying muscle causes necrosis of cardiomyocytes and vasculature. Over 2 to 3 weeks, the necrotic tissue is replaced by a fibrotic scar maintained

by new vasculature. For some time, the fibrous scar tissue was thought to be inert, merely serving as a mechanical patch to prevent rupture (Lodge-Patch, 1951). A large body of evidence now exists demonstrating that the scar tissue is metabolically active and a potential target for therapeutic intervention (Cleutjens et al., 1999; Sun et al., 2002; Rog-Zielinska et al., 2016). Cross-linking collagen fibers make up the majority of the scar, forming a thinner wall than the original myocardium. Myofibroblasts populate the scar as part of the healing process, regulating collagen turnover, as well as possessing the capability to generate sustained mechanical force (Van Den Borne et al., 2010). The gross structure of the scar can vary depending on (i) the anatomical position of the occluded vessel, (ii) the extent of collateral circulation, and (iii) the transmural bias of the coronary circulation (Maxwell et al., 1987). Even after complete occlusion of a coronary artery, the subsequent loss of myocardium is not 100%. Sparse regions of residual myocardium survive through the healing process and can be detected in the scar embedded in fibrous tissue, both histologically (Camelliti et al., 2004; Walker et al., 2007) and using live tissue imaging techniques, including optical coherence tomography and two-photon microscopy (Goergen et al., 2016).

The influence of scar tissue on electrical conduction in the heart has yet to be fully elucidated. There is *in vitro* evidence of myofibroblasts electrically coupling with myocytes in co-cultured preparations (Chilton et al., 2007; Zlochiver et al., 2008; Rohr, 2009; Vasquez et al., 2010; Nguyen et al., 2012), suggesting myoblast/myocyte coupling may occur in scar tissue. Recent studies from transgenic mice have also implicated myocyte/fibroblast coupling in supporting electrical conduction through the border (BZ) and infarct zones (IZ) of the intact heart (Benamer et al., 2013; Mahoney et al., 2016; Rubart et al., 2018). While myocyte/fibroblast coupling may facilitate infarct scar conduction, the ability of such nonexcitable cells to conduct electrical impulses on their own is limited, with the spatial extent of electrical conduction known to be approximately 300 μm (Gaudesius et al., 2003), suggesting conduction through the infarct is still reliant on the presence of remnant myocardium. The degree to which the remnant myocardium is linked to the noninfarcted regions has only recently become clearer. Optical mapping studies of rabbit heart 8 weeks post-MI reported electrical signals from scar tissue that were entrained with the surviving myocardium, suggesting active remnant myocytes (Walker et al., 2007; Saba et al., 2008). In addition, mapping of hearts post-MI using electrogram (EGM) measurements revealed scar tissue characterized by low voltage, fractionated potentials in human patients (Cuculich et al., 2011) and canines (Gardner et al., 1985), indicating a degree of residual electrical activity within the scar tissue; albeit with slow, discontinuous, and nonuniform conduction, and thus a potential source of arrhythmogenic pathways (De Bakker et al., 1993; Crawford et al., 2010).

The objective of this study was to examine the electrical activity of a stable MI scar that developed after complete occlusion of a major coronary artery. This represents the most extreme situation clinically, where a minimum of myocardial tissue is expected to survive. Optical techniques were used to measure electrical activity, enabling membrane potential changes to be studied noninvasively. Our data shows distinct structure/function differences between normal zone (NZ), BZ, and IZ areas of myocardium that have not been seen hitherto in intact hearts.

MATERIALS AND METHODS

All procedures were carried out in accordance with the UK Animals (Scientific Procedures) Act 1986 and conformed to the Guide for the Care and Use of Laboratory Animals (National Institutes of Health publication No. 85-23, revised 2011). Ethical approval for all procedures was granted by the local Glasgow University Ethical committee and the UK Home Office. All chemicals were purchased from Sigma-Aldrich, UK unless otherwise stated. Fluorescent dyes were purchased from Biotium (Hayward, CA, United States) and Thermo-Fisher (Waltham, MA, United States).

Animal Model

MI was induced in male Wistar rats (weight 225–250 g, $n = 10$) by permanent ligation of the left anterior descending coronary artery. Four to five weeks post-procedure a clear IZ was produced (**Figure 1A**). An additional six animals were also used for a subset of experiments, bringing the total number of animals used in the study to 16.

Whole-Heart Langendorff Preparation

Four to five weeks after surgery, rats were euthanized by cervical dislocation. The heart was quickly excised and placed in ice-cold modified Tyrode's solution of composition (in mmol/L) 93 NaCl, 20 $NaHCO_3$, 1 Na_2HPO_4, 1 $MgSO_4$, 5 KCl, 1.8 $CaCl_2$, 20 Na-acetate, 20 glucose. Hearts were mounted via the aorta onto a cannula and retrogradely perfused at 9 ml/min using the same Tyrode's solution at 37°C with pH maintained at 7.4 by bubbling with a 95% O_2/5% CO_2 gas mixture. Perfusate was then switched to a Tyrode's solution containing 10 mmol/L 2,3-butanedione monoxime (BDM) and 10 μmol/L blebbistatin (Enzo Life Sciences, Exeter, United Kingdom) to inhibit contraction and minimize movement artifacts. The heart was positioned horizontally in a custom-built Perspex chamber to enable imaging of the left ventricle (LV) (**Figure 1B**). A pseudo-electrocardiogram (ECG) was monitored throughout the experiment using 2 Ag/AgCl disk electrodes placed close to the heart, with a reference electrode placed in the perfusion bath. Two platinum electrodes connected to an isolated stimulator were positioned on the right atrial (RA) appendage to enable pacing of the hearts via the physiological endocardium to epicardium conduction pathway, at a cycle length of 200 ms (5 Hz).

Optical Measurements of Voltage in NZ, BZ, and IZ

Optical measurements were made as described in detail previously (Kelly et al., 2013). Briefly, hearts were loaded with a 50 μL bolus of 2 mM voltage-sensitive dye di-4-ANEPPS

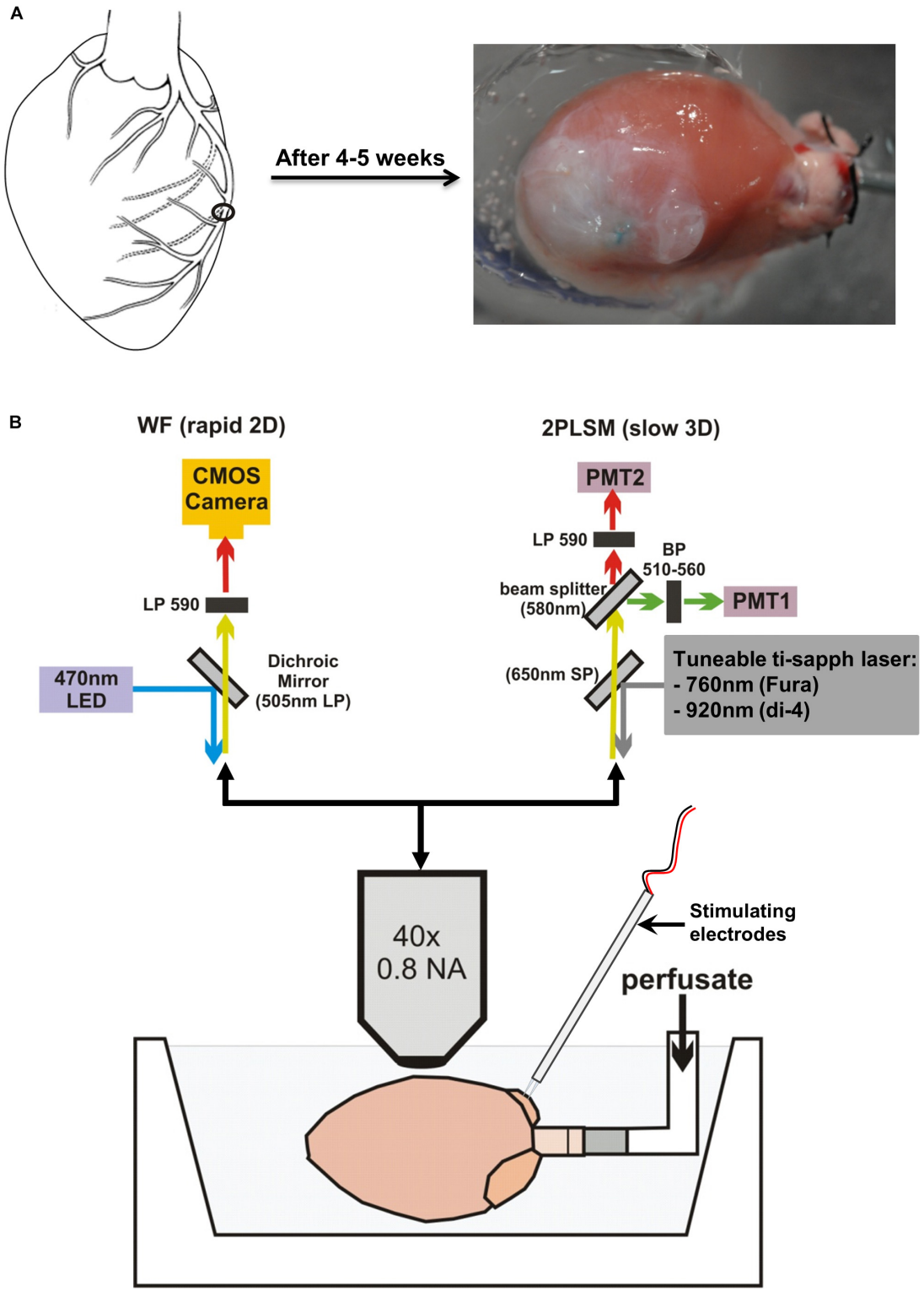

FIGURE 1 | Infarct development and microscope setup. **(A)** Schematic diagram showing the permanent surgical ligation performed on the left anterior descending coronary artery. Four to five weeks post-surgery, a large infarct is produced. **(B)** Langendorff-perfused hearts were positioned horizontally and imaged using an upright microscope. Optical settings were switched between a widefield (WF) system for rapid 2D imaging (top left) and a 2-photon laser scanning microscopy (2PLSM) system for slow 3D imaging (top right).

over a 10 min period. Widefield single-photon epifluorescence recordings from the LV were made using a CardioCMOS-SM128 camera (Redshirt Imaging, Decatur, GA) with a 590 nm long pass emission filter. Excitation was provided by LED light at 470 nm. Image resolution was 128 × 128 pixels/frame, and recordings were made at a frame rate of 2.5 kHz. Two photon (2P) laser scanning microscopy (2PLSM) was carried out using a Zeiss LSM 510 NLO upright microscope (Carl Zeiss, Jena, Germany) equipped with a Ti:Sapphire 690–1080 nm tunable laser (Chameleon Ultra II, Coherent, Santa Clara, CA). These 2P measurements provided a high degree of depth resolution, enabling identification of the discrete tissue layers exhibiting electrical activity (Rubart, 2004). Di-4-ANEPPS was excited at 920 nm, with emission collected by two bi-alkali PMT detectors at 510–560 nm and 590–650 nm, respectively, enabling ratiometric measurements to be made. Line scans, with a scan time of 0.39 ms for short scans and 1.93 ms for long scans, were performed in the direction of cell orientation observed at the epicardial surface. Line scanning was initiated following the arrival of a trigger pulse, synchronized by the electrical stimulus pulse used to pace the hearts. A diagram of the widefield and two photon imaging setup is shown in **Figure 1B**.

Sequential widefield and 2P voltage recordings were made in myocardium remote from the infarct scar in the NZ, in the BZ at the edge of the visible scar, adjacent to the NZ, and within the IZ toward the center of the scar. Widefield electrical mapping using a 10×/0.3 NA objective lens (Carl Zeiss, Jena, Germany) was first used to identify the areas of remnant electrical activity within the BZ and IZ. Widefield electrical mapping was then repeated on regions displaying electrical signals with a 40×/0.8 NA objective (Carl Zeiss, Jena, Germany) to further localize electrically active areas. Finally, structures in the optical plane were imaged using 2P excitation in frame scan mode, then electrical signals recorded using line scan mode at discrete depths below the epicardial surface. A series of recordings were made, starting at 50 μm below the surface and at increasing depths (50–100 μm steps) until the signal-to-noise ratio (S/N) became too low to distinguish a clear action potential (AP) signal. The ability to visualize clear structures decreased at deeper layers; the maximum depth from which discernible images could be obtained depended on the zone, but electrical signals from line scan recordings could always be recorded beyond the layers where structures could be imaged. It was therefore not possible to identify the source of electrical activity directly from images of tissue structure at the deeper layers. A subset of experiments was performed using a modified upright 2P laser scanning setup (Intelligent Imaging Innovations; Denver, CO) utilizing a pair of high sensitivity GaAsP PMT detectors, and using a combination of FluoVolt and Rhod2AM, excited at 840 nm (see **Supplementary Methods** for full details). These were used to verify findings in a higher sensitivity setup.

Determining the Source of Electrical Activity in the Scar

To determine the cellular origin of electrical activity in the scar, measurements of intracellular Ca^{2+} were made in regions where voltage signals were measured by prior loading of the myocardium with Fura-2/AM. If the signals were arising from residual myocytes Ca^{2+} transients (CaTs) would be expected in response to an electrical stimulus. However, if the voltage signals were arising from abnormal myocytes or other cellular entities (i.e., fibroblasts or myofibroblasts), CaTs may not be produced in response to electrical stimulation (Chilton et al., 2007).

Tyrode's solution for these experiments was supplemented with 1 mmol/L probenecid to block anion transporters that excrete Fura-2, thus improving dye retention in the cell (Di Virgilio et al., 1988). Fura-2/AM was prepared as a 1 mmol/L stock in DMSO-pluronic acid F-127 (25% w/v). A 100 μL bolus of dye was injected into a bubble trap in the perfusion line to allow dilution of the dye and slow loading into the heart. Additional boluses of dye were injected if required due to low or time-dependent loss of fluorescence signal. Fura-2/AM was 2P excited at 760 nm, and fluorescence emission was directed through a short-pass 650 nm dichroic mirror and collected at 510–560 nm. Ca^{2+} measurements were made immediately after any voltage signals were detected in the same plane of focus and using the same scan line and 1.93 ms scan time.

Data Analysis and Interpretation

Widefield voltage signals were averaged from 3 × 3 pixel arrays. 2P voltage and Ca^{2+} signals were processed using custom written software that utilized the information from exact cycle length times and line scan rates to align and produce an averaged voltage or Ca^{2+} trace from 25 sequential stimuli (5 s of recordings). AP signal characteristics were analyzed from the averaged trace. These measurements included 10–90% upstroke rise time (TRise) and duration of the AP from 50% activation to 50, 75, and 90% repolarization (APD50, APD75, and APD90, respectively). Activation times were determined as the time of arrival of the AP at that point in the LV wall relative to the time of stimulation.

S/N was calculated as the peak amplitude of the whole trace following a single stimulus pulse (signal) divided by the peak amplitude of the trace during the diastolic period (noise) (**Supplementary Figure S1**). An S/N value of 1 indicated no signal over and above the noise of the baseline. Based on observations of individual traces and corresponding S/N values, an S/N > 1.4, was considered a meaningful transient signal (voltage or Ca^{2+}). All traces with S/N > 1.4 were further scrutinized to rule out artefactual signals produced by movement or noise spikes. All data are expressed as mean ± standard error. Groups of data were compared using Student's *t*-test.

RESULTS

Initial Identification of Areas of Electrical Activity Using Widefield Optics

In the first phase of the protocol, widefield di-4-ANEPPS fluorescence measurements were made within the NZ (**Figure 2A**), BZ (**Figure 3A**), and IZ (**Figure 4A**) with a 10× objective to identify regions of electrical activity over an area of 800 × 800 μm (**Figures 2B**, **3B**, **4B**). This approach was particularly important for measurements within the IZ, as not every recording indicated an electrically active region.

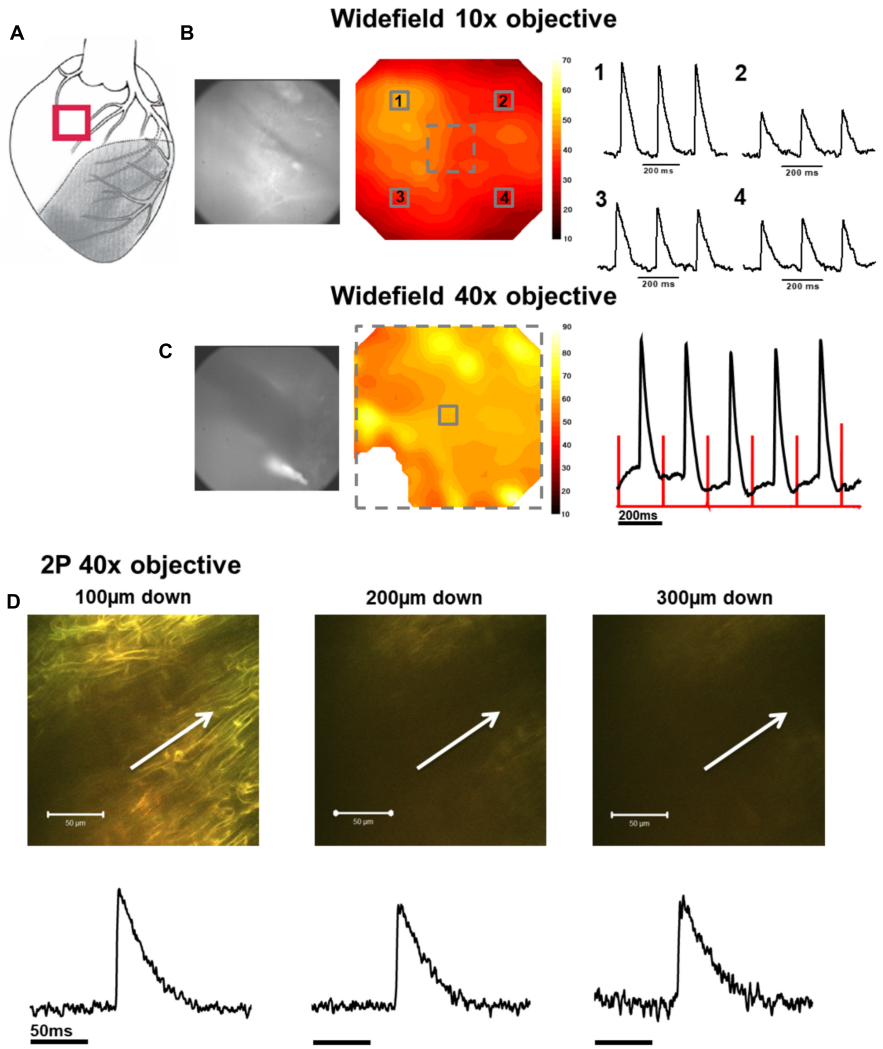

FIGURE 2 | Widefield and 2P signals in the normal zone (NZ). **(A)** Schematic diagram of the infarcted heart. The red square indicates the approximate location of the measurements in the NZ. **(B)** Widefield measurements were first taken from NZ using a 10× objective. CMOS camera image (left) and signal-to-noise ratio contour map (middle) of di-4-ANEPPS fluorescence in the NZ. Line traces on the right show action potentials (APs) from 3 × 3 pixel averaged regions (indicated by numbered solid squares on contour map). **(C)** Measurements were focused to a smaller area using a 40× objective [indicated by the dashed square on contour map in **(B)**]. A CMOS camera (left) image and signal-to-noise ratio contour map (middle) taken from the NZ at 40× magnification. An area in the bottom left of the contour map field was removed due to movement artifact distorting the signal. Right panel: 3 × 3 pixel average of the AP signal in the center of the optical field (defined by the solid square in the contour map). The red lines indicate the timing of the stimulus pulse. **(D)** A series of 2P measurements were made through increasing depth in the same optical field with the 40× objective. Shown here are 2P images and corresponding averaged APs taken (from left to right) 100, 200, and 300 µm below the tissue surface. White arrows in images indicate approximate length and direction of line scans. All the APs shown are an average of 25 APs recorded over a period of ∼5 s.

Contour maps of S/N were constructed to allow comparison of the relative uniformity of the electrical signal in the NZ, BZ, and IZ (**Figures 2B**, **3B**, **4B**, respectively). However, in contrast to NZ and BZ, the IZ displayed only limited regions with AP signals of significant amplitude; large areas of IZ surface had no observable electrical activity (**Figure 4B**).

In the second phase of the protocol, the S/N across a sub-area (250 × 250 µm) of the original field was further examined using a 40× objective (**Figures 2C**, **3C**, **4C**) to pinpoint electrically active regions. In the case of the NZ and the BZ, the relative uniformity of the AP signal recorded with the 10× objective allowed 40× imaging to be made routinely in the center of the field of view. However, due to the nonuniformity of signal in the IZ, the area with the AP signal with the greatest S/N using the 10× objective was chosen for further examination with the 40× objective.

Detailed Examination of Electrical Activity With 2PLSM

In the third phase of the protocol, the variation of the AP signal with depth was examined in a limited central

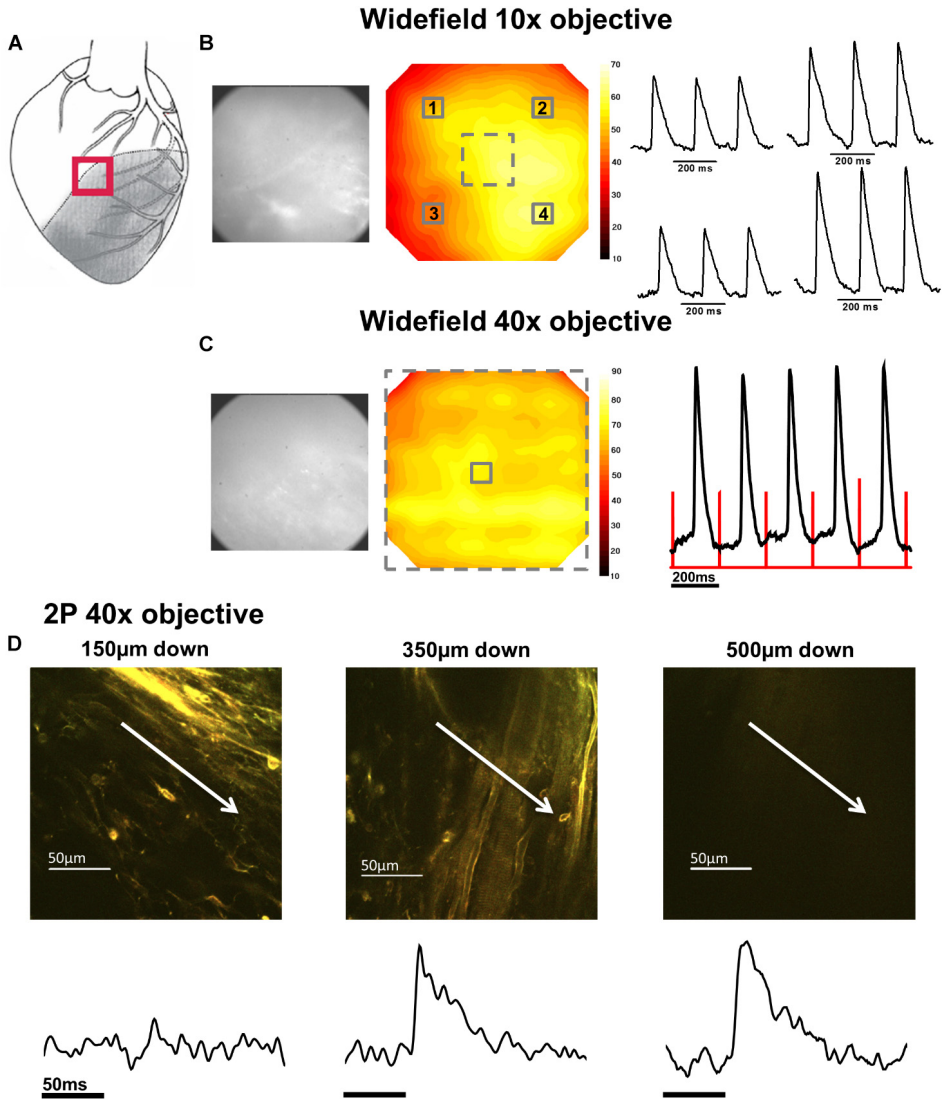

FIGURE 3 | Widefield and 2P signals in the border zone (BZ). **(A)** Schematic diagram of the infarcted heart. The red square indicates the approximate location of the measurements in the BZ. **(B)** Widefield measurements taken from BZ tissue using a 10× objective. From left to right; CMOS camera image of di-4-ANEPPS fluorescence; contour map of di-4-ANEPPS signal-to-noise; 3 × 3 pixel averages (indicated by numbered solid squares in contour map) of action potentials (APs). **(C)** Measurements were then focused to a smaller area using a 40× objective [indicated by the dashed square on contour map in **(B)**]. From left to right; CMOS camera image of di-4-ANEPPS fluorescence in the BZ; Contour map of signal-to-noise in the 40× field of view; 3 × 3 pixel average of the AP signal in the center of the optical field, defined by the solid square in the contour map – red lines indicate timing of the stimulus pulse. A series of 2P measurements were made through increasing depth in the same optical field with the 40× objective. **(D)** 2P images and corresponding voltage measurement taken at (from left to right) 150, 350, and 500 µm below the epicardial surface. Myocardial structures could no longer be identified in 2P images at 500 µm; however, electrical activity was still observed at this depth. White arrows in images indicate approximate length and direction of line scans. All the APs shown are an average of 25 APs recorded over a period of 5 s.

region of the 40× field using 2PLSM. Line scan recordings of APs based on the ratio of di-4-ANEPPS fluorescence were made starting at 50 µm from the epicardial surface and every 50 µm until 500 µm from the surface. In some preparations, the CaT was also recorded from the Fura-2 fluorescence.

AP and CaT Characteristics in NZ

In NZ remote from the infarct, APs had a normal time course at all depths (**Figure 2D**). Myocardial structure and electrical activity could be imaged from 50 µm below the epicardial surface, and AP morphology was unchanged through depth. However, the signals became progressively smaller due to the reduction of fluorescence signal with increasing depth (**Figure 5C**). The limit for recordable images was ∼300 µm, and the limit for AP recordings was ∼500 µm; this was increased to ∼700 µm with the higher sensitivity system. CaT signals, when recorded alongside AP signals, were detected at equivalent depths and were of consistent shape (**Figure 6A**). The amplitude of CaT signal decreased in parallel with

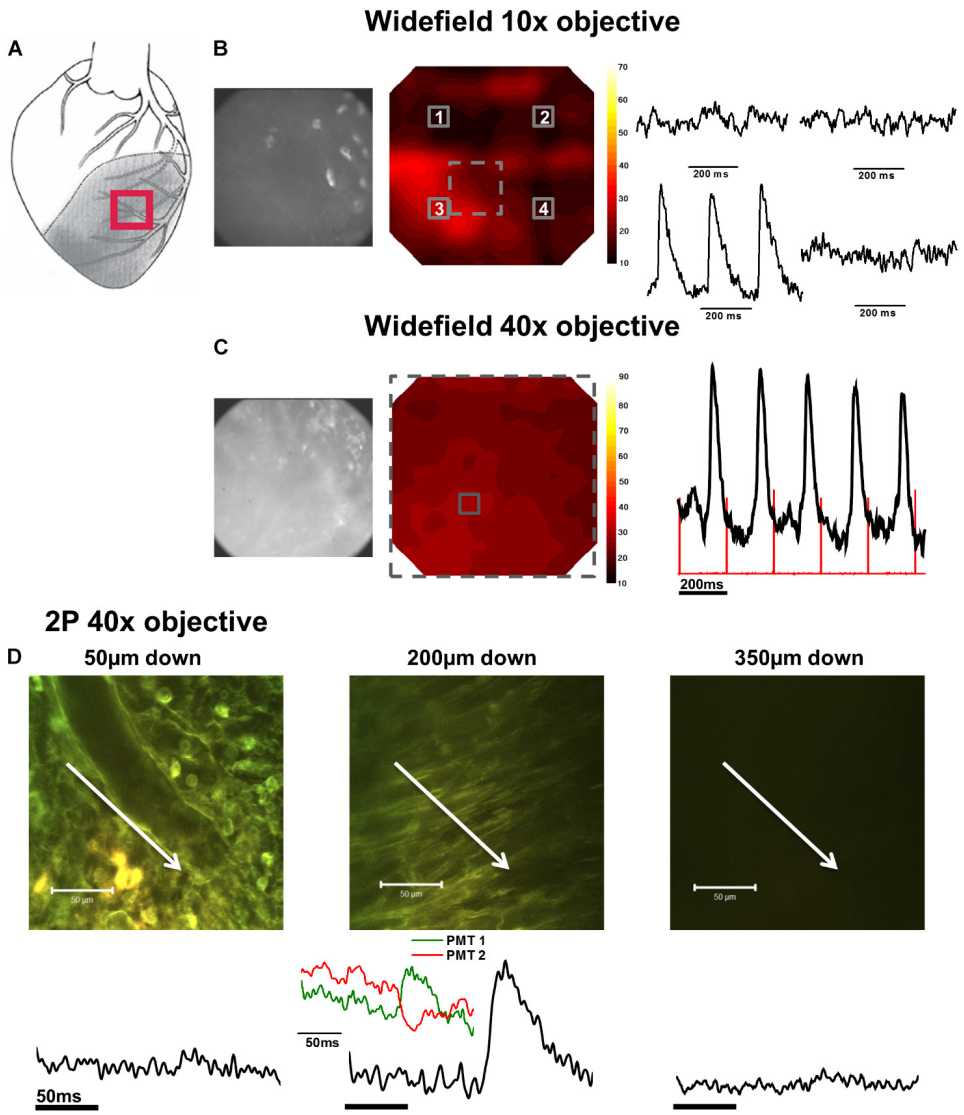

FIGURE 4 | Widefield and 2P signals in the infarct zone (IZ). **(A)** Schematic diagram of the infarcted heart. Red square indicates the approximate location of the measurements in the IZ. **(B)** Widefield measurements taken from the IZ using a 10× objective. From left to right; CMOS camera image of di-4-ANEPPS fluorescence; contour map of di-4-ANEPPS signal-to-noise; 3 × 3 pixel averages (indicated by numbered solid squares in contour map) demonstrated absence of signal in all but one region of the infarct. **(C)** Measurements were then focused to a smaller area using a 40× objective [indicated by the dashed square on the contour map in **(B)**]. From left to right; CMOS camera image of di-4-ANEPPS fluorescence in the IZ; contour map of signal-to-noise in the 40× field of view; 3 × 3 pixel average of the AP signal defined by the solid square in the contour map – red lines indicate timing of the stimulus pulse. **(D)** 2P images and the corresponding voltage signal taken at (from left to right) 50, 200, and 350 µm below the tissue surface. At 200 µm below the tissue surface, tissue structure appears more organized and AP waveforms with slow activation times and upstrokes become apparent from the fluorescence ratio. Closer inspection of the individual PMT signals (inset) demonstrate an increase in fluorescence at the shorter waveband and a decrease in the longer waveband, eliminating the possibility of the fluorescence ratio signal being due to movement artefact. White arrows in images indicate approximate length and direction of line scans. All the APs shown are an average of 25 APs recorded over a period of 5 s.

the AP signal with increasing distance from the epicardial surface.

AP and CaT Characteristics in BZ

Measurements from BZ area, that is, the scar adjacent to the NZ, revealed no AP signals from the layers immediately below the surface (50–100 µm depth), but AP signals were recorded at deeper layers (**Figure 3D**). The exact depth at which electrical signals were first identified varied between preparations but was within the range of 150–300 µm. Normally, AP signals could be detected deeper into the tissue than in the NZ; in two hearts this was up to 1000 µm below the epicardial surface. This indicated that in the scar bordering the NZ, there are layers of connective tissue overlying normal myocardium. The averaged APs recorded in the BZ had a similar time course for repolarization parameters but slower rise times than NZ signals (**Figure 5A**) (3.50 ± 0.50 ms

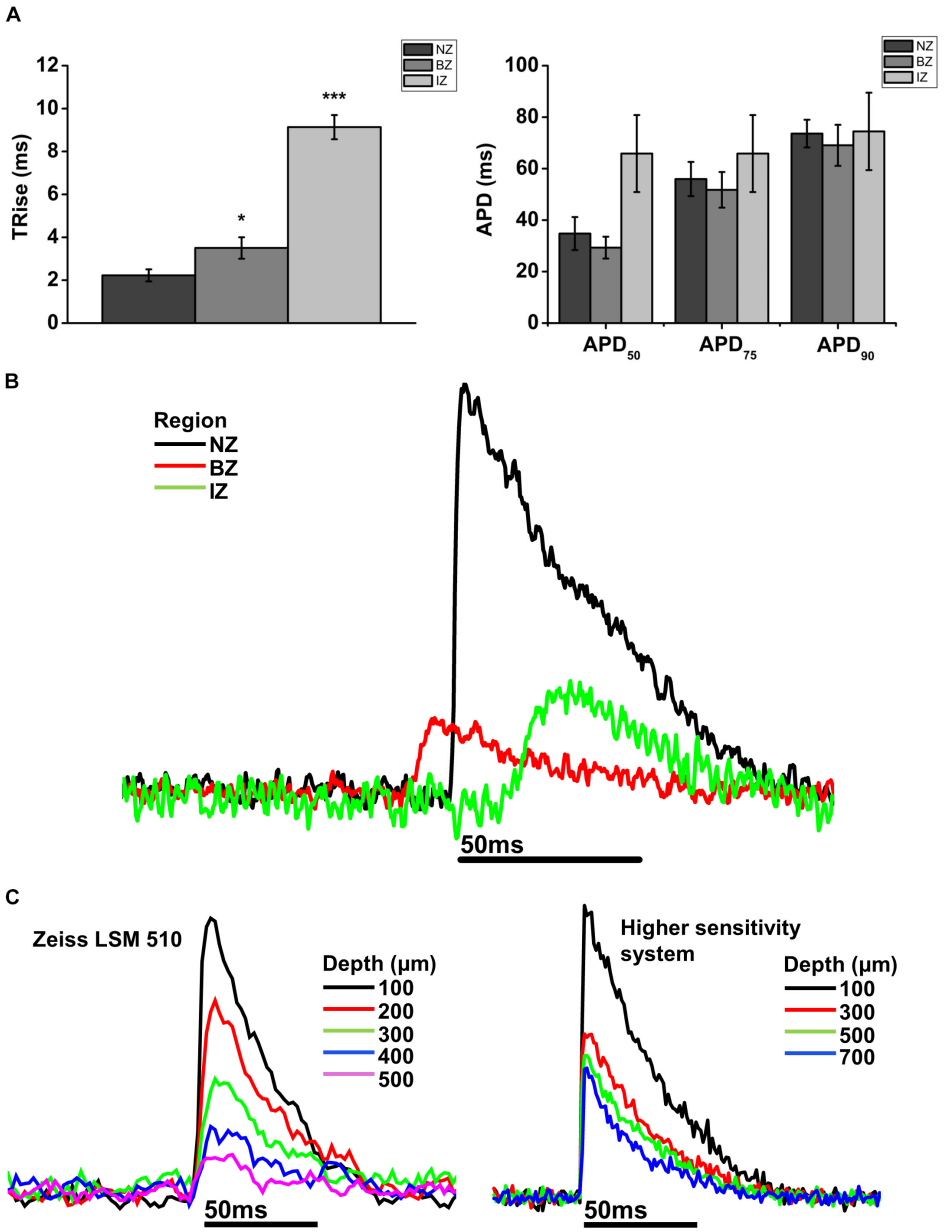

FIGURE 5 | Comparison of AP parameters in normal zone (NZ), border zone (BZ), and infarct zone (IZ). **(A)** Mean 10–90% upstroke rise time (TRise) and mean action potential duration (APD) at 50, 75, and 90% repolarization obtained from 2P signals for each heart in each region. NZ, $n = 6$; BZ, $n = 4$, IZ, $n = 3$. $^{*}p < 0.05$; $^{***}p < 0.001$. **(B)** Representative traces from a rat MI heart showing action potentials recorded using 2PLSM from three imaging zones: Normal zone (NZ), borderzone (BZ), and infarct zone (IZ). AP upstroke was slowed in both BZ and IZ compared to NZ, with no obvious difference in APD. **(C)** Transmural action potentials recorded using two microscope systems: Zeiss LSM 510 (left) and a microscope system featuring optimized detection and optical configuration (right). Note there was no change in AP morphology with either imaging system over the depth range investigated.

vs. 2.23 ± 0.28 ms, $p < 0.05$). This can also be observed in superimposed traces from NZ, BZ, and IZ from an example heart (**Figure 5B**). Activation times were measured from both widefield and 2P AP signals. Widefield measurements of activation delay between NZ and BZ showed no difference (3.36 ± 1.55 ms, $p = 0.41$) indicating absence of a significant activation delay in the BZ. In hearts where CaTs were recorded, the appearance of these signals paralleled AP signals in terms of the depth at which they were detected and the maximum depth that they could be recorded (**Figure 6B**).

AP and CaT Characteristics in IZ

AP and CaT characteristics in IZ were only examined where electrical signals were detected using widefield imaging of di-4-ANEPPS with the 40× objective. This was possible in 5 out of 10 hearts in this configuration. The electrical activity in the

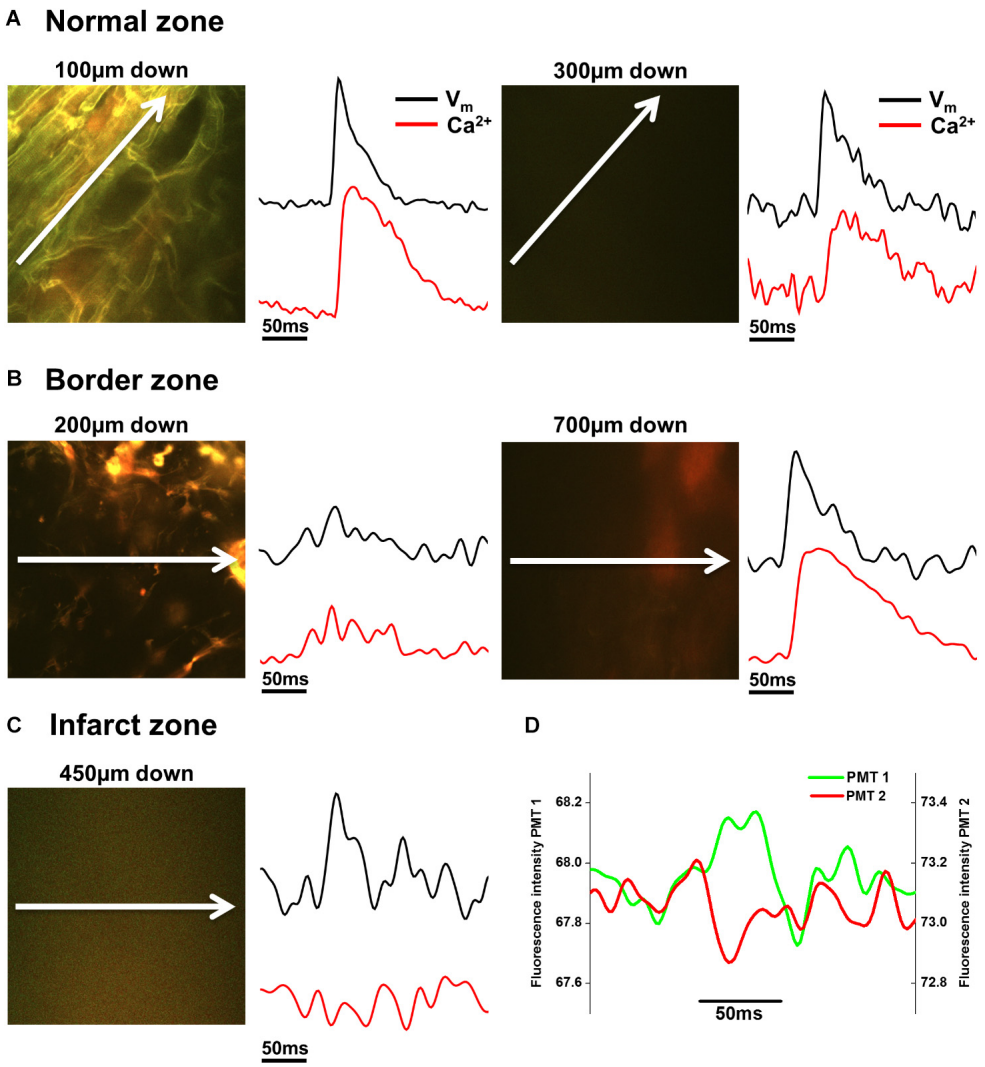

FIGURE 6 | Voltage and Ca^{2+} measurements in normal zone (NZ), border zone (BZ), and infarct zone (IZ). **(A)** 2P image with corresponding voltage (Vm) and intracellular calcium (Ca^{2+}) transients taken from the NZ 100 µm (left panels) and 300 µm (right panels) below the tissue surface. Vm and Ca^{2+} signals were of normal morphology in these areas. **(B)** In the BZ, toward the surface (here at 200 µm down), structures appear to resemble connective tissue and no Vm or Ca^{2+} signals were apparent (left panels). However, deeper into the tissue (700 µm down in this example) fluorescence signal with no defined structures can be detected in the 2P image, and Vm and Ca^{2+} signals with good signal-to-noise were recorded (right panels). **(C)** Within the IZ, in this example, no structures could be resolved in the 2P image at 450 µm down. However, low amplitude voltage signals were detected, with no detectable Ca^{2+} signal in the same region (left panels). **(D)** The individual PMT signals indicate that the voltage signals are not arising from movement artefact, as short and long wavelength signals are not the same. White arrows indicate length and direction of line scan. Vm and Ca^{2+} signals shown are the average of 25 APs/Ca^{2+} transients recorded over a period of 5 s.

IZ differed from that in BZ, as it was only detected in thin layers of tissue approximately 100–300 µm deep and was not found deeper within the tissue (**Figure 4D**). AP morphology was different from that found in NZ (**Figure 5B**), with longer rise times than NZ (9.13 ± 0.56 ms vs. 2.23 ± 0.28 ms, $p < 0.001$; **Figure 5A**). Closer inspection of the fluorescence signals from each channel revealed that this difference in morphology was not due to movement artifact, as the signals collected between 510 and 560 nm (Channel 1) increased upon depolarization but decreased at Channel 2 (collected between 590 and 650 nm), indicating a genuine voltage signal (**Figure 4D** – inset graph in middle panel and **Figure 6D**). Activation times of the widefield signals showed heart-to-heart variation. In two hearts, there were no delays in activation times in IZ relative to NZ. In one heart, there was moderate delay (7 ms) and, in one heart, there was substantial delay (40 ms); mean activation delay was 11.88 ± 9.43 ms. It was not possible to compare activation times in one heart due to differences in the stimulation mode of recordings from NZ and IZ. This variation in activation delay was also observed in the AP signals recorded through depth with 2P excitation. Measurements of AP duration at 50% repolarization (APD_{50}) showed a trend (not significant) toward longer duration in IZ compared to NZ (**Figure 5A**). In contrast to the NZ and BZ, discrete layers within the IZ

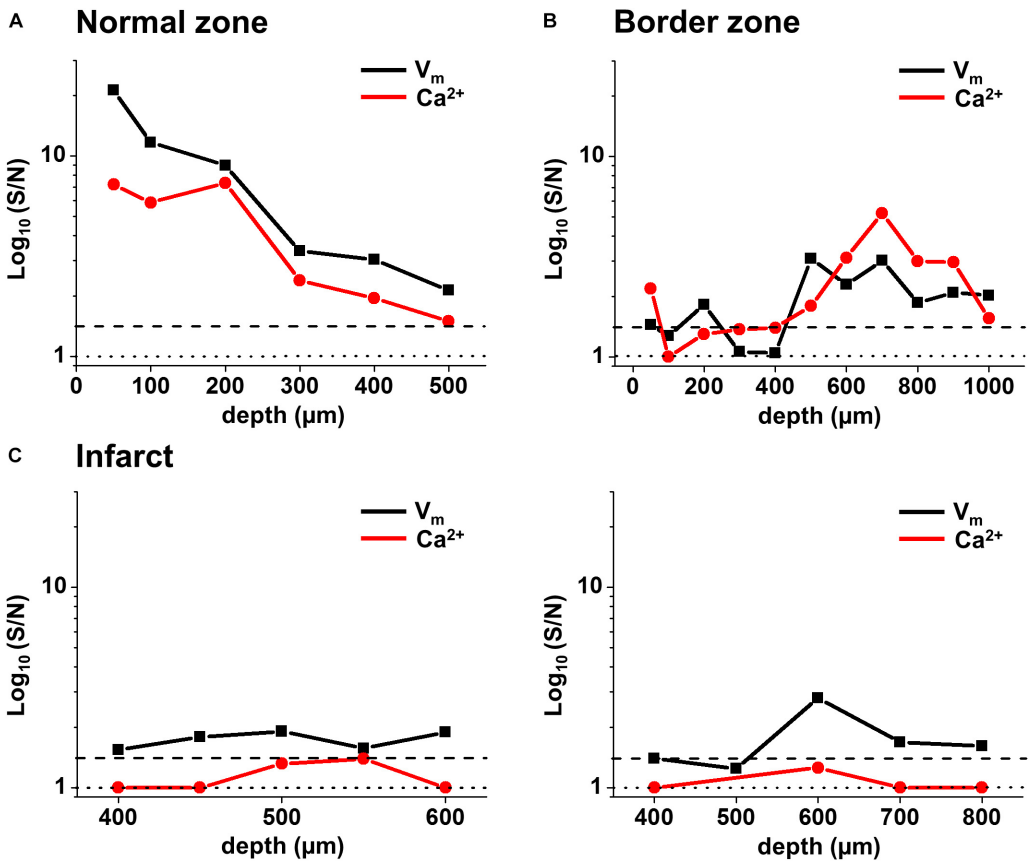

FIGURE 7 | Voltage and Ca^{2+} signal-to-noise in the normal zone (NZ), border zone (BZ), and infarct zone (IZ) from individual hearts. Voltage (black) and Ca^{2+} (red) S/N were plotted through depth for individual hearts in **(A)** NZ, **(B)** BZ, and **(C)** IZ. S/N in the IZ for two hearts [left and right panels in **(C)**] were plotted between depths where a voltage signal was detected. S/N values of 1 (no distinguishable signal) are illustrated by the dotted line. S/N values of 1.4 (indicating a real signal) are illustrated by the dashed line.

at which APs were recorded did not show detectable CaTs (**Figure 6C**).

Signal-to-Noise Profile in the NZ, BZ, and IZ

Values of S/N for voltage and Ca^{2+} signals were plotted against depth for each zone (NZ, BZ, and IZ – **Figure 7**). Plots from a single heart are shown to highlight the characteristics of the signals in the three zones. A distinctive profile of S/N for remote (NZ) tissue was apparent, in which the highest S/N was obtained close to surface, with decreasing S/N through depth. Measurements were not made deeper than 500–600 μm below the surface as the S/N values were close to the detection threshold (1.4). This S/N profile was similar for both voltage and Ca^{2+} signals.

In the BZ, the S/N values of fluorescence signals were <1.4 at the surface indicating the absence of detectable AP signals, but the values of S/N increased deeper into the tissue (to levels similar to those measured in NZ), and remained higher than in remote tissue at 500–1000 μm depth. Again, a similar profile was obtained for both voltage and Ca^{2+}signals. At the deepest layers where no signal could be detected, S/N of recordings was comparable to those obtained in the absence of excitation light (**Supplementary Figures S2A,B**). This indicates that the absence of signal was due to the lack of penetration of excitation light deep into the tissue.

In the IZ, despite a significant widefield signal, the S/N values in the majority of layers were below the value of 1.4 indicating no detectable excitable tissue. However, there were discrete layers within the scar in which voltage S/N exceeded 1.4, but a significant CaT could not be recorded at any of these locations. This profile of S/N was consistent in each of the three zones in all the hearts examined for this study (**Figure 8A**). Very similar results were obtained using a higher sensitivity 2P laser scanning system with improved optics and detector sensitivity (**Figure 8B**). In a subgroup of experiments, improved signal collection allowed significant AP signals to be detected in various subepicardial layers from infarcted tissue in four out of six hearts (**Figure 8B** – top right panel). In a few cases, this improved signal detection also recorded Ca^{2+} transients (s/n ratio > 1.4) in the same layer as an AP. However, for the majority of cases, where an AP was detected within the infarct, no significant Ca^{2+} transient could be detected (**Figure 8B** – bottom right panel). Despite the improved

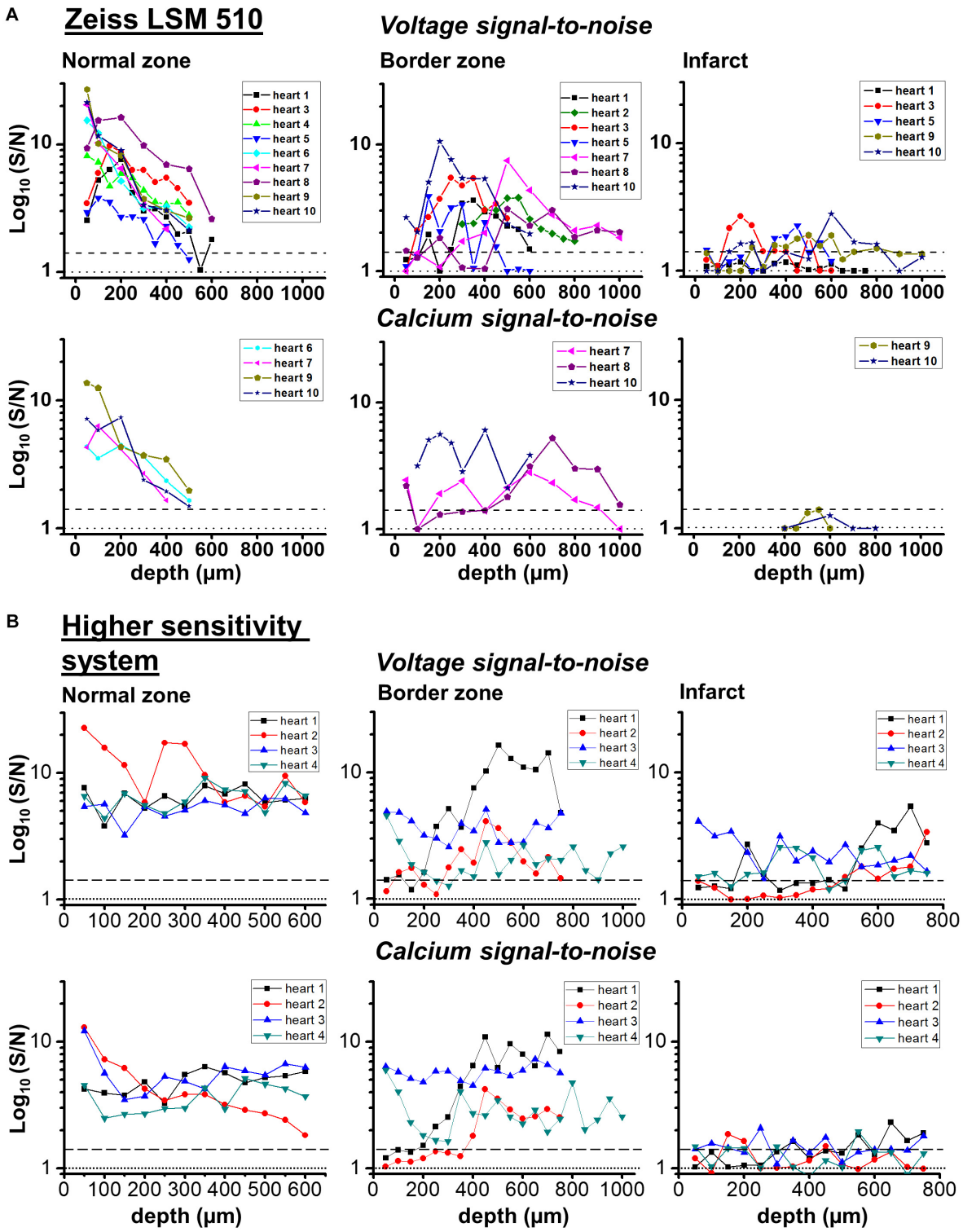

FIGURE 8 | Transmural signal-to-noise in remote, border zone and infarct regions – voltage vs. calcium. S/N values (log10) for voltage (upper row) and calcium (lower row) as a function of tissue depth for individual hearts in two microscope systems: **(A)** Zeiss LSM 510 and **(B)** microscope system featuring optimized detection and optical configuration. From right to left; remote myocardium; border zone; infarct. For border and infarct zones, traces are displayed from hearts which demonstrated significant S/N (>1.4) constituting detection of a signal. Dashed line for each graph indicates threshold for signal detection.

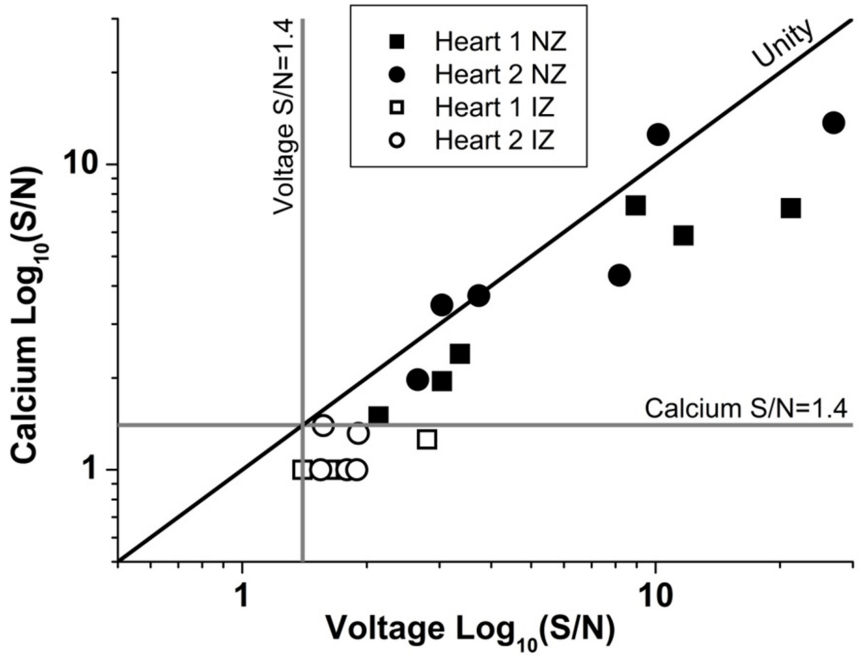

FIGURE 9 | Unity of action potential and calcium transient signal-to-noise. The signal to noise of AP and CaT plotted against one another for two example hearts from normal zone (NZ) (closed symbols) and ischemic zone (IZ – open symbols). CaT signal was on average 76% of the equivalent AP signal at all depths and remained below the detection threshold for calcium signals in the IZ.

transmural AP signal detection afforded using higher sensitivity detectors and an optimized optical configuration, improvement in deep tissue structural imaging was marginal (∼50 μm – data not shown).

DISCUSSION

In this study, optical APs from di-4-ANEPPS fluorescence were recorded from myocardial layers within the homogenous surviving myocardium (NZ), in comparable layers of the scar at the border to the NZ (BZ) and from within the epicardial scar area (IZ). In a sub-group of experiments, the voltage signals were recorded along with intracellular Ca^{2+} signals after loading the heart with Fura-2/AM. The aim of this approach was to identify the cellular origin of the AP using a functional correlate, where conventional imaging would have been unable to resolve structure sufficiently; a voltage signal accompanied by a CaT clearly indicated a myocardial origin of the AP. We hypothesized that a voltage signal with no accompanying CaT suggested that the source of the electrical signal could be substantially modified cardiomyocytes or fibroblasts/myofibroblasts coupled to electrically active cardiomyocytes. From the results presented, we found discrete regions of surviving myocardium within the IZ exhibiting very small voltage signals, but the lack of calcium transient was more likely due to the low S:N ratio of signals arising from such small tissue volumes deep within a scattering structure such as the infarct. Using a higher sensitivity system supported the original findings, with signals only arising from discrete infarct areas and no direct evidence of fibroblast/myofibroblast associated voltage signals.

Characteristics of Signals in Normal Myocardium

As expected, the AP signal in the NZ was homogeneous over the area imaged in widefield and through the depth of the myocardium sampled by the 2P excitation. The S/N of the optical AP decreased with increasing depth due to loss of excitation light power as a consequence of photon scattering in the intervening layers (Kelly et al., 2013; Ghouri et al., 2015), but there were no major changes in AP shape through depth and the activation sequence reflected rapid transmural propagation. In the NZ, voltage signals were detected down to a maximum depth of 500–600 μm below the epicardial surface. In each layer, Ca^{2+} transients accompanied the optical AP even at distances from the epicardial surface where there was insufficient signal to distinguish any structural detail. As shown in **Figure 9**, the S/N of both AP and CaT signals decreased from a value of approximately 30 at the epicardial surface to below the detection threshold (<1.4) at 600 μm. The unity line emphasizes that the S/N of the CaT signal was on average 76% of the equivalent AP signal at all depths (**Figure 9**). These values are a function of the dye loading protocols used in the study.

Characteristics of Signals in the BZ

In the BZ, a layer of electrically inert tissue was present on the epicardial surface of all hearts, although the thickness of this layer varied from heart to heart. The presence of such rim

structures have been reported previously from high resolution histology imaging (Walker et al., 2007). The structure observed from optical sectioning and the lack of electrical activity indicated that this was a layer of connective tissue, which in some hearts was between 300 and 400 μm thick. However, below the connective tissue layer, APs were detected with normal activation times and repolarization characteristics, but with an average time of depolarization that was 150% of the values recorded in the NZ. These electrical signals were recorded at considerably larger distances into the tissue surface than was possible in the NZ (∼1000 μm vs. ∼500 μm). The ability to image and measure optical APs at greater depths is likely due to the lower scatter of excitation light by the upper layers of connective tissue when compared to equivalent layers of compact myocardium (Mourant et al., 1998). Optical properties of normal and infarcted myocardium have been compared previously using tissue from human patients, indicating that infarct scar exhibits a significantly lower scattering coefficient compared to normal healthy myocardium (Splinter et al., 1991).

The voltage signals in the BZ were accompanied by Ca^{2+} transients at all depths. These results are consistent with histological studies of the infarct structure demonstrating the presence of a wedge of myocardium projecting approximately 1 mm into the scar beneath superficial layers of connective tissue in BZ regions (Walker et al., 2007). This increases the apparent size of the scar at the epicardial surface, but covering a volume of tissue in the mid-myocardium with relatively normal histological appearance. Increased thickness of the epicardium has been described in response to MI (Smart et al., 2011; Zhou et al., 2011; Tian et al., 2015), along with the formation of epicardium-derived cells that have both fibroblast and smooth muscle markers. These cells release angiogenic factors to stimulate the recovery of the tissue from infarction. The myocardium below the scar in the BZ had APs with a lower rate of depolarization, suggesting altered excitability of this area of myocardium either through electrical remodeling (i.e., altered sodium current and/or gap-junction function) or altered activation sequence. Walker et al. (2007) reported slowed epicardial conduction at the BZ in response to epicardial stimulation which would be consistent with the slowed AP rise-time observed in these studies. As shown previously, the rate of rise of the AP depends critically on the direction of propagation (Spach et al., 1992; Kelly et al., 2013); APs propagating longitudinally through epicardial tissue along the fiber axis have a slower rate of rise of AP due to reduced resistance of the downstream electrical network when compared to transverse propagation.

Characteristics of Signals in the Infarct

In the IZ, only discrete areas of AP signals were identified with widefield imaging of the epicardial surface of the scar. The AP signals in the IZ were entrained to the stimulus, but the range of activation delays were higher than NZ and BZ, suggesting low conduction velocity and/or altered electrophysiology of the remnant myocardium within the scar. This supports previous findings of low conduction velocity and reduced AP amplitude that has previously been described in optical mapping studies of rabbit hearts post-MI (Saba et al., 2008). The APs recorded were of similar duration to NZ and BZ but with significantly longer rise times (∼400% compared to NZ) indicating altered excitability of this myocardium either through electrical remodeling (i.e., altered sodium current and/gap-junction function) or altered activation sequence. Unlike in the BZ, the electrically active regions of the IZ only occurred in a limited layer (100–300 μm), which suggests that the strands of surviving myocardium remain coupled to the surviving myocardium, despite their narrow dimensions.

The S/N of APs recorded from the IZ was considerably lower than at equivalent depths of NZ or BZ. This supports the idea that the recordings originate from small, possibly sparse layers of myocytes; 2P images from layers of the IZ containing AP signals showed no structural evidence of myocardium (e.g., striated tissue) and were indistinguishable from IZ layers without electrical signals. The average S/N of AP signals in the IZ was 1.75, based on the parallel recording of CaT within the rest of the myocardium (**Figure 8**); these signals would be expected to be accompanied by CaT with an S/N value of approximately 1.3, that is, lower than the threshold for signal detection. This relationship is demonstrated in **Figure 9** and indicates that the values of the AP and CaT signals from the IZ had the same relative values to that in NZ, therefore the absence of detectable CaT signals in the IZ was most likely to be a function of the low amplitude di-4-ANEPPS and Fura-2 signals originating from small volumes of myocardium. Using a higher sensitivity system with improved optics and dyes enabled electrophysiological signal detection from deeper layers in both the remote myocardium (up to 700 μm) and the infarct tissue (up to 1200 μm), revealing a population of cells within the infarct which exhibited resolvable Ca^{2+} transients (**Figure 8B**). However, the majority of AP signals arising from the infarct were not accompanied by a Ca^{2+} transient signal.

Implications for Whole Heart Function After Myocardial Infarction

This study establishes the electrical features of myocardium on the border to the infarct and the remnant myocardium within the IZ. The combined approach of widefield and 2PLSM techniques provides new insight into the presence, abnormality, and transmural localization of functional remnant tissue within and around the scar, increasing our understanding of the potential functional consequences of this activity. Recent studies have highlighted the potential role of fibroblasts/myofibroblasts coupled to surviving myocardium as supporting electrical conduction across the infarct scar (Mahoney et al., 2016). Using a transgenic mouse model with fibroblast-specific Cx43 knockout, Mahoney et al. (2016) reported loss of electrical conduction through ventricular infarct scar tissue in the absence of Cx43 expression in fibroblasts, suggesting that fibroblast coupling is essential for remnant electrical conduction through infarcted myocardium. It is known, however, that fibroblasts can only sustain electrical conduction across a finite distance (approximately 300 μm) (Gaudesius et al., 2003), suggesting that coupled fibroblasts alone would not support electrical propagation in an infarct much larger than this. The combined

presence of remnant myocardium coupled to fibroblasts could therefore be critical in bridging the gap between infarct scar and the normal, noninfarcted tissue, particularly in larger infarcts.

The nonstandard electrical activity adjacent to the surviving myocardium may increase the propensity for arrhythmic behavior by providing regions of electrical heterogeneity in terms of AP characteristics and electrical load. Conversely, the presence of entrained electrical activity within the scar may also be beneficial since conduction within the IZ may prevent a pattern of electrical activation that conducts around an electrically inert region and thus creating the potential for re-entry circuits. Furthermore, this study suggests that even in the situation where the coronary artery is occluded, and the downstream tissue is exposed to complete ischemia, 5 weeks post-MI there are still areas of the IZ with significant remnant myocardium electrically coupled to the surviving myocardium. Identifying these regions containing electrically active remnant myocardium will be important to the success of efforts to repopulate an infarct scar with myocardium using stem-cell derived cardiomyocytes (Laflamme et al., 2007; Templin et al., 2012). Directing the implanted cells toward target regions of the infarct where entrained electrical activity persists could increase the prospect of these cells synchronizing electrically with the surviving myocardium. Indeed, 2PLSM measurements of voltage and Ca^{2+} could prove a useful tool for assessing if implanted cells have formed a functional syncytium with the pre-existing myocardium (Lu and Rubart, 2014; Weinberger et al., 2016).

A limitation of the study was the inability of the optical system to provide sufficient information to allow unequivocal identification of the tissue responsible for the electrical activity arising in the IZ. The 2P excitation mode was able to image the region of myocardium directly below the thick connective tissue layer in the BZ at approximately 500μm from the epicardial surface. However, there were no obvious myocardial structures in regions of the IZ that displayed electrical activity compared to regions that did not. This may be explained by the very small amount of myocardial tissue that generates this signal and/or the distortion of the geometry of the tissue within the infarct. Despite also using a system with improved optics and enhanced signal detection capabilities, resolution of structures within the infarct and normal myocardium was only marginally improved (an increase in structural imaging depth by ∼50 μm). For future studies, mapping of the infarct and BZ regions using a modified functional approach as outlined in this study, combined with subsequent tissue clarification and structural imaging of the same regions in the optically cleared tissue using cell labels may be required to positively identify the cellular structures within the IZ responsible for the remnant electrical activity (Chudakov et al., 2010).

CONCLUSION

The use of 2PLSM has demonstrated myocardial sub-surface functional electrophysiological differences between infarcted, near-infarcted, and noninfarcted regions of the intact MI heart that could not be ascertained by other means. This study has demonstrated that BZ of the infarct consists of an electrically inert scar above relatively normal myocardium and that IZ includes discrete layers displaying entrained APs, but with altered electrophysiology.

AUTHOR CONTRIBUTIONS

IG completed the majority of the experimental work and analysis and contributed to drafting and proofreading the manuscript. AK completed some of the experimental work and analysis and contributed to drafting and proofreading the manuscript. SS and KG completed the supplementary experimental work and analysis. TS complete the supplementary experimental work and analysis and drafting of manuscript. O-JK assisted in planning the study, in experimental work, and editing the text of the manuscript. GS planned the study, assisted in experimental work and some analysis, drafted the manuscript and diagrams.

FUNDING

This work was supported by a European Union Framework Programme 7 grant (Grant No. HEALTH-F2-2009-241526) and a British Heart Foundation project grant (Grant No. PG/09/107). AK is funded by a British Heart Foundation project grant (Grant No. PG/17/12/32847). SS is funded by the Norwegian Council for Cardiac Research.

ACKNOWLEDGMENTS

The authors would like to thank Aileen Rankin and Mike Dunne for their expert technical assistance. The authors would also like to thank Dr. Francis Burton for his assistance with data analysis.

SUPPLEMENTARY MATERIAL

The Supplementary Material for this article can be found online at: https://www.frontiersin.org/articles/10.3389/fphys.2018.01454/full#supplementary-material

REFERENCES

Benamer, N., Vasquez, C., Mahoney, V. M., Steinhardt, M. J., Coetzee, W. A., and Morley, G. E. (2013). Fibroblast KATP currents modulate myocyte electrophysiology in infarcted hearts. *AJP Heart Circ. Physiol.* 304, H1231–H1239. doi: 10.1152/ajpheart.00878.2012

Camelliti, P., Devlin, G. P., Matthews, K. G., Kohl, P., and Green, C. R. (2004). Spatially and temporally distinct expression of fibroblast connexins after sheep

ventricular infarction. *Cardiovasc. Res.* 62, 415–425. doi: 10.1016/j.cardiores.2004.01.027

Chilton, L., Giles, W. R., and Smith, G. L. (2007). Evidence of intercellular coupling between co-cultured adult rabbit ventricular myocytes and myofibroblasts. *J. Physiol.* 583, 225–236. doi: 10.1113/jphysiol.2007.135038

Chudakov, D., Matz, M., Lukyanov, S., and Lukyanov, K. (2010). Fluorescent proteins and their applications in imaging living cells and tissues. *Physiol. Rev.* 90, 1103–1163. doi: 10.1152/physrev.00038.2009

Cleutjens, J. P. M., Blankesteijn, W. M., Daemen, M. J. A. P., and Smits, J. F. M. (1999). The infarcted myocardium: simply dead tissue, or a lively target for therapeutic interventions. *Cardiovasc. Res.* 44, 232–241. doi: 10.1016/S0008-6363(99)00212-6

Crawford, T., Cowger, J., Desjardins, B., Kim, H. M., Good, E., Jongnarangsin, K., et al. (2010). Determinants of postinfarction ventricular tachycardia. *Circ. Arrhythmia Electrophysiol.* 3, 624–631. doi: 10.1161/CIRCEP.110.945295

Cuculich, P. S., Zhang, J., Wang, Y., Desouza, K. A., Vijayakumar, R., Woodard, P. K., et al. (2011). The electrophysiological cardiac ventricular substrate in patients after myocardial infarction: noninvasive characterization with electrocardiographic imaging. *J. Am. Coll. Cardiol.* 58, 1893–1902. doi: 10.1016/j.jacc.2011.07.029

De Bakker, J. M. T., Van Capelle, F. J. L., Janse, M. J., Tasseron, S., Vermeulen, J. T., De Jonge, N., et al. (1993). Slow conduction in the infarcted human heart: "Zigzag" course of activation. *Circulation* 88, 915–926. doi: 10.1161/01.CIR.88.3.915

Di Virgilio, F., Fasolato, C., and Steinberg, T. H. (1988). Inhibitors of membrane transport system for organic anions block fura-2 excretion from PC12 and N2A cells. *Biochem. J.* 256, 959–963. doi: 10.1042/bj2560959

Gardner, P. I., Ursell, P. C., Fenoglio, J. J., and Wit, A. L. (1985). Electrophysiologic and anatomic basis for fractionated electrograms recorded from healed myocardial infarcts. *Circulation* 72, 596–611. doi: 10.1161/01.CIR.72.3.596

Gaudesius, G., Miragoli, M., Thomas, S. P., and Rohr, S. (2003). Coupling of cardiac electrical activity over extended distances by fibroblasts of cardiac origin. *Circ. Res.* 93, 421–428. doi: 10.1161/01.RES.0000089258.40661.0C

Ghouri, I. A., Kelly, A., Burton, F. L., Smith, G. L., and Kemi, O. J. (2015). 2-photon excitation fluorescence microscopy enables deeper high-resolution imaging of voltage and Ca2 + in intact mice, rat, and rabbit hearts. *J. Biophoton.* 8, 112–123. doi: 10.1002/jbio.201300109

Goergen, C. J., Chen, H. H., Sakadžić, S., Srinivasan, V. J., and Sosnovik, D. E. (2016). Microstructural characterization of myocardial infarction with optical coherence tractography and two-photon microscopy. *Physiol. Rep.* 4, 1–10. doi: 10.14814/phy2.12894

Kelly, A., Ghouri, I. A., Kemi, O. J., Bishop, M. J., Bernus, O., Fenton, F. H., et al. (2013). Subepicardial action potential characteristics are a function of depth and activation sequence in isolated rabbit hearts. *Circ. Arrhythmia Electrophysiol.* 6, 809–817. doi: 10.1161/CIRCEP.113.000334

Laflamme, M. A., Chen, K. Y., Naumova, A. V., Muskheli, V., Fugate, J. A., Dupras, S. K., et al. (2007). Cardiomyocytes derived from human embryonic stem cells in pro-survival factors enhance function of infarcted rat hearts. *Nat. Biotechnol.* 25, 1015–1024. doi: 10.1038/nbt1327

Lodge-Patch, I. (1951). The ageing of cardiac infarcts, and its influence on cardiac rupture. *Br. Heart J.* 13, 37–42. doi: 10.1136/hrt.13.1.37

Lu, X. L., and Rubart, M. (2014). Micron-scale voltage and [Ca2 +]i imaging in the intact heart. *Front. Physiol.* 5:451. doi: 10.3389/fphys.2014.00451

Mahoney, V. M., Mezzano, V., Mirams, G. R., Maass, K., Li, Z., Cerrone, M., et al. (2016). Connexin43 contributes to electrotonic conduction across scar tissue in the intact heart. *Sci. Rep.* 6:26744. doi: 10.1038/srep26744

Maxwell, M. P., Hearse, D. J., and Yellon, D. M. (1987). Species variation in the coronary collateral circulation during regional myocardial ischaemia: a critical determinant of the rate of evolution and extent of myocardial infarction. *Cardiovasc. Res.* 21, 737–746. doi: 10.1093/cvr/21.10.737

Mourant, J. R., Freyer, J. P., Hielscher, A. H., Eick, A. A., Shen, D., and Johnson, T. M. (1998). Mechanisms of light scattering from biological cells relevant to noninvasive optical-tissue diagnostics. *Appl. Opt.* 37, 3586–3593. doi: 10.1364/AO.37.003586

Nguyen, T. P., Xie, Y., Garfinkel, A., Qu, Z., and Weiss, J. N. (2012). Arrhythmogenic consequences of myofibroblastmyocyte coupling. *Cardiovasc. Res.* 93, 242–251. doi: 10.1093/cvr/cvr292

Rog-Zielinska, E. A., Norris, R. A., Kohl, P., and Markwald, R. (2016). The Living scar - cardiac fibroblasts and the injured heart. *Trends Mol. Med.* 22, 99–114. doi: 10.1016/j.molmed.2015.12.006

Rohr, S. (2009). Myofibroblasts in diseased hearts: new players in cardiac arrhythmias? *Heart Rhythm.* 6, 848–856. doi: 10.1016/j.hrthm.2009.02.038

Rubart, M. (2004). Two-photon microscopy of cells and tissue. *Circ. Res.* 95, 1154–1166. doi: 10.1161/01.RES.0000150593.30324.42

Rubart, M., Tao, W., Lu, X. L., Conway, S. J., Reuter, S. P., Lin, S. F., et al. (2018). Electrical coupling between ventricular myocytes and myofibroblasts in the infarcted mouse heart. *Cardiovasc. Res.* 114, 389–400. doi: 10.1093/cvr/cvx163

Saba, S., Mathier, M. A., Mehdi, H., Liu, T., Choi, B. R., London, B., et al. (2008). Dual-dye optical mapping after myocardial infarction: does the site of ventricular stimulation alter the properties of electrical propagation? *J. Cardiovasc. Electrophysiol.* 19, 197–202. doi: 10.1111/j.1540-8167.2007.00998.x

Smart, N., Bollini, S., Dubé, K. N., Vieira, J. M., Zhou, B., Davidson, S., et al. (2011). De novo cardiomyocytes from within the activated adult heart after injury. *Nature* 474, 640–644. doi: 10.1038/nature10188

Spach, M. S., Heidlage, J. F., Darken, E. R., Hofer, E., Raines, K. H., and Starmer, C. F. (1992). Cellular Vmax reflects both membrane properties and the load presented by adjoining cells. *Am. J. Physiol.* 263, H1855–H1863.

Splinter, R., Svenson, R. H., Littmann, L., Tuntelder, J. R., Chuang, C. H., Tatsis, G. P., et al. (1991). Optical properties of normal, diseased, and laser photocoagulated myocardium at the Nd: YAG wavelength. *Lasers Surg. Med.* 11, 117–124. doi: 10.1002/lsm.1900110205

Sun, Y., Kiani, M. F., Postlethwaite, A. E., and Weber, K. T. (2002). Infarct scar as living tissue. *Basic Res. Cardiol.* 97, 343–347. doi: 10.1007/s00395-002-0365-8

Templin, C., Zweigerdt, R., Schwanke, K., Olmer, R., Ghadri, J.-R., Emmert, M. Y., et al. (2012). Transplantation and tracking of human-induced pluripotent stem cells in a pig model of myocardial infarction: assessment of cell survival, engraftment, and distribution by hybrid single photon emission computed tomography/computed tomography of sodium Iod. *Circulation* 126, 430–439. doi: 10.1161/CIRCULATIONAHA.111.087684

Tian, X., Pu, W. T., and Zhou, B. (2015). Cellular origin and developmental program of coronary angiogenesis. *Circ. Res.* 116, 515–530. doi: 10.1161/CIRCRESAHA.116.305097

Van Den Borne, S. W. M., Diez, J., Blankesteijn, W. M., Verjans, J., Hofstra, L., and Narula, J. (2010). Myocardial remodeling after infarction: the role of myofibroblasts. *Nat. Rev. Cardiol.* 7, 30–37. doi: 10.1038/nrcardio.2009.199

Vasquez, C., Mohandas, P., Louie, K. L., Benamer, N., Bapat, A. C., and Morley, G. E. (2010). Enhanced fibroblast-myocyte interactions in response to cardiac injury. *Circ. Res.* 107, 1011–1020. doi: 10.1161/CIRCRESAHA.110.227421

Walker, N. L., Burton, F. L., Kettlewell, S., Smith, G. L., and Cobbe, S. M. (2007). Mapping of epicardial activation in a rabbit model of chronic myocardial infarction: response to atrial, endocardial and epicardial pacing. *J. Cardiovasc. Electrophysiol.* 18, 862–868. doi: 10.1111/j.1540-8167.2007.00858.x

Weinberger, F., Breckwoldt, K., Pecha, S., Kelly, A., Geertz, B., Starbatty, J., et al. (2016). Cardiac repair in guinea pigs with human engineered heart tissue from induced pluripotent stem cells. *Sci. Transl. Med.* 8:363ra148.

Zhou, B., Honor, L. B., He, H., Qing, M., Oh, J. H., Butterfield, C., et al. (2011). Adult mouse epicardium modulates myocardial injury by secreting paracrine factors. *J. Clin. Invest.* 121, 1894–1904. doi: 10.1172/JCI45529

Zlochiver, S., Muñoz, V., Vikstrom, K. L., Taffet, S. M., Berenfeld, O., and Jalife, J. (2008). Electrotonic myofibroblast-to-myocyte coupling increases propensity to reentrant arrhythmias in two-dimensional cardiac monolayers. *Biophys. J.* 95, 4469–4480. doi: 10.1529/biophysj.108.136473

Conflict of Interest Statement: The authors declare that the research was conducted in the absence of any commercial or financial relationships that could be construed as a potential conflict of interest.

frontiers in Physiology

CORRECTION
published: 05 April 2019
doi: 10.3389/fphys.2019.00364

Corrigendum: Characterization of Electrical Activity in Post-myocardial Infarction Scar Tissue in Rat Hearts Using Multiphoton Microscopy

*Iffath A. Ghouri[1], Allen Kelly[1], Simona Salerno[2], Karin Garten[2], Tomas Stølen[2], Ole-Johan Kemi[1] and Godfrey L. Smith[1]**

[1] Institute of Cardiovascular & Medical Sciences, University of Glasgow, Glasgow, United Kingdom, [2] Department of Circulation and Medical Imaging, St. Olav's Hospital, Norwegian University of Science and Technology, Trondheim, Norway

Keywords: myocardial infarction, optical mapping, two-photon microscopy, intracellular calcium, border zone

A Corrigendum on

Characterization of Electrical Activity in Post-myocardial Infarction Scar Tissue in Rat Hearts Using Multiphoton Microscopy
by Ghouri, I. A., Kelly, A., Salerno, S., Garten, K., Stølen, T., Kemi, O.-J., et al. (2018). Front. Physiol. 9:1454. doi: 10.3389/fphys.2018.01454

"Ole-Johan Kemi" was not included as an author in the published article. The corrected Author Contributions Statement and Acknowledgments Statement appears below.

AUTHOR CONTRIBUTIONS

IG completed the majority of the experimental work and analysis and contributed to drafting and proofreading the manuscript. AK completed some of the experimental work and analysis and contributed to drafting and proofreading the manuscript. SS and KG completed the supplementary experimental work and analysis. TS complete the supplementary experimental work and analysis and drafting of manuscript. O-JK assisted in planning the study, in experimental work, and editing the text of the manuscript. GS planned the study, assisted in experimental work and some analysis, drafted the manuscript and diagrams.

ACKNOWLEDGMENTS

The authors would like to thank Aileen Rankin and Mike Dunne for their expert technical assistance. The authors would also like to thank Dr. Francis Burton for his assistance with data analysis.

The authors apologize for this error and state that this does not change the scientific conclusions of the article in any way. The original article has been updated.

OPEN ACCESS

Approved by:
Frontiers in Physiology, Frontiers Media SA, Switzerland

***Correspondence:**
Godfrey L. Smith
godfrey.smith@glasgow.ac.uk

Specialty section:
This article was submitted to Cardiac Electrophysiology, a section of the journal Frontiers in Physiology

Received: *12 March 2019*
Accepted: *14 March 2019*
Published: *05 April 2019*

Citation:
Ghouri IA, Kelly A, Salerno S, Garten K, Stølen T, Kemi O-J and Smith GL (2019) Corrigendum: Characterization of Electrical Activity in Post-myocardial Infarction Scar Tissue in Rat Hearts Using Multiphoton Microscopy. Front. Physiol. 10:364. doi: 10.3389/fphys.2019.00364

frontiers in Physiology

ORIGINAL RESEARCH
published: 23 August 2018
doi: 10.3389/fphys.2018.01194

Ca^{2+} Cycling Impairment in Heart Failure Is Exacerbated by Fibrosis: Insights Gained From Mechanistic Simulations

*Maria T. Mora[1], Jose M. Ferrero[1], Juan F. Gomez[1], Eric A. Sobie[2] and Beatriz Trenor[1]**

[1] Centro de Investigación e Innovación en Bioingeniería, Universitat Politècnica de València, Valencia, Spain, [2] Department of Pharmacological Sciences, Icahn School of Medicine at Mount Sinai, New York, NY, United States

Heart failure (HF) is characterized by altered Ca^{2+} cycling, resulting in cardiac contractile dysfunction. Failing myocytes undergo electrophysiological remodeling, which is known to be the main cause of abnormal Ca^{2+} homeostasis. However, structural remodeling, specifically proliferating fibroblasts coupled to myocytes in the failing heart, could also contribute to Ca^{2+} cycling impairment. The goal of the present study was to systematically analyze the mechanisms by which myocyte–fibroblast coupling could affect Ca^{2+} dynamics in normal conditions and in HF. Simulations of healthy and failing human myocytes were performed using established mathematical models, and cells were either isolated or coupled to fibroblasts. Univariate and multivariate sensitivity analyses were performed to quantify effects of ion transport pathways on biomarkers computed from intracellular [Ca^{2+}] waveforms. Variability in ion channels and pumps was imposed and populations of models were analyzed to determine effects on Ca^{2+} dynamics. Our results suggest that both univariate and multivariate sensitivity analyses are valuable methodologies to shed light into the ionic mechanisms underlying Ca^{2+} impairment in HF, although differences between the two methodologies are observed at high parameter variability. These can result from either the fact that multivariate analyses take into account ion channels or non-linear effects of ion transport pathways on Ca^{2+} dynamics. Coupling either healthy or failing myocytes to fibroblasts decreased Ca^{2+} transients due to an indirect sink effect on action potential (AP) and thus on Ca^{2+} related currents. Simulations that investigated restoration of normal physiology in failing myocytes showed that Ca^{2+} cycling can be normalized by increasing SERCA and L-type Ca^{2+} current activity while decreasing Na^{+}–Ca^{2+} exchange and SR Ca^{2+} leak. Changes required to normalize APs in failing myocytes depended on whether myocytes were coupled to fibroblasts. In conclusion, univariate and multivariate sensitivity analyses are helpful tools to understand how Ca^{2+} cycling is impaired in HF and how this can be exacerbated by coupling of myocytes to fibroblasts. The design of pharmacological actions to restore normal activity should take into account the degree of fibrosis in the failing heart.

Keywords: calcium handling, heart failure, fibrosis, sensitivity analysis, electrophysiology

OPEN ACCESS

Edited by:
Elisabetta Cerbai, Università degli Studi di Firenze, Italy

Reviewed by:
Wayne Rodney Giles, University of Calgary, Canada
Stefan Dhein, Leipzig University, Germany

****Correspondence:***
Beatriz Trenor
btrenor@eln.upv.es

Specialty section:
This article was submitted to Cardiac Electrophysiology, a section of the journal Frontiers in Physiology

Received: *01 June 2018*
Accepted: *08 August 2018*
Published: *23 August 2018*

Citation:
Mora MT, Ferrero JM, Gomez JF, Sobie EA and Trenor B (2018) Ca^{2+} Cycling Impairment in Heart Failure Is Exacerbated by Fibrosis: Insights Gained From Mechanistic Simulations. Front. Physiol. 9:1194. doi: 10.3389/fphys.2018.01194

INTRODUCTION

Heart failure (HF) is a major public health problem worldwide (Savarese and Lund, 2017) and the development of appropriate therapies to manage HF requires an in-depth knowledge of this syndrome. HF is classified as HF with reduced ejection fraction (HFrEF) or HF with preserved ejection fraction (HFpEF) according to left ventricular systolic function and the type of remodeling (Fukuta and Little, 2007). In HFrEF, the heart is unable to pump blood efficiently due to a reduction in cardiac contractility after diverse cardiovascular diseases. The complexity of the excitation–contraction sequence and the multiscale problem can be approached through mathematical models, which significantly help to gain insight into the underlying mechanisms of cardiac dysfunction and guide future research lines (O'Hara et al., 2011; Trayanova and Chang, 2016).

Contractile dysfunction in HF has been associated with an altered Ca^{2+} handling in myocytes, since Ca^{2+} homeostasis is crucial for cell contraction and relaxation (Alpert et al., 2000; Bers, 2000). Failing myocytes present a diminished intracellular Ca^{2+} transient (CaT) with a slow rise time and a reduced rate of $[Ca^{2+}]_i$ removal that prolong CaT duration and elevate the diastolic intracellular Ca^{2+} level (Piacentino et al., 2003; Lou et al., 2012). Prolonged action potential duration (APD) and $[Na^+]_i$ increase are other of the hallmark electrophysiological abnormalities in HF and all of them result from ion channel remodeling in myocytes, i.e., changes in the expression and function of proteins involved in the electrical activity of cells (Gomez et al., 2014b).

A tissue-level hallmark of HF is increased fibrosis and proliferation of cardiac fibroblasts. Several *in vitro* studies and mathematical modeling studies have documented that electrical coupling between myocytes and fibroblasts will lead to changes in APD and intracellular Ca^{2+} (Zhan et al., 2014; Li et al., 2017). Experimental evidence suggesting the formation of gap junctions between myocytes and fibroblasts *in vitro* (Gaudesius et al., 2003) has focused researchers attention on the altered electrophysiological properties of myocytes due to this intercellular coupling to explain conduction abnormalities and reentries (Miragoli et al., 2006; Xie et al., 2009a; Majumder et al., 2012). We have already addressed, in a previous work, the consequences on electrical propagation in cardiac tissue under conditions of HF and fibrosis confirming the vulnerability to reentrant activity (Gomez et al., 2014a,b). While electrical changes, with a cellular origin in action potential (AP) properties, have been widely investigated in the heterocellular coupling (Nguyen et al., 2012; Sridhar et al., 2017), changes in Ca^{2+} dynamics have not been explored in depth. It is important, therefore, to understand the role of fibroblasts in the modulation of Ca^{2+} cycling and to progress in the management of HFrEF, improving mechanical contraction.

Therefore, the goal of the present study was to investigate with computational models the effects of fibroblasts on ion transport mechanisms that regulate Ca^{2+} handling in human failing cardiomyocytes. To understand the complex processes taking place in these cells, we made use of sensitivity analyses. Sensitivity calculation has been commonly used for its predictive value in determining electrophysiological properties with parameter variability (Romero et al., 2011; Trenor et al., 2012; Walmsley et al., 2013; Cummins et al., 2014; Mayourian et al., 2016). As univariate and multivariate sensitivity analyses are widely used (Romero et al., 2009; Sobie, 2009), a comparison of both approaches was an initial objective of this work. Inter-subject variability in electrophysiological properties was considered and reproduced by populations of models. Failing populations, with drug-induced alterations in addition to the natural variability, were useful to identify specific combinations of model parameters that could counteract the effects of HF remodeling and fibroblasts. Our results identify the main targets to improve Ca^{2+} dynamics under the pathological conditions explored, improving cardiac contraction recovery.

MATERIALS AND METHODS

Cellular Models

All simulations were performed at the cellular level. To study the electrophysiological behavior of cardiac myocytes, we used the most complete undiseased human ventricular AP model, developed by O'Hara et al. (2011) (ORd model), which comprises 15 sarcolemmal currents, as shown in Eq. 1, known as fast Na^+ current (I_{Na}), late Na^+ current (I_{NaL}), transient outward K^+ current (I_{to}), L-type Ca^{2+} current (I_{CaL}), Na^+ current through the L-type channel (I_{CaNa}), K^+ current through the L-type channel (I_{CaK}), rapid delayed rectifier K^+ current (I_{Kr}), slow delayed rectifier K^+ current (I_{Ks}), inward rectifier K^+ current (I_{K1}), Na^+/Ca^{2+} exchange current (I_{NCX}), Na^+/K^+ ATPase current (I_{NaK}), background currents (I_{Nab}, I_{Cab}, I_{Kb}), and sarcolemmal Ca^{2+} pump current (I_{pCa}). A detailed Ca^{2+} dynamics is also formulated in the model. Properties such as conductances determining ionic densities and membrane kinetics can be found in the original work (O'Hara et al., 2011). We introduced slight modifications in sodium current formulation, as reported in our previous work (Mora et al., 2017) and leading to ORdmm model, which can also be found in **Supplementary Table S1**. To reproduce HFrEF phenotype, specific parameters of the model were modified to represent the downregulation or upregulation of cellular proteins experimentally observed in failing cells. This electrophysiological remodeling involved different ion currents and Ca^{2+} fluxes and has already been described in previous studies of our group (Gomez et al., 2014b; Mora et al., 2017). Specifically, the time constant of inactivation of I_{NaL} (τ_{hL}), I_{NaL} conductance, the maximal flux of I_{NCX} and SR Ca^{2+} leak (J_{leak}), and the fraction of active binding sites of the Ca^{+2} calmodulin-dependent protein kinase II (CaMKa) were upregulated, while conductances of I_{to} and I_{K1}, the maximal flux of I_{NaK}, and Ca^{2+} uptake via SERCA pump (J_{SERCA}), and SR Ca^{2+}-dependence of the steady-state activation of ryanodine receptor release ($K_{rel,Ca}$) were downregulated. Further details

about values and experimental references can be found in **Supplementary Table S2**.

$$I_{ion} = I_{Na} + I_{NaL} + I_{to} + I_{CaL} + I_{CaNa} + I_{CaK} + I_{Kr} + I_{Ks} + I_{K1} + I_{NaCa} + I_{NaK} + I_{Nab} + I_{Cab} + I_{Kb} + I_{pCa} \quad (1)$$

The increase in fibroblasts density due to aging and/or HF, and their interaction with myocytes were modeled using established cell–cell coupling equations. Fibroblasts were resistively coupled to one myocyte (Eq. 2), and a current (I_{gap}) flows from one cell to the other through gap junctions, driven by the potential gradient between the myocyte (V_M) and the fibroblast (V_F) membrane potential and regulated by a junctional conductance (G_{gap}).

$$I_{gap} = G_{gap} \cdot (V_M - V_F) \quad (2)$$

The electrical activity of fibroblasts was formulated using an active fibroblast model (MacCannell et al., 2007). The fibroblast AP model incorporates four transmembrane currents: a time- and voltage-dependent delayed-rectifier K^+ current (I_{Kr}), an inward-rectifying K^+ current (I_{K1}), a Na^+/K^+ ATPase current (I_{NaK}), and a background Na^+ current ($I_{b,Na}$). The membrane potential is governed by the following ordinary differential equation:

$$\frac{dV_F}{dt} = -\frac{1}{C_F}(I_{Kr} + I_{K1} + I_{NaK} + I_{b,Na} - I_{gap}) \quad (3)$$

The electrotonic interaction with the myocyte is included in the term I_{gap}. Regarding fibroblast properties, the membrane capacitance (C_F) was set to 6.3 pF and the resting membrane potential (E_F) had a value of −49.6 mV as in MacCannell et al. (2007). Similarly, the differential equation for the membrane potential of the myocyte, taking into account myocyte–fibroblast coupling, is as follows:

$$\frac{dV_M}{dt} = -\frac{1}{C_M}(I_{ion} + I_{stim} + I_{gap}) \quad (4)$$

Myocyte dimensions are bigger than fibroblasts, which is considered in membrane capacitance differences (C_M = 153.4 pF vs C_F = 6.3 pF). The value of G_{gap} was set to 3 nS for a single fibroblast, considered the nominal value in MacCannell et al. (2007) model. This value is within the range of 0.3–8 nS measured in cultured myocyte–fibroblast pairs (Rook et al., 1992). In our simulations, an elevated degree of fibrosis was considered by setting a myocyte–fibroblast ratio of 1:5, obtained by increasing G_{gap} fivefold (Mayourian et al., 2016; Zimik and Pandit, 2016). In the absence of fibrosis, G_{gap} is 0, and the myocyte is not coupled to fibroblasts.

Both types of myocytes, with and without electrophysiological HF remodeling, were coupled to the same number of fibroblasts with identical properties to simulate the effect of fibrosis on a single myocyte under different conditions. Four basic models were then considered: ORdmm model, ORdmm model with HF remodeling, ORdmm model with five coupled fibroblasts, and HF ORdmm model coupled to five fibroblasts.

Measurement of Biomarkers

To evaluate the electrophysiological activity of myocytes, and particularly Ca^{2+} dynamics, the electrophysiological indicators chosen were APD from maximal upstroke to 90% of repolarization (APD_{90}), calcium transient (CaT) duration from maximal upstroke to 80% of recovery ($CaTD_{80}$), CaT rise time from 10 to 90% of upstroke (t_{10-90}), and systolic and diastolic $[Ca^{2+}]_i$ values. All biomarkers were calculated under steady state conditions after application of 1000 stimuli at 1 Hz.

Population of Models

The aforementioned models were used as the baseline to generate four populations of 300 different individuals. Inter-subject electrophysiological variability was represented by variating maximal ion current conductances with a scale factor, assuming that there are variations in the number of ion channels in the cell membrane between individuals (Muszkiewicz et al., 2016). The variation in these scale factors is also a way to simulate the effects of drugs on ion channels, as a simplified action of pharmacological compounds inhibiting or enhancing ion currents. We selected and modified 13 key variables of the model, accounting for maximal ionic conductances and fluxes of I_{Na}, I_{NaL}, I_{to}, I_{CaL}, I_{Kr}, I_{Ks}, I_{K1}, I_{NaK}, I_{NCX}, the SR Ca^{2+} uptake via SERCA pump (J_{SERCA}), the SR Ca^{2+} release flux via RyR (J_{rel}), the SR Ca^{2+} leak (J_{leak}), and I_{Nab}. These parameters were varied with a scaling factor obtained from a log-normal distribution of standard deviation (σ) equal to 0.3. This led to a 95% (±2σ) of parameters varying between 55 and 182% of its control value, representing inter-individual variability and drug-induced effects. A standard deviation of 0.1 was also considered in different sets of populations.

In order to analyze how failing APs and CaTs could be restored to normal physiological ranges, larger populations of models were generated. Latin Hypercube Sampling (LHS) of parameters in the range of ±60% variation was used for this purpose. In this case, only the basic HF model (with and without coupled fibroblasts) was considered. We set limits for APD_{90} and systolic and diastolic $[Ca^{2+}]_i$ values, in which electrical myocyte activity was considered normal. These limits were obtained from the baseline models as $APD_{90normal} \pm (APD_{90HF} - APD_{90normal})/2$ and after being compared to experimental studies (Drouin et al., 1998; Li et al., 1998; Pereon et al., 2000). **Table 1** shows the considered ranges.

Sensitivity Analysis

Linear regression was employed to analyze biomarker sensitivities to electrophysiological variables. First, a

TABLE 1 | Biomarkers ranges for normal electrophysiological activity.

	Basic ORdmm	Normal range		Basic ORdmm HF
		Min	Max	
APD90 (ms)	290.6	240	341	371.8
systolic $[Ca^{2+}]_i$ (nM)	420	300	1000	190
diastolic $[Ca^{2+}]_i$ (nM)	80	50	200	100

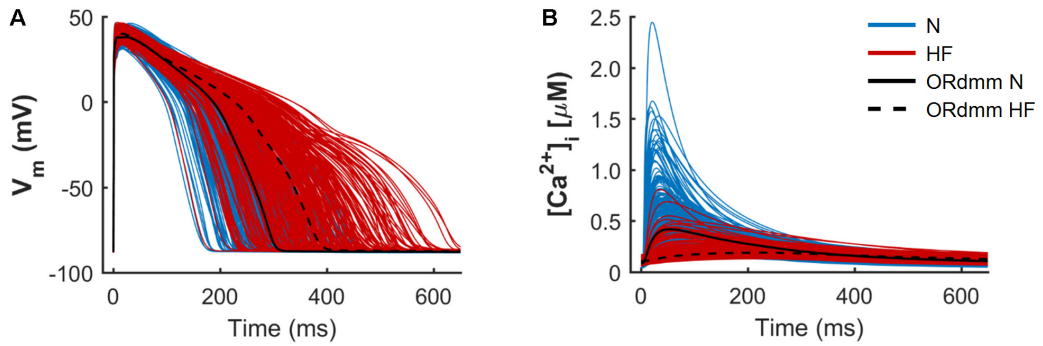

FIGURE 1 | Population of normal (N, blue) and heart failure (HF, red) human ventricular cell models. Simulated action potentials **(A)** and intracellular Ca^{2+} transients **(B)** obtained from a multivariate set of ionic conductances (n = 300), using the baseline ORdmm model in N conditions (black solid line) and with HF ionic remodeling (black dashed line).

univariate sensitivity analysis was conducted varying each parameter individually by a scaling factor of equal magnitude from the baseline models. The individual variation was set to ±60 or ±15% in different sensitivity analyses. This approach was based on our previous work (Mora et al., 2017).

Multivariate regression analyses were then performed using the generated populations of models. We related all the conductance scaling factors configurations (x) to each biomarker (y) with regression coefficients (b) that attempted to predict the indicators (Eq. 5). These coefficients were obtained by applying partial least squares (PLS) method to data as shown in Eq. 6 and after several transformations, such as log-transformations and z-score calculations (Sobie, 2009; Morotti et al., 2017). The obtained coefficients indicate the relative contribution of parameters variation in biomarker changes and can be considered as sensitivities. This methodology takes into account inter-variable effects that cannot be differentiated in the univariate analyses. Coefficients of determination (R^2) indicated the predictive power of the simplified linear model, being R^2 = 1 a good fit.

$$y_{predicted} = \sum b \cdot x \tag{5}$$

$$B_{PLS} = (X^T X)^{-1} \times X^T \times Y \tag{6}$$

Both types of sensitivity analyses were compared with normalized sensitivities to study the similarities and differences in parameter identification as the most important contributors to each electrophysiological characteristic. Normalized sensitivities were calculated as the ratio between each sensitivity and the maximum absolute value obtained for a particular biomarker.

The comparison between isolated and coupled myocytes was performed after adjusting the bar graphs to the standard deviation of the log-transformed biomarkers in N and HF conditions, to ensure equivalent percentages of change.

RESULTS

Comparison of Univariate and Multivariate Sensitivity Analyses in Normal and Failing Conditions

Figure 1 illustrates two populations of models (n = 300) for endocardial human cells paced at 1 Hz, under normal (blue traces) and HF (red traces) conditions, with baseline models for the two respective populations indicated with black solid and dashed lines. The model population calibration process, meant to reproduce natural variability, generates a wide range of physiological AP waveforms and CaTs in both groups. This variability allows us to understand predicted drug effects by considering the HF cells with behavior most similar to normal cells, or vice versa. The electrophysiological remodeling applied to the basic ORdmm model to generate a baseline HF model reproduced the characteristic HF phenotype of prolonged APD and a slower Ca^{2+} dynamics with depressed systolic $[Ca^{2+}]_i$ and elevated diastolic levels. In the generated normal and failing populations, significant differences between both conditions are observed in APs and CaTs, although some traces overlap. To understand the variability within the populations and predict what alterations might cause HF cells to behave more like normal cells, we performed a sensitivity analysis.

Figure 2 represents the sensitivity of quantitative indicators of AP and CaT characteristics to changes in ion channels obtained in the univariate and multivariate sensitivity analyses. Sensitivities helped reveal the most important modulators of a determined electrophysiological property. High regression coefficients highlighted an important effect of a particular transport mechanism on Ca^{2+} indicators, taking into account the synergy between variables in the case of multivariate analysis. Our results showed that I_{Kr} was the parameter with the major impact on APD_{90} (**Figure 2A**), while SERCA had the leading role in Ca^{2+} biomarkers (**Figures 2B–D**). Sensitivities were normalized to allow comparison between the sensitivities obtained through a ± 60% univariate sensitivity analysis (light blue for N conditions and pink bars for HF conditions) with multivariate sensitivity analysis (dark blue for N conditions and

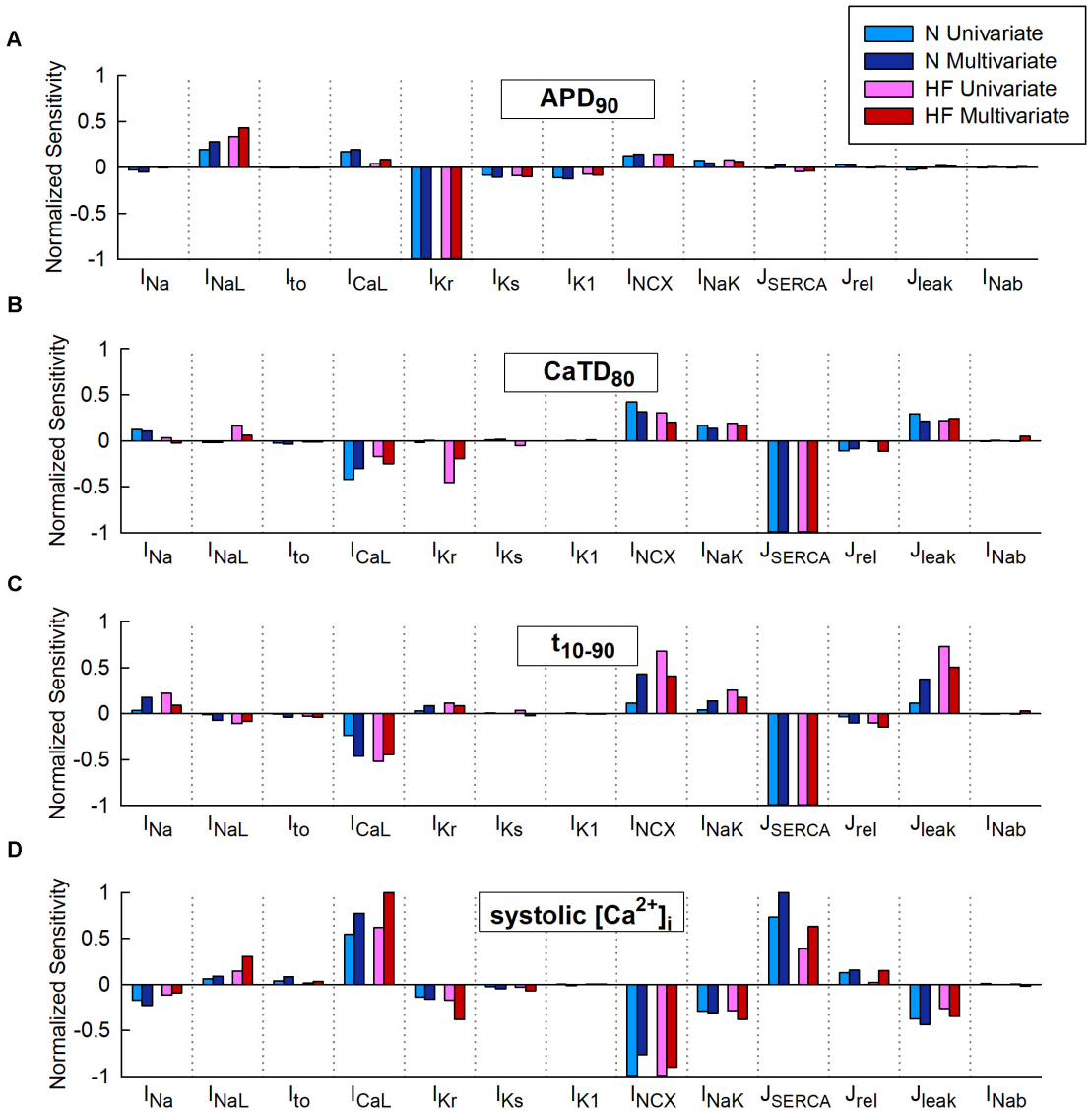

FIGURE 2 | Comparison of univariate and multivariate relative sensitivities in normal (N) and heart failure (HF) conditions. Modulators of **(A)** action potential duration to 90% of repolarization (APD_{90}), **(B)** Ca^{2+}transient (CaT) duration to 80% of recovery ($CaTD_{80}$), **(C)** CaT rise time ($t_{10\text{-}90}$), and **(D)** Systolic peak of CaT. Parameter variability of 60%.

red bars for HF conditions). In this comparison, results from both methodologies were consistent for APD sensitivities (**Figure 2A**). Small differences were though observed in the case of Ca^{2+} biomarkers (**Figures 2B–D**). For instance, **Figure 2B** shows that in HF, I_{Kr} seems to have a moderate impact on $CaTD_{80}$ according to the univariate results (pink bars), while multivariate sensitivity indicates that the effect is lower (red bars). In other cases, with the univariate analysis, the relative importance of parameters can be altered between the N and HF conditions. This was the case for I_{CaL}, I_{NCX}, and J_{leak} on t_{10-90} (**Figure 2C** light blue and pink bars). **Figure 2D** shows how NCX has the main role in modulating systolic Ca^{2+} according to the univariate sensitivity analysis (light blue in N and pink bars in HF), while the multivariate sensitivity highlights SERCA and I_{CaL} as the main modulators in N (dark blue bars) and HF (red bar) conditions, respectively, and the exchanger has a secondary role.

Multivariate and univariate analyses also identified similar changes in parameter sensitivities from N to HF (**Figure 2, light** and **dark** blue vs pink and red), such as an increased impact of I_{NaL} on APD_{90} in HF with respect to normal conditions (**Figure 2A**), a higher I_{Kr} influence on $CaTD_{80}$ (**Figure 2B**), and a decrease of SERCA modulation effect on systolic $[Ca^{2+}]_i$ (**Figure 2D**).

We further investigated the aforementioned discrepancies by performing additional sensitivity analyses with a lower conductance variability. Parameter variability was reduced to 15% in the univariate study and the standard deviation was decreased to 0.1 in the multivariate regression, resulting in

sensitivities slightly different from those described above with higher variability (60% and σ = 0.3, respectively). After reducing parameter variability, negligible differences were found when comparing both methods (see **Supplementary Figures S1**, **S2**, light-colored bars). For example, considering low variability in HF (**Supplementary Figure S2D**, light bars), both analyses (univariate and multivariate) highlighted I_{CaL} as the most important parameter regulating systolic $[Ca^{2+}]_i$, while univariate sensitivities obtained with 60% variability (darker pink bar) highlighted I_{NCX} as the main regulator and underestimated the impact of I_{CaL}.

Coefficients of determination of the multivariable regression are shown in **Table 2** for the different sensitivity analyses. Values were closer to 1 as variability decreased. $CaTD_{80}$ and systolic $[Ca^{2+}]_i$ linear fit significantly improved with lower variability, especially in HF (0.938 vs 0.677 and 0.970 vs 0.792, respectively). This indicates that, with large parameter variability, and in the HF condition, significant non-linear relationships between parameter values and Ca^{2+} handling processes make the multivariable regression model less accurate.

In summary, univariate and multivariate sensitivity analyses yield very similar results for low variability of parameters, which would correspond to natural inter-subject electrophysiological differences. Univariate analysis is less computational expensive and is thus a valid methodology under these conditions. However, when large variability is applied, which would respond to effects of drugs, significant discrepancies arise between both methodologies. Multivariate analysis should be more reliable, at least for biomarkers with coefficients of determination close to one. Indeed, multivariate analysis considers interaction between the different parameters of the ion channels altered.

Effects of Fibroblast–Myocyte Coupling in Normal and Failing Conditions

When simulations were performed to electrically coupled fibroblasts to a myocyte, the myocyte's AP and CaT were significantly changed. **Figure 3** shows APD and systolic $[Ca^{2+}]_i$ reduction in the normal baseline human endocardial model when fibroblasts were coupled (solid vs discontinuous blue trace), as well as in the failing baseline endocardial model (solid vs discontinuous red trace).

When fibroblasts were coupled to myocytes from two populations of models (n = 300) generated for both N and HF conditions, the above-mentioned effects on APD and CaT were maintained, as shown in **Figure 4**. CaT traces in normal conditions (**Figure 4A**) with coupled fibroblasts (discontinuous blue traces) overlapped with CaT traces in the absence of fibroblasts (solid blue traces).

To evaluate whether fibroblasts coupling would significantly change sensitivities of electrophysiological biomarkers to parameters variability, multivariate analyses were conducted on these new populations. When a high variability of parameters was considered (σ = 0.3), our results showed that in the presence of fibroblasts, biomarkers sensitivities to ionic variables slightly changed with respect to uncoupled myocytes. As displayed in **Figure 5**, most of these differences were quantitative, as fibroblasts reduced sensitivities to parameters, but the qualitative role of each parameter was maintained. For instance, SERCA contribution to Ca^{2+} indicators (**Figures 5B–D**) decreased both in normal and failing conditions when fibroblasts were considered (discontinuous bars).

To confirm these results, we decreased parameter variability to σ = 0.1 and obtained more accurate regression coefficients. In the new range of parameter variability (see **Supplementary Figure S3**), sensitivities hardly changed with respect to higher variability.

TABLE 2 | Coefficients of determination (R^2) of the multivariable regression analyses in normal (N) and heart failure (HF).

R^2	APD_{90}	$CaTD_{80}$	t_{10-90}	$[Ca^{2+}]_i$ syst
N (σ = 0.3)	0.987	0.940	0.908	0.954
N (σ = 0.1)	0.994	0.997	0.975	0.994
HF (σ = 0.3)	0.987	0.677	0.871	0.792
HF (σ = 0.1)	0.999	0.938	0.910	0.970

AP and CaT Restoration in HF

To analyze how failing APs and CaTs could be restored and brought to normal ranges, a larger population of failing models was generated (n = 10,000). The population of models approach generates cells exhibiting a wide variety of physiological behaviors, including cells within the HF population that have APs and CaTs similar to those observed in healthy cells. Selecting this subpopulation and examining the distributions of parameters provides guidance for therapeutic targets. We identified parameter combinations restoring APs and CaTs to waveforms within a healthy range shown in **Table 1** in Section "Materials and Methods." In **Figure 6A**, red traces represent all models generated from the baseline ORdmm HF model (black dashed line) and blue lines are models satisfying healthy ranges of both AP and CaT biomarkers. Electrophysiological HF phenotype was restored in around 500 models when I_{Kr}, SERCA, and I_{CaL} activities were enhanced, and NCX function decreased. Interestingly, NCX distribution presented several outliers at high scaling factors. When myocytes were coupled to fibroblasts (**Figure 6B**), the role of SERCA, I_{CaL}, and NCX was similar, whereas I_{Kr} modulation was not important.

Mechanistic Analysis of Calcium Dynamics Impairment in Fibrosis

Fibroblast coupling decreased systolic Ca^{2+} in normal myocytes and exacerbated calcium dynamics impairment in failing myocytes, although parameter sensitivities were hardly affected. To understand the underlying mechanisms, ion currents were carefully analyzed in our simulations. **Figure 7** shows the traces of selected electrophysiological variables of the model in the time course of an AP at steady state for a failing myocyte with (solid line) and without (dashed line) fibroblast coupling. To understand how these steady-state conditions were reached, we analyzed transient changes in myocyte $[Ca^{2+}]$ after fibroblast coupling, as shown in **Figure 8**. In these panels, isolated

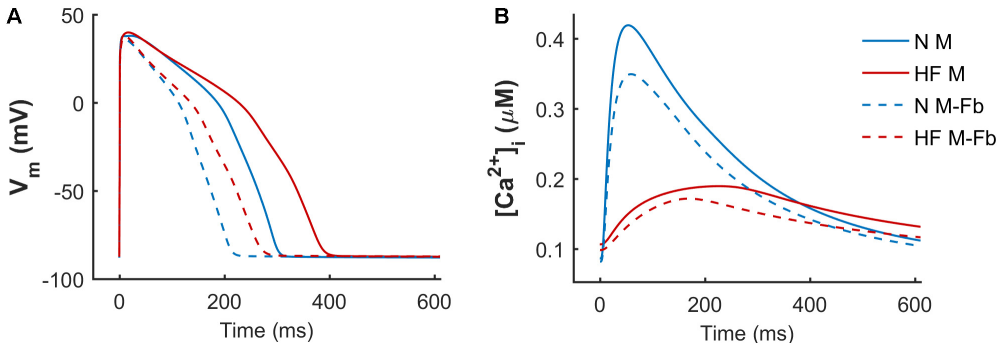

FIGURE 3 | Effect of fibrosis on action potential **(A)** and Ca^{2+} transient **(B)**. Normal (N) and failing (HF) baseline myocyte models in an uncoupled myocyte (M) and a myocyte coupled to five fibroblasts (M-Fb).

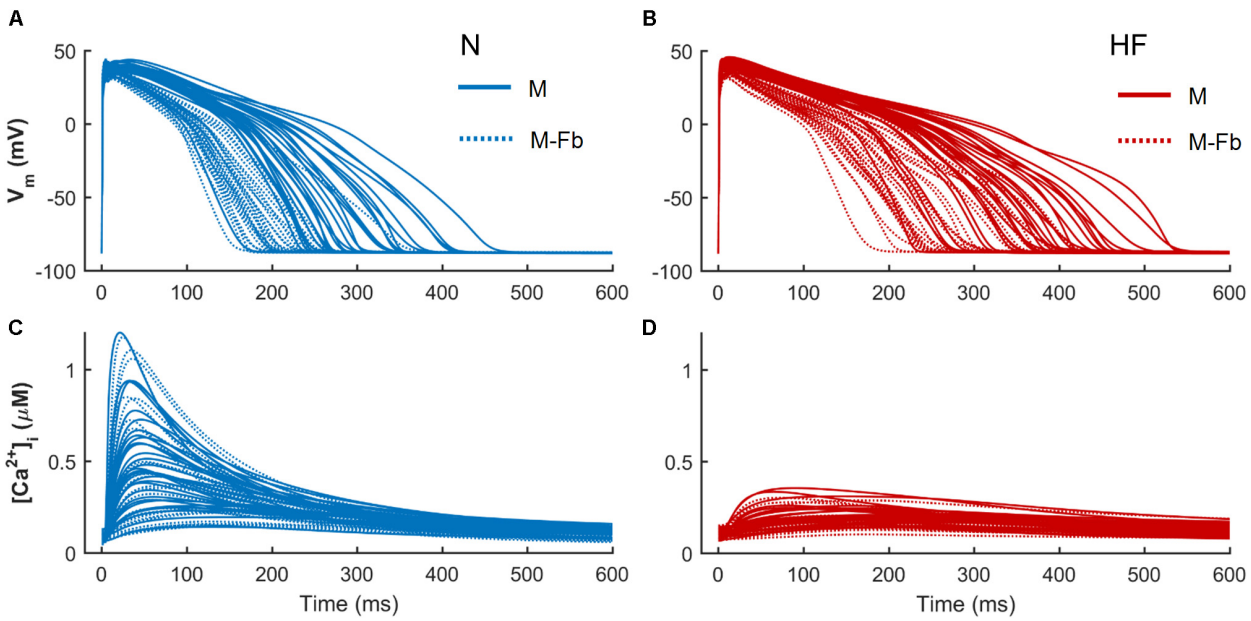

FIGURE 4 | Action potential and Ca^{2+} transient samples (n = 30) of uncoupled myocytes (solid traces) and myocytes coupled to five fibroblasts (discontinuous traces) from two population of models, obtained from a multivariate set of ionic conductances (n = 300), using the basic ORdmm in normal conditions **(A,C)** and the basic HF remodeling model **(B,D)**.

myocytes are initially at steady state, then fibroblasts are coupled beginning on the second beat. As shown in **Figure 7C**, I_{gap} is an outward current flowing from the myocyte to fibroblasts, non-existing in the uncoupled myocyte. This outward current decreases membrane potential and has an indirect effect on voltage dependent currents such as I_{CaL}. Indeed, we can observe that when fibroblasts are coupled (dashed traces) all currents and fluxes present a shorter duration, as well as AP, and a reduced peak (see, for instance, CaT in **Figure 7B**), except I_{CaL}. Despite the reduced duration of this current, the initial I_{CaL} peak contributed to a larger Ca^{2+} influx through these channels (increase from 140 to 146 pC/μF). The integral of NCX was also computed and indicated an increase in inward NCX extruding more Ca^{2+} when fibroblasts were coupled (from 77 to 81 pC/μF). In the transient evolution shown in **Figure 8F**, the peak of I_{CaL} exhibited a maintained increase compared with the uncoupled myocyte (shown in solid red). Due to the increased Ca^{2+} extrusion through NCX, however, $[Ca^{2+}]_{JSR}$ progressively declined, leading to the decrease in $[Ca^{2+}]_i$ peak observed in steady state.

DISCUSSION

Main Findings

In this study, two methodologies were used to perform sensitivity analyses evaluating the effects of fibroblast–myocyte coupling under normal and HF conditions. Our main findings are that (i) univariate and multivariate analyses yield very similar results and low variability of parameters

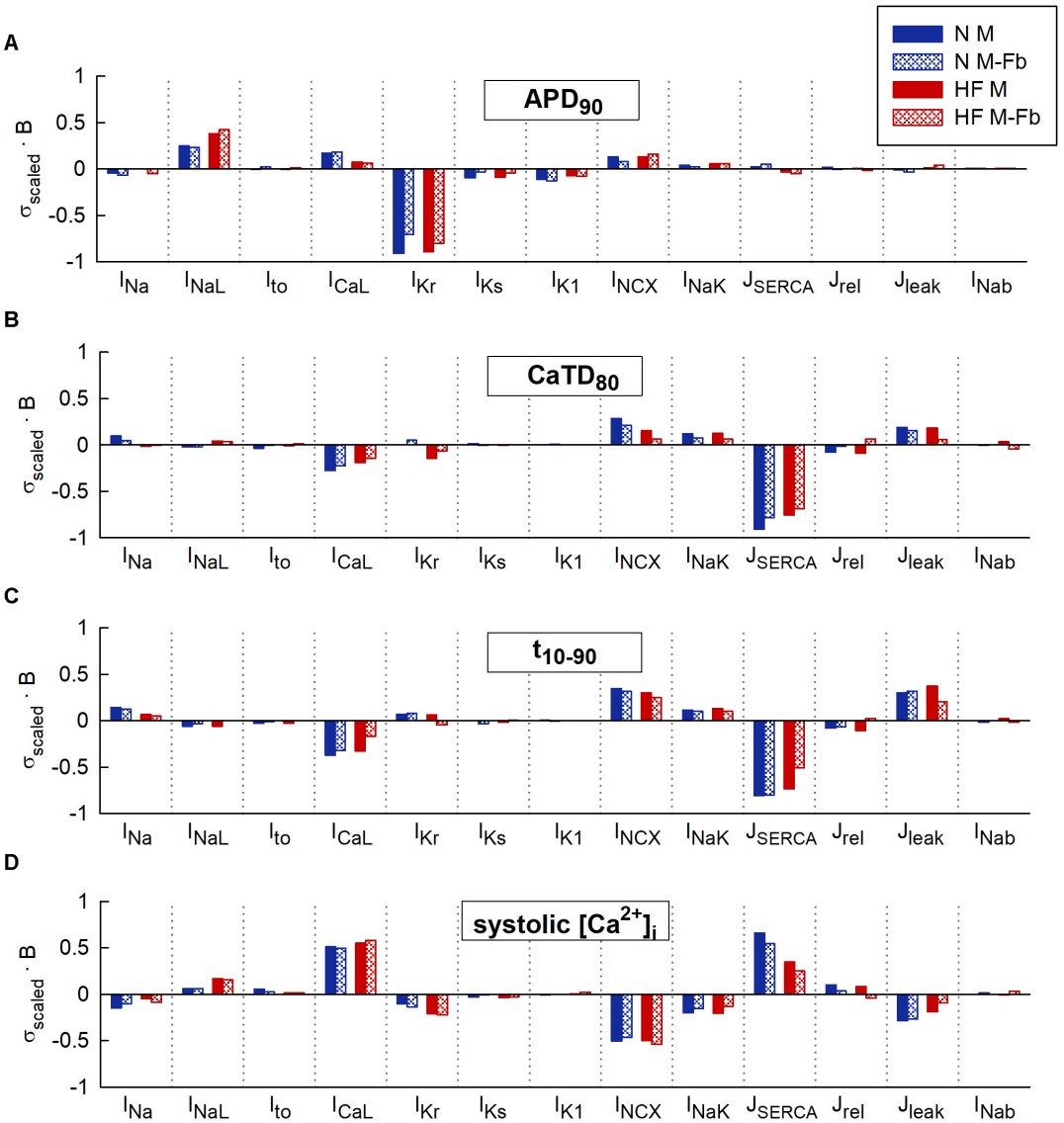

FIGURE 5 | Comparison of sensitivities obtained from 4 multivariable regression analyses: normal (N) and heart failure (HF) conditions with or without coupled fibroblasts (Fb). Modulators of **(A)** action potential duration to 90% of repolarization (APD_{90}), **(B)** Ca^{2+} transient (CaT) duration to 80% of recovery ($CaTD_{80}$), **(C)** CaT rise time ($t_{10\text{-}90}$), and **(D)** Systolic peak of CaT. High parameter variability. Regression coefficients (b) are scaled to the standard deviation (σ) of log-normal distributed biomarkers in uncoupled myocytes (M).

yields more reliable multivariate sensitivity analyses, (ii) despite exacerbating Ca^{2+} impairment in HF, fibroblast to myocyte coupling does not alter the role of the main mechanisms regulating Ca^{2+} dynamics in myocytes, and (iii) drug action on I_{CaL} and SERCA enhancement and NCX block would help CaT restoration in HF regardless of fibrosis presence.

Suitable Sensitivity Analyses

Univariate and multivariate sensitivity analyses were performed using an initial large variability (±60%) and then smaller (±15%). At lower variability, changes in electrophysiological properties behaved linearly, making results from univariate and multivariate analysis more similar. Indeed, ionic currents and fluxes work synergistically to generate AP and CaT. Variables such as membrane potential and ionic concentrations link all ionic mechanisms in a way that a change in one parameter (conductivity in this case) has an effect on other parameters, and final differences in electrophysiological properties are the result of an interaction of all these variations. In addition, within the range of variation of a specific parameter, the effects on biomarkers can be different, and assuming linearity can become less accurate when a wide interval is considered. In fact, as electrophysiological remodeling in HF is simulated by changing parameters, the same scale factor applied in N and HF implies a different range of variation of such parameters, accounting for different sensitivities

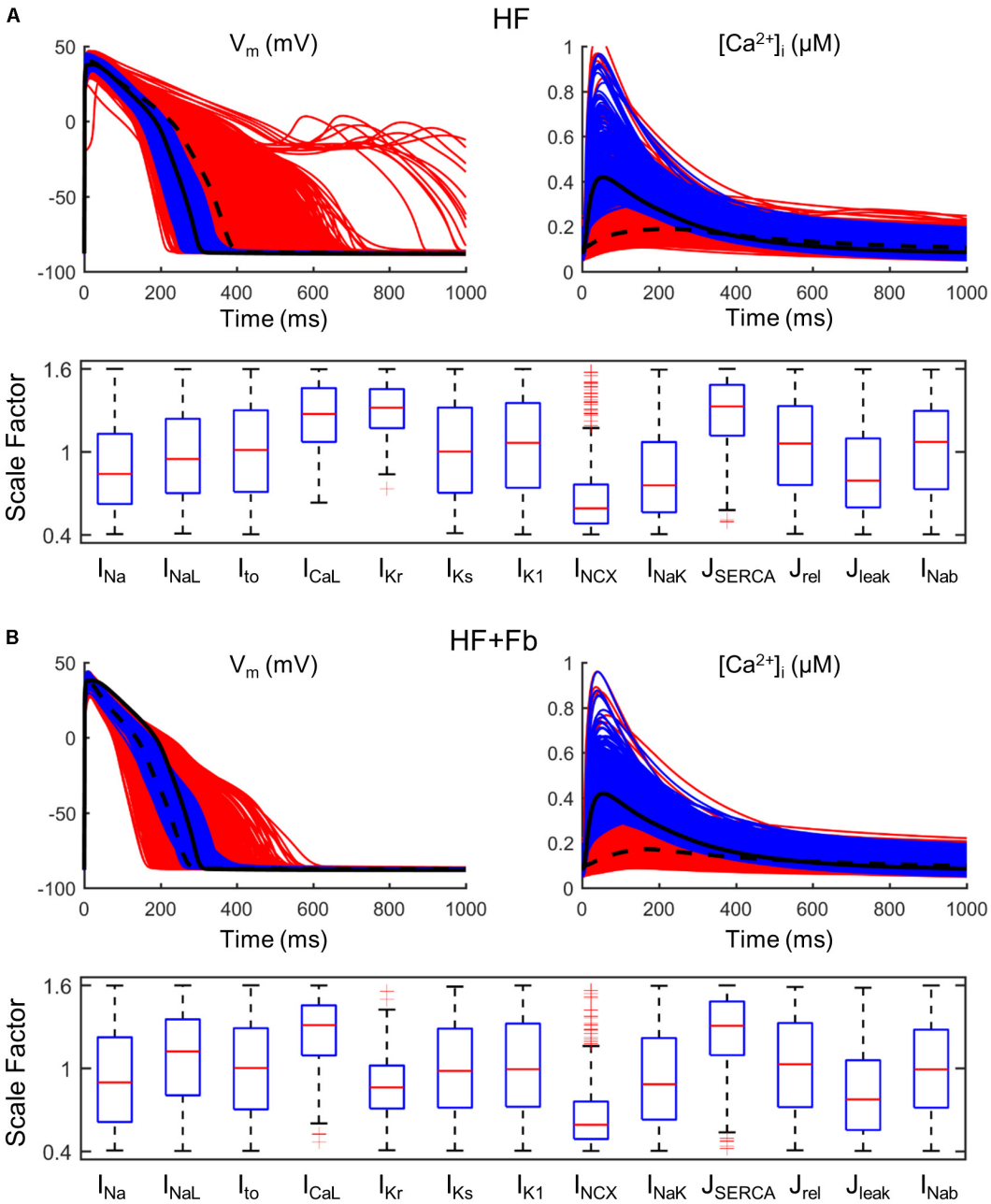

FIGURE 6 | Restoration of normal action potential (AP) and calcium transient (CaT) in a population of failing models (n = 10,000). All simulated models (red traces) are obtained from a HF basic model (black dashed line) in which parameters have been varied ±60%. Calibrated models (blue traces) are within the limits of normal biomarkers (basic ORdmm in black solid line). Distributions of parameter scaling factors for the restored models. **(A)** Population of an uncoupled myocyte. **(B)** Population of a myocyte coupled to five fibroblasts.

to biomarkers. This explains the increase in APD sensitivity to I_{NaL}, or the decrease of systolic $[Ca^{2+}]_i$ sensitivity to SERCA in HF with respect to N conditions.

Multivariate parameter sets, unlike varying one parameter at a time, can provide information about electrophysiological properties in a wide combination of parameters, which could be useful to evaluate the response of a drug in different individuals, instead of on a fixed baseline model. The high physiological or pathological variability of ionic parameters requires the analysis of the behavior in the whole range.

Despite accuracy loss with high parameter variability, sensitivity analyses are a useful systematic tool to determine the most important mechanisms involved in Ca^{2+} dynamics. We observed that univariate and multivariate sensitivities agreed in the most important parameters contributing to each biomarker. For instance, it was observed the strong impact of I_{Kr} on

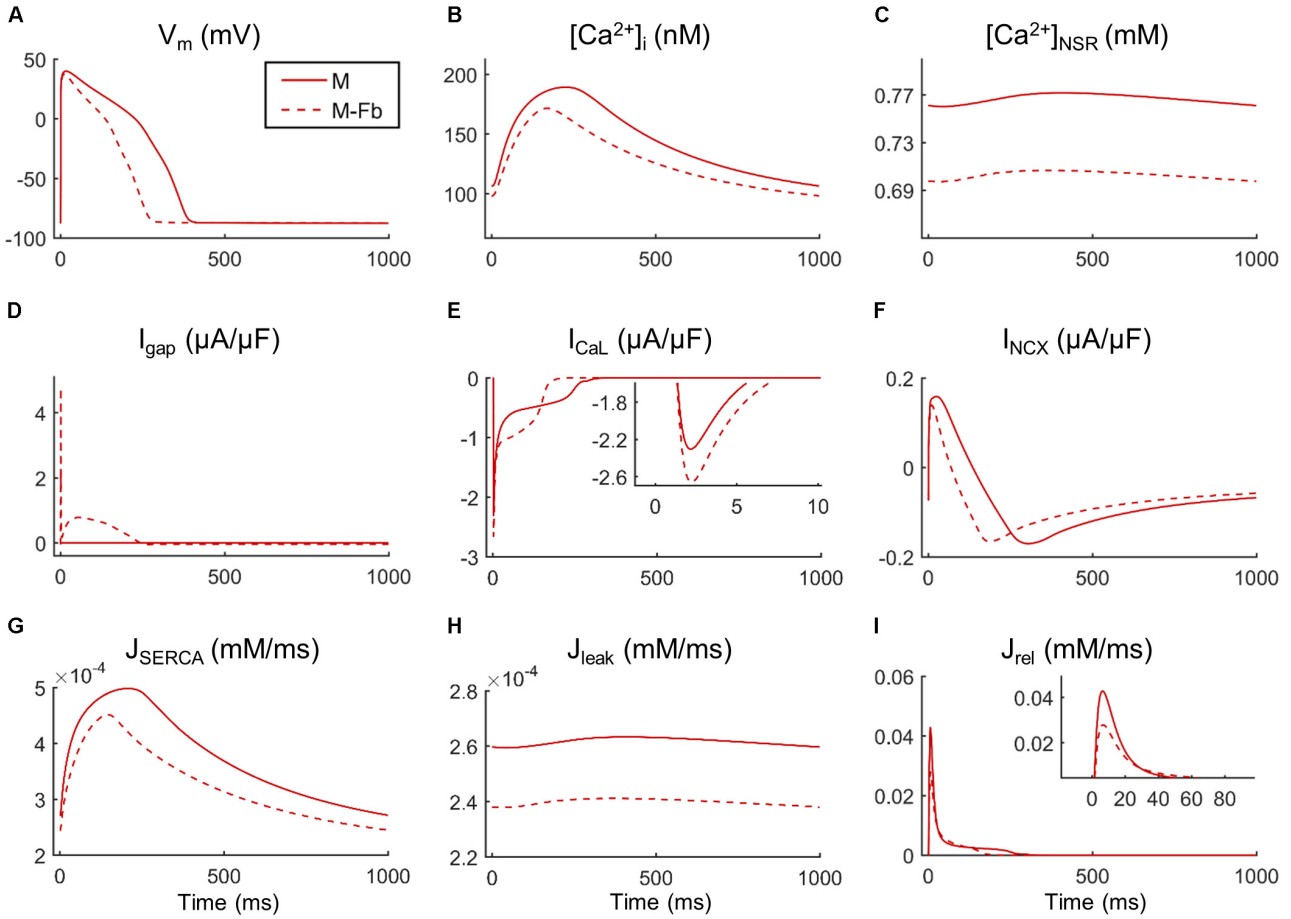

FIGURE 7 | Main ionic properties and mechanisms in steady state of a failing myocyte interacting (M-Fb) or not (M) with fibroblasts. **(A)** Membrane potential (V_m), **(B)** intracellular Ca^{2+} concentration ($[Ca^{2+}]_i$), **(C)** sarcoplasmic reticulum (SR) Ca^{2+} concentration ($[Ca^{2+}]_{SR}$), **(D)** outward positive current circulating from the myocyte to the fibroblast (I_{gap}), **(E)** L-type Ca^{2+} current (I_{CaL}), **(F)** Na^+/Ca^{2+}exchange current (I_{NCX}), **(G)** SR Ca^{2+} uptake via SERCA pump (J_{SERCA}), **(H)** SR Ca^{2+} leak (J_{leak}), and **(I)** SR Ca^{2+} release flux via ryanodine receptors (J_{rel}).

APD_{90}, as O'Hara et al. (2011) described in their model. For CaT indicators, the main role of parameters such as SERCA, NCX, and I_{CaL} was highlighted with both methodologies, agreeing with experimental observations (Ozdemir et al., 2008; Rocchetti et al., 2008; Tamayo et al., 2017), and with a previous study comparing populations of normal and failing myocytes (Walmsley et al., 2013).

In electrophysiological models, biomarker sensitivities are usually calculated within a wide range of variation in ionic conductances, which has been reported experimentally. In their work, Romero et al. (2009) simulated univariate variations up to ±30% to evaluate the arrhythmogenic risk of ionic change, with AP properties falling within the experimental range. In the multivariable regression conducted by Sobie (2009), it was assessed how variability (σ ranging from 0.1 to 0.5) affected the regression model and observed a R^2 reduction with the increase of σ, although many regression coefficients remained constant, being small the decrease in accuracy obtained for APD. This is consistent with our results, highlighting the robustness of sensitivity analysis for AP biomarkers. However, Ca^{2+}-biomarkers sensitivities were more affected by variability. Comparing low and high parameter variability, sensitivities differed more in the univariate case due to changes in parameter–biomarker relation along the variation range, including non-linearities. Sensitivities derived from the multivariate study for HF showed the lowest coefficients of determination, suggesting that HF remodeling enhances non-linearities between variables.

In other modeling studies, experimentally-calibrated populations are first generated with conductances scaled up to ±100%. Constrained biomarkers according to experimental values determine the range of parameters in the subsequent regression analysis (Zhou et al., 2016; Britton et al., 2017). This way, linear fit problem could be solved but natural variability dominates the results and high effects of drugs are not evaluated in this range.

It can be concluded that the roles of the different parameters on electrophysiological biomarkers can be qualitatively estimated using linear methods, including different variability and parameter distributions. Furthermore, our findings highlight that both types of sensitivity studies, univariate and multivariate,

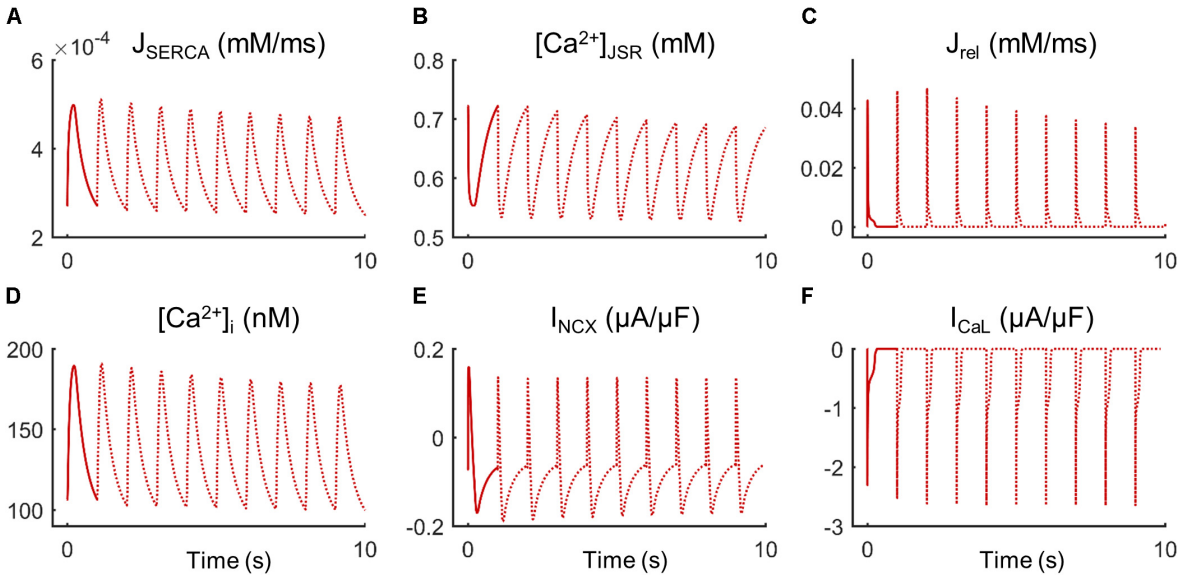

FIGURE 8 | Transient state of ionic mechanisms and Ca^{2+} concentration in cellular compartments of a failing myocyte coupled to five fibroblasts (dashed lines). Initial steady state of an uncoupled myocyte (solid line). **(A)** SR Ca^{2+} uptake via SERCA pump (J_{SERCA}), **(B)** junctional SR Ca^{2+} concentration ($[Ca^{2+}]_{JSR}$), **(C)** SR Ca^{2+} release flux via ryanodine receptors (J_{rel}), **(D)** intracellular Ca^{2+} concentration ($[Ca^{2+}]_i$), **(E)** Na^+/Ca^{2+}exchange current (I_{NCX}), and **(F)** L-type Ca^{2+} current (I_{CaL}).

provide similar results. However, when large variability is considered, discrepancies arising between these methodologies can become notable, affecting Ca^{2+} properties and patholological conditions to a greater extent. Univariate analysis is less computational expensive and is thus a valid methodology within a moderate variability range and for a reasonable number of parameters. Quantitative results from the multivariate analysis should be more reliable, as parameter interaction is considered, but caution should be taken if coefficients of determination are not close to one, which can happen under HF conditions.

Fibrosis Exacerbates Ca^{2+} Transient Impairment in Heart Failure

This computational study shows that the electrical activity of myocytes, including calcium dynamics, is affected by fibroblast coupling. Specifically, CaT peaks are smaller and SR $[Ca^{2+}]$ is reduced when fibroblasts are coupled to myocytes. Despite these alterations, the ionic mechanisms regulating Ca^{2+} cycling are barely affected by the intercellular interaction, indicating that fibroblast coupling does not influence which pathways represent the best drug targets. HF remodeling seems to have a greater impact on the relative role of the different ionic mechanisms that regulate Ca^{2+} cycling. However, our results show that fibroblast coupling could be contributing to the excitation–contraction coupling impairment seen in HF.

An important effect observed when simulating fibroblast–myocyte coupling is the marked APD shortening. Experimental studies showing the existence of gap junctions (connexin43) between fibroblasts and myocytes also revealed changes in AP waveform and conduction velocity due to a modulation of myocyte electrophysiology (Gaudesius et al., 2003; Miragoli et al., 2006; Zlochiver et al., 2008). Previous computational studies exploring fibroblast–myocyte electrophysiological interactions also showed reductions in APD. When MacCannell et al. (2007) developed the mathematical model for the active fibroblast, they coupled it to a human myocyte model and reported an APD shortening, as fibroblasts acted as current sinks. The theoretical work of Jacquemet and Henriquez (2008) also showed that the effect of coupling caused a faster myocyte repolarization, but changing fibroblast properties, such as a less negative fibroblast resting potential, reversed the effect. It is known that fibroblasts differentiate into myofibroblasts in response to inflammation, an activated form which presents contractile proteins, implying the existence of Ca^{2+} cycling (Chilton et al., 2007). To date, no specific models for myofibroblasts have been developed but simulations have been performed increasing the membrane capacitance and depolarizing the resting membrane potential of the fibroblast model (Nguyen et al., 2012; Sridhar et al., 2017). In the present study, we used the fibroblast model by MacCannell et al. (2007) with a resting potential of −49.4 mV, thus the effect in normal and failing myocytes was a reduction in APD. We also conducted some additional simulations (see **Supplementary Figure S4**) changing to myofibroblast phenotype (C_F = 50 pF, E_F = −24.5 mV), and we observed similar effects, i.e., APD shortening and Ca^{2+}-handling impairment. The improvement of myofibroblast models, incorporating Ca^{2+} dynamics, would certainly shed light into the understanding of Ca^{2+} dynamics alterations in the failing tissue.

The number of coupled fibroblasts considered could also alter the results. The uncertainty about the *in vivo* coupling, different degrees of fibrosis, and the difficult to quantify coupled fibroblasts in tissue has led to the exploration of different values of G_{gap} or a range of myocyte–fibroblast

ratios (Jacquemet and Henriquez, 2008; Sachse et al., 2009; Xie et al., 2009a). We compared the effects of coupling one fibroblast to five (results not shown) and we found that the impact on APD and CaT was lower with one fibroblast and increasing the number of fibroblasts to five did not increase the effects fivefold. This finding suggested that the sensitivity of the myocyte to G_{gap} is not linear, saturating for higher values, as observed in other analyses of G_{gap} effects when strong coupling was considered (Jacquemet and Henriquez, 2008). We finally used five fibroblasts in order to represent fibroblast proliferation observed in pathological conditions.

In our simulations, the baseline ORdmm model showed a notable Ca^{2+} impairment when fibroblast interaction was considered in both N and HF conditions, but the population of models revealed that not every individual might have an impaired Ca^{2+} handling in a fibrotic heart. However, in HF, even a minor Ca^{2+}-handling alteration should be considered important because it worsens contractility dysfunction. Only a few studies have measured intracellular Ca^{2+} in myocytes interacting with fibroblasts. In co-culture experiments used to investigate the crosstalk between both cell types, it was found that fibroblasts from normal hearts increased CaT amplitude, while fibroblasts and myofibroblasts from pressure-overloaded hearts led to a smaller amplitude associated with a reduction in SR Ca^{2+} content (Cartledge et al., 2015). A more recent *in vitro* study to explore the influence of heterocellular interactions on cardiomyocyte function showed that only adult fibroblasts had significant consequences on the electrical and mechanical function, by prolonging APD and reducing CaT amplitude (Li et al., 2017). In computational studies, only the work by Zhan et al. (2014) has considered the role of fibroblast proliferation in a mathematical model with Ca^{2+}, and reported a longer APD and CaT width, modulating cardiac electromechanical behavior. This discrepancy with our results, a prediction of APD prolongation rather than shortening, might be due to the use of a passive fibroblast model with a resting membrane potential set to −20 mV. Indeed, when modeling fibroblast electrophysiological behavior, the values of several parameters are crucial in the outcome, including the number of fibroblasts coupled to each myocyte, the resting potential, and the capacitance of each fibroblast (Chilton et al., 2005), and whether myofibroblast properties are considered (Sridhar et al., 2017).

Our sensitivity analysis showed minimal differences in the mechanisms determining APD and CaT waveform between myocytes coupled or not to fibroblasts. This could simplify therapies, as presence or absence of fibrotic tissue would not alter the treatment. The slightly reduced sensitivities in the presence of fibrosis indicate that targeted ion transport pathways require a higher variation to produce the same percentage of change to improve the considered electrophysiological property. I_{Kr} is the main modulator of APD, as O'Hara et al. (2011) reported in their sensitivity analysis, and its enhancement in HF would restore the prolonged APD. However, in myocytes coupled to fibroblasts there is no need to reduce APD via I_{Kr} modulation as fibroblasts act as a current sink and lead to an earlier repolarization. Regarding CaT indicators, HF remodeling seems to be the main cause of Ca^{2+} alteration, which explains why coupled and uncoupled myocytes require the same measures to restore Ca^{2+} cycling: increase of SERCA and I_{CaL}, and NCX reduction.

Finally, the mechanistic analysis of Ca^{2+} cycling with fibroblasts reveals that, despite an increase in I_{CaL} peak with fibroblast coupling, increased NCX Ca^{2+} extrusion leads lower SR content and smaller CaT peaks. In the steady state, there is a balance between fluxes, maintaining constant Ca^{2+} levels, which does not happen in the transient state. In fact, the progressive reduction in intracellular Ca^{2+} is a sign of negative balance between Ca^{2+} influx and efflux in the myocyte, which occurs after a perturbation in the system, i.e., fibroblast coupling. The modulation of all ionic mechanisms including Ca^{2+} cycling is caused by the active role of fibroblasts, becoming a current sink. The new outward current in myocytes, I_{gap}, accelerated AP repolarization and consequently, all voltage-dependent currents were affected, including I_{CaL}. The model used for human endocardial AP does not present a notch with a marked early repolarization phase as in other species. For this reason, I_{gap} does not affect the excitation–contraction coupling by changing the rate of the initial repolarization as in Xie et al. (2009b). In the present study, the implicated mechanism becomes more important in later phases of the AP. We also conducted simulations using the epicardial model of ventricular AP formulated by O'Hara et al. (2011) to see the effect on the early repolarization phase which is indeed present in the epicardial model. As shown in **Supplementary Figure S5**, no important changes are observed in this phase under the effect of coupled fibroblasts.

The static formulation of myocyte–fibroblast coupling differed from the dynamic gap junctions channels modeled by Brown et al. (2016). They observed a reduction in the junctional current during the upstroke of the AP when considering time- and voltage-sensitive gating channels in homotypic and heterotypic channels, i.e., with different connexins combinations (Cx43 and Cx45). Although it did not significantly alter conduction velocity compared to static gap junctions, fibroblasts with a smaller sink impact could have a different effect on Ca^{2+} dynamics.

Our findings showed that a higher I_{CaL} peak introduced more Ca^{2+} in the myocyte but did not trigger a higher SR Ca^{2+} release as expected. According to Shannon et al. (2000), there cannot be a release from the SR with a Ca^{2+} load of less than 50% of its maximal content, explaining that the reduced SR Ca^{2+} content characteristic of failing myocytes contributes to reduce force development. Similarly, changes in SR Ca^{2+} load of 58% have been measured in failing isolated myocytes, and related to a smaller CaT (Piacentino et al., 2003). Therefore, a reduction in SR Ca^{2+} content due to fibroblasts could be the cause of an exacerbated Ca^{2+} impairment. The transient evolution shown in **Figure 8** helps understand the mechanisms leading to cellular Ca^{2+} loss. One of the advantages of mathematical models is the power to analyze hypothetical situations that cannot be measured experimentally,

such as myocyte response to a sudden electrical connection with fibroblasts. In the transient state (**Figure 8**), we observed that I_{CaL} peak increased since the first beat, due to the immediate effects of I_{gap} on AP. Initially, there was also an intracellular Ca^{2+} rise, as SR Ca^{2+} content was still elevated. The mechanisms to remove Ca^{2+} from the cytosol were then activated: SERCA and inward current through NCX (extruding Ca^{2+}). NCX role, extruding Ca^{2+} out of the cell, becomes relevant in the transient state because if there is an imbalance with Ca^{2+} influx through I_{CaL} channels, Ca^{2+} loss occurs. This mechanism might explain the reduced SR Ca^{2+} load in myocytes interacting with fibroblasts.

Our findings suggest that fibroblasts increase Ca^{2+} impairment in HF by further reducing SR Ca^{2+} content in myocytes.

Limitations

Several limitations need to be considered when drawing conclusions from the present study. Although simulations of cellular electrophysiological behavior and systematic analyses of biomarkers complement and enrich experimental research, uncertainties in the development of the mathematical models employed might affect the outcome of the simulations. The limited availability of electrophysiology data from human fibroblasts has led to the use of a fibroblast model developed on the basis of adult rat ventricular tissue data, without taking into consideration potential changes in HF. Fibroblasts with the same characteristics were considered in normal and failing conditions, but electrophysiological remodeling in fibroblast currents could have an additional effect on myocytes (Aguilar et al., 2014). Another limitation is the use of a fibroblast model, instead of using a myofibroblast model (not available to date), which is the characteristic form in pathological conditions, which would take into account Ca^{2+} dynamics in these cells. Ca^{2+} signaling has been observed in human cardiac fibroblasts although with different pathways to those in contractile myocytes (Chen et al., 2010), and myofibroblasts show intracellular CaTs, modulated by intercellular coupling with myocytes (Chilton et al., 2007), but neither of them have been modeled. Specific data for fibroblasts features are still lacking and one of the major concerns in studies focusing myocyte–fibroblast interactions is the use of data from co-cultures and the need of data describing the real electrophysiological behavior *in vivo*.

Gap junctional coupling between a myocyte and a fibroblast has been modeled by a simple conductance as in previous simulation studies of fibroblast-myocyte coupling. However, recent findings suggesting the interaction of connexin45 with CaM (Zou et al., 2017) highlight that some ions such as Ca^{2+} can modulate the coupling current. If the modulation of the intercellular coupling by Ca^{2+} ions was taken into account, larger alterations in Ca^{2+} dynamics mechanisms could be observed. Any mechanism related to Ca^{2+} included into our model, such as realistic Ca^{2+} dynamics in fibroblasts, may affect the regulation of Ca^{2+} cycling in myocytes, and enhance the influence of fibroblasts.

Other structural modifications in HF, concerning myocytes, involve the loss of transverse tubules and reorganization of the cell membrane (Lyon et al., 2009). We have assumed that with the electrophysiological remodeling applied to ionic mechanisms, we qualitatively reproduce the delayed SR Ca^{2+} release resulting from detubulation. However, a detailed model including local changes in membrane structure related to the spatial organization of ion channels in HF could provide more accurate results about Ca^{2+} impairment (Nivala et al., 2015; Sanchez-Alonso et al., 2016).

Although Ca^{2+} homeostasis is related to contraction and relaxation force, other mechanical factors, such as myofibroblast contractility when fibroblasts are differentiated into the activated form or extracellular stiffness due to the excessive accumulation of collagen in HF, can contribute to cardiac dysfunction. Our model only considers intracellular Ca^{2+} in myocytes at a cellular level to evaluate the contraction of the heart. The behavior in tissue or even in the whole organ could also be different. A defined architecture of the myocyte when considering spatial distribution would allow to take into consideration the distribution of gap junctions as well as the extracellular space which could modulate Ca^{2+} homeostasis as it does in electrical propagation (Cabo and Boyden, 2009; Sachse et al., 2009; Seidel et al., 2010; Greisas and Zlochiver, 2016). We consider a natural continuation of the present work the analysis of fibrosis effects on calcium waves in 2D and 3D tissues, in which altered impulse propagation and generation of arrhythmias should develop because of the heterogeneities in tissue, according to other studies (Zlochiver et al., 2008; Sachse et al., 2009; Nguyen et al., 2012; Gomez et al., 2014a; Greisas and Zlochiver, 2016; Zimik and Pandit, 2016).

Regarding sensitivity analyses, the non-linearities are the main issue in quantifying the impact of parameters on biomarkers. To restore the electrical activity and contraction of myocytes, the effect of some drugs can imply a high change in an ionic mechanism, and the predictive value of this methodology decreases with increased variability.

Nonetheless, despite these limitations, cellular simulations can shed light in the causes of Ca^{2+} impairment observed in HF, which together with the arrhythmogenic activity of fibrotic tissue, can compromise the function of the myocardium. In the present study, the measures suggested to restore Ca^{2+} dynamics and contractility at cellular level are reliable because they are supported by experiments and according to our findings, tackling the electrophysiology remodeling in failing myocytes can also improve the effects of fibroblasts interactions.

AUTHOR CONTRIBUTIONS

MM, JF, and BT conceived and designed the study, and analyzed the data. MM performed simulations. JG and ES contributed to the methodology. MM and BT wrote the first draft of the manuscript. All authors contributed to manuscript revision, read, and approved the submitted version.

FUNDING

This work was partially supported by the National Science Foundation (MCB 1615677), the American Heart Association (15GRNT25490006), the "Plan Estatal de Investigación Científica y Técnica y de Innovación 2013–2016 from the Ministerio de Economía, Industria y Competitividad of Spain and Fondo Europeo de Desarrollo Regional (FEDER) DPI2016-75799-R (AEI/FEDER, UE)", and the "Programa de Ayudas de Investigación y Desarrollo (PAID-01-17)" from the Universitat Politècnica de València. The funders had no role in study design, data collection and analysis, decision to publish, or preparation of the manuscript.

SUPPLEMENTARY MATERIAL

The Supplementary Material for this article can be found online at: https://www.frontiersin.org/articles/10.3389/fphys.2018.01194/full#supplementary-material

REFERENCES

Aguilar, M., Qi, X. Y., Huang, H., Comtois, P., and Nattel, S. (2014). Fibroblast electrical remodeling in heart failure and potential effects on atrial fibrillation. *Biophys. J.* 107, 2444–2455. doi: 10.1016/j.bpj.2014.10.014

Alpert, N. R., Hasenfuss, G., Leavitt, B. J., Ittleman, F. P., Pieske, B., and Mulieri, L. A. (2000). A mechanistic analysis of reduced mechanical performance in human heart failure. *Jpn Heart J.* 41, 103–115. doi: 10.1536/jhj.41.103

Bers, D. M. (2000). Calcium fluxes involved in control of cardiac myocyte contraction. *Circ. Res.* 87, 275–281. doi: 10.1161/01.RES.87.4.275

Britton, O. J., Bueno-Orovio, A., Virág, L., Varró, A., and Rodriguez, B. (2017). The electrogenic Na^+/K^+ pump is a key determinant of repolarization abnormality susceptibility in human ventricular cardiomyocytes: a population-based simulation study. *Front. Physiol.* 8:278. doi: 10.3389/fphys.2017.00278

Brown, T. R., Krogh-Madsen, T., and Christini, D. J. (2016). Illuminating myocyte-fibroblast homotypic and heterotypic gap junction dynamics using dynamic clamp. *Biophys. J.* 111, 785–797. doi: 10.1016/j.bpj.2016.06.042

Cabo, C., and Boyden, P. A. (2009). Extracellular space attenuates the effect of gap junctional remodeling on wave propagation: a computational study. *Biophys. J.* 96, 3092–3101. doi: 10.1016/j.bpj.2009.01.014

Cartledge, J. E., Kane, C., Dias, P., Tesfom, M., Clarke, L., Mckee, B., et al. (2015). Functional crosstalk between cardiac fibroblasts and adult cardiomyocytes by soluble mediators. *Cardiovasc. Res.* 105, 260–270. doi: 10.1093/cvr/cvu264

Chen, J.-B., Tao, R., Sun, H.-Y., Tse, H.-F., Lau, C.-P., and Li, G.-R. (2010). Multiple Ca^{2+} signaling pathways regulate intracellular Ca^{2+} activity in human cardiac fibroblasts. *J. Cell. Physiol.* 223, 68–75. doi: 10.1002/jcp.22010

Chilton, L., Giles, W. R., and Smith, G. L. (2007). Evidence of intercellular coupling between co-cultured adult rabbit ventricular myocytes and myofibroblasts. *J. Physiol.* 583, 225–236. doi: 10.1113/jphysiol.2007.135038

Chilton, L., Ohya, S., Freed, D., George, E., Drobic, V., Shibukawa, Y., et al. (2005). K+ currents regulate the resting membrane potential, proliferation, and contractile responses in ventricular fibroblasts and myofibroblasts. *Am. J. Physiol. Circ. Physiol.* 288, H2931–H2939. doi: 10.1152/ajpheart.01220.2004

Cummins, M. A., Dalal, P. J., Bugana, M., Severi, S., and Sobie, E. A. (2014). Comprehensive analyses of ventricular myocyte models identify targets exhibiting favorable rate dependence. *PLoS Comput. Biol.* 10:e1003543. doi: 10.1371/journal.pcbi.1003543

Drouin, E., Lande, G., and Charpentier, F. (1998). Amiodarone reduces transmural heterogeneity of repolarization in the human heart. *J. Am. Coll. Cardiol.* 32, 1063–1067. doi: 10.1016/S0735-1097(98)00330-1

Fukuta, H., and Little, W. C. (2007). Contribution of systolic and diastolic abnormalities to heart failure with a normal and a reduced ejection fraction. *Prog. Cardiovasc. Dis.* 49, 229–240. doi: 10.1016/j.pcad.2006.08.009

Gaudesius, G., Miragoli, M., Thomas, S. P., and Rohr, S. (2003). Coupling of cardiac electrical activity over extended distances by fibroblasts of cardiac origin. *Circ. Res.* 93, 421–428. doi: 10.1161/01.RES.0000089258.40661.0C

Gomez, J. F., Cardona, K., Martinez, L., Saiz, J., and Trenor, B. (2014a). Electrophysiological and structural remodeling in heart failure modulate arrhythmogenesis. 2D simulation study. *PLoS One* 9:e103273. doi: 10.1371/journal.pone.0103273

Gomez, J. F., Cardona, K., Romero, L., Ferrero, J. M., and Trenor, B. (2014b). Electrophysiological and structural remodeling in heart failure modulate arrhythmogenesis. 1D simulation study. *PLoS One* 9:e106602. doi: 10.1371/journal.pone.0106602

Greisas, A., and Zlochiver, S. (2016). The multi-domain fibroblast/myocyte coupling in the cardiac tissue: a theoretical study. *Cardiovasc. Eng. Technol.* 7, 290–304. doi: 10.1007/s13239-016-0266-x

Jacquemet, V., and Henriquez, C. S. (2008). Loading effect of fibroblast-myocyte coupling on resting potential, impulse propagation, and repolarization: insights from a microstructure model. *Am. J. Physiol. Circ. Physiol.* 294, H2040–H2052. doi: 10.1152/ajpheart.01298.2007

Li, G. R., Feng, J., Yue, L., and Carrier, M. (1998). Transmural heterogeneity of action potentials and Ito1 in myocytes isolated from the human right ventricle. *Am. J. Physiol.* 275, H369–H377.

Li, Y., Asfour, H., and Bursac, N. (2017). Age-dependent functional crosstalk between cardiac fibroblasts and cardiomyocytes in a 3D engineered cardiac tissue. *Acta Biomater.* 55, 120–130. doi: 10.1016/j.actbio.2017.04.027

Lou, Q., Janks, D. L., Holzem, K. M., Lang, D., Onal, B., Ambrosi, C. M., et al. (2012). Right ventricular arrhythmogenesis in failing human heart: the role of conduction and repolarization remodeling. *Am. J. Physiol. Heart Circ. Physiol.* 303, H1426–H1434. doi: 10.1152/ajpheart.00457.2012

Lyon, A. R., MacLeod, K. T., Zhang, Y., Garcia, E., Kanda, G. K., Lab, M. J., et al. (2009). Loss of T-tubules and other changes to surface topography in ventricular myocytes from failing human and rat heart. *Proc. Natl. Acad. Sci. U.S.A.* 106, 6854–6859. doi: 10.1073/pnas.0809777106

MacCannell, K. A., Bazzazi, H., Chilton, L., Shibukawa, Y., Clark, R. B., and Giles, W. R. (2007). A mathematical model of electrotonic interactions between ventricular myocytes and fibroblasts. *Biophys. J.* 92, 4121–4132. doi: 10.1529/biophysj.106.101410

Majumder, R., Nayak, A. R., and Pandit, R. (2012). Nonequilibrium arrhythmic states and transitions in a mathematical model for diffuse fibrosis in human cardiac tissue. *PLoS One* 7:e45040. doi: 10.1371/journal.pone.0045040

Mayourian, J., Savizky, R. M., Sobie, E. A., and Costa, K. D. (2016). Modeling electrophysiological coupling and fusion between human mesenchymal stem cells and cardiomyocytes. *PLoS Comput. Biol.* 12:e1005014. doi: 10.1371/journal.pcbi.1005014

Miragoli, M., Gaudesius, G., and Rohr, S. (2006). Electrotonic modulation of cardiac impulse conduction by myofibroblasts. *Circ. Res.* 98, 801–810. doi: 10.1161/01.RES.0000214537.44195.a3

Mora, M. T., Ferrero, J. M., Romero, L., and Trenor, B. (2017). Sensitivity analysis revealing the effect of modulating ionic mechanisms on calcium dynamics in simulated human heart failure. *PLoS One* 12:e0187739. doi: 10.1371/journal.pone.0187739

Morotti, S., Nieves-Cintrón, M., Nystoriak, M. A., Navedo, M. F., and Grandi, E. (2017). Predominant contribution of L-type Cav1.2 channel stimulation to impaired intracellular calcium and cerebral artery vasoconstriction in diabetic hyperglycemia. *Channels* 11, 340–346. doi: 10.1080/19336950.2017.1293220

Muszkiewicz, A., Britton, O. J., Gemmell, P., Passini, E., Sánchez, C., Zhou, X., et al. (2016). Variability in cardiac electrophysiology: using experimentally-calibrated populations of models to move beyond the single virtual physiological human paradigm. *Prog. Biophys. Mol. Biol.* 120, 115–127. doi: 10.1016/j.pbiomolbio.2015.12.002

Nguyen, T. P., Xie, Y., Garfinkel, A., Qu, Z., and Weiss, J. N. (2012). Arrhythmogenic consequences of myofibroblast–myocyte coupling. *Cardiovasc. Res.* 93, 242–251. doi: 10.1093/cvr/cvr292

Nivala, M., Song, Z., Weiss, J. N., and Qu, Z. (2015). T-tubule disruption promotes calcium alternans in failing ventricular myocytes: mechanistic insights from

computational modeling. *J. Mol. Cell. Cardiol.* 79, 32–41. doi: 10.1016/j.yjmcc.2014.10.018

O'Hara, T., Virág, L., Varró, A., and Rudy, Y. (2011). Simulation of the undiseased human cardiac ventricular action potential: model formulation and experimental validation. *PLoS Comput. Biol.* 7:e1002061. doi: 10.1371/journal.pcbi.1002061

Ozdemir, S., Bito, V., Holemans, P., Vinet, L., Mercadier, J. J., Varro, A., et al. (2008). Pharmacological inhibition of Na/Ca exchange results in increased cellular Ca^{2+} load attributable to the predominance of forward mode block. *Circ. Res.* 102, 1398–1405. doi: 10.1161/CIRCRESAHA.108.173922

Pereon, Y., Demolombe, S., Baro, I., Drouin, E., Charpentier, F., and Escande, D. (2000). Differential expression of KvLQT1 isoforms across the human ventricular wall. *Am. J. Physiol. Hear. Circ. Physiol.* 278, H1908–H1915. doi: 10.1152/ajpheart.2000.278.6.H1908

Piacentino, V., Weber, C. R., Chen, X., Weisser-Thomas, J., Margulies, K. B., Bers, D. M., et al. (2003). Cellular basis of abnormal calcium transients of failing human ventricular myocytes. *Circ. Res.* 92, 651–658. doi: 10.1161/01.RES.0000062469.83985.9B

Rocchetti, M., Alemanni, M., Mostacciuolo, G., Barassi, P., Altomare, C., Chisci, R., et al. (2008). Modulation of sarcoplasmic reticulum function by PST2744 [istaroxime; (E,Z)-3-((2-aminoethoxy)imino) androstane-6,17-dione hydrochloride)] in a pressure-overload heart failure model. *J. Pharmacol. Exp. Ther.* 326, 957–965. doi: 10.1124/jpet.108.138701

Romero, L., Carbonell, B., Trenor, B., Rodríguez, B., Saiz, J., and Ferrero, J. M. (2011). Systematic characterization of the ionic basis of rabbit cellular electrophysiology using two ventricular models. *Prog. Biophys. Mol. Biol.* 107, 60–73. doi: 10.1016/J.PBIOMOLBIO.2011.06.012

Romero, L., Pueyo, E., Fink, M., and Rodríguez, B. (2009). Impact of ionic current variability on human ventricular cellular electrophysiology. *Am. J. Physiol. Heart Circ. Physiol.* 297, H1436–H1445. doi: 10.1152/ajpheart.00263.2009

Rook, M. B., van Ginneken, A. C., de Jonge, B., el Aoumari, A., Gros, D., and Jongsma, H. J. (1992). Differences in gap junction channels between cardiac myocytes, fibroblasts, and heterologous pairs. *Am. J. Physiol. Physiol.* 263, C959–C977. doi: 10.1152/ajpcell.1992.263.5.C959

Sachse, F. B., Moreno, A. P., Seemann, G., and Abildskov, J. A. (2009). A model of electrical conduction in cardiac tissue including fibroblasts. *Ann. Biomed. Eng.* 37, 874–889. doi: 10.1007/s10439-009-9667-4

Sanchez-Alonso, J. L., Bhargava, A., O'Hara, T., Glukhov, A. V., Schobesberger, S., Bhogal, N., et al. (2016). Microdomain-specific modulation of L-type calcium channels leads to triggered ventricular arrhythmia in heart failure. *Circ. Res.* 119, 944–945. doi: 10.1161/CIRCRESAHA.116.308698

Savarese, G., and Lund, L. H. (2017). Global public health burden of heart failure. *Card. Fail. Rev.* 3, 7–11. doi: 10.15420/cfr.2016:25:2

Seidel, T., Salameh, A., and Dhein, S. (2010). A simulation study of cellular hypertrophy and connexin lateralization in cardiac tissue. *Biophys. J.* 99, 2821–2830. doi: 10.1016/j.bpj.2010.09.010

Shannon, T. R., Ginsburg, K. S., and Bers, D. M. (2000). Potentiation of fractional sarcoplasmic reticulum calcium release by total and free intra-sarcoplasmic reticulum calcium concentration. *Biophys. J.* 78, 334–343. doi: 10.1016/S0006-3495(00)76596-9

Sobie, E. A. (2009). Parameter sensitivity analysis in electrophysiological models using multivariable regression. *Biophys. J.* 96, 1264–1274. doi: 10.1016/j.bpj.2008.10.056

Sridhar, S., Vandersickel, N., and Panfilov, A. V. (2017). Effect of myocyte-fibroblast coupling on the onset of pathological dynamics in a model of ventricular tissue. *Sci. Rep.* 7:40985. doi: 10.1038/srep40985

Tamayo, M., Manzanares, E., Bas, M., Martín-Nunes, L., Val-Blasco, A., Jesús Larriba, M., et al. (2017). Calcitriol (1,25-dihydroxyvitamin D3) increases L-type calcium current via protein kinase A signaling and modulates calcium cycling and contractility in isolated mouse ventricular myocytes. *Heart Rhythm* 14, 432–439. doi: 10.1016/j.hrthm.2016.12.013

Trayanova, N. A., and Chang, K. C. (2016). How computer simulations of the human heart can improve anti-arrhythmia therapy. *J. Physiol.* 594, 2483–2502. doi: 10.1113/JP270532

Trenor, B., Cardona, K., Gomez, J. F., Rajamani, S., Ferrero, J. M., Belardinelli, L., et al. (2012). Simulation and mechanistic investigation of the arrhythmogenic role of the late sodium current in human heart failure. *PLoS One* 7:e32659. doi: 10.1371/journal.pone.0032659

Walmsley, J., Rodriguez, J. F., Mirams, G. R., Burrage, K., Efimov, I. R., and Rodriguez, B. (2013). mRNA expression levels in failing human hearts predict cellular electrophysiological remodeling: a population-based simulation study. *PLoS One* 8:e56359. doi: 10.1371/journal.pone.0056359

Xie, Y., Garfinkel, A., Camelliti, P., Kohl, P., Weiss, J. N., and Qu, Z. (2009a). Effects of fibroblast-myocyte coupling on cardiac conduction and vulnerability to reentry: a computational study. *Heart Rhythm* 6, 1641–1649. doi: 10.1016/j.hrthm.2009.08.003

Xie, Y., Garfinkel, A., Weiss, J. N., and Qu, Z. (2009b). Cardiac alternans induced by fibroblast-myocyte coupling: mechanistic insights from computational models. *Am. J. Physiol. Circ. Physiol.* 297, H775–H784. doi: 10.1152/ajpheart.00341.2009

Zhan, H., Xia, L., Shou, G., Zang, Y., Liu, F., and Crozier, S. (2014). Fibroblast proliferation alters cardiac excitation conduction and contraction: a computational study. *J. Zhejiang Univ. Sci. B* 15, 225–242. doi: 10.1631/jzus.B1300156

Zhou, X., Bueno-Orovio, A., Orini, M., Hanson, B., Hayward, M., Taggart, P., et al. (2016). In vivo and in silico investigation into mechanisms of frequency dependence of repolarization alternans in human ventricular cardiomyocytes. *Circ. Res.* 118, 266–278. doi: 10.1161/CIRCRESAHA.115.307836

Zimik, S., and Pandit, R. (2016). Instability of spiral and scroll waves in the presence of a gradient in the fibroblast density: the effects of fibroblast-myocyte coupling. *New J. Phys.* 18, 1–13. doi: 10.1088/1367-2630/18/12/123014

Zlochiver, S., Muñoz, V., Vikstrom, K. L., Taffet, S. M., Berenfeld, O., and Jalife, J. (2008). Electrotonic myofibroblast-to-myocyte coupling increases propensity to reentrant arrhythmias in two-dimensional cardiac monolayers. *Biophys. J.* 95, 4469–4480. doi: 10.1529/biophysj.108.136473

Zou, J., Salarian, M., Chen, Y., Zhuo, Y., Brown, N. E., Hepler, J. R., et al. (2017). Direct visualization of interaction between calmodulin and connexin45. *Biochem. J.* 474, 4035–4051. doi: 10.1042/BCJ20170426

Conflict of Interest Statement: The authors declare that the research was conducted in the absence of any commercial or financial relationships that could be construed as a potential conflict of interest.

frontiers in Physiology

ORIGINAL RESEARCH
published: 19 September 2018
doi: 10.3389/fphys.2018.01306

Modulation of Cardiac Alternans by Altered Sarcoplasmic Reticulum Calcium Release: A Simulation Study

Jakub Tomek[1], Markéta Tomková[2], Xin Zhou[1], Gil Bub[3] and Blanca Rodriguez[1]*

[1] Department of Computer Science, British Heart Foundation Centre of Research Excellence, University of Oxford, Oxford, United Kingdom, [2] Nuffield Department of Medicine, University of Oxford, Oxford, United Kingdom, [3] Department of Physiology, McGill University, Montreal, QC, Canada

Background: Cardiac alternans is an important precursor to arrhythmia, facilitating formation of conduction block, and re-entry. Diseased hearts were observed to be particularly vulnerable to alternans, mainly in heart failure or after myocardial infarction. Alternans is typically linked to oscillation of calcium cycling, particularly in the sarcoplasmic reticulum (SR). While the role of SR calcium reuptake in alternans is well established, the role of altered calcium release by ryanodine receptors has not yet been studied extensively. At the same time, there is strong evidence that calcium release is abnormal in heart failure and other heart diseases, suggesting that these changes might play a pro-alternans role.

Aims: To demonstrate how changes to intracellular calcium release dynamics and magnitude affect alternans vulnerability.

Methods: We used the state-of-the-art Heijman–Rudy and O'Hara–Rudy computer models of ventricular myocyte, given their detailed representation of calcium handling and their previous utility in alternans research. We modified the models to obtain precise control over SR release dynamics and magnitude, allowing for the evaluation of these properties in alternans formation and suppression.

Results: Shorter time to peak SR release and shorter release duration decrease alternans vulnerability by improved refilling of releasable calcium within junctional SR; conversely, slow release promotes alternans. Modulating the total amount of calcium released, we show that sufficiently increased calcium release may surprisingly prevent alternans via a mechanism linked to the functional depletion of junctional SR during release. We show that this mechanism underlies differences between "eye-type" and "fork-type" alternans, which were observed in human *in vivo* and *in silico*. We also provide a detailed explanation of alternans formation in the given computer models, termed "sarcoplasmic reticulum calcium cycling refractoriness." The mechanism relies on the steep SR load–release relationship, combined with relatively limited rate of junctional SR refilling.

OPEN ACCESS

Edited by:
Daniel M. Johnson, Maastricht University, Netherlands

Reviewed by:
Thomas Hund, The Ohio State University, United States
Jan Pavel Kucera, Universität Bern, Switzerland
Zhilin Qu, University of California, Los Angeles, United States

****Correspondence:***
Jakub Tomek
jakub.tomek.mff@gmail.com

Specialty section:
This article was submitted to Cardiac Electrophysiology, a section of the journal Frontiers in Physiology

Received: *13 June 2018*
Accepted: *29 August 2018*
Published: *19 September 2018*

Citation:
Tomek J, Tomková M, Zhou X, Bub G and Rodriguez B (2018) Modulation of Cardiac Alternans by Altered Sarcoplasmic Reticulum Calcium Release: A Simulation Study. Front. Physiol. 9:1306. doi: 10.3389/fphys.2018.01306

Conclusion: Both altered dynamics and magnitude of SR calcium release modulate alternans vulnerability. In particular, slow dynamics of SR release, such as those observed in heart failure, promote alternans. Therefore, acceleration of intracellular calcium release, e.g., via synchronization of calcium sparks, may inhibit alternans in failing hearts and reduce arrhythmia occurrence.

Keywords: alternans, calcium handling, calcium release, calcium release dynamics, sarcoplasmic reticulum cycling, computer modeling

INTRODUCTION

Repolarization alternans, the alternation of long and short action potential durations (APD), has been linked to the incidence of ventricular fibrillation and sudden cardiac death (Pastore et al., 1999; Wilson and Rosenbaum, 2007). Episodes of fibrillation were observed to be consistently preceded by alternans formation both in ventricles (Wilson et al., 2009) and atria (Narayan et al., 2011), suggesting that alternans importantly contributes to arrhythmogenesis. At the cellular level, repolarization alternans has been extensively researched both experimentally and computationally (Díaz et al., 2004; Szentesi et al., 2004; Weiss et al., 2006; Livshitz and Rudy, 2007; Kanaporis and Blatter, 2015; Bayer et al., 2016; Qu et al., 2016; Zhou et al., 2016; Tomek et al., 2017). Alternans may be driven primarily by steep APD restitution, or by oscillations in calcium handling (Pruvot et al., 2004). In the calcium-driven alternans hypothesis, calcium alternans consist of calcium transient amplitude oscillation between subsequent beats, which then translate into repolarization alternans via sodium-calcium exchanger and other calcium-sensitive currents (Livshitz and Rudy, 2007; Edwards and Blatter, 2014).

Multiple heart diseases are associated with an increased vulnerability to alternans, particularly heart failure (Kodama et al., 2004; Wilson et al., 2009), as well as hypertrophic cardiomyopathy (Cannon et al., 1986), or myocardial infarction (Gardner et al., 2015). It is known that cardiac remodeling in heart failure and other diseases alters both intracellular calcium release (Lindner et al., 2002) and reuptake (Kho et al., 2012) within cardiomyocytes. While reduced reuptake capacity has been linked to alternans vulnerability (Weiss et al., 2006; Qu et al., 2007), the relationship between altered calcium release and alternans vulnerability is less clear. Ryanodine receptor leakiness has been identified both as a promotor and a suppressor of alternans (Lehnart et al., 2006; Xie et al., 2008). However, the precise mechanisms by which calcium release properties regulate alternans vulnerability in large mammalian hearts are not known. This may be important to better understand pro-arrhythmia mechanisms in diseased hearts with altered calcium release mechanisms.

The main goal of this work is to characterize how altered properties of the sarcoplasmic reticulum (SR) calcium release modulate alternans vulnerability, contributing to the explanation of alternans vulnerability in heart failure and other diseases. We focus at two features of SR release: the dynamics (how quickly is a given amount of calcium released) and magnitude (how much calcium is released in total), showing that both factors modulate alternans. To study the properties of altered calcium release with respect to alternans, we utilize computational modeling of cardiomycytes, which provides excellent observability and control of the studied systems. We used the state-of-the-art model of ventricular myocyte by Heijman et al. (2011), which is the most up-to-date version of the Hund–Rudy model (Hund and Rudy, 2004; Livshitz and Rudy, 2007; Decker et al., 2009) and the ORd model (O'Hara et al., 2011). Both models have been extensively validated against experimental data, contain a detailed model of calcium handling, and were used for study of various aspects of alternans (Livshitz and Rudy, 2007; Zhou et al., 2016; Tomek et al., 2017). The major advantage of these models is the compartmentalization of the SR. This allows the study of calcium cycling within SR, which was suggested to be an important modulator of cellular calcium handling (Ramay et al., 2011) and alternans (Kihara and Morgan, 1991). We demonstrate in this work that this cycling underlies alternans in the studied models and that this is important for the interpretation of our results on alternans and SR release properties.

MATERIALS AND METHODS

Computational Models of Membrane Kinetics and Calcium Handling

The primary model used in this study is Heijman–Rudy (HeRd) (**Figure 1**), a model of canine ventricular myocyte (Heijman et al., 2011); the β-adrenergic component of the model was not used in this study. In addition, we used the O'Hara–Rudy (ORd) model of human ventricular myocyte (O'Hara et al., 2011) in Section Results: Increased and Decreased Magnitude of SR Release Attenuates Alternans to directly link our mechanistic insight to a previously published study utilizing this model. The ORd model has the same compartmentalization as HeRd, but contains human-specific formulations of ionic currents. Codes for both models were downloaded from the website of the lab of Prof. Yoram Rudy[1].

Action potential duration (APD) alternans at a given time point was defined as the difference in APD90 (APD at 90% repolarization level) between two consecutive action potentials.

Below is listed methodology for the respectively numbered "Results" sections.

Stimulation Protocols

At all pacing rates, simulated cells were paced for 2500 beats to reach quasi-stable state as shown previously (Tomek et al., 2017). In a system manifesting alternans, true stability is

[1]http://rudylab.wustl.edu/research/cell/code/AllCodes.html

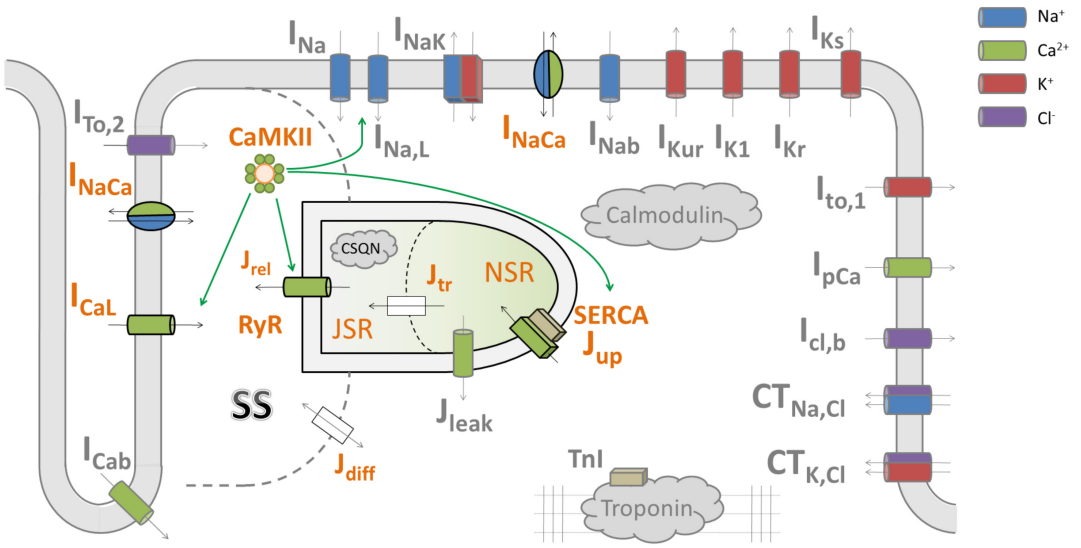

FIGURE 1 | A diagram of the HeRd model of ventricular cardiomyocyte and an overview of calcium handling. Shown are transmembrane currents, compartmentalized sarcoplasmic reticulum and the associated fluxes, and CaMKII signaling. β-adrenergic signaling components in the model were not used in this study. The calcium handling components relevant for alternans are highlighted in orange font. Green arrows indicate which components are regulated by CaMKII, an important regulator of calcium handling. Within an action potential, calcium handling in the model works as follows: L-type calcium current (I_{CaL}) induces an influx of calcium which is sensed by ryanodine receptors (RyR). This induces a large-magnitude release of calcium, J_{rel}, via RyR (this process is termed CICR: calcium-induced calcium release). The amount of calcium released via RyR depends mainly on the calcium stimulus via I_{CaL} and the load–release relationship of junctional sarcoplasmic reticulum containing RyR (JSR): the fuller the JSR is, the more calcium it releases (Shannon et al., 2000). This relationship is steep, as shown in a previous study of the Hund-Rudy model (Livshitz and Rudy, 2007) and experiments (Shannon et al., 2000), i.e., a relatively small increase in JSR contents may increase fractional release considerably. The released calcium then diffuses to the intracellular space (J_{diff}) and eventually to SERCA pumps, which reuptake the calcium back to network sarcoplasmic reticulum containing SERCA pumps (NSR). Ultimately, within sarcoplasmic reticulum, calcium diffuses from NSR to JSR along the concentration gradient (J_{tr}), from where it may be released in the next action potential. SS codes the junctional calcium subspace where the calcium influx via ICaL stimulates ryanodine receptors. The figure is based on Heijman et al. (2011).

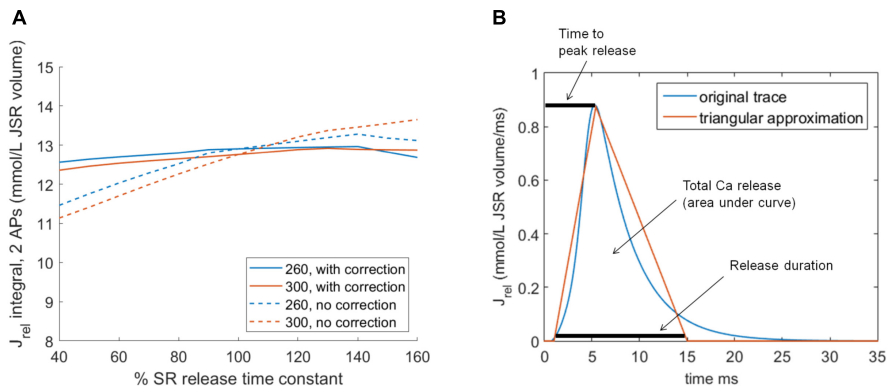

FIGURE 2 | Altering SR release dynamics at bcl 260 and 300 in the HeRd model: **(A)** The relationship between altered time constant of RyR release and total amount of calcium released over two consecutive action potentials at two pacing rates. In solid lines is shown the relationship after the application of compensatory rescaling of I_{CaL} conductance, as described in the main manuscript. The dashed lines show how the relationship between altered SR release time constant and total calcium release would have looked without such scaling. **(B)** An illustration of the approximation of native HeRd J_{rel} using a triangle. Throughout the article, parameters varied are the release duration, time to peak release, and total calcium released.

impossible, given the presence of oscillations in APD and ionic concentrations. We term the cellular model to be in a quasi-stable state when the maximum and minimum of each of the following variables during two consecutive beats change less than 0.2% per 100 beats: membrane potential, intracellular calcium, intracellular potassium, and intracellular sodium. Maxima and minima of beat pairs are used to allow cells manifesting alternans to be considered stabilized. For convenience, "stable state" is used instead of "quasi-stable state" in the rest of the article.

When evaluating the effect of altered time constant of diffusion between the network sarcoplasmic reticulum (NSR) and

the junctional sarcoplasmic reticulum (JSR), cells were first pre-paced for 2500 beats at base cycle lengths 260, 300, and 340. Subsequently, the pre-paced cells were loaded and paced for 2500 more beats with both reduced and increased time constant (60, 70,...,140% of original value) and alternans was measured at the end of the 2500 beats.

Model Modifications to Investigate SR Release Dynamics

To modulate the key features of SR release dynamics, the time to peak release and release duration, we scaled the ryanodine receptor (RyR) release time constant. While changing the RyR release time constant exerts only a small effect on total amount of calcium released (lowering time constant slightly lowers total calcium released and vice versa), it could nevertheless theoretically confound the result achieved. To account for this, we scaled the L-type calcium current (I_{CaL}) conductance in addition to the time constant to achieve a near–flat relationship between the time constant and total calcium released (**Figure 2A**, solid lines; dashed lines show the relationship without I_{CaL} scaling). For time constant multipliers of 0.4, 0.5,...,1.6, the corresponding multipliers of I_{CaL} conductance at base cycle length (bcl) 260 were: 1.0823, 1.0643, 1.0479, 1.0334, 1.0204, 1.0057, 1.0000, 0.9949, 0.9901, 0.9854, 0.9810, 0.9673, and 0.9545. At bcl 300, the corresponding I_{CaL} conductance multipliers were: 1.0949, 1.0772, 1.0593, 1.0425, 1.0269, 1.0129, 1.0000, 0.9882, 0.9772, 0.9690, 0.9650, 0.9605, and 0.9558.

In order to separate two aspects of SR release dynamics, the time to peak release and the release duration, we modified the model to allow a clamp of SR release J_{rel} in the form of a triangle approximating a native release (**Figure 2B**). Concretely, the triangular release starts 1 ms after the stimulus administration (similarly to normal SR release) and has three parameters: release duration (base width of the triangle), time to peak (position of the triangle peak), and total calcium released (area of the triangle).

The triangular clamp was applied after a cell was pre-paced to a stable state using its native SR release formulation. The prepacing was performed for 2500 beats at 400 ms bcl. At this pacing rate the cell does not manifest alternans, but the pacing frequency is fast enough to activate CaMKII and other rate-dependent mechanisms. Calcium leak from JSR ($I_{leak,JSR}$) was set to 0 when the triangular clamp was used so that the total SR release was equal to the value imposed by the triangular clamp and it was not "contaminated" by additional JSR leak.

In order to assess the vulnerability of cells with clamped SR release to alternans, we use a proxy termed "alternans threshold" related to the capability of the cell to refill the JSR following a calcium release. Specifically, we loaded from a file a pre-paced stable-state cell and simulated a single AP with a clamped SR release of given parameters, observing the ability of the cell to refill JSR to the same value as at the beginning of the AP within 400 ms. We searched a range of values of release duration (5–40 ms) and time to peak release (2–35 ms).

- For each of these combinations, we searched a range of values of the total amount of calcium released (effectively stretching the release triangle vertically). Each tested combination of release duration, time to peak release, and total amount of calcium released was simulated after loading a pre-paced stable state, i.e., the simulations were entirely independent.
- "Alternans threshold" is the level of total calcium released above which a cell with the given release duration and time to peak release fails to refill the JSR to the pre-release state within the APD. The intuition underlying the term "alternans threshold" is that in the given family of models, alternans starts following a failure to refill the JSR, which then leads to further oscillation of the calcium handling subsystem.

Modulating SR Release Magnitude

A second change to the release properties performed in this work was changing the total amount of calcium released (SR release integral). In order to control this, we used a proxy in the form of scaling I_{CaL} with a multiplier of its conductance, as there is a near–linear relationship between the scaling factor of I_{CaL} and the respective increase in SR release integral in both considered models (**Figures 3A,B**). Scaling I_{CaL} instead of release properties to control total SR release is appealing, as it is possible to maintain the original formulation of SR release. Consequently, any results achieved may be linked to amount of calcium released, as opposed to other changes to the RyR model which could confound the analysis.

RESULTS

Mechanisms of Alternans Driven by SR Cycling Refractoriness

Cardiac alternans is generally thought to arise predominantly from the oscillation of calcium subsystem of cardiomyocytes (Weiss et al., 2006). Livshitz and Rudy (2007) have also shown that this is the case in the Rudy-family of models. However, it remains to be elucidated how exactly the models enter the calcium oscillations in the first place.

We hypothesized that the rate of diffusion from NSR to JSR could be a key factor in alternans formation. Slow diffusion from NSR to JSR could limit timely refilling of JSR and facilitate alternans, as first proposed by Kihara and Morgan (1991). To test this hypothesis, we varied J_{tr}, the time constant of the NSR→JSR diffusion in simulated cells, observing the impact on APD and calcium transient alternans. Consistent with the hypothesis, a reduction in the diffusion time constant (corresponding to accelerated NSR→JSR diffusion) attenuated alternans in APD and calcium transient (**Figures 4A,B**). Conversely, increased diffusion time constant promoted alternans formation: Even at 300 ms bcl pacing, when a cell with normal diffusion rate did not manifest alternans, sufficiently diminished diffusion rate (high time constant) allowed alternans to occur.

We now reconstruct how alternans is sustained, focusing on two consecutive action potentials during stable-state APD and calcium alternans (**Figures 5A,B**). At the start of the first action potential, the JSR calcium concentration is high (x_1 in

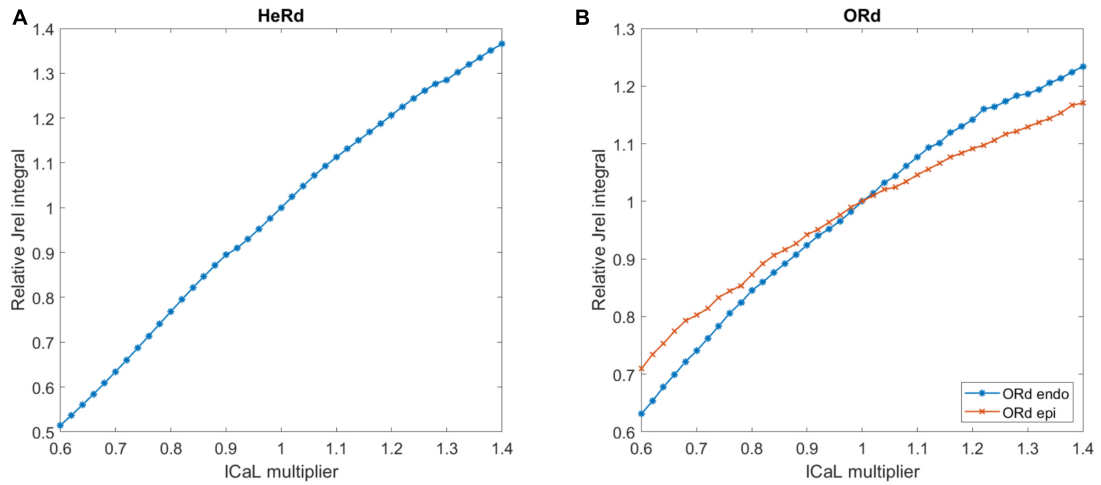

FIGURE 3 | Near-linear relationship between I_{CaL} multiplier and total SR release in the HeRd and ORd models. Shown are results in the HeRd model **(A)** and the ORd model, endocardial, and epicardial **(B)**. Relative increase in total SR release (J_{rel} integral) for a given I_{CaL} scaling factor is given as follows: let *x* be an I_{CaL} scaling factor and *y* be the resulting integral of J_{rel} over two action potentials after stable-state pre-pacing. Let *a* be the integral of J_{rel} over 2 APs for I_{CaL} scaling factor of 1. Then, relative J_{rel} integral is *y*/*b*. Integral over 2 APs is used to accommodate for alternans formation. In all cases, the model was paced until steady state for 2500 beats at bcl 260 ms.

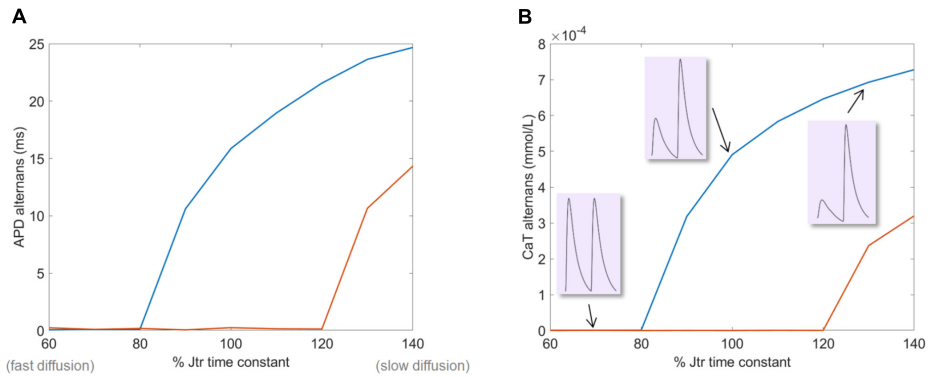

FIGURE 4 | The effect of varying NSR→JSR diffusion time constant on alternans amplitude in the HeRd model. **(A)** The amplitude of APD alternans at two pacing rates: 260 ms (where the baseline model with 100% value of time constant does manifest alternans) and 300 (where the baseline model does not manifest alternans). **(B)** The amplitude of calcium transient (CaT) alternans. In insets are shown examples of calcium transients at the end of the simulation of 260 ms bcl pacing, showing no alternans at 70% time constant, alternans at 100%, and exacerbated alternans at 130%.

Figure 5D), leading to a large release J_{rel} (y_1 in **Figure 5E**). This is followed by calcium diffusion from the junctional subspace to SERCA pumps, allowing for reuptake into NSR (**Figure 5G**). Due to the large depletion of JSR after the first release and a limited rate of diffusion from NSR to JSR (J_{tr}, **Figure 5F**), JSR is refilled to a lower value than at the beginning (x_2 in **Figure 5D**). Crucially, given that the JSR load–release relationship is steep (**Figure 5C**), the following release is small (y_2 in **Figure 5E**). That is, while the JSR calcium concentration at the start of the first action potential (x_1) is not drastically higher than at the start of the second one (x_2), the first peak release y_1 is approximately two times higher than the second one y_2. Total amount of calcium released in the first release is 80% higher than in the second one, causing a pronounced difference in JSR depletion. At the same time, the amount of calcium refilled to the JSR is higher only by 23% during the first action potential compared to the second one. The NSR-JSR flux which may be integrated to obtain the amount of calcium refilled is shown in **Figure 5F**. This insensitivity follows from the fact that the NSR→JSR gradient is relatively high at any point during the simulation (**Figure 5D**) and it is not as strongly affected by JSR depletion. Therefore, the JSR refilling is fast enough to restore JSR calcium concentration back to x_1 within the second AP, perpetuating alternans.

Dynamics of JSR Release and Alternans: Beyond Amount Released

In order to modulate the dynamics of SR release, we modulated the time constant of SR release. Lowering the time constant reduces the time to peak release (**Figure 6A**) and the release

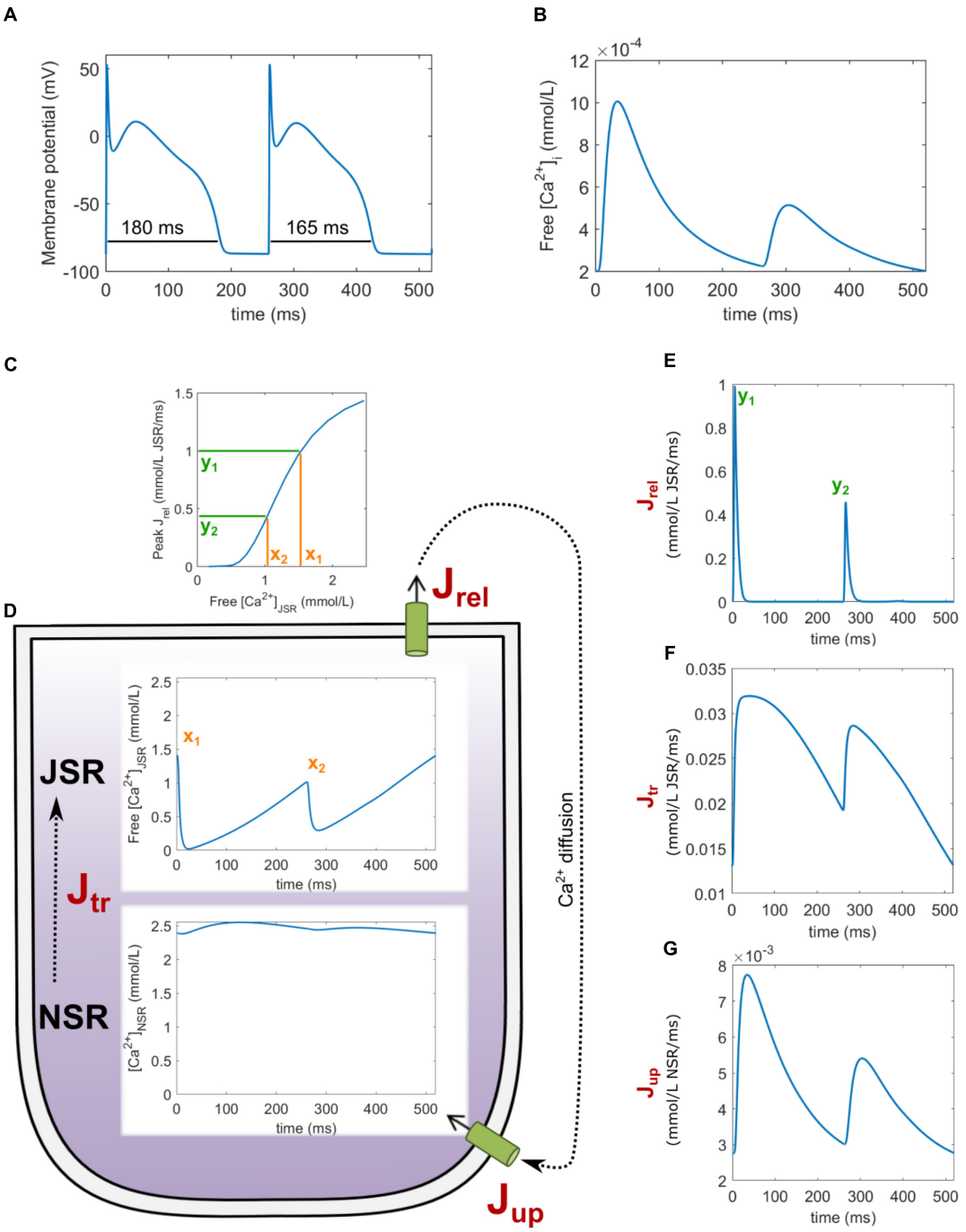

FIGURE 5 | An overview of key variables during alternans in the HeRd model. Two action potentials after reaching the stable state are shown, starting with a prolonged action potential **(A)** with underlying large calcium transient **(B). (C)** The relationship between free JSR calcium and peak J_{rel}. **(D)** Free JSR calcium and NSR calcium. Fluxes associated with SR shown are J_{rel} **(E)**, J_{tr} **(F)**, and J_{up} **(G)**. The free $Ca^{2+}{}_{[JSR]}$ levels x_1, x_2 and peak release values y_1, y_2 are linked with load–release relationship.

duration (**Figure 6B**), while increasing the time constant conversely increases both features of SR release. Crucially, setting the time constant of SR release lower than 80% of the control value abolished alternans in a cell paced at 260 ms bcl (**Figure 6C**). Conversely, sufficiently increased time constant of SR release allowed alternans formation in a cell paced at 300 ms bcl, which does not manifest alternans with baseline value of time constant.

To further separate the influence of shortened time to peak and release duration, we used clamping of SR release to a

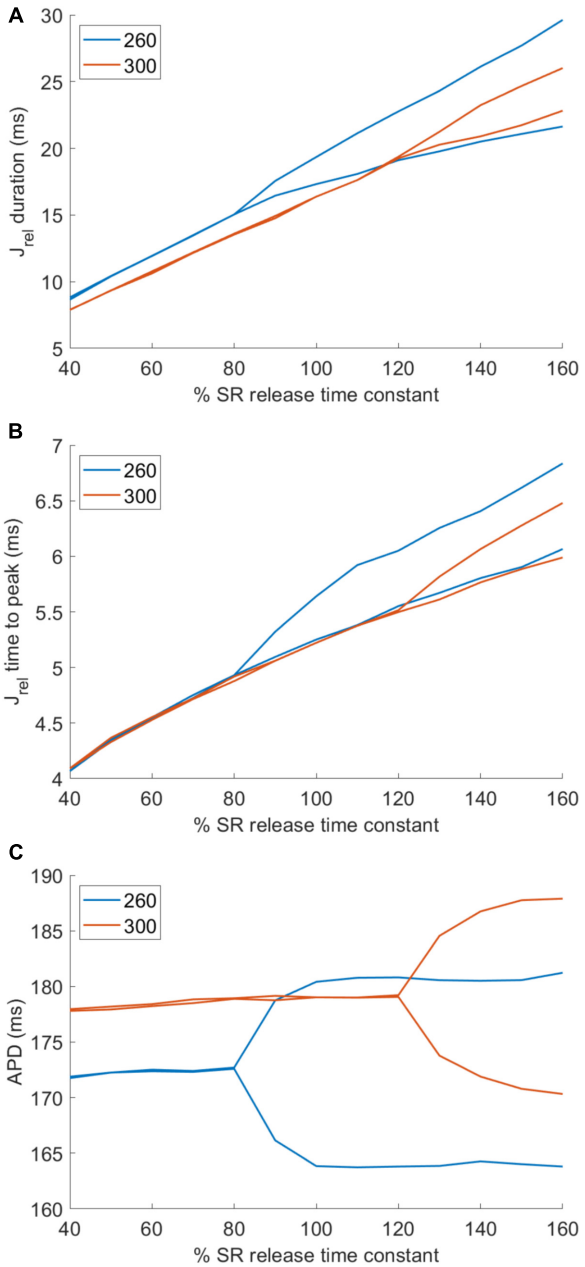

FIGURE 6 | Effect of altering SR release dynamics on alternans at 260 and 300 ms bcl in the HeRd model. Changes in time to peak release **(A)** and duration of release at 90% release recovery **(B)** with scaling of SR release time constant at two pacing rates. The bifurcations correspond to alternans of the respective feature, concurrent with APD alternans **(C)**.

triangular shape of given parameters (section "Materials and Methods"). We assess the vulnerability of cells with a clamped release based on their ability to refill the JSR to the starting value, following a SR release, as this was shown to be a critical determinant of alternans in the previous section. This indirect approach to quantify alternans vulnerability is based on the fact that clamping the SR, necessary for full control over the release, may prevent alternans formation. For every combination of parameters specifying the shape of the triangular release, we search for the highest total JSR release (stretching the triangle vertically), such that JSR is refilled to its initial value within the action potential (details in section "Materials and Methods"). This amount is termed "alternans threshold": cells with a high alternans threshold are more resistant to alternans formation than ones with a low alternans threshold, as they can support a larger release without failing to refill the JSR.

We mapped the alternans threshold over a range of pairs of parameters of the SR release (base width, peak time). It is apparent that both shortened release, as well as the earlier peak release improve JSR refilling and are therefore expected to attenuate alternans, confirming the importance of both aspects of release dynamics (**Figure 7A**). Conversely, prolonged release and longer time to peak facilitate alternans formation. Moreover, for a fixed total calcium release, the amount of refilled calcium (J_{tr} integral) increases with both reduced time to peak release and release duration (**Figure 7B**), in line with increased resistance to alternans. For both parameters, the alternans threshold and amount of refilled calcium are affected even when the other parameter is fixed, suggesting their independence.

In the case of earlier time to peak (**Figure 7C**, solid lines; blue vs. red), the key factor is that JSR is depleted sooner (**Figure 7E**, solid lines), providing more time for SR reuptake and JSR refilling, resulting in higher final JSR concentration in the case of earlier-peak release (**Figure 7E**, inset, solid lines). In the case of short-duration release (**Figure 7C**, dashed lines, orange vs. purple), the earlier JSR depletion plays a similar role (**Figure 7E**, dashed lines). Furthermore, such a fast release of high amplitude increases the extra-SR calcium concentration rapidly, enhancing the SERCA reuptake rate and increasing the NSR loading (**Figure 7F**, dashed lines). This increases the NSR→JSR gradient and therefore also the JSR refilling rate J_{tr}. Consequently, the final concentration of JSR is higher in the case of shorter release (**Figure 7E**, inset, dashed line). We note that in the case where the calcium fails to refill to the original value in **Figure 7E**, the difference of the starting and final state is small – this corresponds to a very early phase of alternans development, where APD alternans would be also minimal. In a cell developing alternans, the amplitude of JSR release oscillation and thus also diastolic SR loading oscillation self-amplifies to greatly increase over subsequent beats; however, this cannot be shown using a model with clamped SR release. Using an unclamped cell without controlled release shows that during stable-state alternans, the difference between JSR calcium concentration at the start and the end of an action potential is much higher (**Figure 5D**, x_1 vs. x_2).

Increased and Decreased Magnitude of SR Release Attenuates Alternans

In the previous section, we characterized how altered release dynamics modulate alternans, given a fixed calcium release magnitude. In this section, we instead maintain given dynamics and study the effect of varying amount of released calcium. We scaled the conductance of the I_{CaL} current in order to manipulate the SR release magnitude within an action potential

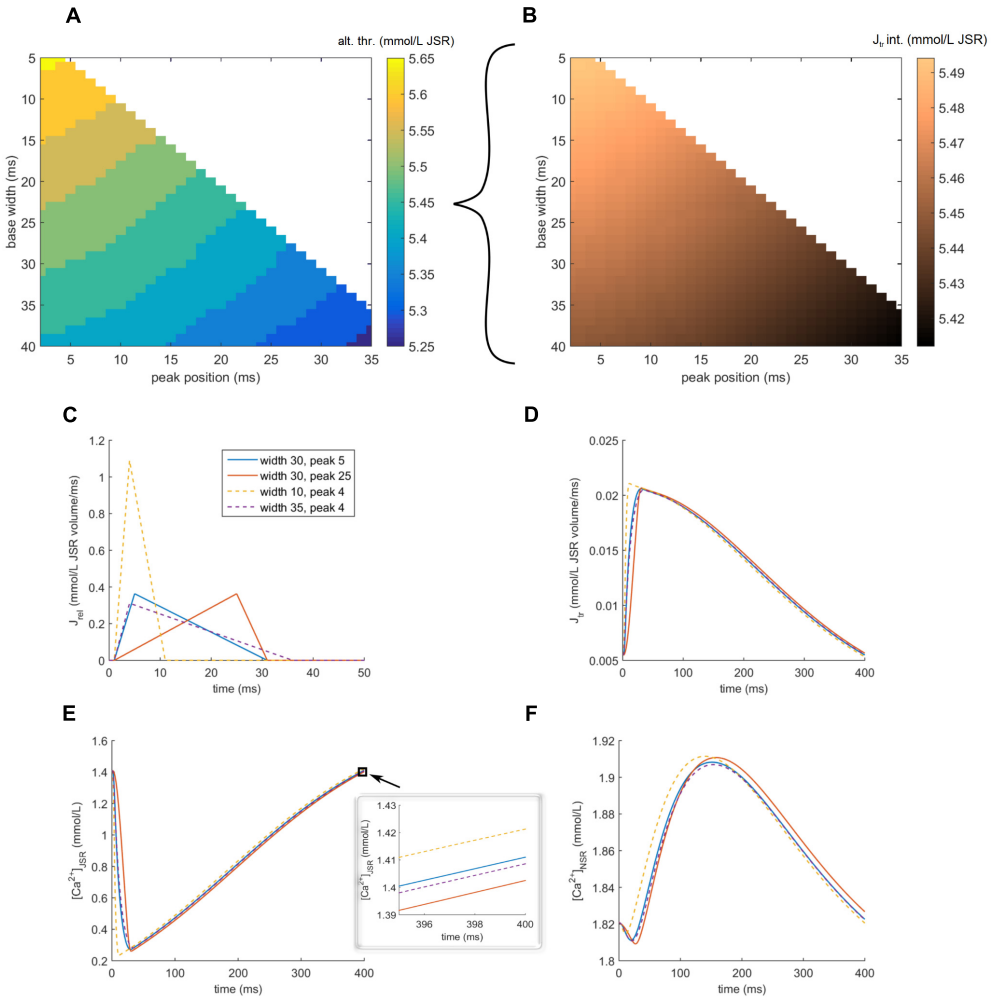

FIGURE 7 | Exploring shapes of SR release and alternans vulnerability in the HeRd model. **(A)** Shown here is the alternans threshold coded by color for various parameters of release triangle. Base width = release duration. Peak time = absolute time after stimulus administration corresponding to time to peak release. Alternans threshold = the level of total calcium released above which a cell with the given release duration and time to peak release fails to refill the JSR to the pre-release state within 400 ms (corresponding to one action potential at the prepacing bcl). **(B)** The integral of J_{tr} (JSR refilling) for a fixed total released calcium of 5.45. **(C)** Shapes of four triangular releases with total released calcium 5.45. The dashed lines vary in release duration, while the solid lines vary in peak position, but have the same duration. **(D)** JSR refilling rate. **(E)** JSR free calcium concentration and an inset of last 5 ms, showing the final calcium concentrations. **(F)** NSR calcium concentration.

(see section "Materials and Methods" for details and validation of near–linear relationship between I_{CaL} conductance and SR release magnitude). The baseline model with control SR release magnitude manifests APD alternans of 17 ms amplitude. In cells with sufficiently decreased SR release (I_{CaL} scaling factor <0.9), the total SR release was inhibited and no alternans was present (**Figure 8A**). This is to be expected: given that alternans in the model arises from an overtly large JSR depletion which cannot be refilled, lowering the SR release overall prevents this event from occurring.

Surprisingly, also sufficiently increased SR release (I_{CaL} scaling factor >1.2) abolished alternans in the stable state after 2500 beats (**Figure 8A**). This is a less expected result: since alternans is driven by SR release oscillations, potentiation of the release might be expected to increase the alternans magnitude. We note that scaling I_{CaL} produced only small effects in J_{rel} dynamics, such as up to 10% change in J_{rel} time to peak. According to results in **Figure 7**, this would have negligible effects on alternans vulnerability, particularly for J_{rel} time to peak of 5 ms as in the ORd/HRd models. Therefore, the effects of I_{CaL} scaling on alternans vulnerability in **Figure 8** are mainly due to alterations in J_{rel} magnitude as quantified in **Figure 3**.

We noticed that alternans did occur in models with increased SR release, but only transiently, i.e., before reaching the stable state (**Figures 8B,E**). Interestingly, after reaching the stable state, JSR was fully depleted in every beat. For intermediate increase in I_{CaL} conductance (scaling factor 1.22, yellow trace in **Figures 8C,D**), the decay of J_{rel} is smooth, similar to the case of cells with low or normal SR release (**Figures 8C,D**). However, for large increase in I_{CaL} conductance (scaling factor 1.3, purple trace

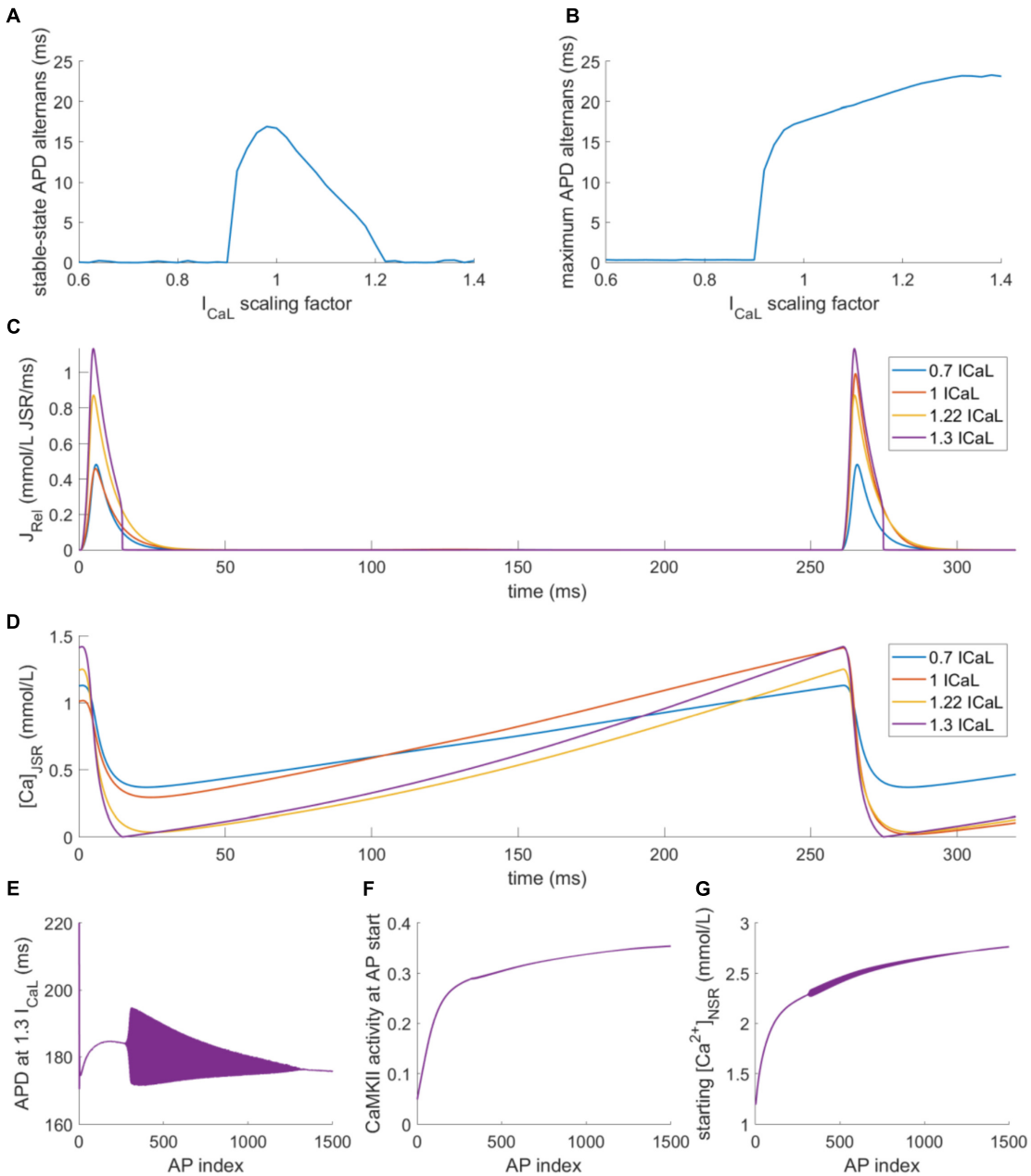

FIGURE 8 | Alternans at 260 ms bcl with varied I_{CaL} conductance in the HeRd model. **(A)** APD alternans amplitude (difference in APD between last two APs) at the end of stable-state pre-pacing. **(B)** Maximum APD alternans (difference in two consecutive APs) at any stage between pre-pacing APs 30–2500 (first 30 APs were omitted as the model may manifest large APD changes at the start of the simulations, which are not due to alternans). **(C)** Examples of J_{rel} for four I_{CaL} scaling factors after stable-state pre-pacing, showing alternans for I_{CaL} scaling factor of 0.7 and 1 but not for 1.22 or 1.3; **(D)** JSR calcium levels aligned with the plot **(C),** showing full depletion in both beats at calcium scaling factors of 1.22 and 1.3. **(E)** Development of APD during pre-pacing for I_{CaL} scaling factor of 1.3, the filled area represents alternans of APD; first 1500 beats of pre-pacing shown. **(F)** Increasing CaMKII activity during pre-pacing for I_{CaL} scaling factor of 1.3. **(G)** Increasing NSR loading during pre-pacing of the model with I_{CaL} scaling factor of 1.3, measured as NSR calcium at the start of an action potential.

in **Figures 8C,D**), the SR release drops to zero abruptly. We are not aware of an experimental study which would report similarly abrupt termination of the SR release and this could be an artifact of the model. It follows from a highly accelerated convergence of the gate variable determining J_{rel} to its steady-state value of zero release when J_{rel} is high, but the JSR loading is low. However, as described below, the aspect crucial for alternans abolishment is the fact of depletion, not of the abrupt termination of release.

The full depletion of JSR leads to disappearance of alternans predominantly by a combination of two factors. The first factor is that when all releasable calcium in the JSR is released, the otherwise steep load–release relationship is flattened: when a JSR

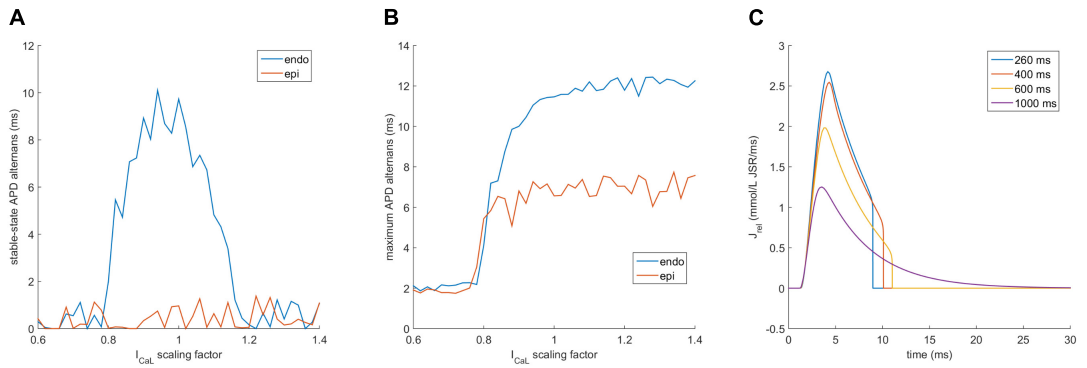

FIGURE 9 | Alternans with varied I_{CaL} conductance in the ORd model. **(A,B)** are an analogy of **Figures 8A,B** obtained using the ORd model paced at 260 ms bcl, showing the data for both endocardial (endo) and epicardial (epi) variant, **(C)** shows traces of J_{rel} in the epicardial variant of ORd after 2500 pre-pacing beats at four different base cycle lengths. The fluctuation in APD alternans amplitude in panels **(A,B)** are due to a higher APD variability of the ORd model at rapid pacing, compared to HeRd.

is depleted during a release, increasing the initial JSR loading further does not translate into considerably increased release given that there is no additional calcium to be released. Second, the refilling of JSR is rapid enough to reach the starting JSR concentration, allowing again for a full depletion in the next AP. During the pacing shown in **Figure 8E**, the CaMKII activity gradually rose (**Figure 8F**), increasing the reuptake rate of SERCA pumps, translating into high NSR loading (**Figure 8G**). In addition, the total reuptake is generally increased in models with high I_{CaL} scaling, given that more calcium enters the cell. The increased NSR loading consequently increases the JSR refilling rate and allows maintaining the depletion of the SR in the stable state.

It can be shown that the mechanism of alternans abolishment via large SR release underlies the difference in alternans vulnerability between different variants (epicardial, endocardial, and midmyocardial) of the highly popular human cardiomyocyte ORd model (O'Hara et al., 2011) used previously to study alternans (Zhou et al., 2016). In this model, only the endocardial variant is able to reproduce alternans in stable state.

We repeated the protocols testing the impact of I_{CaL} modulation on alternans formation in all three variants of the ORd model. Midmyocardial cells generally manifested behavior akin to 2:1 block at fast pacing and did not develop stable behavior, which is why they were excluded from further analysis. While the endocardial variant of ORd developed stable-state alternans for similar values of I_{CaL} modifier as HeRd (extended toward lower values), the epicardial variant was immune to alternans in the stable state altogether (**Figure 9A**). However, observing the maximum alternans amplitude during pre-pacing (**Figure 9B**) revealed that alternans did develop in the epicardial variant of ORd, but only transiently (the baseline alternans amplitude of 2 ms for low I_{CaL} modifier reflects natural APD variability in the ORd model), in a similar fashion to HeRd or endocardial ORd model with highly increased I_{CaL}. Plotting SR release for different bcls in the epicardial ORd variant, it can be clearly seen that up to 600 ms bcl (heart rate of 100 bpm, i.e., relatively normal), SR release becomes zero abruptly, marking functional JSR depletion (**Figure 9C**). Among the differences between the endocardial and epicardial variants of ORd is the increased I_{CaL} conductance and increased SERCA reuptake in the epicardial model, from which the susceptibility to JSR depletion follows naturally.

Understanding the importance of full JSR depletion may be applied to gain insight the disappearance of alternans at rapid pacing in so called "eye-type" alternans, investigated previously by Zhou et al. (2016) using the ORd model. The study used a population of models approach to study the differences between cells manifesting "fork-type" alternans, where the APD bifurcation opens at a certain pacing frequency and is present at all faster frequencies (**Figures 10A–C**), and "eye-type alternans," where the bifurcation opens at a given pacing frequency, but then closes again as the pacing frequency increases (**Figures 10D–F**). A population of ORd model cells based on the epicardial variant with varying channel conductances was simulated. Out of the 2326 simulated cells, 87 manifested alternans: 14 of the eye type and 73 of the fork type. The proposed key difference between cells manifesting these two subtypes of alternans was I_{CaL} conductance. All details of the methodology are given in Zhou et al. (2016).

We repeated the simulation of the population as described in the article, measuring JSR depletion in the last two action potentials, as well as the APD90 and calcium transient. We hypothesized that the functional depletion of JSR may contribute to the eye closing at fast pacing frequencies. Consistent with the hypothesis, we observed that in all the 14 cases of eye-type alternans, the eye closure occurred at the same bcl as the functional JSR depletion in both recorded action potentials. At the same time, in no case of fork alternans did full functional depletion occur in both action potentials. **Figures 10A–C** shows a representative APD, calcium transient, and relative JSR depletion for the fork-type alternans. Corresponding visualization of the given features in eye-type alternans is given in **Figures 10D–F**. Reducing the bcl beyond 500 ms increases the alternans in amplitude both in APD (**Figure 10D**) and calcium transient (**Figure 10E**). However, at 450 ms bcl, one of the two last action

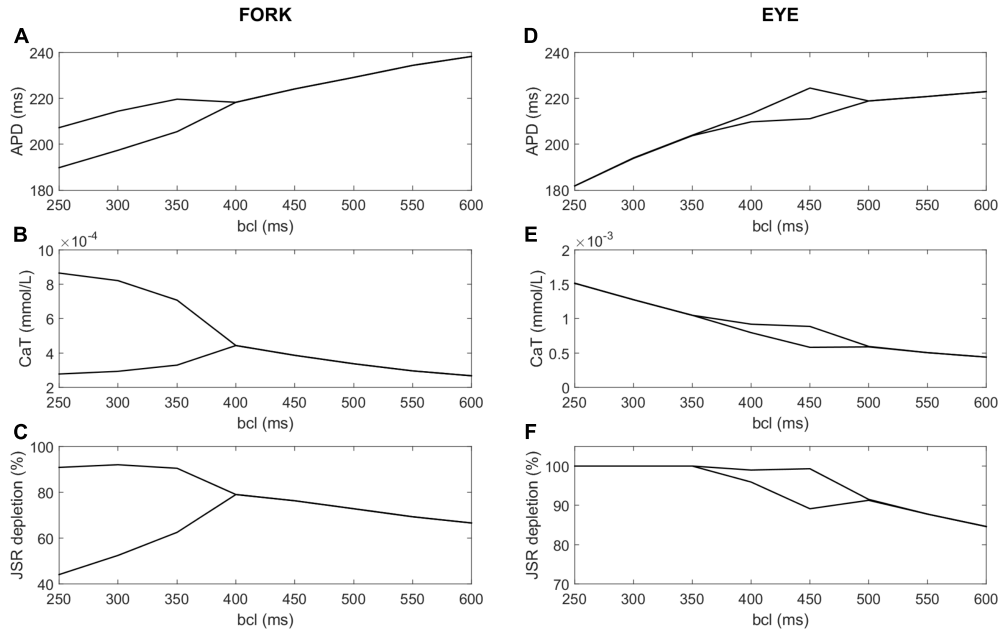

FIGURE 10 | A comparison of fork and eye-type alternans in the ORd model. The left column shows fork alternans in APD **(A)** and calcium transient amplitude **(B)**, with underlying fractional JSR depletion per action potential **(C)**, computed as: $100 * \left(1 - \frac{min(Ca_{JSR})}{Ca_{JSR,start}}\right)$, where $min(Ca_{JSR})$ is the minimum JSR contents per action potential and $Ca_{JSR,start}$ is the starting JSR calcium concentration in the same action potential. In panels **(D–F)** are respectively shown APD, CaT, and depletion in eye-type alternans. All plots show the values of the two last action potentials for every bcl and variable of interest; bifurcation indicates that the last two action potentials differ in the variable of interest, manifesting alternans.

potentials reaches full functional JSR depletion (**Figure 10F**), preventing further divergence of SR release in consecutive beats. With further decreasing bcl, JSR calcium release keeps increasing in the other beat, "catching up" the larger of the two releases. Subsequently, when JSR is fully depleted in both action potentials at bcl 350 ms, the alternans eye closes (**Figures 10D,E**).

DISCUSSION

The main findings of this work are: (1) Accelerated dynamics of SR release attenuate alternans via acceleration of the junctional SR refilling, while slow SR release promotes alternans. (2) A sufficient increase in the magnitude of SR release may attenuate alternans, potentially explaining the formation of "eye-type" alternans. (3) Alternans in the studied models is mainly driven by refractoriness of calcium cycling and junctional SR refilling, supporting SR calcium cycling refractoriness (SRCCR) as a mechanism for alteranans.

Calcium Driven by SR Cycling Refractoriness

Numerous previous studies have investigated the subcellular determinants of calcium transient and repolarization alternans (Qu et al., 2000; Fox et al., 2002; Picht et al., 2006; Weiss et al., 2006; Livshitz and Rudy, 2007). In general, these studies have identified a critical role for SR calcium-cycling properties in calcium transient alternans development, focusing either on refractoriness of release via slow reactivation of RyR (Picht et al., 2006), or slow calcium reuptake resulting in a release-reuptake mismatch (Weiss et al., 2006). Our work highlights the potential importance of a third explanation, "SR calcium cycling refractoriness" (SRCCR).

The explanation of alternans presented in this article relies primarily on steepness of load–release relationship combined with limited rate of diffusion between NSR and JSR preventing timely refilling of releasable calcium. The importance of NSR→JSR diffusion in alternans was first suggested by Kihara and Morgan (1991) and it underlies the alternans formation in the Mahajan model (Mahajan et al., 2008). This process may be enabled by low mobility of calcium diffusing from reuptake to release sites (Swietach et al., 2008). The SRCCR-driven alternans bears similarities with the two major explanations (release-reuptake mismatch and RyR refractoriness), but is distinct at the same time. Similarly to the hypothesis of release-reuptake mismatch, SR calcium oscillations caused by SRCCR play an important role in alternans generation. On the other hand, the release-reuptake hypothesis does not include any form of SR release refractoriness (whether driven by JSR refilling or intrinsic RyR refractoriness), shown to be crucial in alternans generation (Shkryl et al., 2012). Both hypotheses therefore offer a slightly different point of view on the experimental observation that the upregulation of SERCA pumps and thus improved reuptake attenuates alternans (Cutler et al., 2012; Stary et al., 2016).

In the release-reuptake mismatch hypothesis of alternans, upregulation of SERCA pumps directly corrects the mismatch

between release and reuptake, however, the explanation is based on an implicit assumption that the reuptaken calcium is immediately releasable. In models representing intra-SR diffusion of calcium, it can be seen that even if all released calcium is reuptaken, it might not diffuse from the reuptake to the release site in time, failing to prevent alternans. Instead, in the more advanced model including intra-SR diffusion, increased expression of SERCA pumps may be seen as a way of increasing NSR loading. This subsequently translates into larger gradient between NSR and JSR and thus faster NSR→JSR transport and consequently accelerated JSR refilling (reducing release refractoriness). This then attenuates alternans, given alternans formation in SRCCR hypothesis is directly linked to the JSR refilling, rather than SR reuptake.

The SRCCR-driven alternans presented here is similar to the hypothesis on RyR refractoriness driving alternans (Picht et al., 2006) in that both models rely on a form of SR refractoriness. The mechanism of refractoriness is however different. Picht et al. observed alternans without oscillations of diastolic SR calcium in 20% of cells studied. This is hard to explain using the SRCCR alternans mechanism, and thus suggests the existence of an intrinsic RyR refractoriness instead. Consistently with this, Ramay et al. (2011) observed that the frequency of calcium sparks (discrete SR release events) may be increased (via caffeine) or decreased (via tetracaine), supporting the existence of intrinsic RyR refractoriness. At the same time, however, RyR reopening soon after the first opening was associated with considerably diminished spark amplitude, and RyR sensitization via caffeine did not affect its recovery. Even 300 ms after the previous calcium spark, the amplitude of the following calcium spark at a given location was not fully recovered, showing that the time scale of recovery is consistent with a role in alternans during rapid pacing. Similar results were observed in a study by Sobie et al. (2005). This suggests that local JSR refilling might play an important role in refractoriness of overall SR release. In addition, the study by Szentesi et al. (2004) showed that increased SR reuptake accelerates the recovery of SR release from refractoriness. While this is highly consistent with accelerated JSR refilling downstream of altered SR reuptake, it is not immediately obvious how increased SR reuptake would modulate the intrinsic RyR refractoriness. It therefore appears that refractoriness of SR release may be driven both by intrinsic RyR refractoriness and by JSR refilling refractoriness. Taken together, the literature suggests that the two types of refractoriness are not mutually exclusive and that both are physiologically relevant.

Release Dynamics Modulate Alternans Occurrence

Using manipulation of SR release time constant and using a synthetic clamping of SR release, we have shown that accelerating release dynamics improves JSR refilling and acts against alternans formation. These results are linked to our previous work (Tomek et al., 2017), where we have shown that alternans is attenuated when RyR are phosphorylated by β-adrenergic stimulation. The key feature of RyR phosphorylation in this model was altered release dynamics: a shorter-duration release and a shorter time to peak release.

We show that reducing the release time constant (shortening both time to peak release and release duration) attenuates alternans, while increasing the time constant promotes it. In addition, we used a well-controlled SR release clamping approach to show that both changes to dynamics contribute to reduction in alternans independently, explaining why they improve JSR refilling. Conversely, our results show that the combination of JSR release prolongation, time-to-peak prolongation, and amplitude reduction promotes alternans. This could provide a novel explanation of increased alternans vulnerability in cardiac diseases, such as heart failure (Kodama et al., 2004), hypertrophic cardiomyopathy (Cannon et al., 1986), or myocardial infarction (Gardner et al., 2015).

In heart failure, reduced release rate was observed directly by Yamamoto et al. (1999). Moreover, longer time-to-peak, slower decay, and reduced amplitude of calcium sparks were observed (Lindner et al., 2002). Calcium sparks are microscopic releases of calcium from JSR, the sum of which constitutes total SR release at a given time (Collier et al., 2000). Such dynamics of calcium sparks observed in heart failure therefore correspond precisely to the phenotype of longer release, longer time-to-peak, and reduced amplitude, which is expected to be vulnerable to alternans according to our model. Recently, Zhong et al. (2018) similarly observed that reduced expression of ryanodine receptors prolonged the SR release, and that this promoted alternans formation in the hearts.

A further link between alternans vulnerability and release dynamics may be established via the activity of CaMKII, which increases the duration of calcium sparks, prolonging calcium release (Maier et al., 2003; Guo et al., 2006). At the same time, activity of CaMKII is increased in hypertrophy and heart failure (Anderson et al., 2011), as well as within the cardiac post-infarction border zone (Hund et al., 2008), which is a region vulnerable to alternans (Gardner et al., 2015). Therefore, we can conclude that the prolongation of SR release might be contributing to alternans vulnerability in a wide range of cardiac diseases.

We believe that the importance of modulation of SR release dynamics is not limited to the presented mechanism of alternans formation. In the case of alternans driven by the refractoriness of the ryanodine receptors (Picht et al., 2006), early opening of RyR, corresponding to accelerated SR release, provides all ryanodine receptors with more time to recover from refractoriness before the subsequent action potential. Conversely, slow SR release requires late opening of ryanodine receptors, which then have less time to recover, increasing the likelihood of them being refractory at the start of the following action potential, promoting alternans.

Calcium Amount Released and Alternans

In this study, we have shown that sufficiently strong inhibition or potentiation of calcium release can protect the calcium subsystem from alternans. Under inhibited calcium release, the amount of calcium released via RyR is reduced, so that enough JSR calcium can be refilled in time during action potential. In the case of potentiated calcium release, alternans is abolished due to two

factors: functional depletion of JSR in every action potential, flattening the steep load–release relationship, and allowing for rapid JSR refilling through the increased NSR loading.

This phenomenon of full JSR depletion is relevant in understanding the principle of formation of eye-type alternans (APD bifurcation which opens with increasing pacing frequency, then disappearing with further increase in frequency), recently investigated in human data and simulations by Zhou et al. (2016). We show that the disappearance of alternans at fastest pacing frequencies in the eye-type alternans may be caused by functional depletion of JSR in every beat to eliminate alternans at fast pacing. The fact that the eye-type alternans cells in the original study tend to have a higher L-type calcium current conductance compared to fork-type is consistent with our results. First of all, the stronger L-type calcium current translates into higher RyR release, which facilitating functional depletion of JSR at rapid pacing and eye closing. Secondly, the stronger calcium influx mediated via increased L-type calcium current contributes to higher diastolic calcium level, increased SR reuptake, and faster calcium refilling to JSR, allowing maintenance of full JSR release in every beat.

More experimental evidence is needed to clarify the JSR calcium load–release relationship during alternans and whether full functional JSR depletion may occur. Current evidence suggests that functional JSR depletion in myocytes is only 60–80% at most (Bassani et al., 1995; Shannon et al., 2000), even during alternans (Shkryl et al., 2012). However, it is possible that the cells studied in these works represent the fork-type alternans behavior rather than the eye-type. Moreover, it was observed that caffeine-driven release depletes JSR more than a normal release driven by elevated calcium concentration (MacQuaide et al., 2009); it is therefore possible that using caffeine to estimate JSR contents overestimates calcium releasable in a physiological way. Consequently, an 80% depletion of JSR as assessed by caffeine may in fact represent full functional depletion. It is therefore not clear whether the full depletion of JSR in the studied computer models is physiological or if this suggests that the models require further development in this regard. Investigating the slope of JSR load–release relationship in myocytes with a wide range of external calcium stimuli (achievable acutely, e.g., via caged calcium) represents an interesting experiment which could elucidate whether full functional depletion may occur at rapid pacing in myocytes. A potentially important factor to be investigated may be the role of calcium buffering by calsequestrin in the load–release relationship. A recent study suggests that JSR depletion might result in change of calsequestrin conformation and a subsequent closure of the ryanodine receptors (Manno et al., 2017). This provides a mechanism of SR release termination, with possibly similar effect to SR release termination due to JSR depletion.

An indication that the load-release curve may become flatter at high SR contents is provided by the work of Posterino and Lamb (2003) in rat fast-twitch skeletal muscle. The authors show that after the initial steep phase of load–release relationship, increasing SR calcium loading does not translate into an increased SR release (Posterino and Lamb, 2003; Figures 10B,C), flattening the load–release relationship. While it is not explicitly shown that the flattening occurs via functional depletion of JSR, this nevertheless could explain the disappearance of alternans at fast pacing rates in a similar fashion to our depletion-based explanation: at intermediate pacing frequencies where the load–release relationship is steep, alternans may occur. However, with increasing pacing frequency, the load-release flattening may dampen the JSR release oscillation, abolishing alternans and closing the alternans eye. The degree of SR loading at rapid pacing would then be the key feature determining whether a cell manifests alternans of the fork or the eye type.

The eye-type alternans was previously observed also in a mathematical study by Qu et al. (2007). In this work, the closure of the eye at fast pacing rates was linked to rate-dependent attenuation of the function corresponding to the load–release relationship at the very fast pacing rates, assuming rate-independent reuptake. The functional JSR depletion at the fastest pacing rates described in our article may be linked to this mechanism. In our simulations, the reuptake is not rate-independent, but increases with pacing rate (mainly via CaMKII signaling). While the load–release relationship is not strictly reduced at the highest pacing rates, its growth is considerably attenuated by the JSR depletion. This would presumably allow the rate-activated SR reuptake to "overtake" the plateauing SR release, achieving a similar effect to a rate-independent reuptake and rate-inhibited release.

AUTHOR CONTRIBUTIONS

JT conceived and designed most of the study, performed the simulations and analyses, and wrote most of the manuscript. MT contributed to the design of simulations, figure design, and manuscript writing. XZ aided JT with reuse of codes from her previous study and contributed to the manuscript writing. GB and BR supervised the project and strongly contributed to the manuscript writing and structuring.

FUNDING

JT and MT thank the Engineering and Physical Sciences Research Council (EPSRC) for their support of their Ph.D. Programme. JT and XZ are funded via BR's Wellcome Trust Senior Research Fellowship in Basic Biomedical Sciences (100246/Z/12/Z). GB and BR acknowledge support from the British Heart Foundation Centre for Research Excellence at the University of Oxford (RE/08/004). GB was funded by the Heart and Stroke Foundation of Canada. BR was funded by a Wellcome Trust Senior Research Fellowship in Basic Biomedical Sciences (100246/Z/12/Z), an Engineering and Physical Sciences Research Council Impact Acceleration Award (EP/K503769/1), the CompBioMed project (European Commission Grant Agreement No. 675451), and the NC3Rs Infrastructure for Impact award (NC/P001076/1) and Project Grant (NC/P00122X/1).

REFERENCES

Anderson, M. E., Brown, J. H., and Bers, D. M. (2011). CaMKII in myocardial hypertrophy and heart failure. *J. Mol. Cell. Cardiol.* 51, 468–473. doi: 10.1016/j.yjmcc.2011.01.012

Bassani, J. W., Yuan, W., and Bers, D. M. (1995). Fractional SR Ca release is regulated by trigger Ca and SR Ca content in cardiac myocytes. *Am. J. Physiol.* 268(5 Pt 1), C1313–C1319. doi: 10.1152/ajpcell.1995.268.5.C1313

Bayer, J. D., Lalani, G. G., Vigmond, E. J., Narayan, S. M., and Trayanova, N. A. (2016). Mechanisms linking electrical alternans and clinical ventricular arrhythmia in human heart failure. *Heart Rhythm* 13, 1922–1931. doi: 10.1016/j.hrthm.2016.05.017

Cannon, R. O., Schenke, W. H., Bonow, R. O., Leon, M. B., and Rosing, D. R. (1986). Left ventricular pulsus alternans in patients with hypertrophic cardiomyopathy and severe obstruction to left ventricular outflow. *Circulation* 73, 276–285. doi: 10.1161/01.CIR.73.2.276

Collier, M. L., Ji, G., Wang, Y.-X., and Kotlikoff, M. I. (2000). Calcium-induced calcium release in smooth muscle - loose coupling between the action potential and calcium release. *J. Gen. Physiol.* 115, 653–662. doi: 10.1085/jgp.115.5.653

Cutler, M. J., Wan, X., Plummer, B. N., Liu, H., Deschenes, I., Laurita, K. R., et al. (2012). Targeted sarcoplasmic reticulum Ca^{2+} ATPase 2a gene delivery to restore electrical stability in the failing heart. *Circulation* 126, 2095–2104. doi: 10.1161/CIRCULATIONAHA.111.071480

Decker, K. F., Heijman, J., Silva, J. R., Hund, T. J., and Rudy, Y. (2009). Properties and ionic mechanisms of action potential adaptation, restitution, and accommodation in canine epicardium. *AJP Heart Circ. Physiol.* 296, H1017–H1026. doi: 10.1152/ajpheart.01216.2008

Díaz, M. E., O'Neill, S. C., and Eisner, D. A. (2004). Sarcoplasmic reticulum calcium content fluctuation is the key to cardiac alternans. *Circ. Res.* 94, 650–656. doi: 10.1161/01.RES.0000119923.64774.72

Edwards, J. N., and Blatter, L. A. (2014). Cardiac alternans and intracellular calcium cycling. *Clin. Exp. Pharmacol. Physiol.* 41, 524–532. doi: 10.1111/1440-1681.12231

Fox, J. J., McHarg, J. L., and Gilmour, R. F. (2002). Ionic mechanism of electrical alternans. *Am. J. Physiol. Heart Circ. Physiol.* 282, H516–H530. doi: 10.1152/ajpheart.00612.2001

Gardner, R. T., Wang, L., Lang, B. T., Cregg, J. M., Dunbar, C. L., Woodward, W. R., et al. (2015). Targeting protein tyrosine phosphatase sigma after myocardial infarction restores cardiac sympathetic innervation and prevents arrhythmias. *Nat. Commun.* 6:6235. doi: 10.1038/ncomms7235

Guo, T., Zhang, T., Mestril, R., and Bers, D. M. (2006). Ca^{2+}/calmodulin-dependent protein kinase II phosphorylation of ryanodine receptor does affect calcium sparks in mouse ventricular myocytes. *Circ. Res.* 99, 398–406. doi: 10.1161/01.RES.0000236756.06252.13

Heijman, J., Volders, P. G., Westra, R. L., and Rudy, Y. (2011). Local Control of β-adrenergic stimulation: effects on ventricular myocyte electrophysiology and Ca^{2+}-transient. *J. Mol. Cell. Cardiol.* 50, 863–871. doi: 10.1016/j.yjmcc.2011.02.007

Hund, T. J., Decker, K. F., Peter, E. K., Mohler, J., Boyden, P. A., Schuessler, R. B., et al. (2008). Role of activated CaMKII in abnormal calcium homeostasis and INA remodeling after myocardial infarction: insights from mathematical modeling. *J. Mol. Cell. Cardiol.* 45, 420–428. doi: 10.1016/j.yjmcc.2008.06.007

Hund, T. J., and Rudy, Y. (2004). Rate dependence and regulation of action potential and calcium transient in a canine cardiac ventricular cell model. *Circulation* 110, 3168–3174. doi: 10.1161/01.CIR.0000147231.69595.D3

Kanaporis, G., and Blatter, L. A. (2015). The mechanisms of calcium cycling and action potential dynamics in cardiac alternans. *Circ. Res.* 116, 846–856. doi: 10.1161/CIRCRESAHA.116.305404

Kho, C., Lee, A., and Hajjar, R. J. (2012). Altered sarcoplasmic reticulum calcium cycling—targets for heart failure therapy. *Nat. Rev. Cardiol.* 9, 717–733. doi: 10.1038/nrcardio.2012.145

Kihara, Y., and Morgan, J. P. (1991). Abnormal Ca_i^{2+} handling is the primary cause of mechanical alternans: study in ferret ventricular muscles. *Am. J. Physiol.* 261(6 Pt 2), H1746–H1755. doi: 10.1152/ajpheart.1991.261.6.H1746

Kodama, M., Kato, K., Hirono, S., Okura, Y., Hanawa, H., Yoshida, T., et al. (2004). Linkage between mechanical and electrical alternans in patients with chronic heart failure. *Cardiovasc. Electrophysiol.* 15, 295–299. doi: 10.1046/j.1540-8167.2004.03016.x

Lehnart, S. E., Terrenoire, C., Reiken, S., Wehrens, X. H. T., Song, L.-S., Tillman, E. J., et al. (2006). Stabilization of cardiac ryanodine receptor prevents intracellular calcium leak and arrhythmias. *Proc. Natl. Acad. Sci. U.S.A.* 103, 7906–7910. doi: 10.1073/pnas.0602133103

Lindner, M., Brandt, M. C., Sauer, H., Hescheler, J., Böhle, T., and Beuckelmann, D. J. (2002). Calcium sparks in human ventricular cardiomyocytes from patients with terminal heart failure. *Cell Calcium* 31, 175–182. doi: 10.1054/ceca.2002.0272

Livshitz, L. M., and Rudy, Y. (2007). Regulation of Ca^{2+} and electrical alternans in cardiac myocytes: role of CaMKII and repolarizing currents. *Am. J. Physiol. Heart Circ. Physiol.* 292, H2854–H2866. doi: 10.1152/ajpheart.01347.2006

MacQuaide, N., Dempster, J., and Smith, G. L. (2009). Assessment of sarcoplasmic reticulum Ca^{2+} depletion during spontaneous Ca^{2+} waves in isolated permeabilized rabbit ventricular cardiomyocytes. *Biophys. J.* 96, 2744–2754. doi: 10.1016/j.bpj.2008.12.3944

Mahajan, A., Shiferaw, Y., Sato, D., Baher, A., Olcese, R., Xie, L. H., et al. (2008). A rabbit ventricular action potential model replicating cardiac dynamics at rapid heart rates. *Biophys. J.* 94, 392–410. doi: 10.1529/biophysj.106.98160

Maier, L. S., Zhang, T., Chen, L., DeSantiago, J., Brown, J. H., and Bers, D. M. (2003). Transgenic CaMKIIδc overexpression uniquely alters cardiac myocyte Ca^{2+} handling: reduced SR Ca^{2+} load and activated SR Ca^{2+} release. *Circ. Res.* 92, 904–911. doi: 10.1161/01.RES.0000069685.20258.F1

Manno, C., Figueroa, L. C., Gillespie, D., Fitts, R., Kang, C., Franzini-Armstrong, C., et al. (2017). Calsequestrin depolymerizes when calcium is depleted in the sarcoplasmic reticulum of working muscle. *Proc. Natl. Acad. Sci. U.S.A.* 114, E638–E647. doi: 10.1073/pnas.1620265114

Narayan, S. M., Franz, M. R., Clopton, P., Pruvot, E. J., and Krummen, D. E. (2011). Repolarization alternans reveals vulnerability to human atrial fibrillation. *Circulation* 123, 2922–2930. doi: 10.1161/CIRCULATIONAHA.110.977827

O'Hara, T., Virág, L., Varró, A., and Rudy, Y. (2011). Simulation of the undiseased human cardiac ventricular action potential: model formulation and experimental validation. *PLoS Comput. Biol.* 7:e1002061. doi: 10.1371/journal.pcbi.1002061

Pastore, J. M., Girouard, S. D., Laurita, K. R., Akar, F. G., and Rosenbaum, D. S. (1999). Mechanism linking T-wave alternans to the genesis of cardiac fibrillation. *Circulation* 99, 1385–1394. doi: 10.1161/01.CIR.99.10.1385

Picht, E., DeSantiago, J., Blatter, L. A., and Bers, D. M. (2006). Cardiac Alternans do not rely on diastolic sarcoplasmic reticulum calcium content fluctuations. *Circ. Res.* 99, 740–748. doi: 10.1161/01.RES.0000244002.88813.91

Posterino, G. S., and Lamb, G. D. (2003). Effect of sarcoplasmic reticulum Ca^{2+} content on action potential-induced Ca^{2+} release in rat skeletal muscle fibres. *J. Physiol.* 551, 219–237. doi: 10.1113/jphysiol.2003.040022

Pruvot, E. J., Katra, R. P., Rosenbaum, D. S., and Laurita, K. R. (2004). Role of calcium cycling versus restitution in the mechanism of repolarization alternans. *Circ. Res.* 94, 1083–1090. doi: 10.1161/01.RES.0000125629.72053.95

Qu, Z., Garfinkel, A., Chen, P.-S., and Weiss, J. N. (2000). Mechanisms of discordant alternans and induction of reentry in simulated cardiac tissue. *Circulation* 102, 1664–1670. doi: 10.1161/01.CIR.102.14.1664

Qu, Z., Liu, M. B., and Nivala, M. (2016). A unified theory of calcium alternans in ventricular myocytes. *Sci. Rep.* 6:35625. doi: 10.1038/srep35625

Qu, Z., Shiferaw, Y., and Weiss, J. N. (2007). Nonlinear dynamics of cardiac excitation-contraction coupling: an iterated map study. *Phys. Rev. E Stat. Nonlin. Soft Matter Phys.* 75(1 Pt 1), 011927. doi: 10.1103/PhysRevE.75.011927

Ramay, H. R., Liu, O. Z., and Sobie, E. A. (2011). Recovery of cardiac calcium release is controlled by sarcoplasmic reticulum refilling and ryanodine receptor sensitivity. *Cardiovasc. Res.* 91, 598–605. doi: 10.1093/cvr/cvr143

Shannon, T. R., Ginsburg, K. S., and Bers, D. M. (2000). Potentiation of fractional sarcoplasmic reticulum calcium release by total and free intra-sarcoplasmic reticulum calcium concentration. *Biophys. J.* 78, 334–343. doi: 10.1016/S0006-3495(00)76596-76599

Shkryl, V. M., Maxwell, J. T., Domeier, T. L., and Blatter, L. A. (2012). Refractoriness of sarcoplasmic reticulum Ca^{2+} release determines Ca^{2+} alternans in atrial myocytes. *AJP Heart Circ. Physiol.* 302, H2310–H2320. doi: 10.1152/ajpheart.00079.2012

Sobie, E. A., Song, L.-S., and Lederer, W. J. (2005). Local recovery of Ca^{2+} release in rat ventricular myocytes. *J. Physiol.* 565(Pt 2), 441–447. doi: 10.1113/jphysiol.2005.086496

Stary, V., Puppala, D., Scherrer-Crosbie, M., Dillmann, W. H., and Armoundas, A. A. (2016). SERCA2a upregulation ameliorates cellular alternans induced by metabolic inhibitions. *J. Appl. Physiol.* 120, 865–875. doi: 10.1152/japplphysiol.00588.2015

Swietach, P., Spitzer, K. W., and Vaughan-Jones, R. D. (2008). Ca^{2+}-mobility in the sarcoplasmic reticulum of ventricular myocytes is low. *Biophys. J.* 95, 1412–1427. doi: 10.1529/biophysj.108.130385

Szentesi, P., Pignier, C., Egger, M., Kranias, E. G., and Niggli, E. (2004). Sarcoplasmic reticulum Ca^{2+} refilling controls recovery from Ca^{2+}-induced Ca^{2+} release refractoriness in heart muscle. *Circ. Res.* 95, 807–813. doi: 10.1161/01.RES.0000146029.80463.7d

Tomek, J., Rodriguez, B., Bub, G., and Heijman, J. (2017). β-adrenergic receptor stimulation inhibits proarrhythmic alternans in post-infarction border zone cardiomyocytes: a computational analysis. *Am. J. Physiol. Heart Circ. Physiol.* 313, H338–H353. doi: 10.1152/ajpheart.00094.2017

Weiss, J. N., Karma, A., Shiferaw, Y., Chen, P. S., Garfinkel, A., and Qu, Z. (2006). From pulsus to pulseless: the saga of cardiac alternans. *Circ. Res.* 98, 1244–1253. doi: 10.1161/01.RES.0000224540.97431.f0

Wilson, L. D., Jeyaraj, D., Wan, X., Hoeker, G. S., Said, T. H., Gittinger, M., et al. (2009). Heart failure enhances susceptibility to arrhythmogenic cardiac alternans. *Heart Rhythm* 6, 251–259. doi: 10.1016/j.hrthm.2008.11.008

Wilson, L. D., and Rosenbaum, D. S. (2007). Mechanisms of arrythmogenic cardiac alternans. *Europace* 9(Suppl. 6), 77–82. doi: 10.1093/europace/eum210

Xie, L.-H., Sato, D., Garfinkel, A., Qu, Z., and Weiss, J. N. (2008). Intracellular Ca alternans: coordinated regulation by sarcoplasmic reticulum release, uptake, and leak. *Biophys. J.* 95, 3100–3110. doi: 10.1529/biophysj.108.130955

Yamamoto, T., Yano, M., Kohno, M., Hisaoka, T., Ono, K., Tanigawa, T., et al. (1999). Abnormal Ca^{2+} release from cardiac sarcoplasmic reticulum in tachycardia-induced heart failure. *Cardiovasc. Res.* 44, 146–155. doi: 10.1016/S0008-6363(99)00200-X

Zhong, X., Vallmitjana, A., Sun, B., Xiao, Z., Guo, W., Wei, J., et al. (2018). Reduced expression of cardiac ryanodine receptor protects against stress-induced ventricular tachyarrhythmia, but increases the susceptibility to cardiac alternans. *Biochem. J.* 475, 169–183. doi: 10.1042/BCJ20170631

Zhou, X., Bueno-Orovio, A., Orini, M., Hanson, B., Hayward, M., Taggart, P., et al. (2016). In vivo and in silico investigation into mechanisms of frequency dependence of repolarization alternans in human ventricular cardiomyocytes. *Circ. Res.* 118, 266–278. doi: 10.1161/CIRCRESAHA.115.307836

Conflict of Interest Statement: The authors declare that the research was conducted in the absence of any commercial or financial relationships that could be construed as a potential conflict of interest.

frontiers in Physiology

REVIEW
published: 27 September 2018
doi: 10.3389/fphys.2018.01379

The Histidine-Rich Calcium Binding Protein in Regulation of Cardiac Rhythmicity

*Demetrios A. Arvanitis[1], Elizabeth Vafiadaki[1], Daniel M. Johnson[2], Evangelia G. Kranias[1,3] and Despina Sanoudou[1,4]**

[1] Molecular Biology Division, Biomedical Research Foundation, Academy of Athens, Athens, Greece, [2] Department of Cardiothoracic Surgery, Cardiovascular Research Institute Maastricht, Maastricht University, Maastricht, Netherlands, [3] Department of Pharmacology and Systems Physiology, University of Cincinnati College of Medicine, Cincinnati, OH, United States, [4] Clinical Genomics and Pharmacogenomics Unit, 4th Department of Internal Medicine, Attikon Hospital, Medical School, National and Kapodistrian University of Athens, Athens, Greece

Sudden unexpected cardiac death (SCD) accounts for up to half of all-cause mortality of heart failure patients. Standardized cardiology tools such as electrocardiography, cardiac imaging, electrophysiological and serum biomarkers cannot accurately predict which patients are at risk of life-threatening arrhythmic episodes. Recently, a common variant of the histidine-rich calcium binding protein (HRC), the Ser96Ala, was identified as a potent biomarker of malignant arrhythmia triggering in these patients. HRC has been shown to be involved in the regulation of cardiac sarcoplasmic reticulum (SR) Ca^{2+} cycling, by binding and storing Ca^{2+} in the SR, as well as interacting with the SR Ca^{2+} uptake and release complexes. The underlying mechanisms, elucidated by studies at the molecular, biochemical, cellular and intact animal levels, indicate that transversion of Ser96 to Ala results in abolishment of an HRC phosphorylation site by Fam20C kinase and dysregulation of SR Ca^{2+} cycling. This is mediated through aberrant SR Ca^{2+} release by the ryanodine receptor (RyR2) quaternary complex, due to the impaired HRC/triadin interaction, and depressed SR Ca^{2+} uptake by the sarco/endoplasmic reticulum Ca^{2+} ATPase (SERCA2) pump, due to the impaired HRC/SERCA2 interaction. Pharmacological intervention with KN-93, an inhibitor of Ca^{2+}/calmodulin-dependent protein kinase II (CaMKII), in the HRC Ser96Ala mouse model, reduced the occurrence of malignant cardiac arrhythmias. Herein, we summarize the current evidence on the pivotal role of HRC in the regulation of cardiac rhythmicity and the importance of HRC Ser96Ala as a genetic modifier for arrhythmias in the setting of heart failure.

Keywords: calcium, homeostasis, contractility, ion channels, arrhythmia

OPEN ACCESS

Edited by:
Gaetano Santulli,
Columbia University, United States

Reviewed by:
Crystal M. Ripplinger,
University of California, Davis, United States
Yoram Etzion,
Ben-Gurion University of the Negev, Israel
Pietro Mesirca,
Centre National de la Recherche Scientifique (CNRS), France

***Correspondence:**
Despina Sanoudou
dsanoudou@med.uoa.gr;
dsanoudou@bioacademy.gr

Specialty section:
This article was submitted to Cardiac Electrophysiology, a section of the journal Frontiers in Physiology

Received: *21 July 2018*
Accepted: *11 September 2018*
Published: *27 September 2018*

Citation:
Arvanitis DA, Vafiadaki E, Johnson DM, Kranias EG and Sanoudou D (2018) The Histidine-Rich Calcium Binding Protein in Regulation of Cardiac Rhythmicity. Front. Physiol. 9:1379. doi: 10.3389/fphys.2018.01379

INTRODUCTION

Arrhythmias are potentially life-threatening electrical manifestations of the heart, which are difficult to predict and treat. The underlying molecular and cellular mechanisms leading to arrhythmia triggering are only partly known. Previously, Na^+ and K^+ ion channels, which are known to modulate depolarization and repolarization, had been a focus of studies on arrhythmia pathogenesis (Remme and Bezzina, 2010; Schmitt et al., 2014). However, many cases cannot be explained by impairments in these two types of channels, suggesting that additional genes, such

as calcium (Ca^{2+}) homeostasis regulators, are implicated in cardiac arrhythmias (London, 2013). Indeed, abnormal Ca^{2+} handling by the sarcoplasmic reticulum (SR) has emerged as a significant contributor to arrhythmogenesis. This is based on accumulating evidence on the crucial role of SR Ca^{2+} homeostasis in cardiac contraction, the direct association of human mutations in SR Ca^{2+} release components with arrhythmias, as well as alterations in the expression levels and activity of key Ca^{2+} handling proteins in human heart failure (Antoons and Sipido, 2008; Pritchard and Kranias, 2009; Lompre et al., 2010; Landstrom et al., 2017). One of these proteins, namely histidine-rich calcium binding protein (HRC) has attracted considerable attention over the past decade, since the identification of the HRC Ser96Ala gene variant was associated with increased risk for malignant arrhythmias and sudden cardiac death (SCD) in dilated cardiomyopathy patients (Arvanitis et al., 2008, 2011; Pritchard and Kranias, 2009). Deciphering the fine mechanisms of HRC contribution to cardiac physiology and pathophysiology could hold answers for the treatment of arrhythmias.

Herein, we summarize the major evidence on the crucial role of HRC in the regulation of cardiac rhythmicity through modulation of SR Ca^{2+} homeostasis, the clinical and molecular defects associated with the HRC genetic variant Ser96Ala, as well as potential therapeutic approaches targeting the underlying molecular defects in Ser96Ala carriers to prevent arrhythmia triggering.

THE HISTIDINE-RICH CALCIUM BINDING PROTEIN

Histidine-rich calcium binding protein is a 170 kDa protein that is primarily expressed in striated muscles and arteriolar smooth muscle cells (Hofmann et al., 1989a,b; Pathak et al., 1992; Anderson et al., 2004). It is a highly charged molecule, with over 30% of the protein composed of acidic residues and 13% of histidine (Hofmann et al., 1989b). Based on its deduced amino acid sequence, HRC contains the following structural features: (1) an amino-terminal 27-residue signal sequence that is believed to target the protein to the SR; (2) a highly repetitive region containing 9 nearly identical tandem repeats of 29 residues, each consisting of a histidine-rich sequence HRHRGH and a stretch of 10–11 acidic amino acids that is believed to have Ca^{2+} binding properties; (3) a 13-residue stretch of polyglutamic acid; and (4) a cluster of 14 closely spaced cysteine residues, with the repeating pattern of Cys-X-X-Cys suggestive of a heavy metal binding domain, at the carboxyl terminus (Hofmann et al., 1989b). Detailed biochemical analysis has established that HRC is a low-affinity, high capacity Ca^{2+} binding protein. Although there is no Ca^{2+} binding motif in HRC, it is presumed that the acidic repeats constitute its Ca^{2+} binding sites (Hofmann et al., 1989b). It is noteworthy that HRC contains more acidic clusters than the other major SR Ca^{2+} binding protein, calsequestrin (CSQ), indicating the high capacity of HRC for Ca^{2+} binding (Hofmann et al., 1989a; Picello et al., 1992). These structural features render HRC an important regulator of cardiomyocyte SR Ca^{2+} homeostasis, as revealed by in depth investigations at the *in vitro*, *ex vivo*, and *in vivo* levels.

THE ROLE OF HRC AS A PROGNOSTIC MARKER OF ARRHYTHMIAS

Heart failure is characterized by impaired cytosolic Ca^{2+} handling, a process predominantly governed by the SR, which leads to diastolic and systolic dysfunction of the cardiomyocyte and ultimately of the heart pump (Morgan et al., 1990). Early reports on the association of HRC with cardiac pathophysiology proposed a role in dystrophic cardiac calcification of inbred mouse strains (van den Broek et al., 1998). HRC has been previously associated with two human autosomal dominant cardiac diseases, the isolated cardiac conduction (de Meeus et al., 1995) and the familial heart block type 1 (Brink et al., 1995). Further studies in end-stage human heart failure reported a significant decrease in HRC protein levels (Fan et al., 2004), a finding also observed in experimental heart failure in mice (Fan et al., 2004) and dogs (Gupta et al., 2009). Collectively, these observations implicated HRC in cardiac pathophysiology and raised the need for further investigations on its precise role and value in the clinical setting.

In 2008 our group was the first to show a direct association of the HRC Ser96Ala polymorphism with malignant ventricular arrhythmias. Through the study of 123 idiopathic dilated cardiomyopathy (DCM) patients (referred to hospital for diagnosis or treatment of heart failure, including implantable cardioverter-defibrillator (ICD) implantation) and 96 healthy controls, the HRC genetic variant Ser96Ala was found to have a statistically significant association with malignant ventricular arrhythmias and SCD in the patients (Arvanitis et al., 2008). Specifically, idiopathic DCM patients harboring the Ala/Ala variant had a fourfold increased risk of SCD compared to homozygotes for the Ser allele. The HRC Ser96Ala polymorphism was an independent predictor of life-threatening ventricular arrhythmias controlled by age, sex, left ventricular ejection fraction, atrial fibrillation, left bundle branch block or medication. Interestingly, further genetic analysis showed that approximately 60% of the general population has at least one copy of Ser96Ala, however, only those individuals suffering from DCM and carrying this polymorphism appear to be susceptible to arrhythmogenesis. Consequently, the HRC Ser96Ala polymorphism has a significant prognostic value.

UNDERSTANDING THE ROLE OF HRC IN ARRHYTHMIAS THROUGH *IN VITRO* AND *IN VIVO* RODENT MODELS

One of the first studies to explore the role of HRC in SR Ca^{2+} handling, employed rat cardiomyocytes overexpressing HRC, and demonstrated that increased HRC levels lead to a 30% increase in SR Ca^{2+}, accompanied by a 40% decrease in SR Ca^{2+} release, ultimately resulting in depressed cardiomyocyte shortening and re-lengthening. The depressed contraction

of the HRC-infected cardiomyocytes remained even after maximal isoproterenol stimulation. At the molecular level, HRC overexpresssion was accompanied by increase of the ryanodine receptor (RyR2) quaternary complex components junctin and triadin (Fan et al., 2004).

This study was followed by the generation of a transgenic mouse model overexpressing HRC (by 3-fold). Genetically modified mouse models, as well as their explanted hearts and isolated cardiomyocytes, have long been used to delineate the effects of various genes and mutations thereof on cardiac arrhythmogenesis. Although these models have a number of limitations, they remain one of the major tools available for in depth cellular and physiological studies at the *in vivo*, *ex vivo*, and *in vitro* levels (Davis et al., 2012; Huang, 2017).

In this setting, the increased cardiac HRC levels were associated with impaired SR Ca^{2+} uptake (by 35%) and attenuated cardiomyocyte Ca^{2+} transient decay (by nearly 40%). Possibly as a compensatory mechanism, there was a marked increase of the $Na^{+}-Ca^{2+}$ exchanger (NCX) and triadin protein levels in myocytes isolated from these mice. At the cellular level, however, neither NCX mediated Ca^{2+} extrusion nor RyR2 SR Ca^{2+} release was elevated. In fact, the depressed SR Ca^{2+} sequestration was associated with an attenuated rate of Ca^{2+} extrusion. Interestingly, as the mice aged, they presented with impaired cardiomyocyte Ca^{2+} cycling, leading to abnormal cardiac remodeling and congestive heart failure (Gregory et al., 2006).

Similarly, the implications of the lack of HRC were investigated at the *in vitro* and *in vivo* levels. Initially, HRC was knocked-down in neonatal rat ventricular cells and HL-1 cells, using *in vitro* siRNA technology. This led to increased activity of RyR2 and SERCA2 whilst SR Ca^{2+} load was unaffected. The *in vivo* adeno-associated virus (AAV)-mediated HRC knock-down in mice with or without transverse aortic constriction (TAC)-induced heart failure, led to decreased fractional shortening and increased cardiac fibrosis compared with control. At the molecular level these findings were associated with increased phosphorylation of RyR2, CaMKII, p38 MAPK, and phospholamban (PLN). Thus, down-regulation of HRC led to significant deterioration of cardiac function following TAC-induced heart failure (Park et al., 2012).

Following these studies, HRC-knockout (KO) mice were generated. Although morphologically and histologically they were normal, compared to wild-type, at the cellular level, the HRC-KO mouse cardiomyocytes exhibited significantly enhanced contractility, Ca^{2+} transients, and maximal SR Ca^{2+} uptake rates. They also presented with an increased number of spontaneous SR Ca^{2+} releases and delayed afterdepolarizations, perhaps driven by the increased number of Ca^{2+} sparks seen in KO mice compared to controls. Under stress conditions of 1 μmol/L isoproterenol and 5 Hz stimulation, the HRC-KO isolated cardiomyocytes were found to be five-fold more prone to after-contractions compared to wild-type mice. After TAC the HRC-KO mice developed severe cardiac hypertrophy, fibrosis, pulmonary edema and premature death compared to wild-types. Isolated cardiomyocytes from TAC treated HRC-KO hearts exhibited poor contractility and impaired Ca^{2+}-cycling, possibly due to reduced SERCA2 expression. These data underline the importance of HRC in the normal physiology of SR Ca^{2+} handling, as well as in maintaining the integrity of normal cardiac performance (Park et al., 2013).

Since HRC Ser96Ala has been associated with malignant ventricular arrhythmias (Arvanitis et al., 2008), the cellular mechanisms of pathogenesis were investigated initially in isolated adult rat ventricular cardiomyocytes infected with adenoviruses encoding the human HRC (hHRC) Ser96 or Ala96. The hHRC Ala96 exacerbated the inhibitory effects of hHRC Ser96 on the amplitude of Ca^{2+} transients, the prolongation of Ca^{2+} decay, and the caffeine-induced SR Ca^{2+} release, indicating a higher SR Ca^{2+} load. hHRC Ala96 had a stronger suppressive effect on the maximal SR Ca^{2+} uptake rate compared to hHRC Ser96. Furthermore, hHRC Ala96 increased the frequency of spontaneous Ca^{2+} sparks, while the hHRC Ser96 reduced them compared to GFP expressing controls. Importantly, expression of hHRC Ala96 in cardiomyocytes from a rat model of post-myocardial infarction heart failure induced dramatic disturbances of rhythmic Ca^{2+} transients. These findings reproduce the arrhythmogenic propensity of the human HRC Ser96Ala variant carriers when their cardiac function is compromised in the setting of heart failure (Han et al., 2011).

A recent study was carried out on a 'humanized' mouse of HRC Ser96Ala, where the murine HRC gene was replaced by the human homolog, and therefore carried either the wild-type gene with serine at position 96, or the alanine variant. The hHRC Ala96 mice displayed poor contractility and Ca^{2+} cycling compared to hHRC Ser96, in the absence of any structural or histological abnormalities. The occurrence of Ca^{2+} waves was significantly higher but the SR Ca^{2+} load was lower in hHRC Ala96 compared to hHRC Ser96. At the molecular level these findings were attributed to the poor interaction of HRC Ala96 with triadin, and ultimately with RyR2 (through triadin). Indeed, the open probability of RyR2 was significantly increased in hHRC Ala96 cardiomyocytes. Under stress conditions of 1 μmol/L isoproterenol and 5 Hz stimulation, isolated cardiomyocytes from hHRC Ala96 hearts presented with 6-fold more aftercontractions and 3-fold more delayed afterdepolarizations when compared to hHRC Ser96 cardiomyocytes. RyR2 was found to be hyperphoshorylated by CaMKII at Ser2814. Importantly, treatment of the hHRC Ala96 derived cardiomyocytes with KN93, a specific inhibitor of CaMKII, reversed the increase of Ca^{2+} sparks and waves (Singh et al., 2013).

Although these studies provided important insights into the potential arrhythmogenic mechanisms of the Ser96Ala mutation, they had an inherent issue – a non-murine protein being produced in the mouse. This could result in interactions of the human HRC with mouse proteins that may not necessarily take place when exclusively murine HRC is present. We therefore pursued an alternative, and perhaps more physiologically relevant approach, where the mutation was directly introduced in the mouse gene, at the equivalent site. This led to the development of the HRC Ser81Ala mouse model, which recapitulated the human Ser96Ala mutation directly in the mouse HRC protein

(Tzimas et al., 2017). The HRC Ser81Ala mice presented with increased mortality over a 12-month period, with 50% of the Ser81Ala mice dead by 10 months, compared to only 15% of the wild-type animals. Interestingly, no abnormalities were noted in the Ser81Ala mouse hearts in terms of cardiac structure and fibrosis, at least as far as 3–5 months of age, similar to data from the humanized Ser96Ala mouse. In addition, cardiac contraction, both *in vivo* and *ex vivo* (as measured by Langendorff preparation), was shown to be significantly decreased in 3–4-month-old Ser81Ala mice, when compared to the wild-types, whilst the Ser81Ala mice showed a slight decrease in intraventricular septum and left ventricular posterior wall thickness. Further age-related decreases in contractile function were similar between the two strains. Taken together, these data indicated that the increased mortality observed in HRC Ser81Ala mice was unlikely due to acute heart failure, and other factors should be considered (Tzimas et al., 2017).

Due to the fact that ventricular arrhythmias have been previously noted in the patient population with the Ser96Ala variant (Arvanitis et al., 2008), we hypothesized that SCD as a result of arrhythmias may also be the reason for the increased mortality in the Ser81Ala mice. We therefore performed a series of electrophysiological examinations on these mice *in vivo*. This work revealed an increased sensitivity of the Ser81Ala mice to an arrhythmogenic challenge (caffeine/epinephrine administration) when compared to the wild-type, with more than 50% of Ser81Ala mice going into ventricular tachycardia, compared to none of the wild-type animals. We extended these studies by carrying out experiments in isolated myocytes, where an increase in aftercontractions, calcium after-transients and delayed afterdepolarizations were observed in Ser81Ala derived cells, further supporting the hypothesis that the increase in mortality is due to arrhythmogenic events (Tzimas et al., 2017). Interestingly, contraction in myocytes from the Ser81Ala mouse was not increased, indicating that Ca^{2+} overload, *per se*, was not a driving force for the arrhythmogenic phenotype, as has been seen in a number of other models and digitalis-induced arrhythmias (Sipido, 2006; van den Hoogenhof et al., 2018).

Interestingly in heart failure, where arrhythmias may also ensue, it has been shown that SR Ca^{2+} load is not increased (Hasenfuss and Pieske, 2002). In this case arrhythmogenesis may be due to a variety of other factors, including increased activity of RyR2 or altered activity of NCX. For these reasons we went on to investigate if there was an increased spontaneous Ca^{2+} release in the Ser81Ala cardiomyocytes. Despite the fact we did not observe any alterations in Ca^{2+} spark properties, we did see an increase in total Ca^{2+} leak in myocytes isolated from the Ser81Ala mice, and an increase in Ca^{2+} wave speed. Furthermore, an increase in phosphorylation of RyR2 was noted at the CaMKII phosphorylation site (Ser-2814) under baseline conditions in Ser81Ala myocytes, whilst no differences were observed at the protein kinase A (PKA) site of RyR2, or in PLN phosphorylation.

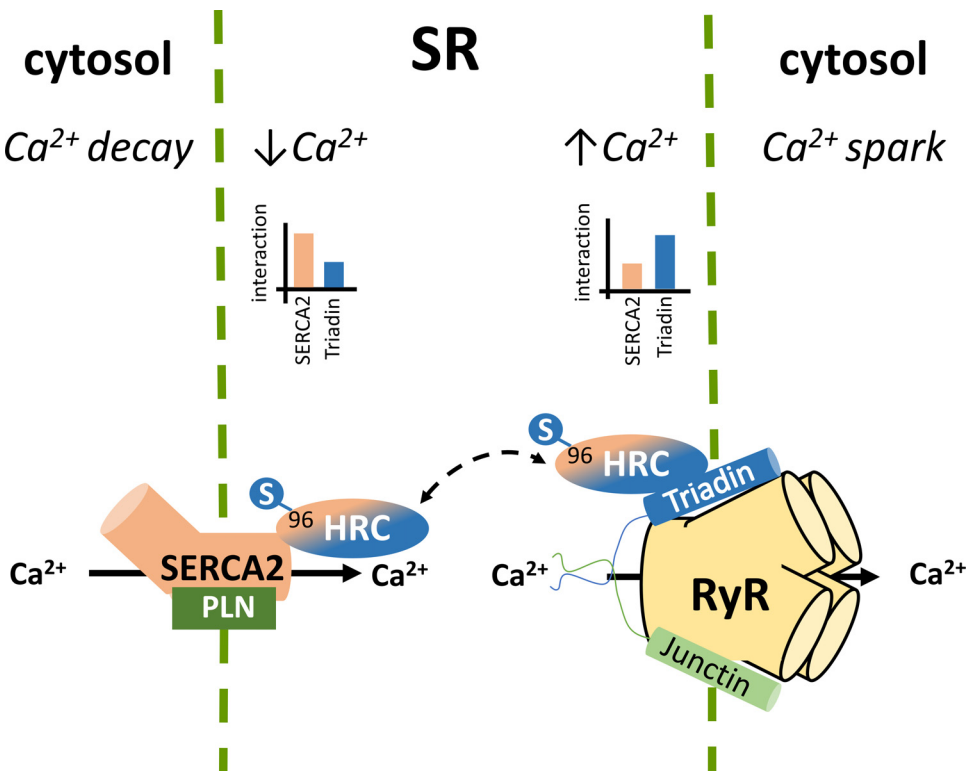

FIGURE 1 | Histidine-rich calcium binding protein complex cellular interactions within the cardiomyocytes. Local SR Ca^{2+} changes alter the dynamics of HRC interactions with triadin and SERCA2.

However, there were no alterations in the levels of the RyR2 protein, whilst an increase was seen in junctin and NCX, and a decrease in triadin. Additionally, increases in action potential (AP) duration were noted in the Ser81Ala myocytes, which went along with an increase in inward (Ca^{2+}) current. Taking all of these data together, we hypothesized that CaMKII played a key role in the arrhythmogenic phenotype in the Ser81Ala mouse. At both the cellular and *in vivo* levels, inhibition of CaMKII with KN-93 was indeed able to reduce the number of arrhythmogenic events.

Despite the fact that further studies should be carried out in this model, including the potential dyadic structural remodeling in myocytes, we can summarize that the HRC Ser81Ala mutation causes arrhythmia via increased spontaneous Ca^{2+} leak and longer APs, and this is, at least in part due to CaMKII activity. This alteration of CaMKII activity could be driven by the alterations in the local Ca^{2+} concentration, although the exact mechanisms of CaMKII activation in this model remains to be elucidated. Taking all of these data into account, CaMKII inhibition could be a potential therapeutic target in patients with similar polymorphisms/mutations.

HRC BINDING PARTNERS AND THEIR ROLE IN MEDIATING HRC EFFECTS ON Ca^{2+} HOMEOSTASIS AND ARRHYTHMOGENESIS

The SR holds a pivotal role in Ca^{2+} compartmentalization within the cardiomyocyte. During each cycle of cardiomyocyte activation Ca^{2+} fluxes rapidly back and forth between the cytosol and the sarcoplasmic reticulum. The SR Ca^{2+} release occurs through the opening of the gigantic RyR2 multiprotein complex under the regulation of triadin and junctin (Gambardella et al., 2018; Santulli et al., 2018; Slabaugh et al., 2018), while the energetic transport of cytosolic Ca^{2+} to the SR is achieved by SERCA2 under the regulation of PLN (Vafiadaki et al., 2009; Wang et al., 2011; Kranias and Hajjar, 2012). The HRC protein interacts with both systems mediating a fine cross talk between cytosolic Ca^{2+}— spark and decay (**Figure 1**; Arvanitis et al., 2007). HRC has been previously shown to be localized to the SR lumen in cardiac and skeletal muscles (Hofmann et al., 1989a; Shoshan-Barmatz et al., 1996; Suk et al., 1999) and based on its structural similarities with CSQ, it was initially suggested to be functionally associated with SR Ca^{2+} release (Hofmann et al., 1989a; Damiani and Margreth, 1991). This was supported by several studies, clearly demonstrating the direct interaction of HRC with triadin, an integral SR membrane protein forming a quaternary complex with the RyR2, CSQ, and junctin (Kim et al., 1990; Sacchetto et al., 1999, 2001; Lee et al., 2001). HRC binds to triadin in a Ca^{2+}-dependent manner, with increases in Ca^{2+} concentration leading to enhanced interaction between the two proteins (Sacchetto et al., 2001; Arvanitis et al., 2007; Rani et al., 2016). Multiple domains of HRC, including the C-terminal cysteine-rich domain (Sacchetto et al., 1999, 2001; Arvanitis et al., 2007) and the histidine-rich and acidic repeats (Lee et al., 2001), have been shown to interact with triadin. Interestingly, HRC interacts with triadin's luminal KEKE motif, a region which is also implicated in CSQ and RyR2 binding (Lee et al., 2001; Rani et al., 2016). Given this overlap on triadin's minimal binding region, a biochemical study recently examined the potential competition between CSQ, HRC and RyR2 for triadin binding. Using increasing concentrations of RyR2 or CSQ peptides in immunoprecipitation assays, HRC was demonstrated to compete with RyR2 and CSQ for binding to triadin (Rani et al., 2016). These findings, indicate the regulatory nature of these protein associations that are tightly controlled by Ca^{2+} concentration toward effective regulation of RyR2 function and SR Ca^{2+} release. The possibility that HRC can bind to RyR2 independently of triadin, was suggested by a study utilizing the HEK293 cell culture system which lacks endogenous triadin protein (Zhang et al., 2014). However, as these findings were obtained solely from microscopy-based assays, and no further evidence has emerged since then to support this notion, additional work is required to establish this association. Overall, based on its association with triadin, HRC is believed to modulate RyR2 function and SR Ca^{2+} release by conferring refractoriness to SR Ca^{2+} release and exerting a presumably beneficial effect on SR Ca^{2+} reloading at intermediate Ca^{2+} concentrations (Rani et al., 2016).

In addition to triadin, we have demonstrated that HRC directly interacts with SERCA2a, the key enzyme mediating SR Ca^{2+} uptake (Arvanitis et al., 2007). Similarly to the HRC-triadin, the HRC-SERCA2 interaction is also Ca^{2+}-dependent, but with maximal binding occurring at low Ca^{2+} concentration, and a diminishing HRC-SERCA2 association with increasing Ca^{2+} concentrations (Arvanitis et al., 2007). The protein domains involved in this interaction include the amino-terminal fragment of SERCA2 that projects into the SR lumen (amino acid residues 74–90) and the second histidine- and glutamic acid-rich domain of HRC (amino acids 320–460) (Arvanitis et al., 2007).

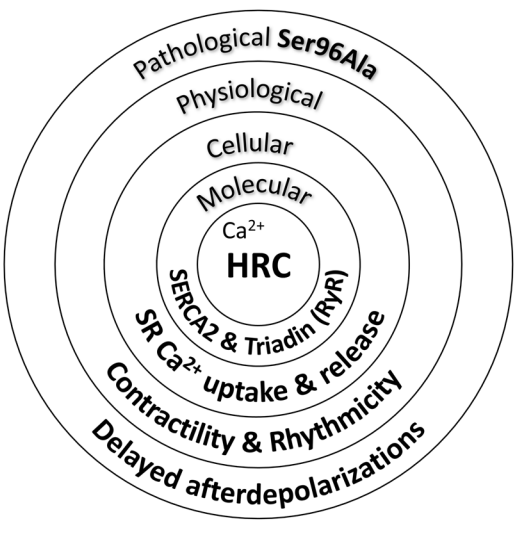

FIGURE 2 | Histidine-rich calcium binding protein functional significance in cardiac physiology and pathophysiology.

Interestingly, the HRC domain binding to triadin is distinct, and involves its cysteine-rich domain (amino acids 609–699) at the carboxyl terminal fragment (Sacchetto et al., 2001; Arvanitis et al., 2007). The choice of HRC binding partner, which is tightly controlled by Ca^{2+} concentrations, determines the HRC effect on SR Ca^{2+} cycling. At low SR Ca^{2+} load HRC interacts with SERCA2 and inhibits its activity. However, upon increases in SR Ca^{2+} concentration, HRC dissociates from SERCA2, exhibits enhanced binding to triadin, and modulates SR Ca^{2+} release (Arvanitis et al., 2011). Through this dual association with SERCA2 and triadin, HRC is implicated in both SR Ca^{2+} uptake and Ca^{2+} release, with defects in both processes observed upon HRC overexpression or ablation (Gregory et al., 2006; Park et al., 2013). HRC may therefore represent a key mediator of the fine cross-talk between these two processes in cardiomyocyte contraction and relaxation. Any factors modulating HRC, such as post-translational modifications (see section below) or gene sequence variations (e.g., the genetic variant Ser96Ala), could affect these protein associations with direct implications in SR Ca^{2+} cycling and arrhythmogenesis.

Indeed, acute overexpression of the HRC Ser96Ala human variant in cell culture systems significantly increased the binding of HRC Ser96Ala to SERCA2, an effect that was associated with enhanced inhibition of SERCA2 activity and thus reduced maximal SR Ca^{2+} uptake rate (Han et al., 2011). Importantly, HRC Ser96Ala increased the frequency of spontaneous Ca^{2+} sparks, suggesting enhanced RyR2 activity, and leading to increased uncontrolled SR Ca^{2+} release (Han et al., 2011). Similarly, as mentioned above, cardiomyocytes from the humanized HRC Ser96Ala mouse model exhibited increased RyR2 activity, enhanced propensity for spontaneous SR Ca^{2+} release and arrhythmias (Singh et al., 2013). Collectively, these studies have clearly demonstrated the functional significance of HRC interactions with SERCA2 and triadin toward effective regulation of SR Ca^{2+} uptake and release (**Figure 2**). Defects in HRC function due to genetic mutations lead to aberrant SR Ca^{2+} cycling and enhanced propensity toward arrhythmia triggering.

HRC POST-TRANSLATIONAL MODIFICATION

Initial reports on the HRC gene and protein functions described the phosphorylation of HRC by multiple kinases, including PKA and CaMKII (Damiani and Margreth, 1991; Damiani et al., 1995), as well as casein kinase II (CKII), an endogenous kinase which associates with SR membranes (Orr and Shoshan-Barmatz, 1996; Shoshan-Barmatz et al., 1996). Although PKA and CaMKII can phosphorylate HRC *in vitro*, these phosphorylations may not occur *in vivo* since HRC is a luminal protein and is not accessible to these cytoplasmic kinases (Hofmann et al., 1989a; Suk et al., 1999). It has been postulated that phosphorylation of HRC by CKII decreased the affinity of RyR2 for Ca^{2+}, although it was

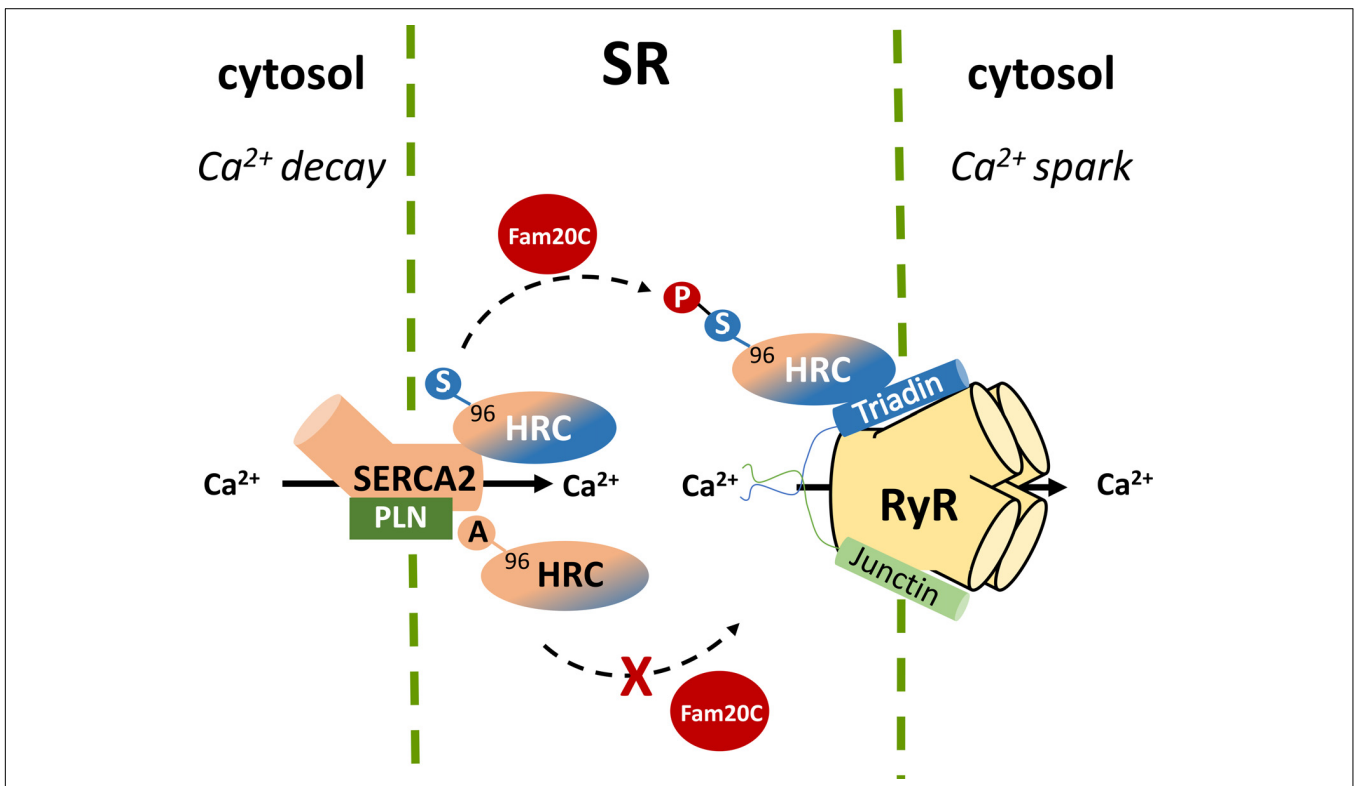

FIGURE 3 | Histidine-rich calcium binding protein phosphorylation by Fam20C at Ser96 affects the affinity of HRC interactions with SERCA2 and triadin while the Ala96 variant remains unaffected.

not clear whether this phosphorylation mediates a direct effect on RyR2 activity (Orr and Shoshan-Barmatz, 1996; Shoshan-Barmatz et al., 1996).

The discovery of the HRC Ser96Ala variant association with life-threatening ventricular arrhythmias in the setting of dilated cardiomyopathy, led to the hypothesis of abolishment of a potential phosphorylation site on HRC, with direct implication in downstream molecular and cellular processes. Indeed, bioinformatical analysis showed that HRC Ser96, an evolutionary conservative amino-acid position, could be phosphorylated (Arvanitis et al., 2008). *In vivo* phosphoproteomic studies of healthy human skeletal muscle found that HRC is phosphorylated at six serine amino acid residues, namely Ser119, Ser431, Ser563, Ser567, Ser157/Ser159, and Ser170/Ser171 (Hojlund et al., 2009). The authors predicted, using bioinformatical analysis, that the majority of these sites, (Ser119, Ser170 or Ser171, Ser431, and Ser567), could be phosphorylated by the luminally located CKII, while Ser157 or Ser159 may be phosphorylated by protein kinase B (PKB), and Ser563 by the mitogen-activated protein kinase 8 (MAPK8) or the glycogen synthase kinase 3 beta (GSK3B). Another study, which focused on *in vitro* dephosphorylation of cardiac proteins, demonstrated that HRC is phosphorylated at five positions (Ser104, Ser129, Ser249, Ser324, and Ser466) in wild-type hearts and can be dephosphorylated *in vitro* by alkaline phosphatase (Husberg et al., 2012). Although these studies were valuable for achieving a deeper understanding on post-translational modifications of wild-type HRC in healthy human skeletal and cardiac muscles, the status of HRC Ser96 remained unaddressed.

Recently, a new kinase, family with sequence similarity 20C (Fam20C) that phosphorylates S-x-E/pS motifs on proteins was found to be responsible for the majority of the extracellular phosphoproteome (Tagliabracci et al., 2015). Located within the ER and the Golgi apparatus, Fam20C phosphorylates a multitude of proteins including HRC Ser96, Ser119, Ser145, Ser358, Ser409, Ser431, Ser494, and Ser567. These findings not only identify Fam20C as the predominant kinase involved in the protein secretory pathway of cells but also suggest that Fam20C is a potential pharmacological target, affecting a multiple of cellular processes ranging from cell adhesion and migration to treatment against HRC driven life-threatening ventricular arrhythmias. Further proteomic and biochemical investigations under native or post-phosphatase treated whole-cardiac homogenates, clearly demonstrated that Fam20C is the kinase for HRC *in vivo* (Tagliabracci et al., 2015). These findings were supported by cell culture studies of co-expression of HRC and Fam20C in rat cardiomyoblasts, and expression of HRC in human osteosarcoma cells with CRISPR/Cas9 knockout of Fam20C. The importance of HRC phosphorylation at position 96 was demonstrated when HRC KO mouse heart derived primary cardiomyocytes, which exhibit increased arrhythmogenicity, were infected with pseudo-phosphorylated (HRC-Asp96) encoding adenoviruses, which alleviated the arrhythmias. In addition, the Fam20C-phosphorylated HRC showed a stronger interaction with triadin and a weaker interaction with SERCA2 by co-immunoprecipitation studies, while the unphosphorylated HRC showed a stronger interaction with SERCA2 (**Figure 3**). Collectively, these data suggest that Fam20C is, at least in part, responsible for HRC phosphorylation, and that the variant Ser96Ala changes the affinity of HRC interactions with triadin and SERCA2 (Pollak et al., 2017). Further experiments with specific inhibitors of Fam20 will be required to clarify the role of Fam20-phosphorylation in arrhythmia generation.

CONCLUSION

Studies on HRC function over the past decade, using *in vitro* and *in vivo* approaches at the molecular, cellular, tissue, organ, and whole organism levels have demonstrated its importance in cardiomyocyte physiology and pathophysiology. HRC mediates a cross-talk between SR Ca^{2+} uptake and release, regulating both systems and acting as a Ca^{2+} sensor. Importantly, the function of HRC is regulated by its phosphorylation at Ser96 and human carriers with the Ser96Ala variant are predisposed to cardiac arrhythmias under stress conditions. Thus this variant may serve as a biomarker for the identification of cardiovascular disease patients at risk for SCD.

AUTHOR CONTRIBUTIONS

All authors contributed in manuscript preparation and approved the final version of the manuscript.

REFERENCES

Anderson, J. P., Dodou, E., Heidt, A. B., De Val, S. J., Jaehnig, E. J., Greene, S. B., et al. (2004). HRC is a direct transcriptional target of MEF2 during cardiac, skeletal, and arterial smooth muscle development in vivo. *Mol. Cell. Biol.* 24, 3757–3768. doi: 10.1128/MCB.24.9.3757-3768.2004

Antoons, G., and Sipido, K. R. (2008). Targeting calcium handling in arrhythmias. *Europace* 10, 1364–1369. doi: 10.1093/europace/eun271

Arvanitis, D. A., Sanoudou, D., Kolokathis, F., Vafiadaki, E., Papalouka, V., Kontrogianni-Konstantopoulos, A., et al. (2008). The Ser96Ala variant in histidine-rich calcium-binding protein is associated with life-threatening ventricular arrhythmias in idiopathic dilated cardiomyopathy. *Eur. Heart J.* 29, 2514–2525. doi: 10.1093/eurheartj/ehn328

Arvanitis, D. A., Vafiadaki, E., Fan, G. C., Mitton, B. A., Gregory, K. N., Del Monte, F., et al. (2007). Histidine-rich Ca-binding protein interacts with sarcoplasmic reticulum Ca-ATPase. *Am. J. Physiol. Heart Circ. Physiol.* 293, H1581–H1589. doi: 10.1152/ajpheart.00278.2007

Arvanitis, D. A., Vafiadaki, E., Sanoudou, D., and Kranias, E. G. (2011). Histidine-rich calcium binding protein: the new regulator of sarcoplasmic reticulum calcium cycling. *J. Mol. Cell Cardiol.* 50, 43–49. doi: 10.1016/j.yjmcc.2010.08.021

Brink, P. A., Ferreira, A., Moolman, J. C., Weymar, H. W., van der Merwe, P. L., and Corfield, V. A. (1995). Gene for progressive familial heart block type I maps to chromosome 19q13. *Circulation* 91, 1633–1640. doi: 10.1161/01.CIR.91.6.1633

Damiani, E., and Margreth, A. (1991). Subcellular fractionation to junctional sarcoplasmic reticulum and biochemical characterization of 170 kDa Ca(2+)-

and low-density-lipoprotein-binding protein in rabbit skeletal muscle. *Biochem. J.* 277(Pt 3), 825–832. doi: 10.1042/bj2770825

Damiani, E., Picello, E., Saggin, L., and Margreth, A. (1995). Identification of triadin and of histidine-rich Ca(2+)-binding protein as substrates of 60 kDa calmodulin-dependent protein kinase in junctional terminal cisternae of sarcoplasmic reticulum of rabbit fast muscle. *Biochem. Biophys. Res. Commun.* 209, 457–465. doi: 10.1006/bbrc.1995.1524

Davis, J., Maillet, M., Miano, J. M., and Molkentin, J. D. (2012). Lost in transgenesis: a user's guide for genetically manipulating the mouse in cardiac research. *Circ. Res.* 111, 761–777. doi: 10.1161/CIRCRESAHA.111.262717

de Meeus, A., Stephan, E., Debrus, S., Jean, M. K., Loiselet, J., Weissenbach, J., et al. (1995). An isolated cardiac conduction disease maps to chromosome 19q. *Circ. Res.* 77, 735–740. doi: 10.1161/01.RES.77.4.735

Fan, G. C., Gregory, K. N., Zhao, W., Park, W. J., and Kranias, E. G. (2004). Regulation of myocardial function by histidine-rich, calcium-binding protein. *Am. J. Physiol. Heart Circ. Physiol.* 287, H1705–H1711. doi: 10.1152/ajpheart.01211.2003

Gambardella, J., Trimarco, B., Iaccarino, G., and Santulli, G. (2018). New insights in cardiac calcium handling and excitation-contraction coupling. *Adv. Exp. Med. Biol.* 1067, 373–385. doi: 10.1007/5584_2017_106

Gregory, K. N., Ginsburg, K. S., Bodi, I., Hahn, H., Marreez, Y. M., Song, Q., et al. (2006). Histidine-rich Ca binding protein: a regulator of sarcoplasmic reticulum calcium sequestration and cardiac function. *J. Mol. Cell Cardiol.* 40, 653–665. doi: 10.1016/j.yjmcc.2006.02.003

Gupta, R. C., Mishra, S., Rastogi, S., Wang, M., Rousso, B., Mika, Y., et al. (2009). Ca(2 +)-binding proteins in dogs with heart failure: effects of cardiac contractility modulation electrical signals. *Clin. Transl. Sci.* 2, 211–215. doi: 10.1111/j.1752-8062.2009.00097.x

Han, P., Cai, W., Wang, Y., Lam, C. K., Arvanitis, D. A., Singh, V. P., et al. (2011). Catecholaminergic-induced arrhythmias in failing cardiomyocytes associated with human HRCS96A variant overexpression. *Am. J. Physiol. Heart Circ. Physiol.* 301, H1588–H1595. doi: 10.1152/ajpheart.01153.2010

Hasenfuss, G., and Pieske, B. (2002). Calcium cycling in congestive heart failure. *J. Mol. Cell Cardiol.* 34, 951–969. doi: 10.1006/jmcc.2002.2037

Hofmann, S. L., Brown, M. S., Lee, E., Pathak, R. K., Anderson, R. G., and Goldstein, J. L. (1989a). Purification of a sarcoplasmic reticulum protein that binds Ca2 + and plasma lipoproteins. *J. Biol. Chem.* 264, 8260–8270.

Hofmann, S. L., Goldstein, J. L., Orth, K., Moomaw, C. R., Slaughter, C. A., and Brown, M. S. (1989b). Molecular cloning of a histidine-rich Ca2 + -binding protein of sarcoplasmic reticulum that contains highly conserved repeated elements. *J. Biol. Chem.* 264, 18083–18090.

Hojlund, K., Bowen, B. P., Hwang, H., Flynn, C. R., Madireddy, L., Geetha, T., et al. (2009). In vivo phosphoproteome of human skeletal muscle revealed by phosphopeptide enrichment and HPLC-ESI-MS/MS. *J. Proteome Res.* 8, 4954–4965. doi: 10.1021/pr9007267

Huang, C. L. (2017). Murine electrophysiological models of cardiac arrhythmogenesis. *Physiol. Rev.* 97, 283–409. doi: 10.1152/physrev.00007.2016

Husberg, C., Agnetti, G., Holewinski, R. J., Christensen, G., and Van Eyk, J. E. (2012). Dephosphorylation of cardiac proteins in vitro – A matter of phosphatase specificity. *Proteomics* 12, 973–978. doi: 10.1002/pmic.201100116

Kim, K. C., Caswell, A. H., Talvenheimo, J. A., and Brandt, N. R. (1990). Isolation of a terminal cisterna protein which may link the dihydropyridine receptor to the junctional foot protein in skeletal muscle. *Biochemistry* 29, 9281–9289. doi: 10.1021/bi00491a025

Kranias, E. G., and Hajjar, R. J. (2012). Modulation of cardiac contractility by the phospholamban/SERCA2a regulatome. *Circ. Res.* 110, 1646–1660. doi: 10.1161/CIRCRESAHA.111.259754

Landstrom, A. P., Dobrev, D., and Wehrens, X. H. T. (2017). Calcium signaling and cardiac arrhythmias. *Circ. Res.* 120, 1969–1993. doi: 10.1161/CIRCRESAHA.117.310083

Lee, H. G., Kang, H., Kim, D. H., and Park, W. J. (2001). Interaction of HRC (histidine-rich Ca(2 +)-binding protein) and triadin in the lumen of sarcoplasmic reticulum. *J. Biol. Chem.* 276, 39533–39538. doi: 10.1074/jbc.M010664200

Lompre, A. M., Hajjar, R. J., Harding, S. E., Kranias, E. G., Lohse, M. J., and Marks, A. R. (2010). Ca2 + cycling and new therapeutic approaches for heart failure. *Circulation* 121, 822–830. doi: 10.1161/CIRCULATIONAHA.109.890954

London, B. (2013). Searching for sudden death snps in calcium handling genes. *J. Am. Heart Assoc.* 2:e000541. doi: 10.1161/JAHA.113.000541

Morgan, J. P., Erny, R. E., Allen, P. D., Grossman, W., and Gwathmey, J. K. (1990). Abnormal intracellular calcium handling, a major cause of systolic and diastolic dysfunction in ventricular myocardium from patients with heart failure. *Circulation* 81, III21–III32.

Orr, I., and Shoshan-Barmatz, V. (1996). Modulation of the skeletal muscle ryanodine receptor by endogenous phosphorylation of 160/150-kDa proteins of the sarcoplasmic reticulum. *Biochim. Biophys. Acta* 1283, 80–88. doi: 10.1016/0005-2736(96)00078-8

Park, C. S., Cha, H., Kwon, E. J., Jeong, D., Hajjar, R. J., Kranias, E. G., et al. (2012). AAV-mediated knock-down of HRC exacerbates transverse aorta constriction-induced heart failure. *PLoS One* 7:e43282. doi: 10.1371/journal.pone.0043282

Park, C. S., Chen, S., Lee, H., Cha, H., Oh, J. G., Hong, S., et al. (2013). Targeted ablation of the histidine-rich Ca(2 +)-binding protein (HRC) gene is associated with abnormal SR Ca(2 +)-cycling and severe pathology under pressure-overload stress. *Basic Res. Cardiol.* 108:344. doi: 10.1007/s00395-013-0344-2

Pathak, R. K., Anderson, R. G., and Hofmann, S. L. (1992). Histidine-rich calcium binding protein, a sarcoplasmic reticulum protein of striated muscle, is also abundant in arteriolar smooth muscle cells. *J. Muscle Res. Cell Motil.* 13, 366–376. doi: 10.1007/BF01766464

Picello, E., Damiani, E., and Margreth, A. (1992). Low-affinity Ca(2 +)-binding sites versus Zn(2 +)-binding sites in histidine-rich Ca(2 +)-binding protein of skeletal muscle sarcoplasmic reticulum. *Biochem. Biophys. Res. Commun.* 186, 659–667. doi: 10.1016/0006-291X(92)90797-O

Pollak, A. J., Haghighi, K., Kunduri, S., Arvanitis, D. A., Bidwell, P. A., Liu, G. S., et al. (2017). Phosphorylation of serine96 of histidine-rich calcium-binding protein by the Fam20C kinase functions to prevent cardiac arrhythmia. *Proc. Natl. Acad. Sci. U.S.A.* 114, 9098–9103. doi: 10.1073/pnas.1706441114

Pritchard, T. J., and Kranias, E. G. (2009). Junctin and the histidine-rich Ca2 + binding protein: potential roles in heart failure and arrhythmogenesis. *J. Physiol.* 587(Pt 13), 3125–3133. doi: 10.1113/jphysiol.2009.172171

Rani, S., Park, C. S., Sreenivasaiah, P. K., and Kim, D. H. (2016). Characterization of Ca(2 +)-dependent protein-protein interactions within the Ca(2 +) release units of cardiac sarcoplasmic reticulum. *Mol. Cells* 39, 149–155. doi: 10.14348/molcells.2016.2284

Remme, C. A., and Bezzina, C. R. (2010). Sodium channel (dys)function and cardiac arrhythmias. *Cardiovasc. Ther.* 28, 287–294. doi: 10.1111/j.1755-5922.2010.00210.x

Sacchetto, R., Damiani, E., Turcato, F., Nori, A., and Margreth, A. (2001). Ca(2 +)-dependent interaction of triadin with histidine-rich Ca(2 +)-binding protein carboxyl-terminal region. *Biochem. Biophys. Res. Commun.* 289, 1125–1134. doi: 10.1006/bbrc.2001.6126

Sacchetto, R., Turcato, F., Damiani, E., and Margreth, A. (1999). Interaction of triadin with histidine-rich Ca(2 +)-binding protein at the triadic junction in skeletal muscle fibers. *J. Muscle Res. Cell Motil.* 20, 403–415. doi: 10.1023/A:1005580609414

Santulli, G., Lewis, D., des Georges, A., Marks, A. R., and Frank, J. (2018). Ryanodine receptor structure and function in health and disease. *Subcell. Biochem.* 87, 329–352. doi: 10.1007/978-981-10-7757-9_11

Schmitt, N., Grunnet, M., and Olesen, S. P. (2014). Cardiac potassium channel subtypes: new roles in repolarization and arrhythmia. *Physiol. Rev.* 94, 609–653. doi: 10.1152/physrev.00022.2013

Shoshan-Barmatz, V., Orr, I., Weil, S., Meyer, H., Varsanyi, M., and Heilmeyer, L. M. (1996). The identification of the phosphorylated 150/160-kDa proteins of sarcoplasmic reticulum, their kinase and their association with the ryanodine receptor. *Biochim. Biophys. Acta* 1283, 89–100. doi: 10.1016/0005-2736(96)00079-X

Singh, V. P., Rubinstein, J., Arvanitis, D. A., Ren, X., Gao, X., Haghighi, K., et al. (2013). Abnormal calcium cycling and cardiac arrhythmias associated with the human Ser96Ala genetic variant of histidine-rich calcium-binding protein. *J. Am. Heart Assoc.* 2:e000460. doi: 10.1161/JAHA.113.000460

Sipido, K. R. (2006). Calcium overload, spontaneous calcium release, and ventricular arrhythmias. *Heart Rhythm.* 3, 977–979. doi: 10.1016/j.hrthm.2006.01.013

Slabaugh, J. L., Brunello, L., Elnakish, M. T., Milani-Nejad, N., Gyorke, S., and Janssen, P. M. L. (2018). Synchronization of Intracellular Ca(2 +) release

in multicellular cardiac preparations. *Front. Physiol.* 9:968. doi: 10.3389/fphys.2018.00968

Suk, J. Y., Kim, Y. S., and Park, W. J. (1999). HRC (histidine-rich Ca2 + binding protein) resides in the lumen of sarcoplasmic reticulum as a multimer. *Biochem. Biophys. Res. Commun.* 263, 667–671. doi: 10.1006/bbrc.1999.1432

Tagliabracci, V. S., Wiley, S. E., Guo, X., Kinch, L. N., Durrant, E., Wen, J., et al. (2015). A single kinase generates the majority of the secreted phosphoproteome. *Cell* 161, 1619–1632. doi: 10.1016/j.cell.2015.05.028

Tzimas, C., Johnson, D. M., Santiago, D. J., Vafiadaki, E., Arvanitis, D. A., Davos, C. H., et al. (2017). Impaired calcium homeostasis is associated with sudden cardiac death and arrhythmias in a genetic equivalent mouse model of the human HRC-Ser96Ala variant. *Cardiovasc. Res.* 113, 1403–1417. doi: 10.1093/cvr/cvx113

Vafiadaki, E., Papalouka, V., Arvanitis, D. A., Kranias, E. G., and Sanoudou, D. (2009). The role of SERCA2a/PLN complex, Ca(2 +) homeostasis, and anti-apoptotic proteins in determining cell fate. *Pflugers. Arch.* 457, 687–700. doi: 10.1007/s00424-008-0506-5

van den Broek, F. A., Bakker, R., den Bieman, M., Fielmich-Bouwman, A. X., Lemmens, A. G., van Lith, H. A., et al. (1998). Genetic analysis of dystrophic cardiac calcification in DBA/2 mice. *Biochem. Biophys. Res. Commun.* 253, 204–208. doi: 10.1006/bbrc.1998.9776

van den Hoogenhof, M. M. G., Beqqali, A., Amin, A. S., van der Made, I., Aufiero, S., Khan, M. A. F., et al. (2018). RBM20 mutations induce an arrhythmogenic dilated cardiomyopathy related to disturbed calcium handling. *Circulation*. doi: 10.1161/CIRCULATIONAHA.117.031947

Wang, H. S., Arvanitis, D. A., Dong, M., Niklewski, P. J., Zhao, W., Lam, C. K., et al. (2011). SERCA2a superinhibition by human phospholamban triggers electrical and structural remodeling in mouse hearts. *Physiol. Genomics* 43, 357–364. doi: 10.1152/physiolgenomics.00032.2010

Zhang, J. Z., McLay, J. C., and Jones, P. P. (2014). The arrhythmogenic human HRC point mutation S96A leads to spontaneous Ca(2 +) release due to an impaired ability to buffer store Ca(2 +). *J. Mol. Cell Cardiol.* 74, 22–31. doi: 10.1016/j.yjmcc.2014.04.019

Conflict of Interest Statement: The authors declare that the research was conducted in the absence of any commercial or financial relationships that could be construed as a potential conflict of interest.

frontiers in Physiology

REVIEW
published: 07 November 2018
doi: 10.3389/fphys.2018.01500

Hypokalemia-Induced Arrhythmias and Heart Failure: New Insights and Implications for Therapy

Jonas Skogestad[1]* *and Jan Magnus Aronsen*[2,3]

[1] Division of Cardiovascular and Pulmonary Diseases, Institute of Experimental Medical Research, University of Oslo and Oslo University Hospital, Oslo, Norway, [2] Department of Pharmacology, Faculty of Medicine, University of Oslo and Oslo University Hospital, Oslo, Norway, [3] Bjørknes College, Oslo, Norway

Routine use of diuretics and neurohumoral activation make hypokalemia (serum K^+ < 3. 5 mM) a prevalent electrolyte disorder among heart failure patients, contributing to the increased risk of ventricular arrhythmias and sudden cardiac death in heart failure. Recent experimental studies have suggested that hypokalemia-induced arrhythmias are initiated by the reduced activity of the Na^+/K^+-ATPase (NKA), subsequently leading to Ca^{2+} overload, Ca^{2+}/Calmodulin-dependent kinase II (CaMKII) activation, and development of afterdepolarizations. In this article, we review the current mechanistic evidence of hypokalemia-induced triggered arrhythmias and discuss how molecular changes in heart failure might lower the threshold for these arrhythmias. Finally, we discuss how recent insights into hypokalemia-induced arrhythmias could have potential implications for future antiarrhythmic treatment strategies.

Keywords: calcium, arrhythmia (heart rhythm disorders), Na^+ - K^+-ATPase, hypokalaemia, heart failure

OPEN ACCESS

Edited by:
Daniel M. Johnson, University of Birmingham, United Kingdom

Reviewed by:
Fadi G. Akar, Icahn School of Medicine at Mount Sinai, United States
Davor Pavlovic, University of Birmingham, United Kingdom

***Correspondence:**
Jonas Skogestad
jonas.skogestad@medisin.uio.no

Specialty section:
This article was submitted to Cardiac Electrophysiology, a section of the journal Frontiers in Physiology

Received: *06 July 2018*
Accepted: *05 October 2018*
Published: *07 November 2018*

Citation:
Skogestad J and Aronsen JM (2018) Hypokalemia-Induced Arrhythmias and Heart Failure: New Insights and Implications for Therapy. Front. Physiol. 9:1500. doi: 10.3389/fphys.2018.01500

INTRODUCTION

Despite continuous improvements in therapies, long-term prognosis in heart failure (HF) remains poor, with overall 5-year mortality reaching 50% (Yancy et al., 2013), and even higher in more advanced stages (NYHA III-IV) (Arnold et al., 2013). Sudden cardiac death (SCD), mostly due to ventricular tachyarrhythmias (VTs), contributes to ∼50% of HF deaths (Tomaselli and Zipes, 2004). Hypokalemia is a well-recognized risk factor for VT, and hypokalemia is both common and independently associated with worse clinical outcomes in HF patients (Cleland et al., 1987; Ahmed et al., 2007; Bowling et al., 2010; Kjeldsen, 2010; Aldahl et al., 2017; Nunez et al., 2018), as well as increasing the risk of ventricular arrhythmias and mortality during acute myocardial infarction (Goyal et al., 2012; Colombo et al., 2018; Hoppe et al., 2018).

Here, we review the current evidence for mechanisms of triggered hypokalemia-induced arrhythmias, how cardiac remodeling in HF might lower the threshold for these arrhythmias, and use this to propose future antiarrhythmic drug targets.

Hypokalemia in HF: Etiology and Prevalence

Hypokalemia is defined as serum K^+ levels (serum-[K^+]) <3.5 mM (Unwin et al., 2011), but several studies report increased risk of SCD and all-cause mortality in HF patients with serum-[K^+] <4 mM (Nolan et al., 1998; Macdonald and Struthers, 2004; Bowling et al., 2010; Aldahl et al., 2017).

The prevalence of hypokalemia in HF patients varies between 19 and 54%, depending on the definition of hypokalemia and patient characteristics (Wester and Dyckner, 1986; Guo et al., 2005; Ahmed et al., 2007; Bowling et al., 2010; Collins et al., 2017). The prevalence was more likely to be higher in patient populations that were studied before the introduction of beta-blockers, ACE-inhibitors, and AT_1-antagonists as standard HF therapy, as all of these drugs increase serum K^+ levels and thus counteract hypokalemia. In addition, the prevalence of hypokalemia is generally higher in hospitalized patients compared to nonhospitalized patients (Unwin et al., 2011).

The main causes of hypokalemia in HF are use of diuretics and activation of the renin-angiotensin-aldosterone system that causes loss of K^+ in the urine (Leier et al., 1994). Increased levels of catecholamines also contribute by shifting K^+ into the intracellular compartment (Packer, 1990; Osadchii, 2010; Urso et al., 2015), whereas volume overload in more progressive HF could cause a dilution effect (Leier et al., 1994).

It has long been recognized that diuretics, both thiazides and loop-diuretics, increase the risk of hypokalemia and cardiac arrhythmias in patients receiving digitalis (Steiness and Olesen, 1976; Kaplan, 1984). Hypertensive men with baseline ECG abnormalities following an intensive diuretics regime displayed increased mortality compared to the standard regime in the Multiple Risk Factor Intervention Trial (1982). Later trials found no increased mortality with intensive diuretics treatment (1984) or when comparing diuretics to other anti-hypertensive agents (Officers et al., 2002), leading some authors to argue that the anti-hypertensive effect of diuretics compensates for the suggested pro-arrhythmic effect by diuretics alone (Papademetriou, 2006). Nevertheless, one study noted that a minority of patients using thiazides developed marked hypokalemia and cardiac arrhythmias (Siegel et al., 1992), and a case-control study found a dose-response relationship between thiazide dosage and the risk of SCD (Siscovick et al., 1994). Importantly, in patients with left ventricular dysfunction there was 30–40% increased risk of arrhythmic death among patients who used diuretics (Cooper et al., 1999). These results collectively suggest that, even though diuretics are important drugs for blood pressure reduction and prevention of volume overload in HF, being aware of the risk of hypokalemia and cardiac arrhythmias, in particular in the setting of heart disease, is important.

In contrast to thiazides and loop diuretics, mineralocorticoid receptor antagonists limit the renal excretion of K^+, increase serum-[K^+], and limit the risk for cardiac arrhythmias induced by hypokalemia (Siscovick et al., 1994; Cooper et al., 1999). ACE inhibitors, aldosterone receptor blockers, and beta blockers could potentially prevent hypokalemia by opposing the neurohumoral activation associated with HF that lowers serum-[K^+] (Macdonald and Struthers, 2004).

Serum [K^+] is altered during and after intensive exercise. During exercise, marked hyperkalemia may develop due to the release of K^+ from skeletal muscles (Sejersted and Sjogaard, 2000). Increased levels of catecholamines counteract and decrease recovery time from exercise-induced hyperkalemia (Williams et al., 1985) by stimulating Na^+/K^+-ATPase (NKA) (Despa et al., 2008). Interestingly, serum-[K^+] undershoots during the recovery phase after physical exercise, leading to postexercise hypokalemia (Medbo and Sejersted, 1990; Lindinger, 1995). The combination of hyperkalemia and subsequent hypokalemia with increased catecholamines during physical exercise could potentially contribute to the increased risk of cardiac arrhythmias and SCD observed during exercise in patients with structural or ischemic heart diseases (Siscovick et al., 1984; Thompson et al., 2007). Intriguingly, the risk of arrhythmias is particularly high in the recovery phase after exercise (Young et al., 1984), which coincides with postexercise hypokalemia (Medbo and Sejersted, 1990; Lindinger, 1995). Low serum-[K^+] might thus be a cause of arrhythmias in patients even without clinically recognized hypokalemia.

Triggered Ventricular Arrhythmias

Ventricular tachyarrhythmias are highly prevalent in HF, with 50–80% of patients having nonsustained VT on ambulatory cardiac monitoring (Singh et al., 1997; Teerlink et al., 2000). Re-entry and triggered arrhythmias are the two main types of tachyarrhythmias (Antzelevitch and Burashnikov, 2011). Fibrosis, scarring, and conduction abnormalities promote mechanical and electrophysiological re-entry, whereas reduced repolarization reserve, Ca^{2+} dysregulation, and altered transmembrane ion currents cause triggered arrhythmias (Tomaselli and Zipes, 2004; Ebinger et al., 2005; Jin et al., 2008).

Triggered arrhythmias are reported to initiate most VTs in nonischemic HF and even half of the VTs in ischemic HF (Pogwizd et al., 1992; Pogwizd and Bers, 2004). Triggered arrhythmias are caused by either early or delayed afterdepolarizations (EADs or DADs), abnormal depolarizations of the membrane potential that could give rise to a spontaneous action potential (AP) between two regular APs (Volders et al., 2000). DADs are caused by spontaneous Ca^{2+} release in a feed forward reaction that propagates as Ca^{2+} waves along the sarcoplasmic reticulum (SR) membrane as illustrated in **Figure 1**. Ca^{2+} waves can occur due to overload of Ca^{2+} in the SR and/or reduced threshold for Ca^{2+} leak through the ryanodine receptors (RyRs) (Venetucci et al., 2008). The spontaneously released Ca^{2+} activates inward currents named I_{ti} (mainly consisting of I_{NCX}), leading to a depolarization of the resting membrane potential (Clusin, 2003; Venetucci et al., 2008). The Ca^{2+} wave-induced depolarization triggers an extra AP if the resulting inward current depolarizes the membrane sufficiently to trigger opening of voltage-gated Na^+ channels.

EADs typically develop in situations with reduced repolarization reserve, either due to increased inward currents, reduced outward currents, or both (Weiss et al., 2010). EADs occur when inward currents, the L-type Ca^{2+} current (I_{Ca}) or I_{ti} derived from Ca^{2+} waves during the AP, are larger than the outward currents (mainly K^+ currents) during late phases of the AP (Zhao et al., 2012).

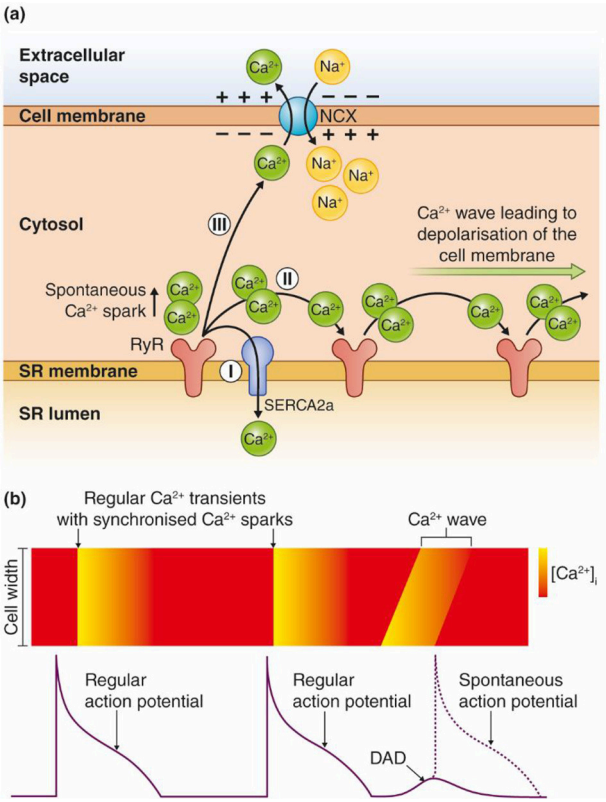

FIGURE 1 | Model for transformation of a Ca^{2+} wave into an afterdepolarization. **(a)** Ca^{2+} ions are released spontaneously from the SR, either due to Ca^{2+} overload or increased RyR conductance (reduced threshold). The Ca^{2+} ions released from RyRs have three possible routes: (I) SERCA2 pumps the Ca^{2+} ions directly back into the SR. The Ca^{2+} wave is interrupted and no afterdepolarizations occur. (II) The Ca^{2+} ions diffuse to the neighboring RyRs, which leads to release of new Ca^{2+} ions. Repetitive events where Ca^{2+} ions are released and activate the next cluster of RyRs along the SR membrane lead to a Ca^{2+} wave. (III) Ca^{2+} can be extruded across the sarcolemma through the Na^+/Ca^{2+} exchanger (NCX). This causes an inward, depolarizing current due to the inward flux of three positively charged Na^+ ions per one Ca^{2+} that is extruded over the cell membrane. **(b)** Regular APs trigger synchronous Ca^{2+} release, which leads to cardiomyocyte contraction. Ca^{2+} waves can lead to DADs between two regular APs, and trigger a spontaneous AP as shown in the figure. Ca^{2+} waves during an AP can trigger EADs.

MECHANISMS FOR HYPOKALEMIA-INDUCED TRIGGERED ARRHYTHMIAS

Clinically, hypokalemia is associated with triggered arrhythmias such as Torsades De Pointes (TDP), polymorphic VT, ventricular fibrillation (VF), and ventricular ectopy (Nordrehaug et al., 1985). Hypokalemia has been shown to cause regional alterations in conduction velocity (Chah et al., 1982; Smeets et al., 1986; Wolk et al., 1998) and regional action potential duration (APD) heterogeneity (Poelzing and Veeraraghavan, 2007) that establish functional reentry circuits, although a recent study in postinfarction pigs with increased afterload only found slowed conduction velocity with no regional differences in APD (Motloch et al., 2017). Hypokalemia promotes triggered arrhythmias by a reduction in cardiac repolarization reserve and increased intracellular Ca^{2+} in cardiomyocytes (Weiss et al., 2017). Here, we review evidence for mechanisms coupling hypokalemia to induction of triggered arrhythmias, and argue that this is primarily due to inhibition of NKA (in particular the NKAα2 isoform) leading to development of afterdepolarizations as proposed in **Figure 2**.

The Relative Role of NKA VS. K^+ Channels in Induction of Hypokalemia-induced Ventricular Arrhythmias

The pro-arrhythmic effects of hypokalemia have been linked to reduced outward K^+ currents such as I_{K1}, I_{Kr}, I_{Ks}, and I_{to} (Yang et al., 1997; Bouchard et al., 2004; Killeen et al., 2007; Osadchii, 2010) and recently to reduced NKA currents (Aronsen et al., 2015; Pezhouman et al., 2015). Reduced outward K^+ currents decrease the repolarization reserve, prolong the APD, and increase the risk of afterdepolarizations (Weiss et al., 2017). Low extracellular K^+ (K_e^+) leads to hyperpolarization of the resting membrane potential, which paradoxically increases excitability of cardiomyocytes. This effect is ascribed to an increased number of available Na^+ channels and the reduced ability of I_{K1} to generate outward current that protects against membrane depolarization (Bers, 2001).

Pezhouman, Singh, and coworkers observed in an elegant study that reduced NKA activity was necessary and sufficient to develop hypokalemia-induced ventricular arrhythmias. Reduced K^+ channel conductance in itself caused only a modest increase in APD and no afterdepolarizations, but potentiated the pro-arrhythmic effect of NKA inhibition in this study (Pezhouman et al., 2015). Comparably, we found that NKA inhibition was necessary and sufficient to increase Ca^{2+} levels in a factorial analysis where we compared the relative effect of lowering NKA activity vs. all other ion channels and transporters sensitive to K_e^+. Several lines of evidence suggest that Ca^{2+} overload caused by NKA inhibition is the main initiating event in hypokalemia-induced ventricular arrhythmias, as discussed in the next sections.

NCX: The Link Between NKA Inhibition and Ca^{2+} Overload in Hypokalemia

Na^+ and Ca^{2+} homeostasis are coupled through the Na^+/Ca^{2+}-exchanger (NCX) that uses the electrochemical gradient of Na^+ and Ca^{2+} to exchange 3 Na^+ for 1 Ca^{2+}. This allows NKA to indirectly regulate cardiac Ca^{2+} fluxes through the regulation of $[Na^+]_i$. NKA is an ATP- and voltage-dependent ion transporter that exchanges 3 Na^+ ions from the cytosol with 2 K^+ ions from the extracellular compartment, leading to a net outward current (Stanley et al., 2015). NKA is the only major Na^+ efflux mechanism in cardiomyocytes, and regulates intracellular $[Na^+]$ by balancing Na^+ efflux against Na^+ influx (Aronsen et al., 2013; Despa and Bers, 2013).

NKA activity is regulated by extracellular K^+ levels, intracellular Na^+ levels, the membrane potential (Glitsch, 2001), posttranslational modifications (Figtree et al., 2009; Poulsen et al.,

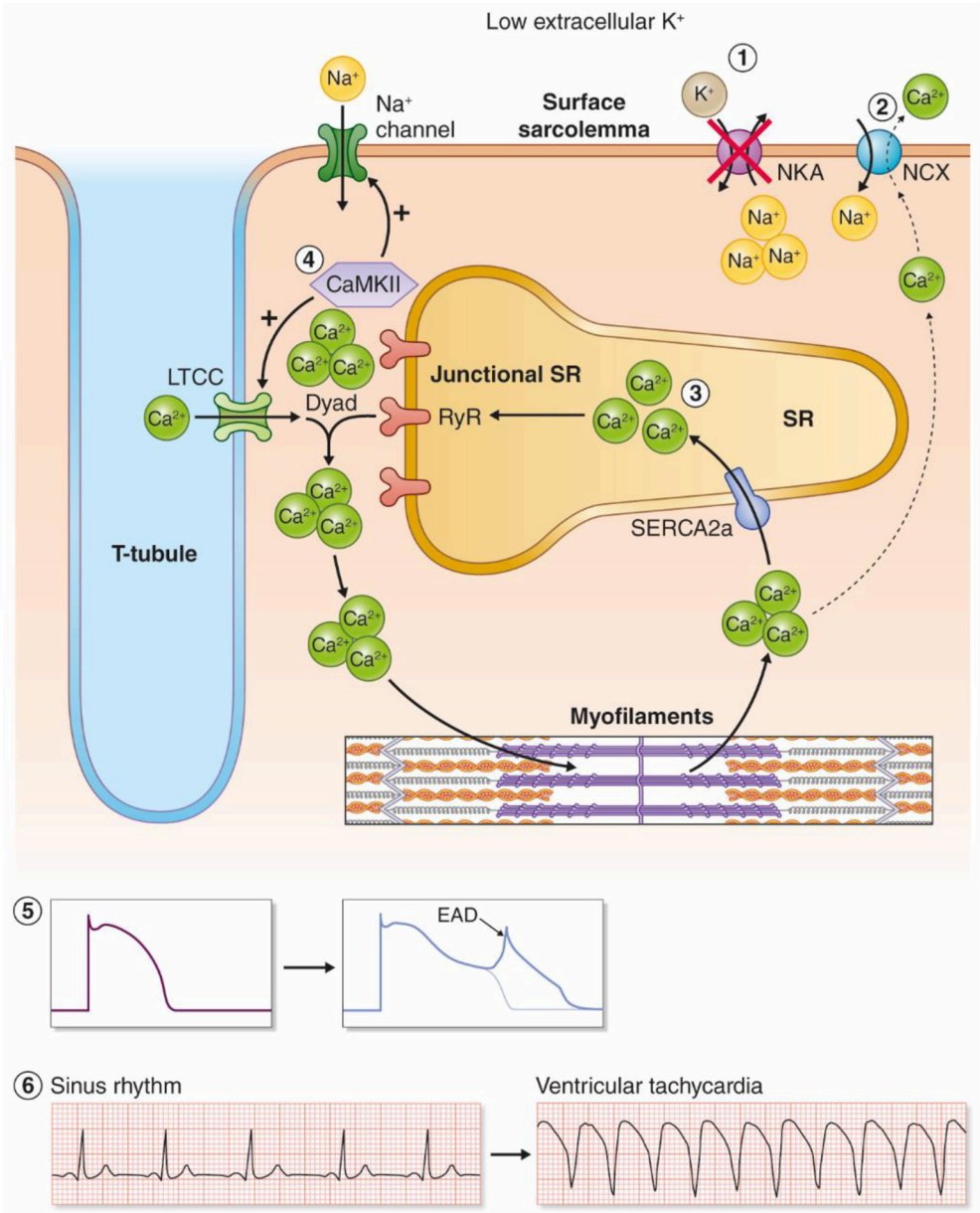

FIGURE 2 | Proposed model for hypokalemia-induced triggered arrhythmias. **(1)** Low K_e^+ reduces the activity of the NKAα2 isoform. **(2)** Intracellular Na^+ accumulates and leads to reduced inward NCX current, and by this less extrusion of Ca^{2+}. **(3)** Intracellular and SR Ca^{2+} increases as a result. **(4)** Ca^{2+} overload increases the activity of the Ca^{2+}/calmodulin-dependent kinase (CaMKII), which leads to a vicious cycle by phosphorylation of voltage-gated Na^+ channels and L-type Ca^{2+} channels. **(5)** Increased influx of Na^+ and Ca^{2+} amplifies Ca^{2+} overload and triggers EADs. **(6)** Hypokalemia-induced EADs can trigger ventricular tachyarrhythmias.

2010), and the accessory protein phospholemman (PLM), which binds to and inhibits NKA activity (Pavlovic et al., 2007, 2013a). β-adrenergic stimulation leads to phosphorylation of PLM, which relieves PLM inhibition of NKA (Despa et al., 2005; Khafaga et al., 2012). This provides a link between circulating catecholamines and fluxes of Na^+ and K^+ over the cell membrane. NKA is composed of αβ dimers, where both isoforms exist in three different isoforms (α1-3 and β1-3) (Lingrel and Kuntzweiler, 1994; Sweadner et al., 1994; McDonough et al., 1996; Bers and Despa, 2009). NKAα1 and NKAα2 contribute to 70–95% and 5–30% of the total NKA activity in cardiomyocytes respectively (Lucchesi and Sweadner, 1991; James et al., 1999; Berry et al., 2007; Despa and Bers, 2007; Swift et al., 2007; Despa et al., 2012). Despite being less abundant than NKAα1, several studies strongly suggest that NKAα2, and not NKAα1, is the main NKA isoform that regulates NCX activity and Ca^{2+} fluxes in cardiomyocytes by limiting the $[Na^+]_i$ sensed by the NCX (Berry et al., 2007; Despa and Bers, 2007; Swift et al., 2007, 2010; Despa et al., 2012).

According to this scheme, reduced activity of NKAα2 increases cellular Ca^{2+} levels by limiting forward mode NCX activity (that extrudes Ca^{2+}) and by increasing reverse mode NCX activity, which mediates Ca^{2+} influx during a short time during the early phases of the AP (Bers, 2002; Lines et al., 2006).

Despa et al. demonstrated that a similar degree of NKAα1 and NKAα2 inhibition yielded a comparable rise in intracellular Na^+, but only NKAα2 inhibition increased the Ca^{2+} levels in cardiomyocytes (Despa et al., 2012). This study and others (James et al., 1999; Swift et al., 2007) suggest that the ability of NKAα2 to regulate Ca^{2+} fluxes and cardiac contractility is most likely due to close localization with NCX, but this remains to be shown. NKAα1 is more abundant at the sarcolemma, whereas NKAα2 preferentially localizes to the transverse T-tubules (Berry et al., 2007; Swift et al., 2007; Yuen et al., 2017). The anchoring protein Ankyrin B coordinates a NKA/NCX microdomain, but both NKAα1 and NKAα2 coprecipitate with Ankyrin-B (Mohler et al., 2005). More studies are needed to determine the precise mechanism through which NKAα2 specifically can control Ca^{2+} homeostasis and cardiac contractility.

We studied the effect of low K_e^+ (2.7 mM) on intracellular Ca^{2+} in rat ventricular myocytes, and found that steady-state Ca^{2+} transients were increased compared to normal K_e^+ (5.0 mM). The increase in Ca^{2+} was not present in cells pretreated with a low dose of ouabain to selectively inhibit NKAα2 (Aronsen et al., 2015). This result could be explained by the finding that NKAα2 preferentially regulates intracellular Ca^{2+}, as discussed above, and the different sensitivity to extracellular K^+ $[K^+]_e$. Changes in $[K^+]_e$ within the clinical range of hypokalemia are expected to modulate primarily NKAα2 ($k_{0.5} = 2.7$ mM) and have relatively small effects on NKAα1 ($k_{0.5} = 1.5$ mM) (Han et al., 2009).

These results suggest that moderate hypokalemia reduces NKAα2 activity and leads to arrhythmogenic Ca^{2+} overload by decreased forward mode and/or reduced reverse mode NCX activity (Aronsen et al., 2015). In addition, chronic hypokalemia has been reported to downregulate the expression of cardiac NKAα2, but not the NKAα1 isoform (Azuma et al., 1991). It cannot be excluded that inhibition of NKAα1 also contributes to the arrhythmogenesis in cells exposed K_e^+, but given the established role of NKAα2 as a regulator of Ca^{2+} levels in cardiomyocytes, in combination with the present evidence, inhibition of NKAα2 is the most likely mechanism leading to Ca^{2+} overload in hypokalemia.

In addition to NKA inhibition, which reduces inward NCX current, hypokalemia also alters the NCX activity through hyperpolarization of the resting membrane potential. Hyperpolarization increases the inward NCX current and is associated with reduced intracellular Ca^{2+} levels (Bouchard et al., 2004), opposing reduced inward NCX current and the increased intracellular Ca^{2+} following NKA inhibition (Eisner and Lederer, 1979; Aronsen et al., 2013). Both we (Aronsen et al., 2015) and others (Eisner and Lederer, 1979; Bouchard et al., 2004) have reported that myocardial contractility and Ca^{2+} transients are first reduced, and then subsequently increase to above the basal level after switching from normal to low K_e^+. In the intact organism, changes in K_e^+ are much slower than in experimental settings, and the Ca^{2+} levels most likely reach steady state without a biphasic response. Still, it is important to appreciate the biphasic cardiomyocyte response to low K_e^+, as the steady state in myocardium exposed to low K_e^+ probably reflects the combined effect of membrane hyperpolarization (that reduces Ca^{2+} levels) and NKA inhibition (that increases Ca^{2+} levels).

Afterdepolarizations Due to Ca^{2+} Overload in Hypokalemia

Two studies have reported Ca^{2+} overload in intact, beating hearts perfused with low K^+. One study found that the Ca^{2+}-induced K^+ channel was active in hearts exposed to low K_e^+ (corresponding to clinical hypokalemia) and not in hearts exposed to normal K_e^+ (Chan et al., 2015). This was further supported in another study that observed that hearts perfused with normal extracellular Ca^{2+} levels, in addition to low K_e^+, developed VT/VF, but not if the hearts were perfused with low extracellular Ca^{2+}. In the latter study, both EADs and DADs appeared in rat hearts exposed to moderate hypokalemia, but only the EADs were followed by episodes of sustained ventricular arrhythmias (Pezhouman et al., 2015). Comparably, only EADs were present in rabbit hearts exposed to moderate hypokalemia (Pezhouman et al., 2015), indicating that that EADs and not DADs are the main trigger of VT/VFs in otherwise normal hearts exposed to hypokalemia.

In addition to the reduction of NKAα2 activity as discussed in the previous sections, other mechanisms contribute to hypokalemia-induced Ca^{2+} overload in the system-based mechanism presented by Pezhouzman, Singh, and coworkers (Pezhouman et al., 2015). First, hypokalemia reduces outward repolarizing currents, both K^+ currents and the NKA current. This increases the APD, allowing more Ca^{2+} influx through the L-type Ca^{2+} channels during the plateau phase (Weiss et al., 2017). Second, the initial increase in Ca^{2+} caused by NKA inhibition and reduced inward NCX currents, combined with APD prolongation, initiates a positive feedback loop (Pezhouman et al., 2015). According to this model, the initial increase in Ca^{2+} activates CaMKII, which phosphorylates and activates the late Na^+ current (I_{NaL}) and increases I_{Ca}. Activation of I_{NaL} and I_{Ca} further amplifies the intracellular overload of Na^+ and Ca^{2+}, eventually activating CaMKII, in a detrimental, downward spiral, ultimately leading to afterdepolarizations and ventricular arrhythmias. Mathematical modeling supported this model, and both CaMKII inhibitors and inhibitor of I_{NaL} prevented development of VT/VF in hearts exposed to hypokalemia. Altogether, the collective data suggest that reduced NKAα2 activity initiates cellular Ca^{2+} overload in hypokalemia, which further leads to ventricular arrhythmias through a feed forward spiral where the activation of CaMKII amplifies intracellular Na^+ and Ca^{2+} overload, ultimately leading to EADs (**Figure 2**).

A Possible Role for NKA Inhibition in Other Types of Ventricular Arrhythmias

Some evidence suggests that reduced NKA activity and subsequent development of Ca^{2+} overload and CaMKII

activity could be involved in the arrhythmogenesis in other cardiac diseases besides hypokalemia. Transgenic mice with unphosphorylatable PLM have increased incidence of pacing-induced arrhythmias (Pavlovic et al., 2013b), corresponding to the finding that PLM KO have increased amount of triggered arrhythmias after beta-adrenergic stimulation, as PLM phosphorylation protects against Na^+ and Ca^{2+} overload (Despa et al., 2008). Reduced NKA activity, increased intracellular Na^+, and reduced inward NCX current are the main mechanisms of digitalis-induced arrhythmias (Wasserstrom and Aistrup, 2005). It has also been reported that digitalis increases CaMKII activity with pro-arrhythmogenic downstream effects, which is a further indication that the pathophysiological mechanisms of digitalis- and hypokalemia-induced arrhythmias are similar (Gonano et al., 2011). The same model could also explain the triggered arrhythmias observed in the Ankyrin B syndrome (LQTS4), a rare genetic syndrome characterized by conductance abnormalities and high risk of ventricular tachyarrhythmias (Cunha and Mohler, 2009). NKA expression is mildly reduced in Ankyrin $B^{+/-}$ mice (Mohler et al., 2003, 2005), and the NKA current is lower than in healthy controls (Camors et al., 2012). Further, forward mode NCX is reduced (Camors et al., 2012), leading to increased CaMKII activity (Popescu et al., 2016) and higher frequency of Ca^{2+} waves (Camors et al., 2012) in Ankyrin $B^{+/-}$ mice, suggesting that the mechanisms discussed for hypokalemia also partly could explain induction of ventricular arrhythmias in the Ankyrin B syndrome.

CELLULAR ALTERATIONS IN HEART FAILURE AND HYPOKALEMIA-INDUCED ARRHYTHMIAS

Molecular remodeling (e.g., transcriptional alterations, posttranscriptional regulation, and posttranslation regulation of proteins) and structural remodeling (cardiac hypertrophy and fibrosis) are hallmarks of HF (Fedak et al., 2005; Kehat and Molkentin, 2010). The remodeling is associated with increased risk of arrhythmias, and might potentiate the pro-arrhythmic effects of hypokalemia. However, there is a paucity of mechanistic data on hypokalemia in HF. Given the high prevalence of hypokalemia in HF patients, more studies are needed to clarify how the remodeling-associated HF influences the risk of hypokalemia-induced arrhythmias. Here, we discuss key alterations in HF that we consider relevant for the expected effect of hypokalemia in failing hearts.

Factors That Promote Na^+ and Ca^{2+} Overload in HF

Intracellular Na^+ is increased in both human and animal models of hypertrophy and HF (Pieske et al., 2002; Pogwizd et al., 2003), and one study also found increased Na^+ in the subsarcolemmal space in cells from dogs with cardiac hypertrophy (Verdonck et al., 2003). In theory, the increased Na^+ levels could be due to increased Na^+ influx or less Na^+ extrusion. Although NKA expression and/or activity generally is shown to be reduced in HF, for example by reducing the phosphorylation of PLM (Shamraj et al., 1993; Semb et al., 1998; Bossuyt et al., 2005; Boguslavskyi et al., 2014), one study found no alterations in NKA activity (Despa et al., 2002). Several studies have also reported upregulated I_{NaL} in HF cardiomyocytes (Undrovinas et al., 1999; Moreno and Clancy, 2012), indicating increased Na^+ influx in HF cardiomyocytes. In a study designed to determine the mechanism for increased Na^+ concentration in HF, Despa and coworkers found that increased $[Na^+]_i$ in failing rabbit cardiomyocytes (that more closely resembles human cardiomyocytes than rodents) primarily is due to higher TTX-sensitive Na^+ influx and not due to reduced NKA activity (Despa et al., 2002). Altogether, it seems likely that increased Na^+ influx and possibly reduced Na^+ efflux could contribute to the increased intracellular Na^+ during HF.

Increased intracellular Na^+ in HF leads to increased intracellular Ca^{2+}, by favoring less Ca^{2+} extrusion through forward mode NCX and/or more Ca^{2+} influx through reverse mode NCX. NCX is often upregulated in human (Studer et al., 1994; Reinecke et al., 1996) and experimental (Pogwizd et al., 1999; Sipido et al., 2000) HF, whereas Sarco(Endo)plasmic Reticulum Calcium ATPase 2 (SERCA2) expression and activity are reduced in HF (Lipskaia et al., 2014; Roe et al., 2015). Since intracellular Na^+ is already higher at baseline and the NCX/SERCA2 balance is shifted in HF, a less pronounced NKA inhibition (e.g., by hypokalemia) could cause sufficient rise in Na^+ to cause Ca^{2+} overload and spontaneous SR Ca^{2+} release. In addition, one study found pronounced reduction in the NKAα2 isoform expression and function despite only minor changes in the NKAα1 isoform (Swift et al., 2008). Increased expression and activity of CaMKII are also consistently observed in HF (Hoch et al., 1999; Kirchhefer et al., 1999; Zhang et al., 2003), and contribute to increased intracellular Na^+ and Ca^{2+} by increasing I_{Na-L} (Anderson et al., 2011) and Ca^{2+} leak through RyRs (Ai et al., 2005). On the basis of these observations, we speculate that HF patients are "sensitized" and tolerate less changes in serum-$[K^+]$ compared to patients without cardiac diseases. This might help explain why HF patients with serum-$[K^+] < 4$ mM have increased risk of SCD and death (Macdonald and Struthers, 2004; Bowling et al., 2010), compared to the conventional cut-off at 3.5 mM (Unwin et al., 2011).

Factors That Promote Afterdepolarizations in HF

Spontaneous Ca^{2+} waves induce DADs by activating an inward current mainly consisting of I_{NCX} (Clusin, 2003). Since NCX typically is upregulated in HF, a given amount of spontaneously released Ca^{2+} generates more depolarizing inward current, reducing the threshold for DADs (Pogwizd and Bers, 2004). I_{K1} acts as a "safety valve" and counterbalances depolarizing inward currents caused by spontaneous Ca^{2+} release during the resting phase of the AP. I_{K1} is downregulated in HF (Fauconnier

et al., 2005; Bers, 2006), thus increasing the likelihood that a spontaneous AP occurs through generation of EADs and/or DADs. In line with the typical observation of prolonged APD and reduced repolarization reserve (Wang and Hill, 2010), in addition to the earlier described factors that possibly contribute to Na^+ and Ca^{2+} overload in HF, it is likely that there is a reduced threshold for hypokalemia-induced afterdepolarizations in HF.

FUTURE TARGETED THERAPIES FOR HYPOKALEMIA-INDUCED TRIGGERED ARRHYTHMIAS

No treatment that directly targets the underlying mechanism for hypokalemia-induced arrhythmias is currently available. The current treatment of hypokalemia in itself is potassium replacement (Cohn et al., 2000), and in patients with TDP, magnesium sulfate injection is used to prevent EADs and DADs through an unknown mechanism (Fazekas et al., 1993). TDP can also be treated with cardiac pacing or isoproterenol injection to shorten the APD (Banai and Tzivoni, 1993).

Ideally, new treatments against hypokalemia-induced arrhythmias should aim at (1) preventing EADs/DADs, (2) shortening the APD, and (3) directly targeting the underlying mechanism. On the basis of the model for hypokalemia-induced ventricular arrhythmias in **Figure 2**, we suggest CaMKII inhibition, NKA activation, and in particular NKAα2 activation, to be further investigated as future antiarrhythmic strategies. CaMKII inhibition prevents hypokalemia-induced EADs (Pezhouman et al., 2015), Ca^{2+} overload, and DADs in catecholaminergic polymorphic ventricular tachycardia (CPVT) (Di Pasquale et al., 2013) and in HF (Ai et al., 2005; Sag et al., 2009), in addition to hypokalemia-induced VT/VF (Pezhouman et al., 2015). CaMKII inhibition also shortens APD (Li et al., 2006; Bourgonje et al., 2012), although this effect might be species-dependent (Wagner et al., 2009). We are currently unaware of any drug that specifically activates the NKA. Theoretically, this could prove to be an effective antiarrhythmic strategy, as NKA inhibition causes Ca^{2+} overload, afterdepolarizations, and ventricular arrhythmias (Faggioni and Knollmann, 2015).

HF is also characterized by APD prolongation (Wang and Hill, 2010) and increased risk of afterdepolarizations (Pogwizd and Bers, 2004; Weiss et al., 2010), and we speculate that CaMKII inhibitors and NKA activators might be future antiarrhythmic options in HF even in the absence of hypokalemia.

AUTHOR CONTRIBUTIONS

Both authors listed have made a substantial, direct and intellectual contribution to the work, and approved it for publication.

ACKNOWLEDGMENTS

We are grateful to Debbie Maizels (www.scientific-art.com) for the artwork included in this review and to Dr. Emma L. Robinson for valuable inputs.

REFERENCES

(1982). Multiple risk factor intervention trial. Risk factor changes and mortality results. The Multiple Risk Factor Intervention Trial Research Group. *JAMA* 248, 1465–1477.

(1984). The effect of antihypertensive drug treatment on mortality in the presence of resting electrocardiographic abnormalities at baseline: the HDFP experience. The hypertension detection and Folow-up Program Cooperative Research Group. *Circulation* 70, 996–1003.

Ahmed, A., Zannad, F., Love, T. E., Tallaj, J., Gheorghiade, M., Ekundayo, O. J., et al. (2007). A propensity-matched study of the association of low serum potassium levels and mortality in chronic heart failure. *Eur. Heart J.* 28, 1334–1343. doi: 10.1093/eurheartj/ehm091

Ai, X., Curran, J. W., Shannon, T. R., Bers, D. M., and Pogwizd, S. M. (2005). Ca^{2+}/calmodulin-dependent protein kinase modulates cardiac ryanodine receptor phosphorylation and sarcoplasmic reticulum Ca^{2+} leak in heart failure. *Circ. Res.* 97, 1314–1322. doi: 10.1161/01.RES.0000194329.41863.89

Aldahl, M., Jensen, A. C., Davidsen, L., Eriksen, M. A., Moller Hansen, S., Nielsen, B. J., et al. (2017). Associations of serum potassium levels with mortality in chronic heart failure patients. *Eur. Heart J.* 38, 2890–2896. doi: 10.1093/eurheartj/ehx460

Anderson, M. E., Brown, J. H., and Bers, D. M. (2011). CaMKII in myocardial hypertrophy and heart failure. *J. Mol. Cell. Cardiol.* 51, 468–473. doi: 10.1016/j.yjmcc.2011.01.012

Antzelevitch, C., and Burashnikov, A. (2011). Overview of basic mechanisms of cardiac arrhythmia. *Card. Electrophysiol. Clin.* 3, 23–45. doi: 10.1016/j.ccep.2010.10.012

Arnold, J. M. O., Liu, P., Howlett, J., Ignaszewski, A., Leblanc, M. H., Kaan, A., et al. (2013). Ten year survival by NYHA functional class in heart failure outpatients referred to specialized multidisciplinary heart failure clinics 1999 to 2011. *Eur. Heart J.* 34, 291–291. doi: 10.1093/eurheartj/eht308.P1505

Aronsen, J. M., Skogestad, J., Lewalle, A., Louch, W. E., Hougen, K., Stokke, M. K., et al. (2015). Hypokalaemia induces Ca^{2+} overload and Ca^{2+} waves in ventricular myocytes by reducing Na^+,K^+-ATPase α_2 activity. *J. Physiol.* 593, 1509–1521. doi: 10.1113/jphysiol.2014.279893

Aronsen, J. M., Swift, F., and Sejersted, O. M. (2013). Cardiac sodium transport and excitation-contraction coupling. *J. Mol. Cell. Cardiol.* 61, 11–19. doi: 10.1016/j.yjmcc.2013.06.003

Azuma, K. K., Hensley, C. B., Putnam, D. S., and McDonough, A. A. (1991). Hypokalemia decreases Na^+-K^+-ATPase α_2- but not alpha 1-isoform abundance in heart, muscle, and brain. *Am. J. Physiol.* 260(5 Pt 1), C958–C964.

Banai, S., and Tzivoni, D. (1993). Drug therapy for torsade de pointes. *J. Cardiovasc. Electrophysiol.* 4, 206–210. doi: 10.1111/j.1540-8167.1993.tb01224.x

Berry, R. G., Despa, S., Fuller, W., Bers, D. M., and Shattock, M. J. (2007). Differential distribution and regulation of mouse cardiac Na^+/K^+-ATPase α_1 and α_2 subunits in T-tubule and surface sarcolemmal membranes. *Cardiovasc. Res.* 73, 92–100. doi: 10.1016/j.cardiores.2006.11.006

Bers, D. M. (2001). *Excitation-Contraction Coupling and Cardiac Contractile Force*, 2nd Edn. Dordrecht; Boston, MA: Kluwer Academic Publishers.

Bers, D. M. (2002). Cardiac excitation-contraction coupling. *Nature* 415, 198–205. doi: 10.1038/415198a

Bers, D. M. (2006). Altered cardiac myocyte Ca regulation in heart failure. *Physiology (Bethesda)* 21, 380–387. doi: 10.1152/physiol.00019.2006

Bers, D. M., and Despa, S. (2009). Na^+ transport in cardiac myocytes; Implications for excitation-contraction coupling. *IUBMB Life* 61, 215–221. doi: 10.1002/iub.163

Boguslavskyi, A., Pavlovic, D., Aughton, K., Clark, J. E., Howie, J., Fuller, W., et al. (2014). Cardiac hypertrophy in mice expressing unphosphorylatable phospholemman. *Cardiovasc. Res.* 104, 72–82. doi: 10.1093/cvr/cvu182

Bossuyt, J., Ai, X., Moorman, J. R., Pogwizd, S. M., and Bers, D. M. (2005). Expression and phosphorylation of the na-pump regulatory subunit phospholemman in heart failure. *Circ. Res.* 97, 558–565. doi: 10.1161/01.RES.0000181172.27931.c3

Bouchard, R., Clark, R. B., Juhasz, A. E., and Giles, W. R. (2004). Changes in extracellular K^+ concentration modulate contractility of rat and rabbit cardiac myocytes via the inward rectifier K^+ current IK1. *J. Physiol.* 556(Pt *3*), 773–790. doi: 10.1113/jphysiol.2003.058248

Bourgonje, V. J., Schoenmakers, M., Beekman, J. D., van der Nagel, R., Houtman, M. J., Miedema, L. F., et al. (2012). Relevance of calmodulin/CaMKII activation for arrhythmogenesis in the AV block dog. *Heart Rhythm.* 9, 1875–1883. doi: 10.1016/j.hrthm.2012.07.023

Bowling, C. B., Pitt, B., Ahmed, M. I., Aban, I. B., Sanders, P. W., Mujib, M., et al. (2010). Hypokalemia and outcomes in patients with chronic heart failure and chronic kidney disease: findings from propensity-matched studies. *Circ. Heart Fail.* 3, 253–260. doi: 10.1161/CIRCHEARTFAILURE.109.899526

Camors, E., Mohler, P. J., Bers, D. M., and Despa, S. (2012). Ankyrin-B reduction enhances Ca spark-mediated SR Ca release promoting cardiac myocyte arrhythmic activity. *J. Mol. Cell. Cardiol.* 52, 1240–1248. doi: 10.1016/j.yjmcc.2012.02.010

Chah, Q. T., Braly, G., Bouzouita, K., and Faucon, G. (1982). Effects of hypokalemia on the various parts of the conduction system of the dog heart *in situ*. Naunyn Schmiedebergs. *Arch. Pharmacol.* 319, 178–183. doi: 10.1007/BF00503934

Chan, Y. H., Tsai, W. C., Ko, J. S., Yin, D., Chang, P. C., Rubart, M., et al. Chen, P. S. (2015). Small-conductance calcium-activated potassium current is activated during hypokalemia and masks short-term cardiac memory induced by ventricular pacing. *Circulation* 132, 1377–1386. doi: 10.1161/CIRCULATIONAHA.114.015125

Cleland, J. G., Dargie, H. J., and Ford, I. (1987). Mortality in heart failure: clinical variables of prognostic value. *Br. Heart J.* 58, 572–582. doi: 10.1136/hrt.58.6.572

Clusin, W. T. (2003). Calcium and cardiac arrhythmias: DADs, EADs, and alternans. *Crit. Rev. Clin. Lab. Sci.* 40, 337–375. doi: 10.1080/713609356

Cohn, J. N., Kowey, P. R., Whelton, P. K., and Prisant, L. M. (2000). New guidelines for potassium replacement in clinical practice: a contemporary review by the National Council on Potassium in Clinical Practice. *Arch. Intern. Med.* 160, 2429–2436. doi: 10.1001/archinte.160.16.2429

Collins, A. J., Pitt, B., Reaven, N., Funk, S., McGaughey, K., Wilson, D., et al. (2017). Association of serum potassium with all-cause mortality in patients with and without heart failure, chronic kidney disease, and/or diabetes. *Am. J. Nephrol.* 46, 213–221. doi: 10.1159/000479802

Colombo, M. G., Kirchberger, I., Amann, U., Dinser, L., and Meisinger, C. (2018). Association of serum potassium concentration with mortality and ventricular arrhythmias in patients with acute myocardial infarction: a systematic review and meta-analysis. *Eur. J. Prev. Cardiol.* 25, 576–595. doi: 10.1177/2047487318759694

Cooper, H. A., Dries, D. L., Davis, C. E., Shen, Y. L., and Domanski, M. J. (1999). Diuretics and risk of arrhythmic death in patients with left ventricular dysfunction. *Circulation* 100, 1311–1315. doi: 10.1161/01.CIR.100.12.1311

Cunha, S. R., and Mohler, P. J. (2009). Ankyrin protein networks in membrane formation and stabilization. *J. Cell. Mol. Med.* 13, 4364–4376. doi: 10.1111/j.1582-4934.2009.00943.x

Despa, S., and Bers, D. M. (2007). Functional analysis of Na^+/K^+-ATPase isoform distribution in rat ventricular myocytes. *Am. J. Physiol. Cell Physiol.* 293, C321–C327. doi: 10.1152/ajpcell.00597.2006

Despa, S., and Bers, D. M. (2013). Na^+ transport in the normal and failing heart-remember the balance. *J. Mol. Cell. Cardiol.* 61, 2–10. doi: 10.1016/j.yjmcc.2013.04.011

Despa, S., Bossuyt, J., Han, F., Ginsburg, K. S., Jia, L. G., Kutchai, H., et al. (2005). Phospholemman-phosphorylation mediates the beta-adrenergic effects on Na/K pump function in cardiac myocytes. *Circ. Res.* 97, 252–259. doi: 10.1161/01.RES.0000176532.97731.e5

Despa, S., Islam, M. A., Weber, C. R., Pogwizd, S. M., and Bers, D. M. (2002). Intracellular Na^+ concentration is elevated in heart failure but Na/K pump function is unchanged. *Circulation* 105, 2543–2548. doi: 10.1161/01.CIR.0000016701.85760.97

Despa, S., Lingrel, J. B., and Bers, D. M. (2012). Na^+/K^+-ATPase α_2-isoform preferentially modulates Ca^{2+} transients and sarcoplasmic reticulum Ca^{2+} release in cardiac myocytes. *Cardiovasc. Res.* 95, 480–486. doi: 10.1093/cvr/cvs213

Despa, S., Tucker, A. L., and Bers, D. M. (2008). Phospholemman-mediated activation of Na/K-ATPase limits [Na]i and inotropic state during beta-adrenergic stimulation in mouse ventricular myocytes. *Circulation* 117, 1849–1855. doi: 10.1161/CIRCULATIONAHA.107.754051

Di Pasquale, E., Lodola, F., Miragoli, M., Denegri, M., Avelino-Cruz, J. E., Buonocore, M., et al. (2013). CaMKII inhibition rectifies arrhythmic phenotype in a patient-specific model of catecholaminergic polymorphic ventricular tachycardia. *Cell Death Dis.* 4:e843. doi: 10.1038/cddis.2013.369

Ebinger, M. W., Krishnan, S., and Schuger, C. D. (2005). Mechanisms of ventricular arrhythmias in heart failure. *Curr. Heart Fail. Rep.* 2, 111–117. doi: 10.1007/s11897-005-0018-y

Eisner, D. A., and Lederer, W. J. (1979). The role of the sodium pump in the effects of potassium-depleted solutions on mammalian cardiac muscle. *J. Physiol.* 294, 279–301.

Faggioni, M., and Knollmann, B. C. (2015). Arrhythmia protection in hypokalemia: a novel role of Ca^{2+}-Activated K^+ currents in the ventricle. *Circulation* 132, 1371–1373. doi: 10.1161/CIRCULATIONAHA.115.018874

Fauconnier, J., Lacampagne, A., Rauzier, J. M., Vassort, G., and Richard, S. (2005). Ca^{2+}-dependent reduction of IK1 in rat ventricular cells: a novel paradigm for arrhythmia in heart failure? *Cardiovasc. Res.* 68, 204–212. doi: 10.1016/j.cardiores.2005.05.024

Fazekas, T., Scherlag, B. J., Vos, M., Wellens, H. J., and Lazzara, R. (1993). Magnesium and the heart: antiarrhythmic therapy with magnesium. *Clin. Cardiol.* 16, 768–774. doi: 10.1002/clc.4960161105

Fedak, P. W., Verma, S., Weisel, R. D., and Li, R. K. (2005). Cardiac remodeling and failure: from molecules to man (Part I). *Cardiovasc. Pathol.* 14, 1–11. doi: 10.1016/j.carpath.2004.12.002

Figtree, G. A., Liu, C. C., Bibert, S., Hamilton, E. J., Garcia, A., White, C. N., et al. (2009). Reversible oxidative modification: a key mechanism of Na^+-K^+ pump regulation. *Circ. Res.* 105, 185–193. doi: 10.1161/CIRCRESAHA.109.199547

Glitsch, H. G. (2001). Electrophysiology of the sodium-potassium-ATPase in cardiac cells. *Physiol. Rev.* 81, 1791–1826. doi: 10.1152/physrev.2001.81.4.1791

Gonano, L. A., Sepulveda, M., Rico, Y., Kaetzel, M., Valverde, C. A., Dedman, J., et al. (2011). Calcium-calmodulin kinase II mediates digitalis-induced arrhythmias. *Circ. Arrhythm. Electrophysiol.* 4, 947–957. doi: 10.1161/CIRCEP.111.964908

Goyal, A., Spertus, J. A., Gosch, K., Venkitachalam, L., Jones, P. G., Van den Berghe, G., et al. (2012). Serum potassium levels and mortality in acute myocardial infarction. *JAMA* 307, 157–164. doi: 10.1001/jama.2011.1967

Guo, H., Lee, J. D., Ueda, T., Wang, J., Lu, D., He, H., et al. (2005). Different clinical features, biochemical profiles, echocardiographic and elctrocardiographic findings in older and younger patients with idiopathic dilated cardiomyopathy. *Acta Cardiol.* 60, 27–31. doi: 10.2143/AC.60.1.2005045

Han, F., Tucker, A. L., Lingrel, J. B., Despa, S., and Bers, D. M. (2009). Extracellular potassium dependence of the Na^+-K^+-ATPase in cardiac myocytes: isoform specificity and effect of phospholemman. *Am. J. Physiol,. Cell Physiol.* 297, C699–C705. doi: 10.1152/ajpcell.00063.2009

Hoch, B., Meyer, R., Hetzer, R., Krause, E. G., and Karczewski, P. (1999). Identification and expression of delta-isoforms of the multifunctional Ca2+/calmodulin-dependent protein kinase in failing and nonfailing human myocardium. *Circ. Res.* 84, 713–721. doi: 10.1161/01.RES.84.6.713

Hoppe, L. K., Muhlack, D. C., Koenig, W., Carr, P. R., Brenner, H., and Schottker, B. (2018). Association of abnormal serum potassium levels with arrhythmias and cardiovascular mortality: a systematic review and meta-analysis of observational studies. *Cardiovasc. Drugs Ther.* 32, 197–212. doi: 10.1007/s10557-018-6783-0

James, P. F., Grupp, I. L., Grupp, G., Woo, A. L., Askew, G. R., Croyle, M. L., et al. (1999). Identification of a specific role for the Na,K-ATPase alpha 2 isoform as a regulator of calcium in the heart. *Mol. Cell* 3, 555–563. doi: 10.1016/S1097-2765(00)80349-4

Jin, H., Lyon, A. R., and Akar, F. G. (2008). Arrhythmia mechanisms in the failing heart. *Pacing Clin. Electrophysiol.* 31, 1048–1056. doi: 10.1111/j.1540-8159.2008.01134.x

Kaplan, N. M. (1984). Our appropriate concern about hypokalemia. *Am. J. Med.* 77, 1–4. doi: 10.1016/0002-9343(84)90427-3

Kehat, I., and Molkentin, J. D. (2010). Molecular pathways underlying cardiac remodeling during pathophysiological stimulation. *Circulation* 122, 2727–2735. doi: 10.1161/CIRCULATIONAHA.110.942268

Khafaga, M., Bossuyt, J., Mamikonian, L., Li, J. C., Lee, L. L., Yarov-Yarovoy, V., et al. (2012). Na(+)/K(+)-ATPase E960 and phospholemman F28 are critical for their functional interaction. *Proc. Natl. Acad. Sci. U.S.A.* 109, 20756–20761. doi: 10.1073/pnas.1207866109

Killeen, M. J., Gurung, I. S., Thomas, G., Stokoe, K. S., Grace, A. A., and Huang, C. L. (2007). Separation of early afterdepolarizations from arrhythmogenic substrate in the isolated perfused hypokalaemic murine heart through modifiers of calcium homeostasis. *Acta Physiol. (Oxf).* 191, 43–58. doi: 10.1111/j.1748-1716.2007.01715.x

Kirchhefer, U., Schmitz, W., Scholz, H., and Neumann, J. (1999). Activity of cAMP-dependent protein kinase and Ca^{2+}/calmodulin-dependent protein kinase in failing and nonfailing human hearts. *Cardiovasc. Res.* 42, 254–261. doi: 10.1016/S0008-6363(98)00296-X

Kjeldsen, K. (2010). Hypokalemia and sudden cardiac death. *Exp. Clin. Cardiol.* 15, e96–99.

Leier, C. V., Dei Cas, L., and Metra, M. (1994). Clinical relevance and management of the major electrolyte abnormalities in congestive heart failure: hyponatremia, hypokalemia, and hypomagnesemia. *Am. Heart J.* 128, 564–574. doi: 10.1016/0002-8703(94)90633-5

Li, J., Marionneau, C., Zhang, R., Shah, V., Hell, J. W., Nerbonne, J. M., et al. (2006). Calmodulin kinase II inhibition shortens action potential duration by upregulation of K^+ currents. *Circ. Res.* 99, 1092–1099. doi: 10.1161/01.RES.0000249369.71709.5c

Lindinger, M. I. (1995). Potassium regulation during exercise and recovery in humans: implications for skeletal and cardiac muscle. *J. Mol. Cell. Cardiol.* 27, 1011–1022. doi: 10.1016/0022-2828(95)90070-5

Lines, G. T., Sande, J. B., Louch, W. E., Mork, H. K., Grottum, P., and Sejersted, O. M. (2006). Contribution of the Na^+/Ca^{2+} exchanger to rapid Ca^{2+} release in cardiomyocytes. *Biophys. J.* 91, 779–792. doi: 10.1529/biophysj.105.072447

Lingrel, J. B., and Kuntzweiler, T. (1994). Na^+,K^+-ATPase. *J. Biol. Chem.* 269, 19659–19662.

Lipskaia, L., Keuylian, Z., Blirando, K., Mougenot, N., Jacquet, A., Rouxel, C., et al. (2014). Expression of sarco (endo) plasmic reticulum calcium ATPase (SERCA) system in normal mouse cardiovascular tissues, heart failure and atherosclerosis. *Biochim. Biophys. Acta* 1843, 2705–2718. doi: 10.1016/j.bbamcr.2014.08.002

Lucchesi, P. A., and Sweadner, K. J. (1991). Postnatal changes in Na,K-ATPase isoform expression in rat cardiac ventricle. Conservation of biphasic ouabain affinity. *J. Biol. Chem.* 266, 9327–9331.

Macdonald, J. E., and Struthers, A. D. (2004). What is the optimal serum potassium level in cardiovascular patients? *J. Am. Coll. Cardiol.* 43, 155–161. doi: 10.1016/j.jacc.2003.06.021

McDonough, A. A., Zhang, Y., Shin, V., and Frank, J. S. (1996). Subcellular distribution of sodium pump isoform subunits in mammalian cardiac myocytes. *Am. J. Physiol.* 270(4 Pt 1), C1221–C1227.

Medbo, J. I., and Sejersted, O. M. (1990). Plasma potassium changes with high intensity exercise. *J. Physiol.* 421, 105–122.

Mohler, P. J., Davis, J. Q., and Bennett, V. (2005). Ankyrin-B coordinates the Na/K ATPase, Na/Ca exchanger, and InsP3 receptor in a cardiac T-tubule/SR microdomain. *PLoS Biol.* 3:e423. doi: 10.1371/journal.pbio.0030423

Mohler, P. J., Schott, J. J., Gramolini, A. O., Dilly, K. W., Guatimosim, S., duBell, W. H., et al. (2003). Ankyrin-B mutation causes type 4 long-QT cardiac arrhythmia and sudden cardiac death. *Nature* 421, 634–639. doi: 10.1038/nature01335

Moreno, J. D., and Clancy, C. E. (2012). Pathophysiology of the cardiac late Na current and its potential as a drug target. *J. Mol. Cell. Cardiol.* 52, 608–619. doi: 10.1016/j.yjmcc.2011.12.003

Motloch, L. J., Ishikawa, K., Xie, C., Hu, J., Aguero, J., Fish, K. M., et al. (2017). Increased afterload following myocardial infarction promotes conduction-dependent arrhythmias that are unmasked by hypokalemia. *JACC Basic Trans. Sci.* 2, 258–269. doi: 10.1016/j.jacbts.2017.02.002

Nolan, J., Batin, P. D., Andrews, R., Lindsay, S. J., Brooksby, P., Mullen, M., et al. (1998). Prospective study of heart rate variability and mortality in chronic heart failure: results of the United Kingdom heart failure evaluation and assessment of risk trial (UK-heart). *Circulation* 98, 1510–1516. doi: 10.1161/01.CIR.98.15.1510

Nordrehaug, J. E., Johannessen, K. A., and von der Lippe, G. (1985). Serum potassium concentration as a risk factor of ventricular arrhythmias early in acute myocardial infarction. *Circulation* 71, 645–649. doi: 10.1161/01.CIR.71.4.645

Nunez, J., Bayes-Genis, A., Zannad, F., Rossignol, P., Nunez, E., Bodi, V., et al. (2018). Long-term potassium monitoring and dynamics in heart failure and risk of mortality. *Circulation* 137, 1320–1330. doi: 10.1161/CIRCULATIONAHA.117.030576

Officers, A., Coordinators for the, A. C. R. G. T. A., and Lipid-Lowering Treatment to Prevent Heart Attack, T. (2002). Major outcomes in high-risk hypertensive patients randomized to angiotensin-converting enzyme inhibitor or calcium channel blocker vs. diuretic: the Antihypertensive and Lipid-Lowering Treatment to Prevent Heart Attack Trial (ALLHAT). *JAMA* 288, 2981–2997. doi: 10.1001/jama.288.23.2981

Osadchii, O. E. (2010). Mechanisms of hypokalemia-induced ventricular arrhythmogenicity. *Fundam. Clin. Pharmacol.* 24, 547–559. doi: 10.1111/j.1472-8206.2010.00835.x

Packer, M. (1990). Potential role of potassium as a determinant of morbidity and mortality in patients with systemic hypertension and congestive heart-failure. *Am. J. Cardiol.* 65, E45–E51. doi: 10.1016/0002-9149(90)90251-U

Papademetriou, V. (2006). Diuretics, hypokalemia, and cardiac arrhythmia: a 20-year controversy. *J. Clin. Hypertens. (Greenwich)* 8, 86–92. doi: 10.1111/j.1524-6175.2005.04722.x

Pavlovic, D., Fuller, W., and Shattock, M. J. (2007). The intracellular region of FXYD1 is sufficient to regulate cardiac Na/K ATPase. *FASEB J.* 21, 1539–1546. doi: 10.1096/fj.06-7269com

Pavlovic, D., Fuller, W., and Shattock, M. J. (2013a). Novel regulation of cardiac Na pump via phospholemman. *J. Mol. Cell. Cardiol.* 61:83–93. doi: 10.1016/j.yjmcc.2013.05.002

Pavlovic, D., Hall, A. R., Kennington, E. J., Aughton, K., Boguslavskyi, A., Fuller, W., et al. (2013b). Nitric oxide regulates cardiac intracellular Na^+ and Ca^{2+} by modulating Na/K ATPase via PKCepsilon and phospholemman-dependent mechanism. *J. Mol. Cell. Cardiol.* 61, 164–171. doi: 10.1016/j.yjmcc.2013.04.013

Pezhouman, A., Singh, N., Song, Z., Nivala, M., Eskandari, A., Cao, H., et al. (2015). Molecular basis of hypokalemia-induced ventricular fibrillation. *Circulation* 132, 1528–1537. doi: 10.1161/CIRCULATIONAHA.115.016217

Pieske, B., Maier, L. S., Piacentino, V. III., Weisser, J., Hasenfuss, G., and Houser, S. (2002). Rate dependence of [Na+]i and contractility in nonfailing and failing human myocardium. *Circulation* 106, 447–453. doi: 10.1161/01.CIR.0000023042.50192.F4

Poelzing, S., and Veeraraghavan, R. (2007). Heterogeneous ventricular chamber response to hypokalemia and inward rectifier potassium channel blockade underlies bifurcated T wave in guinea pig. *Am. J. Physiol. Heart Circ. Physiol.* 292, H3043–H3051. doi: 10.1152/ajpheart.01312.2006

Pogwizd, S. M., and Bers, D. M. (2004). Cellular basis of triggered arrhythmias in heart failure. *Trends Cardiovasc. Med.* 14, 61–66. doi: 10.1016/j.tcm.2003.12.002

Pogwizd, S. M., Hoyt, R. H., Saffitz, J. E., Corr, P. B., Cox, J. L., and Cain, M. E. (1992). Reentrant and focal mechanisms underlying ventricular tachycardia in the human heart. *Circulation* 86, 1872–1887. doi: 10.1161/01.CIR.86.6.1872

Pogwizd, S. M., Qi, M., Yuan, W., Samarel, A. M., and Bers, D. M. (1999). Upregulation of Na^+/Ca^{2+} exchanger expression and function in an arrhythmogenic rabbit model of heart failure. *Circ. Res.* 85, 1009–1019. doi: 10.1161/01.RES.85.11.1009

Pogwizd, S. M., Sipido, K. R., Verdonck, F., and Bers, D. M. (2003). Intracellular Na in animal models of hypertrophy and heart failure: contractile function and arrhythmogenesis. *Cardiovasc. Res.* 57, 887–896. doi: 10.1016/S0008-6363(02)00735-6

Popescu, I., Galice, S., Mohler, P. J., and Despa, S. (2016). Elevated local [Ca^{2+}] and CaMKII promote spontaneous Ca^{2+} release in ankyrin-B-deficient hearts. *Cardiovasc. Res.* 111, 287–294. doi: 10.1093/cvr/cvw093

Poulsen, H., Morth, P., Egebjerg, J., and Nissen, P. (2010). Phosphorylation of the Na^+,K^+-ATPase and the H^+,K^+-ATPase. *FEBS Lett.* 584, 2589–2595. doi: 10.1016/j.febslet.2010.04.035

Reinecke, H., Studer, R., Vetter, R., Holtz, J., and Drexler, H. (1996). Cardiac Na^+/Ca^{2+} exchange activity in patients with end-stage heart failure. *Cardiovasc. Res.* 31, 48–54. doi: 10.1016/S0008-6363(95)00176-X

Roe, A. T., Frisk, M., and Louch, W. E. (2015). Targeting cardiomyocyte Ca^{2+} homeostasis in heart failure. *Curr. Pharm. Des.* 21, 431–448. doi: 10.2174/1381612821041412041241 29

Sag, C. M., Wadsack, D. P., Khabbazzadeh, S., Abesser, M., Grefe, C., Neumann, K., et al. (2009). Calcium/calmodulin-dependent protein kinase II contributes to cardiac arrhythmogenesis in heart failure. *Circ. Heart Fail.* 2, 664–675. doi: 10.1161/CIRCHEARTFAILURE.109.865279

Sejersted, O. M., and Sjogaard, G. (2000). Dynamics and consequences of potassium shifts in skeletal muscle and heart during exercise. *Physiol. Rev.* 80, 1411–1481. doi: 10.1152/physrev.2000.80.4.1411

Semb, S. O., Lunde, P. K., Holt, E., Tonnessen, T., Christensen, G., and Sejersted, O. M. (1998). Reduced myocardial Na^+, K^+-pump capacity in congestive heart failure following myocardial infarction in rats. *J. Mol. Cell. Cardiol.* 30, 1311–1328. doi: 10.1006/jmcc.1998.0696

Shamraj, O. I., Grupp, I. L., Grupp, G., Melvin, D., Gradoux, N., Kremers, W., et al. (1993). Characterisation of Na/K-ATPase, its isoforms, and the inotropic response to ouabain in isolated failing human hearts. *Cardiovasc. Res.* 27, 2229–2237. doi: 10.1093/cvr/27.12.2229

Siegel, D., Hulley, S. B., Black, D. M., Cheitlin, M. D., Sebastian, A., Seeley, D. G., et al. (1992). Diuretics, serum and intracellular electrolyte levels, and ventricular arrhythmias in hypertensive men. *JAMA* 267, 1083–1089. doi: 10.1001/jama.1992.03480080053026

Singh, S. N., Carson, P. E., and Fisher, S. G. (1997). Nonsustained ventricular tachycardia in severe heart failure. *Circulation* 96, 3794–3795.

Sipido, K. R., Volders, P. G., de Groot, S. H., Verdonck, F., Van de Werf, F., Wellens, H. J., et al. (2000). Enhanced Ca^{2+} release and Na/Ca exchange activity in hypertrophied canine ventricular myocytes: potential link between contractile adaptation and arrhythmogenesis. *Circulation* 102, 2137–2144. doi: 10.1161/01.CIR.102.17.2137

Siscovick, D. S., Raghunathan, T. E., Psaty, B. M., Koepsell, T. D., Wicklund, K. G., Lin, X., et al. (1994). Diuretic therapy for hypertension and the risk of primary cardiac arrest. *N. Engl. J. Med.* 330, 1852–1857. doi: 10.1056/NEJM199406303302603

Siscovick, D. S., Weiss, N. S., Fletcher, R. H., and Lasky, T. (1984). The incidence of primary cardiac arrest during vigorous exercise. *N. Engl. J. Med.* 311, 874–877. doi: 10.1056/NEJM198410043111402

Smeets, J. L., Allessie, M. A., Lammers, W. J., Bonke, F. I., and Hollen, J. (1986). The wavelength of the cardiac impulse and reentrant arrhythmias in isolated rabbit atrium. The role of heart rate, autonomic transmitters, temperature, and potassium. *Circ Res* 58, 96–108. doi: 10.1161/01.RES.58.1.96

Stanley, C. M., Gagnon, D. G., Bernal, A., Meyer, D. J., Rosenthal, J. J., and Artigas, P. (2015). Importance of the voltage dependence of cardiac Na/K ATPase isozymes. *Biophys. J.* 109, 1852–1862. doi: 10.1016/j.bpj.2015.09.015

Steiness, E., and Olesen, K. H. (1976). Cardiac arrhythmias induced by hypokalaemia and potassium loss during maintenance digoxin therapy. *Br. Heart J.* 38, 167–172. doi: 10.1136/hrt.38.2.167

Studer, R., Reinecke, H., Bilger, J., Eschenhagen, T., Bohm, M., Hasenfuss, G., et al. (1994). Gene expression of the cardiac Na^+-Ca^{2+} exchanger in end-stage human heart failure. *Circ. Res.* 75, 443–453. doi: 10.1161/01.RES.75.3.443

Sweadner, K. J., Herrera, V. L., Amato, S., Moellmann, A., Gibbons, D. K., and Repke, K. R. (1994). Immunologic identification of Na^+,K^+-ATPase isoforms in myocardium. Isoform change in deoxycorticosterone acetate-salt hypertension. *Circ. Res.* 74, 669–678. doi: 10.1161/01.RES.74.4.669

Swift, F., Birkeland, J. A., Tovsrud, N., Enger, U. H., Aronsen, J. M., Louch, W. E., et al. (2008). Altered Na^+/Ca^{2+}-exchanger activity due to downregulation of Na^+/K^+-ATPase α_2-isoform in heart failure. *Cardiovasc. Res.* 78, 71–78. doi: 10.1093/cvr/cvn013

Swift, F., Tovsrud, N., Enger, U. H., Sjaastad, I., and Sejersted, O. M. (2007). The Na^+/K^+-ATPase α_2-isoform regulates cardiac contractility in rat cardiomyocytes. *Cardiovasc. Res.* 75, 109–117. doi: 10.1016/j.cardiores.2007.03.017

Swift, F., Tovsrud, N., Sjaastad, I., Sejersted, O. M., Niggli, E., and Egger, M. (2010). Functional coupling of α_2-isoform Na^+/K^+-ATPase and Ca^{2+} extrusion through the Na^+/Ca^{2+}-exchanger in cardiomyocytes. *Cell Calcium.* 48, 54–60. doi: 10.1016/j.ceca.2010.06.006

Teerlink, J. R., Jalaluddin, M., Anderson, S., Kukin, M. L., Eichhorn, E. J., Francis, G., et al. (2000). Ambulatory ventricular arrhythmias in patients with heart failure do not specifically predict an increased risk of sudden death. PROMISE (Prospective Randomized Milrinone Survival Evaluation) Investigators. *Circulation* 101, 40–46. doi: 10.1161/01.CIR.101.1.40

Thompson, P. D., Franklin, B. A., Balady, G. J., Blair, S. N., Corrado, D., Estes, N. A. III., et al. (2007). Exercise and acute cardiovascular events placing the risks into perspective: a scientific statement from the American Heart Association Council on Nutrition, Physical Activity, and Metabolism and the Council on Clinical Cardiology. *Circulation* 115, 2358–2368. doi: 10.1161/CIRCULATIONAHA.107.181485

Tomaselli, G. F., and Zipes, D. P. (2004). What causes sudden death in heart failure? *Circ. Res.* 95, 754–763. doi: 10.1161/01.RES.0000145047.14691.db

Undrovinas, A. I., Maltsev, V. A., and Sabbah, H. N. (1999). Repolarization abnormalities in cardiomyocytes of dogs with chronic heart failure: role of sustained inward current. *Cell. Mol. Life Sci.* 55, 494–505. doi: 10.1007/s000180050306

Unwin, R. J., Luft, F. C., and Shirley, D. G. (2011). Pathophysiology and management of hypokalemia: a clinical perspective. *Nat. Rev. Nephrol.* 7, 75–84. doi: 10.1038/nrneph.2010.175

Urso, C., Brucculeri, S., and Caimi, G. (2015). Acid-base and electrolyte abnormalities in heart failure: pathophysiology and implications. *Heart Fail. Rev.* 20, 493–503. doi: 10.1007/s10741-015-9482-y

Venetucci, L. A., Trafford, A. W., O'Neill, S. C., and Eisner, D. A. (2008). The sarcoplasmic reticulum and arrhythmogenic calcium release. *Cardiovasc. Res.* 77, 285–292. doi: 10.1093/cvr/cvm009

Verdonck, F., Volders, P. G., Vos, M. A., and Sipido, K. R. (2003). Increased Na^+ concentration and altered Na/K pump activity in hypertrophied canine ventricular cells. *Cardiovasc. Res.* 57, 1035–1043. doi: 10.1016/S0008-6363(02)00734-4

Volders, P. G., Vos, M. A., Szabo, B., Sipido, K. R., de Groot, S. H., Gorgels, A. P., et al. (2000). Progress in the understanding of cardiac early afterdepolarizations and torsades de pointes: time to revise current concepts. *Cardiovasc. Res.* 46, 376–392. doi: 10.1016/S0008-6363(00)00022-5

Wagner, S., Hacker, E., Grandi, E., Weber, S. L., Dybkova, N., Sossalla, S., et al. (2009). Ca/calmodulin kinase II differentially modulates potassium currents. *Circ. Arrhythm. Electrophysiol.* 2, 285–294. doi: 10.1161/CIRCEP.108.842799

Wang, Y., and Hill, J. A. (2010). Electrophysiological remodeling in heart failure. *J. Mol. Cell. Cardiol.* 48, 619–632. doi: 10.1016/j.yjmcc.2010.01.009

Wasserstrom, J. A., and Aistrup, G. L. (2005). Digitalis: new actions for an old drug. *Am. J. Physiol. Heart Circ. Physiol.* 289, H1781–H1793. doi: 10.1152/ajpheart.00707.2004

Weiss, J. N., Garfinkel, A., Karagueuzian, H. S., Chen, P. S., and Qu, Z. (2010). Early afterdepolarizations and cardiac arrhythmias. *Heart Rhythm* 7, 1891–1899. doi: 10.1016/j.hrthm.2010.09.017

Weiss, J. N., Qu, Z., and Shivkumar, K. (2017). Electrophysiology of hypokalemia and hyperkalemia. *Circ. Arrhythm. Electrophysiol.* 10:e004667. doi: 10.1161/CIRCEP.116.004667

Wester, P. O., and Dyckner, T. (1986). Intracellular electrolytes in cardiac failure. *Acta Med. Scand. Suppl.* 707, 33–36.

Williams, M. E., Gervino, E. V., Rosa, R. M., Landsberg, L., Young, J. B., Silva, P., et al. (1985). Catecholamine modulation of rapid potassium shifts during exercise. *N. Engl. J. Med.* 312, 823–827. doi: 10.1056/NEJM198503283121304

Wolk, R., Kane, K. A., Cobbe, S. M., and Hicks, M. N. (1998). Regional electrophysiological effects of hypokalaemia, hypomagnesaemia and hyponatraemia in isolated rabbit hearts in normal and ischaemic conditions. *Cardiovasc. Res.* 40, 492–501. doi: 10.1016/S0008-6363(98)00200-4

Yancy, C. W., Jessup, M., Bozkurt, B., Butler, J., Casey, D. E. Jr., Drazner, M. H., et al. (2013). 2013 ACCF/AHA guideline for the management of heart failure: executive summary: a report of the American College of Cardiology Foundation/American Heart Association Task Force on practice guidelines. *Circulation* 128, 1810–1852. doi: 10.1161/CIR.0b013e31829e8807

Yang, T., Snyders, D. J., and Roden, D. M. (1997). Rapid inactivation determines the rectification and [K+]o dependence of the rapid component of the delayed rectifier K^+ current in cardiac cells. *Circ. Res.* 80, 782–789. doi: 10.1161/01.RES.80.6.782

Young, D. Z., Lampert, S., Graboys, T. B., and Lown, B. (1984). Safety of maximal exercise testing in patients at high risk for ventricular arrhythmia. *Circulation* 70, 184–191. doi: 10.1161/01.CIR.70.2.184

Yuen, G. K., Galice, S., and Bers, D. M. (2017). Subcellular localization of Na/K-ATPase isoforms in ventricular myocytes. *J. Mol. Cell. Cardiol.* 108:158–169. doi: 10.1016/j.yjmcc.2017.05.013

Zhang, T., Maier, L. S., Dalton, N. D., Miyamoto, S., Ross, J. Jr., Bers, D. M., et al. (2003). The deltaC isoform of CaMKII is activated in cardiac hypertrophy and induces dilated cardiomyopathy and heart failure. *Circ. Res.* 92, 912–919. doi: 10.1161/01.RES.0000069686.31472.C5

Zhao, Z., Wen, H., Fefelova, N., Allen, C., Baba, A., Matsuda, T., et al. (2012). Revisiting the ionic mechanisms of early afterdepolarizations in cardiomyocytes: predominant by Ca waves or Ca currents? *Am. J. Physiol. Heart Circ. Physiol.* 302, H1636–H1644. doi: 10.1152/ajpheart.00742.2011

Conflict of Interest Statement: The authors declare that the research was conducted in the absence of any commercial or financial relationships that could be construed as a potential conflict of interest.

frontiers in Physiology

ORIGINAL RESEARCH
published: 09 January 2019
doi: 10.3389/fphys.2018.01893

Action Potential Prolongation, β-Adrenergic Stimulation, and Angiotensin II as Co-factors in Sarcoplasmic Reticulum Instability

*Carlotta Ronchi, Beatrice Badone, Joyce Bernardi and Antonio Zaza**

Laboratory of Cardiac Cellular Physiology, Department of Biotechnology and Bioscience, University of Milano-Bicocca, Milan, Italy

Introduction: Increases in action potential duration (APD), genetic or acquired, and arrhythmias are often associated; nonetheless, the relationship between the two phenomena is inconstant, suggesting coexisting factors. β-adrenergic activation increases sarcoplasmic reticulum (SR) Ca^{2+}-content; angiotensin II (ATII) may increase cytosolic Ca^{2+} and ROS production, all actions stimulating RyRs opening. Here we test how APD interacts with β-adrenergic and AT-receptor stimulation in facilitating spontaneous Ca^{2+} release events (SCR).

Methods: Under "action potential (AP) clamp", guinea-pig cardiomyocytes (CMs) were driven with long (200 ms), normal (150 ms), and short (100 ms) AP waveforms at a CL of 500 ms; in a subset of CMs, all the 3 waveforms could be tested within the same cell. SCR were detected as inward current transients (I_{TI}) following repolarization; I_{TI} incidence and repetition within the same cycle were measured under increasing isoprenaline concentration ([ISO]) alone, or plus 100 nM ATII (30 min incubation+superfusion).

Results: I_{TI} incidence and repetition increased with [ISO]; at longer APs the [ISO]-response curve was shifted upward and I_{TI} coupling interval was reduced. ATII increased I_{TI} incidence more at low [ISO] and under normal (as compared to long) APs. Efficacy of AP shortening in suppressing I_{TI} decreased in ATII-treated myocytes and at higher [ISO].

Conclusions: AP prolongation sensitized the SR to the destabilizing actions of ISO and ATII. Summation of ISO, ATII and AP duration effects had a "saturating" effect on SCR incidence, thus suggesting convergence on a common factor (RyRs stability) "reset" by the occurrence of spontaneous Ca^{2+} release events.

Keywords: action potential duration, angiotensin II, SR stability, arrhythmias, repolarization reserve, β-adrenergic activation

OPEN ACCESS

Edited by:
Daniel M. Johnson, University of Birmingham, United Kingdom

Reviewed by:
Andrew F. James, University of Bristol, United Kingdom
Senka Holzer, Medical University of Graz, Austria

****Correspondence:***
Antonio Zaza
antonio.zaza@unimib.it

Specialty section:
This article was submitted to Cardiac Electrophysiology, a section of the journal Frontiers in Physiology

Received: *06 September 2018*
Accepted: *14 December 2018*
Published: *09 January 2019*

Citation:
Ronchi C, Badone B, Bernardi J and Zaza A (2019) Action Potential Prolongation, β-Adrenergic Stimulation, and Angiotensin II as Co-factors in Sarcoplasmic Reticulum Instability. Front. Physiol. 9:1893. doi: 10.3389/fphys.2018.01893

INTRODUCTION

Prolonged ventricular repolarization, whether caused by myocardial remodeling (Nattel et al., 2007), genetic defects (Schwartz et al., 2001), or drugs (Yang et al., 2001), may reduce myocardial electrical stability. Prolonged action potential duration (APD) may be a reporter of reduced "repolarization reserve," but it can also be causally linked to arrhythmogenesis through several mechanisms. Along with purely electrophysiological consequences (e.g., increased repolarization

heterogeneity) (Winter and Shattock, 2016), APD prolongation affects the sarcolemmal Ca^{2+} influx/efflux balance (Bers, 2001), thus it represents a stress-condition for intracellular Ca^{2+} homeostasis requiring robust compensatory mechanisms. This might be critical under conditions, such as heart failure, in which intracellular Ca^{2+} homeostasis is primarily impaired; indeed, "triggered activity" is common in the failing myocardium (Pogwizd, 1995).

On the other hand, prolonged repolarization *per se* may be insufficient to induce arrhythmias, which might require the concomitance of multiple factors. This may be true also for primarily electrical disorders, such as genetic (Napolitano et al., 2015) and drug-induced (Redfern et al., 2003) repolarization abnormalities. After the early identification of sympathetic activation as a powerful triggering mechanism (Malliani et al., 1980), relatively little attention has been devoted to other biological variables that might theoretically converge with prolonged repolarization in reducing electrical stability. Their identification might pave the way to risk stratification and development of relatively simple preventive measures.

Myocardial and systemic production of angiotensin II (ATII) is increased in response to stress. Beside its well-known role in long-term structural remodeling of the failing heart, ATII has a couple of actions at the cellular level that might acutely compromise the compensations required to cope with prolonged repolarization.

AT-1 receptors (AT1R) stimulation by ATII induces Ca^{2+} release from the sarcoplasmic reticulum (SR) through inositol 1,4,5-trisphospate-receptor channels (IP_3R) and IP_3R are functionally coupled to RYR2 in atrial myocytes (Kockskamper et al., 2008; Wullschleger et al., 2017). Although, in ventricular myocytes IP_3R are less expressed (Garcia and Boehning, 2017), IP_3R activation (by endothelin 1) has been reported to enhance CICR in rabbit ventricular myocytes (Domeier et al., 2008). Secondly, AT1R stimulation activates production of radical O_2 species (ROS) by sarcolemmal NADPH-oxydases (Kawai et al., 2017); peroxydation destabilizes RyR2 closed state and is well-known to facilitate spontaneous Ca^{2+} release events (SCR) and related arrhythmias (Prosser et al., 2013).

While an antiarrhythmic effect of ATII antagonism has been reported (Garg et al., 2006), acute proarrhythmia does not stand out as a direct consequence of increased ATII signaling, but what happens if the functional reserve provided by Ca^{2+}-homeostatic mechanisms is concomitantly decreased by prolonged repolarization?

Based on the above information, we hypothesize that stimulation of ATII receptors, may facilitate the occurrence of SCR events induced by APD prolongation and β-adrenergic stimulation. The aim of this study was to test such hypothesis.

The practical interest in this question also lies in the availability of widely used drugs limiting ATII cellular effects (AT1R antagonists), which might then be considered as complements in the prevention of ventricular arrhythmias under conditions of prolonged repolarization.

MATERIALS AND METHODS

The investigation conforms to the Guide of the Care and Use of Laboratory Animals published by the US National Institute of Health (NIH publication No, 85-23). This study was reviewed and approved by the Animal Care Committee endorsed by University Milano-Bicocca.

Cell Isolation

Dunkin-Hartley guinea pigs left ventricular cardiomyocytes were isolated by using a retrograde coronary perfusion method previously published (Zaza et al., 1998), with minor modifications. Rod-shaped, Ca^{2+}-tolerant myocytes were used within 12 h from dissociation. No measure was taken to dissociate myocytes selectively from either the left or the right ventricle.

Action Potential Clamp Recordings

Measurements were performed during superfusion with Tyrode's solution at 36.5°C. Pre-recorded guinea-pig action potential (AP) waveforms were applied in V-clamp mode, as previously described (Sala et al., 2017), at a cycle length of 2 Hz. Three AP waveforms (obtained from previous I-clamp recordings under appropriate conditions) with different APD_{90} (APD measured at 90% of repolarization) values were used: 200 ms (Long AP), 150 ms (Normal AP), and 100 ms (Short AP). APD_{90} in the Long AP is 40% longer than in Normal AP, a change proportionally compatible with repolarization abnormalities seen in the clinical setting (Schwartz et al., 1995) (it would simulate a QTc change from e.g., 370–518 ms). According to the experimental protocol, the different AP waveforms were applied to different myocytes (group comparison) or within the same myocyte (internal control). Because of their design, internal control experiments involved application of both AP waveforms in a fixed sequence, thus requiring to exclude the dependence of I_{TI} properties on the sequence itself. This was ruled out in preliminary experiments by applying Long-Short-Long AP sequences within the same myocyte. Characteristics of AP waveforms are summarized in **Table S1**.

Total membrane current (I_m) during the AP-clamp cycle (**Figure 1A** and **Figure S1**) was recorded. Because the AP waveforms were not recorded within the same myocyte, I_m during the AP was not null as expected under proper "self" AP-clamp conditions (Zaza et al., 1997); nonetheless, changes in the balance between I_m inward and outward components could still be used as a gross estimate of interventions effect on systolic currents.

SCR events were detected as the occurrence of diastolic inward current transients (I_{TI}), known to result from activation of Na^+/Ca^{2+} exchange by intracellular Ca^{2+} transients. This method was preferred to direct recording of intracellular Ca^{2+} because free from the contaminating effect of Ca^{2+} buffering by fluorescent Ca^{2+} probes; furthermore, I_m is sensitive to sub-sarcolemmal Ca^{2+} changes, which are relevant to membrane electrophysiology but poorly detected by epifluorescence measurements. Based on the baseline variance of diastolic current, I_{TI} events were defined I_{TI} exceeding a threshold of 15 pA; their incidence was defined as the percentage of myocytes

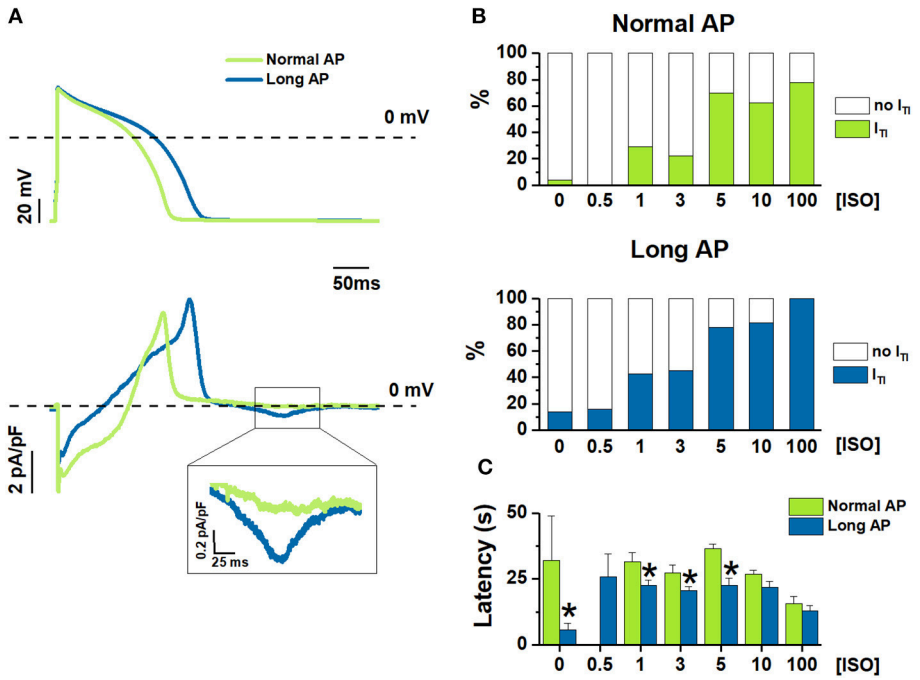

FIGURE 1 | [ISO]-dependency effect on I_{TI} incidence under Normal AP and Long AP. **(A)** Examples of Long AP and Normal AP waveforms used as a command in AP clamp (top) and the corresponding I_m (bottom) during 1nM ISO. **(B)** I_{TI} incidence, and **(C)** latency before I_{TI} onset from starting ISO challenge at different ISO concentrations (nM). $N > 10$ for all data points. *$P < 0.05$ vs. Normal AP.

in which at least 1 event was observed. Peak I_{TI} amplitude (pA/pF) and I_{TI} integral (Q_{TI}, in μC), which reports the charge moved by Na^+/Ca^{2+} exchange, was used to quantify the magnitude of SCR events. Other parameters considered were I_{TI} coupling interval after the preceding AP (CI in ms) and I_{TI} latency (in sec) after the beginning of ISO infusion.

β-adrenergic stimulation was achieved by exposure to increasing isoprenaline concentrations [ISO]; ATII-receptors were stimulated by 30 min preincubation in 100 nM ATII, which was also added to the superfusate.

Whether the effect of ATII was due to modulation of IP_3R was tested by (5 min) exposure to 2 μM 2-aminoethyl diphenylborinate (2APB), an antagonist of IP_3R. Nifedipine 5 μM (NIFE) was used to compare 2APB effect on I_m to that of L type Ca^{2+} current (I_{CaL}) blockade.

Experimental Solutions

Tyrode's solution contained (in mM): 154 NaCl, 4 KCl, 2 $CaCl_2$, 1 $MgCl_2$, 5 HEPES-NaOH, 5.5 D-glucose, adjusted to pH 7.35 with NaOH. Myocytes were patch-clamped with borosilicate glass pipettes containing (mM): K^+-aspartate 110, KCl 23, $MgCl_2$ 3, HEPES KOH 5, EGTA KOH 1, GTP Na^+-salt 0.4, ATP Na^+-salt 5, creatine phosphate Na^+-salt 5, $CaCl_2$ 0.4 (calculated free-Ca^{2+} = 10^{-7} M), adjusted to pH 7.3.

ISO and ATII were dissolved in water, NIFE in ethanol, and 2APB in DMSO. When used, compound solvents (ethanol or DMSO) were added to all solutions at the same final concentration, which never exceed 0.1%. All chemicals were purchased from Sigma.

Statistical Analysis

Student's paired or unpaired *t*-test was applied to compare means of continuous variables (latency, amplitudes etc). Difference between categorical variables (expressed as incidence %) was tested by chi-square (group comparison) or McNemar analysis (internal control) applied to absolute numbers; GLM regression for binomial data (R statistical package) was used to compare vectors of categorical variables (incidence in ISO dose-response curves). Statistical significance was defined as $P < 0.05$. Sample size (n, number of cells) is specified for each experimental condition in the respective figure legend.

Categorical variables are expressed in percentages while the continuous variables are expressed as average ± standard error of the mean.

RESULTS

Effect of APD Prolongation on ISO-Induced I_{TI} Events

The experimental protocol was optimized to test the effect of multiple [ISO] in each myocyte; because of limitations inherent to preparation stability, the effect of changing APD on the [ISO] vector had to be tested by comparing myocyte groups. Thus, the incidence of I_{TI} events was compared between myocytes clamped with either the Normal AP or the Long AP (group comparison)

at baseline and during exposure to increasing ISO concentrations ([ISO]) (**Figure 1**).

I_{TI} incidence dose-dependently increased with [ISO] under both AP waveforms (**Figure 1B**); the Long APD moved the ISO concentration-response curve to significantly higher I_{TI} incidences ($p < 0.05$ at binomial GLM regression) and reduced the threshold concentration for ISO effect (lower vs. upper panel in **Figure 1B**). As compared to Normal AP, Long AP shortened the time of I_{TI} appearance after the beginning of ISO (or control) solution challenge; however, this effect became smaller as [ISO] was increased (**Figure 1C**).

Effect of Adding ATII

The above experiments were repeated in cells treated with 100 nM ATII (ATII) and compared with untreated cells (no ATII) (**Figure 2**).

ATII alone [[ISO] = 0] had a very small effect on I_{TI} incidence under Normal AP ($p < 0.05$) and failed to change I_{TI} significantly under Long AP (**Figure 2A**). Within each AP waveform, ATII moved the ISO concentration-response curve to significantly higher I_{TI} incidences. ATII effect was present with both AP waveforms, ($p < 0.05$ at binomial GLM regression), but it was smaller and limited to low [ISO] during the Long AP (**Figure 2A**). ATII tended to shorten the time of I_{TI} appearance (latency) after the beginning of ISO challenge, but did so only under the Normal AP (**Figure 2B**).

Effect of APD Changes on I_{TI} Occurrence and Properties

This set of experiments was designed to test whether APD shortening would effectively modify I_{TI} events induced by receptor stimulation. To this end, each myocyte in which I_{TI} events occurred during the Long AP (incidence = 100% by default) was subsequently clamped with the Normal AP (internal control). This was repeated in myocyte groups, each exposed to a different [ISO] alone, or in the presence of ATII (**Figures 3**, **4**). I_{TI} incidence and properties were measured.

Without ATII, (**Figure 3A**), switching from Long AP to Normal AP caused I_{TI} to cease within several beats in 88% of the cells in basal conditions, in 46% under 1 nM ISO and in 33% under 10 nM ISO ($p < 0.05$ for ΔAPD_{90} differences along the [ISO] vector). In ATII-treated myocytes, APD shortening terminated I_{TI} in 55% of cells under basal conditions and termination rate decreased with increasing [ISO] (**Figure 3B**). The effect of APD shortening on I_{TI} incidence was not significantly modified by ATII.

In the absence of ATII, occurrence of two I_{TI} events within the same cycle was not significantly affected by ISO. Surprisingly, ATII did not increase the occurrence of double I_{TI} events and, if anything, tended to reduce it (**Figure 3C**).

Similarly, I_{TI} properties were affected by APD shortening (in the direction of smaller SCR with greater latency) only in the absence of β-adrenergic stimulation. ATII increased I_{TI} magnitude (Q_{TI} and peak amplitude), but the effect of APD shortening was preserved (**Figure 4**).

To test whether APD affected I_{TI} occurrence only if increased above its normal value, in a subset of myocytes the Short AP waveform was also tested (again by internal control) (**Figure 5**). I_{TI} incidence and properties were incrementally modified by AP waveforms of shorter duration, suggesting that SR stability depends on APD in a continuous fashion. High [ISO] minimized the effect of APD shortening.

Overall, internal control experiments confirmed that APD shortening may counter the arrhythmogenic effect of receptor stimulation, but its impact was reduced at high levels of neurohumoral stimulation.

IP_3R Contribution to ATII Effect

The contribution of IP_3 signaling to I_{TI} facilitation by ATII was investigated by blocking IP_3R (by 2APB) (**Figure 6**). To this end I_{TI} incidence was measured, during Normal and Long APs, in the presence of 1 nM or 10 nM ISO + ATII only and after adding 2APB to the superfusate.

With 1 nM ISO, 2APB similarly reduced I_{TI} incidence during Normal APD and Long APD (**Figure 6A**); the same was true for I_{TI} charge (Q) (**Figure 6C**). When [ISO] was increased to 10 nM 2APB still reduced I_{TI} incidence during Normal AP (by 60%) but had a much smaller effect during the Long AP (**Figure S2**).

This would suggest that IP_3R stimulation significantly contributed to ATII-induced increment in SCR events; however, a substantial outward shift of I_m during the AP (**Figure 6B**) opens the possibility of decreased Ca^{2+} influx as the mechanism for I_{TI} suppression. To test the hypothesis of direct I_{CaL} blockade by 2APB, we compared the kinetics of its action on I_m during the AP plateau to that of a saturating concentration of NIFE (**Figure S3**). The much slower kinetics of 2APB argues against direct I_{CaL} blockade by 2APB.

DISCUSSION

The main findings of the present study were: ISO concentration-dependently induced SCR events and APD prolongation enhanced ISO effect; ATII increased SCR incidence preferentially when it was still far from 100%, i.e., with normal APD and in the lower range of [ISO].

While APD prolongation typically facilitates EADs through a mechanism at least partially independent of SCR (January and Riddle, 1989; Song et al., 2015), its association with SCR is less straightforward. An increase in intracellular Ca^{2+} content (both on the cytosolic and luminal sides of SR membrane) facilitates SCR (Egdell et al., 2000; Venetucci et al., 2008). Because of net charge transport by the Na^+/Ca^{2+} exchanger, Ca^{2+} extrusion from the cell is favored at diastolic potentials; thus, assuming a constant cycle length (CL), APD prolongation can increase intracellular Ca^{2+} content simply by decreasing the proportion of the cycle occupied by diastole (Bers, 2001). Accordingly, modeling studies indicate that the amplitude and prematurity of DADs is expectedly related to APD because of APD-dependency of SR Ca^{2+} load (Song et al., 2015). Nonetheless, blockade of a repolarizing current (I_{Ks}) in canine myocytes prolonged ventricular APD (by ∼15%) but failed to induce DADs unless associated with β-adrenergic stimulation (Burashnikov and Antzelevitch, 2000). In the present study, APD prolongation (by 40%) alone slightly increased

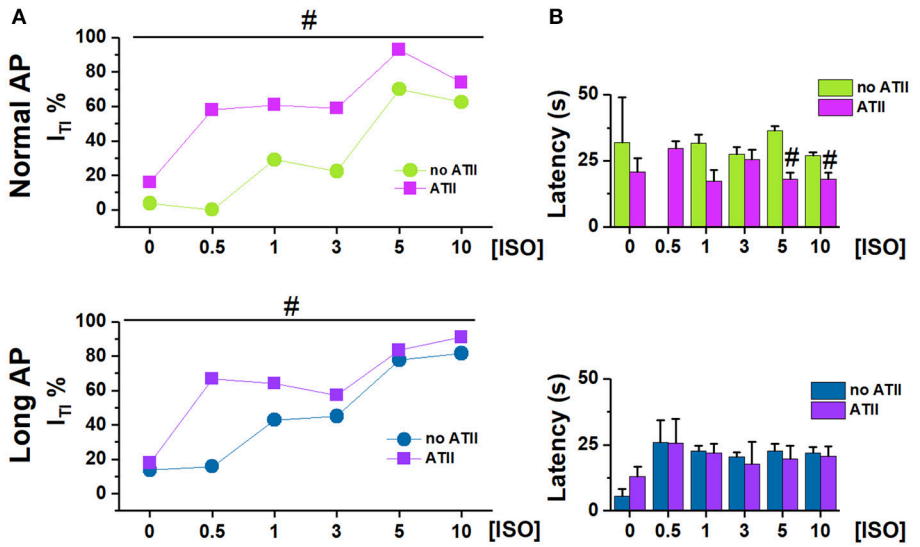

FIGURE 2 | Effect of adding ATII on I_{TI} incidence under Normal AP and Long AP. **(A)** I_{TI} incidence and **(B)** latency at different ISO concentrations (nM) in untreated (noATII) and ATII- treated (ATII) CMs. $N > 20$ for all groups. #$p < 0.05$ vs. ISO group.

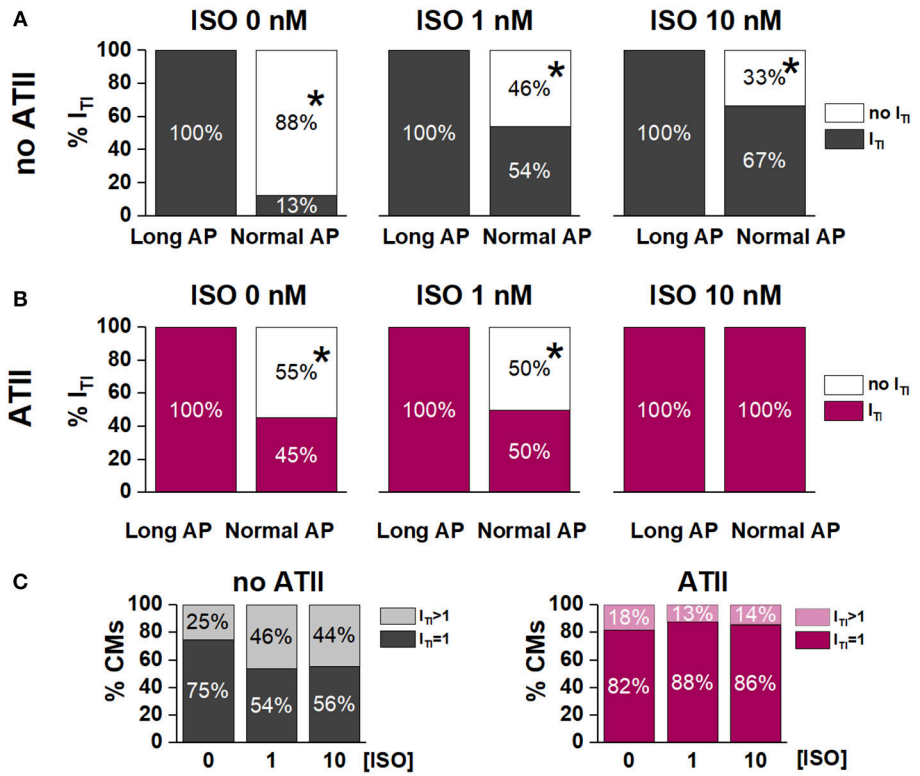

FIGURE 3 | Effect of APD shortening on I_{TI} incidence within the same cardiomyocyte in the absence (no ATII) **(A)** or presence of ATII (ATII) **(B)**. **(C)** Percent of cardiomyocytes with 1 I_{TI} event or >1 I_{TI} events in the absence (no ATII) or presence (ATII) of ATII (Long AP; 0, 1,10 nM ISO). CMs: cardiomyocytes. $N > 8$ for all groups. *$p < 0.05$ vs. Long AP.

I_{TI} incidence also in the absence of ISO; this effect was smaller than that previously reported in rabbit myocytes using more pronounced APD prolongation (Wu et al., 1999). APD prolongation had a much larger effect in the presence of very low (nanomolar) ISO concentrations (**Figure 1**). This suggests that APD prolongation by amounts more relevant to the clinical

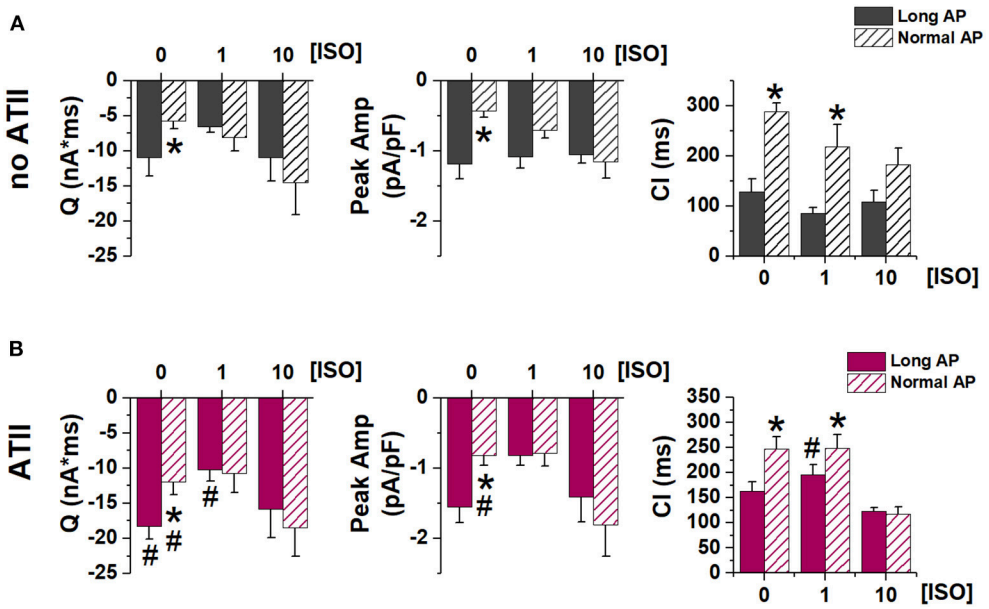

FIGURE 4 | Effect of APD shortening on I_{TI} properties. Statistics (mean ± S.E.) of I_{TI} charge (Q), peak I_{TI} amplitude (Peak Amp) and coupling interval (CI) **(A)** in the absence of ATII (no ATII); **(B)** in the presence of ATII (ATII). $N > 8$ for all groups. $^*p < 0.05$ vs. Long AP; $\#p < 0.05$ vs. no ATII CMs.

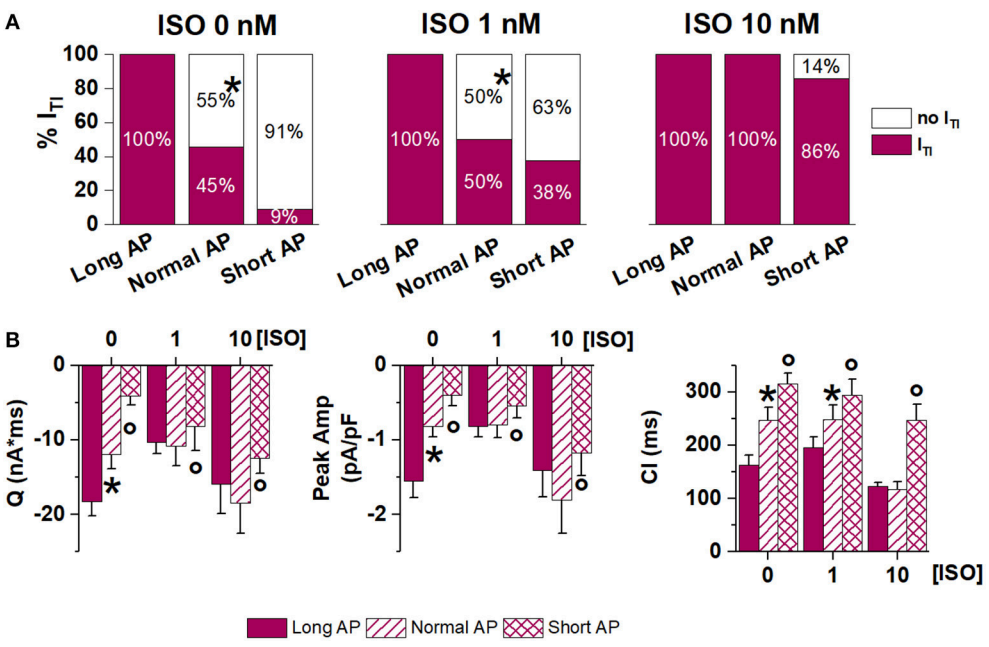

FIGURE 5 | Effect of APD shortening within the same ATII-treated cardiomyocyte (Long AP, Normal AP and Short AP waveforms). **(A)** I_{TI} incidence in basal condition (ISO 0) and in 1 nM and 10 nM ISO. **(B)** statistics (mean ± S.E.) of I_{TI} charge (Q), peak I_{TI} amplitude (Peak Amp) and coupling interval (CI). $N > 8$ for all groups $^*p < 0.05$ vs. Long AP; $^\circ p < 0.05$ vs. Normal AP.

setting may be relatively inconsequential on its own but becomes a powerful co-factor in the induction of SCR by adrenergic stimulation.

In the present experiments, APD was changed at a constant cycle length, thus reciprocally affecting diastolic interval. This implies that membrane "duty cycle" (the ratio between systolic and diastolic times), rather than APD itself, was considered. This approach was motivated by the consideration that repolarization abnormalities are defined as changes of the rate-corrected QT interval, which implies that they are

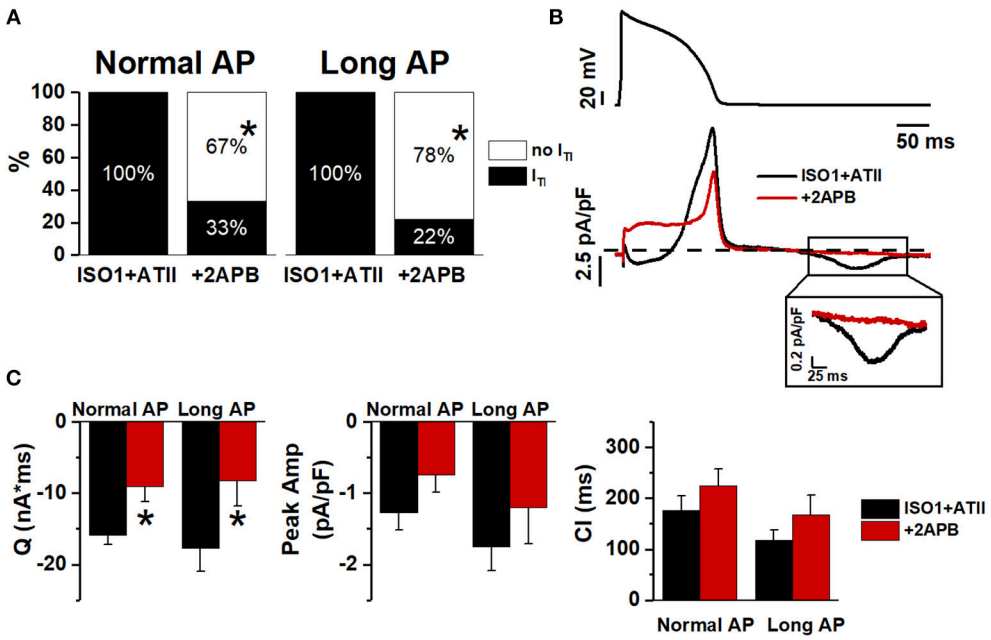

FIGURE 6 | Effect of 2APB on I_{TI} induced by ISO+ATII. **(A)** I_{TI} incidence in ISO1+ATII alone and with 2APB. **(B)** Examples of Normal AP (top) and I_m corresponding (bottom). **(C)** statistic (mean ± S.E.) of I_{TI} charge (Q); peak I_{TI} amplitude (Peak Amp) and coupling interval (CI). $N = 9$ for both groups. *$p > 0.05$ vs. ISO1+ATII.

not accompanied by a commensurate change in cycle length. Furthermore, from a mechanistic standpoint, the sarcolemmal Ca^{2+} flux balance depends on membrane duty cycle, rather than on APD alone (Bers, 2001). Nonetheless, it is fair to stress that the present data may not describe the effect of changes in APD alone (i.e., with constant diastolic interval).

In the presence of normal APD, ATII significantly facilitated I_{TI} induction at all levels of β-adrenergic stimulation (**Figure 2**). ATII has been reported to exert "enhanced antagonism" of I_{CaL} activation by β1-AR, reflecting inhibition of pre-activated adenylate cyclase (Ai et al., 1998). Thus, I_{TI} facilitation by ATII in the context of β1-AR activation may look contradictory. However, it should be noted that, in the present experiments, I_{TI} facilitation by ATII prevailed at low ISO concentrations, which failed to induce I_{TI} events on their own (**Figure 2**). Overall, this may suggest that ATII facilitated I_{TI} events by mechanisms other than those triggered by β1-AR activation, but converging with them to impair SR stability.

ATII activates membrane phospholipase C (PLC) resulting in production of IP_3 and diacylglycerol. SR Ca^{2+} release through IP_3R channels is central in smooth muscle physiology and significantly contributes to intracellular Ca^{2+} dynamics of atrial myocytes (Li et al., 2005; Wullschleger et al., 2017). Expression of IP_3R in ventricular myocytes is lower, largely perinuclear and likely devoted to excitation-transcription coupling (Lipp et al., 2000; Wu et al., 2006; Domeier et al., 2008); therefore, their role in intracellular Ca^{2+} dynamics is debated. Nevertheless, IP_3-dependent enhancement of excitation-contraction coupling has been observed in rabbit ventricular myocytes (Domeier et al., 2008). Functional crosstalk between neighboring IP_3R and RyR2 channels, caused by local Ca^{2+} diffusion and amounting to direct activation of Ca^{2+} release units, has been demonstrated in atrial myocytes (Wullschleger et al., 2017). In ventricular myocytes (including human ones), enhanced IP_3R-mediated SR Ca^{2+} leak has been reported not to affect RyR2 function directly, but rather secondary to APD prolongation by the increment in Na^+/Ca^{2+} exchanger current (I_{NCX}) (Signore et al., 2013). Consistent with this interpretation, IP_3R overexpression in a transgenic mouse model substantially enhanced SR Ca^{2+} leak without affecting the incidence of organized SCR events (Ca^{2+} sparks or puffs) (Blanch and Egger, 2018).

IP_3R activation likely contributed to SCR facilitation by ATII in the present experiments, as suggested by the effect of 2APB (**Figure 6**). 2APB also shifted the current balance during the AP in the outward direction, a change compatible with an increased contribution of I_{NCX} during IP_3R activation (Signore et al., 2013). Direct I_{CaL} blockade by 2APB is unlikely because of the slow kinetics of 2APB effect (**Figure 6**) and of failure 2APB alone to affect Ca^{2+} dynamics in ventricular myocytes (Peppiatt et al., 2003). The present results suggest that IP_3R activation, possibly through an increment of cytosolic Ca^{2+}, may indeed facilitate Ca^{2+} waves under the conditions generated by APD prolongation and β-adrenergic stimulation.

Albeit not investigated in the present work, activation of ROS production by ATII is a further mechanism potentially contributing to RyR2 destabilization (Prosser et al., 2013).

Seen in the context of previous findings, the present results suggest that, albeit potentially inconsequential on its own,

ATII may substantially facilitate SCR induction by β-adrenergic stimulation in ventricular myocytes.

Apparently in contrast with the hypothesis of a facilitatory role of APD prolongation, when APD was prolonged, ATII effect was smaller and limited to very low ISO concentrations (**Figure 2**). However, this can be viewed as "saturation" of the mechanisms responsible for SCR by APD prolongation (i.e., intracellular Ca^{2+} load) and strong β-adrenergic stimulation. Notably, even at saturation, I_{TI} incidence did not achieve 100% and events per cycle were limited to one or two. Such pattern is expected from convergence of the three co-factors (APD, ISO and ATII) on a common mechanism (RyR2 facilitation) with a "ceiling" effect. The ceiling can be conceivably caused by the SCR itself, which resets SR Ca^{2+} content (Venetucci et al., 2008). Considering that ATII facilitated SCR, we expected it to increase the occurrence of double I_{TI} events within a cycle. The finding that the opposite was true can be tentatively interpreted by considering that ATII increased the magnitude of the first SCR event (Q in **Figure 4**); by causing larger SR Ca^{2+} depletion, this might reduce the probability of a second SCR event.

The relevance of APD on I_{TI} induction is highlighted by the ability of APD shortening to abrogate I_{TI} once it was induced by either ISO alone or ISO plus ATII (**Figure 5**). Even when I_{TI} persisted after AP normalization, its charge and amplitude were reduced, indicating that APD may affect the amount of Ca^{2+} released by the SCR and, with it, the likelihood of triggering a propagated beat. In keeping with the convergence of factors, the ability of APD normalization to affect I_{TI} occurrence and properties was reduced at high ISO concentrations and, further, in the presence of ATII.

CONCLUSION

From the data obtained it is possible to conclude that ATII may act as a co-factor to facilitate the occurrence of SCR in the presence of AP prolongation and β-adrenergic stimulation.

LIMITATIONS

Among small animals, guinea-pigs have an action potential contour which is closest to the human one; this justifies their adoption as experimental model. However, as compared to canine (and, possibly, human) myocytes, guinea-pig ones do not express I_{TO} (Nakajima et al., 2002) and have a prominent sustained I_{CaL}, which likely supports a more positive action potential plateau (Sala et al., 2017). This might exaggerate the impact of changes in APD in facilitating SCR events.

While I_{TI} (measured under V-clamp) is a suitable reporter of SCR, the direct cause of arrhythmogenesis by SCR are DADs. Albeit I_{TI} is the cause of DAD, their features do not necessarily coincide because V-clamp prevents the positive feed-back loop between depolarization and further current activation; moreover, the amplitude of DADs caused by a given I_{TI} amplitude depends on membrane diastolic resistance and, thus, on the currents determining it (mostly I_{K1}). While absence of positive feed-back would lead to underestimate DADs amplitude, the effect of the interventions tested on diastolic membrane resistance is unknown.

PRATICAL IMPLICATIONS

ATII signaling is part of an homeostatic control system central to physiological adaptations; furthermore, ATII is also synthetized locally (cardiomyocytes, fibroblasts, vascular cells) in response to stress (Varagic and Frohlich, 2002); its production and its receptors (AT1R) are upregulated in cardiac disease (Szczepanska-Sadowska et al., 2018). Therefore, the extent of ATII signaling may well vary among subjects and, within a subject, in response to physiological and pathological states. The present results in cardiomyocytes suggest that ATII signaling might act as a variable co-factor in determining the impact of repolarization abnormalities on SR stability and the resulting arrhythmias. Thus, ATII antagonism might have an antiarrhythmic significance beyond prevention of myocardial remodeling, potentially extended to genetic and drug-induced conditions of prolonged repolarization. Considering that myocardial ATII production may be independent of the angiotensin converting enzyme (ACE) (Varagic and Frohlich, 2002), direct antagonism of AT1 receptors should be considered as the logical intervention.

AUTHOR CONTRIBUTIONS

CR planned, performed, analyzed the majority of experiments and wrote the first manuscript draft; BB and JB contributed to part of the experiments and to data analysis. AZ supervised the study and contributed to the manuscript final version.

FUNDING

This work was funded by Fondo di Ateneo per la Ricerca (FAR 2018) to AZ.

SUPPLEMENTARY MATERIAL

The Supplementary Material for this article can be found online at: https://www.frontiersin.org/articles/10.3389/fphys.2018.01893/full#supplementary-material

REFERENCES

Ai, T., Horie, M., Obayashi, K., and Sasayama, S. (1998). Accentuated antagonism by angiotensin II on guinea-pig cardiac L-type Ca-currents enhanced by β-adrenergic stimulation. *Pflügers Archiv.* 436, 168–174.

Bers, D. M. (2001). *Excitation-Contraction Coupling and Cardiac Contractile Force*. Boston, MA: Kluwer Academic Publishers.

Blanch, I. Salvador. J., and Egger, M. (2018). Obstruction of ventricular Ca^{2+} -dependent arrhythmogenicity by inositol 1,4,5-trisphosphate-triggered sarcoplasmic reticulum Ca^{2+} release. *J. Physiol.* 596, 4323–4340. doi: 10.1113/JP276319

Burashnikov, A., and Antzelevitch, C. (2000). Block of I(Ks) does not induce early afterdepolarization activity but promotes beta-adrenergic agonist-induced delayed afterdepolarization activity. *J. Cardiovasc. Electrophysiol.* 11, 458–465. doi: 10.1111/j.1540-8167.2000.tb00342.x

Domeier, T. L., Zima, A. V., Maxwell, J. T., Huke, S., Mignery, G. A., and Blatter, L. A. (2008). IP3 receptor-dependent Ca^{2+} release modulates excitation-contraction coupling in rabbit ventricular myocytes. *Am. J. Physiol. Heart Circ. Physiol.* 294, H596–H604. doi: 10.1152/ajpheart.01155.2007

Egdell, R. M., De Souza, A. I., and MacLeod, K. T. (2000). Relative importance of SR load and cytoplasmic calcium concentration in the genesis of aftercontractions in cardiac myocytes. *Cardiovasc. Res.* 47, 769–777. doi: 10.1016/s0008-6363(00)00147-4

Garcia, M. I., and Boehning, D. (2017). Cardiac inositol 1, 4, 5-trisphosphate receptors. *Biochim. Biophys. Acta (BBA)-Mol. Cell Res.* 1864, 907–914. doi: 10.1016/j.bbamcr.2016.11.017

Garg, S., Narula, J., Marelli, C., and Cesario, D. (2006). Role of angiotensin receptor blockers in the prevention and treatment of arrhythmias. *Am. J. Cardiol.* 97, 921–925. doi: 10.1016/j.amjcard.2005.10.028

January, C. T., and Riddle, J. M. (1989). Early afterdepolarizations: mechanism of induction and block. A role for L-type Ca^{2+} current. *Circ. Res.* 64, 977–990.

Kawai, T., Forrester, S. J., O'Brien, S., Baggett, A., Rizzo, V., and Eguchi, S. (2017). AT1 receptor signaling pathways in the cardiovascular system. *Pharmacol. Res.* 125 (Pt A), 4–13. doi: 10.1016/j.phrs.2017.05.008

Kockskämper, J., Zima, A. V., Roderick, H. L., Pieske, B., Blatter, L. A., and Bootman, M. D. (2008). Emerging roles of inositol 1,4,5-trisphosphate signaling in cardiac myocytes. *J. Mol. Cell Cardiol.* 45, 128–147. doi: 10.1016/j.yjmcc.2008.05.014

Li, X., Zima, A. V., Sheikh, F., Blatter, L. A., and Chen, J. (2005). Endothelin-1-induced arrhythmogenic Ca^{2+} signaling is abolished in atrial myocytes of inositol-1,4,5-trisphosphate(IP3)-receptor type 2-deficient mice. *Circ. Res.* 96, 1274–1281. doi: 10.1161/01.RES.0000172556.05576.4c

Lipp, P., Laine, M., Tovey, S. C., Burrell, K. M., Berridge, M. J., Li, W., et al. (2000). Functional InsP3 receptors that may modulate excitation-contraction coupling in the heart. *Curr. Biol.* 10, 939–942. doi: 10.1016/s0960-9822(00)00624-2

Malliani, A., Schwartz, P. J., and Zanchetti, A. (1980). Neural mechanisms in life-threatening arrhythmias. *Am. Heart J.* 100, 705–715.

Nakajima, I., Watanabe, H., Iino, K., Saito, T., and Miura, M. (2002). Ca^{2+} overload evokes a transient outward current in guinea-pig ventricular myocytes. *Circ. J.* 66, 87–92. doi: 10.1253/circj.66.87

Napolitano, C., Novelli, V., Francis, M. D., and Priori, S. G. (2015). Genetic modulators of the phenotype in the long QT syndrome: state of the art and clinical impact. *Curr. Opin. Genet. Dev.* 33, 17–24. doi: 10.1016/j.gde.2015.06.009

Nattel, S., Maguy, A., Le Bouter, S., and Yeh, Y. H. (2007). Arrhythmogenic ion-channel remodeling in the heart: heart failure, myocardial infarction, and atrial fibrillation. *Physiol. Rev.* 87, 425–456. doi: 10.1152/physrev.00014.2006

Peppiatt, C. M., Collins, T. J., Mackenzie, L., Conway, S. J., Holmes, A. B., Bootman, M. D., et al. (2003). 2-Aminoethoxydiphenyl borate (2-APB) antagonises inositol 1, 4, 5-trisphosphate-induced calcium release, inhibits calcium pumps and has a use-dependent and slowly reversible action on store-operated calcium entry channels. *Cell Calcium* 34, 97–108. doi: 10.1016/s0143-4160(03)00026-5

Pogwizd, S. M. (1995). Nonreentrant mechanism underlying spontaneous ventricular arrhythmias in a model of nonischemic heart failure in rabbits. *Circulation* 192, 1034–1048.

Prosser, B. L., Khairallah, R. J., Ziman, A. P., Ward, C. W., and Lederer, W. J. (2013). X-ROS signaling in the heart and skeletal muscle: stretch-dependent local ROS regulates $[Ca^{2+}]$i. *J. Mol. Cell Cardiol.* 58, 172–181. doi: 10.1016/j.yjmcc.2012.11.011

Redfern, W. S., Carlsson, L., Davis, A. S., Lynch, W. G., MacKenzie, I., Palethorpe, S., et al. (2003). Relationships between preclinical cardiac electrophysiology, clinical QT interval prolongation and torsade de pointes for a broad range of drugs: evidence for a provisional safety margin in drug development. *Cardiovasc. Res.* 58, 32–45. doi: 10.1016/s0008-6363(02)00846-5

Sala, L., Hegyi, B., Bartolucci, C., Altomare, C., Rocchetti, M., Váczi, K., et al. (2017). Action potential contour contributes to species differences in repolarization response to β-adrenergic stimulation. *Europace* 20, 1543–1552. doi: 10.1093/europace/eux236

Schwartz, P. J., Priori, S. G., Locati, E. H., Napolitano, C., Cantù, F., Towbin, J. A., et al. (1995). Long QT syndrome patients with mutations of the SCN5A and HERG genes have differential responses to Na^{+} channel blockade and to increases in heart rate. *Circulation* 92, 3381–3386. doi: 10.1161/01.Cir.92.12.3381

Schwartz, P. J., Priori, S. G., Spazzolini, C., Moss, A. J., Vincent, G. M., Napolitano, C., et al. (2001). Genotype-phenotype correlation in the long-QT syndrome: gene-specific triggers for life-threatening arrhythmias. *Circulation* 103, 89–95. doi: 10.1161/01.cir.103.1.89

Signore, S., Sorrentino, A., Ferreira-Martins, J., Kannappan, R., Shafaie, M., Del Ben, F., et al. (2013). Inositol 1, 4, 5-trisphosphate receptors and human left ventricular myocytes. *Circulation* 128, 1286–1297. doi: 10.1161/CIRCULATIONAHA.113.002764

Song, Z., Ko, C. Y., Nivala, M., Weiss, J. N., and Qu, Z. (2015). Calcium-voltage coupling in the genesis of early and delayed afterdepolarizations in cardiac myocytes. *Biophys. J.* 108, 1908–1921. doi: 10.1016/j.bpj.2015.03.011

Szczepanska-Sadowska, E., Czarzasta, K., and Cudnoch-Jedrzejewska, A. (2018). Dysregulation of the renin-angiotensin system and the vasopressinergic system interactions in cardiovascular disorders. *Curr. Hypertens. Rep.* 20:19. doi: 10.1007/s11906-018-0823-9

Varagic, J., and Frohlich, E. D. (2002). Local cardiac renin–angiotensin system: hypertension and cardiac failure. *J. Mol. Cell. Cardiol.* 34, 1435–1442. doi: 10.1006/jmcc.2002.2075

Venetucci, L. A., Trafford, A. W., O'Neill, S. C., and Eisner, D. A. (2008). The sarcoplasmic reticulum and arrhythmogenic calcium release. *Cardiovasc. Res.* 77, 285–292. doi: 10.1093/cvr/cvm009

Winter, J., and Shattock, M. J. (2016). Geometrical considerations in cardiac electrophysiology and arrhythmogenesis. *Europace* 18, 320–331. doi: 10.1093/europace/euv307

Wu, X., Zhang, T., Bossuyt, J., Li, X., McKinsey, T. A., Dedman, J. R., et al. (2006). Local InsP3-dependent perinuclear Ca^{2+} signaling in cardiac myocyte excitation-transcription coupling. *J. Clin. Invest.* 116, 675–682. doi: 10.1172/JCI27374

Wu, Y., Roden, D. M., and Anderson, M. E. (1999). Calmodulin kinase inhibition prevents development of the arrhythmogenic transient inward current. *Circ. Res.* 84, 906–912.

Wullschleger, M., Blanch, J., and Egger, M. (2017). Functional local crosstalk of inositol 1,4,5-trisphosphate receptor- and ryanodine receptor-dependent Ca^{2+} release in atrial cardiomyocytes. *Cardiovasc. Res.* 113, 542–552. doi: 10.1093/cvr/cvx020

Yang, T., Snyders, D., and Roden, D. M. (2001). Drug block of I(kr): model systems and relevance to human arrhythmias. *J. Cardiovasc. Pharmacol.* 38, 737–744. doi: 10.1097/00005344-200111000-00010

Zaza, A., Micheletti, M., Brioschi, A., and Rocchetti, M. (1997). Ionic currents during sustained pacemaker activity in rabbit sino-atrial myocytes. *J. Physiol.* 505, 677–688.

Zaza, A., Rocchetti, M., Brioschi, A., Cantadori, A., and Ferroni, A. (1998). Dynamic Ca^{2+}-induced inward rectification of K^{+} current during the ventricular action potential. *Circ. Res.* 82, 947–956.

Conflict of Interest Statement: The authors declare that the research was conducted in the absence of any commercial or financial relationships that could be construed as a potential conflict of interest.

frontiers in Physiology

ORIGINAL RESEARCH
published: 08 August 2018
doi: 10.3389/fphys.2018.01086

An Augmented Negative Force-Frequency Relationship and Slowed Mechanical Restitution Are Associated With Increased Susceptibility to Drug-Induced Torsade de Pointes Arrhythmias in the Chronic Atrioventricular Block Dog

David J. Sprenkeler, Alexandre Bossu, Jet D. M. Beekman, Marieke Schoenmakers and Marc A. Vos*

Department of Medical Physiology, Division of Heart and Lungs, University Medical Center Utrecht, Utrecht, Netherlands

OPEN ACCESS

Edited by:
Daniel M. Johnson, Maastricht University, Netherlands

Reviewed by:
Carlos L. del Rio, QTest Labs, United States
Milan Stengl, Charles University, Czechia
Atsushi Sugiyama, Toho University, Japan

***Correspondence:**
David J. Sprenkeler
D.J.Sprenkeler@umcutrecht.nl

Specialty section:
This article was submitted to Cardiac Electrophysiology, a section of the journal Frontiers in Physiology

Received: *29 May 2018*
Accepted: *23 July 2018*
Published: *08 August 2018*

Citation:
Sprenkeler DJ, Bossu A, Beekman JDM, Schoenmakers M and Vos MA (2018) An Augmented Negative Force-Frequency Relationship and Slowed Mechanical Restitution Are Associated With Increased Susceptibility to Drug-Induced Torsade de Pointes Arrhythmias in the Chronic Atrioventricular Block Dog. Front. Physiol. 9:1086. doi: 10.3389/fphys.2018.01086

Introduction: In the chronic AV-block (CAVB) dog model, structural, contractile, and electrical remodeling occur, which predispose the heart to dofetilide-induced Torsade de Pointes (TdP) arrhythmias. Previous studies found a relation between electrical remodeling and inducibility of TdP, while structural remodeling is not a prerequisite for arrhythmogenesis. In this study, we prospectively assessed the relation between *in vivo* markers of contractile remodeling and TdP inducibility.

Methods: In 18 anesthetized dogs, the maximal first derivative of left ventricular pressure (LV dP/dt_{max}) was assessed at acute AV-block (AAVB) and after 2 weeks of chronic AV-block (CAVB2). Using pacing protocols, three markers of contractile remodeling, i.e., force-frequency relationship (FFR), mechanical restitution (MR), and post-extrasystolic potentiation (PESP) were determined. Infusion of dofetilide (0.025 mg/kg in 5 min) was used to test for TdP inducibility.

Results: After infusion of dofetilide, 1/18 dogs and 12/18 were susceptible to TdP-arrhythmias at AAVB and CAVB2, respectively ($p = 0.001$). The inducible dogs at CAVB2 showed augmented contractility at a CL of 1200 ms (2354 ± 168 mmHg/s in inducible dogs versus 1091 ± 59 mmHg/s in non-inducible dogs, $p < 0.001$) with a negative FFR, while the non-inducible dogs retained their positive FFR. The time constant (TC) of the MR curve was significantly higher in the inducible dogs (158 ± 7 ms versus 97 ± 8 ms, $p < 0.0001$). Furthermore, a linear correlation was found between a weighted score of the number and severity of arrhythmias and contractile parameters, i.e., contractility at CL of 1200 ms ($r = 0.73$, $p = 0.002$), the slope of the FFR ($r = -0.58$, $p = 0.01$) and the TC of MR ($r = 0.66$, $p = 0.003$). Thus, more severe arrhythmias were seen in dogs with the most pronounced contractile remodeling.

Conclusion: Contractile remodeling is concomitantly observed with susceptibility to dofetilide-induced TdP-arrhythmias. The inducible dogs show augmented contractile remodeling compared to non-inducible dogs, as seen by a negative FFR, higher maximal response of MR and PESP and slowed MR kinetics. These altered contractility parameters could reflect disrupted Ca^{2+} handling and Ca^{2+}-overload, which predispose the heart to delayed- and early afterdepolarizations that could trigger TdP-arrhythmias.

Keywords: force-frequency relationship, mechanical restitution, post-extrasystolic potentiation, Torsade de Pointes, contractile remodeling, chronic AV-block dog

INTRODUCTION

Despite advances in treatment and prevention strategies, sudden cardiac death caused by ventricular arrhythmias remains a common cause of death in patients with heart failure or compensated hypertrophy (Tomaselli and Zipes, 2004). In response to certain stressors, these patients exhibit ventricular remodeling, an adaptive process that initially helps to maintain normal cardiac function, but eventually becomes maladaptive, causing electrical instability and an increased risk of life-threatening ventricular arrhythmias (Konstam et al., 2011).

The chronic AV-block (CAVB) dog model is a widely used animal model to study ventricular remodeling and its relation with ventricular arrhythmias (Oros et al., 2008; Zhou et al., 2008; Wada et al., 2016). In this model, creation of third degree AV-block results in bradycardia and volume overload. To compensate for the resulting drop in cardiac output, ventricular remodeling occurs (Volders et al., 1998; Vos et al., 1998). This remodeling process reduces the so called "repolarization reserve," the ability of the heart to cope with stressors on repolarization (Roden, 1998). When repolarization is then further challenged by anesthesia and administration of a pro-arrhythmic drug such as dofetilide, early afterdepolarizations (EADs), ectopic beats, and TdP arrhythmias start to occur (Dunnink et al., 2010).

Ventricular remodeling is a complex process and can be divided into multiple components, such as structural, electrical, and contractile remodeling. However, the contribution of each of the three different components to arrhythmogenesis is not fully elucidated. Previous studies have shown that electrical remodeling is an important contributor to the susceptibility of TdP, (Vos et al., 1998) while structural remodeling is not a prerequisite (Schoenmakers et al., 2003). Electrical remodeling, which is reflected by prolongation of the action potential duration (APD) and increased spatial and temporal dispersion of repolarization, (Verduyn et al., 1997a,b; Thomsen et al., 2006, 2007) develops in synchrony with TdP-inducibility: both are present after 2 weeks of CAVB (Vos et al., 1998; Schoenmakers et al., 2003). Structural remodeling, on the other hand, follows a much slower path and is fully present after 16 weeks of CAVB (Schoenmakers et al., 2003; Peschar et al., 2004; Donker et al., 2005).

Yet, the time course of contractile remodeling and its relation to TdP-inducibility is less well described. Contractile adaptations, as a result of changes in Ca^{2+} handling, can be measured *in vivo* by three physiological mechanisms of the heart: force-frequency relationship (FFR), mechanical restitution (MR) and post-extrasystolic potentiation (PESP). The FFR accounts for potentiation of contractility when heart rate is increased. MR and PESP relate to changes in contractile force of the extrasystolic beat and post-extrasystolic beat, respectively, when a basic stimulation train is interrupted with extrastimuli. MR represents the restoration of contractile force of the extrasystolic beat when the CI of the extrastimulus is lengthened. PESP displays the opposite behavior: when CI is shortened, the contractility of the post-extrasystolic beat is enhanced. Thus, the earlier an extrasystole occurs, the lower the contractility of the extrasystolic beat and the higher the contractility of the post-extraystolic beat.

de Groot et al. (2000) showed that FFR and PESP are altered in the CAVB-dogs after 6 weeks of remodeling and that these contractile parameters are associated with delayed afterdepolarizations (DADs) *in vivo*. Furthermore, in isolated cardiomyocytes from CAVB-dogs, Ca^{2+}-overload of the sarcoplasmic reticulum (SR) can result in spontaneous Ca^{2+} release, which triggers EADs/DADs (Sipido, 2006). However, it is unknown whether these macroscopic measures of Ca^{2+}-handling (FFR, MR, PESP) also reflect the propensity for sustained TdP-arrhythmias. If contractility and arrhythmogenesis are intertwined, contractile parameters could function as markers of pro-arrhythmia and might eventually help to identify the patient at risk for life-threatening arrhythmias. Therefore, we aimed to investigate the relation between *in vivo* contractility measures and susceptibility to TdP-arrhythmias in the CAVB dog. We assessed these measures after 2 weeks of remodeling, since CAVB-dogs are susceptible to TdP-arrhythmias from that moment onward.

Abbreviations: AAVB, acute AV-block; CAVB, chronic AV-block; CI, coupling interval; CL, cycle length; DAD, delayed afterdepolarization; EAD, early afterdepolarization; FFR, force-frequency relationship; MAPD, monophasic action potential duration; MR, mechanical restitution; NCX, Na^{+}–Ca^{2+} exchanger; PESP, post-extrasystolic potentiation; RyR2, ryanodine receptor 2; SERCA2a, sarcoplasmic reticulum Ca^{2+}-ATPase 2a; SR, sinus rhythm; STV, short-term variability; TdP, Torsade de Pointes.

MATERIALS AND METHODS

Animal handling was in accordance with the "Directive 2010/63/EU of the European Parliament and of the Council of 22 September 2010 on the protection of animals used for scientific purposes" and the Dutch law, laid down in the Experiments

on Animals Act. All experiments were performed with approval of the Central Authority for Scientific Procedures on Animals (CCD), registered as project AVD115002016531.

Animal Preparation

Eighteen adult purpose-bred mongrel dogs of either sex (Marshal, United States; 5 females, 13 males; bodyweight 26 ± 0.63 kg) were included. Experiments were performed under general anesthesia with mechanical ventilation at 12 breaths/min. The dogs were premedicated with a mixture of 0.5 mg/kg methadone, 0.5 mg/kg vetranquil and 0.02 mg/kg atropine i.m.. General anesthesia was induced with 25 mg/kg pentobarbital i.v. and maintained by isoflurane (1.5%) in a mixture of O_2 and N_2O (1:2). Periprocedurally antibiotics (ampicillin 1000 mg i.v. preoperatively and ampicillin 1000 mg i.m. postoperatively) and analgesics (metacam 0.2 mg/kg s.c. preoperatively and buprenorphine 0.3 mg i.m. postoperatively) were administered.

Ten surface-ECG leads (six limb leads, four precordial leads) were recorded throughout the experiment and stored on hard disk. Under aseptic conditions, the femoral artery and vein and carotid artery were dissected and sheaths were placed by Seldinger technique. Right and left ventricular monophasic action potential (RV and LV MAP) catheters (Hugo Sachs Elektronik GmbH, March, Germany) and a left ventricular 7F pressure catheter (CD Leycom Inc., Zoetermeer, Netherlands) were positioned under fluoroscopic guidance.

Experimental Protocol

Two serial experiments were performed. In the first experiment, baseline surface ECG, LV, and RV MAPD and left ventricular pressure during SR were recorded. Subsequently, His bundle ablation was done as described previously (Schoenmakers et al., 2003). When the idioventricular rhythm (IVR) was too low, a pacemaker was implanted subcutaneously with a transvenous lead in the RV apex. At AAVB, a pacing protocol (see below) was performed and the effects on LV pressure were recorded. Next, susceptibility to TdP was tested by a pro-arrhythmic challenge with the I_{Kr} blocker dofetilide (0.025 mg/kg i.v, infused during 5 min or until the first TdP occurred). TdP was defined as a run of five or more ectopic beats, with twisting morphology of the QRS-complexes. When ≥3 TdP occurred in the first 10 min after start of dofetilide administration, the dog was considered inducible.

During the second experiment, after 2 weeks of remodeling at CAVB2, baseline ECG, LV and RV MAPD and left ventricular pressure were recorded and the pacing protocol and susceptibility test with dofetilide were repeated.

Pacing Protocol

FFR, MR, and PESP were measured during a pacing protocol from the LV MAP catheter. The FFR protocol consisted of 3 min of steady-state pacing at three different CLs of 300 ms, 750 ms, and 1200 ms. For the MR and PESP protocol, the LV was paced with a basic CL of 600 ms, which was interrupted every 20th beat by an extrastimulus with an incremental CI ranging from 250 ms up to 800 ms, with steps of 50 ms.

Data Analysis

Contractility Measures

As a measure of contractility, the maximal slope of left ventricular pressure rise (LV dP/dt_{max}) was calculated offline with computer software (Conduct NT, CD Leycom). For the FFR, the mean LV dP/dt_{max} of five consecutive beats was used at the three stimulation frequencies. A straight line was fitted through these points and its slope was calculated to quantify the orientation of the FFR. MR and PESP were defined as the LV dP/dt_{max} of the extrasystolic and post-extrasystolic beat, respectively (**Figure 1**). In addition, normalized MR and PESP were calculated by taking the ratio of LV dP/dt_{max} of the extrasystolic and post-extrasystolic beat, respectively, to the mean LV dP/dt_{max} of the five beats immediately preceding the extrasystole. Both MR and PESP were fitted to monoexponential functions using non-linear least squares regression, with the equation: $y = a–b^{*}e^{-\frac{x}{TC}}$ for MR and $y = a + b^{*}e^{-\frac{x}{TC}}$ for PESP to calculate the time constant (TC) of MR and PESP.

Electrophysiological Measures

Measurement of RR-interval and QT-interval was performed with calipers on lead II of the surface ECG by use of a software program (EPTracer, Cardiotek, Heilbronn, Germany). QT-interval was corrected for heart rate (QT_c) with the van der Water formula (Van de Water et al., 1989), which gives a better estimate than Bazett formula in anesthetized dogs.

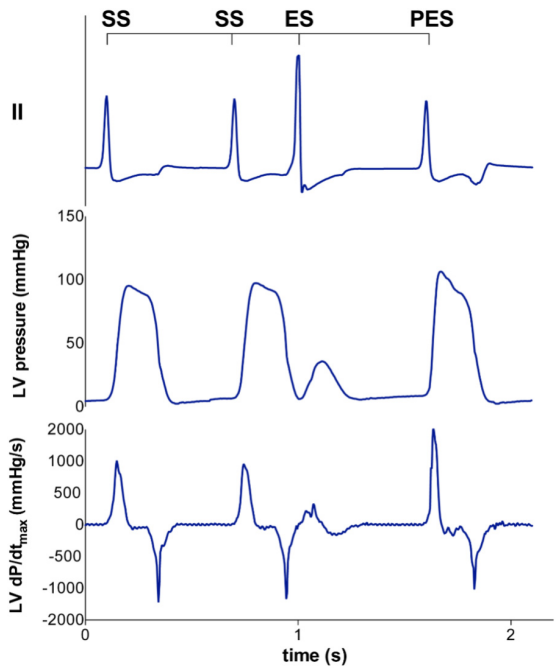

FIGURE 1 | Representative tracing of LV pressure and LV dP/dt_{max} of the extrasystolic and postextrasystolic beat. A steady state stimulation train (SS) is interrupted with an extrasystolic beat (ES) at different coupling interval (CI), followed by a post-extrasystolic beat (PES) at a fixed CI. With decremental CI of the ES, the LV dP/dt_{max} of the ES decreases, while the LV dP/dt_{max} of the PES increases.

LV and RV MAPD were measured from the initial peak to 80% of repolarization in a custom-made MATLAB software program. We defined interventricular dispersion (ΔMAPD) as the difference between LV MAPD and RV MAPD. STV of LV MAPD (STV) was calculated over 31 consecutive beats using the formula: $\mathrm{STV} = \sum |D_{n+1} - D_n|/30 \times \sqrt{2}$, where D represents LV MAPD. STV after dofetilide challenge was measured just prior to the first ectopic beat.

Statistical Analysis

Data are expressed as mean ± standard error of the mean (SEM). Serial data were analyzed with a paired Student's *t*-test or a repeated measure analysis of variance (ANOVA) with *post hoc* Bonferroni correction. Group analysis was performed with an unpaired Student's *t*-test. Correlation analysis was done with Pearson's correlation coefficient. All statistical analyses were performed with GraphPad Prism 6.0 (GraphPad Software Inc., La Jolla, CA, United States). A p-value < 0.05 was considered as statistically significant.

RESULTS

Contractile Remodeling

Contractile parameters at AAVB and CAVB are shown in **Figure 2**. Contractile remodeling was present after 2 weeks of CAVB, as seen by a significant increase in LV dP/dt_{max} during IVR compared to AAVB (**Figure 2A**). At AAVB, a positive FFR was observed with augmentation of LV dP/dt_{max} at higher frequencies (**Figure 2B**). This relationship was blunted at CAVB2. At AAVB, the MR curve demonstrated a monoexponential rise in LV dP/dt_{max} toward a plateau with lengthening of the CI. The PESP curve displayed the opposite behavior. (**Figures 2C,D**). Both these parameters were increased at CAVB2.

Electrical Remodeling

The course of electrical remodeling is depicted in **Table 1**. At AAVB, all electrophysiological parameters have adapted to the sudden drop in heart rate. When challenged with dofetilide, a further significant increase was seen in QT, LV and RV MAPD, and STV. After 2 weeks of CAVB, electrical remodeling was present, as seen by a significant increase in QT, QTc, and LV MAPD under baseline conditions compared to AAVB. RV MAPD did not increase to the same extent as LV MAPD, thus creating a high interventricular dispersion (ΔMAPD). Finally, also STV showed a significant increase, which was further augmented after infusion of dofetilide.

Contractile and Electrical Remodeling and Susceptibility to TdP

Of the 18 dogs tested, one was susceptible to dofetilide-induced TdP at AAVB. After 2 weeks of CAVB, 12/18 dogs (67%, $p = 0.002$ compared to AAVB) were inducible after dofetilide infusion. Separate measurement of contractile parameters of the

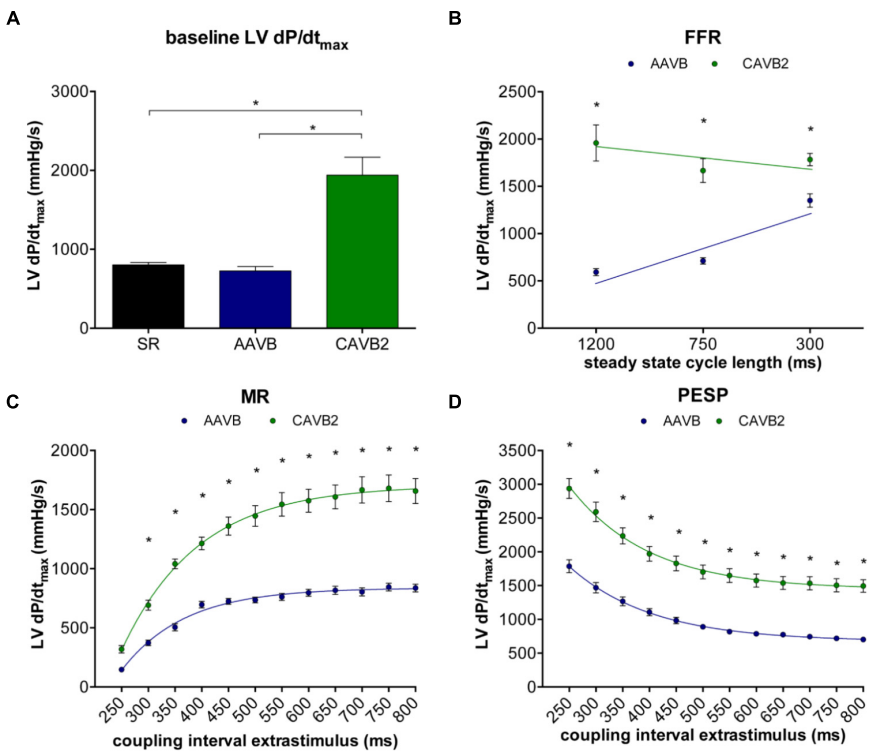

FIGURE 2 | Contractile parameters at acute AV-block (AAVB) and chronic AV-block (CAVB2). **(A)** LV dP/dtmax at baseline. **(B)** Force-frequency relationship (FFR). **(C)** Mechanical restitution (MR). **(D)** Post-extrasystolic potentiation (PESP). *$p < 0.05$ compared to AAVB.

TABLE 1 | Electrophysiological parameters.

	SR	AAVB	AAVB + dof	CAVB2	CAVB2 + dof
RR (ms)	571 ± 11	1048 ± 72*	1229 ± 75	1262 ± 47†	1452 ± 62§
QT (ms)	261 ± 4	327 ± 9*	552 ± 22†	421 ± 16†	593 ± 19§
QTc (ms)	298 ± 3	319 ± 9*	543 ± 30†	398 ± 14†	553 ± 19§
LV MAPD (ms)	193 ± 3	240 ± 6*	454 ± 23†	302 ± 12†	470 ± 30§
RV MAPD (ms)	190 ± 14	216 ± 6*	345 ± 10†	245 ± 6	341 ± 22§
ΔMAPD (ms)	9 ± 2	24 ± 5*	138 ± 24†	56 ± 8†	130 ± 25§
STV (ms)	0.36 ± 0.02	0.72 ± 0.10*	1.91 ± 0.22†	1.51 ± 0.31†	2.66 ± 0.34§

*$p < 0.05$ versus SR. †$p < 0.05$ versus AAVB. § $p < 0.05$ versus CAVB2.

inducible and non-inducible dogs are depicted in **Figure 3**. At AAVB, no differences were found in contractile measures between the two groups. However, at CAVB2, the inducible dogs demonstrated a completely different pattern of contractile remodeling compared to the non-inducible dogs. At low stimulation frequency with a CL of 1200 ms, the inducible subjects had augmentation of contractility compared to the non-inducible dogs (2354 ± 168 mmHg/s versus 1091 ± 59 mmHg/s, $p < 0.001$; **Figure 3A**). Furthermore, the slope of the FFR-curve was inverted in the inducible dogs, while the non-inducible dogs retained their positively oriented FFR (slope of −0.51 ± 0.19 in inducible dogs versus 0.89 ± 0.06 in non-inducible dogs, $p < 0.001$). As seen from **Table 2**, these differences in LV dP/dt_{max} between inducible and non-inducible dogs are not due to differences in end-diastolic pressure (EDP). A significantly higher end-systolic pressure (ESP) is seen in the inducible dogs at low stimulation rate.

At small CIs, MR was similar in both groups, but diverged when the CI of the extrasystole rised above 450 ms, after which the susceptible dogs showed a significantly higher LV dP/dt_{max} (1483 ± 96 mmHg/s versus 1117 ± 31 mmHg/s, $p = 0.01$, **Figure 3B**). PESP, on the other hand, was increased in the inducible dogs at whole range of CIs (**Figure 3C**). When MR was normalized to the LV dP/dt_{max} of the preceding beats, the TC of MR appeared significantly higher in the inducible dogs (TC = 158 ± 7 ms versus TC = 97 ± 8 ms in non-inducible dogs, $p < 0.001$, **Figure 4A**). Normalized PESP was similar between the groups and had equal TC (143 ± 9 ms versus 153 ± 4 ms, $p = 0.46$, **Figure 4B**).

Electrically, no differences were found between the two groups at AAVB. At CAVB, the RR-interval, QT- and QTc-interval, LV MAPD, RV MAPD, and ΔMAPD were similar between the inducible and non-inducible dogs (**Table 3**). Only STV could distinguish between inducible and non-inducible dogs both at baseline and when challenged with dofetilide. Dogs that were inducible to drug-induced TdP had significantly higher STV at baseline (1.98 ± 0.41 ms versus 0.61 ± 0.08 ms, $p = 0.009$) which increased even more when challenged with dofetilide (3.18 ± 0.36 ms versus 1.35 ± 0.08 ms, $p = 0.001$).

Relation of Contractile and Electrical Remodeling With Severity of Arrhythmias

In order to quantify the severity of arrhythmias, we developed a new weighted scoring system, which takes into account both the number of arrhythmias in 10 min and whether the arrhythmias were sustained or defibrillations were needed (**Table 4**). This weighted score was correlated with both contractile and electrical remodeling. As illustrated in **Figure 5**, a linear correlation was found between this weighted score and LV dP/dt_{max} at CL of 1200 ms ($r = 0.71$, $p = 0.002$), the slope of FFR ($r = -0.58$, $p = 0.01$) and TC of MR ($r = 0.66$, $p = 0.003$). Of the electrical parameters, STV at baseline was also correlated with the weighted score of arrhythmic severity ($r = 0.74$, $p = 0.0006$).

The Effect of Ouabain on Contractility and TdP-Inducibility

As a proof of principle of the importance of contractile remodeling and Ca^{2+}-overload for the inducibility of TdP-arrhythmias in the CAVB dog model, we attempted to pharmacologically increase Ca^{2+}-load to alter FFR and potentially convert an initial non-inducible dog into an inducible one. Four non-inducible dogs were given a single dose of the cardiac glycoside ouabain (0.045 mg/kg i.v. in 1 min) prior to administration of dofetilide. In **Figure 6**, the effects of ouabain administration on FFR are depicted. In all dogs, ouabain resulted in a rise in contractility. Ouabain itself did not induce any arrhythmias. Unfortunately, in three out of four dogs, contractility at a CL of 1200 ms could not reach a level comparable to that of the inducible dogs and retained a positive FFR. As expected, these three dogs remained non-inducible after additional dofetilide infusion. Nevertheless, in one dog, contractility after ouabain administration increased to a level similar to that of the inducible dogs, with a more blunted FFR. Interestingly, this dog did become inducible to TdP-arrhythmias after infusion of dofetilide (**Figure 7**).

DISCUSSION

The results of this study demonstrate that contractile remodeling is already present after 2 weeks of CAVB and that this remodeling process differs substantially between TdP-susceptible and TdP-resistant dogs. Moreover, the more contractile or electrical remodeling have occurred, the higher the number and severity of arrhythmias after dofetilide challenge. Alterations in Ca^{2+}-homeostasis may be the common denominator that explains the observed relation between contractile remodeling and arrhythmogenesis in the CAVB-dog model.

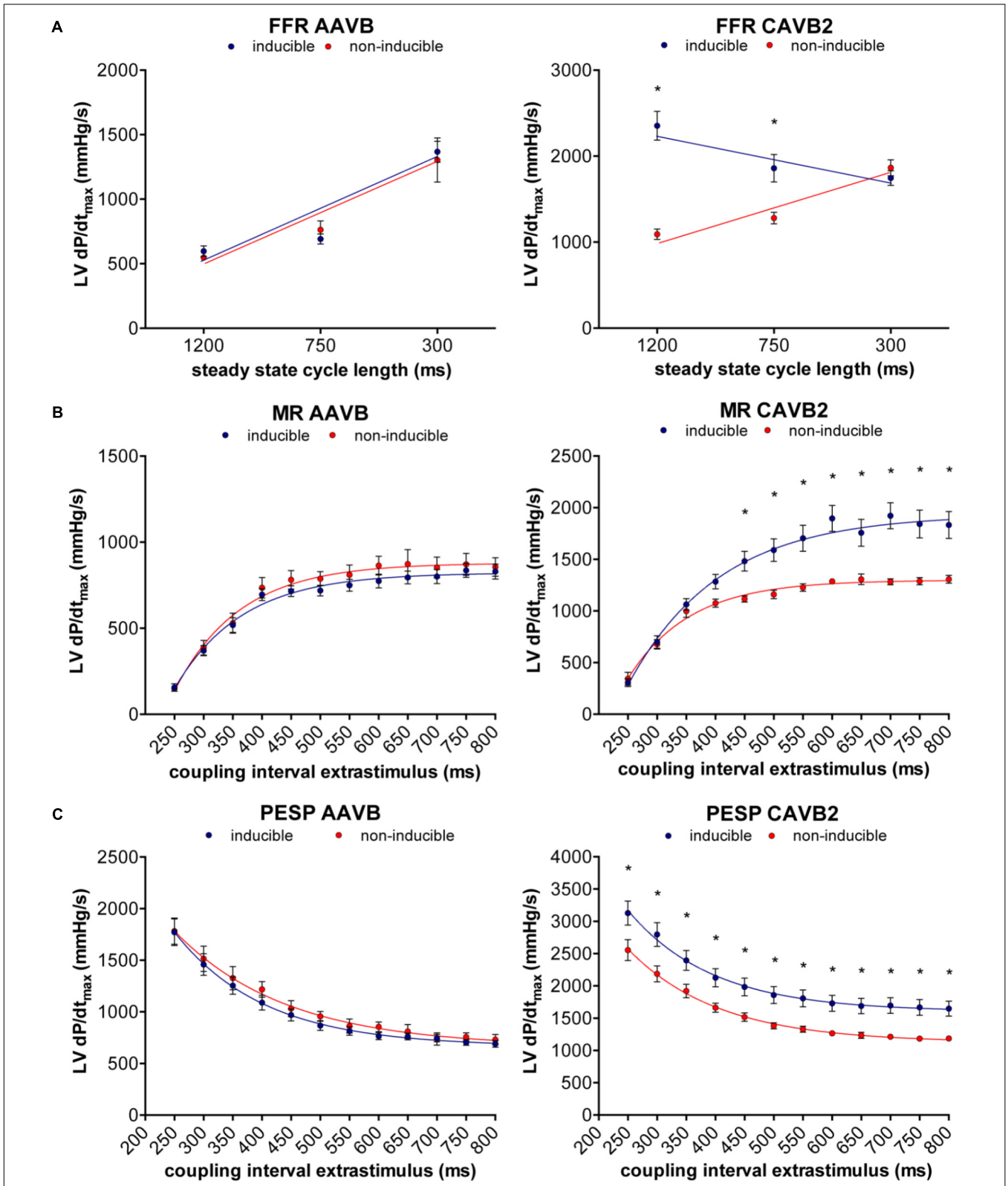

FIGURE 3 | Relation between contractile remodeling and susceptibility to TdP. **(A)** FFR, **(B)** MR, and **(C)** PESP of inducible dogs (blue line) and non-inducible dogs (red line) at AAVB (left) and at CAVB2 (right). *$p < 0.05$ compared to non-inducible.

TABLE 2 | Hemodynamic parameters of non-inducible and inducible dogs.

		AAVB		CAVB	
		non-inducible	inducible	non-inducible	Inducible
LV EDP (mmHg)	CL 1200 ms	14 ± 2	16 ± 1	12 ± 2	11 ± 1
	CL 750 ms	14 ± 2	16 ± 1	10 ± 2	10 ± 1
	CL 300 ms	14 ± 1	15 ± 1	11 ± 3	9 ± 1
LV ESP (mmHg)	CL 1200 ms	60 ± 4	55 ± 4	73 ± 3	88 ± 2*
	CL 750 ms	63 ± 9	62 ± 2	85 ± 3	85 ± 3
	CL 300 ms	69 ± 9	69 ± 4	87 ± 6	77 ± 4
LV dP/dtmax (mmHg/s)	CL 1200 ms	547 ± 10	597 ± 42	1091 ± 59	2354 ± 168*
	CL 750 ms	763 ± 69	692 ± 39	1280 ± 68	1860 ± 160*
	CL 300 ms	1304 ± 170	1368 ± 81	1865 ± 94	1745 ± 86

$p < 0.05$ versus non-inducible during dofetilide infusion.

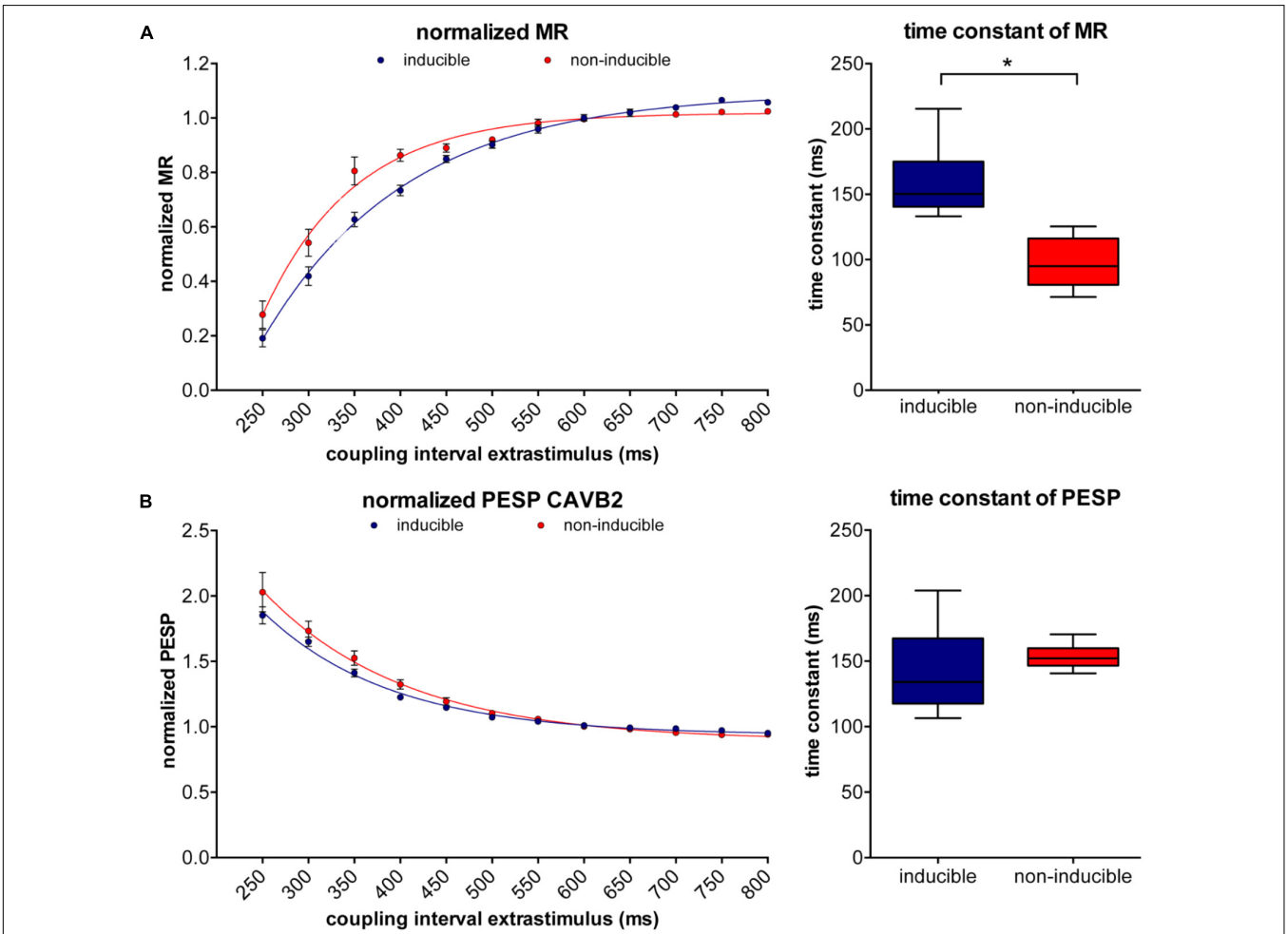

FIGURE 4 | Normalized MR and PESP curves of inducible and non-inducible dogs. **(A)** The inducible dogs show slower restitution compared to the non-inducible dogs (left) with significantly higher time constants (TCs; right). **(B)** Normalized PESP curves are similar in inducible dogs and non-inducible dogs. *$p < 0.05$.

Ca^{2+} Overload, DADs, and EADs in the CAVB-Dog

The present study is, to our knowledge, the first to show a direct relation between *in vivo* measurements of contractility and inducibility of TdP-arrhythmias. Nevertheless, the relation between disturbances of Ca^{2+}-homeostasis and arrhythmogenesis on a cellular level is well established. Previous *in vitro* studies have demonstrated altered Ca^{2+} handling in isolated cardiomyocytes of CAVB-dogs with increased amplitude

TABLE 3 | Electrophysiological parameters of non-inducible and inducible dogs.

	Baseline		Dofetilide	
	Non-inducible	**Inducible**	**Non-inducible**	**Inducible**
RR (ms)	1272 ± 33	1257 ± 69	1507 ± 107	1373 ± 72
QT (ms)	383 ± 19	439 ± 20	596 ± 50	587 ± 25
LV MAPD (ms)	292 ± 23	308 ± 14	494 ± 48	460 ± 39
RV MAPD (ms)	236 ± 9	249 ± 8	378 ± 53	328 ± 23
ΔMAPD (ms)	57 ± 10	56 ± 9	116 ± 14	135 ± 35
STV (ms)	0.61 ± 0.08	1.98 ± 0.41*	1.35 ± 0.08	3.18 ± 0.36†

*$p < 0.05$ versus non-inducible in baseline. †$p < 0.05$ versus non-inducible during dofetilide infusion.

TABLE 4 | Custom-made weighted score of the number and severity of arrhythmias.

Arrhythmia	**Points**
Single ectopic beat	1
Double ectopic beats	2
Triple ectopic beats	3
Four ectopic beats	4
nsTdP (<50 complexes)	10
Sustained TdP (>50 complexes) or defibrillation	100
>1 consecutive defibrillations	200

Score is the total number of points during 10 min after start of dofetilide infusion.

and duration of Ca^{2+}-transients along with a higher Ca^{2+}-content of the SR (Sipido et al., 2002). Furthermore, NCX is upregulated, which contributes to further loading of the SR via "reverse mode" Ca^{2+}-influx (Sipido et al., 2000). The resulting SR Ca^{2+} overload is associated with spontaneous SR Ca^{2+} release, which can generate a DAD via "forward mode" function of NCX (exchange of 1 Ca^{2+}-ion for 3 Na^{+}-ions, creating an inward current) (Pogwizd and Bers, 2002). Furthermore, it has become more and more evident that altered Ca^{2+} cycling and upregulation of NCX also play a role in the formation of EADs, which has been regarded as the most important trigger of TdP arrhythmias (Volders et al., 2000; Němec et al., 2010; Horváth et al., 2015).

Our results are consistent with the study by de Groot et al. (2000) which showed that the highest LV dP/dt_{max} postpacing, which reflects an increased SR-load, was associated with the occurrence of DADs on MAP recordings. Since DADs and EADs share a common molecular mechanism, we expected to find the same relation between enhanced contractility and susceptibility of TdP-arrhythmias.

Force-Frequency Relationship and TdP-Arrhythmias

A blunted or inverted FFR has been observed in isolated muscle preparations of failing myocardium (Pieske et al., 1995, 1999, 2002) as well as in animal models (Eising et al., 1994; Neumann et al., 1998) or patients with cardiac dysfunction (Feldman et al., 1988; Hasenfuss et al., 1994; Schotten et al., 1999). In the CAVB-dog, FFR has also shown to be inverted, with increased contractility at low heart rates (de Groot et al., 2000; Peschar et al., 2004).

In the present study we observed the inverted FFR only in the inducible dogs, while the FFR of the non-inducible dogs remained positive (**Figure 3A**). There is strong evidence that increased $[Na]_i$ during diastole plays a central role in the inversion of the FFR (Mubagwa et al., 1997; Mills et al., 2007). A study on rabbit papillary muscle strips examined the effect of increased $[Na]_i$ on FFR and showed that treatment with the Na^+ ionophore monensin, which increases diastolic $[Na]_i$, could convert a positive FFR into a negative FFR, mainly by increasing contractility at lower heart rates (Mubagwa et al., 1997). The high diastolic $[Na]_i$ will favor Ca^{2+} influx via NCX and since the ratio of diastole to systole is highest at low heart rates, Ca^{2+} loading of the SR will be enhanced, resulting in increased contractility. Dogs with CAVB have approximately 4 mM higher $[Na]_i$, compared to controls, probably due to reduced $[Na]_i$-affinity of the Na^+-K^+-ATPase and increased Na^+-influx via the Na^+-H^+-exchanger type 1 (NHE-1) (Verdonck et al., 2003; van Borren et al., 2013). However, in these studies, no dofetilide challenge was performed, therefore it is unknown whether the $[Na]_i$ is higher in inducible dogs compared to non-inducible dogs.

Nevertheless, we could hypothesize that in the inducible dogs a high $[Na]_i$ in combination with enhanced NCX activity results in Ca^{2+}-overload, spontaneous Ca^{2+} release, and subsequent EADs and TdP-arrhythmias. Supporting this hypothesis, it has been shown that lowering $[Na]_i$ by administration of the selective late Na^+-current blocker ranolazine could reduce the number of EADs *in vitro* and TdP-arrhythmias *in vivo* (Antoons et al., 2010). In addition, blockade of NCX by SEA-0400 is effective in prevention of TdP-arrhythmias in the CAVB dog (Bourgonje et al., 2013).

As a proof of concept, we tried to increase $[Na]_i$ in the non-inducible dogs by blockade of the Na^+-K^+-ATPase with ouabain. In contrast to the cardiac glycoside digitalis, ouabain has a fast onset of action, reaching his maximum after 5 min of administration (Fuerstenwerth, 2014). The increased $[Na]_i$ caused by inhibition of the Na-K-ATPase will be exchanged for Ca^{2+}, causing Ca^{2+}-overload of the cardiomyocyte that is responsible for both the inotropic and potential arrhythmogenic effects. As we have shown, only the dog that could reach the contractility level of the inducible dogs and developed a more

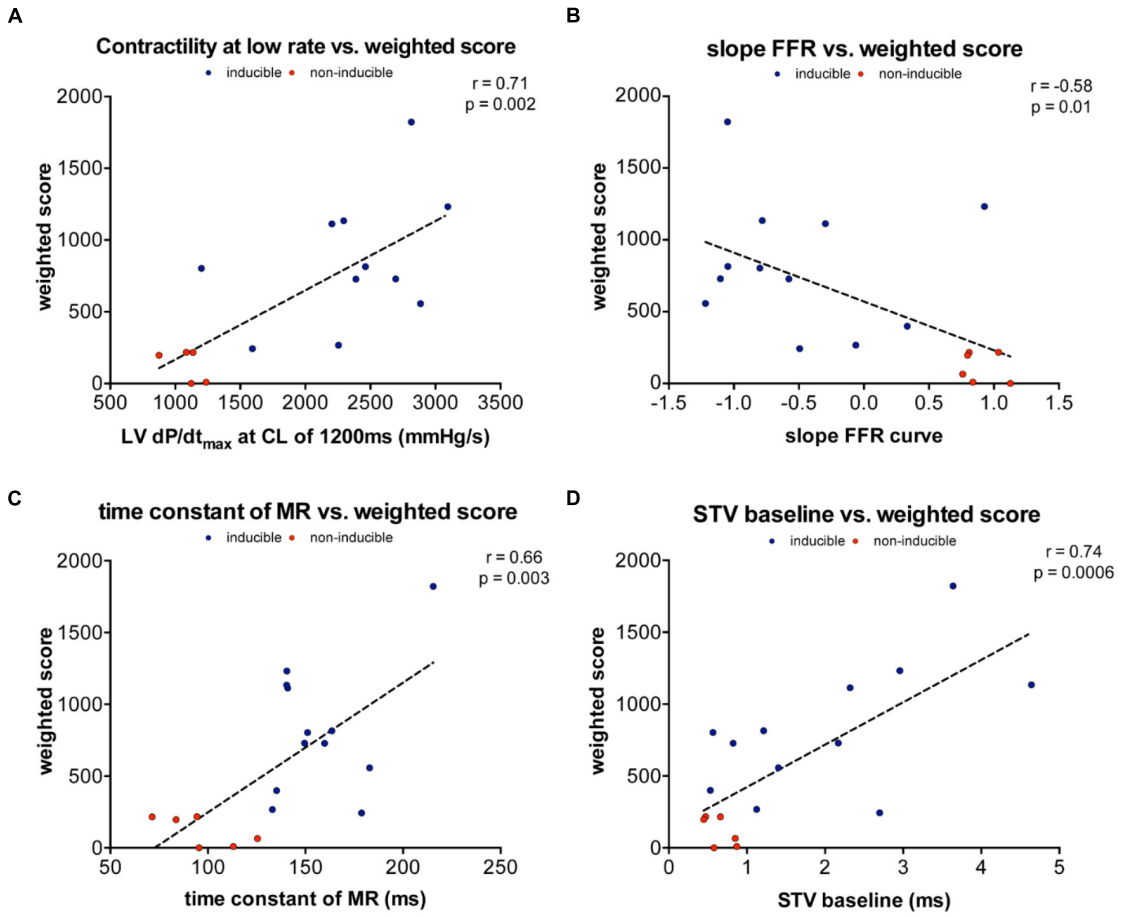

FIGURE 5 | Linear correlations between weighted arrhythmia score and contractile and electrical remodeling. **(A)** Linear correlation between weighted and contractility at 1200 ms (r = 0.71, p = 0.002). **(B)** Linear correlation between weighted score and slope of FFR (r = –0.58, p = 0.01). **(C)** Linear correlation between weighted score and TC of MR (r = 0.66, p = 0.003). **(D)** Linear correlation between weighted score and STV at baseline (r = 0.74, p = 0.0006).

blunted FFR, became susceptible to dofetilide-induced TdP, which further illustrates the importance of $[Na]_i$ and $[Ca^{2+}]_i$ for the initiation of TdP-arrhythmias.

Mechanical Restitution/Post-extrasystolic Potentiation and TdP-Arrhythmias

We have demonstrated that inducible dogs have a higher MR and PESP and slower MR kinetics compared to the non-inducible dogs. In previous studies altered MR and PESP have been found in patients with hypertrophy and heart failure. (Beck et al., 1971; Merillon et al., 1979; Seed et al., 1984; Prabhu and Freeman, 1995). Both phenomena are explained by time-dependent availability of releasable Ca^{2+} due to gradual translocation of releasable Ca^{2+} from an uptake compartment to a release compartment or because of a time-dependent recovery of the SR Ca^{2+}-release channel, the RyR2.

Discussion on the mechanism of slower MR in the CAVB dog remains speculative, since the kinetics of RyR2 have never been investigated. Furthermore, the precise molecular mechanism behind inactivation and recovery of RyR2 remains controversial (Bers, 2008). First, it can be hypothesized that the intrinsic gating properties of the RyR2 have been altered by the remodeling process. Secondly, changes in cytosolic $[Ca^{2+}]$ have been proposed to influence the inactivation of RyR2, referred to as Ca^{2+}-dependent inactivation. It is hypothesized that increased dyadic $[Ca]_i$, which is responsible for RyR2 activation, might also play a role in RyR2 inactivation (Laver, 2005). Thirdly, RyR refractoriness might be caused by "functional depletion" of Ca^{2+} of the SR after global Ca^{2+}-release. Refilling of the SR during Ca^{2+}-reuptake increases the sensitivity of RyR2 to cytosolic Ca^{2+} and accelerates recovery from inactivation (Szentesi et al., 2004). Since Ca^{2+} homeostasis is an interplay between RyR2, SERCA2a, and NCX, we can assume that alterations in expression and function of one of these proteins, will subsequently affect normal function of the others. Increased NCX function could result in "relatively" diminished activity of SERCA2a, by changing the ratio of Ca^{2+} extrusion versus reuptake. In this regard, a study in a transgenic mouse model showed that overexpression of phospholamban, the main inhibitor of SERCA2a, caused a reduced reuptake of Ca^{2+} in the SR, but also resulted in a

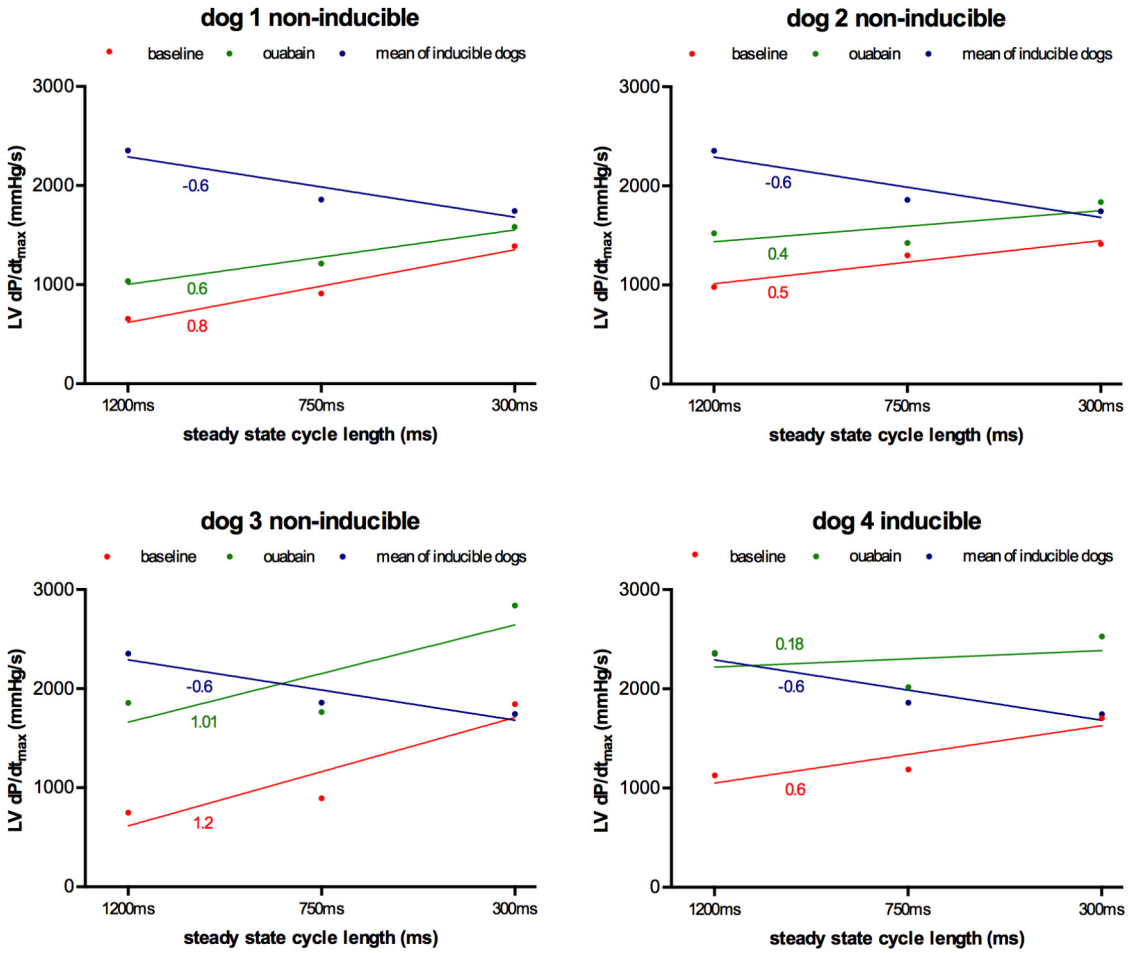

FIGURE 6 | Effect of ouabain on force-frequency relationship in non-inducible subjects (n = 4). Contractility at CL of 1200, 750, and 300 ms at baseline (red line) and after ouabain (green line) in four non-inducible dogs. As comparison, the mean of the inducible dogs is shown (blue line). Only dog 4 became inducible after ouabain in combination with dofetilide. TCs of the different curves are given.

higher TC of MR and increased PESP compared to control, just as we found in the inducible dogs (Hoit et al., 1999, 2000). Furthermore, in isolated cardiomyocytes, inhibition of SERCA2a could significantly slow down recovery from inactivation of RyR2 (Szentesi et al., 2004). Thus, increased NCX function, which contributes to susceptibility to triggered arrhythmias in the CAVB-dog, might indirectly influence SERCA2a and RyR2 function, and thus alter MR and PESP *in vivo*.

Electrical Remodeling and TdP-Arrhythmias

Electrically, we found that only STV can distinguish between inducible and non-inducible subjects. This is in line with previous studies on STV in the CAVB dog model, which show that STV both at baseline and after dofetilide infusion is a more powerful predictor of drug-induced TdP arrhythmias compared to the QT-interval or LV MAPD itself (Thomsen et al., 2004, 2006, 2007). The molecular basis of STV is not fully elucidated, but have been attributed to alterations in Ca^{2+} handling. In isolated cardiomyocytes, β-adrenergic stimulation during reduced repolarization reserve (blockade of the repolarization current I_{Ks}) resulted in increased cellular Ca^{2+} load and spontaneous Ca^{2+} release, which was associated with increased STV and the occurrence of DADs and EADs (Johnson et al., 2010, 2013). Buffering of Ca^{2+} by BAPTA-AM, blockade of SR Ca^{2+} release with ryanodine or inhibition of NCX by SEA0400 led to a drastic reduction of STV and eliminated all DADs and EADs (Johnson et al., 2010, 2013). A study by Antoons et al. (2015) showed that STV is highly dependent on SR Ca^{2+} release, which can modulate Ca^{2+}-dependent currents making the heart more prone to EADs. These data support the hypothesis that increased STV reflects disrupted Ca^{2+}-homeostasis as the underlying mechanism of EADs and TdP-arrhythmias in the CAVB-dog.

Clinical Implications

Since the CAVB dog model is a specific model of compensated hypertrophy caused by volume overload, extrapolation to a population of patients with heart failure with reduced

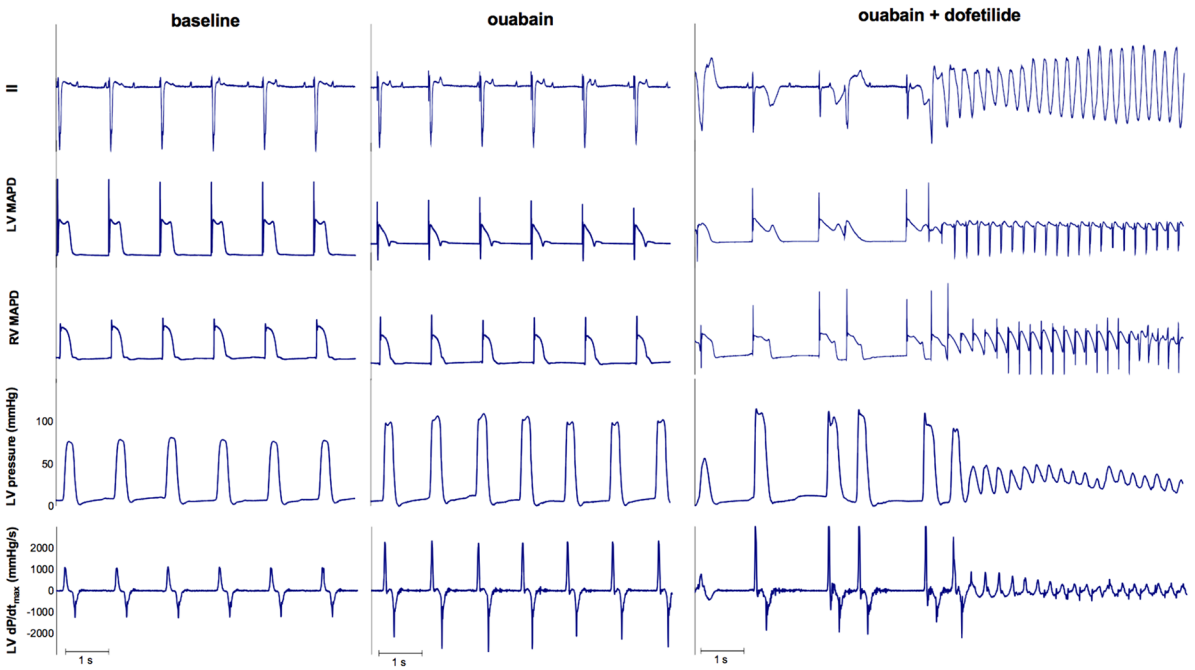

FIGURE 7 | ECG, LV MAP, RV MAP, LV pressure, and LV dP/dt_{max} of dog 4. Administration of ouabain did not cause any arrhythmias. However, the combination of ouabain and dofetilide resulted in Torsade de Pointes arrhythmias.

ejection fraction should be done with caution. Nevertheless, since contractile remodeling and arrhythmogenesis are related, contractile parameters might be used in risk stratification of ventricular arrhythmias and sudden cardiac death. In addition, patients with heart failure with preserved ejection fraction (HF-pEF) have also been shown to exhibit disrupted Ca^{2+}-handling, therefore the contractile parameters investigated in this study could also be used in these patients. Recently, a study of a non-invasive measurement of PESP of blood pressure, measured via a photoplethysmographic device, showed that higher PESP was correlated with increased mortality in myocardial infarction survivors (Sinnecker et al., 2014). The cause of death was not stratified in this study, however, increased PESP may be associated with increased arrhythmia risk. The currently ongoing "EUropean Comparative Effectiveness Research to assess the use of primary prophylacTic Implantable Cardioverter Defibrillators" (EU-CERT-ICD) study evaluates the relationship between non-invasive measured PESP and the incidence of ICD-shocks in a primary prevention ICD-population. This study will give further insight if non-invasive measures of contractility could function as predictors of life-threatening arrhythmias.

Limitations

No direct measurements of Ca^{2+} transients or SR function have been done, therefore hypotheses on mechanism of contractile remodeling and the relation with TdP-arrhythmias are based on assumptions derived from previous molecular work. Explanations other than related to Ca^{2+}-handling may also be possible, such as mechano-electrical feedback, i.e., direct effects of altered loading conditions on repolarization. Secondly, LV dP/dt_{max} has important limitations as a measure of contractility, since it is also dependent on ventricular loading. While we did not measure ventricular volumes, we have shown that EDP are not different between inducible and non-inducible dogs. Therefore, we can assume the differences found in LV dP/dt_{max} are predominantly caused by changes in contractility. Finally, the relation between contractile remodeling and TdP was only measured at CAVB2, therefore no conclusion can be made on this association later in the remodeling process.

CONCLUSION

In the CAVB dog model, contractile and electrical remodeling are already present after 2 weeks of AV-block and develop concomitantly with susceptibility to dofetilide-induced TdP. Furthermore, contractile parameters are altered to a far larger extent in inducible dogs, as seen by development of an augmented negative FFR, higher maximal response of MR and PESP and slowed MR kinetics.

AUTHOR CONTRIBUTIONS

DS did experimental work, analysis of data, and wrote the manuscript. JB delivered technical support during experiments. MS contributed to experimental concepts and design of the study. MV was responsible for organization of experiments and revised the manuscript thoroughly. All authors approved the submitted version.

FUNDING

The research leading to these results has received funding from the European Community's Seventh Framework Programme FP7/2007-2013 under grant agreement no. 602299, EU-CERT-ICD. The results have been presented as an abstract at the European Heart Rhythm Association (EHRA) congress 2018 and Heart Rhythm annual scientific sessions 2018.

REFERENCES

Antoons, G., Johnson, D. M., Dries, E., Santiago, D. J., Ozdemir, S., Lenaerts, I., et al. (2015). Calcium release near L-type calcium channels promotes beat-to-beat variability in ventricular myocytes from the chronic AV block dog. *J. Mol. Cell. Cardiol.* 89, 326–334. doi: 10.1016/j.yjmcc.2015.10.008

Antoons, G., Oros, A., Beekman, J. D. M., Engelen, M. A., Houtman, M. J. C., Belardinelli, L., et al. (2010). Late Na+ current inhibition by ranolazine reduces torsades de pointes in the chronic atrioventricular block dog model. *J. Am. Coll. Cardiol.* 55, 801–809. doi: 10.1016/j.jacc.2009.10.033

Beck, W., Chesler, E., and Schrire, V. (1971). Postextrasystolic ventricular pressure responses. *Circulation* 44, 523–533. doi: 10.1161/01.CIR.44.4.523

Bers, D. M. (2008). Calcium cycling and signaling in cardiac myocytes. *Annu. Rev. Physiol.* 70, 23–49. doi: 10.1146/annurev.physiol.70.113006.100455

Bourgonje, V. J. A., Vos, M. A., Ozdemir, S., Doisne, N., Acsai, K., Varro, A., et al. (2013). Combined Na+/Ca2+ exchanger and l-type calcium channel block as a potential strategy to suppress arrhythmias and maintain ventricular function. *Circ. Arrhythm. Electrophysiol.* 6, 371–379. doi: 10.1161/CIRCEP.113.000322

de Groot, S. H., Schoenmakers, M., Molenschot, M. M., Leunissen, J. D., Wellens, H. J., and Vos, M. A. (2000). Contractile adaptations preserving cardiac output predispose the hypertrophied canine heart to delayed afterdepolarization-dependent ventricular arrhythmias. *Circulation* 102, 2145–2151. doi: 10.1161/01.CIR.102.17.2145

Donker, D. W., Volders, P. G., Arts, T., Bekkers, B. C., Hofstra, L., Spätjens, R. L., et al. (2005). End-diastolic myofiber stress and ejection strain increase with ventricular volume overload–Serial in-vivo analyses in dogs with complete atrioventricular block. *Basic Res. Cardiol.* 100, 372–382. doi: 10.1007/s00395-005-0525-8

Dunnink, A., Sharif, S., Oosterhoff, P., Winckels, S., Montagne, D., Beekman, J., et al. (2010). Anesthesia and arrhythmogenesis in the chronic atrioventricular block dog model. *J. Cardiovasc. Pharmacol.* 55, 601–608. doi: 10.1097/FJC.0b013e3181da7768

Eising, G. P., Hammond, H. K., Helmer, G. A., Gilpin, E., and Ross, J. (1994). Force-frequency relations during heart failure in pigs. *Am. J. Physiol.* 267, H2516–H2522. doi: 10.1152/ajpheart.1994.267.6.H2516

Feldman, M. D., Alderman, J. D., Aroesty, J. M., Royal, H. D., Ferguson, J. J., Owen, R. M., et al. (1988). Depression of systolic and diastolic myocardial reserve during atrial pacing tachycardia in patients with dilated cardiomyopathy. *J. Clin. Invest.* 82, 1661–1669. doi: 10.1172/JCI113778

Fuerstenwerth, H. (2014). On the differences between ouabain and digitalis glycosides. *Am. J. Ther.* 21, 35–42. doi: 10.1097/MJT.0b013e318217a609

Hasenfuss, G., Holubarsch, C., Hermann, H. P., Astheimer, K., Pieske, B., and Just, H. (1994). Influence of the force-frequency relationship on haemodynamics and left ventricular function in patients with non-failing hearts and in patients with dilated cardiomyopathy. *Eur. Heart J.* 15, 164–170. doi: 10.1093/oxfordjournals.eurheartj.a060471

Hoit, B. D., Kadambi, V. J., Tramuta, D. A., Ball, N., Kranias, E. G., and Walsh, R. A. (2000). Influence of sarcoplasmic reticulum calcium loading on mechanical and relaxation restitution. *Am. J. Physiol. Heart Circ. Physiol.* 278, H958–H963. doi: 10.1152/ajpheart.2000.278.3.H958

Hoit, B. D., Tramuta, D. A., Kadambi, V. J., Dash, R., Ball, N., Kranias, E. G., et al. (1999). Influence of transgenic overexpression of phospholamban on postextrasystolic potentiation. *J. Mol. Cell. Cardiol.* 31, 2007–2015. doi: 10.1006/jmcc.1999.1031

Horváth, B., Hegyi, B., Kistamás, K., Váczi, K., Bányász, T., Magyar, J., et al. (2015). Cytosolic calcium changes affect the incidence of early afterdepolarizations in canine ventricular myocytes 1. *Can. J. Physiol. Pharmacol.* 93, 527–534. doi: 10.1139/cjpp-2014-0511

Johnson, D. M., Heijman, J., Bode, E. F., Greensmith, D. J., van der Linde, H., Abi-Gerges, N., et al. (2013). Diastolic spontaneous calcium release from the sarcoplasmic reticulum increases beat-to-beat variability of repolarization in canine ventricular myocytes after β-adrenergic stimulation. *Circ. Res.* 112, 246–256. doi: 10.1161/CIRCRESAHA.112.275735

Johnson, D. M., Heijman, J., Pollard, C. E., Valentin, J.-P., Crijns, H. J. G. M., Abi-Gerges, N., et al. (2010). IKs restricts excessive beat-to-beat variability of repolarization during beta-adrenergic receptor stimulation. *J. Mol. Cell. Cardiol.* 48, 122–130. doi: 10.1016/j.yjmcc.2009.08.033

Konstam, M. A., Kramer, D. G., Patel, A. R., Maron, M. S., and Udelson, J. E. (2011). Left ventricular remodeling in heart failure: current concepts in clinical significance and assessment. *JACC Cardiovasc. Imaging* 4, 98–108. doi: 10.1016/j.jcmg.2010.10.008

Laver, D. R. (2005). Coupled calcium release channels and their regulation by luminal and cytosolic ions. *Eur. Biophys. J.* 34, 359–368. doi: 10.1007/s00249-005-0483-y

Merillon, J. P., Motte, G., Aumont, M. C., Masquet, C., Lecarpentier, Y., and Gourgon, R. (1979). Post-extrasystolic left ventricular peak pressure with and without left ventricular failure. *Cardiovasc. Res.* 13, 338–344. doi: 10.1093/cvr/13.6.338

Mills, G. D., Harris, D. M., Chen, X., and Houser, S. R. (2007). Intracellular sodium determines frequency-dependent alterations in contractility in hypertrophied feline ventricular myocytes. *Am. J. Physiol. Heart Circ. Physiol.* 292, H1129–H1138. doi: 10.1152/ajpheart.00375.2006

Mubagwa, K., Lin, W., Sipido, K., Bosteels, S., and Flameng, W. (1997). Monensin-induced reversal of positive force–frequency relationship in cardiac muscle: role of intracellular sodium in rest-dependent potentiation of contraction. *J. Mol. Cell. Cardiol.* 29, 977–989. doi: 10.1006/jmcc.1996.0342

Němec, J., Kim, J. J., Gabris, B., and Salama, G. (2010). Calcium oscillations and T-wave lability precede ventricular arrhythmias in acquired long QT type 2. *Heart Rhythm* 7, 1686–1694. doi: 10.1016/j.hrthm.2010.06.032

Neumann, T., Ravens, U., and Heusch, G. (1998). Characterization of excitation-contraction coupling in conscious dogs with pacing-induced heart failure. *Cardiovasc. Res.* 37, 456–466. doi: 10.1016/S0008-6363(97)00246-0

Oros, A., Beekman, J. D. M., and Vos, M. A. (2008). The canine model with chronic, complete atrio-ventricular block. *Pharmacol. Ther.* 119, 168–178. doi: 10.1016/j.pharmthera.2008.03.006

Peschar, M., Vernooy, K., Cornelussen, R. N., Verbeek, X. A. A., Reneman, R. S., Vos, M. A., et al. (2004). Structural, electrical and mechanical remodeling of the canine heart in AV-block and LBBB. *Eur. Heart J. Suppl.* 6, D61–D65. doi: 10.1016/j.ehjsup.2004.05.017

Pieske, B., Kretschmann, B., Meyer, M., Holubarsch, C., Weirich, J., Posival, H., et al. (1995). Alterations in intracellular calcium handling associated with the inverse force-frequency relation in human dilated cardiomyopathy. *Circulation* 92, 1169–1178. doi: 10.1161/01.CIR.92.5.1169

Pieske, B., Maier, L. S., Bers, D. M., and Hasenfuss, G. (1999). Ca2+ handling and sarcoplasmic reticulum Ca2+ content in isolated failing and nonfailing human myocardium. *Circ. Res.* 85, 38–46. doi: 10.1161/01.RES.85.1.38

Pieske, B., Maier, L. S., Piacentino, V., Weisser, J., Hasenfuss, G., and Houser, S. (2002). Rate dependence of [Na+]i and contractility in nonfailing and failing human myocardium. *Circulation* 106, 447–453. doi: 10.1161/01.CIR.0000023042.50192.F4

Pogwizd, S. M., and Bers, D. M. (2002). Calcium cycling in heart failure: the arrhythmia connection. *J. Cardiovasc. Electrophysiol.* 13, 88–91. doi: 10.1046/j.1540-8167.2002.00088.x

Prabhu, S. D., and Freeman, G. L. (1995). Effect of tachycardia heart failure on the restitution of left ventricular function in closed-chest dogs. *Circulation* 91, 176–185. doi: 10.1161/01.CIR.91.1.176

Roden, D. M. (1998). Taking the "idio" out of "idiosyncratic": predicting torsades de pointes. *Pacing Clin. Electrophysiol.* 21, 1029–1034. doi: 10.1111/j.1540-8159.1998.tb00148.x

Schoenmakers, M., Ramakers, C., van Opstal, J. M., Leunissen, J. D. M., Londoño, C., and Vos, M. A. (2003). Asynchronous development of electrical

remodeling and cardiac hypertrophy in the complete AV block dog. *Cardiovasc. Res.* 59, 351–359. doi: 10.1016/S0008-6363(03)00430-9

Schotten, U., Voss, S., Wiederin, T. B., Voss, M., Schoendube, F., Hanrath, P., et al. (1999). Altered force-frequency relation in hypertrophic obstructive cardiomyopathy. *Basic Res. Cardiol.* 94, 120–127. doi: 10.1007/s003950050134

Seed, W. A., Noble, M. I., Walker, J. M., Miller, G. A., Pidgeon, J., Redwood, D., et al. (1984). Relationships between beat-to-beat interval and the strength of contraction in the healthy and diseased human heart. *Circulation* 70, 799–805. doi: 10.1161/01.CIR.70.5.799

Sinnecker, D., Dirschinger, R. J., Barthel, P., Muller, A., Morley-Davies, A., Hapfelmeier, A., et al. (2014). Postextrasystolic blood pressure potentiation predicts poor outcome of cardiac patients. *J. Am. Heart Assoc.* 3:e000857. doi: 10.1161/JAHA.114.000857

Sipido, K. R. (2006). Calcium overload, spontaneous calcium release, and ventricular arrhythmias. *Heart Rhythm* 3, 977–979. doi: 10.1016/j.hrthm.2006.01.013

Sipido, K. R., Volders, P. G., de Groot, S. H., Verdonck, F., Van de Werf, F., Wellens, H. J., et al. (2000). Enhanced Ca(2+) release and Na/Ca exchange activity in hypertrophied canine ventricular myocytes: potential link between contractile adaptation and arrhythmogenesis. *Circulation* 102, 2137–2144. doi: 10.1161/01.CIR.102.17.2137

Sipido, K. R., Volders, P. G. A., Schoenmakers, M., De Groot, S. H. M., Verdonck, F., and Vos, M. A. (2002). Role of the Na/Ca exchanger in arrhythmias in compensated hypertrophy. *Ann. N. Y. Acad. Sci.* 976, 438–445. doi: 10.1111/j.1749-6632.2002.tb04773.x

Szentesi, P., Pignier, C., Egger, M., Kranias, E. G., and Niggli, E. (2004). Sarcoplasmic reticulum Ca2+ refilling controls recovery from Ca2+-induced Ca2+ release refractoriness in heart muscle. *Circ. Res.* 95, 807–813. doi: 10.1161/01.RES.0000146029.80463.7d

Thomsen, M., Oros, A., Schoenmakers, M., van Opstal, J., Maas, J., Beekman, J., et al. (2007). Proarrhythmic electrical remodelling is associated with increased beat-to-beat variability of repolarisation. *Cardiovasc. Res.* 73, 521–530. doi: 10.1016/j.cardiores.2006.11.025

Thomsen, M. B., Verduyn, S. C., Stengl, M., Beekman, J. D. M., de Pater, G., van Opstal, J., et al. (2004). Increased short-term variability of repolarization predicts d-sotalol-induced torsades de pointes in dogs. *Circulation* 110, 2453–2459. doi: 10.1161/01.CIR.0000145162.64183.C8

Thomsen, M. B., Volders, P. G. A., Beekman, J. D. M., Matz, J., and Vos, M. A. (2006). Beat-to-Beat variability of repolarization determines proarrhythmic outcome in dogs susceptible to drug-induced torsades de pointes. *J. Am. Coll. Cardiol.* 48, 1268–1276. doi: 10.1016/j.jacc.2006.05.048

Tomaselli, G. F., and Zipes, D. P. (2004). What causes sudden death in heart failure? *Circ. Res.* 95, 754–763. doi: 10.1161/01.RES.0000145047.14691.db

van Borren, M. M. G. J., Vos, M. A., Houtman, M. J. C., Antoons, G., and Ravesloot, J. H. (2013). Increased sarcolemmal Na+/H+ exchange activity in hypertrophied myocytes from dogs with chronic atrioventricular block. *Front. Physiol.* 4:322. doi: 10.3389/fphys.2013.00322

Van de Water, A., Verheyen, J., Xhonneux, R., and Reneman, R. S. (1989). An improved method to correct the QT interval of the electrocardiogram for changes in heart rate. *J. Pharmacol. Methods* 22, 207–217. doi: 10.1016/0160-5402(89)90015-6

Verdonck, F., Volders, P. G. A., Vos, M. A., and Sipido, K. R. (2003). Increased Na+ concentration and altered Na/K pump activity in hypertrophied canine ventricular cells. *Cardiovasc. Res.* 57, 1035–1043. doi: 10.1016/S0008-6363(02)00734-4

Verduyn, S. C., Vos, M. A., van der Zande, J., Kulcsàr, A., and Wellens, H. J. (1997a). Further observations to elucidate the role of interventricular dispersion of repolarization and early afterdepolarizations in the genesis of acquired torsade de pointes arrhythmias: a comparison between almokalant and *d*-sotalol using the dog as its own control. *J. Am. Coll. Cardiol.* 30, 1575–1584. doi: 10.1016/S0735-1097(97)00333-1

Verduyn, S. C., Vos, M. A., van der Zande, J., van der Hulst, F. F., and Wellens, H. J. (1997b). Role of interventricular dispersion of repolarization in acquired torsade-de-pointes arrhythmias: reversal by magnesium. *Cardiovasc. Res.* 34, 453–463.

Volders, P. G., Sipido, K. R., Vos, M. A., Kulcsár, A., Verduyn, S. C., and Wellens, H. J. (1998). Cellular basis of biventricular hypertrophy and arrhythmogenesis in dogs with chronic complete atrioventricular block and acquired torsade de pointes. *Circulation* 98, 1136–1147. doi: 10.1161/01.CIR.98.11.1136

Volders, P. G., Vos, M. A., Szabo, B., Sipido, K. R., de Groot, S. H., Gorgels, A. P., et al. (2000). Progress in the understanding of cardiac early afterdepolarizations and torsades de pointes: time to revise current concepts. *Cardiovasc. Res.* 46, 376–392. doi: 10.1016/S0008-6363(00)00022-5

Vos, M. A., de Groot, S. H., Verduyn, S. C., van der Zande, J., Leunissen, H. D., Cleutjens, J. P., et al. (1998). Enhanced susceptibility for acquired torsade de pointes arrhythmias in the dog with chronic, complete AV block is related to cardiac hypertrophy and electrical remodeling. *Circulation* 98, 1125–1135. doi: 10.1161/01.CIR.98.11.1125

Wada, T., Ohara, H., Nakamura, Y., Yokoyama, H., Cao, X., Izumi-Nakaseko, H., et al. (2016). Impacts of surgically performed renal denervation on the cardiovascular and electrophysiological variables in the chronic atrioventricular block dogs– comparison with those of amiodarone treatment. *Circ. J.* 80, 1556–1563. doi: 10.1253/circj.CJ-16-0198

Zhou, S., Jung, B.-C., Tan, A. Y., Trang, V. Q., Gholmieh, G., Han, S.-W., et al. (2008). Spontaneous stellate ganglion nerve activity and ventricular arrhythmia in a canine model of sudden death. *Heart Rhythm* 5, 131–139. doi: 10.1016/j.hrthm.2007.09.007

Conflict of Interest Statement: The authors declare that the research was conducted in the absence of any commercial or financial relationships that could be construed as a potential conflict of interest.

Advantages of publishing in Frontiers

OPEN ACCESS
Articles are free to read for greatest visibility and readership

FAST PUBLICATION
Around 90 days from submission to decision

HIGH QUALITY PEER-REVIEW
Rigorous, collaborative, and constructive peer-review

TRANSPARENT PEER-REVIEW
Editors and reviewers acknowledged by name on published articles

Frontiers
Avenue du Tribunal-Fédéral 34
1005 Lausanne | Switzerland

Visit us: www.frontiersin.org
Contact us: info@frontiersin.org | +41 21 510 17 00

REPRODUCIBILITY OF RESEARCH
Support open data and methods to enhance research reproducibility

DIGITAL PUBLISHING
Articles designed for optimal readership across devices

FOLLOW US
@frontiersin

IMPACT METRICS
Advanced article metrics track visibility across digital media

EXTENSIVE PROMOTION
Marketing and promotion of impactful research

LOOP RESEARCH NETWORK
Our network increases your article's readership